UCLA
UCLA Electronic Theses and Dissertations

Title

Total Syntheses of Akuammiline Alkaloids and Nickel-Catalyzed Heck Cyclizations of Amide Derivatives

Permalink

https://escholarship.org/uc/item/67b824zf

Author

Moreno, Jesus

Publication Date

2017

Peer reviewed|Thesis/dissertation

eScholarship.org Powered by the California Digital Library
University of California

UNIVERSITY OF CALIFORNIA

Los Angeles

Total Syntheses of Akuammiline Alkaloids and Nickel-Catalyzed Heck Cyclizations of Amide Derivatives

A dissertation submitted in partial satisfaction of the

requirements for the degree Doctor of Philosophy

in Chemistry

by

Jesus Moreno

2017

© Copyright by

Jesus Moreno

2017

ABSTRACT OF THE DISSERTATION

Total Syntheses of Akuammiline Alkaloids and Nickel-Catalyzed Heck Cyclizations of Amide Derivatives

by

Jesus Moreno

Doctor of Philosophy in Chemistry

University of California, Los Angeles, 2017

Professor Neil Kamal Garg, Chair

This dissertation is divided into two projects concerning natural product synthesis and methodology development. The importance of natural product synthesis in chemistry and medicine cannot be overstated. In addition to providing a complex setting to test and apply new synthetic methodologies, natural products play a vital role in public health. Their influence in the pharmaceutical industry is profound, as approximately half of all chemical entities to treat disease come from natural product mimics, derivatives, or natural products themselves. With new natural products being discovered daily, there exists an ongoing need to develop efficient syntheses of these compounds and their derivatives.

Chapters One, Two, and Three focus on a particularly interesting and important class of indole-containing natural products called the akuammiline alkaloids. Specifically, Chapter One provides a historical overview of this family of compounds that ultimately demonstrates how these challenging structures, along with their encouraging pharmacological profiles, render them

formidable synthetic targets that have been the subject of synthetic chemists' efforts for the past decade.

Chapters Two and Three describe our lab's own synthetic efforts to members of the akuammiline family: picrinine, strictamine, 2(*S*)-cathafoline, and aspidophylline A. Central to our approach was the use of modern variants of the classic Fischer indolization reaction to generate high levels of complexity and the cores of the natural products. Ultimately, these efforts culminated in the first total synthesis of picrinine, strictamine, and 2(*S*)-cathafoline, as well as an enantioselective, second-generation synthesis of aspidophylline A.

Chapter Four describes the development of the first Mizoroki–Heck cyclizations of amide derivatives. This work highlights the potential of amides, which were once thought to be unreactive due to their resonance stability, as building blocks to prepare complex structures. Through this method, various products containing quaternary centers can be formed.

The dissertation of Jesus Moreno is approved.

Yi Tang

Robert Michael van Dam

Neil Kamal Garg, Committee Chair

University of California, Los Angeles

2017

"I know that you think it's fake, (but) maybe fake's what I like."

– Tame Impala, 'New Person, Same Old Mistakes'

For my parents: Carlos and Maria Moreno

TABLE OF CONTENTS

LIST OF FIGURES

CHAPTER ONE

CHAPTER TWO

CHAPTER FOUR

LIST OF SCHEMES

CHAPTER ONE

CHAPTER TWO

CHAPTER THREE

LIST OF TABLES

CHAPTER THREE

CHAPTER FOUR

LIST OF ABBREVIATIONS

α	alpha
$[\alpha]_D$	specific rotation at wavelength of sodium D line
Å	angstrom
β	beta
c	concentration for specific rotation measurements
γ	gamma
m/z	mass to charge ratio
μ	micro
π	pi
Ac	acetyl, acetate
AcOH	acetic acid
AIBN	azobisisobutyronitrile
app.	apparent
aq.	aqueous
BHT	butylated hydroxytoluene
Boc	*tert*-butoxycarbonyl
Boc_2O	di-*tert*-butyl dicarbonate
Bn	benzyl
br	broad
BTPP	(*tert*-butylimino)tris(pyrrolidino)phosphorane
Bu	butyl
i-Bu	isobutyl
n-Bu	butyl (linear)
t-Bu	*tert*-butyl
t-BuOH	*tert*-butyl alcohol
Bz	benzoyl
°C	degrees Celsius
calcd	calculated
CAN	cerium (IV) ammonium nitrate
cat.	catalytic
CCDC	Cambridge Crystallographic Data Centre
cod	1,5-cyclooctadiene

d	doublet
DCB	1,2-dichlorobenzene
DCE	1,2-dichloroethane
Dess–Martin	Dess–Martin Periodinane
$(DHQ)_2PHAL$	hydroquinine 1,4-phthalazinediyl diether
DIBAL-H	diisobutylaluminium hydride
DIC	*N,N*′-diisopropylcarbodiimide
dig	digonal
DMA	Dimethylacetamide
DMAP	4-dimethylaminopyridine
DMF	*N*,*N*-dimethylformamide
DMPU	1,3-dimethyl-3,4,5,6-tetrahydro-2(1H)-pyrimidinone
DMSO	dimethyl sulfoxide
dppf	1,1′-bis(diphenylphosphino)ferrocene
ee	enantiomeric excess
equiv	equivalent
EDC•HCl	1-ethyl-3-(3-dimethylaminopropyl)carbodiimide hydrochloride
ESI	electrospray ionization
Et	ethyl
g	gram(s)
Glc	glucosyl
h	hour(s)
HMPA	hexamethylphosphoramide
HOBt	hydroxybenzatriazole
HRMS	high resolution mass spectroscopy
Hz	hertz
imid.	imidazole
IBX	2-iodoxybenzoic acid
IR	infrared (spectroscopy)
J	coupling constant
L	liter
LiHMDS	lithium hexamethyldisilazide
m	meta
m-CPBA	3-chloroperbenzoic acid

m	multiplet or milli
min	minute(s)
mol	mole(s)
mp	melting point
M	molecular mass
Me	methyl
MHz	megahertz
MOM	methoxymethyl ether
MS	molecular sieves
NF-κB	nuclear Factor kappa B
NIS	*N*-iodosuccinimide
NMO	4-methylmorpholine *N*-oxide
NMR	nuclear magnetic resonance
Ns	2-nitrobenzenesulfonyl
[O]	oxidation
OTf	trifluoromethanesulfonate (triflate)
p	para-toluenesulfonic acid
pH	hydrogen ion concentration in aqueous solution
ppm	parts per million
PCC	pyridinium chlorochromate
Ph	phenyl
Piv	pivaloyl
Pr	propyl
i-Pr	isopropyl
PMP	1,2,2,6,6-pentamethylpiperidine
PPTS	pyridinium *p*-toluenesulfonate
PSI	Pounds per square inch
q	quartet
quint.	quintet
R_f	retention factor
s	singlet
sat.	saturated
sext.	sextet
SGLT2	sodium-glucose linked transporter 2

t	triplet
trig	trigonal
TBAB	tetra-*n*-butylammonium bromide
TBDPS	*tert*-butyldiphenylsilyl
TBS	*tert*-butyldimethylsilyl
TBSCl	*tert*-butyldimethylsilyl chloride
TEBA	benzyltriethylammonium
TES	triethylsilyl
Tf	trifluoromethanesulfonyl (trifyl)
TFA	trifluoroacetic acid
THF	tetrahydrofuran
TLC	thin layer chromatography
TMS	trimethylsilyl
TMSCl	trimethylsilyl chloride
TMSOTf	trimethylsiyl triflate
Trost Ligand	(*R*, *R*)-DACH-phenyl Trost ligand
Ts	*p*-toluenesulfonyl (tosyl)
UV	ultraviolet

ACKNOWLEDGEMENTS

First and foremost, I would like to thank my advisor, Professor Neil K. Garg. Throughout the years, I've always been asked by many people about what it's like to work with Neil. Whether I'm answering to other graduate students (prospective or current), potential employers, or even friends and family, my answer has remained the same: "He is very good at what he does." Despite the nebulous connotation, I believe this statement is positively all-encompassing on many levels. For example, his reputation as an educator speaks for itself. But for me, as one of his graduate students, the preceding statement is most true when considering that he, through thick and thin, is the lab's biggest advocate. Graduate school is very tough, and there is no shortage of bad patches. In spite of this, I am proud to characterize the relationship I've developed with Neil over the years as one based on constant communication and mutual respect. He has been essential to my professional and scientific development, and I am very grateful for his constant support, understanding, and encouragement at all stages of graduate school, dating from allowing me to join his lab, to helping me secure a job.

Of course, I would also like to acknowledge the rest of my doctoral committee (both certifying and non-certifying members): Professors Miguel A. García-Garibay, Yi Tang, and Robert Michael van Dam. They have been constant supporters of Neil's lab in many ways, and I thank them for taking the time to personally support me by serving on my committee.

I'd also like to thank other people who were instrumental in my professional and scientific development en route towards graduate school. Barbara Sawrey at the University of California, San Diego was a great mentor who helped enrich my undergraduate studies by introducing me to many research opportunities. At UCSD, my first undergraduate research experience was conducted

in Professor Thomas Hermann's laboratory. I thank Thomas for his willingness to take me in as an undergraduate researcher, when it seemed like I had just about contacted every professor in the chemistry department, desperately looking for a lab to join. In his lab, I interacted with a talented group of graduate students, a couple of whom I would like to specifically mention. Maia Carnevali, Emily Garcia Sega, and Kevin Rynearson were all excellent mentors and I thank them for their patience. Furthermore, I thank Kevin for introducing me to the concept of graduate school and identifying the things that were most important in selecting a lab. His mentorship and friendship truly motivated me to go to graduate school, in hopes that I could emulate an ounce of the exemplary chemist that he is.

Dr. Sawrey also introduced me to a Summer Undergraduate Research Fellowship program at the Scripps Research Institute, where I had the pleasure of working in Professor Ryan Shenvi's laboratory. Ryan is by far one the most intelligent people I've ever interacted with. His optimism and love for science, in collaboration with the mentorship I received from graduate student Dan Jansen, provided a positive experience that I wished to carry on through my own doctoral studies.

As I prepare to embark onto the next stage of my professional career as a medicinal chemist at Merck & Co., Inc. in Boston, I can't help but think how different my path would be had I not randomly stumbled upon an internship application at Vertex Pharmaceuticals, and was subsequently fortunate enough to actually obtain the position. My experience at Vertex affirmed my interest in returning to the pharmaceutical industry after graduate school. At Vertex, Corey Anderson was a great supervisor that provided me with copious amounts of objective advice going into my graduate studies that continued even as I looked for jobs at other companies (since Vertex wasn't hiring, unfortunately). In addition, the positive interactions I had with many of the other staff at Vertex made me very excited at the prospect of being involved in a highly collaborative

environment to potentially solve many problems in human health. This, after all was a major reason as to why I became interested in organic chemistry in the first place.

They say that players are nothing without their teammates, and this is certainly true when thinking about the projects I've worked on throughout my graduate studies. I feel extremely fortunate to have been able to closely work on the two projects disclosed in this thesis with the following people: Joel M. Smith, Elias Picazo, Lucas A. Morrill, Jose M. Medina, Sophie Racine, and Shuaijing Du.

Like Ryan Shevi, Joel belongs to the short list of the most intelligent people I've ever met. It was truly an honor to learn so much from and work alongside him. I thought we made an extremely effective team to tackle one of the most longstanding challenges of our lab's research program. Outside the lab, I'll always appreciate our friendship, which focused on a common passion for soccer and a very particular sense of humor. After finishing the total synthesis of picrinine, our dynamic duo doubled in size and we were joined by Elias (AKA: *Mamas*) and Lucas (AKA: Doofy). Their excitement and intuition upon joining this project was extremely impressive to the point where it didn't feel like I was mentoring them, rather we were all just taking turns learning from each other. I am also very grateful for their friendship. Through Elias and our similar experiences, I have gotten to learn about myself more than I ever thought I could, and I feel honored to serve as one of the groomsmen in his wedding. Despite our constant bickering like an old married couple, I thank Lucas for helping me assimilate in countless ways in preparation for my move to Boston. I now realize that it was always his ulterior motive to get me to take a job out there, but I couldn't be happier with that decision, and look forward to catching up with him about it in the years to come.

I'll always regard Jose as one of the hardest working people I've ever met. I admire the way he approaches and thinks about chemistry, especially because I think it complemented my own perspective and ultimately created another successful partnership. I also regard Jose as someone with an extremely good taste in music. I appreciated the eagerness in which he constantly introduced me to new bands, even when it appeared that the music I previously listened to was garbage. I had fun going to many great concerts with him, especially the *three* Tame Impala shows! I honestly can't thank him enough for introducing me to them. The culmination of the project we started working on could not have been possible without Sophie and Shuaijing. We were extremely fortunate to have a postdoctoral student as experienced as Sophie join us when finishing the project was of utmost priority. In addition, Sophie is a great person who constantly reminded me to never depreciate my self-worth as a chemist, and more importantly, as a person. I am also obliged to Shuaijing Du for being a respectful undergraduate student on this project who helped me learn how to become a more effective mentor.

Apart from the colleagues I worked the closest with, I am indebted to the rest of the members of Neil's lab that I interacted with, as they definitely made my experience in and outside of the lab more enjoyable. I've always enjoyed the group's dynamic as a whole, and this characteristic was one of the main reasons as to why I ultimately wanted to join the lab.

As a younger student, I had the pleasure of getting to know older students who have since moved on to bigger and better things. I thank the likes of Alex Schammel, Ben Boal, Alex Huters, Grace Chiou, Adam Goetz, and Stephen Ramgren for being welcoming and exemplary older students at the time. Evan Styduhar was a great person to work next to upon joining the lab. He was an invaluable resource as I got myself situated with research in the group, as well as a good friend who also shared his love of music with me, in return for my sharing of love for Mexican

food with him. I would argue that Noah Fine Nathel is responsible for a huge part of my personal development. Aside from his unique sense of humor (more so than Joel's) and passion for horror movies, both of which I grew to love, Noah was a compassionate, but objective listener during some of my toughest times. Ultimately, he taught me how use logic and reason when I thought it wasn't possible, and that there were many productive ways to battle the demons we all have to deal with from time to time. Tejas Shah was the best "first roomie" anyone could ask for. I am glad to have spent a lot of my most fun nights in Los Angeles with him as members of the "drink team." In addition, he is a very supportive person, although he can be quite the contrarian sometimes… Liana Hie is one of the sweetest people I've ever met. What's even more impressive than her dedicated work ethic is the fact that she managed to survive her last years in graduate school by being in a room with loud and outspoken guys, myself included. In spite of this, she still managed to always provide the lab with positive reinforcement. I personally appreciated the kind comments about my hair and the enabling of stress-eating.

Some of the older students I interacted with during my time at UCLA were not just graduate students of the lab, but other postdoctoral students. I feel like Travis McMahon's arrival revamped the lab's general interest for sports and beer, and I thank him for that. Aside from that, he was very helpful and extremely constructive with chemistry and presentation feedback. There are an infinite number of things I can say with respect to Marie Hoffmann. To be honest, she's probably heard most of these things, whether or not she remembers them. As another founding member of the "drink team," she was a fantastic friend that I could always count on to keep me grounded and to remind me that my happiness should always come first. Most recently, it was nice to have interacted with Evan Darzi, who in my opinion is a very well-rounded person. It would've been great to work with him more, as I admire his fascination for all areas of chemistry, rap, and sports.

I am extremely grateful to the sense of comradery I felt with the rest of my cohort in the lab. I thank Mike Corsello (*Hi!*) for showing me nothing but empathy as we concurrently tried to carve our own paths in graduate school. I feel a sense of pride when I think about just how much we've each grown since we started the program, because it wouldn't have been possible without each others' support. It's safe to say that Nick Weires provided the majority of the comic relief necessary to survive in graduate school. I'll always have fond memories of him making Mike laugh until he cried, especially during our year's trip to the ACS conference in Philadelphia.

It's baffling to think how much I'll miss someone like Junyong Kim (AKA: Junie, Jun-ya, Jun-puppy, etc.) when all he did was refuse to hang out with me and defeat me in the lab's search for the "best dressed" guy at the holiday parties. Still, I thank him for all the good times stemming from his contagious laugh, love for puppies, countless nicknames (*vide supra*), and karaoke sessions in lab. I am happy to have met Emma Baker, who also shares a love for horror movies. By the end of my doctoral studies, it was her who was graciously inviting me and Noah to watch the next scary movie, so I thank her for her inclusion.

I am happy to have gotten close with even some of the younger students of the lab. My interactions with Bryan Simmons (A.K.A: Money) have been nothing but positive since the first day I met him at his recruitment weekend. I'd like to think I had something to do with his decision to join our lab. Regardless whether that's true or not, I'm glad he joined the lab as he has been an important part of it. His support throughout my studies should've definitely warranted him an acknowledgment in all my manuscripts, but I suppose this will do. I thank him for getting me into hockey and for all the good times we've had going to concerts and just hanging out (without Chloe of course… kidding!). I think about how much my friendship with Joyann Barber has grown and almost regret it… only because she is now just as sassy with me as I have been with everyone else

in the lab! But at the end of the day, I'm happy she decided to join our "lunch crew" and, like Liana, I thank her for patience in dealing with a bunch of outspoken people, although she is one of us now!

I explicitly remember (jokingly) telling everyone that I was done befriending younger students, beginning with the class that blessed us with the likes of Robert Susick (AKA: Bobby), Michael Yamano (AKA: Roboto) and Jacob Dander. However, after about a year of pestering, to everyone's disbelief, I have grown to appreciate these guys as well. I first brought my guard down for Robert, not only because he was my roommate, but because he is a genuinely nice guy that was absolutely essential to balancing out my cynical demeanor. I can't believe I allowed myself to humor someone with as bad jokes as Michael, but still cherish all the random hangouts involving all the things he bought off of Craigslist (e.g. foosball, craps, spikeball, etc.) I also have to thank him and Robert for introducing me to Rick and Morty, as that currently comprises 90% of my humor ("*wubba lubba dub dub!*"). Despite constantly referring to him as my antithesis, I thank Jacob for being a pleasant person to talk to. I've enjoyed collectively hanging out with him, Robert and Michael doing the most of the things listed above, as he balances the trio by being the most level-headed person of the group.

It is disappointing to realize that I won't get the chance to interact with the lab's current first year students as much as I would've like to. Still, I am obliged to Sarah Anthony (AKA: Sonya), Margeaux (AKA: Marjorie) Miller, Tim Boit, and Melissa Ramirez for taking me back in time and helping me see a little bit of my past self in them, especially in Sarah's eagerness and Margeaux's sarcasm. It's a nice reminder of how scary, but exciting graduate school can be as an incoming first year, even when you aren't entirely aware of how much you'll grow throughout the journey. I am looking forward to hearing about their growth in the future, and wish them, as well

as the rest of my dear colleagues, the best of luck on their future endeavors. Never forget that at the end of the day, you are more in control than you think you might be.

I would also like to thank the friends outside of the realm of my research group. I've made many friendships with people at UCLA and thank them for their support and memories: Jessica Grandner, Janice Lin, Tim Chung, Jeong Hoon Ko (J.K.), and Austin Asari. I am also extremely happy with the groups of friends I've made in Los Angeles (outside of UCLA), and those that I have sustained from San Diego and beyond. As such, I thank all members of both "Shy Boyz FC" and "The B**** Crew." Both groups provided me not just with countless memories of soccer games, inside jokes, and nights out, but with the constant reminder of my culture and heritage, which is something that I will continue to proudly express wherever I go. I am grateful for the type of relationship I continue to have with Tomas Hernandez. We have gone months, or even years without seeing each other, but his support and friendship remains the same. I appreciate the mutual understanding we have for our individual lives and goals, and I am proud of the strides he has made. Soon we will be able to sit back and fondly reflect on things more often, as we do so well.

I was lucky enough to have had extended family support me here in Los Angeles, which immensely helped my transition at the beginning of my graduate studies. To that end, I would like to thank my Tios Rudy and Teresa Ramirez, Jorge Silva and Gloria Moreno for always welcoming me into their home and taking me in like one of their own. I am grateful for my cousins Rudy, Noemi, and Jonathan. I thank Noemi for bringing my Godson Damien into this world and for giving me the opportunity to be his Godfather. I am especially proud to have seen Jonathan grow up to be the level-headed man he is today. I'd like to think I had something to do with that, but in all honesty, I feel privileged to have grown with him these past years because he has taught me more than I think I have taught him. He is without a doubt the little brother I never had.

It would be a disservice to not take ample time to directly thank my biggest support system: my immediate family. Vanesa, I am so excited to have the chance to celebrate both of our accomplishments together. I couldn't be a prouder older brother and I am looking forward to watch you start your own life with Jando (*Hi Jando!*) next year. I thank you and him for never giving up on me, even when I felt like all I did was bombard you guys with my problems. Melina, one of the reasons I am thankful for my struggles is because it brought me closer to you. Even if we don't see eye to eye on a lot of things, I am happy that I can at least understand you for who you are as you have always been towards me. I, too, am proud of you for how far you come and hope that you continue on the right path towards your happiness because you deserve it. Mom and Dad, I've said this time and time again: *nothing* that I have accomplished has been for anyone but me and you, because you are the only ones who have literally made it possible. I have been humbly astounded at the amount of support you have provided in every conceivable way. No matter how difficult of an adjustment graduate school was for me and you, both of you graciously kept your composure and showed me nothing but unconditional love and understanding. Just as you have relayed how proud you are of me, I am equally proud of you for being selfless parents and best friends to me and my sisters. I will try to continue to make you proud in the years to come, with the intention of repaying you for all you have done for our family. *Gracias Ama y Apa, otra vez lo logramos*.

Finally, I directly thank my girlfriend, Liliana Briseño. You don't know how much your reentry into my life means to me. Rather than attempting to do so here, I promise to show you in the many days that await us. I couldn't be more excited and happier to start the next chapter of my life with you. *I love you, always*.

Chapter One is a version of Smith, J. M.; Moreno, J.; Boal, B. W.; Garg, N. K. *Angew. Chem., Int. Ed.* **2015**, *54*, 400–412. Smith, Moreno, Boal, and Garg were responsible for writing the manuscript.

Chapter Two is a blend of Smith, J. M.; Moreno, J.; Boal, B. W.; Garg, N. K. *J. Am. Chem. Soc.* **2014**, *136*, 4504–4507 and Smith, J. M.; Moreno, J.; Boal, B. W.; Garg, N. K. *J. Org. Chem.* **2015**, *80*, 8954–8967. Smith, Moreno, and Boal were responsible for experimental work.

Chapter Three is a version of Moreno, J. Picazo, E.; Morrill, L. A.; Smith, J. M.; Garg, N. K. *J. Am. Chem. Soc.* **2016**, *138*, 1162–1165. Moreno, Picazo, Morrill, and Smith were responsible for experimental work.

Chapter Four is a version of Medina, J. M.; Moreno, J.; Racine, S.; Du, S.; Garg, N. K. *Angew. Chem, Int. Ed. Soc.* [Online early access]. DOI: 10.1002/anie.201703174R1. Medina, Moreno, Racine, and Du were responsible for experimental work.

These studies were supported by a predoctoral fellowship from the NIH (F31-GM113642).

BIOGRAPHICAL SKETCH

Education:

University of California, Los Angeles, CA

- Ph.D Candidate in Organic Chemistry, September 2014 – May 2017
- Graduate Research Assistant, November 2012 – May 2017
- Current GPA: 3.935/4.0

University of California, San Diego, CA

- Bachelor of Science in Molecular Synthesis, June 2012.
- Cumulative GPA: 3.39/4.00

Professional and Academic Experience:

Graduate Research Assistant: University of California, Los Angeles, CA

- November 2012 – May 2017; Advisor: Prof. Neil K. Garg
- Synthesized over half a gram of a tricyclic ketone intermediate for synthetic studies toward the total synthesis of picrinine.
- Implemented intricate late-stage synthetic strategies and completed the first total synthesis of the polycyclic akuammiline alkaloid picrinine.
- Developed a unified approach to access several structural subclasses of the akuammiline alkaloids from common late-stage intermediates.
- Achieved a second-generation, enantioselective total synthesis of the MDR-reversing agent aspidophylline A.
- Optimized late-stage manipulations to enable the first, enantioselective total syntheses of 2(*S*)-cathafoline and strictamine.
- Developed the nickel-catalyzed Heck cyclization of aryl amide derivatives.

Graduate Teaching Assistant: University of California, Los Angeles, CA.

- Fall 2012 – Spring 2013.
- Led discussion sections for undergraduate general and organic chemistry.

Chemistry Intern: Vertex Pharmaceuticals, San Diego, CA

- April 2012 to August 2012; Mentor: Dr. Corey Anderson
- Developed a facile one-pot process for the addition of nitriles to substituted heterocycles.

Summer Undergraduate Research Fellow: Scripps Research Institute, San Diego, CA

- June 2011 – August 2011; Advisor: Prof. Ryan A. Shenvi
- Synthesized multigram amounts of a key triene intermediate en route to the total synthesis of the quinolizidine alkaloid, castoramine.
- Optimized several key steps of the aforementioned synthetic route to improve yields, efficiency, and practicality.

Undergraduate Research Assistant: University of California, San Diego, CA

- September 2010 – April 2012; Advisor: Prof. Thomas Hermann

- Synthesized three different classes of compounds to be investigated as potential small molecular inhibitors of the internal ribosomal entry site (IRES) of the Hepatitis C virus.
- Implemented robust synthetic routes to access derivatives of each class of compounds for subsequent biological studies.

Honors and Awards:

- American Chemical Society Scholars Program, 2008–2012.
- The Scripps Research Institute Summer Undergraduate Research Fellowship, 2011.
- UCLA Hanson–Dow Award for Excellence in Teaching, 2013.
- UCLA Christopher S. Foote Fellowship in Organic Chemistry, 2015.
- NIH – Ruth L. Kirschstein National Research Service Award (NRSA) Predoctoral Fellowship to Promote Diversity in Health-Related Research, 2015–present.
- Invitee – 2016 Dow BEST Symposium, August 2016.

Publications:

7. **Mizoroki–Heck Cyclizations of Amide Derivatives for the Introduction of Quaternary Centers.** Jose M. Medina,[†] Jesus Moreno,[†] Sophie Racine, Shuaijing Du, and Neil K. Garg. *Angew. Chem, Int. Ed. Soc.* [Online early access]. DOI: 10.1002/anie.201703174R1. *([†] Denotes equal authorship)*

6. **Enantioselective Total Syntheses of Akuammiline Alkaloids (+)-Strictamine, (–)-2(*S*)-Cathafoline, and (–)-Aspidophylline A.** Jesus Moreno,[†] Elias Picazo,[†] Lucas A. Morrill, Joel M. Smith, and Neil K. Garg. *J. Am. Chem. Soc.* **2016**, *138*, 1162–1165. *([†] Denotes equal authorship)*

5. **The Fischer Indolization Reaction as a Strategic Platform for the Total Synthesis of Picrinine.** Joel M. Smith, Jesus Moreno, Ben W. Boal, and Neil K. Garg. *J. Org. Chem.* **2015**, *80*, 8954–8967. *(Feature article and journal cover)*

4. **Cascade Reactions: A Driving Force in Akuammiline Alkaloid Total Synthesis (Review).** Joel M. Smith[†], Jesus Moreno[†], Ben W. Boal, and Neil K. Garg. *Angew. Chem., Int. Ed.* **2015**, *54*, 400–412. *([†]Denotes equal authorship)*

3. **Total Synthesis of the Akuammiline Alkaloid Picrinine.** Joel M. Smith, Jesus Moreno, Ben W. Boal, and Neil K. Garg. *J. Am. Chem. Soc.* **2014**, *136*, 4504–4507.

2. **2-Aminobenzoxazole Ligands of the Hepatitis C Virus Internal Ribosomal Entry Site.** Kevin D. Rynearson, Brian Charrette, Christopher Gabriel, Jesus Moreno, Mark A. Boerneke, Sergey M. Dibrov, and Thomas Hermann. *Bioorg. Med. Chem. Lett.* **2014**, *24, 3521–3525.*

1. **Addition of α-Lithiated Nitriles to Azaheterocycles.** Corey Anderson, Jesus Moreno, and Sabine Hadida. *Synlett* **2014**, *25*, 677–680.

CHAPTER ONE

The Akuammiline Alkaloids: Origins and Synthetic Achievements

Adapted from: Joel M. Smith, Jesus Moreno, Ben W. Boal, and Neil K. Garg.

Angew. Chem., Int. Ed. **2015**, *54*, 400–412.

1.1 Abstract

The akuammiline alkaloids are a family of intricate natural products that have received considerable attention from scientists worldwide. Despite that many members of this alkaloid class were discovered over 50 years ago, synthetic chemistry has been unable to address their architectures until recently. This chapter provides a brief overview of the rich history of the akuammiline alkaloids, including their isolation, structural features, biological activity, and proposed biosyntheses. Furthermore, several recently completed total syntheses are discussed in detail. These examples not only serve to highlight modern achievements in alkaloid total synthesis, but also demonstrate how many the molecular scaffolds of the akuammilines have provided inspiration for the discovery and implementation of innovative cascade reactions for the rapid assembly of complex structures.

1.2 Introduction

Natural products belonging to the akuammiline family of alkaloids have provided a fruitful area of scientific discovery for over one century.[1] Initial interest in the akuammilines stemmed from their role in traditional medicine, where inhabitants of southern and southeastern Asia utilized

the leaves of native plants such as *Alstonia scholaris* to treat various ailments in humans and livestock.[2] As a result, scientists have investigated the pharmacological effects of akuammiline alkaloids and discovered their wide range of biological properties, which range from anti-cancer to analgesic effects. For example, echitamine (**1.1**), which was first isolated in 1875,[3] displays both in vitro and in vivo cytotoxicity,[4] whereas strictamine (**1.2**)[5] inhibits the transcription factor NF-κB (Figure 1.1).[6] Additionally, derivatives of picraline (**1.3**)[7] inhibit the renal cortex protein SGLT2,[8] while aspidophylline A (**1.4**) reverses drug-resistance in cancerous cell lines.[9]

Figure 1.1 Representative Biologically Active Akuammiline Alkaloids.

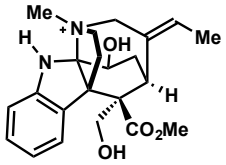

(–)-Echitamine (1.1)
(1875)

displays in vivo and
in vitro cytotoxicity

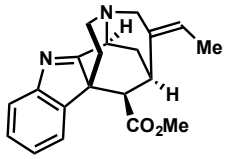

(+)-Strictamine (1.2)
(1966)

inhibits transcription
factor NF-kB

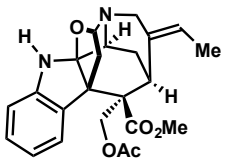

(+)-Picraline (1.3)
(1954)

derivatives inhibit
SGLT2 protein

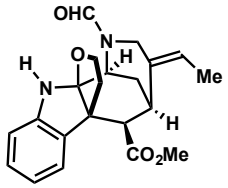

(–)-Aspidophylline A (1.4)
(2007)

reverses drug resistance
in cancer cells

As is apparent from the representative family members shown in Figure 1.1, there is a great deal of complexity and structural diversity amongst the >30 akuammiline alkaloids that have been isolated to date.[1] Although detailed biosynthetic studies have not been performed, the proposed biogenesis of various akuammilines sheds light on how nature likely assembles these intricate

scaffolds. As shown in Figure 1.2, the union of tryptamine (**1.5**) and the monoterpenoid secologanin (**1.6**) first results in the formation of the natural product geissoschizine (**1.7**). In turn, **1.7** serves as the progenitor to many different alkaloid frameworks including the strychnos, mavacurine, and akuammiline varieties.[10] For example, the strychnos alkaloid preakuammicine (**1.8**) would arise from a cyclization between C2 and C16, whereas the mavacurine alkaloid pleiocarpamine (**1.9**) stems from a cyclization between N1 and C16. The akuammiline framework, on the other hand, derives from an intramolecular oxidative coupling between C7 and C16 of geissoschizine (**1.7**). This constructs the caged indolenine framework of rhazimal (**1.10**).[11]

Figure 1.2 Proposed Biosynthesis of Several Monoterpenoid Indole Alkaloid Classes.

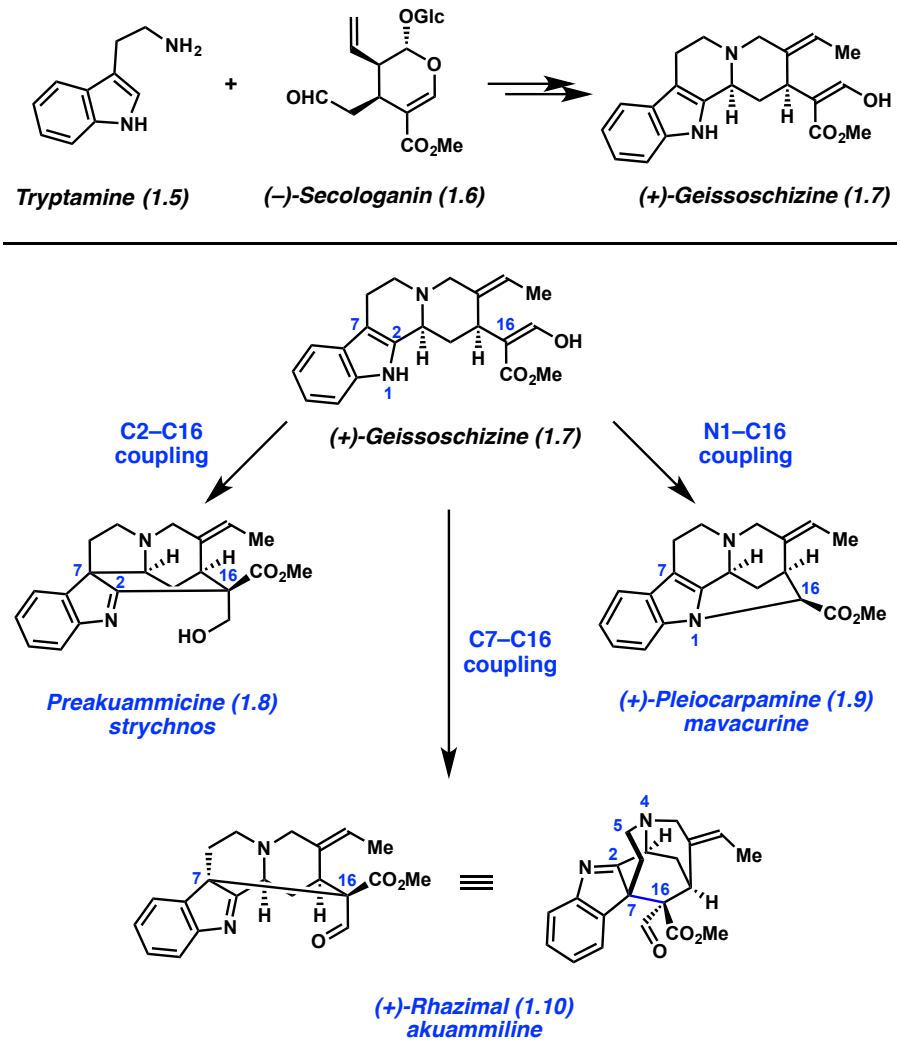

The polycyclic natural product rhazimal (**1.10)** is thought to serve as a molecular platform to access to all the other akuammiline family members through redox transformations, acylations, alkylations or skeletal migrations (Scheme 1.1). For example, pseudoakuammigine (**1.11**)[12] is thought to arise from aldehyde reduction, *N*-methylation, and tetrahydrofuran ring formation from **1.10**. Alternatively, akuammiline (**1.12**),[12] the namesake of the family, forms from reduction and acylation of the C17 carbonyl. Strictamine (**1.2**), on the other hand, forms from C16 deformylation.[5] Oxidation of akuammiline (**1.12**) at C5 would provide picraline (**1.3**),[7,7b] while the analogous transformation from **1.2** would yield picrinine (**1.13**).[13] Both scholarisine A (**1.14**) and aspidophylline A (**1.4**) are believed to arise from picrinine (**1.13**). Aspidophylline A (**1.4**)[9] could be generated by reduction at C5 and N4 formylation, whereas scholarisine A (**1.14**) is proposed to come from a redox isomerization and skeletal reconfiguration.[14] Finally, the pyrrolidinoindoline scaffold of vincorine (**1.15**)[15] is thought to stem from strictamine (**1.2**) via N4 migration from C3 to C2.[5]

Scheme 1.1 Divergent Biosynthetic Relationship of the Akuammiline Alkaloids.

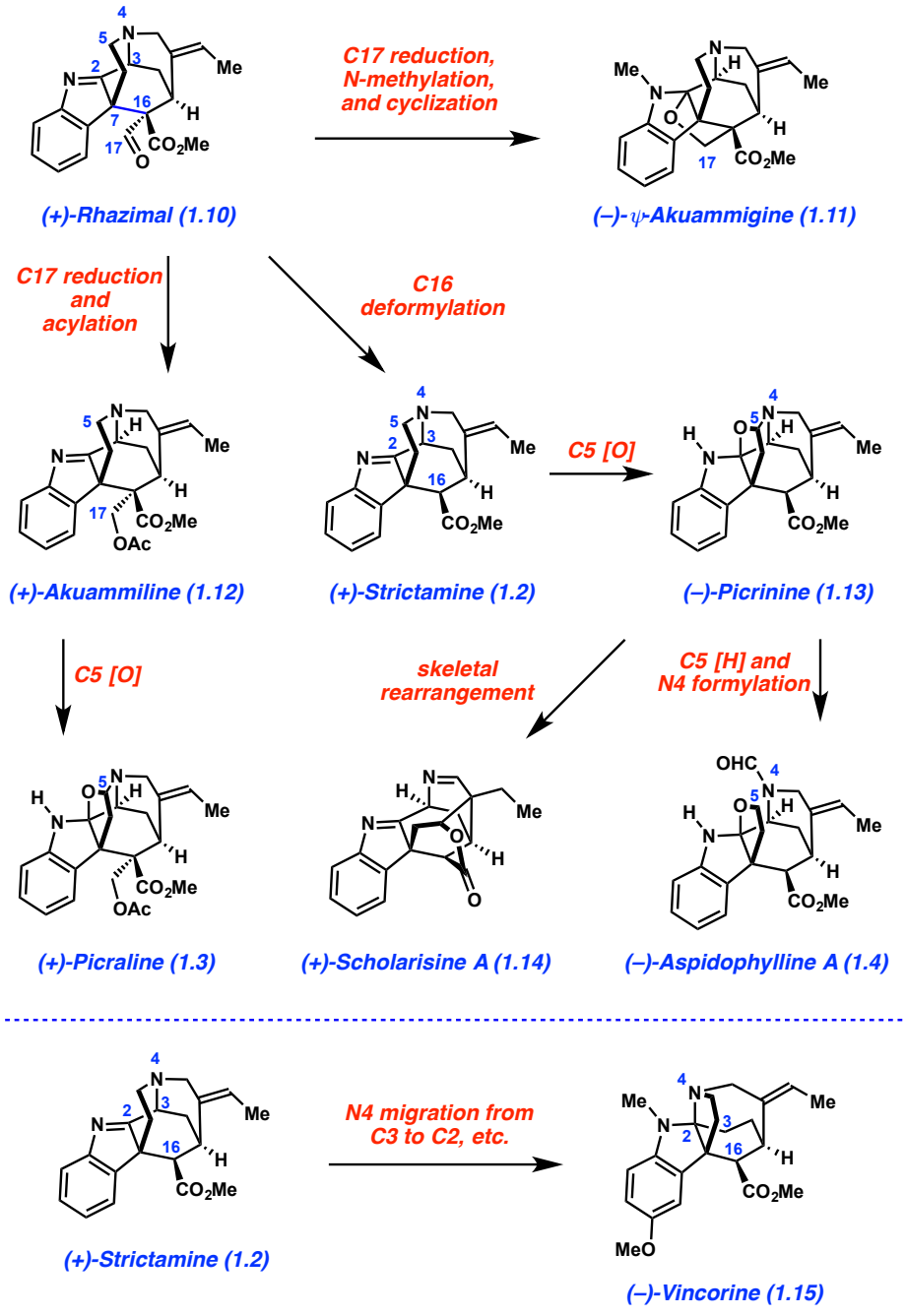

Research concerning the akuammilines has historically focused on isolation and pharmacological studies[1a] with relatively less emphasis on synthetic chemistry. However, synthetic studies by Dolby in the 1970's brought some attention to the akuammilines and provided

some noteworthy lessons on synthetic strategies for accessing these challenging natural products.[16] Since then, many research groups have reported promising strategies toward the akuammilines, including those of Sakai,[17] Toupet,[18] Bosch,[19] Takemoto,[20] Higuchi,[21] Shi,[22] and Zhu.[23]

Although many akuammiline alkaloids have yet to succumb to laboratory synthesis, synthetic efforts spanning from 2009–2015 have led to the completed total synthesis of four daunting akuammilines: vincorine (**1.15**),[24,25,26] aspidophylline A (**1.4**),[27,28,29] picrinine (**1.13**),[30] and scholarisine A (**1.14**).[31,32] Although the synthetic routes towards these alkaloids contain a variety of creative elements, one unifying theme is their utilization of innovative cascade reactions to elegantly and efficiently forge their intricate architectures. This chapter provides a perspective on the key transformations that construct multiple chemical bonds in one process, and how these cascades have fueled achievements in akuammiline total synthesis. Additionally, other important bond formations are highlighted, specifically those that played instrumental roles in enabling the completed syntheses.

1.3 Total Synthesis of Vincorine

(–)-Vincorine (**1.15**, Scheme 1.1) was first isolated in 1962 from *Vinca minor* by Šefčovič and co-workers.[15] As mentioned above, this alkaloid contains a pyrrolidinoindoline core that arises from a nitrogen migration within the parent akuammiline architecture. This migration results in a pentacyclic scaffold that includes one seven-membered ring and four contiguous stereocenters, one of which is quaternary. This section highlights the three completed total syntheses of **1.15** that have been reported to date by the groups of Qin,[24] Ma,[25] and MacMillan.[26]

1.3.1 Qin's Cyclopropanation Approach

The first breakthrough in the total synthesis of akuammilines came from Qin and co-workers, who reported the total synthesis of (±)-vincorine (**1.15**) in 2009.[24] The Qin group targeted two key challenges: assembly of the cyclohexyl-fused pyrrolidinoindoline framework and construction of the seven-membered ring. To address the former difficulty, Qin and co-workers employed an elegant cyclopropanation/fragmentation cascade sequence, which had earlier proven useful in their synthesis of the *strychnos* alkaloid minfiensine.[33]

As depicted in Scheme 1.2, a three-step sequence was used to convert ester **1.16**, a readily available intermediate,[34] to α-diazoester **1.17**, the substrate for the key cascade reaction. Using 5 mol% of copper(I) triflate, α-diazoester **1.17** underwent the desired cyclopropanation/fragmentation sequence to furnish tetracycle **1.20** in 52% yield. The transformation is thought to proceed by initial cyclopropanation of the indole moiety. Subsequent fragmentation of the cyclopropane (transition structure **1.18)** to the corresponding indoleninium species presumably occurs rapidly by virtue of the indoline nitrogen. Subsequent trapping by the tosyl-protected amine (transition structure **1.19**) then delivers the tetracyclic product. Notably, this cascade reaction concisely builds one carbon–nitrogen bond and one carbon–carbon bond. Moreover, the key C7 quaternary stereocenter is introduced, in addition to the pyrrolidinoindoline scaffold. From tetracycle **1.20**, four steps were used to access allylic alcohol **1.21**.

Scheme 1.2 Qin's Key Cyclopropanation Step to Construct **1.21**.

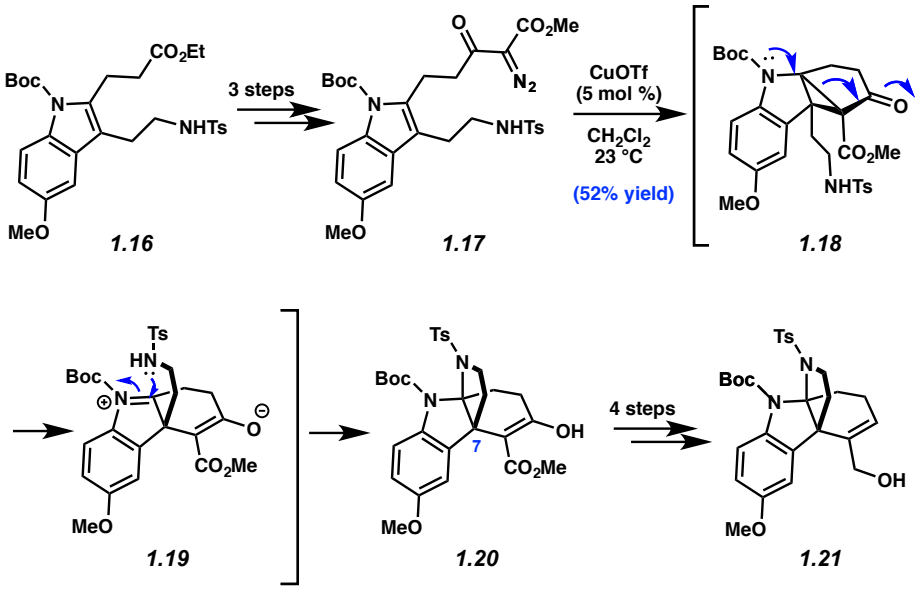

An abbreviated sequence illustrating the endgame to Qin's synthesis of (±)-vincorine (**1.15**) is shown in Scheme 1.3. Upon treatment with pivalic acid and trimethyl orthoacetate, alcohol **1.21** was converted into ester **1.23** in a 74% yield of the desired diastereomer, via a Johnson–Claisen rearrangement (transition structure **1.22**).[35] Ester **1.23** was elaborated in six steps to acid **1.24**, an important precursor towards constructing the natural product's seven-membered ring. The tosyl protecting group on the fused pyrrolidine was removed with Na/naphthalene, which set the stage for amide bond formation using Mukaiyama's reagent. Impressively, amide **1.25** was accessed in 39% yield from alcohol **1.21** (nine steps). Further manipulation provided silyl ether **1.26** over six steps, which included introduction of the exocylic olefin. A final six-step sequence was used to convert silyl ether **1.26** to (±)-vincorine (**1.15**) via deprotection and redox manipulations of the alcohol, and a deprotection and *N*-methylation of the indole nitrogen.

Scheme 1.3 Qin's Synthetic Endgame and Completion of (±)-Vincorine (**1.15**).

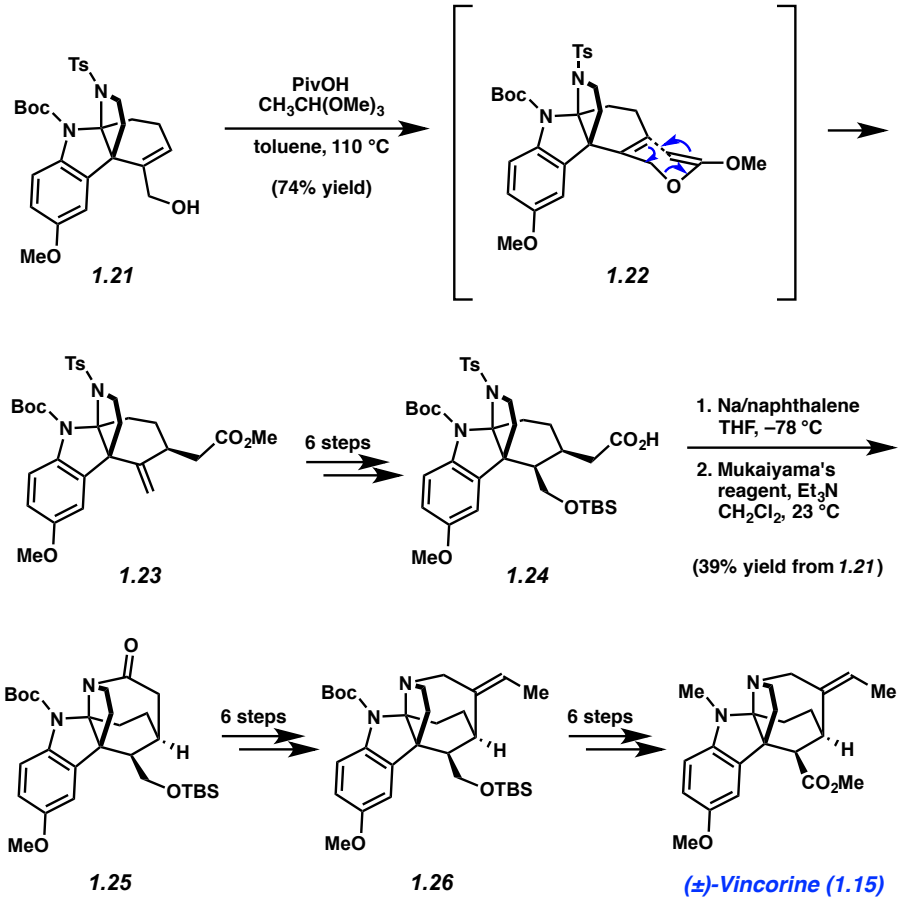

Qin's synthesis of (±)-vincorine (**1.15**) proceeded in 31 steps from known intermediate **1.16**, in roughly 1% overall yield. Of note, this was the first reported total synthesis of any akuammiline alkaloid, which marked a major achievement in the field. Qin's approach relied on intermediate tetracycle **1.20**, which was synthesized using a copper-catalyzed cyclopropanation/fragmentation cascade. This sequence built an important quaternary center, part of the compound's distinct fused pyrrolidinoindoline scaffold. Qin's efforts toward (±)-vincorine (**1.15**) also served to reveal the many challenges associated with assembling the natural product's core, such as constructing the seven-membered ring of the natural product. These seminal studies

provided significant groundwork for future syntheses of vincorine (**1.15**) and other akuammiline alkaloids.

1.3.1 Ma's Oxidative Coupling Approach

In 2012, Ma and co-workers reported the first enantioselective synthesis of (–)-vincorine (**1.15**).[25] Similar to the approach of Qin, Ma elected to forge the pyrrolidinoindoline scaffold early in the synthesis. Ma's approach utilizes a bioinspired intramolecular oxidative coupling to introduce all of the requisite carbon atoms of the natural product, prior to building the seven-membered ring. It should be noted that the Ma laboratory had previously developed a similar oxidative coupling strategy for their enantioselective synthesis of communesin F.[36]

Ma's synthesis of the key oxidative cyclization precursor, diester **1.31**, is summarized in Scheme 1.4. α,β-Unsaturated ester **1.27**, an intermediate readily accessed from tryptophan, was elaborated to malonate **1.28** in four steps. Toward installing the ethylidene unit, the Ma laboratory implemented an organocatalyzed enantioselective Michael addition of **1.29** using a proline-derived catalyst on the basis of precedent.[37] Although both aldehyde **1.29** and malonate **1.28** were both more complex than substrates reported in the literature, the desired coupling proceeded smoothly to deliver selenide **1.30** in 75% yield as a 5:1 diastereomeric mixture. Selenide **1.30** was then converted to the oxidative intramolecular coupling substrate **1.31** over a five-step sequence.

Scheme 1.4 Ma's Enantioselective Synthesis of Intermediate **1.31**.

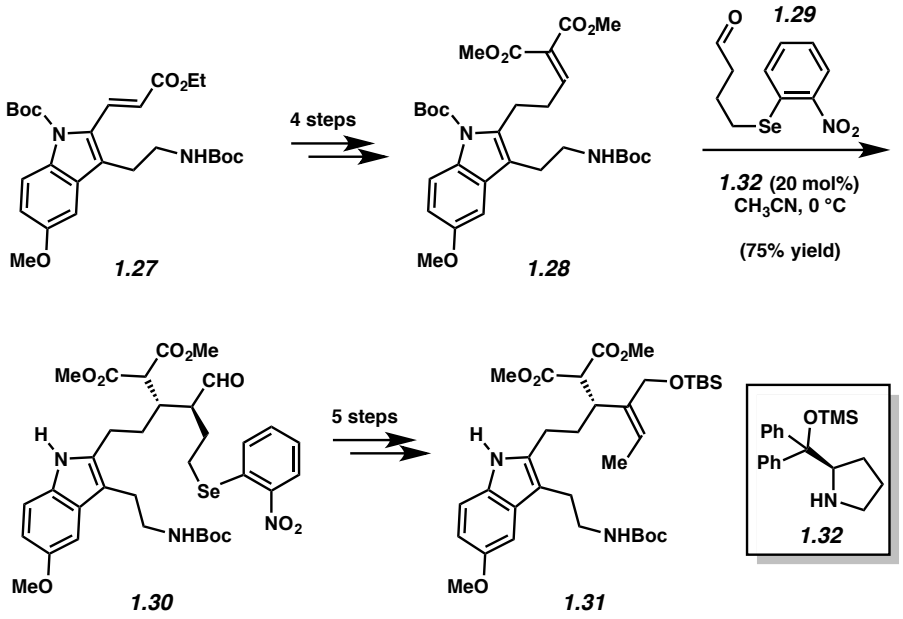

Having established an efficient synthesis of diester **1.31**, the focus turned to forming the fused pyrrolidinoindoline core of the natural product. As shown in Scheme 1.5, diester **1.31** underwent oxidative cyclization in the presence of two equivalents of lithium hexamethyldisilazide (LiHMDS) and a solution of iodine to give indoline **1.35**. This key cascade sequence presumably proceeds through formation of tricyclic indolenine intermediate, followed by subsequent trapping by the Boc-protected amine (see transition structure **1.34**). The stereochemical outcome of this transformation can be attributed to the chair-like transition structure **1.33** shown in Scheme 1.5. In this orientation, the axial ester avoids repulsive interactions with the indole moiety, thus resulting in the desired stereochemical outcome. It should be noted that initial attempts at –78 ºC gave minor amounts of the desired indoline **1.35**, but when the reaction was started at –40 ºC and allowed to warm to room temperature, the yield improved to an impressive 67%. Starting the reaction at a higher temperature did not improve the yield. It should also be noted that the use of other oxidants such as Fe(III) salts, Cu(II) salts, or *N*-iodosuccinimide in place of iodine,[38] had detrimental effects

on the reaction. Nonetheless, this bioinspired cascade transformation resulted in the construction of the key C7 quaternary center and three of the natural product's four stereogenic centers. In addition, the oxidative coupling was highly diastereoselective, translating the stereoselectivity of the organocatalyzed Michael addition into the enantioenriched pyrrolidinoindoline product.

To complete the total synthesis, Krapcho decarboxylation[39] of diester **1.35**, followed by treatment with triphenylphosphine dichloride[40] delivered alkyl chloride **1.36** in 61% yield over two steps. This intermediate was then quickly elaborated to (–)-vincorine (**1.15**) after a final three-step sequence involving deprotection, cyclization to forge the seven-membered ring, and methylation.

Scheme 1.5 Ma's Oxidative Cyclization and Completion of (–)-Vincorine (**1.15**).

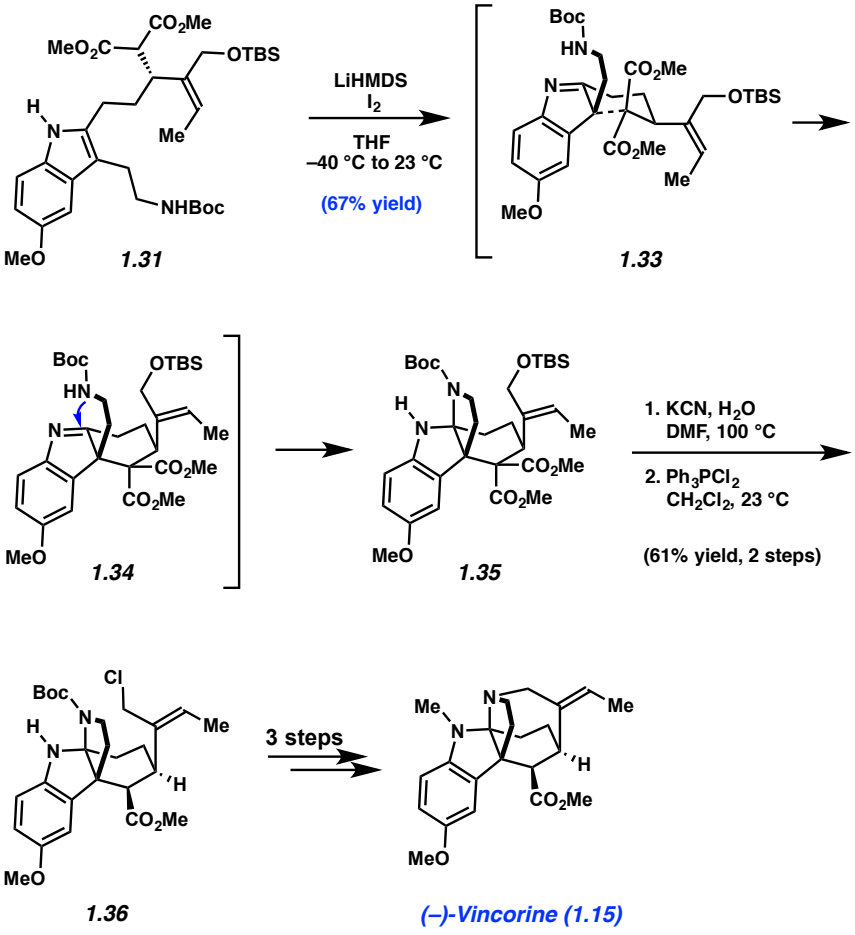

Ma's total synthesis of (–)-vincorine (**1.15**) stands as the first asymmetric route to this complex natural product. A key feature of the synthesis is the use of an oxidative cyclization to construct the quaternary center of **1.15** and two of its complex rings. Of note, this cascade also builds the compound's carbon framework, which greatly facilitated late-stage transformations. Ma's approach to (–)-vincorine (**1.15**) proceeds in 18 steps from commercially available starting materials in a striking overall yield of 5%.

1.3.2 MacMillan's Organocatalytic Approach

Most recently, the MacMillan laboratory successfully completed a concise enantioselective total synthesis of (–)-vincorine (**1.15**).[26] Similar to the overall bond construction strategy pursued by the Qin and Ma laboratories, MacMillan opted to first assemble the pyrrolidinoindoline framework of the natural product, before building the seven-membered ring. However, in the interest of creating a general strategy toward (–)-vincorine (**1.15**) and related natural products, MacMillan and co-workers designed an enantioselective organocatalytic Diels–Alder/iminium ion cyclization cascade sequence[41] to construct the fused pyrrolidinoindoline tetracyclic core, which, in turn, enabled the efficient introduction of the seven-membered ring.

The details of the key cascade reaction are presented in Scheme 1.6. Vinyl tryptamine **1.37**, a readily accessible intermediate from 5-methoxy-*N′*-Boc tryptamine, was combined with enal **1.38** and treated with catalyst **1.39** at –20 °C to afford tetracycle **1.42** in 70% yield and 95% *ee*. It is proposed that the activated iminium species approaches the vinyl tryptamine as depicted in transition structure **1.40** in an *endo* fashion with the facial selectivity controlled by the catalyst's steric environment. Following tandem catalyst dissociation and acid-promoted protonation, an indoleninium is formed. Trapping of this ion by the tethered carbamate (see transition structure

1.41) afforded the tetracyclic product **1.42**. It should be emphasized that this remarkable cascade reaction establishes the relative and absolute configuration of four stereocenters, three of which reside in the natural products' architecture. From there, tetracycle **1.42** was transformed to telluride **1.43** over two steps in preparation of constructing the seven-membered ring.

Scheme 1.6 MacMillan's Key Cascade Transformation.

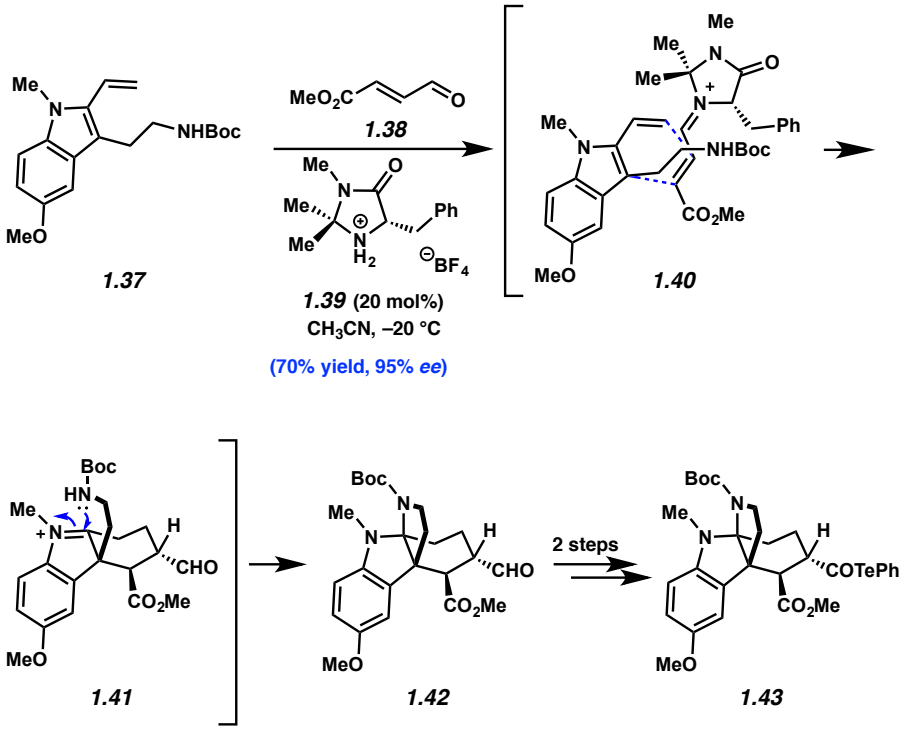

The elaboration of telluride **1.43** to the natural product is depicted in Scheme 1.7. Removal of the *N*-Boc group was effected with TFA and the resultant pyrrolidine nitrogen was alkylated under reductive amination conditions with aldehyde **1.44** to furnish **1.45** in 65% yield over two steps. Upon heating this substrate to 200 °C for 10 h, the desired 7-*exo*-dig cyclization (see transition structure **1.46**) took place, furnishing the exocyclic allene product **1.47**.[42] The authors propose that homolysis of the C–Te bond leads to extrusion of carbon monoxide and formation of

a putative secondary radical. This radical is then poised to undergo the desired cyclization with the pendant π-acceptor to form the final ring system of the natural product. The authors noted that the corresponding transformation was less effective using other radical precursors, such as thiohydroxamic acids and acyl selenides, under a variety of radical initiation conditions. Nonetheless, the successful conversion of **1.43** to **1.45** represents the first example of an acyl telluride being used as an alkyl radical precursor, and provides a bold and creative solution to the formation of the challenging seven-membered ring. With intermediate **1.47** in hand, selective hydrogenation of the allene terminus delivered (–)-vincorine (**1.15**) in 80% yield.

Scheme 1.7 MacMillan's Radical Cyclization and Completion of (–)-Vincorine (**1.15**).

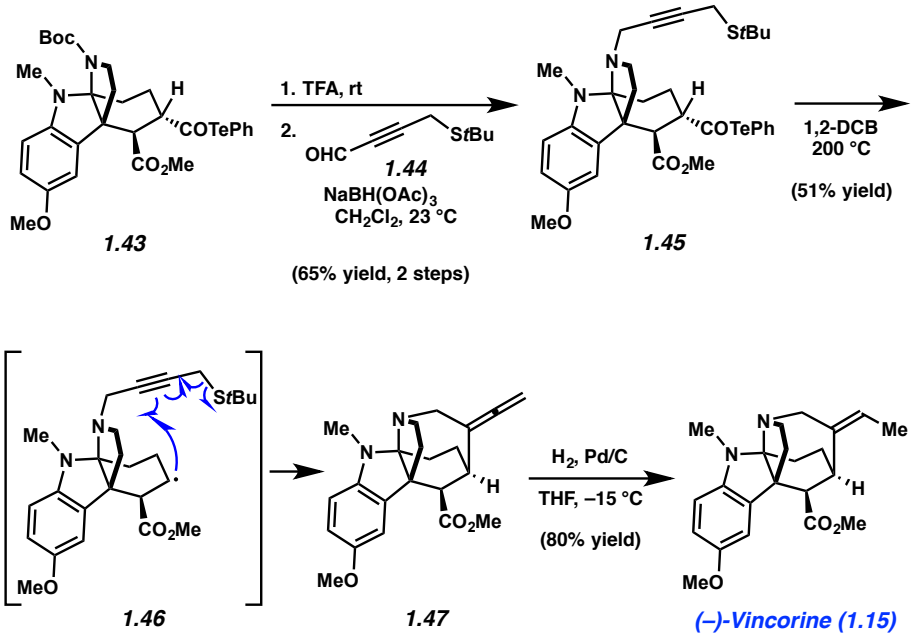

MacMillan's synthesis of (–)-vincorine, which is just nine steps beginning from commercially available starting materials, is the most concise route to **1.15** reported to date. Furthermore, it proceeds in the highest overall yield, which is an impressive 9%. The brevity of

the synthesis can be attributed to the elegant cascade reaction employed: the enantioselective organocatalytic Diels–Alder/iminium ion cyclization, which generates almost all of the natural product's framework with control of relative and absolute stereochemistry. This reaction is a testament to the power of asymmetric organocatalysis for the generation of high molecular complexity in a single synthetic step from achiral starting materials.

1.4 Total Syntheses of Aspidophylline A and Picrinine

1.4.1 Garg's Interrupted Fischer Approach

The akuammiline alkaloids aspidophylline A (**1.4**) and picrinine (**1.13**) were isolated in 2007[9] and 1965,[27] respectively (Scheme 1.1). Aspidophylline A (**1.4**) was found to reverse drug resistance in cancer cells, while picrinine (**1.13**) has been shown to have mild analgesic activity.[43] Each natural product contains a furoindoline motif embedded within a polycyclic framework. Additionally, both compounds contain multiple stereogenic centers, including quaternary centers at C7, thus rendering them daunting synthetic targets. This section includes a summary of total syntheses of aspidophylline A (**1.4**) reported by Garg,[27] Zhu,[28] and Ma,[29] as well as the total synthesis of picrinine (**1.13**).[30]

In 2011, the Garg laboratory reported the first synthesis of aspidophylline A (**1.4**), which was carried out in racemic form.[27] Central to their strategy for building the pentacyclic framework of the natural product was the construction of the fused indoline moiety through an interrupted Fischer indolization cascade reaction.[44] Of note, the authors were able to execute this challenging approach at a late stage in the total synthesis.

The synthesis of the substrate for the aforementioned cascade reaction is illustrated in Scheme 1.8. [2.2.2]-bicyclic lactam **1.48** was elaborated overfive steps to vinyl iodide **1.49**, which,

upon treatment with palladium (0) and pentamethylpiperidine, cleanly underwent a regioselective Heck cyclization[45] to forge the [3.3.1]-azabicycle and furnish **1.50** in excellent yield. Next, in a series of transformations, [3.3.1]-azabicycle **1.50** was converted to ester **1.51** in three steps, which was subsequently carried forward to tricyclic lactone **1.52** in five steps.

Scheme 1.8 Garg's Synthesis of Lactone **1.52**.

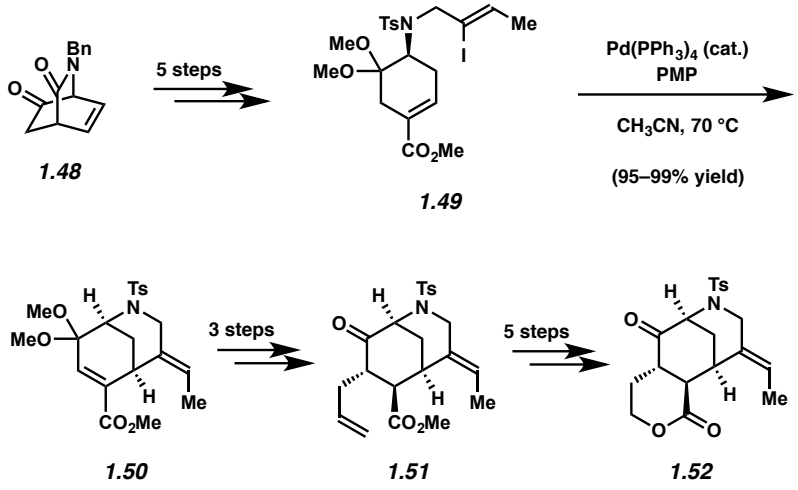

As previously mentioned, tricyclic lactone **1.52** was identified as a suitable substrate for the key intended interrupted Fischer indolization cascade reaction, the details of which are shown in Scheme 1.9. Tricyclic lactone **1.52** was treated with phenylhydrazine (**1.53**) and trifluoroacetic acid in dichloroethane at 40 °C. The resulting ene-hydrazine underwent a charge-accelerated [3,3]-sigmatropic rearrangement (see transition structure **1.54**) and subsequent ammonia extrusion to furnish indolenine **1.55**. This intermediate was not isolated, but rather was subjected to base-promoted methanolysis to generate an alkoxide intermediate. In situ cyclization (see transition structure **1.56**) gave **1.57** in 70% yield, which contains the pentacyclic framework of (±)-aspidophylline A (**1.4**). Notably, this cascade reaction assembles two new C–heteroatom bonds,

one new C–C bond, and one quaternary center, and also proceeds with complete diastereoselectivity. Following construction of pentacycle **1.57**, removal of the tosyl protecting group and *N*-formylation delivered (±)-aspidophylline A (**1.4**).

Scheme 1.9 Interrupted Fischer Indolization and Completion of Aspidophylline A (**1.4**).

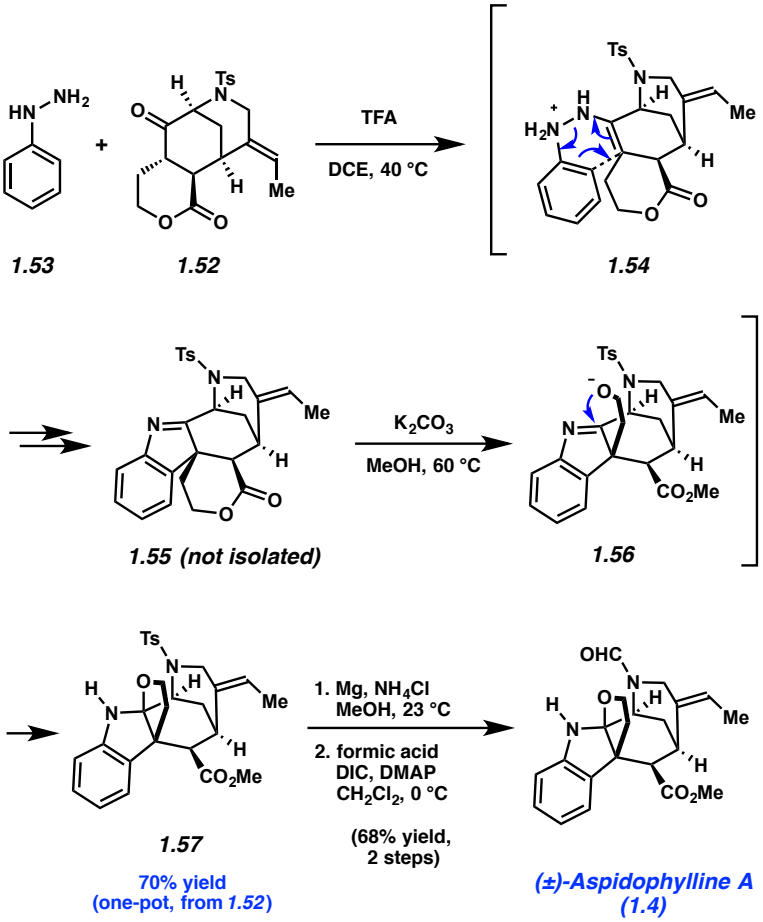

Garg's synthesis of (±)-aspidophylline A (**1.4**) marked the second total synthesis of any akuammiline alkaloid, preceded only by Qin's synthesis of (±)-vincorine (**1.15**). The synthesis proceeds in 7.5% overall yield, and requires 20 steps from commercially available starting materials. In particular, the hallmark of the synthesis is the use of the interrupted Fischer

indolization cascade at a late stage to assemble the compound's complex pentacyclic architecture and introduce two stereogenic centers. This late-stage reaction demonstrates the efficiency of cascade reactions for swiftly generating and manipulating high molecular complexity, while also highlighting the virtues of the venerable Fischer indolization reaction.

Subsequently in 2016, Garg and co-workers disclosed a second-generation, asymmetric synthesis of (–)-aspidophylline A (**1.4**).[46] The details of this account is part of Chapter Three of this dissertation and can be found in this respective section.

1.4.2 Garg's Synthesis of Picrinine

An account of Garg's synthetic efforts towards picrinine (**1.13**)[30] is the main subject matter of Chapter Two of this dissertation and can be found in this respective section.

1.4.3 Zhu's Oxidative Azidoalkoxylation Approach

Earlier this year, Zhu and co-workers reported the second synthesis of (±)-aspidophylline A (**1.4**).[28] Zhu's synthesis hinged upon an oxidative azidoalkoxylation reaction[47] to install N2 of the alkaloid's scaffold while concurrently establishing the furoindoline moiety.[48] This contrasted with Garg's strategy described earlier, where installation of the [3.3.1]-azabicycle was accomplished early in the synthesis, followed by late-stage introduction of the furoindoline.

As shown in Scheme 1.10, Zhu's synthesis commenced from readily available cyclohexanedione **1.58**,[49] which was elaborated to tricycle **1.59** through a triflation.[50] reduction,[51] and carbamoylation sequence. Next, chemoselective oxidation of the terminal olefin with osmium tetroxide and sodium periodate,[52] followed by sodium borohydride reduction, provided furoindoline **1.60** in 71% yield over two steps. This intermediate was then elaborated to silyl ether

1.61, the substrate for the key oxidative cyclization cascade. In the event, treatment of silyl ether **1.61** with ceric ammonium nitrate and sodium azide in acetone delivered azidofuroindoline **1.64** in 53% yield. Mechanistically, it is thought that ceric ammonium nitrate serves as a mild oxidant to first promote single electron transfer and putatively form radical cation **1.62**. Then, this radical cation is trapped by azide, with tandem loss of another electron, to afford an indoleninium species, which undergoes in situ cyclization (see transition structure **1.63**). This umpolung cascade transformation efficiently forges the tetracyclic furoindoline core of the natural product. Additionally, it successfully installs three contiguous stereocenters and the important nitrogen substituent at C3 of the natural product.

Scheme 1.10 Zhu's Oxidative Key Azidoalkoxylation Transformation.

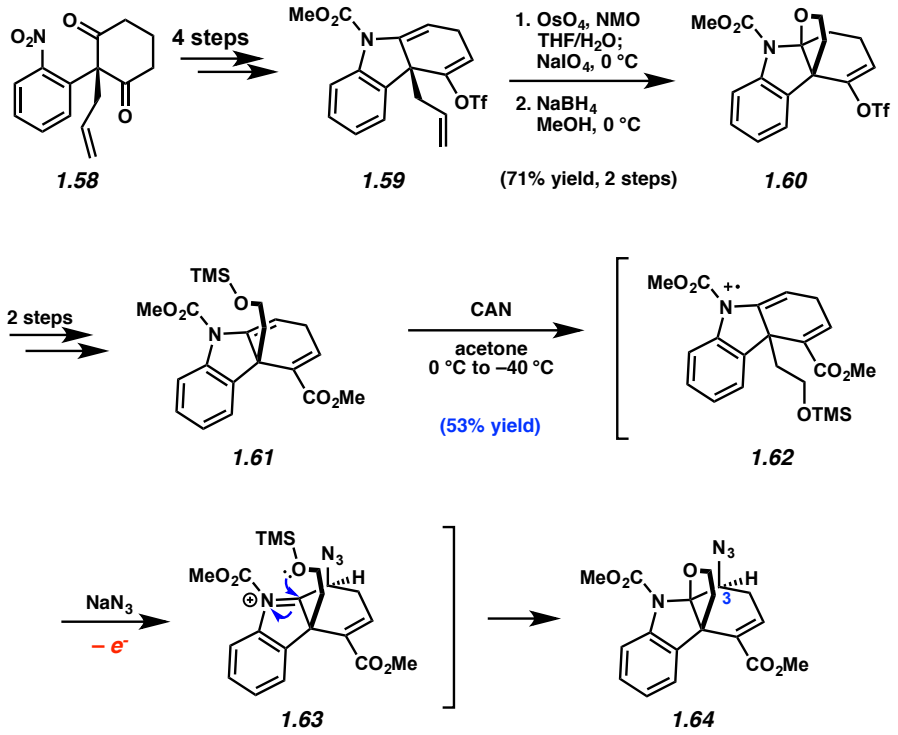

The remainder of Zhu's synthesis is depicted in Scheme 1.11. In a two-step azide reduction and alkylation sequence,[53] furoindoline **1.64** was elaborated to iodide **1.65**. Iodide **1.65** was the utilized as the substrate for a challenging intramolecular Michael addition into the embedded enoate. After much optimization, the authors found that treatment of **1.65** with *t*-BuLi and TMSCl in HMPA and THF at low temperature delivered adduct **1.66** in 51% yield, thus forging the pentacyclic scaffold of the natural product.[54] Subsequent formylation and cleavage of the methyl carbamate delivered (±)-aspidophylline A (**1.4**).

Scheme 1.11 Zhu's Completion of (±)-Aspidophylline A (**1.4**).

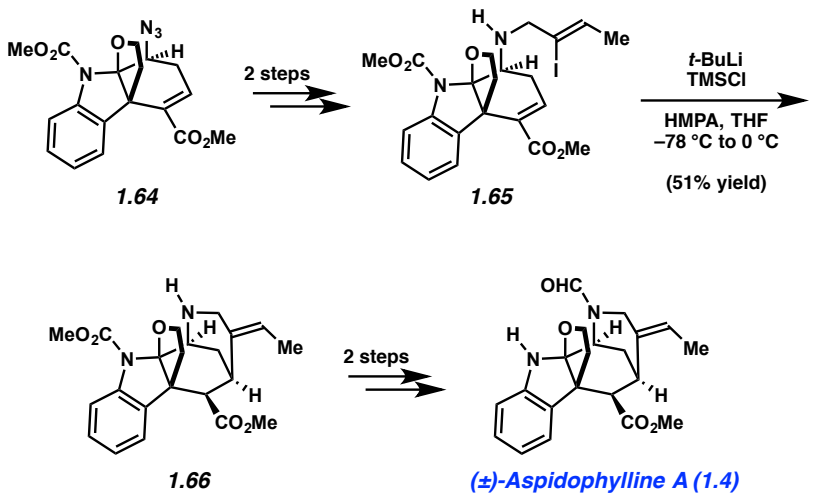

Zhu's impressive total synthesis of (±)-**1.4** proceeds in just 14 steps from known cyclohexanedione **1.58**. The key oxidative azidoalkoxylation cascade reaction employed in the synthesis provides an elegant means to construct the natural product's densely substituted cyclohexane ring. Additionally, Zhu's swift approach demonstrates the enabling power of umpolung reactivity as a functionalization strategy in complex molecule synthesis.

1.4.4 Ma's Oxidative Coupling Approach

Very recently, Ma and co-workers were also successful in completing a total synthesis of (±)-aspidophylline A (**1.4**).[29] Similar to their completed synthesis of (–)-vincorine (**1.15**), the authors sought to employ an intramolecular oxidative coupling[36] to build the core tetracyclic furoindoline scaffold of the natural product. Then, analogous to the overall strategy executed by Zhu, Ma envisioned construction of the piperidine ring through a late-stage cyclization strategy.

The synthesis began by elaborating indole **1.67** to azide **1.68**, which was the substrate for the key intermolecular oxidative coupling cascade reaction (Scheme 1.12). Although the substrate for this coupling appeared less complex than the coupling substrate in the authors' synthesis of vincorine, the transformation proved to be quite challenging.[55] After optimization, it was discovered that treatment of **1.68** with LiHMDS in THF at –40 °C promoted formation of the putative lithium complex **1.69**. Quenching with iodine and warming to 0 °C led to oxidative C–C bond formation, thus furnishing an indolenine intermediate. In turn, this underwent in situ imine trapping (see transition structure **1.70**) to deliver furoindoline **1.71** in 36% yield. Ma and co-workers noted that the addition of additives to this reaction, such as HMPA, resulted mostly in oxidative coupling of the diester to the indole nitrogen, presumably as a result of HMPA disrupting the formation of complex **1.69**. Although the oxidative coupling was not as high yielding as the analogous reaction in Ma's vincorine synthesis, the transformation is quite impressive in that it provides the furoindoline scaffold of the natural product, with three contiguous stereocenters including the quaternary center at C7.

Scheme 1.12 Ma's Key Oxidative Coupling to Forge Furoindoline **1.71**.

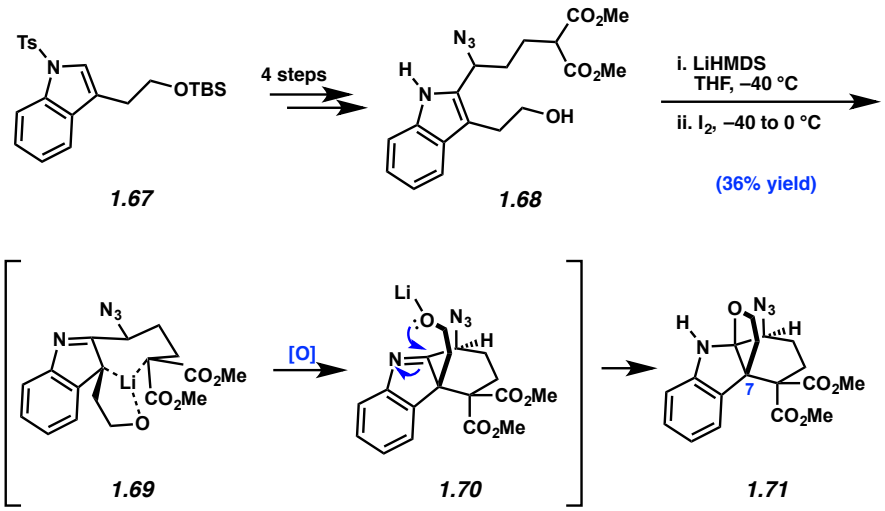

Ma's synthetic endgame is shown in Scheme 1.13. Furoindoline **1.71** was converted to tetracyclic enoate **1.72** through a protection, decarboxylation, and oxidation sequence. Similar to the approach taken by Zhu, vinyl iodide **1.74** was synthesized from enoate **1.72** in two steps including Staudinger reduction and alkylation with bromide **1.73**. Next, formylation of the secondary nitrogen with formic acid and *N,N'*-diisopropylcarbodiimide delivered formamide **1.75**. Following this acylation event, cyclization of the iodide with the pendant enoate was mediated by $Ni(cod)_2$ in the presence of triethylamine and BHT to deliver pentacycle **1.76** in 27% yield.[56] Following this difficult cyclization, cleavage of the Boc group was achieved in nearly quantitative yield to afford (±)-aspidophylline A (**1.4**).

Scheme 1.13 Ma's Completion of (±)-Aspidophylline A (**1.4**).

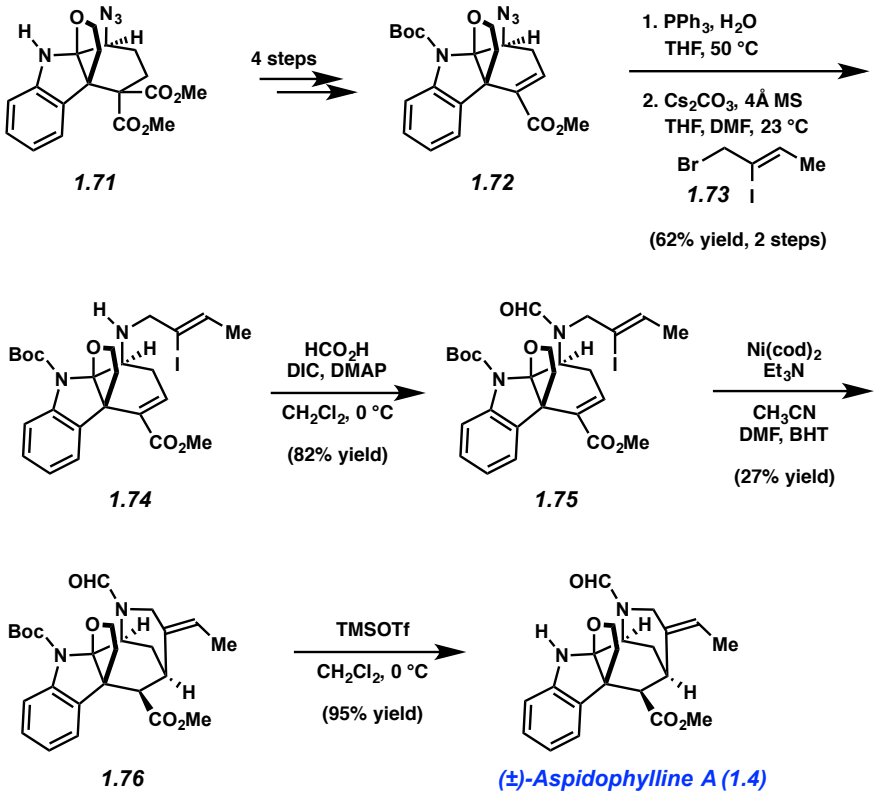

Ma's total synthesis of (±)-aspidophylline A (**1.4**) requires only 15 steps. Critical to the brevity of the synthesis is the use of an innovative intramolecular oxidative cascade coupling to rapidly assemble the furoindoline core of the natural product. This unique strategy, along with the concise construction of the piperidine ring, provides useful synthetic tools that should prove useful in assembling other complex molecules.

1.5 Total Syntheses of Scholarisine A

The natural product scholarisine A (**1.14**) is one of the most recently discovered akuammilines. Reported in 2008, Luo and co-workers isolated **1.14** from the tree *Alstonia scholaris*.[14] Scholarisine A (**1.14**) contains a rearranged akuammiline skeleton with six fused rings

and six stereogenic centers, including two quaternary centers. In addition, its unusual [2.2.2]-bicyclic lactone moiety provides a unique synthetic challenge in akuammiline alkaloid total synthesis. The valiant efforts of the Smith[31] and Snyder[32] laboratories have recently led to two completed total syntheses, both of which harness the power of cascade reactions to access **1.14**.

1.5.1 Smith's Reductive Cyclization Approach

In 2012, the Smith laboratory reported the first total synthesis of (+)-scholarisine A (**1.14**).[31] Their route relied on the use of a reductive cyclization cascade to introduce three rings of the natural product. In addition, the authors utilized a late-stage Fischer indolization reaction to install the indole nucleus en route to forging the [2.2.2]-bicyclic lactone of the natural product.

The synthesis of ketone **1.81** is depicted in Scheme 1.14. Lactone **1.77**, a known compound synthesized from commercially available cis-4-cyclohexene-1,2-dicarboxylic anhydride,[57] was elaborated to nitrile **1.78** in three steps. Upon treatment of **1.78** with H_2 and rhodium on alumina, the desired reductive cyclization cascade occurred to deliver tricyclic amine **1.80** in 64% yield. This cascade sequence presumably proceeds via reduction of the nitrile,[58] followed by intramolecular epoxide opening by the resulting amine.[59] Of note, the authors observed that this cyclization is the first of its kind and, importantly, forges the [3.3.1]-bicyclic moiety contained within the natural product's structure. In addition, the opening of the epoxide elegantly provided a secondary alcohol functional group handle that could be used to later install the indole nucleus. The authors performed two additional steps to convert amine **1.80** to ketone **1.81**, which involved amine protection and alcohol oxidation.

Scheme 1.14 Smith's Key Reductive Cyclization Cascade Reaction.

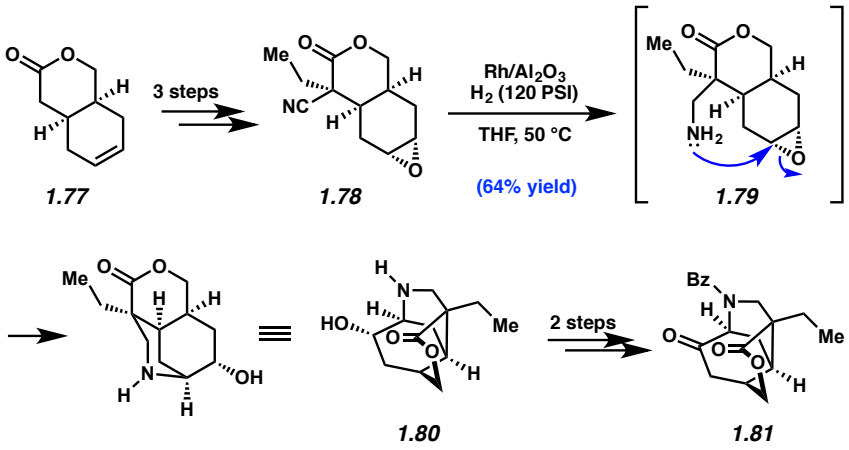

The remainder of Smith's synthetic efforts are highlighted in Scheme 1.15. Treatment of ketone **1.81** with benzyl protected phenylhydrazine (**1.82**) and HCl in pyridine[60] facilitated the key Fischer indolization to provide indole **1.83** in 70% yield. Of note, indole **1.83** possesses most of the scholarisine A framework. A three-step sequence was used to elaborate indole **1.83** to aldehyde **1.84**, which, in turn, was treated with in situ-generated benzyloxy-methyllithium.[61] Subsequent base-mediated desilylation in the same pot afforded diol **1.85**. Diol **1.85** was carried forward to mesylate **1.86** over six steps and subjected to *tert*-butyliminotri(pyrrolidino)-phosphorane (BTPP).[62] This resulted in cyclization to provide indolenine **1.87** in 19% yield from diol **1.85**. Indolenine **1.87** was quickly elaborated to (+)-scholarisine A (**1.14**) using a two-step sequence.

Scheme 1.15 Smith's Completion of (+)-Scholarisine A (**1.14**).

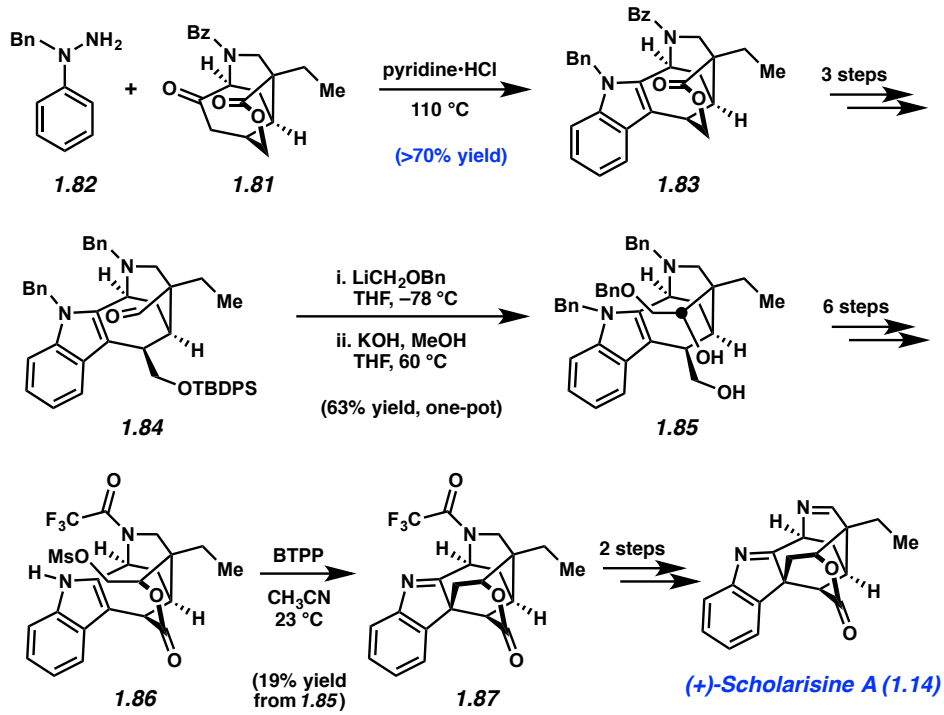

Smith's elegant synthesis of (+)-scholarisine A (**1.14**) marked the first asymmetric synthesis of an akuammiline alkaloid. The longest linear reaction sequence to arrive at the intricate natural product structure is just 20 steps from known lactone **1.77**. A major highlight of the synthesis is Smith's use of a reductive cyclization cascade of nitrile **1.78** to smoothly construct the [3.3.1]-bicycle of the natural product. This key reaction provided the groundwork for the late-stage efforts, thus illustrating the importance of cascade reactions not solely for generating complexity, but also for providing properly functionalized synthetic intermediates for subsequent manipulations.

1.5.2 Snyder's Radical Functionalization Approach

The Snyder laboratory reported the most recent synthesis of (+)-scholarisine A (**1.14**) in 2013.[32] Their strategy differed greatly from that of Smith's and relied heavily on radical cascade processes to forge the natural product's polycyclic skeleton. In particular, two cascade reactions were utilized to construct the two quaternary centers and, in turn, the important indolenine moiety.

Shown in Scheme 1.16 is the key radical cascade used to construct tetracyclic lactam **1.93**. Starting from bicyclic lactone **1.88**, the substrate for the radical cascade (**1.89**) was synthesized in two steps via an acetonide hydrolysis[63] and bromination sequence. Subsequent treatment of **1.89** with triethyl borane in the presence of air at 75 °C promoted homolysis of the carbon bromine bond which putatively revealed a primary radical.[64] This radical then underwent a 6-exo-trig cyclization (see transition structure **1.90**) resulting in tertiary radical compound **1.91**, which was trapped in situ with allyltributylstannane to give tricycle **1.92** with full diastereoselectivity. Notably, this cyclization/trapping cascade sequence forged two key carbon–carbon bonds with remarkable stereocontrol, and allowed for swift access to the natural product's core. This tricyclic intermediate was further elaborated over three steps to lactam **1.93** through a redox epimerization of the nitrogen substituent and intramolecular amide formation.

Scheme 1.16 Snyder's Radical Cyclization/Keck Allylation cascade.

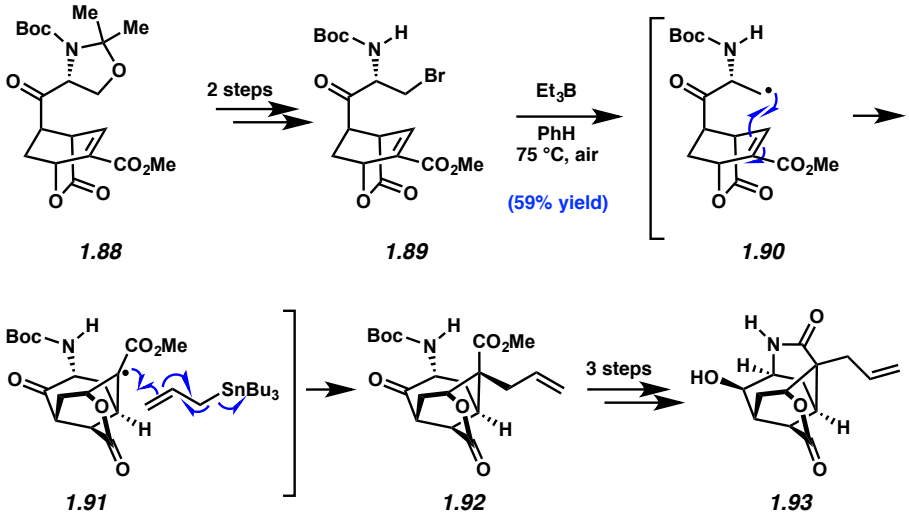

The construction of tetracyclic lactam **1.93** allowed for the second radical cascade to be executed en route to **1.14**, as shown in Scheme 1.17. First, oxidation of the secondary alcohol gave the corresponding ketone. Subsequent condensation with 2-iodoaniline provided imine **1.94** as a mixture of geometrical isomers. Upon heating **1.94** with tributylstannane and 1,1'-azobis(cyclohexane-carbonitrile) in toluene, the authors obtained indolenine **1.98**[65] (18% over the three steps from lactam **1.93**). The transformation is thought to proceed by initial homolysis of the C–I bond to give an aryl radical. 1,5-hydrogen atom transfer (see transition structure **1.95**) then yields an isomeric bridgehead radical intermediate. 5-exo-trig homolytic aromatic substitution on the pendant aryl ring, as suggested in transition structure **1.96**, would then forge the C7–C8 linkage and deliver intermediate **1.97**. Oxidation of the cyclohexadienyl radical provides indolenine **1.98**. This key synthetic intermediate was then used to complete the synthesis (+)-scholarisine A (**1.14**).

Scheme 1.17 Snyder's Radical C–H Activation and Completion of (+)-Scholarisine A (**1.14**).

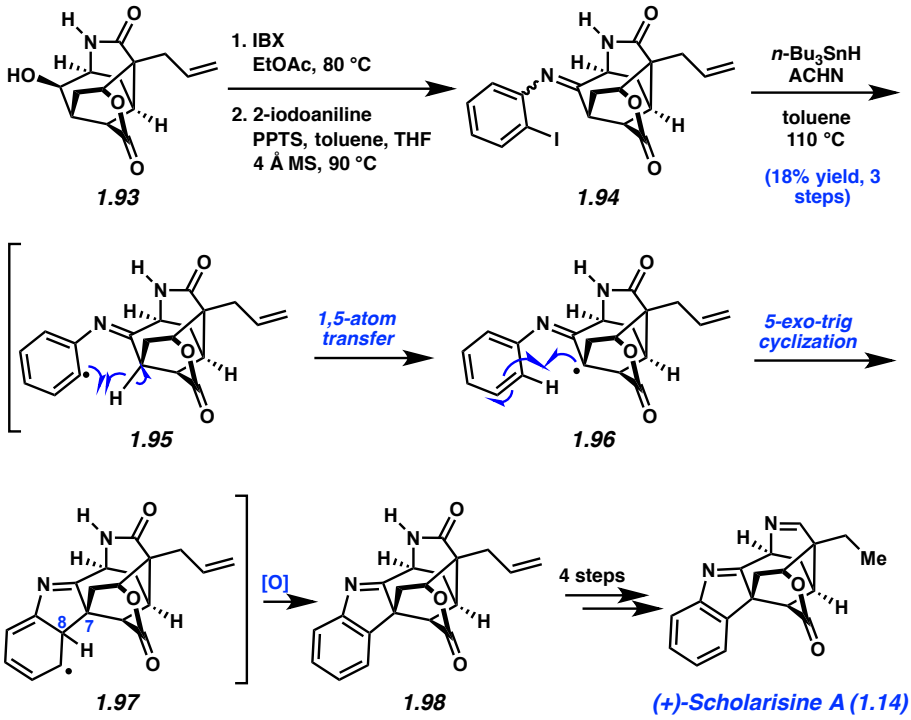

Snyder's approach to (+)-scholarisine A (**1.14**) is currently the most concise approach to this complex alkaloid (14 steps). The synthesis was enabled by the daring use of two challenging radical cascades, which highlights their importance and utility in building complex molecular architectures.

1.6 Most Recent Synthetic Achievements

Not surprisingly, the complex structures and promising pharmacological properties of the akuammiline alkaloids have continued to make them attractive synthetic targets. In fact, since 2016, the number of completed syntheses of akuammiline alkaloids has more than doubled than the amount reported from 2009–2015. Among those synthesized are (+)-strictamine (**1.2**),[46,66] (–)-2(*S*)-cathafoline (**1.99**),[46] calophyline A (**1.100**),[67] (–)-aspidodasycarpine (**1.101**),[68] (–)-lonicerine

(**1.102**),[68] (–)-lanciferine (**1.103**),[68] (+)-scholarisine K (**1.104**),[69] and (–)-alstolactine A (**1.105**),[69] as shown on Figure 1.3. With the exception of Garg's synthetic efforts towards (+)-strictamine (**1.2**)[46] and (–)-2(*S*)-cathafoline (**1.99**),[46] which are the main subject matter of Chapter Three of this dissertation, a detailed account of these most recent synthetic achievements won't be disclosed. However, it should be noted that prior to these reports, none of these natural products had previously succumb to total synthesis.[70]

Figure 1.3 Most Recent Achievements in Akuammiline Alkaloid Total Synthesis.

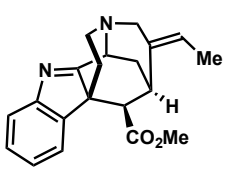

(+)-Strictamine (1.2)

Garg (2016), Zhu (2016)
Ohno (2016), Gaich (2016)
Snyder (2017)

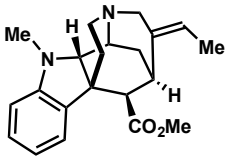

(–)-2(S)-Cathafoline (1.99)

Garg (2016)

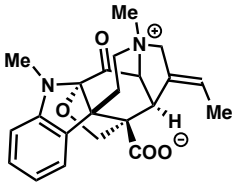

(+)-Calophyline A (1.100)

Zu (2016)

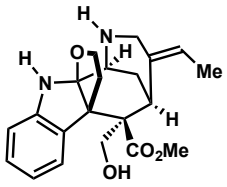

(–)-Aspidodasycarpine (1.101)

Li (2016)

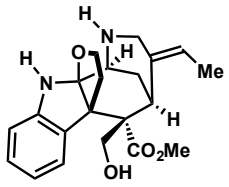

(–)-Lonicerine (1.102)

Li (2016)

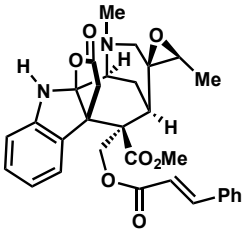

(–)-Lanciferine (1.103)

Li (2016)

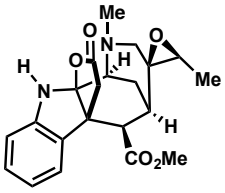

(+)-Scholarisine K (1.104)

Gao (2017)

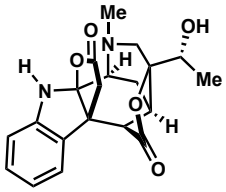

(–)-Alstolactine A (1.105)

Gao (2017)

1.7 Conclusion

In summary, the akuammiline alkaloid natural products have been the subject of many recent synthetic endeavors, despite being known for many decades. Their intricate structures, along with their promising biological activities, have made them attractive targets amongst the chemical community. Various approaches towards making these natural products have been reported, of which the successful routes are highlighted herein. These successful routes have utilized cascade reactions to construct the cores of these compounds, demonstrating that these innovative techniques are useful for the construction of exceedingly complex structural manifolds. The collective efforts of the many laboratories involved in this area have not only provided a solid groundwork for making other akuammilines and their derivatives, but has also set the stage for using modern cascade reactions in the synthesis of other intricate molecular scaffolds.

1.8 Notes and References

(1) (a) Ramírez, A.; García−Rubio, S. *Curr. Med. Chem.* **2003**, *10*, 1891−1915. (b) Eckermann, R.; Gaich, T. *Synthesis* **2013**, *45*, 2813−2823.

(2) Baliga, M. S. *Chin. J. Integr. Med.* **2012**, 1–14.

(3) Gorup-Besanez, v. *Justus Liebigs Ann. Chem.* **1875**, *176*, 88−89.

(4) Jagetia, G. C.; Baliga, M. S.; Venkatesh, P.; Ulloor, J. N.; Mantena, S. K.; Genebriera, J.; Mathuram, V. *J. Pharm. Pharmacol.* **2005**, *57*, 1213−1219.

(5) Schnoes, H.; Biemann, K.; Mokrý, J.; Kompis, I.; Chatterjee, A.; Ganguli, G. *J. Org. Chem.* **1966**, *31*, 1641–1642.

(6) Yuanyuan, H.; Xuelin, C.; Liqiang, W.; Binfeng, C.; Linyi, D.; Xiaodong, L.; Gang, B.; Wenyuan, G. *J. Chromatogr. B* **2012**, *908*, 98–104.

(7) For initial isolation, see: (a) Thomas, A. F. D. Phil. Thesis, Oxford, England, 1954. (b) Subsequent Isolation: Britten, A. Z.; Smith, G. F. *J. Chem. Soc.* **1963**, 3850–3854.

(8) (a) Arai, H.; Hirasawa, Y.; Rahman, A.; Kusumawati, I.; Zaini, N. C.; Sato, S.; Aoyama, C.; Takeo, J.; Morita, H. *Bioorg. Med. Chem.* **2010**, *18*, 2152−2158. (b) Meng, W.; Ellsworth, B. A.; Nirschl, A. A.; McCann, J.; Patel, M.; Girotra, R. N.; Wu, G.; Sher, P. M.; Morrison, E. P.; Biller, S. A.; Zahler, R.; Deshpande, P. P.; Pullockaran, A.; Hagan, D. L.; Morgan, N.; Taylor, J. R.; Obermeier, M. T.; Humphreys, W. G.; Khanna, A.; Discenza, L.; Robertson, J. G.; Wang, A.; Han, S.; Wetterau, J. R.; Janovitz, E. B.; Flint, O. P.; Whaley, J. M.; W. N. Washburn, *J. Med. Chem.* **2008**, *51*, 1145−1149.

(9) Subramanian, G.; Hiraku, O.; Hayashi, M.; Koyano, T.; Komiyama, K.; Kam, T.-S. *J. Nat. Prod.* **2007**, *70*, 1783–1789.

(10) (a) Battersby, A. R.; Thompson, M.; Glüsenkamp, K.-H.; Tietze, L.-F. *Chem. Ber.* **1981**, *114*, 3430–3438. (b) Battersby, A. R.; Westcott, N. D.; Glüsenkamp, K.-H.; Tietze, L.-F. *Chem. Ber.* **1981**, *114*, 3439–3447. (c) Scott, A. I. *Acc. Chem. Res.* **1970**, *3*, 151–157. (d) Stöckigt, J.; Barleben, L.; Panjikar, S.; Loris, E. A. *Plant Physiol. Biochem.* **2008**, *46*, 340–355.

(11) Ahmad, Y.; Fatima, K.; Le Quesne, P. W.; Atta-Ur-Rahman *Phytochemistry* **1983**, *22*, 1017–1019.

(12) (a) Henry, T. A. *J. Chem. Soc.* **1932**, 2759–2768. (b) Olivier, L.; Lévy, J.; Le Men, J.; Janot, M. M.; Budzikiewicz, H.; Djerassi, C. *Bull. Soc. Chim. Fr.* **1965**, 868–876.

(13) Chatterjee, A.; Mukherjee, B.; Ray, A. B.; Das, B. *Tetrahedron Lett*. **1965**, *6*, 3633–3637.

(14) Cai, X.-H.; Tan, Q.-G.; Liu, Y.-P.; Feng, T.; Du, Z.-Z.; Li, W.-Q.; Luo, X.-D. *Org. Lett.* **2008**, *10*, 577–580.

(15) Mokrý, J.; Dúbravková, L.; Šefčovič, P. *Experientia* **1962**, *18*, 564–565.

(16) (a) Dolby, L. J.; Esfandiari, Z. *J. Org. Chem.* **1972**, *37*, 43–46. (b) Dolby, L. J.; Nelson, S. J. *J. Org. Chem.* **1973**, *38*, 2882–2887.

(17) Hoike, T.; Takayama, H.; Sakai, S. *Chem. Pharm. Bull.* **1991**, *39*, 1677–1681.

(18) Lévy, J.; Sapi, J.; Laronze, J.-Y.; Royer, D.; Toupet, L. *Synlett* **1992**, 601–602.

(19) Bennasar, M.-L.; Zulaica, E.; Ramrez, A.; Bosch, J. *J. Org. Chem.* **1996**, *61*, 1239–1251.

(20) Yasui, Y.; Kinugawab, T.; Takemoto, Y. *Chem. Commun.* **2009**, 4275–4277.

(21) Watanabe, T.; Kato, N.; Umezawa, N.; Higuchi, T. *Chem. Eur. J.* **2013**, *19*, 4255–4261.

(22) Li, Q.; Li, G.; Ma, S.; Feng, P.; Shi, Y. *Org. Lett.* **2013**, *15*, 2601–2603.

(23) Ren, W.; Tappin, N.; Wang, Q.; Zhu, J. *Synlett* **2013**, 1941–1944.

(24) Zhang, M.; Huang, X.; Shen, L.; Qin, Y. *J. Am. Chem. Soc.* **2009**, *131*, 6013–6020.

(25) Zi, W.; Xie, W.; Ma, D. *J. Am. Chem. Soc.* **2012**, *134*, 9126–9129.

(26) Horning, B. D.; MacMillan, D. W. C. *J. Am. Chem. Soc.* **2013**, *135*, 6442–6445.

(27) Zu, L.; Boal, B. W.; Garg, N. K. *J. Am. Chem. Soc*. **2011**, *133*, 8877–8879.

(28) Ren, W.; Wang, Q.; Zhu, J. *Angew. Chem., Int. Ed.* **2014**, *53*, 1818–1821.

(29) Teng, M.; Zi, W.; Ma, D. *Angew. Chem., Int. Ed.* **2014**, *53*, 1814–1817.

(30) Smith, J. M.; Moreno, J.; Boal, B. W.; Garg, N. K. *J. Am. Chem. Soc.* **2014**, *136*, 4504–4507.

(31) (a) Adams, G. L.; Caroll, P. J.; Smith, A. B. *J. Am. Chem. Soc.* **2012**, *134*, 4037–4040. (b) Adams, G. L.; Caroll, P. J.; Smith, A. B. *J. Am. Chem. Soc.* **2013**, *135*, 519–528.

(32) Smith, M. W.; Snyder, S. A. *J. Am. Chem. Soc.* **2013**, *135*, 12964–12967.

(33) (a) He, B.; Song, H.; Y. Du, Y. Qin, *J. Org. Chem.* **2009**, *74*, 298–304. (b) J. Yang, H. Wu, L. Shen, Y. Qin, *J. Am. Chem. Soc.* **2007**, *129*, 13794–13795. (c) Song, H.; Yang, J.; Chen, W.; Qin, Y. *Org. Lett.* **2006**, *8*, 6011–6014. (d) Yang, J.; Song, H.; Xiao, X.; Wang, J.; Qin, Y. *Org. Lett.* **2006**, *8*, 2187–2190.

(34) Vercauteren, J.; Lavaud, C.; Lévy, J.; Massiot, G. *J. Org. Chem.* **1984**, *49*, 2278–2279.

(35) (a) Schlama, T.; Baati, R.; Gouverneur, V.; Valleix, A.; Falck, J. R.; Mioskowski, C. *Angew. Chem., Int. Ed.* **1998**, *37*, 2085–2087. (b) Ng, F. W.; Lin, H.; Danishefsky, S. J. *J. Am. Chem. Soc.* **2002**, *124*, 9812–9824. (c) Birman, V. B.; Danishefsky, S. J. *J. Am. Chem. Soc.* **2002**, *124*, 2080–2081. (d) Kim, D.; Lee, J.; Shim, P. J.; Lim, J. I.; Jo, H.; Kim, S. *J. Org. Chem.* **2002**, *67*, 764–771. (e) Shigeyama, T.; Katakawa, K.; Kogure, N.; Kitajima, M.; Takayama, H. *Org. Lett.* **2007**, *9*, 4069–4072.

(36) (a) Zuo, Z.; Xie, W.; Ma, D. *J. Am. Chem. Soc.* **2010**, *132*, 13226–13228. (b) Zuo, Z.; Ma, D. *Angew. Chem., Int. Ed.* **2011**, *50*, 12008–12011.

(37) (a) Zhao, G.-L.; Vesely, J.; Sun, J.; Christensen, K. E.; Bonneau, C.; Córdova, A. *Adv. Synth. Catal.* **2008**, *350*, 657–661. (b) Wen, L.; Shen, Q.; Lu, L. *Org. Lett.* **2010**, *12*, 4655–4657. (c) Chowdhury, R.; Ghosh, S. K. *Tetrahedron: Asymmetry* **2010**, *21*, 2696–2702.

(38) (a) Baran, P. S.; Richter, J. M. *J. Am. Chem. Soc.* **2004**, *126*, 7450–7451. (b) Baran, P. S.; Richter, J. M. *J. Am. Chem. Soc.* **2005**, *127*, 15394–15396. (c) Baran, P. S.; Guerrero, C. A.; Ambhaikar, N. B.; Hafensteiner, B. D. *Angew. Chem., Int. Ed.* **2005**, *44*, 606–609.

(39) Krapcho, A. P.; Weimaster, J. F.; Eldridge, J. M.; Jahngen, Jr., E. G. E.; Lovey, A. J.; Stephens, W. P. *J. Org. Chem.* **1978**, *43*, 138–147.

(40) Aizpurua, J. M.; Cossio, F. P.; Palomo, C. *J. Org. Chem.* **1986**, *51*, 4941–4943.

(41) (a) Jones, S. B.; Simmons, B.; MacMillan, D. W. C. *J. Am. Chem. Soc.* **2009**, *131*, 13606–13607. (b) Jones, S. B.; Simmons, B.; Mastracchio, A.; MacMillan, D. W. C. *Nature* **2011**, *475*, 183–188.

(42) Chen, C.; Crich, D.; Papadatos, A. *J. Am. Chem. Soc.* **1992**, *114*, 8313–8314.

(43) Shang, J.-H.; Cai, X.-H.; Feng, T.; Zhao, Y.-L.; Wang, J.-K.; Zhang, L.-Y.; Yan, M.; Luo, X.-D. *J. Ethnopharmacol.* **2010**, *129*, 174–181.

(44) (a) Boal, B. W.; Schammel, A. W.; Garg, N. K. *Org. Lett.* **2009**, *11*, 3458–3461. (b) Schammel, A. W.; Boal, B. W.; Zu, L.; Mesganaw, T.; Garg, N. K. *Tetrahedron* **2010**, *66*, 4687–4695. (c) Çelebi-Ölçüm, N.; Boal, B. W.; Huters, A. D.; Garg, N. K.; Houk, K. N. *J. Am. Chem. Soc.* **2011**, *133*, 5752–5755. (d) Schammel, A. W.; Chiou, G.; Garg, N. K. *J. Org. Chem.* **2012**, *77*, 725–728. (e) Schammel, A. W.; Chiou, G.; Garg, N. K. *Org. Lett.* **2012**, *14*, 4556–4559.

(45) (a) Rawal, V. H.; Michoud, C.; Monestel, R. F. *J. Am. Chem. Soc.* **1993**, *115*, 3030–3031. (b) Rawal, V. H.; Iwasa, S. *J. Org. Chem.* **1994**, *59*, 2685–2686. (c) Martin, D. B. C.; Vanderwal, C. D. *J. Am. Chem. Soc.* **2009**, *131*, 3472–3473.

(46) Moreno, J.; Picazo, E.; Morrill, L. A.; Smith, J. M.; Garg, N. K. *J. Am. Chem. Soc.* **2016**, *138*, 1162–1165.

(47) For examples of oxidative azidoalkoxylation, see: (a) Chavan, S. P.; Subbarao, Y. T.; *Tetrahedron Lett.* **1999**, *40*, 5073–5074. (b) Norton Matos, M. R. P.; Alfonso, C. A. M.; Batey,

R. A. *Tetrahedron Lett.* **2001**, *42*, 7007–7010. (c) Le Corre, L.; Kizirian, J.-C.; Levraud, C.; Boucher, J.-L.; Bonnet, V.; Dhimane, H. *Org. Biomol. Chem.* **2008**, *6*, 3388–3398.

(48) Li, Q.; Li, G.; Ma, S.; Feng, P.; Shi, Y. *Org. Lett.* **2013**, *15*, 2601–2603.

(49) Solé, D.; Bosch, J.; Bonjoch, J. *Tetrahedron* **1996**, *52*, 4013–4028.

(50) Mi, Y.; Schreiber, J. V.; Corey, E. J. *J. Am. Chem. Soc.* **2002**, *124*, 11290–11291.

(51) Kozmin, S. A.; Iwama, T.; Huang, Y.; Rawal, V. H. *J. Am. Chem. Soc.* **2002**, *124*, 4628–4641.

(52) Trost, B. M.; Pissot-Soldermann, C.; Chen, I.; Schroeder, G. M. *J. Am. Chem. Soc.* **2004**, *126*, 4480–4481.

(53) Sirasani, G.; Andrade, R. B. *Org. Lett.* **2011**, *13*, 4736–4737.

(54) (a) Cooke, Jr., M. P.; Widener, R. K. *J. Org. Chem.* **1987**, *52*, 1381–1396. (b) Piers, E.; Harrison, C. L.; Zetina-Rocha, C. *Org. Lett.* **2001**, *3*, 3245–3247. (c) Dieter, R. K.; Oba, G.; Chandupatla, K. R.; Topping, C. M.; Lu, K.; Watson, R. T. *J. Org. Chem.* **2004**, *69*, 3076–3086. (d) Martin, D. B. C.; Vanderwal, C. D. *Chem. Sci.* **2011**, *2*, 649–651. (e) Martin, D. B. C.; Nguyen, L. Q.; Vanderwal, C. D. *J. Org. Chem.* **2012**, *77*, 17–46.

(55) Zhu and co-workers attempted a similar type of oxidative coupling in efforts towards strictamine, see ref. 23.

(56) (a) Solé, D.; Cancho, Y.; Llebaria, A.; Moretó, J. M.; Delgado, A. *J. Am. Chem. Soc.* **1994**, *116*, 12133–12134. (b) Bonjoch, J.; Solé, D.; Bosch, J. *J. Am. Chem. Soc.* **1995**, *117*, 11017–11018. c) Solé, D.; Bonjoch, J.; Bosch, J. *J. Org. Chem.* **1996**, *61*, 4194–4195. (d) Bonjoch, J.; Solé, D.; García-Rubio, S.; Bosch, J. *J. Am. Chem. Soc.* **1997**, *119*, 7230–7240. (e) Ma, J.;

Yin, W.; Zhou, H.; Cook, J. M. *Org. Lett.* **2007**, *9*, 3491–3494. (f) Yu, F.; Cheng, B.; Zhai, H. *Org. Lett.* **2011**, *13*, 5782–5783.

(57) (a) Danieli, B.; Lesma, G.; Mauro, M.; Palmisano, G.; Passarella, D. *J. Org. Chem.* **1995**, *60*, 2506–2513. (b) Danieli, B.; Lesma, G.; Mauro, M.; Palmisano, G.; Passarella, D. *Tetrahedron* **1994**, *50*, 8837–8852. (c) Danieli, B.; Lesma, G.; Mauro, M.; G. Palmisano, D. Passarella *Tetrahedron: Asymmetry* **1990**, *1*, 793–800. For a modified procedure to access lactone **1.77** on gram scale, see reference 31b.

(58) Freifelder, M. *J. Am. Chem. Soc.* **1960**, *82*, 2386–2389.

(59) Schultz, R. J.; Staas, W. H.; Spurlock, L. A. *J. Org. Chem.* **1973**, *38*, 3091–3093.

(60) Welch, W. M. *Synthesis* **1977**, 645–646.

(61) Still, W. C. *J. Am. Chem. Soc.* **1978**, *100*, 1481–1487.

(62) Schwesinger, R.; Willaredt, J.; Schlemper, H.; Keller, M.; Schmitt, D.; Fritz, H. *Chem. Ber.* **1994**, *127*, 2435–2454.

(63) Yonezawa, Y.; Tani, N.; Shin, C.-G. *Heterocycles* **2005**, *65*, 95–105.

(64) For use of Et_3B as a radical initiator, see: (a) Reddy, L. R.; Fournier, J.-F.; Reddy, B. V. S.; Corey, E. J. *J. Am. Chem. Soc.* **2005**, *127*, 8974–8976. (b) Lambert, T. H.; Danishefsky, S. J. *J. Am. Chem. Soc.* **2006**, *128*, 426–427.

(65) For examples of radical cyclizations to form indole derivatives, see: (a) Beckwith, A. L.; Storey, J. M. D. *J. Chem. Soc., Chem. Comm.* **1995**, 977–978. (b) Beckwith, A. L.; Bowry, V. W.; Bowman, W. R.; Mann, E.; Parr, J.; Storey, J. M. D. *Angew. Chem., Int. Ed.* **2004**, *43*, 95–98. (c) Jia, Y.-X.; Kündig, E. P. *Angew. Chem., Int. Ed.* **2009**, *48*, 1636–1639.

(66) (a) Ren, W.; Wang, Q.; Zhu, J.; *Angew. Chem., Int. Ed.* **2016**, *55*, 3500–3503. (b) Nishiyama, D.; Ohara, A.; Chiba, H.; Kumagai, H.; Oishi, S.; Fujii, N.; Ohno, H. *Org. Lett.* **2016**, *18*, 1670–1673. (c) Eckermann, R.; Breunig, M.; Gaich, T. *Chem. Commun.* **2016**, *52*, 11363–11365. (d) Eckermann, R.; Breunig, M.; Gaich, T. *Chem. Eur. J.* **2017**, *23*, 1–13. (e) Smith, M. W.; Zhou, Z.; Gao, A. X.; Shimbayashi, T.; Snyder, S. A. *Org. Lett.* **2017**, *19*, 1004–1007.

(67) Li, G.; Xie, X.; Zu, L. *Angew. Chem., Int. Ed.* **2016**, *55*, 10483–10486.

(68) Li, Y.; Zhu, S.; Li, J.; Li, A. *J. Am. Chem. Soc.* **2016**, *138*, 3982–3985.

(69) Wang, D.; Hou, M.; Ji, Y.; Gao, S. *Org. Lett.* **2017**, *19*, 1922–1925.

(70) In addition to these recent syntheses, two formal, asymmetric syntheses of (–)-aspidophylline A (**1.4**) have been reported. See: (a) Jiang, S.-Z.; Zeng, X.-Y.; Liang, Z.; Lei, T.; Wei, K.; Yang, Y.-R. *Angew. Chem., Int Ed.* **2016**, *55*, 4044–4048. (b) Wang, T.; Duan, X.; Zhao, H.; Zhai, S.; Tao, C.; Wang, H.; Li, Y.; Cheng, B.; Zhai, H. *Org. Lett.* **2017**, *19*, 1650–1653.

CHAPTER TWO

The Fischer Indolization as a Strategic Platform for the Total Synthesis of Picrinine

Adapted from: Joel M. Smith, Jesus Moreno, Ben W. Boal, and Neil K. Garg.

J. Am. Chem. Soc. **2014**, *136*, 4504–4507 and *J. Org. Chem.* **2015**, *80*, 8954–8967.

2.1 Abstract

This chapter describes a second-generation approach to the akuammiline alkaloid picrinine. Central to the success of our approach is the use of a Fischer indolization reaction on a cyclopentene-containing substrate to circumvent the previously encountered roadblocks. Additionally, a more concise and scalable synthetic strategy towards building the natural product scaffold is detailed, which ultimately fueled a thorough investigation of late-stage chemistry. Furthermore, various roadblocks encountered in our experimental efforts are described, which were successfully overcome to complete the total synthesis.

2.2 Introduction

Although not described here,[1] our initial route to picrinine (**2.1**) was met with many setbacks. Among these difficulties was that the route provided inefficient material throughput due to scale limitations. This impediment provided for little faculty in the investigation of the final synthetic manipulations. Thus, we were prompted to devise a new, concise, and efficient strategy that allowed for scalability, while addressing the strategic hurdles encountered in the later stages of our first-generation route.

2.3 Second-Generation Retrosynthetic Analysis

Our second-generation retrosynthetic analysis of **2.1** is shown in Scheme 2.1. Identical to our first strategy, we envisioned picrinine (**2.1**) arising from cyclization of the penultimate lactol **2.2**. However, we now sought to access this lactol from indolenine **2.3**, which bears a cyclopentene moiety. The cyclopentene would serve as a "tethered" variant of the previously problematic allyl sidechain.[1] Specifically, we envisaged that the oxidative cleavage of cyclopentene **2.3**[2] would not be hampered by cyclization of the presumed diol intermediate due to geometric constraints; accordingly, C–C bond cleavage could occur. Indolenine **2.3** would come from a late-stage Fischer indolization of phenylhydrazine (**2.4**) and ketone **2.5**, the latter of which would be derived from enone **2.6**. Although **2.6** had been previously accessed,[1] the route was significantly hampered by poor material throughput. Thus, we took the opportunity to design a new and scalable synthetic route to this key intermediate. We envisioned that enone **2.6** could be accessed from bicyclic ketone **2.7**,[3] the product of an intramolecular Pd-catalyzed enolate coupling of vinyl iodide **2.8**. Finally, the iodide would be prepared from readily available fragments cyclohexanone **2.9** and tosylate **2.10**.

Scheme 2.1 Second-generation Retrosynthetic Analysis of Picrinine (**2.1**).

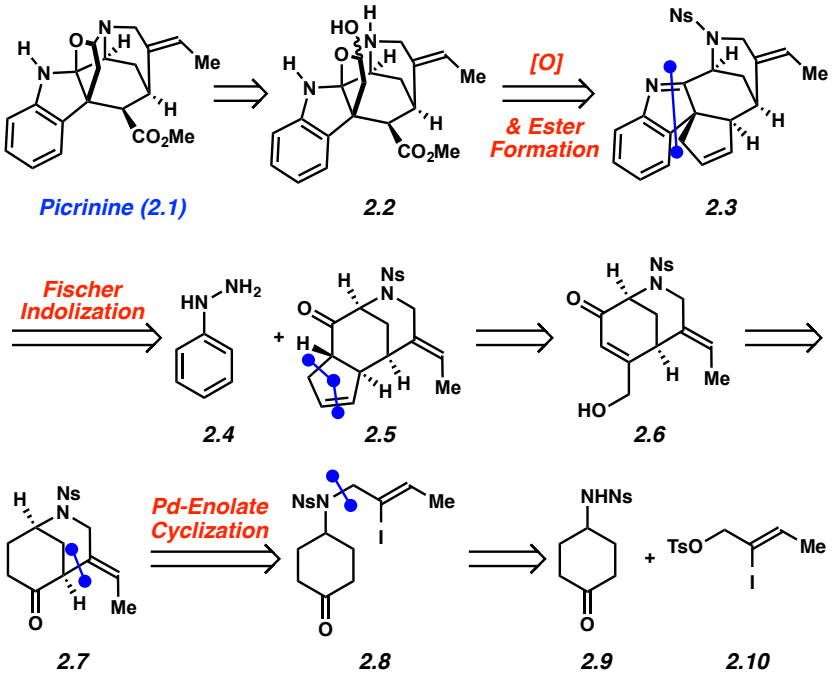

2.4 Development of a Synthetic Route to Access Fischer Indolization Substrate 2.5

Scheme 2.2 shows the successful synthesis of bicyclic ketone **2.7** and our initial attempt to elaborate it to enone **2.13**. Starting with cyclohexanone **2.9**,[4] alkylation with tosylate **2.10**[5] in the presence of Cs_2CO_3 provided vinyl iodide **2.8** in excellent yield. When treated with $PdCl_2(dppf)•CH_2Cl_2$ (20 mol%) and K_2CO_3 in methanol at 65 °C, iodide **2.8** underwent efficient conversion to bicyclic ketone **2.7** in 63% yield.[6] This transformation was performed on multigram scale and allowed access to the important [3.3.1]-azabicycle in just two steps from **2.9**, which was a notable improvement compared to our earlier approach to assembling the azabicycle.[1] With ketone **2.7** in hand, IBX oxidation provided enone **2.11** in 60% yield.[7] Enone **2.11** was treated with a preformed MOM-protected alkyllithium species at low temperature to give tertiary allylic alcohol **2.12**, albeit in low yield.[8] Unfortunately, all attempts made by my colleague Joel Smith to oxidatively rearrange allylic alcohol **2.12** to enone **2.13** were unsuccessful. The use of various

Cr(VI)[9] reagents, hypervalent iodine reagents,[10] or *N*-oxoammonium salts[11] were ineffective, and largely resulted in the recovery of starting material or decomposition. Attempts to isomerize the allylic alcohol without oxidation were also unsuccessful. We surmise that the difficulties encountered in our attempts to manipulate **2.12** are due to the tertiary alcohol being sterically hindered.

Scheme 2.2 Assembly of the [3.3.1]-Azabicycle and Attempted Elaboration to Enone **2.13**.

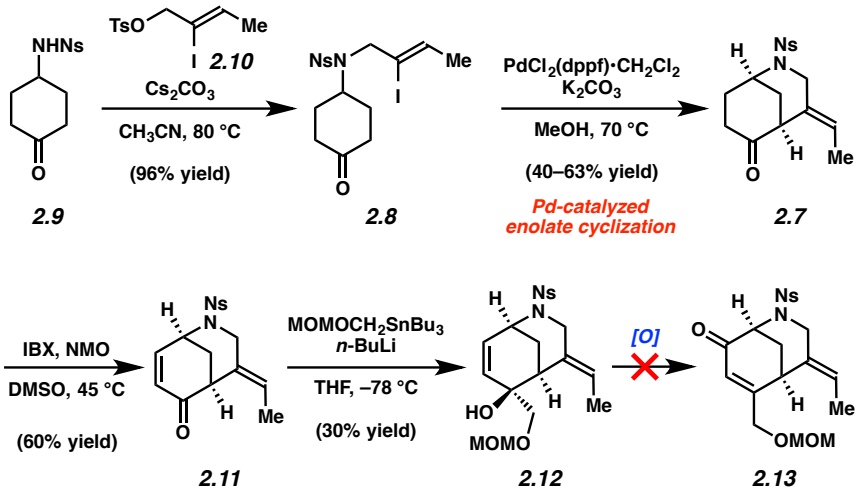

To sidestep our inability to utilize allylic alcohol **2.12**, we pursued the epoxidation/fragmentation sequences shown in Scheme 2.3. Of note, these studies were also investigated by my colleague, Joel Smith. First, enone **2.11** was exposed to a Corey-Chaykovsky homologation with a preformed sulfur ylide to produce spiroepoxide **2.14**.[12] With the goal of introducing oxygenation through an S_N2'-type substitution process, epoxide **2.14** was treated with $Pd(PPh_3)_4$ in the presence of AcOH.[13] However, the only product obtained was enal **2.15**, which presumably arises by initial formation of a π-allylpalladium complex and subsequent β-hydride elimination and tautomerization. A second effort to open epoxide **2.14** was attempted using dilute

sulfuric acid,[14] but this also delivered the undesired enal **2.15**. In an alternate strategy, we returned to enone **2.11** and performed an oxidation using sodium perborate tetrahydrate in THF and water,[15] which furnished epoxide **2.16** in 89% yield. This epoxide was subsequently treated with methoxymethyltriphenylphosphonium chloride in the presence of base to furnish enal **2.18** in 82% yield.[16] Presumably this transformation proceeds via Wittig olefination and spontaneous epoxide fragmentation and hydrolysis (see transition structure **2.17**). Using this sequence, gram quantities of enal **2.18** were accessible.

Scheme 2.3 Approaches to Homologate and Oxidize Enone **2.11**.

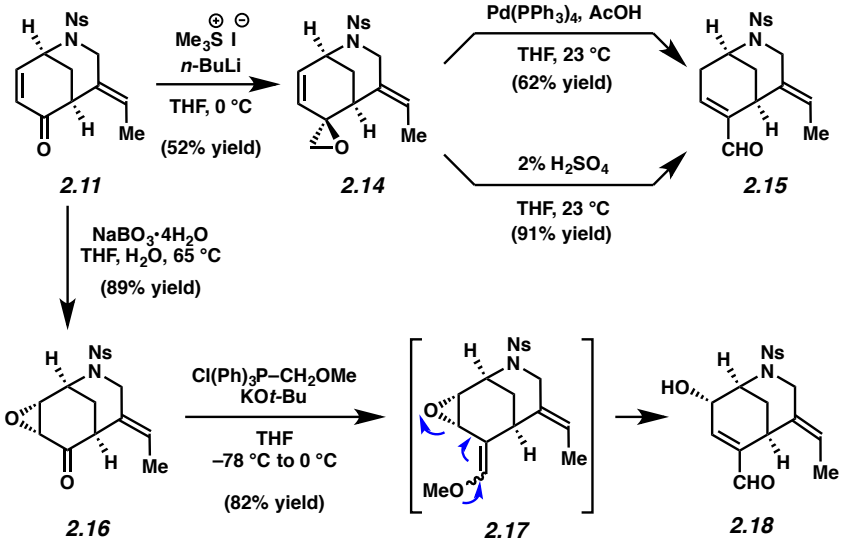

En route to the desired Fischer indolization substrate, we sought to perform a conjugate reduction of the enal (Scheme 2.4). Our initial attempts involved treatment of enal **2.18** with a number of copper[17] or rhodium-based reducing agents,[18] however these efforts were ineffective. Hypothesizing that the secondary alcohol was problematic, we silyl protected it to give **2.21** in 83% yield. Reduction of **2.21** in the presence of $Pd(PPh_3)_4$, Bu_3SnH, and $ZnCl_2$ in THF[19] proceeded in 62% yield, although with a 5:1 ratio of diastereoselectivity, favoring the undesired epimer **2.23**.

The diastereoselectivity of this process is thought to be governed by the bulky triethylsilyl ether, which sterically hinders protonation (see **2.22**).[20] Although further attempts to reduce **2.21** were also unsuccessful, we found that treatment of unprotected enal **2.18** under the Pd-catalyzed reduction conditions gave the desired hydroxyaldehyde **2.20** in 90% yield (dr = 7:1). The favorable selectivity presumably arises from protonation of the intermediate enolate on the sterically more accessible face of the [3.3.1]-azabicycle (see **2.19**).

Scheme 2.4 Diastereoselective Reduction of Enal **2.18**.

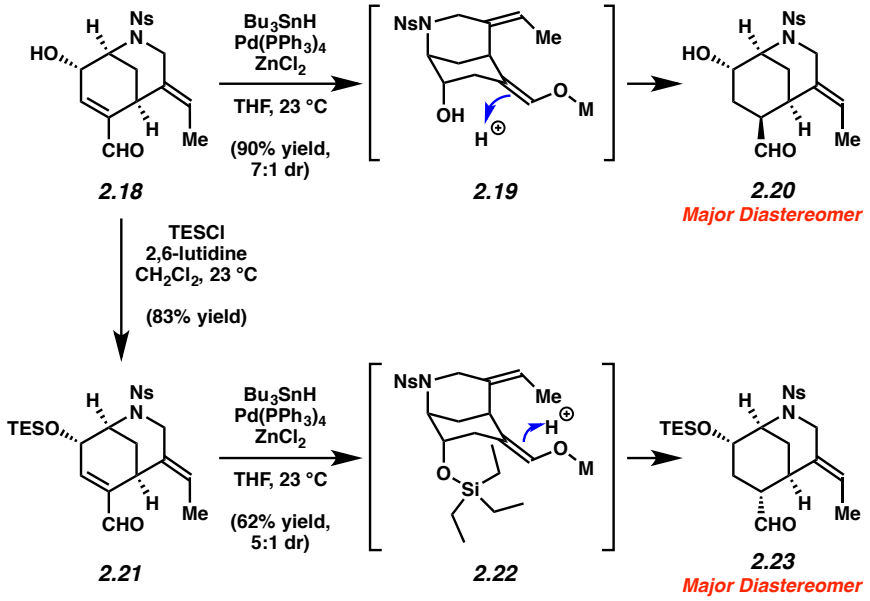

As shown in Scheme 2.5, aldehyde **2.20** could be readily elaboratored to the desired Fischer indolization substrate **2.5**. Wittig olefination of the aldehyde, followed by oxidation of the secondary alcohol with Dess–Martin periodinane, afforded ketone **2.24** in 80% over two steps. Next, allylic alkylation of **2.24** with allyl iodide in the presence of strong base and *N,N′*-dimethylpropyleneurea (DMPU) furnished **2.25** in 55% yield, along with 31% recovered ketone **2.24**. To arrive at the desired Fischer indolization substrate, **2.25** was treated with the Grubbs–

Hoveyda 2nd Generation catalyst (**2.26**) in CH_2Cl_2 at reflux to give cyclopentene **2.5** in good yield.[21] It is worth noting that epimerization was not observed in this reaction and the *trans*-hydrindenone product (**2.5**) was the only product observed. To our delight, reaction of ketone **2.5** with phenylhydrazine (**2.4**) and TFA delivered indolenine **2.3** in 74% yield via late-stage Fischer indolization. Of note, only a single diastereomer was observed in this complexity-generating step. The transformation required only 2 hours, which compares favorably to our earlier Fischer indolization studies. It is hypothesized that the rigidity of the substrate is responsible for the facile nature of the [3,3]-sigmatropic rearrangement. Nonetheless, our ability to access **2.3** marked a critical juncture in our synthetic efforts, as we expected that oxidative cleavage of the cyclopentene could lead to assembly of the important furanoindoline motif present in the natural product.

Scheme 2.5 Synthesis of Cyclopentene **2.5** and Fischer Indolization.

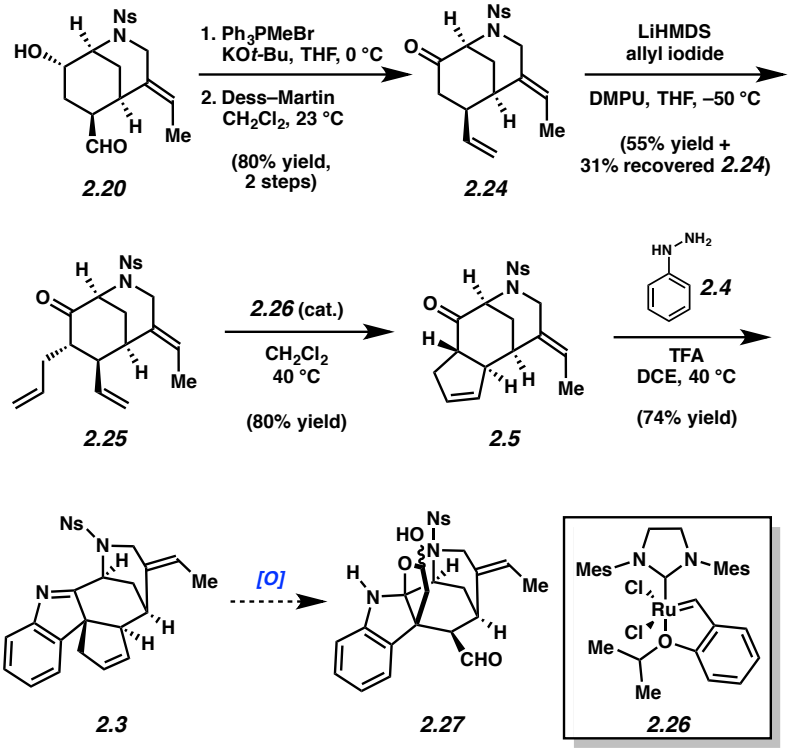

2.5 Failed Oxidation and Modification of Synthetic Route

Our excitement in having accessed Fischer indolization product **2.3** was quickly thwarted by our inability to oxidatively cleave the cyclopentene ring. Figure 2.1 summarizes a variety of reaction conditions that were tested by my colleague Joel Smith as a means to selectively oxidize the endocyclic olefin. Each of these efforts resulted in the recovery of starting material or substantial nonspecific decomposition of substrate **2.3**. Osmium-,[22,23] along with ruthenium-[24] and manganese-based oxidations,[25] were deemed ineffective. Similarly, attempted epoxidation with *m*-CPBA or direct oxidative cleavage using ozonolysis conditions resulted in decomposition of the starting material.

Figure 2.1 Attempted Olefin Oxidation of Indolenine Substrate **2.3**.

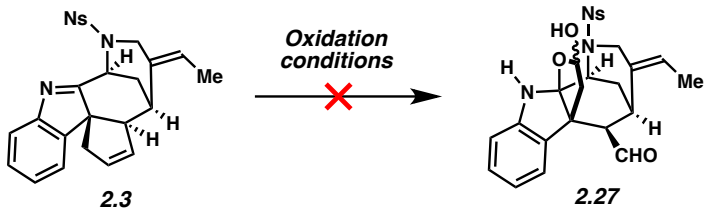

2.3 ***2.27***

Oxidant	*Additive(s)*	*Result*
OsO_4 (cat.), $NaIO_4$	2,6-lutidine	recovery of ***2.3*** + decomposition
$KMnO_4$	TEBA-Cl	recovery of ***2.3***
m-CPBA	–	decomposition
OsO_4	pyridine	recovery of ***2.3***
$RuCl_3 \cdot 3H_2O$ (cat.), $NaIO_4$	H_2O	recovery of ***2.3***
K_2OsO_4 (cat.), $NaIO_4$	–	recovery of ***2.3***
O_3	–	decomposition
OsO_4	DMAP	decomposition
K_2OsO_4 (cat.), $K_3Fe(CN)_6$	$MeSO_2NH_2$, $(DHQ)_2PHAL$	recovery of ***2.3***

Figure 2.2 suggests a reasonable hypothesis for the difficulties we experienced in attempting to oxidatively cleave cyclopentene **2.3**. A three-dimensional depiction of **2.3** shows

that approach to the olefin is severely obstructed on both faces. On one hand, the proximal ethylidene moiety blocks approach of an oxidant, whereas approach to the other face is impeded by the hydrogen at C9. As a workaround, we considered performing the oxidative functionalization of cyclopentene **2.5** prior to performing the Fischer indolization. Although the ethylidene similarly blocks approach of one face of the olefin in **2.5**, the other face appeared accessible.

Figure 2.2 Hypothesis for Oxidation Difficulties and Revision of Strategy.

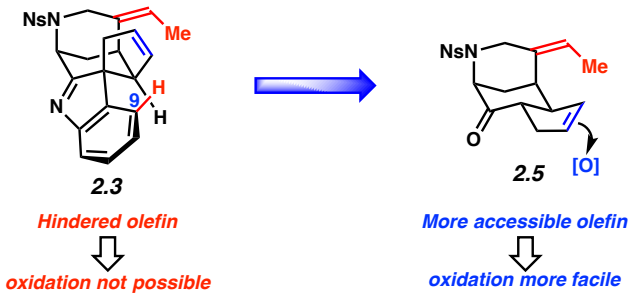

2.6 Earlier Oxidation, Successful Fischer indolization, and Late-Stage Challenges

Our efforts to carry out the revised endgame strategy are depicted in Scheme 2.6. First, chemo- and diastereoselective Upjohn dihydroxylation[26] of the *trans*-hydrindenone **2.5**, followed by protection of the resultant diol as the cyclic carbonate,[27] gave tetracyclic intermediate **2.28** in 78% yield over two steps. The success of this sequence validated our hypothesis shown in Figure 2.2 and allowed us to attempt the key Fischer indolization step. In the event, treatment of **2.28** with phenylhydrazine (**2.4**) and TFA at 80 °C in DCE gave a mixture of two products in a combined yield of 69%. After careful separation and 2D-NMR analysis of each compound in C_6D_6, the two products were identified as indolenine **2.29** and hydrate **2.30**.[28] These compounds could be taken forward as an inconsequential mixture. It is worth noting that the Fischer indolization of substrate **2.28** is one of the most complex examples in the literature to date.[29]

The next late-stage maneuver involved revealing the diol moiety and performing oxidative cleavage. This was achieved by treating the mixture of **2.29** and **2.30** with NaOH,[30] followed by exposure of the intermediate diol to $NaIO_4$. The resulting lactol, **2.27**, was obtained in 81% yield over two steps.[31] Thus, by installing oxidation prior to the Fischer indolization, our problematic oxidation of cyclopentene **2.3** (see Figures 2.1 and 2.2) had been successfully circumvented. Having synthesized lactol **2.27**, all that remained was conversion of the exocyclic aldehyde to a methyl ester, cleavage of the sulfonamide, and construction of the *N,O*-acetal. In our first efforts, we attempted to cleave the sulfonamide group using thiol-based denosylation conditions.[32] Unfortunately, these attempts led to the formation of multiple products that proved difficult to isolate. To facilitate purification, the deprotection of **2.27** was tried using a resin-bound thiol (MetSThiol) in the presence of Cs_2CO_3.[33] Although it appeared that cleavage of the nosyl protecting group had occurred,[34] we regrettably did not detect formation of the desired product **2.31**. Thus, our efforts to access the natural product (**2.1**) had again been foiled.

Scheme 2.6 Synthesis of Lactol **2.27** and Failed Late-stage *N,O*-Acetal Formation.

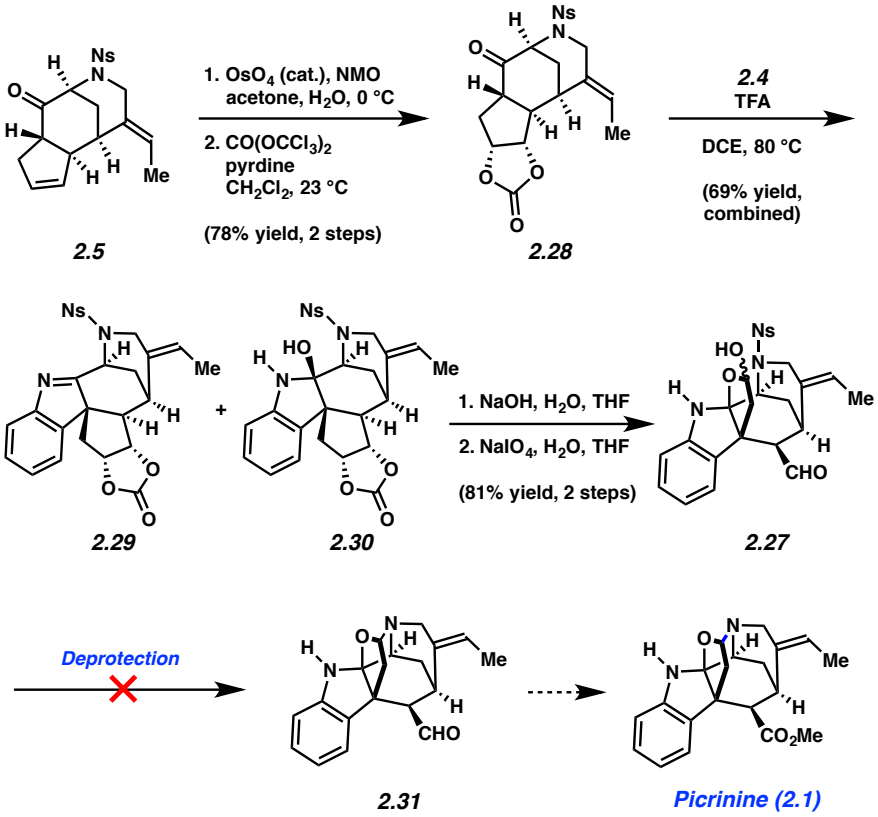

2.7 Completion of the Total Synthesis of Picrinine (2.1)

With limited options available, we decided to change the order of late-stage transformations by introducing the ester prior to denosylation (Scheme 2.7). Toward this end, Lindgren oxidation of **2.27** gave an intermediate carboxylic acid, which was methylated with trimethylsilyldiazomethane to afford ester **2.32** in 58% yield over two steps.[35] This delicate oxidation is noteworthy in that it occurred without any competitive oxidation of the lactol. With ester **2.32** in hand, we attempted the nosyl removal using the solid-supported conditions mentioned previously. Much to our pleasure, picrinine (**2.1**) was obtained as the sole product.[36] It is likely that the formation of **2.1** occurs via cyclization of intermediate **2.2** due to the constrained proximity

of N4 and C5. Our synthetic sample of picrinine (**2.1**) was found to be identical to a natural sample.[37]

Scheme 2.7 Completion of the Total Synthesis of Picrinine (**2.1**).

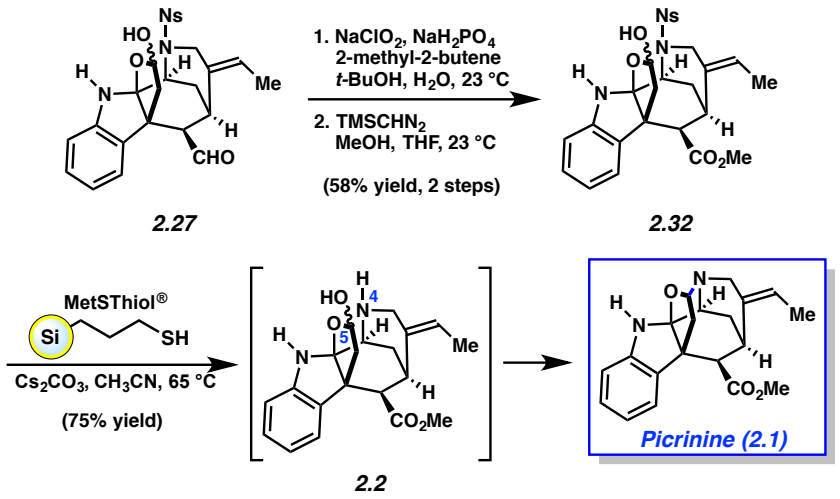

2.8 Conclusion

In conclusion, we have developed the first total synthesis of the daunting, polycyclic akuammiline alkaloid picrinine (**2.1**). Our initial synthetic efforts, which were largely inspired by our earlier total synthesis of aspidophylline A, were plagued by late-stage difficulties and material throughput problems. However, these challenges prompted us to develop a revised synthesis of the [3.3.1]-azabicyclic core of the natural product, which proved far more robust and scalable compared to our initial route. In turn, efficient access to the azabicyclic core permitted the design and testing of substrates for late-stage Fischer indolization reactions. In fact, the substrates utilized in our synthetic forays toward **2.1** represent some of the most complex examples of Fischer indolizations to date. It is hoped that the lessons learned in the course of our total synthesis of picrinine (**2.1**) will help guide synthetic studies pertaining to akuammilines and other classes of complex indole alkaloids.

2.9 Experimental Section

2.9.1 Materials and Methods

Unless stated otherwise, reactions were conducted in flame-dried glassware under an atmosphere of nitrogen using anhydrous solvents (either freshly distilled or passed through activated alumina columns). $Pd(PPh_3)_4$ and (OsO_4 were obtained from Strem. Phenylhydrazine (**2.4**) was purified by flash chromatography (4:1 hexanes:EtOAc) prior to use. Unless stated otherwise, reactions were performed at room temperature (approximately 23 °C). Thin-layer chromatography (TLC) was conducted with EMD gel 60 F254 pre-coated plates (0.25 mm) and visualized using a combination of UV, anisaldehyde, and iodine staining. SiliCycle silica gel 60 (particle size 0.040–0.063 mm) was used for flash column chromatography. ^{1}H NMR spectra were recorded on 300 and 500 MHz spectrometers. Data for ^{1}H spectra are reported as follows: chemical shift (δ ppm), multiplicity, coupling constant (Hz), integration and are referenced to the residual solvent peak 7.26 ppm for $CDCl_3$, and 7.16 ppm for C_6D_6. ^{13}C NMR spectra are reported in terms of chemical shift (at 125 MHz) and are referenced to the residual solvent peak 77.16 ppm for $CDCl_3$, and 128.06 ppm for C_6D_6. IR spectra are reported in terms of frequency absorption (cm^{-1}). High-resolution mass spectra were obtained from the UC Irvine and UCLA Mass Spectrometry Facilities using TOF and Orbitrap mass analyzers, respectively.

2.9.2 Experimental Procedures

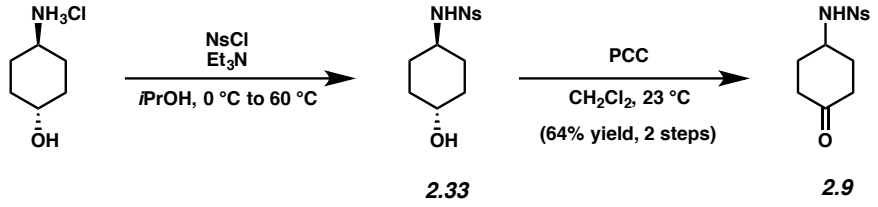

Nosyl Ketone 2.9. To a solution of *trans*-4-aminocyclohexanol•HCl (10.0 g, 66.0 mmol) in *i*-PrOH (120 mL) was added NsCl (14.6 g, 66.0 mmol) and Et_3N (36.7 mL, 263.8 mmol) at 0 °C. The mixture was heated to 60 °C and after 2 h, the reaction was filtered and the filtrate was concentrated under reduced pressure. The resulting residue was dissolved in EtOAc (200 mL) and washed successively with 0.5 M HCl (50 mL) and H_2O (100 mL). The aqueous layer was extracted with EtOAc (50 mL) and the organic layers were combined, dried over $MgSO_4$, and evaporated under reduced pressure to afford the crude product **2.33**, which was used in the subsequent step without further purification.

To a solution of PCC (26.0 g, 120.9 mmol) and celite (9.5 g) in CH_2Cl_2 (202 mL) was added **2.33** at room temperature. After 12 h, the reaction was diluted with Et_2O (300 mL), filtered over a pad of layered celite, alumina, and sand, and washed with EtOAc (1 L). The filtrate was concentrated under reduced pressure to afford nosyl ketone **2.9** (12.5 g, 64% yield, two steps) as a beige solid. Nosyl ketone **2.9**: mp: 145–147 °C; R_f 0.25 (1:1 hexanes:EtOAc); ^{1}H NMR (500 MHz, $CDCl_3$): δ 8.21 (m, 1H), 7.90 (m, 1H), 7.78 (m, 2H), 5.41 (d, J = 7.0), 3.79 (m, 1H), 2.47–2.32 (m, 4H), 2.12 (m, 2H), 1.86 (m, 2H); ^{13}C NMR (125 MHz, $CDCl_3$): δ 208.6, 148.1, 134.5, 134.0, 133.2, 130.9, 125.7, 51.1, 38.5, 32.6; IR (film) 3305, 2952, 1710, 1538, 1443, 1343, 1163 cm^{-1}; HRMS–APCI (*m/z*) $[M + H]^+$ calcd for $C_{12}H_{15}N_2O_5S^+$, 299.06962; found 299.06911.

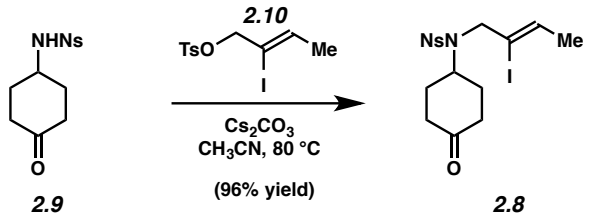

Iodide 2.8. To a suspension of ketone **2.9** (15.0 g, 50.3 mmol) and Cs_2CO_3 (24.6 g, 75.5 mmol) in CH_3CN (250 mL) was added tosylate **2.10**[5] (21.3 g, 60.5 mmol). The reaction was refluxed at 80 °C. After 1.5 h, the reaction was cooled to room temperature and excess CH_3CN was removed under reduced pressure. The residue was poured into deionized water (100 mL) and the resulting mixture was diluted with CH_2Cl_2 (250 mL). The layers were separated and the aqueous layer was extracted with CH_2Cl_2 (3 x 100 mL). The organic layers were combined, dried over $MgSO_4$, and evaporated under reduced pressure. The resulting residue was purified via flash chromatography (1.5:1 hexanes:EtOAc) to afford iodide **2.8** (23.1 g, 96% yield) as a yellow solid. Iodide **2.8**: mp: 58–61 °C; R_f 0.53 (1:1 hexanes:EtOAc); ^{1}H NMR (500 MHz, $CDCl_3$): δ 8.02–8.00 (m, 1H), 7.75–7.65 (m, 3H), 6.00 (qt, J = 6.4, 1.3, 1H), 4.42 (tt, J = 12.1, 3.6, 1H), 4.20 (t, J = 1.3, 2H), 2.51 (td, J = 14.6, 6, 2H), 2.42 (dt, J = 14.6, 2.4, 2H), 2.23–2.17 (m, 2H), 1.89 (qd, J = 12.8, 4.7, 2H), 1.66 (dt, J = 6.4, 1.3, 3H); ^{13}C NMR (125 MHz, $CDCl_3$): δ 208.8, 147.9, 134.4, 134.2, 133.9, 131.8 (2 carbons), 124.6, 105.3, 56.5, 55.8, 40.1, 30.6, 22.0; IR (film): 2957, 1716, 1541, 1369, 1345, 1160 cm^{-1}; HRMS–ESI (*m/z*) $[M + Na]^+$ calcd for $C_{16}H_{19}IN_2O_5SNa^+$, 500.9952; found 500.9960.

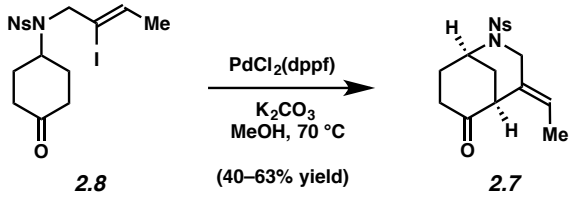

Ketone 2.7. A solution of iodide **2.8** (500 mg, 1.05 mmol) in MeOH (20 mL) was cooled to –100 °C. After stirring for 5 min, the solution was put under vacuum. After 5 additional min of stirring, the reaction was sparged with N_2 for 10 min, followed by the addition of $PdCl_2$(dppf) (171 mg, 0.209 mmol) and K_2CO_3 (570 mg, 4.18 mmol) (Note: The variable amount of oxygen present in the reaction can alter the yield, thus rigorous deoxygenation is required). The cooling bath was removed from the reaction and continued to be degassed while warming up to room temperature, at which point the reaction was refluxed at 70 °C. After 45 min, the reaction was cooled to room temperature and the excess MeOH was removed under reduced pressure. The resulting residue was diluted with deionized water (100 mL) and CH_2Cl_2 (100 mL). The layers were separated and the aqueous layer was extracted with CH_2Cl_2 (2 x 100 mL). The organic layers were combined, dried over Na_2SO_4, and evaporated under reduced pressure. The resulting residue was purified via flash chromatography (1.5:1 hexanes:EtOAc) to afford ketone **2.7** (195 mg, 53% yield) as a brown solid. Ketone **2.7**: mp: 125–129 °C; R_f 0.29 (1:1 hexanes:EtOAc); ^{1}H NMR (300 MHz, $CDCl_3$): δ 8.07–8.03 (m, 1H), 7.77–7,68 (m, 2H), 7.67–7.60 (m, 1H), 5.68 (q, *J* = 7.0, 1H), 4.30 (t, *J* = 5.8, 1H), 4.15 (d, *J* = 13.9, 1H), 3.90 (dt, *J* = 13.9, 0.9, 1H), 3.49 (br. s, 1H), 2.90–2.79 (m, 1H), 2.33–2.24 (m, 2H), 2.03 (dt, *J* = 14.1, 2.7, 1H), 1.97–1.85 (m, 1H), 1.61 (dt, *J* = 7.0, 0.9, 3H); ^{13}C NMR (125 MHz, $CDCl_3$): δ 208.1, 148.5, 134.0, 132.0, 131.8, 131.3, 128.8, 126.6, 124.4, 49.0, 48.2. 46.7. 35.0, 32.9, 31.4, 13.2; IR (film): 2956, 1713, 1543, 1373, 1164 cm^{-1}; HRMS–ESI (*m/z*) [M + Na]$^+$ calcd for $C_{16}H_{18}N_2O_5SNa^+$, 373.0829; found 373.0836.

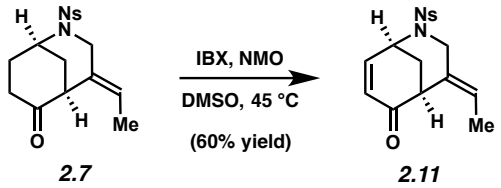

2.7 *2.11*

Enone 2.11. To a dram vial charged with IBX (0.128 g, 0.457 mmol) and NMO (0.056 g, 0.476 mmol) was added DMSO (0.5 mL). The mixture was stirred for 10 min at room temperature at which point a solution of ketone **2.7** (0.050 g, 0.143 mmol) in DMSO (0.64 mL) was added and the reaction was heated to 45 °C. After 20 h, the reaction was cooled to room temperature and washed with a 5% aq. $NaHCO_3$ solution (2 mL) and extracted with Et_2O (4 x 20 mL). The organic layers were combined, dried over $MgSO_4$, and evaporated under reduced pressure. The resulting residue was purified via flash chromatography (1.5:1 hexanes:EtOAc) to afford enone **2.11** (0.030 g, 60% yield) as a white solid. Enone **2.11**: mp: 122.5–124 ºC; R_f 0.48 (1.5:1 hexanes:EtOAc); ^{1}H NMR (500 MHz, $CDCl_3$): δ 8.08 (dd, *J* = 7.4, 2, 1H), 7.67–7.67 (m, 3H), 6.85 (ddd, *J* = 10.0, 6.1, 1.8, 1H), 6.26 (dd, *J* = 10.0, 1.1), 5.58 (q, *J* = 7.2, 1H), 4.74 (dt *J* = 6.1, 3.1, 1H), 4.00 (d, *J* = 14.7, 1H), 3.85 (dt, *J* = 14.7, 2.1, 1H), 3.67 (t, *J* = 3.0, 1H), 2.36 (dt, *J* = 13.1, 3.1, 1H), 2.05 (m, 1H), 1.73 (dd, *J* = 6.8, 2.1, 3H); ^{13}C NMR (125 MHz, $CDCl_3$): δ 197.2, 147.9, 142.3, 134.0, 133.2, 133.1, 132.1, 131.0, 128.0, 124.9, 124.7, 47.6, 47.1, 44.2, 32.8, 12.9; IR (film): 2925, 1686, 1542, 1370, 1165 cm^{-1}; HRMS–ESI (*m/z*) $[M + Na]^+$ calcd for $C_{16}H_{16}N_2O_5SNa^+$, 371.0677; found 371.0672.

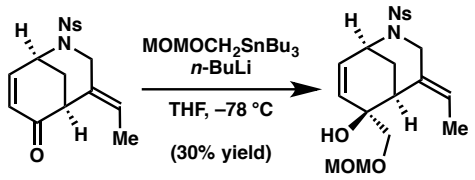

2.11 *2.12*

Alcohol 2.12. To a solution of $CH_3OCH_2OCH_2SnBu_3$ (39 mg, 0.11 mmol)[8a] in THF (1 mL) was added a solution of *n*-BuLi (0.046 mL, 2.05 M in hexanes) at –78 °C. The reaction mixture was stirred for 20 min, at which point a solution of enone **2.11** (25 mg, 0.072 mmol) in THF (1 mL) was added dropwise over 1 min at –78 °C. After 1 h, the reaction mixture was quenched with a solution of sat. aqueous NH_4Cl (3 mL) and allowed to warm to room temperature. The layers were separated, and the aqueous layer was extracted with EtOAc (4 x 10 mL). The combined organic layers were dried over $MgSO_4$, filtered, and evaporated under reduced pressure. The resulting residue was purified via flash chromatography (2:1 hexanes:EtOAc) to afford alcohol **2.12** (9 mg, 30% yield) as a pale yellow oil. Alcohol **2.12**: R_f 0.28 (2:1 hexanes:EtOAc); ^{1}H NMR (500 MHz, $CDCl_3$): δ 8.02 (m, 1H), 7.68 (m, 2H), 7.62, (m, 1H), 5.86 (dd, *J* = 10.0, 1.3, 1H), 5.73 (ddd, *J* = 10.0, 5.7, 1.3, 1H), 5.66 (q, *J* = 6.9, 1H), 4.68–4.48 (m, 3H), 3.97 (d, *J* = 14.1, 1H), 3.90 (dt, *J* = 14.1, 2.0, 1H), 3.58 (d, *J* = 10.4, 1H), 3.48 (d, *J* = 10.4, 1H), 3.38 (s, 3H), 3.23 (t, *J* = 3.8, 1H), 2.49 (s, 1H), 1.99 (dt, *J* = 13.4, 3.0, 1H), 1.82 (dt, *J* = 13.4, 3.4, 1H), 1.66 (dd, *J* = 6.9, 2.0, 3H); ^{13}C NMR (125 MHz, $CDCl_3$): δ 148.0, 136.2, 133.7, 133.6, 131.8, 131.2, 130.8, 125.6, 124.8, 124.4, 97.3, 72.8, 71.5, 55.7, 47.9, 47.7, 35.0, 30.9, 12.9; IR (film): 3526, 2931, 1543, 1442, 1372, 1352, 1213, 1164, 1108, 1036 cm^{-1}; HRMS–APCI (*m/z*) $[M + H]^+$ calcd for $C_{19}H_{25}N_2O_7S^+$, 425.13770; found 425.13565.

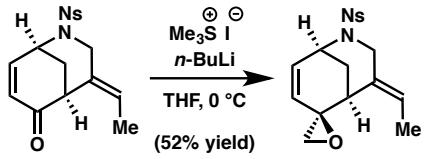

2.11 *2.14*

Epoxide 2.14. To a suspension of Me_3SI (39 mg, 0.19 mmol) in THF (1 mL) was added *n*-BuLi (65 µL, 2.65 M in hexanes) at 0 °C. After 5 min, a solution of enone **2.11** (56 mg, 0.16 mmol) in THF (0.6 mL) was added dropwise over 1 min at 0 °C. After 30 min, the reaction was warmed to room temperature and poured into a brine solution (3 mL). The layers were separated, and the aqueous layer was extracted with EtOAc (3 x 10 mL). The combined organic layers were dried over $MgSO_4$, filtered, and evaporated under reduced pressure. The resulting residue was purified via flash chromatography (2:1 hexanes:EtOAc) to afford epoxide **2.14** (30 mg, 52% yield) as a pale yellow oil. Epoxide **2.14**: R_f 0.58 (2:1 hexanes:EtOAc); ^{1}H NMR (500 MHz, $CDCl_3$): δ 8.04 (m, 1H), 7.69 (m, 2H), 7.63 (m, 1H), 5.94 (ddd, *J* = 1.5, 5.9, 9.9, 1H), 5.56 (q, *J* = 6.8, 12), 5.55 (dd, *J* = 1.2, 9.9, 1H), 4.61(dt, *J* = 3.0, 5.9, 1H), 4.00 (m, 2H), 2.96 (d, *J* = 5.2, 1H), 2.85 (d, *J* = 5.2, 1H), 2.73 (br. s, 1H), 2.16 (dt, *J* = 3.1, 12.9, 1H), 1.99 (ddt, *J* = 1.6, 3.4, 12.9, 1H), 1.56 (dd, *J* = 1.5, 6.3, 3H); ^{13}C NMR (125 MHz, $CDCl_3$): δ 148.0, 135.8, 133.6, 133.7, 131.9, 131.0, 130.8, 129.1, 124.4, 123.5, 58.3, 56.4, 47.6, 47.3, 34.9, 32.3, 12.7; IR (film): 2924, 1543, 1440, 1372, 1165, 1127, 1075 cm^{-1}; HRMS–APCI (*m/z*) $[M + H]^+$ calcd for $C_{17}H_{19}N_2O_5S^+$, 363.10090; found 369.10024.

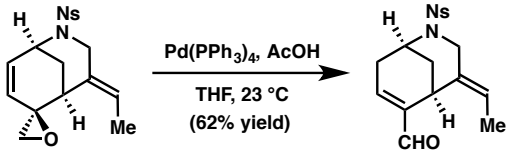

2.14 *2.15*

Enal 2.15. To a solution of $Pd(PPh_3)_4$ (1 mg, 0.00030 mmol) and AcOH (2 μL, 0.033 mmol) in THF (0.25 mL) was added a solution of epoxide **3.14** (0.011 g, 0.030 mmol) dropwise over 1 min. After 30 min, the reaction was filtered over a plug of SiO_2, washed with EtOAc (25 mL) and the filtrate was concentrated under reduced pressure. The resulting residue was purified via preparative TLC (2:1 hexanes:EtOAc) to afford enal **2.15** (7 mg, 62% yield) as a colorless oil. Enal **2.15**: R_f 0.38 (2:1 hexanes:EtOAc); ^{1}H NMR (500 MHz, $CDCl_3$): δ 9.37 (s, 1H), 8.05 (m, 1H), 7.74–7.63 (m, 3H), 6.91 (t, *J* = 3.7, 1H), 5.43 (q, *J* = 6.9, 1H), 4.45 (br. s, 1H), 3.96 (br. s, 1H), 3.85 (d, *J* = 14.3, 1H), 3.71 (d, *J* = 14.3, 1H), 2.82 (ddd, *J* = 3.4, 5.9, 21.5, 1H), 2.59 (dd, *J* = 3.9, 21.5, 1H), 1.92 (dt, *J* = 3.4, 12.8, 1H), 1.78 (dd, *J* = 1.8, 6.8, 3H), 1.69 (dt, *J* = 3.1, 12.8, 1H); ^{13}C NMR (125 MHz, $CDCl_3$): δ 191.8, 149.1, 148.0, 142.5, 133.7, 133.6, 131.9, 131.0, 130.7, 124.5, 122.7, 48.0, 47.0, 33.2, 30.9, 26.6, 12.9; IR (film): 2923, 1682, 1542, 1440, 1371, 1340, 1164, 1126, 1081 cm^{-1}; HRMS–APCI (*m/z*) $[M + H]^+$ calcd for $C_{17}H_{19}N_2O_5S^+$, 363.10090; found 363.10022.

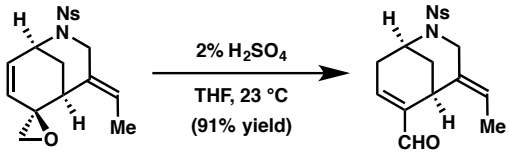

2.14 *2.15*

Enal 2.15. To a solution of epoxide **2.14 (**11 mg, 0.030 mmol) in THF (0.30 mL) was added an aqueous solution of H_2SO_4 (0.2 mL, 2% w/w). After 5 min, the reaction mixture was diluted with EtOAc (5 mL) and poured into a solution of sat. aq. $NaHCO_3$ (5 mL). The layers were separated and the aqueous layer was extracted with EtOAc (3 x 10 mL). The combined organic layers were

dried over $MgSO_4$, filtered, and evaporated under reduced pressure. The resulting residue was purified via flash chromatography (2:1 hexanes:EtOAc) to afford enal **2.15** (10 mg, 91% yield) as a colorless oil.

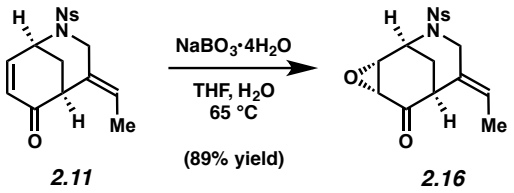

2.11 *2.16*

Epoxide 2.16. To two individual, but identical solutions of enone **2.11** (422 mg, 1.21 mmol) in 1:1 THF:H_2O (4 mL) was added $NaBO_3$•$4H_2O$ (375 mg, 3.76 mmol). Each reaction was heated to 65 °C. After stirring for 12 h, each reaction was cooled to room temperature and poured into deionized water (150 mL) and diluted with EtOAc (150 mL). The layers were separated and the aqueous layer was extracted with EtOAc (2 x 150 mL). The organic layers from both reactions were combined, dried over $MgSO_4$, and evaporated under reduced pressure. The combined residue was purified via flash chromatography (2:1 hexanes:EtOAc) to afford epoxide **2.16** (785 mg, 89% yield) as a yellow solid. Epoxide **2.16**: mp: 147–149 °C; R_f 0.45 (1:1 hexanes:EtOAc); ^{1}H NMR (500 MHz, $CDCl_3$): δ 8.13–8.11 (m, 1H), 7.77–7.69 (m, 3H), 5.60 (q, J = 6.9, 1H), 4.72 (q, J = 2.9, 1H), 4.06 (d, J = 15.1, 1H), 3.97 (dt, J = 15.1, 1.8), 3.62 (t, J = 3.2, 1H), 3.52 (t, J = 2.7, 1H), 3.38 (d, J = 3.2, 1H), 2.33 (dt, J = 13.7, 2.9, 1H), 1.71–1.68 (m, 4H); ^{13}C NMR (125 MHz, $CDCl_3$): δ 201.7, 147.8, 134.1, 133.0, 132.1, 131.0, 128.3, 125.1, 124.7, 54.2, 51.7, 48.4, 47.6, 42.0, 23.6, 12.8; IR (film): 2919, 1716, 1542, 1371, 1163 cm^{-1}; HRMS–ESI (*m/z*) $[M + Na]^+$ calcd for $C_{16}H_{16}N_2O_6SNa^+$, 387.0621; found 387.0630.

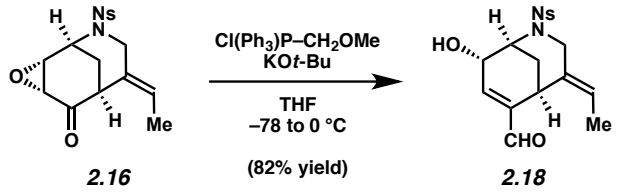

2.16 *2.18*

Enal 2.18. In a glovebox, a round-bottom flask was charged with methoxymethyl-triphenylphosphonium chloride (0.659 g, 1.93 mmol), and a dram vial was charged with KO*t*-Bu (0.198 g, 1.76 mmol). The contents were removed from the glovebox, placed under N_2 pressure, and THF was added to the flask and vial (8 mL and 2 mL, respectively). The solution of methoxymethyltriphosphonium chloride in THF was cooled to –78 °C and the solution of KO*t*-Bu in THF was added dropwise over 1 min. The mixture was stirred at –78 °C for 30 min, at which point a solution of epoxide **2.16** (0.585 g, 1.60 mmol) in THF (6 mL) was added dropwise over 1 min. The reaction was warmed to 0 °C, and after stirring for 15 min, the reaction was quenched with a solution of sat. aq. NH_4Cl (15 mL). The resulting mixture was poured into deionized water (100 mL) and diluted with EtOAc (100 mL). The layers were separated and the aqueous layer was extracted with EtOAc (2 x 100 mL). The organic layers were combined, dried over $MgSO_4$, and evaporated under reduced pressure. The resulting residue was purified via flash chromatography (1:1 hexanes:EtOAc) to afford enal **2.18** (0.500 g, 82% yield) as a clear wax. Enal **2.18**: R_f 0.15 (1:1 hexanes: EtOAc); ^{1}H NMR (500 MHz, $CDCl_3$): δ 9.47 (s, 1H), 8.05 (dd, *J* = 1.7, 7.5, 1H), 7.76–7.65 (m, 3H), 6.86 (d, *J* = 3.8, 1H), 5.45 (q, *J* = 6.8, 1H), 4.42 (d, *J* = 2.7, 1H), 4.26 (s, 1H), 3.93 (s, 1H), 3.84 (d, *J* = 14.5, 1H), 3.60 (d, *J* = 14.5, 1H), 2.70 (s, 1H), 1.91 (dt, *J* = 13.3, 3.2), 1.81–1.73 (m, 4H); ^{13}C NMR (125 MHz, $CDCl_3$): δ 192.3, 147.9, 146.7, 143.6, 133.9, 133.3, 132.1, 131.0, 129.4, 124.6, 123.5, 67.6, 55.1, 47.2, 27.1, 26.6, 12.9; IR (film): 3406, 2926, 2859, 1686, 1541, 1370, 1160, 1127 cm^{-1}; HRMS–ESI (*m/z*) $[M - H]^-$ calcd for $C_{17}H_{17}N_2O_6S^-$, 377.0807; found 377.0821.

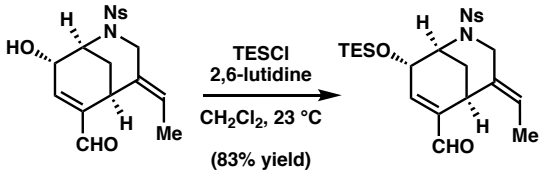

2.18 *2.21*

Enal 2.21. To a solution of enal **2.18** (25 mg, 0.066 mmol) in CH_2Cl_2 (1 mL) was added 2,6-lutidine (0.046 mL, 0.40 mmol) and TESCl (33 µL, 0.20 mmol). After stirring for 17 h, the reaction mixture was diluted with CH_2Cl_2 (5 mL) and poured into H_2O (5 mL). The layers were separated, and the aqueous layer was extracted with CH_2Cl_2 (2 x 10 mL). The combined organic layers were dried over $MgSO_4$, filtered, and evaporated under reduced pressure. The resulting residue was purified via preparative TLC (1:1 hexanes:EtOAc) to afford enal **2.21** (27 mg, 83% yield) as a colorless oil. Enal **2.21**: R_f 0.31 (4:1 hexanes:EtOAc); ^{1}H NMR (500 MHz, $CDCl_3$): δ 9.44 (s, 1H), 8.06 (m, 1H), 7.73–7.65 (m, 3H), 6.75 (dd, *J* = 4.0, 1.2, 1H), 5.41 (q, *J* = 6.7, 1H), 4.41 (d, *J* = 4.0, 1H), 4.06 (br. s, 1H), 2.90 (t, *J* = 2.9, 1H), 3.81 (d, *J* = 14.5, 1H), 3.67 (dt, *J* = 14.5, 1.9, 1H), 1.95 (dt, *J* = 13.0, 3.1, 1H), 1.76 (dd, *J* = 6.8, 1.9, 3H), 1.66 (dt, *J* = 13.0, 3.2, 1H), 0.96 (t, *J* = 8.1, 9H), 0.66 (q, *J* = 8.1, 6H); ^{13}C NMR (125 MHz, $CDCl_3$): δ 192.6, 148.0 (2 carbons), 142.1, 133.8, 133.4, 131.9, 131.1, 129.7, 124.7, 122.9, 67.9, 55.1, 47.2, 27.1, 26.2, 12.8, 6.9, 4.7; IR (film): 2957, 2877, 1690, 1543, 1457, 1440, 1370, 1343, 1240, 1164, 1126, 1071, 1009 cm^{-1}; HRMS–APCI (*m/z*) [M + H]$^+$ calcd for $C_{23}H_{32}N_2O_6SSi^+$, 493.18231; found 493.17800.

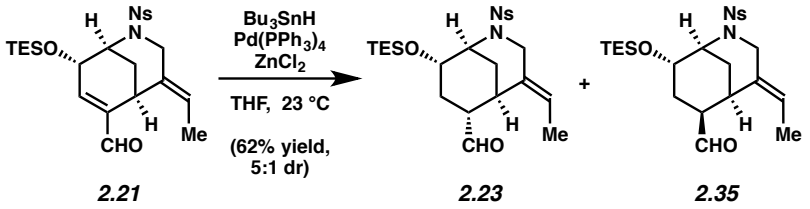

Aldehyde 2.23 and Aldehyde 2.35. In the glovebox, a vial was charged with $Pd(PPh_3)_4$ (2 mg, 0.0016 mmol) and $ZnCl_2$ (17 mg, 0.125 mmol). The flask was removed from the glovebox, placed under N_2 pressure, and THF (1.5 mL) was added. To this solution was added a solution of enal **2.21** (27 mg, 0.054 mmol) in THF (1.2 mL). The resulting mixture was sparged with N_2 for 10 min, at which point Bu_3SnH (0.029 mL, 0.11 mmol) was added. After 20 h, the reaction mixture was diluted with EtOAc (10 mL) and poured into H_2O (10 mL). The layers were separated, and the aqueous layer was extracted with EtOAc (2 x 10 mL). The combined organic layers were dried over $MgSO_4$, filtered, and evaporated under reduced pressure. The resulting residue was purified via preparative TLC (18:1:1 benzene:Et_2O:CH_2Cl_2) to afford aldehyde **2.23** (14 mg, 52% yield) and aldehyde **2.35** (3 mg, 10% yield) as colorless oils. The stereochemical assignment of **2.23** and **2.35** were determined by analysis of ^{1}H NMR coupling constants. Aldehyde **2.23**: R_f 0.48 (2:1 hexanes:EtOAc); ^{1}H NMR (500 MHz, $CDCl_3$): δ 9.72 (s, 1H), 7.96 (m, 1H), 7.70 (m, 2H), 7.61 (m, 1H), 5.48 (q, J = 7.0, 1H), 4.14 (app. q, J = 3.1, 1H), 4.06 (d, J = 14.1, 1H), 3.75 (m, 2H), 3.36 (br. s, 1H), 2.35 (ddd, J = 14.8, 6.8, 2.5, 1H), 2.30 (dt, J = 14.2, 2.7, 1H), 2.25 (d, J = 6.8, 1H), 2.03 (d, J = 14.8, 1H), 1.57 (d, J = 7.0, 3H), 1.50 (dt, J = 14.2, 3.7, 1H), 0.96 (t, J = 8.1, 9H), 0.62 (q, J = 8.1, 6H); ^{13}C NMR (125 MHz, $CDCl_3$): δ 202.6, 148.7, 134.4, 133.8, 131.61, 131.57, 131.2, 124.4, 121.9, 68.9, 54.3, 48.61, 48.60, 27.19, 27.17, 20.4, 13.2, 6.9, 4.7; IR (film): 2955, 2921, 2876, 1720, 1544, 1467, 1439, 1373, 1356, 1242, 1168, 1105, 1082, 1069 cm^{-1}; HRMS–APCI (*m/z*) $[M + H]^+$ calcd for $C_{23}H_{34}N_2O_6SSi^+$, 495.19796; found 495.19705.

Aldehyde **2.35**: R_f 0.48 (2:1 hexanes:EtOAc); ^{1}H NMR (500 MHz, $CDCl_3$): δ 9.64 (s, 1H), 8.04 (m, 1H), 7.69 (m, 3H), 5.45 (q, *J* = 6.9, 1H), 4.19 (app. q, *J* = 2.7, 1H), 4.13 (dt, *J* = 15.3, 2.4, 1H), 3.90 (d, *J* = 15.3, 1H), 3.85 (app. q, *J* = 3.5, 1H), 3.35 (app. q, *J* = 3.5, 1H), 3.02 (dt, *J* = 12.7, 4.4, 1H), 2.41 (dt, *J* = 13.2, 3.1, 1H), 2.10 (ddd, *J* = 15.7, 13.0, 3.4, 1H), 1.85 (dd, *J* = 15.7, 4.8, 1H), 1.60 (dd, *J* = 6.9, 1.6, 3H), 1.56 (dt, *J* = 13.2, 3.6, 1H), 0.95 (t, *J* = 8.1, 9H), 0.61 (q, *J* = 8.1, 6H); ^{13}C NMR (125 MHz, $CDCl_3$): δ 203.4, 148.1, 133.7, 133.0, 131.8, 131.3, 130.7, 124.7, 122.5, 68.5, 53.3, 49.7, 48.7, 29.0, 28.8, 26.7, 13.2, 7.0, 4.7; IR (film): 2955, 2920, 2876, 1723, 1543, 1459, 1440, 1369, 1243, 1164, 1127, 1099, 1067, 1045, 1006 cm^{-1}; HRMS–ESI (*m/z*) $[M + H]^+$ calcd for $C_{23}H_{34}N_2O_6SSi^+$, 495.19796; found 495.19642.

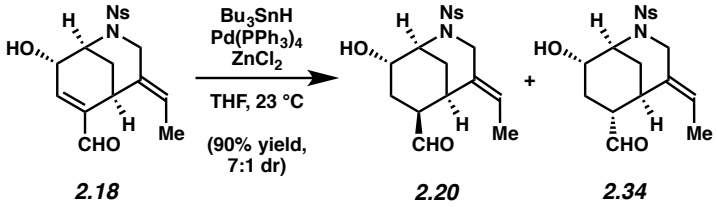

Aldehyde 2.20 and Aldehyde 2.34. In a glovebox, a round-bottom flask was charged with $Pd(PPh_3)_4$ (68.0 mg, 0.059 mmol) and $ZnCl_2$ (370 mg, 2.71 mmol). The flask was removed from the glovebox, placed under N_2 pressure, and THF (11 mL) was added. To this solution was added a solution of enal **2.18** (430 mg, 1.17 mmol) in THF (11 mL). The resulting mixture was sparged with N_2 for 10 min, at which point Bu_3SnH (0.63 ml, 2.35 mmol) was added. After stirring for 12 h, the reaction was quenched with a solution of sat. aq. NH_4Cl (30 mL). The resulting mixture was diluted with EtOAc (65 mL). The layers were separated and the aqueous layer was extracted with EtOAc (2 x 65 mL). The combined organic layers were washed with sat. aq. NH_4Cl (30 mL), dried over MgSO4, filtered and evaporated under reduced pressure. The resulting residue was purified via flash chromatography (1.5:1 hexanes:EtOAc → 1:1.5 hexanes:EtOAc) to afford aldehyde **2.20**

(0.341 g, 79% yield) as a yellow solid and aldehyde **2.34** (0.049 g, 9% yield) as a colorless foam. The stereochemical assignment of **2.20** and **2.34** were determined by analysis of ^{1}H NMR coupling constants. Aldehyde **2.20**: mp: 52–55 °C; R_f 0.12 (1:1 hexanes:EtOAc); ^{1}H NMR (500 MHz, $CDCl_3$): δ 9.60 (s, 1H), 8.06–8.04 (m, 1H), 7.73–7.68 (m, 2H), 7.77–7.64 (m, 1H), 5.46 (q, J = 6.8, 1H), 4.25 (br. s, 1H), 4.12 (dt, J = 15.3, 2.0, 1H), 4.03–4.01 (m, 1H), 3.92 (d, J = 15.3, 1H), 3.41–3.39 (m, 1H), 3.04 (dt, J = 13.0, 4.6, 1H), 2.41 (dt, J = 13.3, 3.0, 1H), 2.15 (ddd, J = 15.9, 13, 3.9, 1H), 1.97 (dd, J = 15.9, 4.6, 1H), 1.87 (d, J = 3.4, 1H), 1.64 (dt, J = 13.3, 3.4, 1H), 1.61 (dd, J = 6.8, 2.0, 3H); ^{13}C NMR (125 MHz, $CDCl_3$): δ 202.6, 147.9, 133.7, 132.7, 131.8, 131.1, 130.2, 124.5, 122.8, 67.9, 52.7, 49.7, 48.4 28.8, 27.7, 26.8, 13.0; IR (film): 3432, 2924, 2851, 1720, 1542, 1371, 1164 cm^{-1}; HRMS–APCI (*m/z*) $[M + H]^+$ calcd for $C_{17}H_{21}N_2O_6S^+$, 381.11148; found 381.11309.

Aldehyde **2.34.** R_f 0.12 (1:1 hexanes:EtOAc); ^{1}H NMR (500 MHz, $CDCl_3$): δ 9.79 (s, 1H), 8.01 (m, 1H), 7.71 (m, 2H), 7.61 (m, 1H), 5.53 (q, *J* = 6.9, 1H), 4.16 (t, *J* = 3.0, 1H), 4.11 (d, *J* = 14.2, 1H), 3.88 (app. q, *J* = 3.4, 1H), 3.82 (d, *J* = 14.2, 1H), 3.35 (br. s, 1H), 2.45 (d, *J* = 6.9, 1H), 2.37 (d, *J* = 4.1, 1H), 2.30 (ddd, *J* = 15.3, 6.9, 3.2, 1H), 2.16 (dt, *J* = 14.9, 2.9, 1H), 2.13 (d, *J* = 15.3, 1H), 1.62 (d, *J* = 6.9, 3H), 1.55 (dt, *J* = 14.9, 3.8, 1H); ^{13}C NMR (125 MHz, $CDCl_3$): δ 203.7, 148.7, 134.0, 133.9, 131.7, 131.5, 131.3, 124.3, 122.4, 68.0, 53.8, 49.1, 48.6, 27.2, 25.5, 20.5, 13.2; IR (film): 3516, 2926, 2854, 1716, 1542, 1467, 1440, 1373, 1352, 1165, 1127, 1102, 1078, 1066 cm^{-1}; HRMS–APCI (*m/z*) $[M + H]^+$ calcd for $C_{17}H_{21}N_2O_6S^+$, 381.11148; found 381.11041.

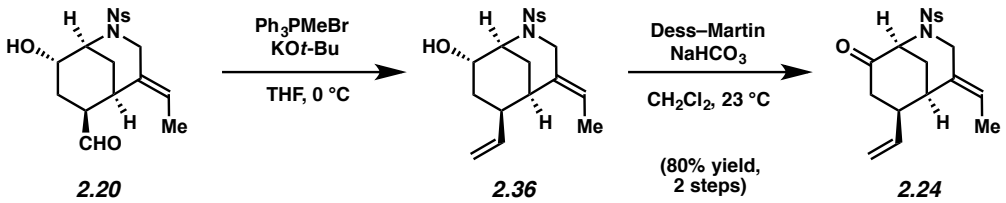

Vinyl Ketone 2.24. In a glovebox, a dram vial was charged with KO*t*-Bu (125 mg, 1.10 mmol). The vial was removed from the glovebox and placed under N_2 pressure. To a suspension of methyltriphenylphosphonium bromide (417 mg, 1.16 mmol) in THF (2 mL) at 0 °C was added a solution of the KO*t*-Bu in THF (2 mL) dropwise over 1 min. The mixture was stirred at 0 C° for 30 min, at which point a solution of aldehyde **2.20** (200 mg, 0.526 mmol) in THF (8 mL) was added dropwise over 1 min. After 10 min of stirring at 0 °C, the reaction was quenched with acetone (6 mL) and deionized water (6 mL). The resulting mixture was diluted with EtOAc (50 mL). The layers were separated and the aqueous layer was extracted with EtOAc (2 x 50 mL). The organic layers were combined and dried over $MgSO_4$. Evaporation of the solvent under reduced pressure afforded vinyl alcohol **2.36**, which was used in the subsequent step without further purification.

To a solution of crude vinyl alcohol **2.36** and $NaHCO_3$ (420 mg, 4.96 mmol) in CH_2Cl_2 (5 mL) was added Dess–Martin Periodinane (631 mg, 1.49 mmol). After stirring for 1.5 h, the reaction mixture was quenched with a solution of sat. aq. $NaHCO_3$ (10 mL) and diluted with CH_2Cl_2 (65 mL). The layers were separated and the aqueous layer was extracted with CH_2Cl_2 (2 x 65 mL). The organic layers were combined, dried over $MgSO_4$, and evaporated under reduced pressure. The resulting residue was purified via flash chromatography (1.5:1 hexanes:EtOAc) to afford vinyl ketone **2.24** (159 mg, 80% yield, two steps) as a white solid. Vinyl ketone **2.24**: mp: 159–161 °C; R_f 0.47 (1:1 hexanes:EtOAc); ^{1}H NMR (500 MHz, $CDCl_3$): 8.08–8.06 (m, 1H), 7.76–7.68 (m, 2H), 7.64–7.62 (m, 1H), 5.75–5.66 (m, 2H), 5.07–5.02 (m, 2H), 4.26–4.17 (m, 3H), 3.07

(q, J = 3.6, 1H), 2.78 (dd, J = 12.2, 6.4, 1H), 2.54 (dd, J = 15.7, 12.4, 1H), 2.46 (dd, J = 15.7, 6.4, 1H), 2.20 (dt, J = 14.0, 3.6, 1H), 2.03 (dt, J = 14.0, 2.9, 1H), 1.63 (dq, J = 6.9, 1, 3H); ^{13}C NMR (125 MHz, $CDCl_3$): δ 205.7, 148.1, 139.2, 134.1, 132.23, 132.20, 131.9, 130.2, 124.3, 124.0, 115.6, 58.7, 49.6, 46.6, 43.9, 33.6, 33.0, 13.5; IR (film): 2921, 2851, 1721, 1633, 1542, 1370, 1166 cm^{-1}; HRMS–APCI (m/z) $[M + H]^+$ calcd for $C_{18}H_{21}N_2O_5S^+$, 377.1166; found 377.11588.

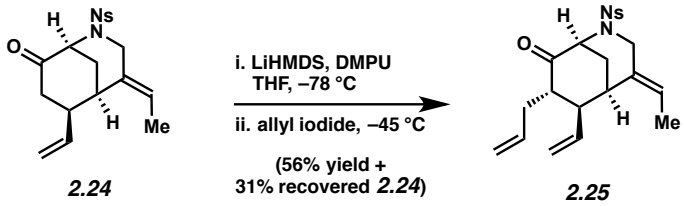

Allyl–vinyl Ketone 2.25. In a glovebox, a dram vial was charged with LiHMDS (129 mg, 0.77 mmol). The vial was removed from the glovebox, placed under N_2 pressure, and THF was added (4 mL). To a solution of ketone **2.24** (288 mg, 0.77 mmol) in THF (4 mL) at –78 ºC was added the solution of LiHMDS dropwise over 1 min. The resulting mixture was stirred for 20 min at –78 ºC, at which point DMPU (2 mL) was added. After 15 min of additional stirring at –78 ºC, a solution of allyl iodide (210 µL, 2.30 mmol) in THF (3 mL) was added and the reaction was subsequently warmed to –45 ºC. Following 1 h, an additional solution of allyl iodide (210 µL, 2.30 mmol) in THF (3 mL) was added at –45 ºC. Following 2 h, an additional solution of allyl iodide (210 µL, 2.30 mmol) in THF (3 mL) was added at –45 ºC. After 1 further h, the reaction was quenched with a solution of sat. aq. NH_4Cl (9 mL) and warmed to room temperature. The resulting mixture was poured into deionized water (6 mL) and diluted with EtOAc (75 mL). The layers were separated and the aqueous layer was extracted with EtOAc (2 x 75 mL). The organic layers were combined, dried over $MgSO_4$, and evaporated under reduced pressure. The resulting residue was purified via flash chromatography (4:1 hexanes:EtOAc → 1:1.5 hexanes:EtOAc) to afford recovered vinyl–

ketone **2.24** (88 mg, 31% yield) and allyl–vinyl ketone **2.25** (179 mg, 56% yield) as a clear oil. Allyl–vinyl ketone **2.25**: R_f 0.64 (1:1 hexanes:EtOAc); ^{1}H NMR (500 MHz, $CDCl_3$): 8.07–8.02 (m, 1H), 7.72–7.67 (m, 2H), 7.64–7.59 (m, 1H), 5.69 (q, *J* = 7.0, 1H) 5.65–5.52 (m, 2H), 5.12–5.07 (m, 2H), 4.92–4.86 (m, 2H), 4.31 (dt, *J* = 15.1, 1.9, 1H), 4.26 (dt, *J* = 15.1, 1.2, 1H) 4.23 (dd, *J* = 4.0, 2.8, 1H), 3.05 (q, *J* = 3.4, 1H), 2.60 (ddd, *J* = 11.4, 7.1, 3.5, 1H), 2.46 (ddd, *J* = 12.7, 9.3, 4.6, 1H), 2.26–2.18 (m, 2H), 2.16 (ddd, *J* = 13.9, 4.0, 3.1, 1H), 2.00 (dt, *J* = 13.9, 3.1, 1H), 1.61 (dt, *J* = 7.0, 1.2, 3H); ^{13}C NMR (125 MHz, $CDCl_3$): δ 206.9, 148.1, 138.8, 135.6, 134.0, 132.3, 132.1, 132.0, 130.4, 124.3, 123.9, 117.5, 116.8, 59.7, 52.4, 50.5, 49.4, 34.1, 33.9, 30.9, 13.6; IR (film): 2922, 1718, 1542, 1358, 1166 cm^{-1}; HRMS–APCI (*m/z*) $[M + H]^+$ calcd for $C_{21}H_{25}N_2O_5S^+$, 417.14787; found 417.14670.

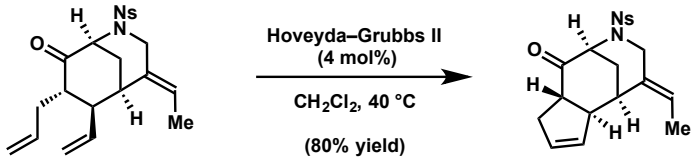

2.25 ***2.5***

Cyclopentene 2.5. In a glovebox, a dram vial was charged with Hoveyda–Grubbs second generation catalyst (9.8 mg, 0.016 mmol). The vial was removed from the glovebox, placed under N_2 pressure, and CH_2Cl_2 (1 mL) was added. A solution of allyl vinyl ketone **2.25** (93 mg, 0.22 mmol) in CH_2Cl_2 (10 ml) was added to the solution of Hoveyda–Grubbs second generation catalyst. The resulting mixture was heated to 40 °C. After 24 h, the reaction was cooled to room temperature and directly purified by flash chromatography (1:5:1 hexanes:EtOAc) to afford cyclopentene **2.5** (69 mg, 80% yield) as a white solid. Cyclopentene **2.5**: mp: 144–147 °C; R_f 0.37 (1:1 hexanes:EtOAc); ^{1}H NMR (500 MHz, $CDCl_3$): 8.04–8.00 (m, 1H), 7.73–7.68 (m, 2H), 7.66–7.64 (m, 1H), 5.83–5.81 (m, 1H), 5.77–5.73 (m, 2H), 4.41 (d, *J* = 15.0, 1H), 4.09 (ddd, *J* = 15.0,

2.4, 1.2, 1H), 4.04 (dd, J = 4.1, 2.4, 1H), 3.53 (ddd, J = 17.5, 10.8, 6.8, 1H), 3.38 (br. s, 1H), 2.72–2.68 (m, 1H), 2.47–2.43 (m, 1H), 2.42–2.37 (m, 1H), 2.05–2.00 (m, 1H), 1.94 (dt, 14.3, 2.7, 1H), 1.69 (dd, 7.1, 2.4, 3H); ^{13}C NMR (125 MHz, $CDCl_3$): δ 207.9, 148.0, 134.0, 132.5, 132.02, 132.00, 131.9, 131.7, 131.5, 124.6, 124.3 61.0, 60.3, 50.5, 48.4, 34.9, 31.6, 29.0, 14.9; IR (film): 2923, 2854, 1733, 1543, 373, 1166 cm^{-1}; HRMS–APCI (m/z) $[M + H]^+$ calcd for $C_{19}H_{21}N_2O_5S^+$, 389.11657; found 389.11773.

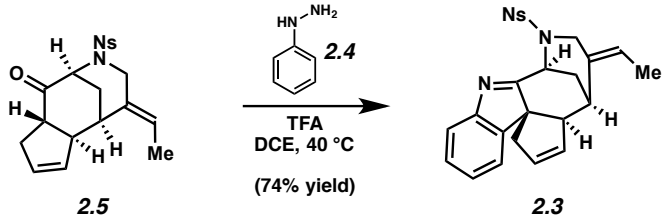

Indolenine 2.3. To a solution of cyclopentene **2.5** (6 mg, 0.015 mmol) in DCE (0.40 mL) was added phenylhydrazine (**2.4**) (4.6 µL, 0.046 mmol), followed by TFA (9.5 µL, 0.124 mmol). The reaction was heated to 40 °C. After 2.5 h, the reaction was cooled to room temperature and quenched with a solution of sat. aq. $NaHCO_3$ (10 mL). The resulting mixture was diluted with EtOAc (10 mL). The layers were separated and the aqueous layer was extracted with EtOAc (2 x 10 mL). The organic layers were combined, dried over $MgSO_4$, and evaporated under reduced pressure. The resulting residue was purified by flash chromatography (2:1 hexanes:EtOAc → 1:2 hexanes:EtOAc) to afford indolenine **2.3** (5.3 mg, 74% yield) as a brown solid. Indolenine **2.3**: mp: 98–101 °C; R_f 0.48 (3:1 EtOAc:hexanes); ^{1}H NMR (500 MHz, $CDCl_3$): δ 8.19–8.17 (m, 1H), 7.69–7.65 (m, 2H), 7.62–7.60 (m, 2H), 7.36 (d, J = 7.5, 1H), 7.31 (dt, J = 7.6, 1.0, 1H), 7.13 (dt, J = 7.5, 1.0, 1H), 6.05–6.03 (m, 1H), 5.96–5.94 (m, 1H), 5.62 (q, J = 6.2, 1H), 5.07 (dd, J = 4.4, 2.0, 1H), 4.29 (d, J = 15.2, 1H), 4.09 (dt, J = 15.2, 2, 1H), 3.10 (dq, J = 17.0, 2.4, 1H), 3.02 (m, 2H), 2.48 (ddd, J = 14.0, 4.4, 3, 1H), 2.17 (dd, J = 17.0, 2.4, 1H), 1.87 (dt, J = 14.0, 2.4, 1H), 1.61 (d,

J = 6.2, 3H); ^{13}C NMR (125 MHz, $CDCl_3$): δ 185.6, 152.8, 148.4, 148.3, 133.9, 132.7, 132.3 132.1, 131.8 (2 carbons), 131.7, 128.0, 126.2, 124.2, 123.3, 120.89, 120.87, 62.2, 60.2, 54.7, 48.0, 40.7, 36.4, 31.6, 15.0; IR (film): 2920, 2851, 1544, 1440, 1358, 1169 cm^{-1}; HRMS–APCI (m/z) $[M + H]^+$ calcd for $C_{25}H_{24}N_3O_4S^+$, 462.1482, found 462.14698.

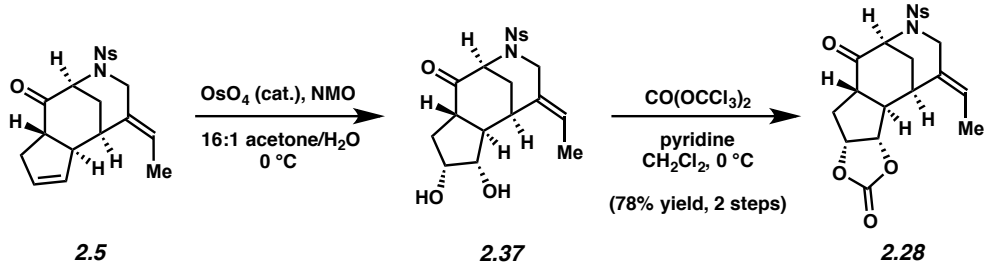

Carbonate 2.28. To a solution of cyclopentene **2.5** (27.2 mg, 0.070 mmol) in 16:1 acetone:H_2O (0.58 mL) was added a solution of NMO (8.6 mg, 0.0073 mmol) in acetone (0.82 mL). The solution was cooled to 0 ºC. After stirring for 5 min, a solution of OsO_4 in water (45 μL of a 20 mg /1 mL solution, 0.0036 mmol) was added. The reaction was stirred at 0 ºC for one additional hour before being warmed to room temperature. After 4 h, the reaction mixture was poured into deionized water (10 mL) and brine (5 mL) and the resulting mixture was diluted with EtOAc (15 mL). The layers were separated and the aqueous layer was extracted with EtOAc (2 x 15 mL). The organic layers were combined and dried over $MgSO_4$. Evaporation of the solvent under reduced pressure afforded diol **2.37**, which was used in the subsequent step without further purification.

To a solution of crude diol **2.37** (23 mg, 0.054 mmol) in CH_2Cl_2 (2.0 mL) and pyridine (0.20 mL) was added a solution of triphosgene (15.3 mg, 0.051 mmol) in CH_2Cl_2 (0.5 mL) dropwise. After stirring for 10 min, the volatiles were removed under reduced pressure and the resulting residue was purified by flash chromatography (1:1 hexanes:EtOAc → 100% EtOAc) to afford carbonate **2.28** (24.5 mg, 78% yield, two steps) as a brown solid. Carbonate **2.28**: mp: 121–

124 °C; R_f 0.23 (3:1 EtOAc:hexanes); ^{1}H NMR (500 MHz, $CDCl_3$): 8.06 (dd, *J* = 7.3, 2, 1H) 7.74 (m, 2H), 7.68 (dd, *J* = 7.3, 2, 1H), 5.69 (q, *J* = 6.7, 1H), 5.11 (dd, *J* = 6, 3.6, 1H), 5.07 (t, *J* = 6.0, 1H), 4.40 (dt, 15.5, 1.6, 1H), 4.25 (dd, *J* = 4.2, 2.4, 1H), 4.11 (dt, *J* = 15.5, 1.4, 1H), 3.41–3.38 (m, 2H), 2.26 (ddd, *J* = 14.1, 4.2, 3, 1H), 2.13 (dd, *J* = 15.1, 5.8, 1H), 2.00 (m, 1H), 1.94 (dt, *J* = 14.1, 3, 1H), 1.81 (dt, *J* = 14.0, 3.6, 1H), 1.73 (dt, *J* = 6.7, 1.4, 3H); ^{13}C NMR (125 MHz, $CDCl_3$): δ 205.3, 154.6, 148.1, 134.4, 132.3, 132.0, 131.5, 128.8, 125.1, 124.7, 81.3, 79.3, 59.9, 55.1, 48.5, 46.1, 35.9, 31.6, 29.5, 13.6; IR (film): 2923, 2851, 1799, 1730, 1543, 1373, 1167 cm^{-1}; HRMS–APCI (*m/z*) $[M + H]^+$ calcd for $C_{20}H_{21}N_2O_8S^+$, 449.10131, found 449.10056.

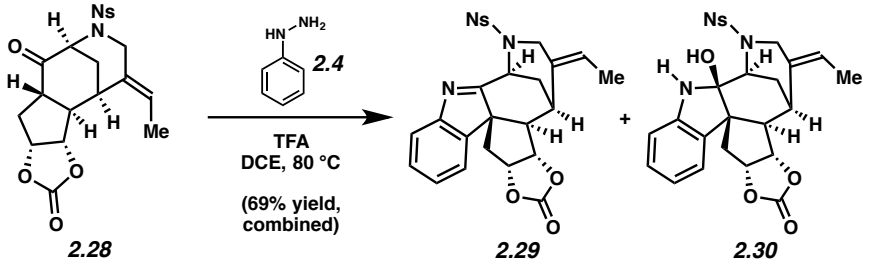

Indolenine 2.29 and Indoline 2.30. To a solution of carbonate **2.28** (14.7 mg, 0.033 mmol) in 1,2-DCE (1.1 mL) was added phenylhydrazine (**2.4**) (10 µL, 0.098 mmol), followed by TFA (20 µL, 0.26 mmol). The reaction was heated to 80 °C. After stirring for 2 h, the reaction mixture was cooled to room temperature and quenched with a solution of sat. aq. $NaHCO_3$ (15 mL). The resulting mixture was diluted with EtOAc (15 mL). The layers were separated and the aqueous layer was extracted with EtOAc (2 x 15 mL). The combined organic layers were dried over $MgSO_4$, filtered, and evaporated under reduced pressure. The resulting residue was purified via flash chromatography (2:1 hexanes:EtOAc → 1:2 hexanes:EtOAc) to afford indolenine **2.29** and indoline **2.30** (12.0 mg, 69% yield) as a red oil. Indolenine **2.29**: R_f 0.39 (3:1 EtOAc:hexanes); ^{1}H NMR (500 MHz, C_6D_6): 7.85 (dd, *J* = 7.9, 1.3, 1H), 7.69 (d, *J* = 7.7, 1H), 7.09 (dt, *J* = 7.7, 1.0,

1H), 6.89 (dt, *J* = 7.5, 1.0, 1H), 6.62 (dd, *J* = 7.9, 1.3, 1H), 6.57 (dt, *J* = 7.7, 1.3, 1H), 6.42 (dt, *J* = 7.7, 1.3, 1H), 6.24 (d, *J* = 7.5, 1H), 5.43 (dd, *J* = 4.2, 2.7, 1H), 5.29 (q, *J* = 7.0, 1H), 4.61 (dt, *J* = 15.5, 2.4, 1H), 4.38 (app. t, *J* = 8.8, 1H), 4.31–4.25 (m, 1H), 3.94 (dt, *J* = 15.5, 1.2, 1H), 2.78 (dd, *J* = 15.3 5.9, 1H), 2.55 (quin, *J* = 3.1, 1H), 1.79 (ddd, *J* = 13.8, 4.2, 3, 1H), 1.72 (dd, *J* = 7.0, 1.2, 3H), 1.53 (m, 2H), 1.31 (dt, *J* = 13.8, 3.1, 1H); ^{13}C NMR (23 of 26 observed, 125 MHz, C_6D_6): δ 183.0, 154.3, 153.8, 148.4, 146.5, 133.4, 132.4, 131.7, 130.8, 126.2, 123.9, 122.3, 120.9, 80.7, 80.4, 61.8, 54.4, 53.4, 48.8, 38.5, 36.8, 28.2, 13.9; IR (film): 2923, 2851, 1802, 1543, 1373, 1166 cm^{-1}; HRMS–ESI (*m/z*) $[M + Na]^+$ calcd for $C_{26}H_{23}N_3O_7SNa^+$, 544.1149; found 544.1160.

Indoline **2.30**: R_f 0.77 (3:1 EtOAc:hexanes); ^{1}H NMR (500 MHz, C_6D_6): 7.71 (dd, *J* = 7.9, 1.3, 1H), 7.06 (td, *J* = 7.6, 1.1, 1H), 6.68–6.61 (m, 3H), 6.45 (td, *J* = 7.7, 1.3, 1H), 6.38 (d, *J* = 7.6, 1H), 6.1 (d, *J* = 7.5, 1H), 5.35 (q, *J* = 7.7, 1H), 4.39–4.34 (m, 3H), 4.23 (t, *J* = 3.1, 1H), 3.80 (d, *J* = 15.4, 1H), 3.09 (s, br, 1H), 3.05 (s, br, *J* = 1H), 2.90 (dd, *J* = 16.0, 2.9, 1H), 2.49 (dd, *J* = 3.5, 3.0, 1H), 2.17 (m, 1H), 1.91 (dt, *J* = 13.4, 3.1, 1H), 1.76 (dt, *J* = 13.4, 3.5, 1H), 1.55–1.53 (m, 1H) 1.65 (dd, *J* = 7.7, 2.1, 3H); ^{13}C NMR (500 MHz, C_6D_6): δ 154.7, 147.8, 145.1, 138.7, 133.3, 133.2, 131.5, 131.2, 129.4, 129.1, 127.5, 124.1, 121.4, 119.5, 109.9, 94.2, 81.1, 80.3, 55.7, 55.3, 53.7, 50.5, 37.1, 32.3, 27.2, 13.4; IR (film): 3475, 3359, 1803, 1731, 1599, 1542, 1372, 1163 cm^{-1}; HRMS–ESI (*m/z*) $[M + Na]^+$ calcd for $C_{26}H_{25}N_3O_8SNa^+$, 562.1255; found 562.1262.

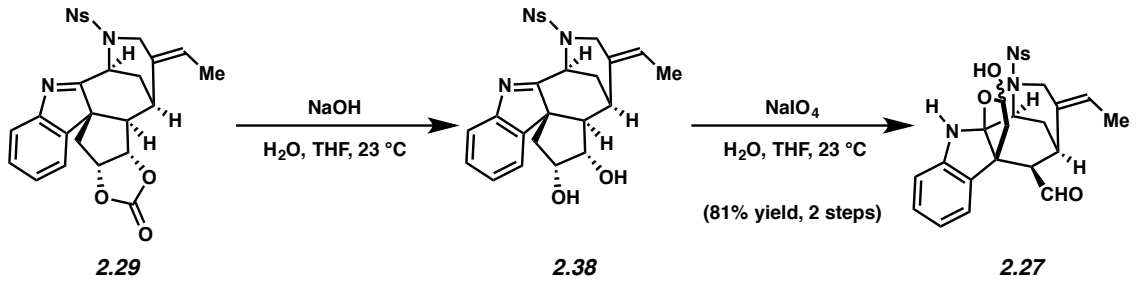

2.29 *2.38* *2.27*

Aldehyde 2.27. To a solution of indolenine **2.29** (9.0 mg, 0.017 mmol) in THF (0.17 mL) was added an aqueous solution of NaOH (0.5 N, 0.17 mL). After vigorous stirring for 45 min, the reaction mixture was poured into deionized water (10 mL) and the resulting mixture was diluted with EtOAc (10 mL). The layers were separated and the aqueous layer was extracted with EtOAc (2 x 10 mL). The organic layers were combined and dried over $MgSO_4$. Evaporation of the solvent under reduced pressure afforded diol **2.38**, which was used in the subsequent step without further purification.

To a solution of crude diol **2.38** in 1:1 THF:H_2O (0.34 mL) was added $NaIO_4$ (10.9 mg, 0.051 mmol). After stirring for 1.5 h, the reaction mixture was poured into deionized water (5 mL) and brine (5 mL), and the resulting mixture was diluted with EtOAc (10 mL). The layers were separated and the aqueous layer was extracted with EtOAc (2 x 10 mL). The organic layers were combined and dried over $MgSO_4$. The resulting residue was purified via flash chromatography (2:1 hexanes:EtOAc) to afford aldehyde **2.27** (7.1 mg, 81% yield) as an orange solid and as an inseparable mixture of diastereomers (2:1). These compounds were characterized as a mixture. **2.27 (major diastereomer)**: ^{1}H NMR (500 MHz, C_6D_6): 9.27 (d, J = 0.6, 1H), 7.85 (dd, J = 8.0, 1.3, 1H), 7.23 (d, J = 7.4, 1H), 6.96 (dd, J = 7.7, 1.2, 1H), 6.78–6.67 (m, 3H), 6.53 (dt, J = 7.7, 1.4, 1H), 6.30 (d, J = 7.7, 1H), 5.30–5.24 (m, 1H), 4.96 (q, J = 7.0, 1H), 4.58 (app. s, 1H), 4.04 (s, 1H), 3.74 (app. d, 1H), 3.61 (dt, J = 15.2, 2.2, 1H), 2.75 (d, J = 14.4, 1H), 2.68–2.65 (m, 1H), 2.35 (dd, J = 14.4, 5.6, 1H), 1.96 (app. d, 1H), 1.89 (dt, J = 13.5, 3.8, 1H), 1.66 (d, J = 8.5, 1H), 1.63

(dt, J = 13.6, 2.9, 1H), 1.16 (dd, J = 7.0, 1.7, 3H); **2.27 (minor diastereomer)**: ^{1}H NMR (500 MHz, C_6D_6): 9.29 (d, J = 1.1, 1H), 7.78 (dd, J = 8.0, 1.3, 1H), 7.02 (dd, J = 7.7, 1.2, 1H), 6.78–6.67 (m, 3H), 6.64 (dt, J = 7.7, 1.3, 1H), 6.49 (dt, J = 7.7, 1.4, 1H), 6.35 (d, J = 7.7, 1H), 5.30–5.24 (m, 1H), 4.85 (q, J = 7.0, 1H), 4.58 (app. s, 1H), 4.15 (dt, J = 15.4, 2.3, 1H), 3.74 (app. d, 1H), 3.71 (d, J = 8.1, 1H), 3.52 (d, J = 15.4, 1H), 3.03 (dd, J = 13.7, 4.9, 1H), 2.68–2.65 (m, 1H), 2.21 (dd, J = 13.7, 7.6, 1H), 2.00 (dd, J = 13.5, 3.8, 1H), 1.96 (app. d, 1H), 1.76 (dd, J = 13.7, 2.9, 1H), 1.14 (dd, J = 7.0, 1.6, 3H); Aldehyde **2.27** (**mixture**): mp: 145–148 °C; R_f 0.50 (1.5:1 EtOAc:hexanes); ^{13}C NMR (125 MHz, $CDCl_3$): δ 201.1, 200.9, 148.1 (2 carbons), 145.8, 144.8, 136.7, 135.8, 133.8, 133.6, 133.5, 133.0, 132.4, 132.0, 131.7, 131.5, 129.23, 129.15, 129.12, 128.9, 125.3, 125.1, 124.9, 124.6, 124.1, 123.8, 120.8, 120.5, 110.4, 110.1, 104.0, 101.2, 101.0, 99.0, 77.4, 77.2, 76.9, 62.6, 61.8, 54.0, 53.8, 52.0, 51.3, 48.3, 48.2, 43.9, 43.8, 30.4, 30.1, 28.0 (2 carbons), 13.7, 13.6; IR (film): 3371, 2925, 2851, 1721, 1542, 1468, 1370, 1263, 1162 cm^{-1}; HRMS–ESI (*m/z*) $[M + Na]^+$ calcd for $C_{25}H_{25}N_3O_7SNa^+$, 534.1311; found 534.1324.

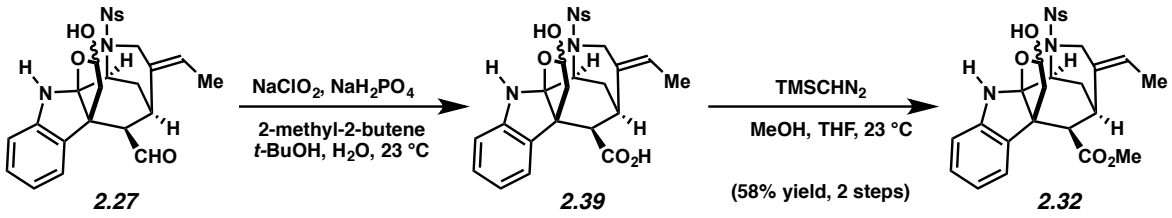

Ester 2.32. To a solution of aldehyde **2.27** (5.2 mg, 0.010 mmol) in *t*-BuOH (0.39 mL) and 2-methyl-2-butene (0.26 mL) at 0 °C was added a solution of sodium chlorite (5.1 mg, 0.056 mmol) and monobasic sodium phosphate (7.9 mg, 0.066 mmol) in H_2O (0.39 mL). The reaction was allowed to warm to room temperature while stirring. After vigorous stirring for 1 h, the reaction mixture was poured into deionized water (10 mL) and the resulting mixture was diluted with EtOAc (10 mL). The layers were separated and the aqueous layer was extracted with EtOAc (2 x

10 mL). The organic layers were combined and dried over $MgSO_4$. Evaporation of the solvent under reduced pressure afforded acid **2.39**, which was used in the subsequent step without further purification.

To a solution of crude acid **2.39** in 5:3 THF/MeOH (1.0 mL) was added $TMSCHN_2$ (20 μL of a 0.6 M solution in hexanes, 0.012 mmol). After stirring for 30 min, the reaction mixture was poured into deionized water (10 mL) and the resulting mixture was diluted with CH_2Cl_2 (10 mL). The layers were separated and the aqueous layer was extracted with CH_2Cl_2 (2 x 10 mL). The organic layers were combined and dried over $MgSO_4$. The resulting residue was purified via flash chromatography (2:1 hexanes:EtOAc) to afford ester **2.32** (3.2 mg, 58% yield) as a brown solid and as an inseparable mixture of diastereomers (1.5:1). These compounds were characterized as a mixture. **2.32** (**major diastereomer)**: ^{1}H NMR (26 of 27 observed, 500 MHz, $CDCl_3$): δ 8.11–8.07 (m, 1H), 7.74–7.72 (m, 1H), 7.70–7.64 (m, 2H), 7.16–7.08 (m, 2H), 6.81 (dt, *J* = 7.5, 0.7, 1H), 6.71 (d, *J* = 7.8, 1H), 5.55–5.46 (m, 1H), 5.29 (dd, *J* = 8.7, 5.5, 1H), 4.76 (s, 1H), 4.48–4.45 (m, 1H), 3.92 (dt, *J* = 15.2. 2.1 1H), 3.85 (d, *J* = 15.2, 1H), 3.70 (s, 3H), 3.34–3.28 (m, 1H), 3.07–3.00 (m, 1H), 2.79 (d, *J* = 4.5, 1H), 2.74 (d, *J* = 14.9, 1H), 2.23–2.13 (m, 1H), 2.11–2.08 (app. t, *J* = 3.3, 1H), 1.56 (app. d, 3H); **2.32 (minor diastereomer)**: ^{1}H NMR (26 of 27 observed, 500 MHz, $CDCl_3$): δ 8.18–8.15 (m, 1H), 7.74–7.72 (m, 1H), 7.70–7.64 (m, 2H), 7.16–7.08 (m, 2H), 6.79 (dt, *J* = 7.5, 0.7, 1H), 6.67 (d, *J* = 7.8, 1H), 5.55–5.46 (m, 1H), 5.17–5.12 (m, 1H), 4.59 (s, 1H), 4.48–4.45 (m, 1H), 4.29 (dt, *J* = 14.9. 2.0, 1H), 3.68 (s, 3H), 3.34–3.28 (m, 1H), 3.07–3.00 (m, 1H), 2.77 (d, *J* = 4.5, 1H), 2.54 (dd, *J* = 14.1, 7.8, 1H), 2.23–2.13 (m, 1H), 2.11–2.08 (app. t, *J* = 3.3, 1H), 1.86 (d, *J* = 9.0, 1H), 1.56 (app. s, 3H); Ester **2.32** (**mixture**): mp: 78–82 °C; R_f 0.51 (1.5:1 EtOAc:hexanes); ^{13}C NMR (125 MHz, $CDCl_3$): δ 172.02, 171.97, 148.2, 148.1, 145.9, 144.9, 136.8, 136.1, 133.8, 133.6, 133.5, 132.9, 132.6, 132.0, 131.69, 131.67, 129.1, 128.94, 128.90,

128.84, 125.8, 125.4, 124.9, 124.5, 123.4, 123.1, 120.7, 120.4, 110.7, 110.4, 103.9, 101.3, 101.1 99.0, 54.5, 54.1, 53.8, 52.7, 51.92, 51.89, 51.84, 48.2, 48.1, 43.8, 43.7, 30.8, 30.5, 29.9, 29.8, 13.02, 12.99; IR (film): 3497, 3365, 2917, 2850, 1737, 1542, 1441, 1364, 1261, 1162 cm^{-1}; HRMS–APCI (*m/z*) $[M + H]^+$ calcd for $C_{26}H_{28}N_3O_8SH^+$, 542.15916; found 542.15948.

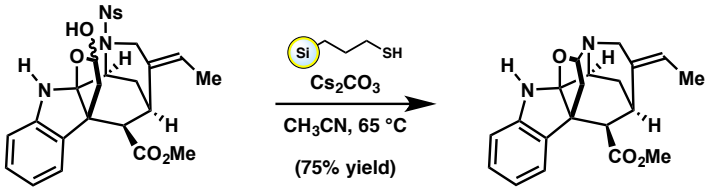

2.32 *Picrinine (2.1)*

Picrinine (**2.1**). To a suspension of ester **2.32** (6.3 mg, 0.012 mmol) and Cs_2CO_3 (11.4 mg, 0.035 mmol) in CH_3CN (0.39 mL) was added SiliaMetS® Thiol (35.0 mg, 0.047 mmol). The reaction was heated to 65 °C. After 1 h, the reaction was cooled to room temperature, and directly purified by flash chromatography (30:1 EtOAc:MeOH → 9:1 *i*-PrOH:CH_2Cl_2) to afford picrinine **2.1** (2.9 mg, 75% yield) as a white solid. Spectral data for ^{1}H NMR for synthetic **2.1** was consistent with literature reports[37] and a natural sample of **2.1** obtained from Prof. T.-S. Kam. Spectral data for ^{13}C NMR for synthetic **2.1** was consistent with literature reports.[37] Picrinine (**2.1**): ^{1}H NMR (500 MHz, $CDCl_3$): δ 7.14 (d, *J* = 7.5, 1H), 7.09 (dt, *J* = 7.7, 1.3, 1H), 6.79 (dt, *J* = 7.5, 1.0, 1H), 6.76 (d, *J* = 7.7, 1H), 5.40 (q, *J* = 7.0, 1H), 4.82 (d, *J* = 2.6, 1H), 4.72 (s, 1H), 3.76 (dt, *J* = 17.6, 2.5, 1H), 3.65 (s, 3H), 3.59 (d, *J* = 4.9, 1H), 3.42 (d, *J* = 13.7, 1H) 3.28 (app. d, *J* = 2.8, 1H), 3.09 (d, *J* = 17.0, 1H), 2.44 (d, *J* = 3.5, 1H), 2.26 (dd, *J* = 13.7, 2.6, 1H), 2.15 (ddd, *J* = 14.1, 4.9, 3.5, 1H), 1.86 (dd, *J* = 14.1, 2.8, 1H), 1.49 (dd, *J* = 7.0, 2.5, 3H). ^{13}C NMR (125 MHz, $CDCl_3$): δ 172.6, 147.7, 136.4, 135.4, 128.1, 125.3, 121.0, 120.5, 110.7, 106.4, 87.5, 52.1, 52.0, 51.6, 51.3, 46.5, 40.7, 31.2, 26.2, 12.9.

2.10 Spectra Relevant to Chapter Two:

The Fischer Indolization as a Strategic Platform for the Total Synthesis of Picrinine

Adapted from: Joel M. Smith, Jesus Moreno, Ben W. Boal, and Neil K. Garg

J. Am. Chem. Soc. **2014**, *136*, 4504–4507 and *J. Org. Chem.* **2015**, *80*, 8954–8967.

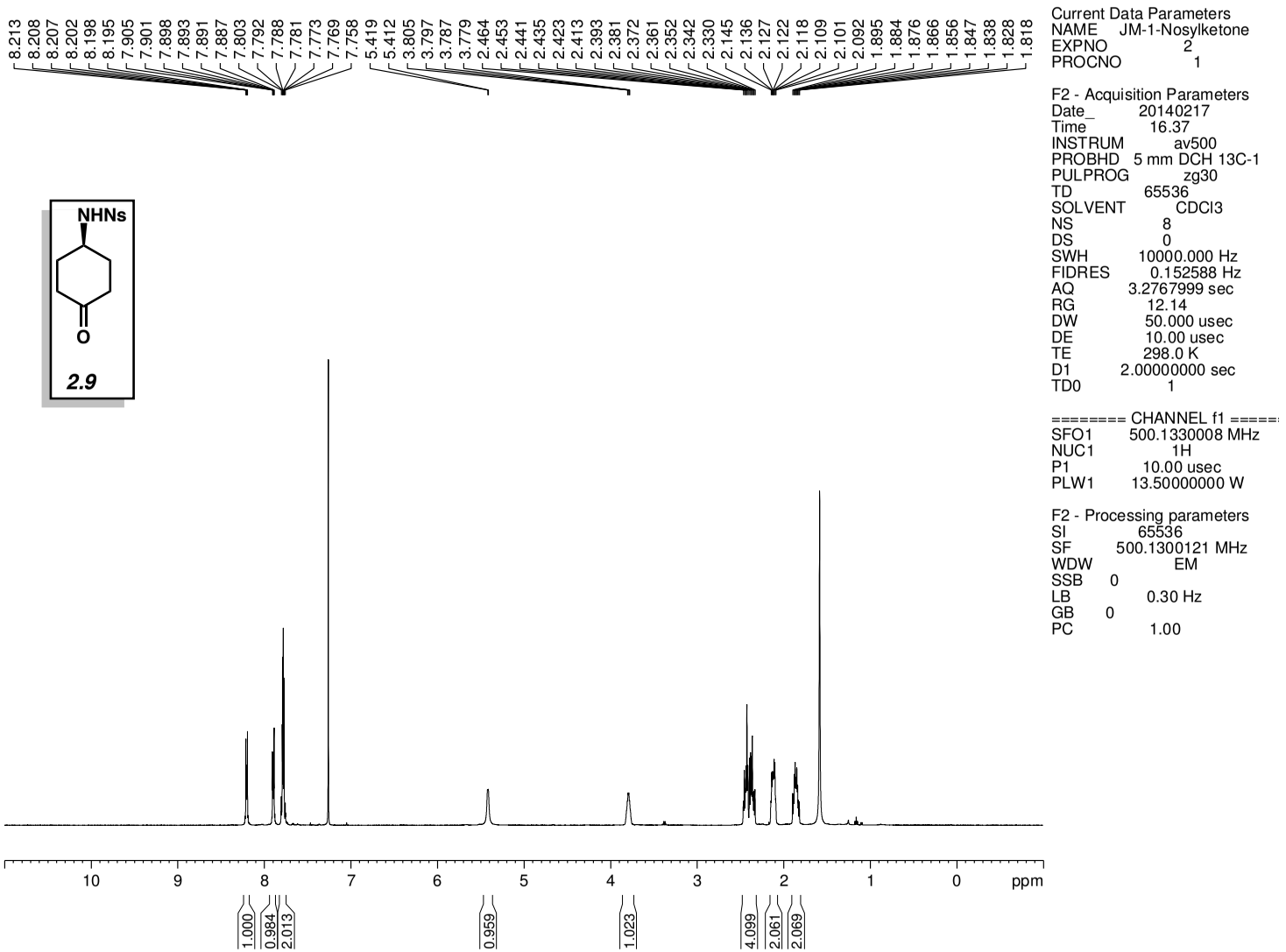

Figure 2.3 ^{1}H NMR (500 MHz, $CDCl_3$) of compound **2.9**.

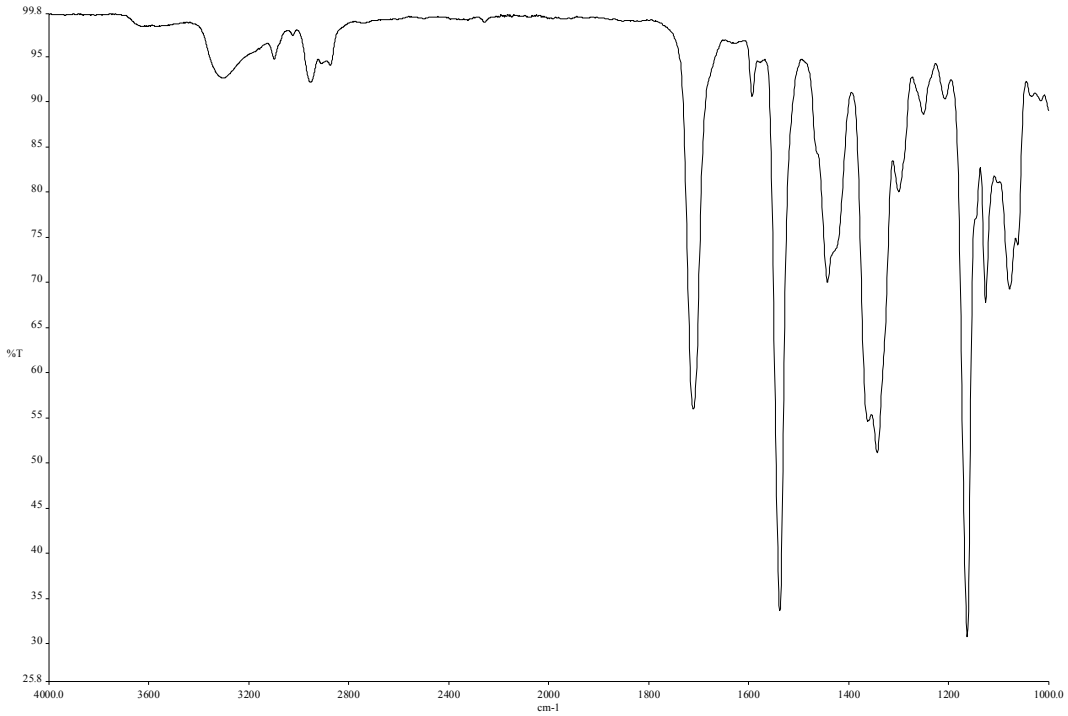

Figure 2.4 Infrared spectrum of compound **2.9**.

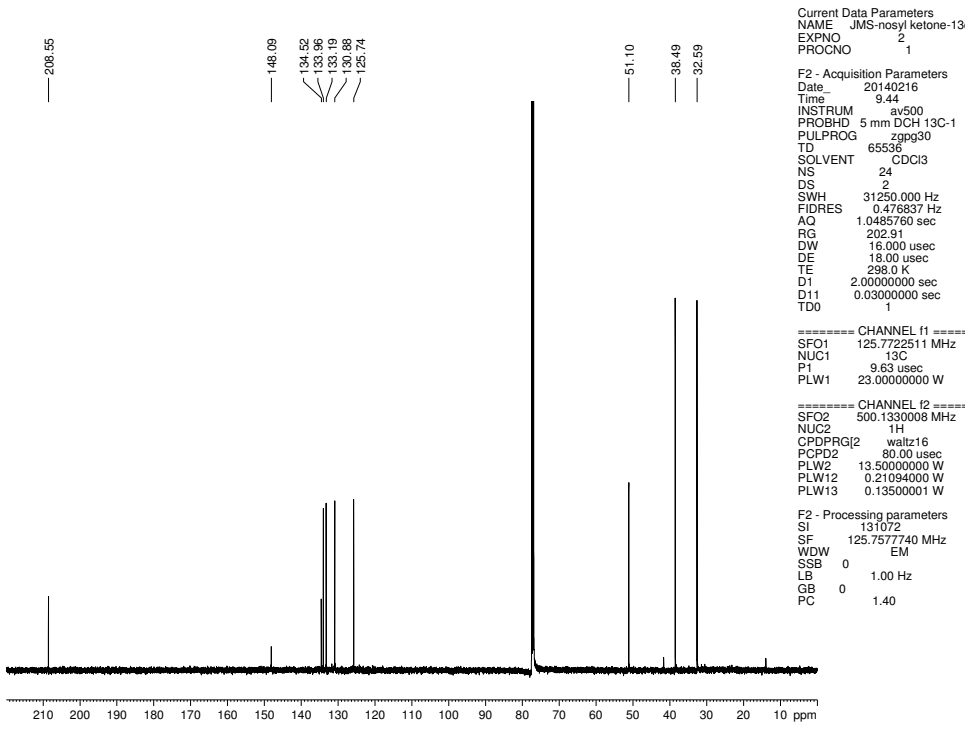

Figure 2.5 ^{13}C NMR (125 MHz, $CDCl_3$) of compound **2.9**.

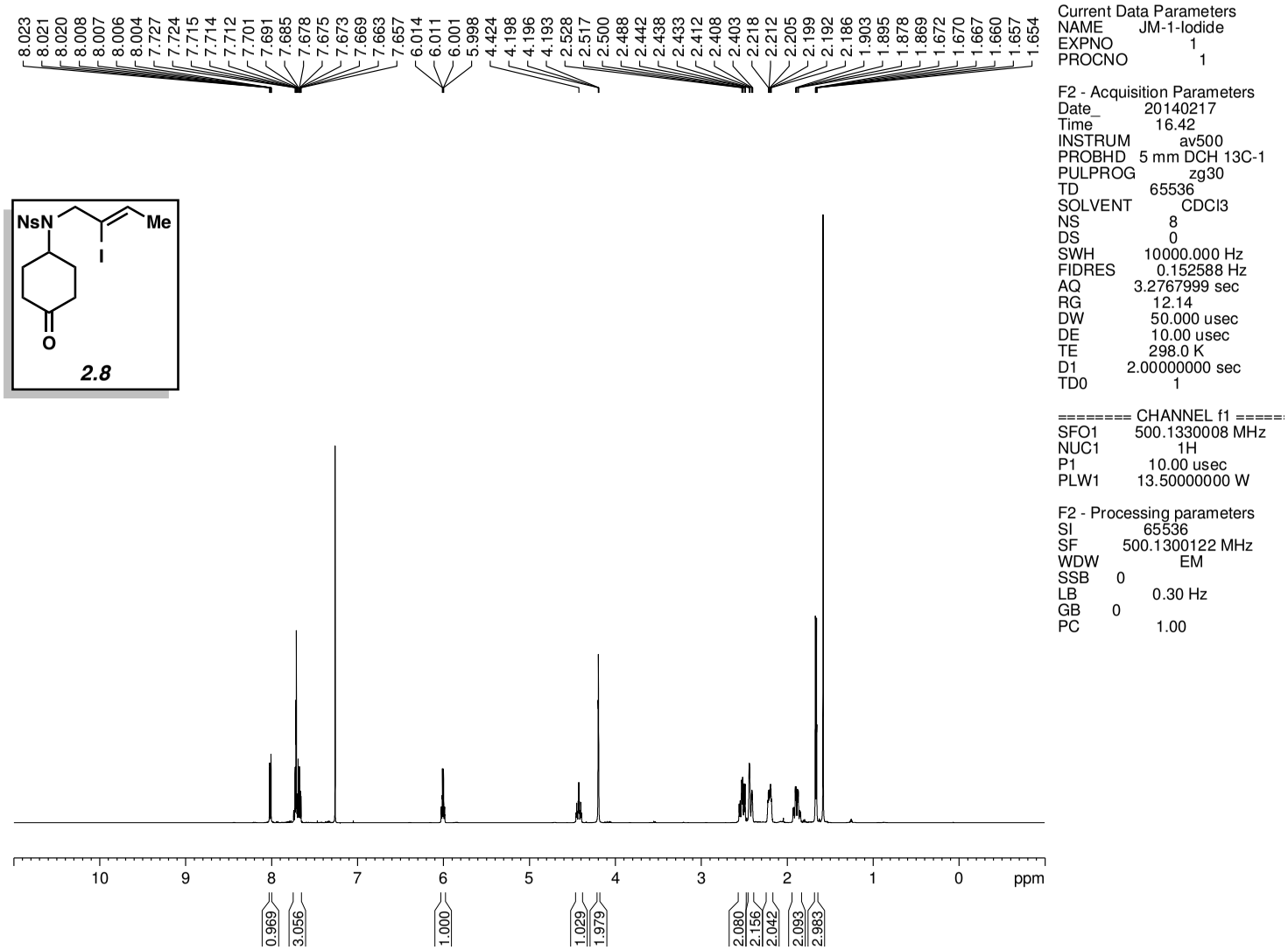

Figure 2.6 ^{1}H NMR (500 MHz, $CDCl_3$) of compound **2.8**.

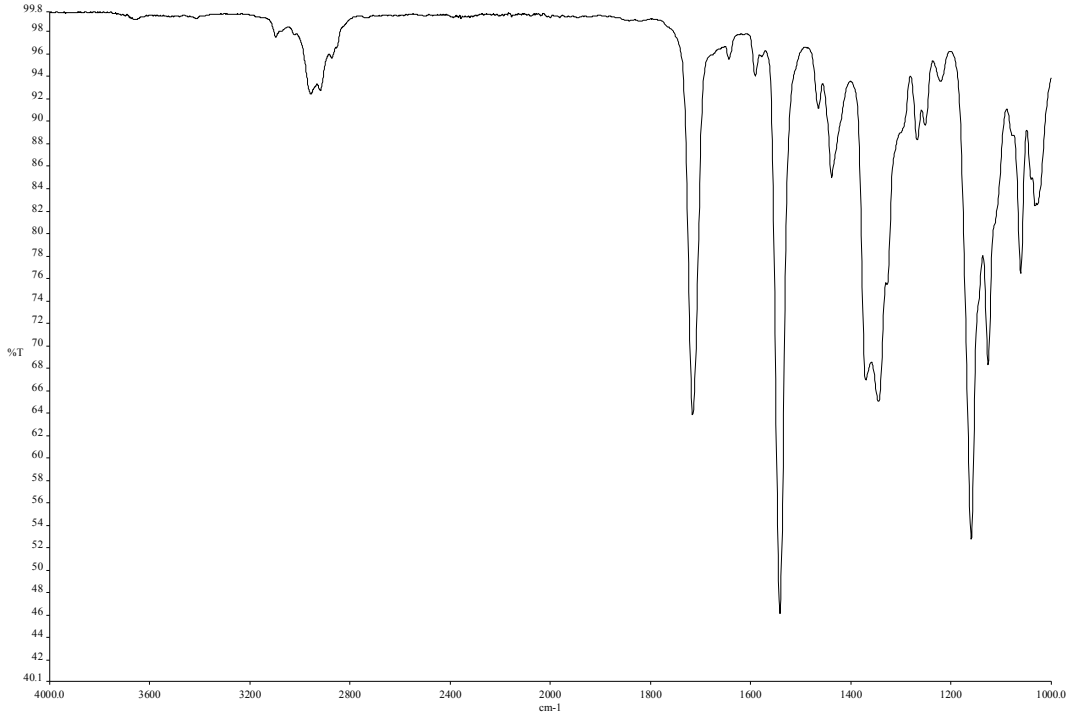

Figure 2.7 Infrared spectrum of compound **2.8**.

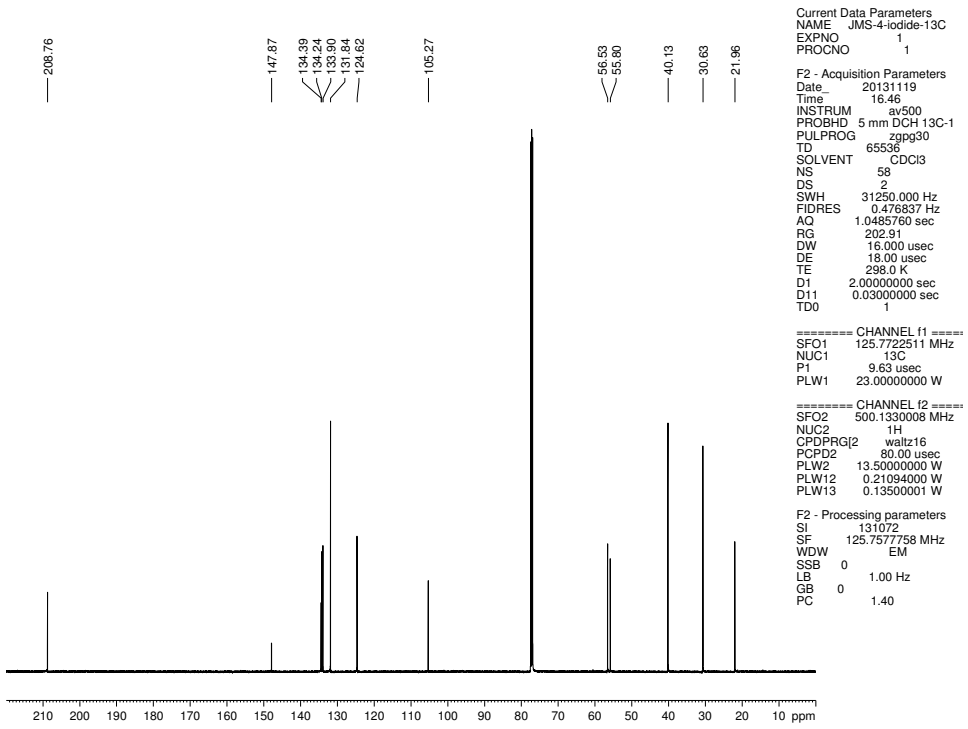

Figure 2.8 ^{13}C NMR (125 MHz, $CDCl_3$) of compound **2.8**.

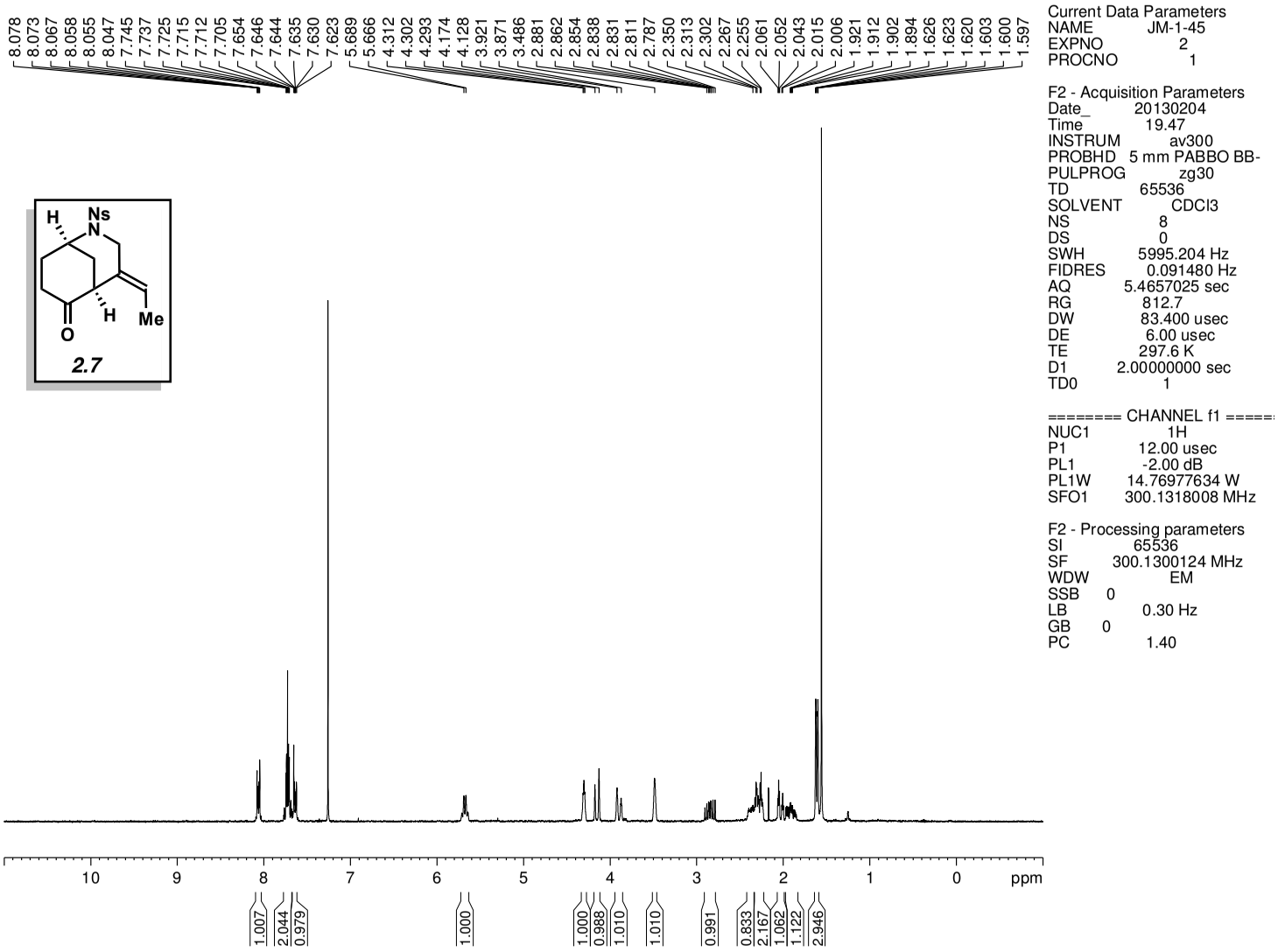

Figure 2.9 ^{1}H NMR (300 MHz, $CDCl_3$) of compound **2.7**.

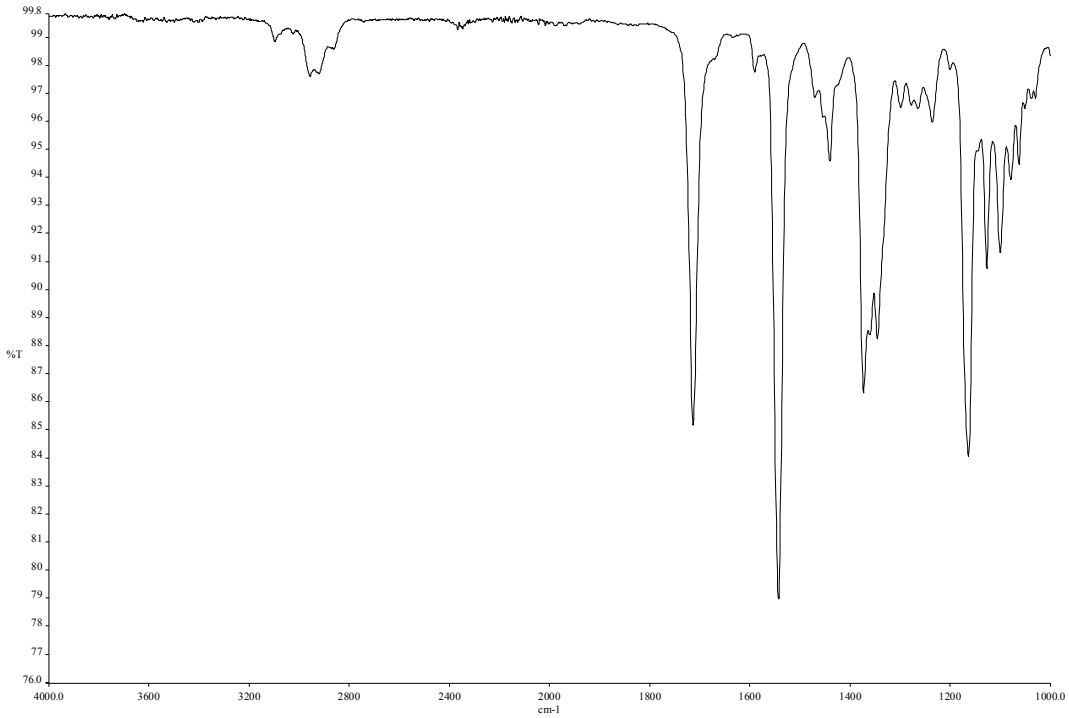

Figure 2.10 Infrared spectrum of compound **2.7**.

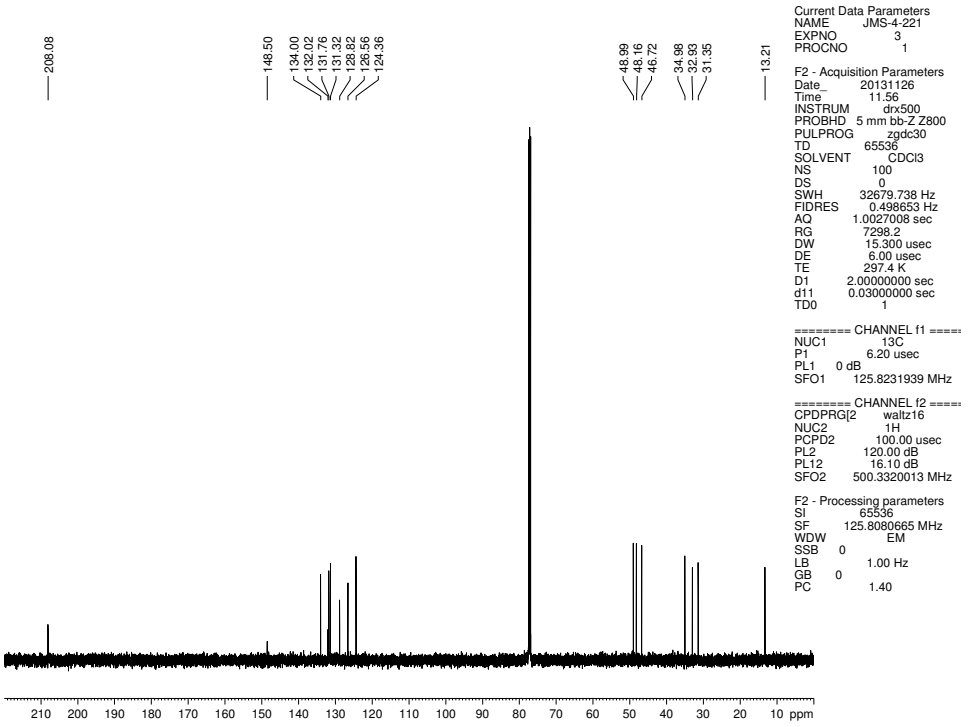

Figure 2.11 ^{13}C NMR (125 MHz, $CDCl_3$) of compound **2.7**.

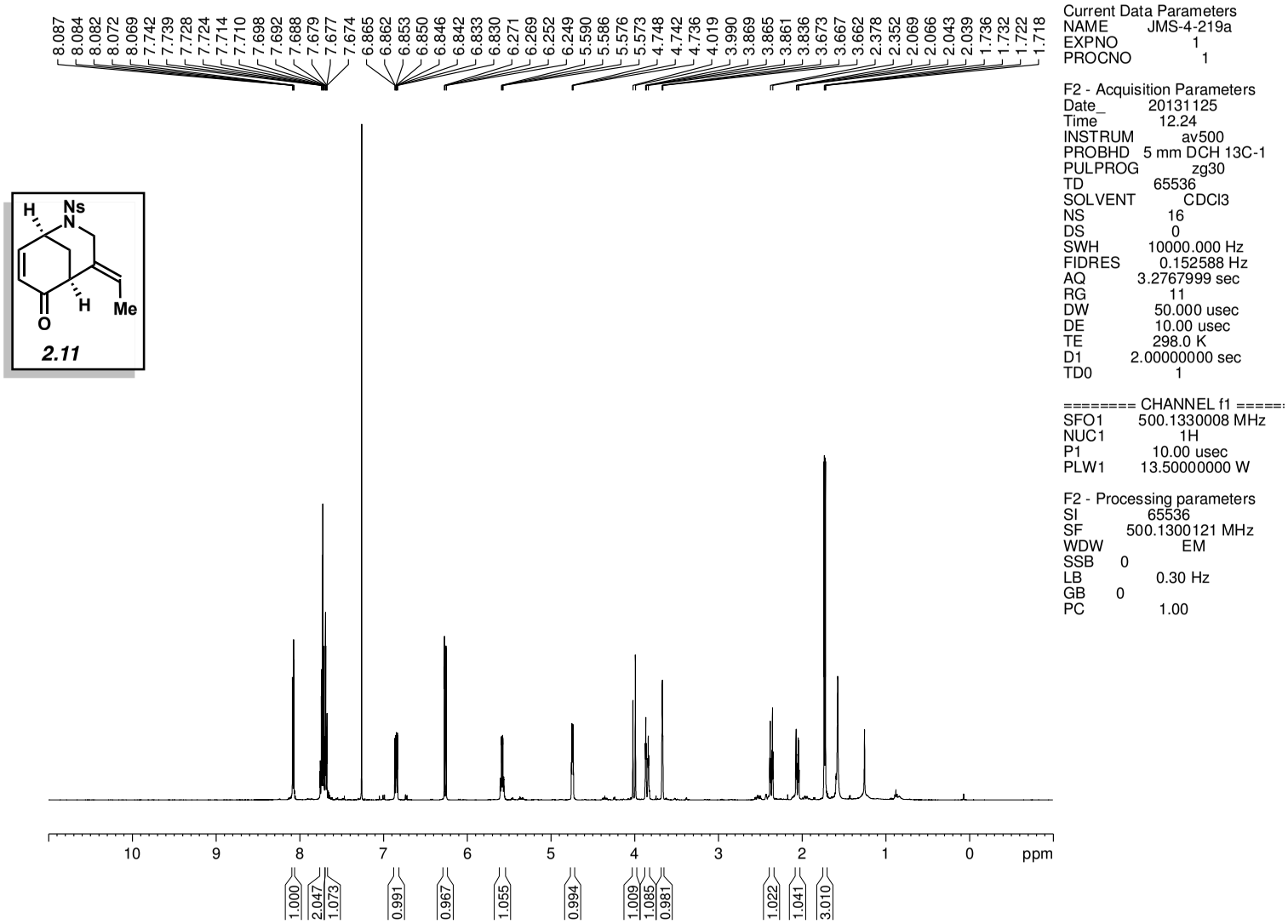

Figure 2.12 ^{1}H NMR (500 MHz, $CDCl_3$) of compound **2.11**.

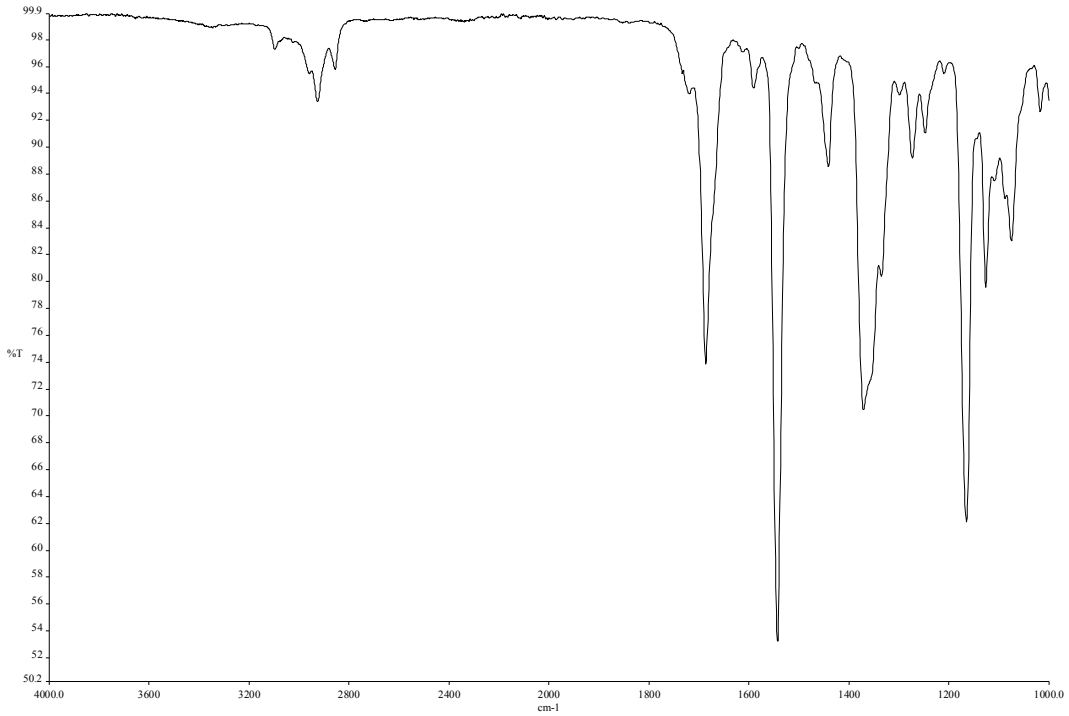

Figure 2.13 Infrared spectrum of compound **2.11**.

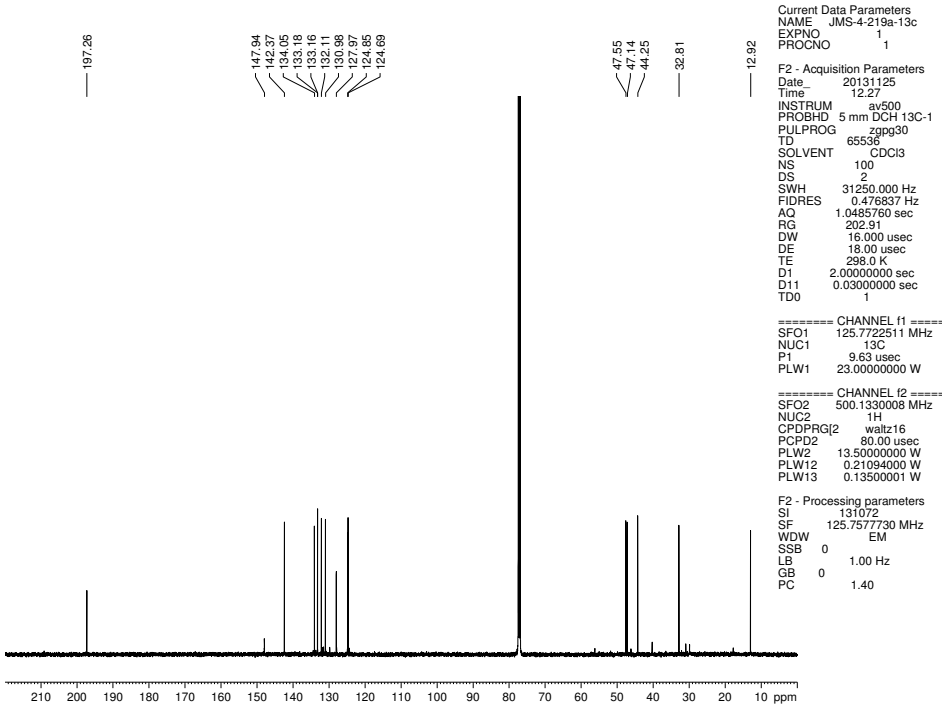

Figure 2.14 ^{13}C NMR (125 MHz, $CDCl_3$) of compound **2.11**.

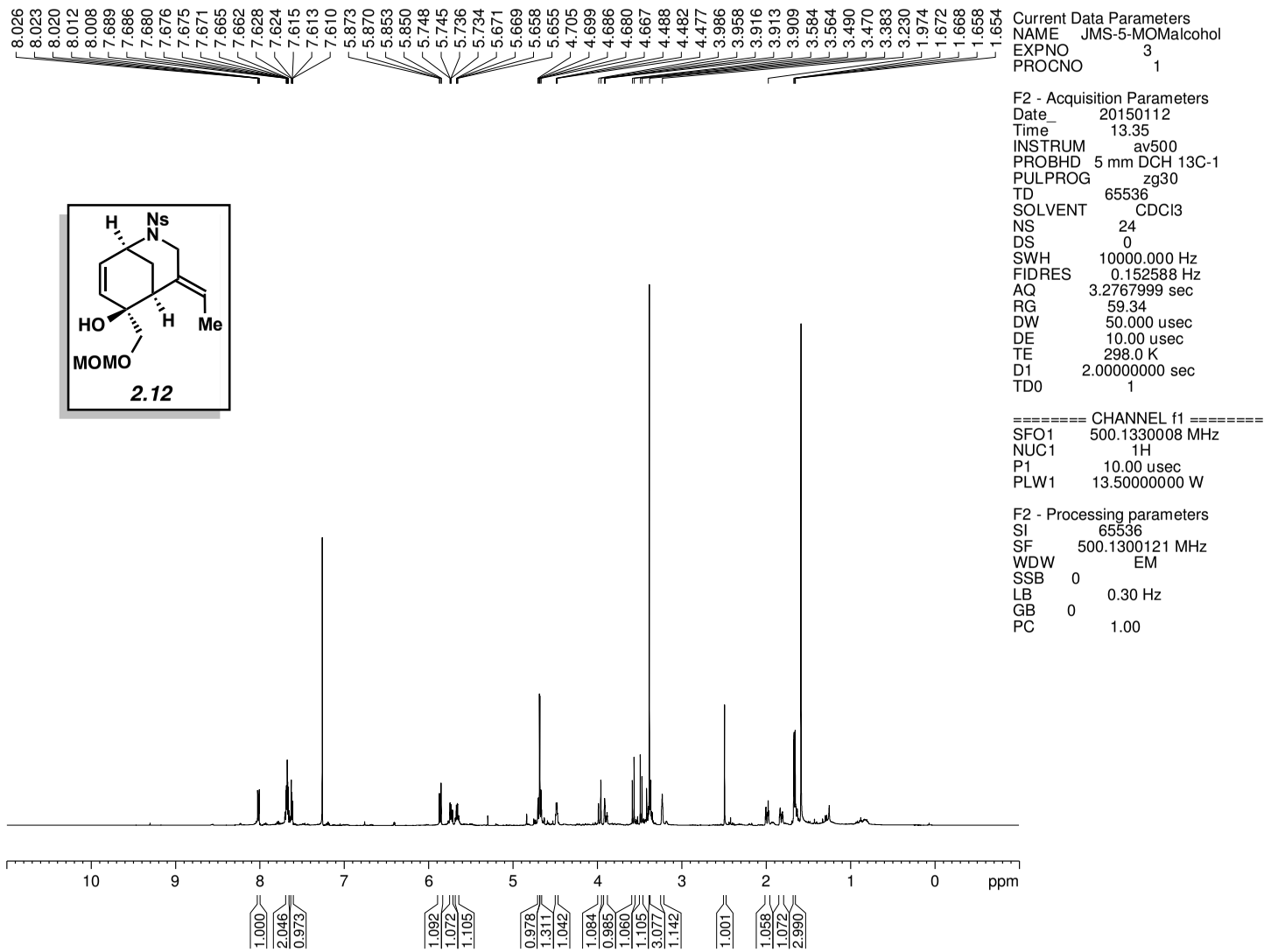

Figure 2.15 ^{1}H NMR (500 MHz, $CDCl_3$) of compound **2.12**.

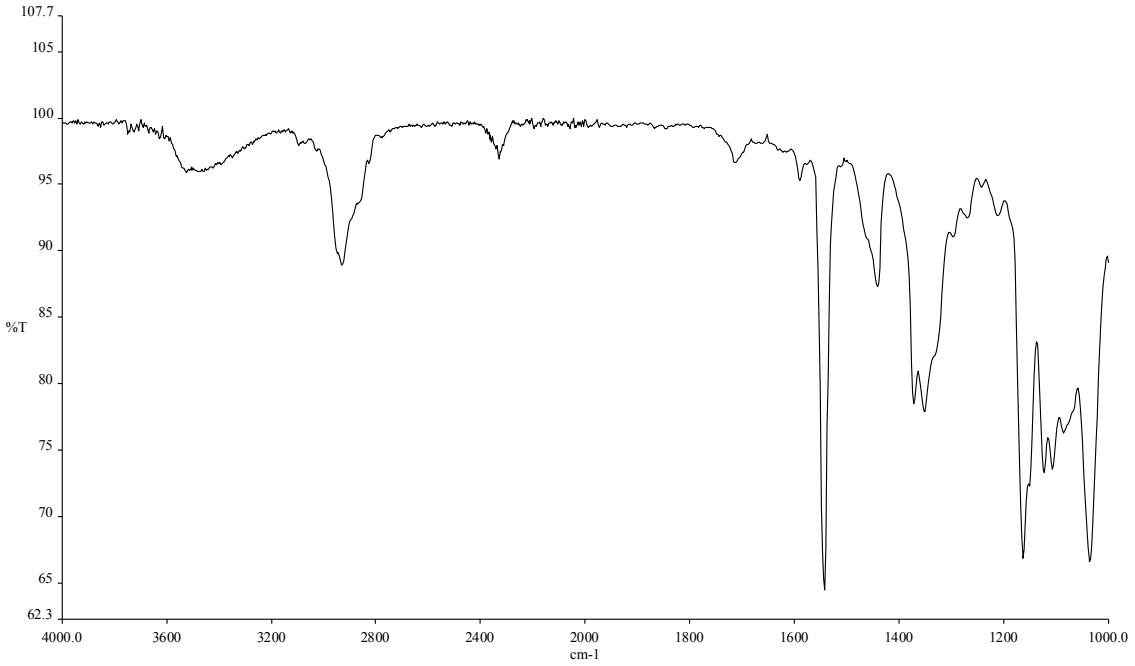

Figure 2.16 Infrared spectrum of compound **2.12**.

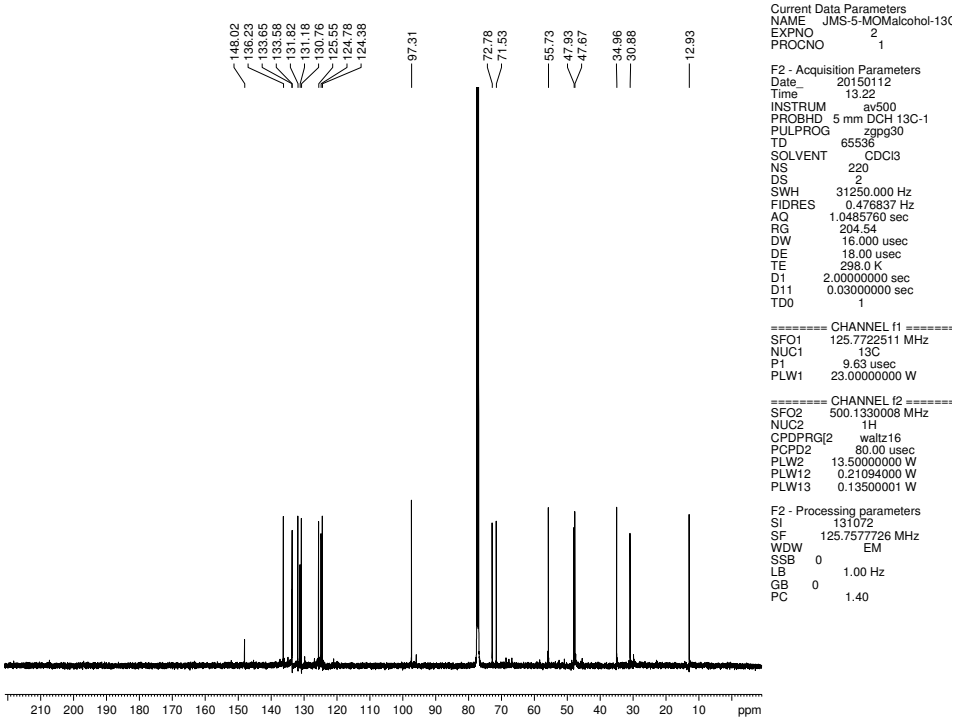

Figure 2.17 ^{13}C NMR (125 MHz, $CDCl_3$) of compound **2.12**.

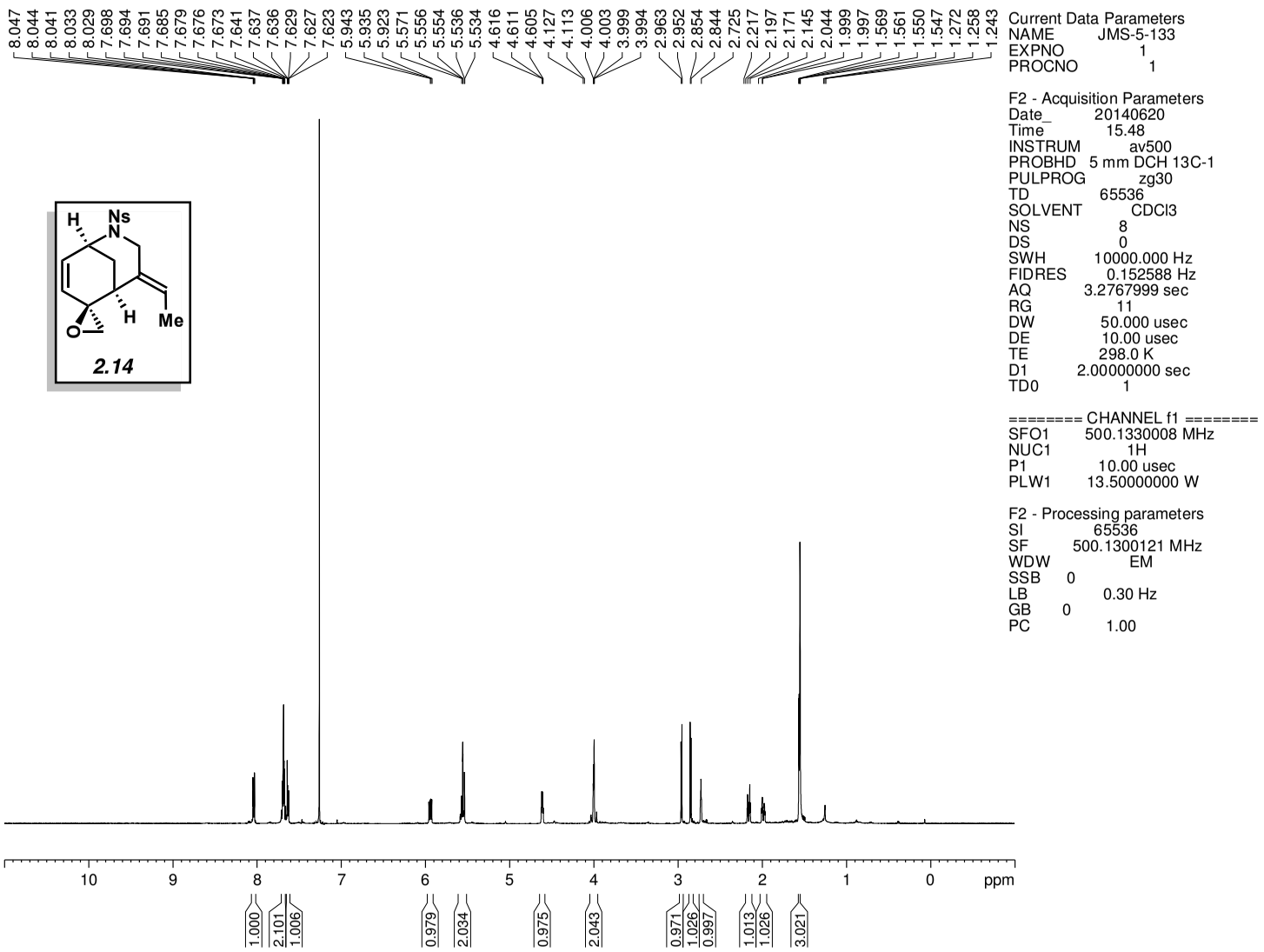

Figure 2.18 ^{1}H NMR (500 MHz, $CDCl_3$) of compound **2.14**.

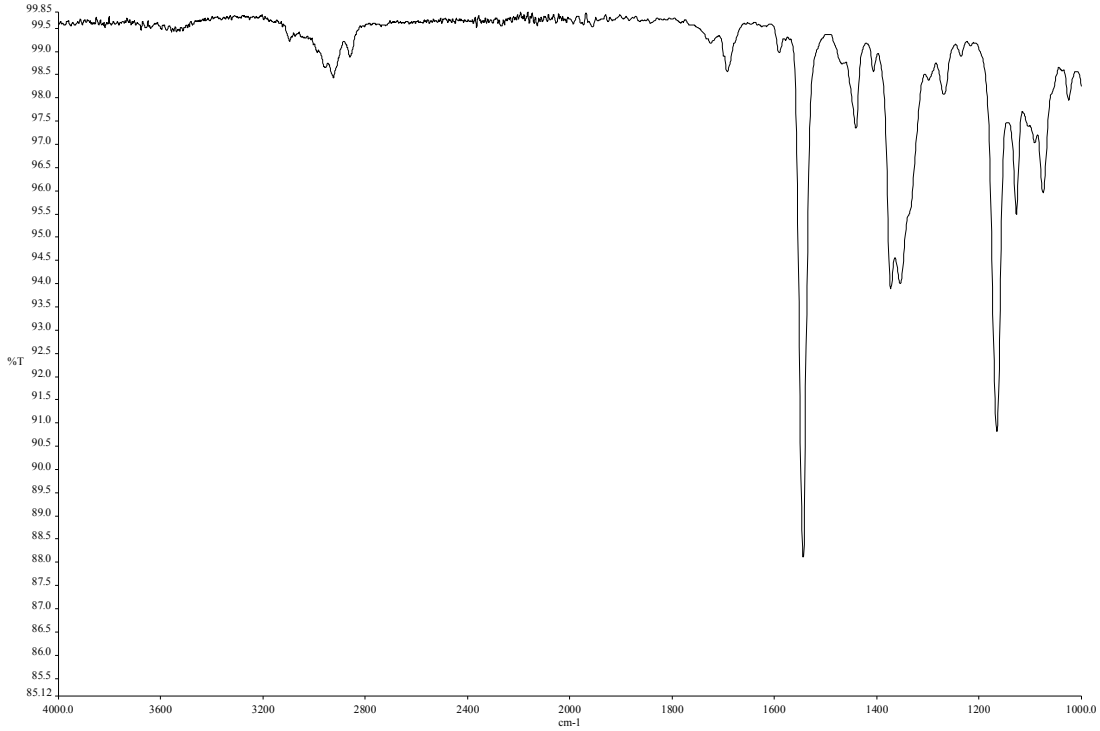

Figure 2.19 Infrared spectrum of compound **2.14**.

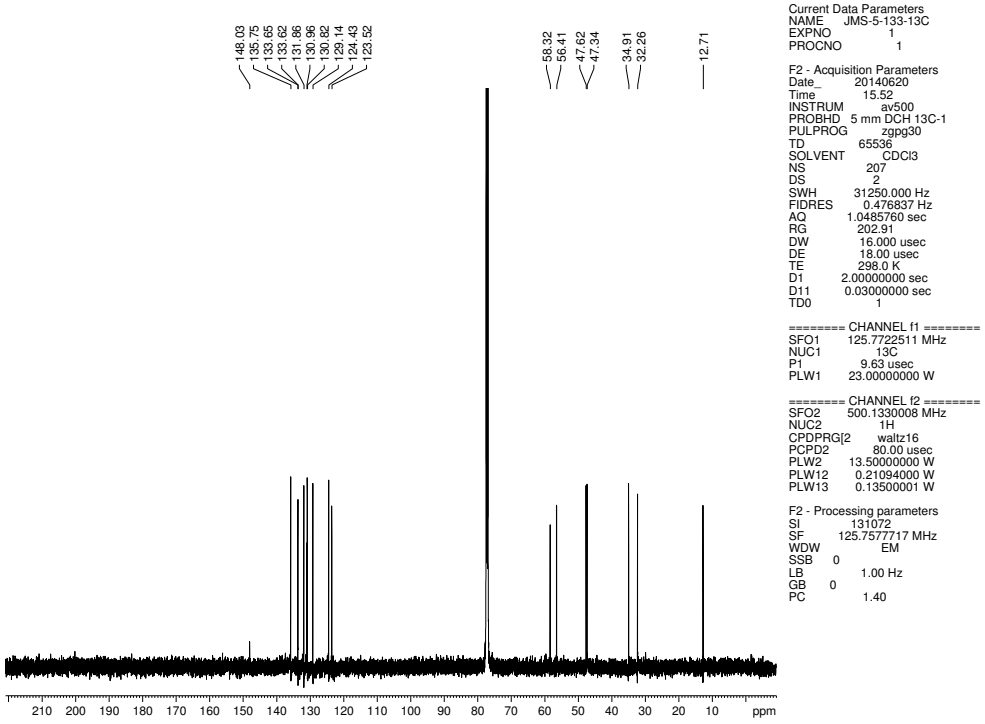

Figure 2.20 ^{13}C NMR (125 MHz, $CDCl_3$) of compound **2.14**.

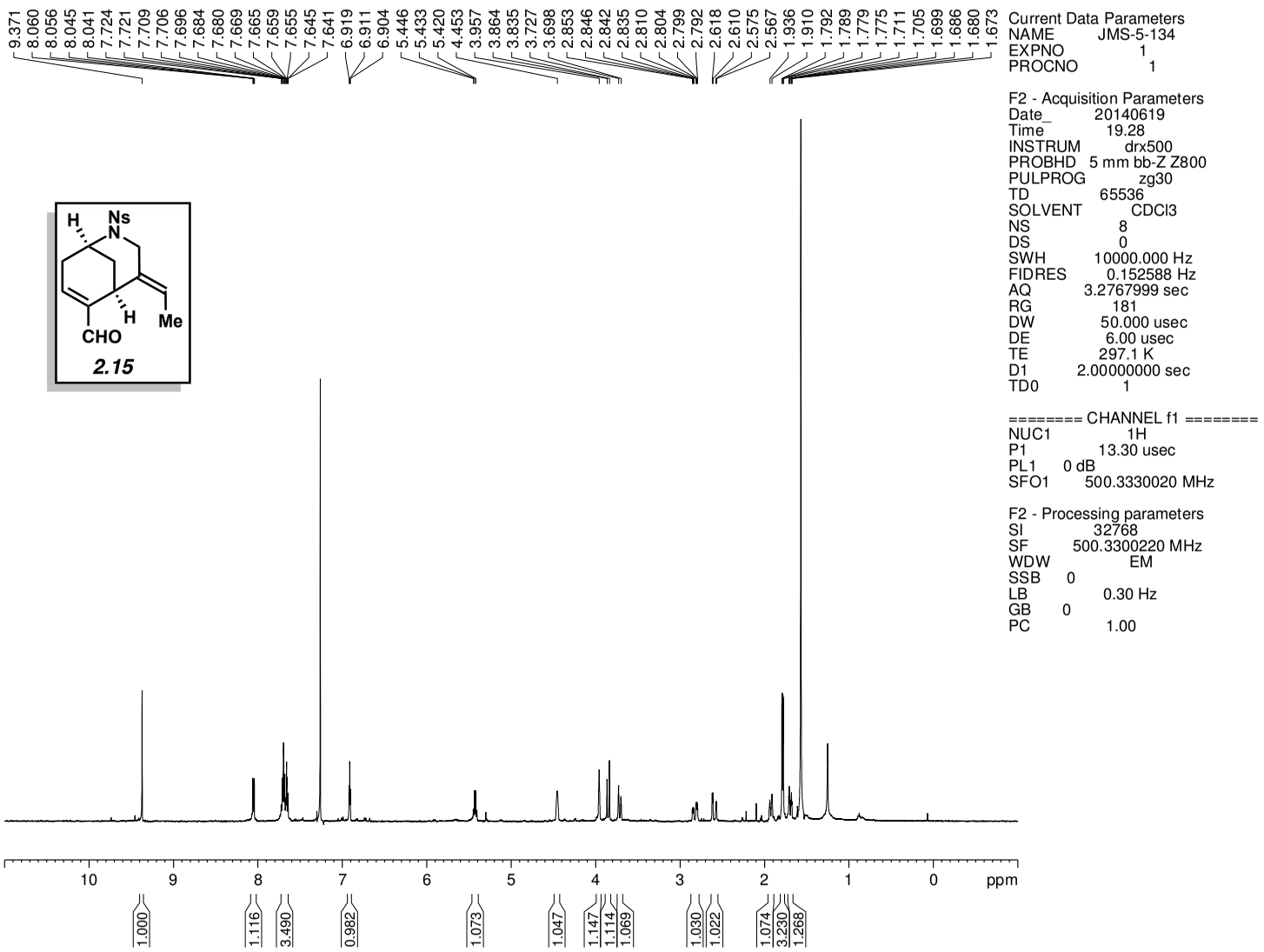

Figure 2.21 ^{1}H NMR (500 MHz, $CDCl_3$) of compound **2.15**.

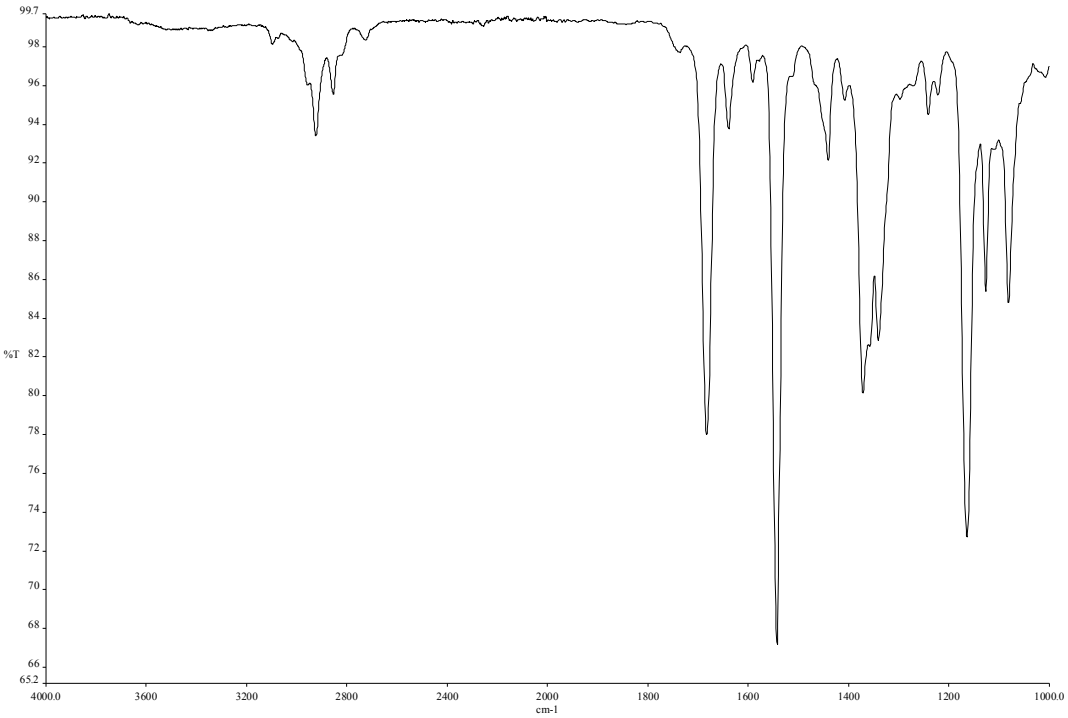

Figure 2.22 Infrared spectrum of compound **2.15**.

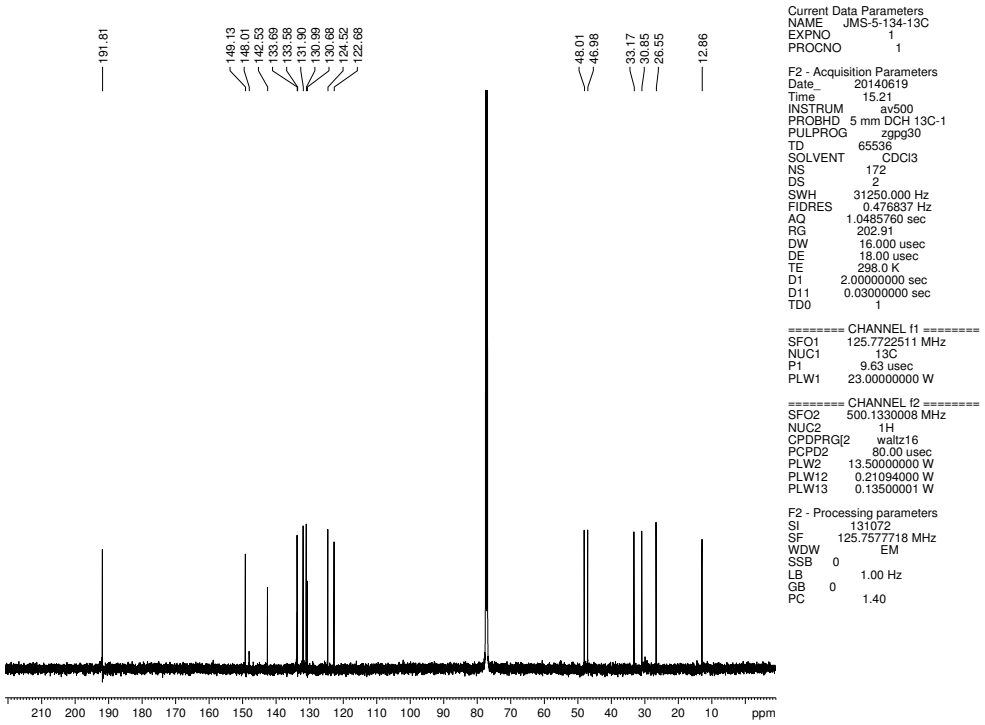

Figure 2.23 ^{13}C NMR (125 MHz, $CDCl_3$) of compound **2.15**.

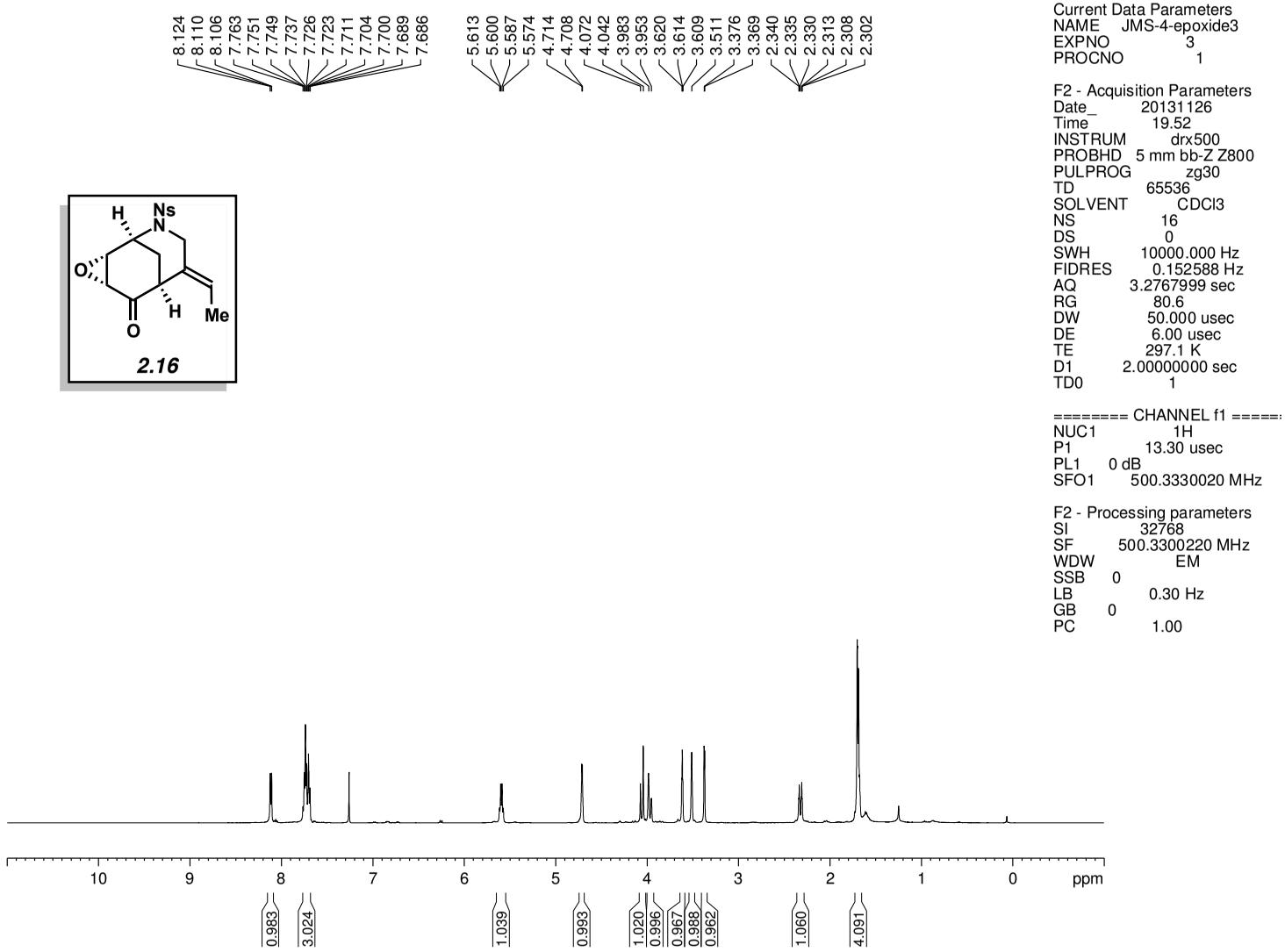

Figure 2.24 ^{1}H NMR (500 MHz, $CDCl_3$) of compound **2.16**.

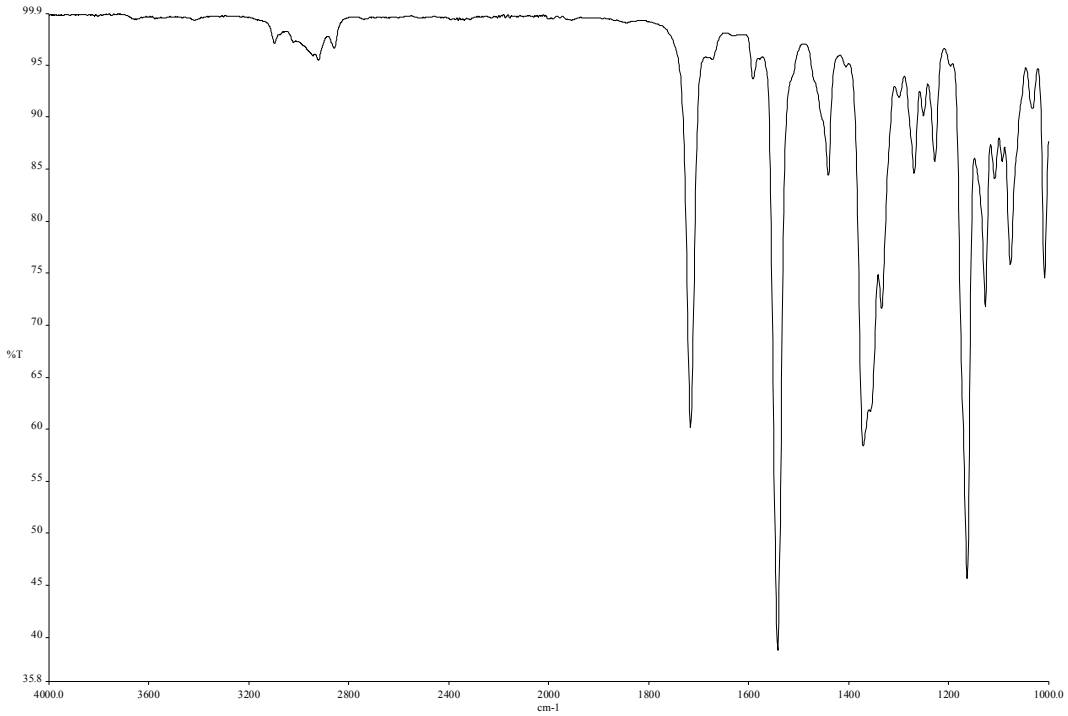

Figure 2.25 Infrared spectrum of compound **2.16**.

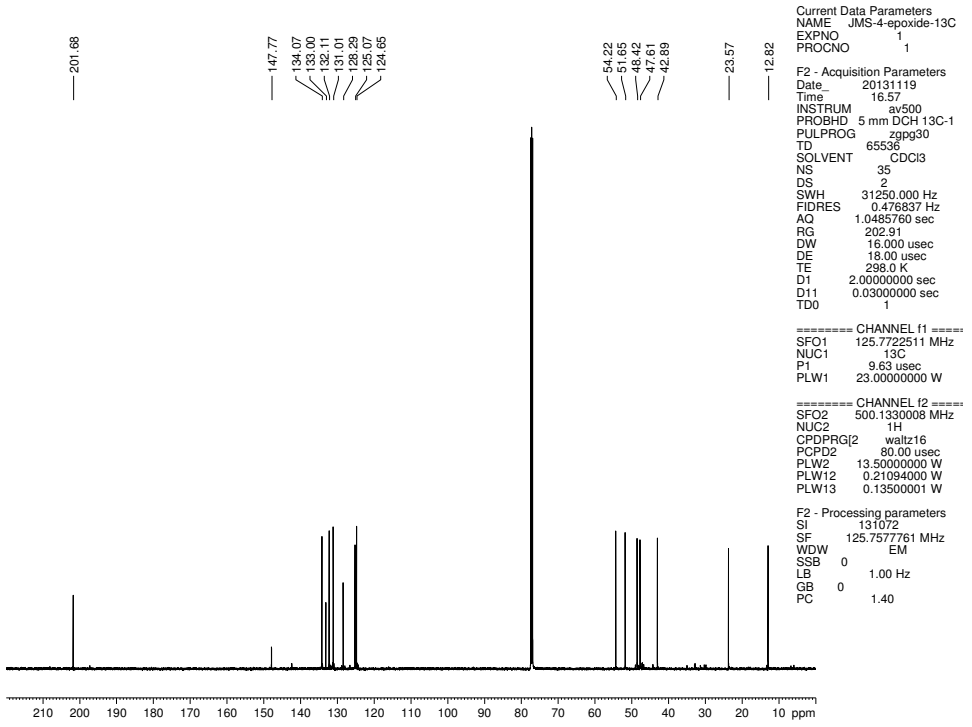

Figure 2.26 ^{13}C NMR (125 MHz, $CDCl_3$) of compound **2.16**.

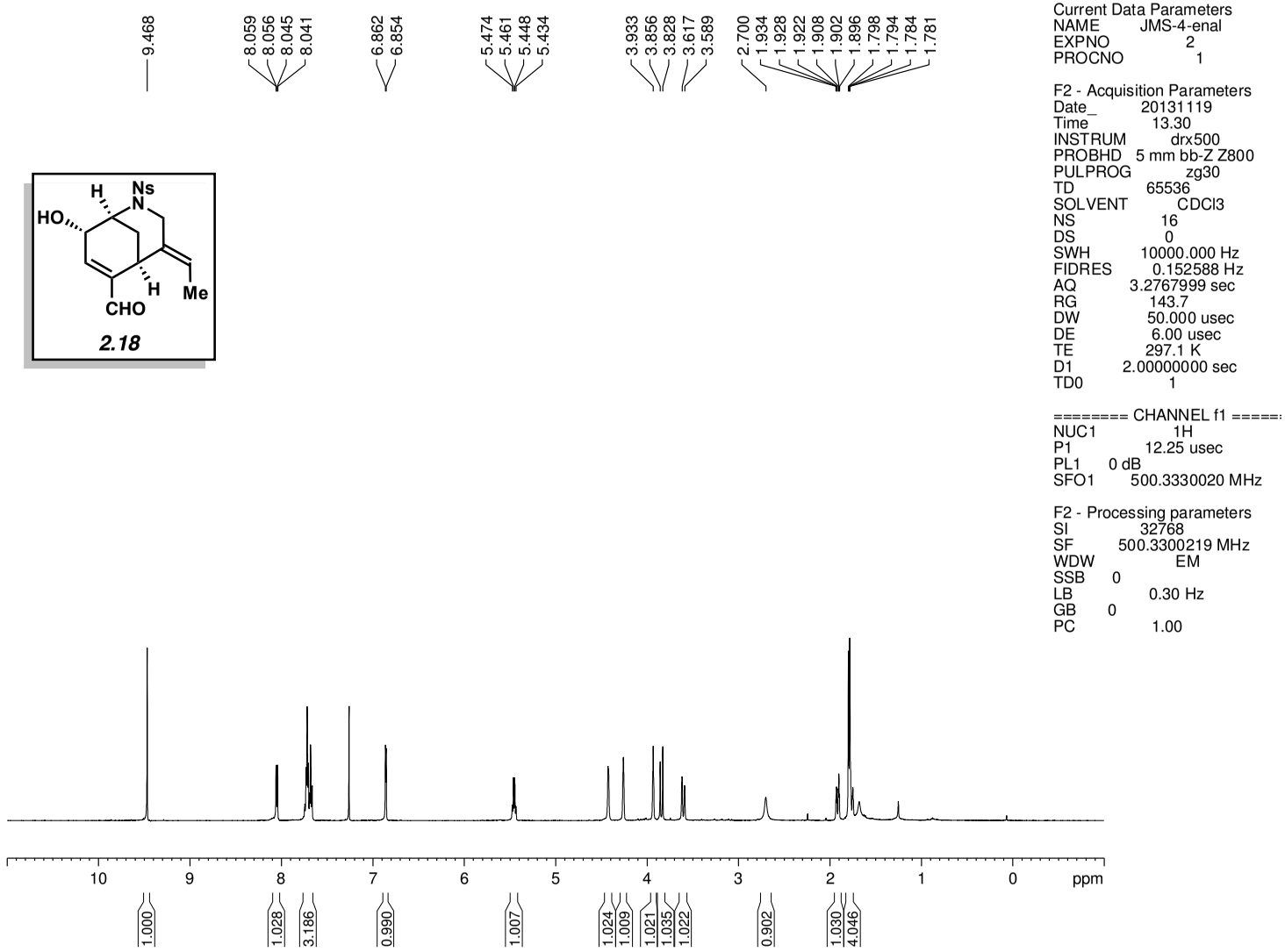

Figure 2.27 ^{1}H NMR (500 MHz, $CDCl_3$) of compound **2.18**.

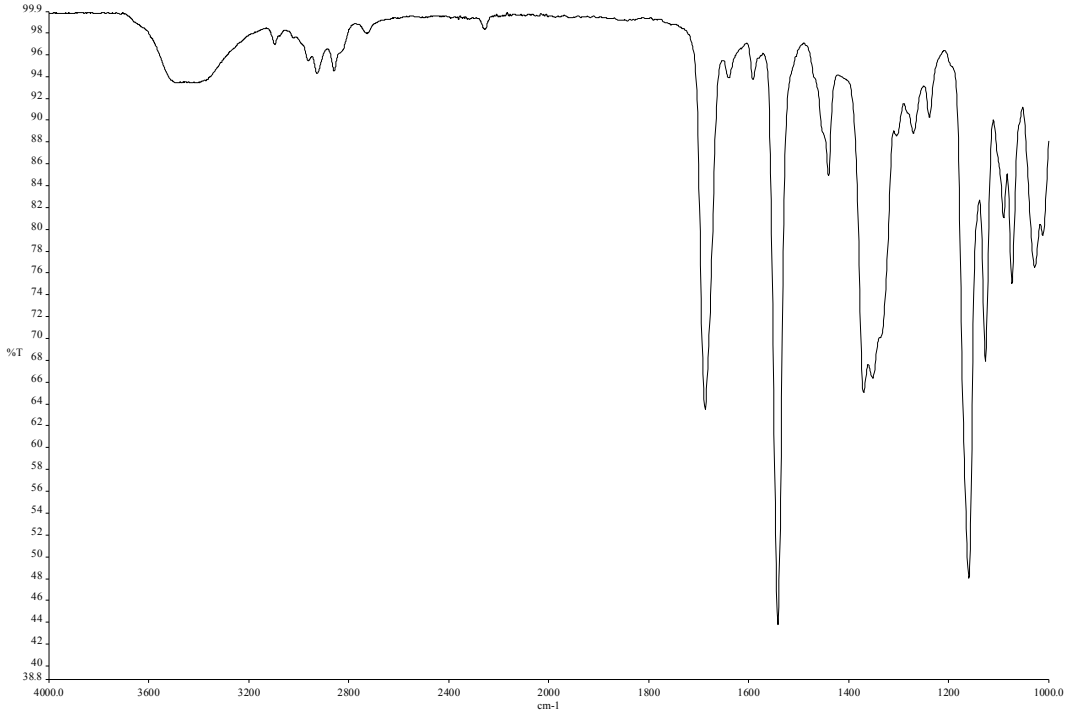

Figure 2.28 Infrared spectrum of compound **2.18**.

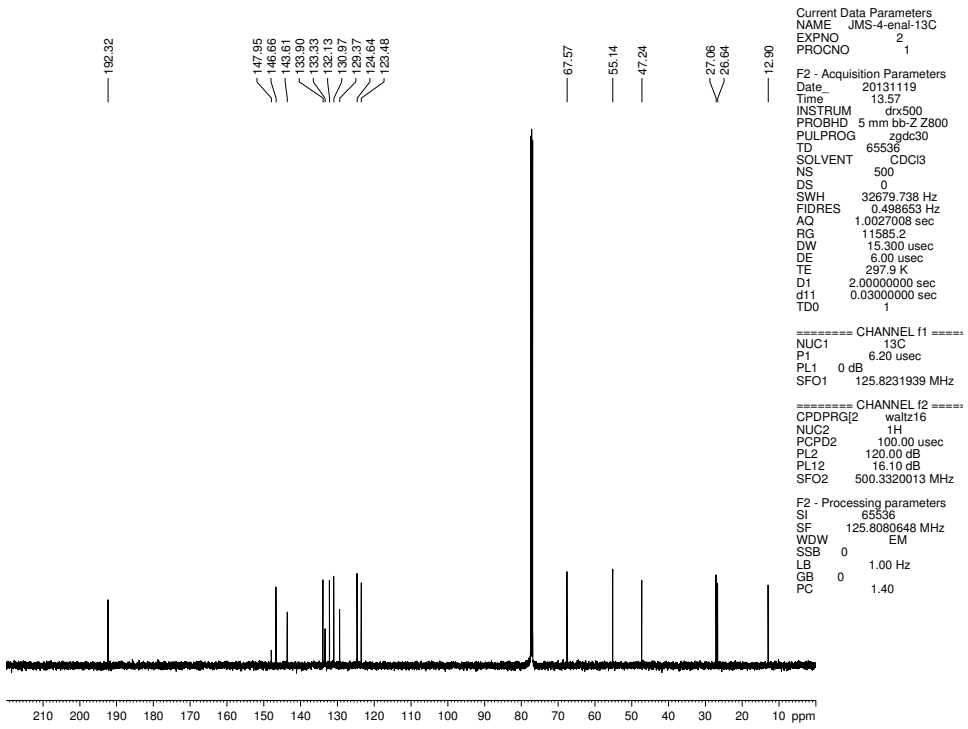

Figure 2.29 ^{13}C NMR (125 MHz, $CDCl_3$) of compound **2.18**.

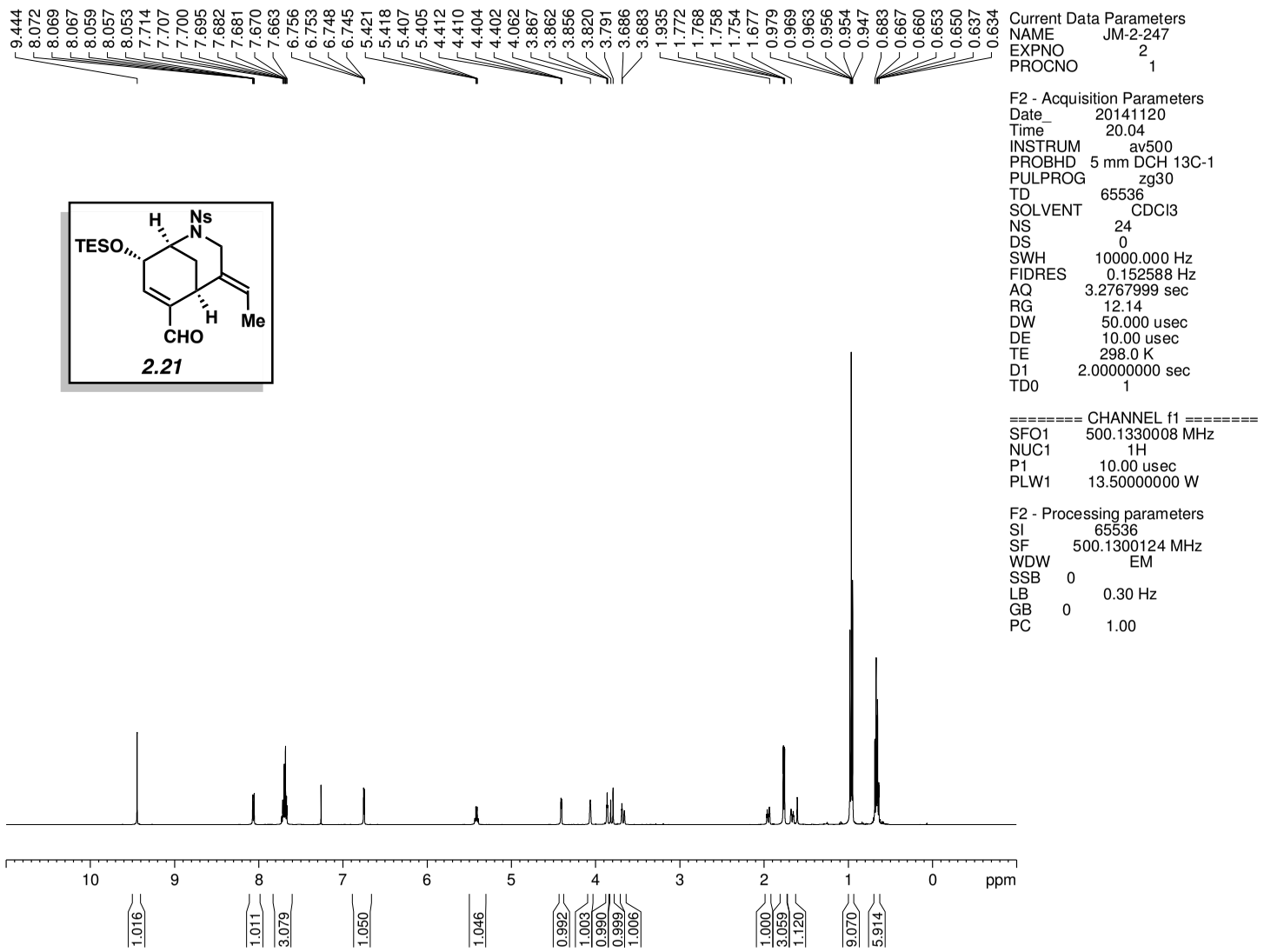

Figure 2.30 ^{1}H NMR (500 MHz, $CDCl_3$) of compound **2.21**.

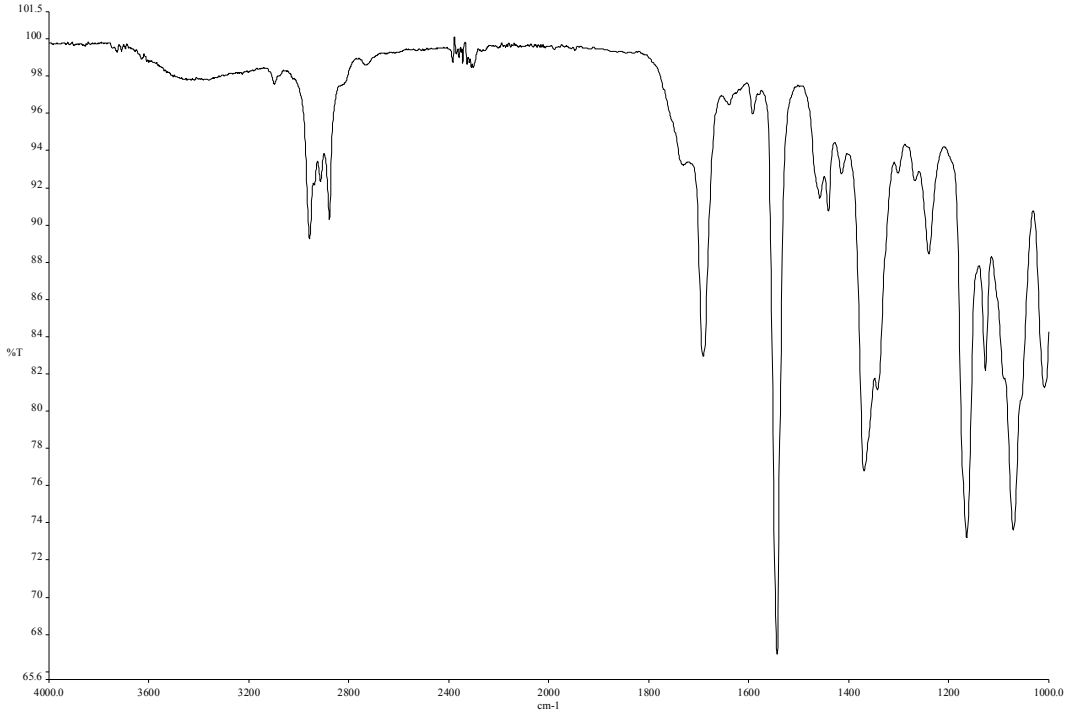

Figure 2.31 Infrared spectrum of compound **2.21**

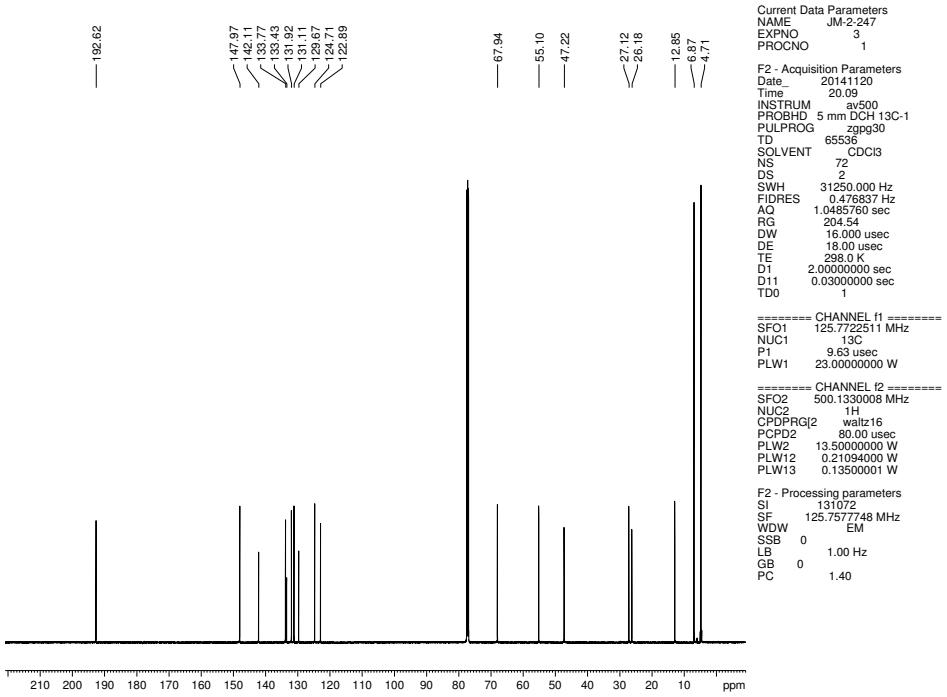

Figure 2.32 ^{13}C NMR (125 MHz, $CDCl_3$) of compound **2.21**.

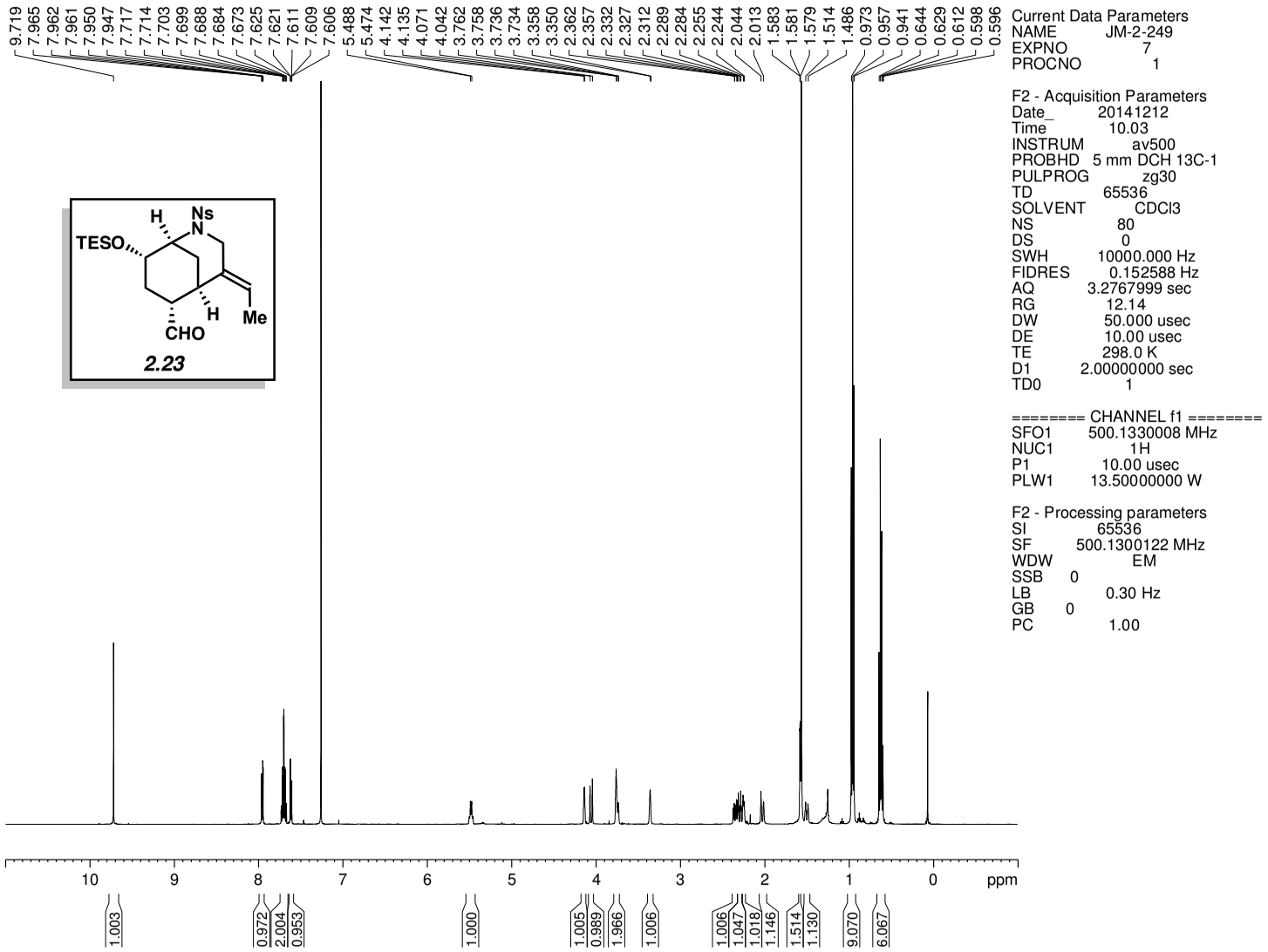

Figure 2.33 ^{1}H NMR (500 MHz, $CDCl_3$) of compound **2.23**.

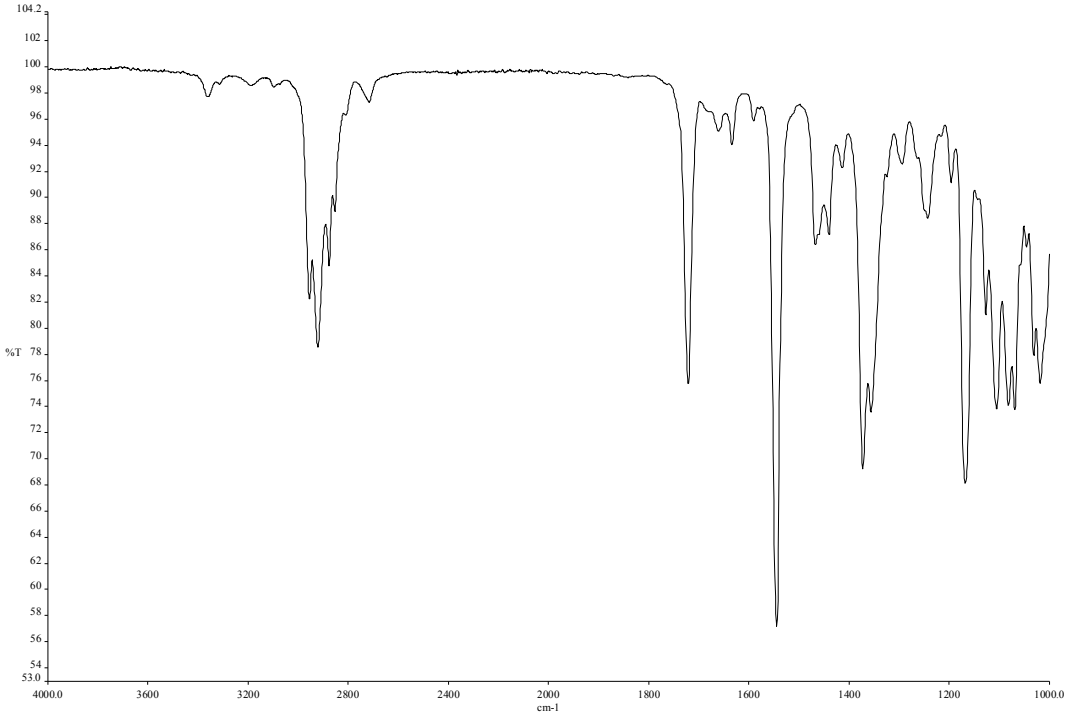

Figure 2.34 Infrared spectrum of compound **2.23**.

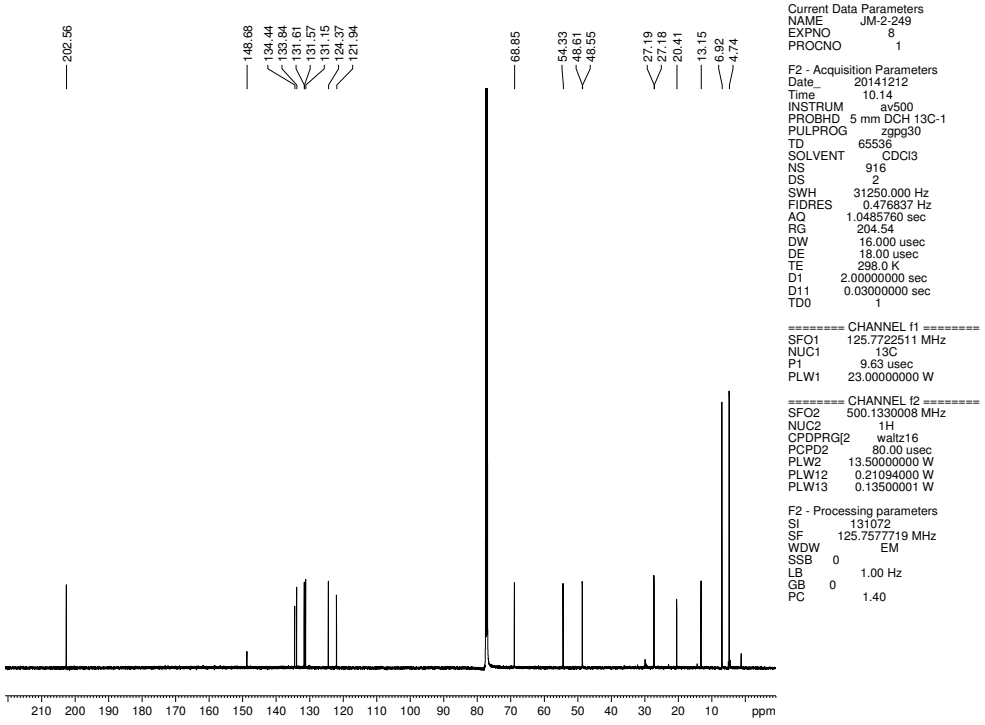

Figure 2.35 ^{13}C NMR (125 MHz, $CDCl_3$) of compound **2.23**.

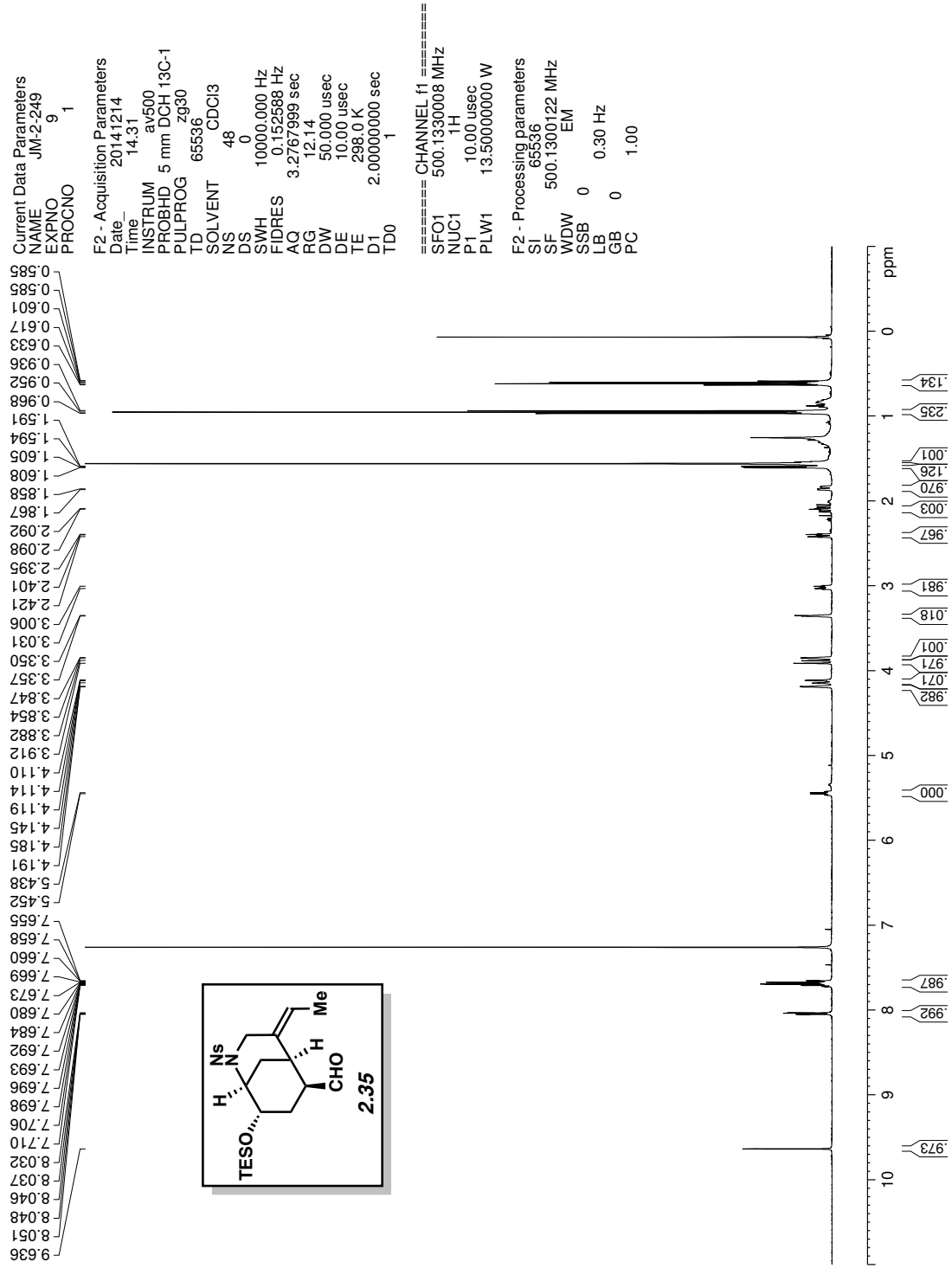

Figure 2.36 ^{1}H NMR (500 MHz, $CDCl_3$) of compound **2.35**.

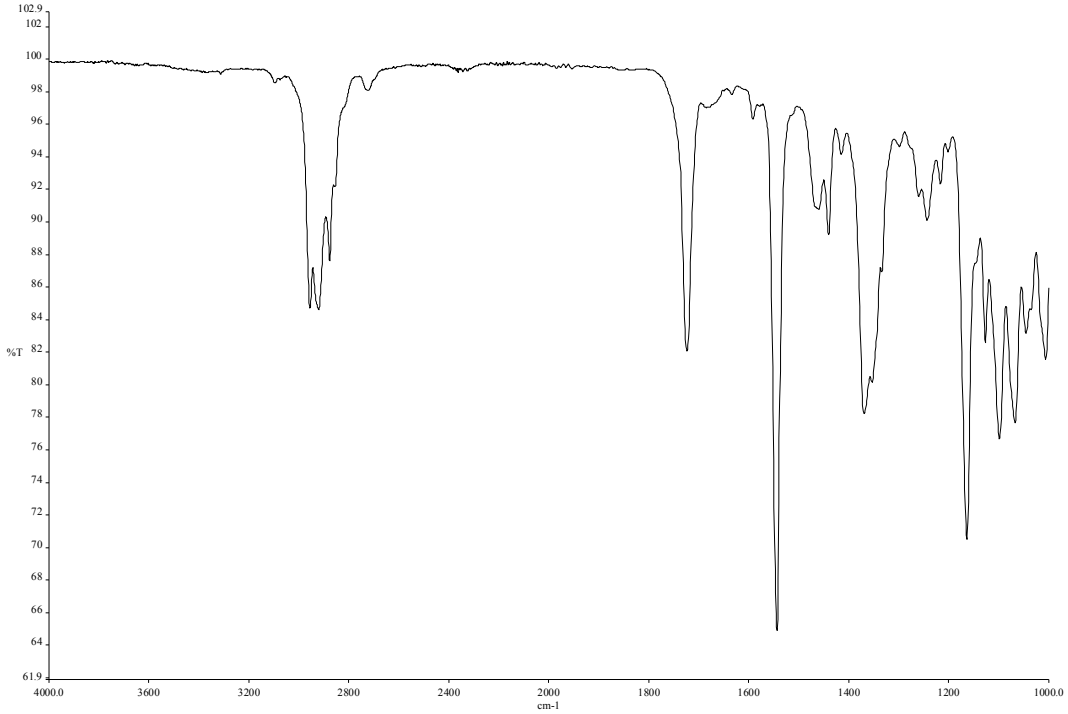

Figure 2.37 Infrared spectrum of compound **2.35**.

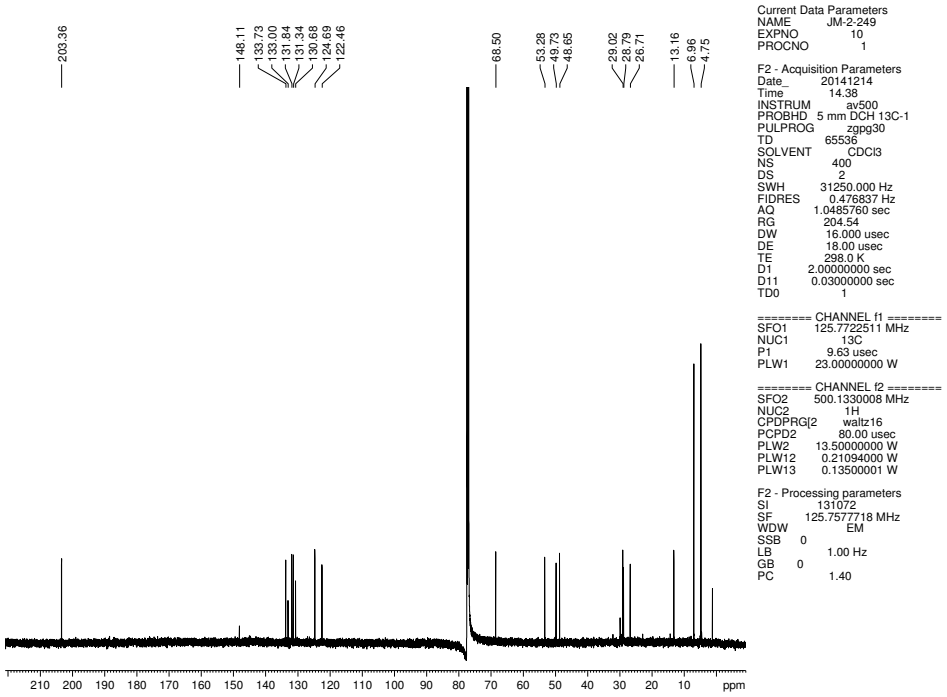

Figure 2.38 ^{13}C NMR (125 MHz, $CDCl_3$) of compound **2.35**.

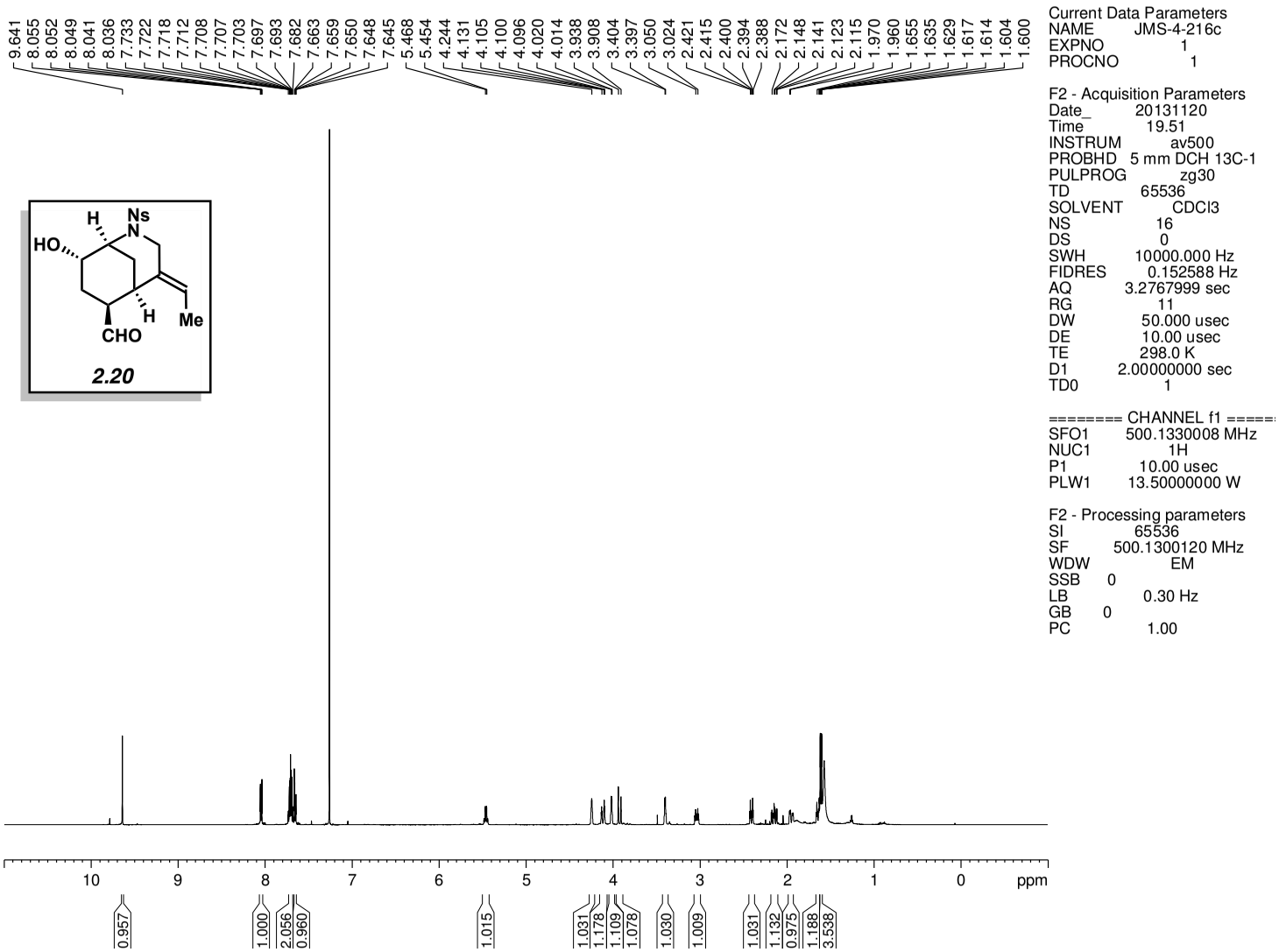

Figure 2.39 ^{1}H NMR (500 MHz, $CDCl_3$) of compound **2.20**.

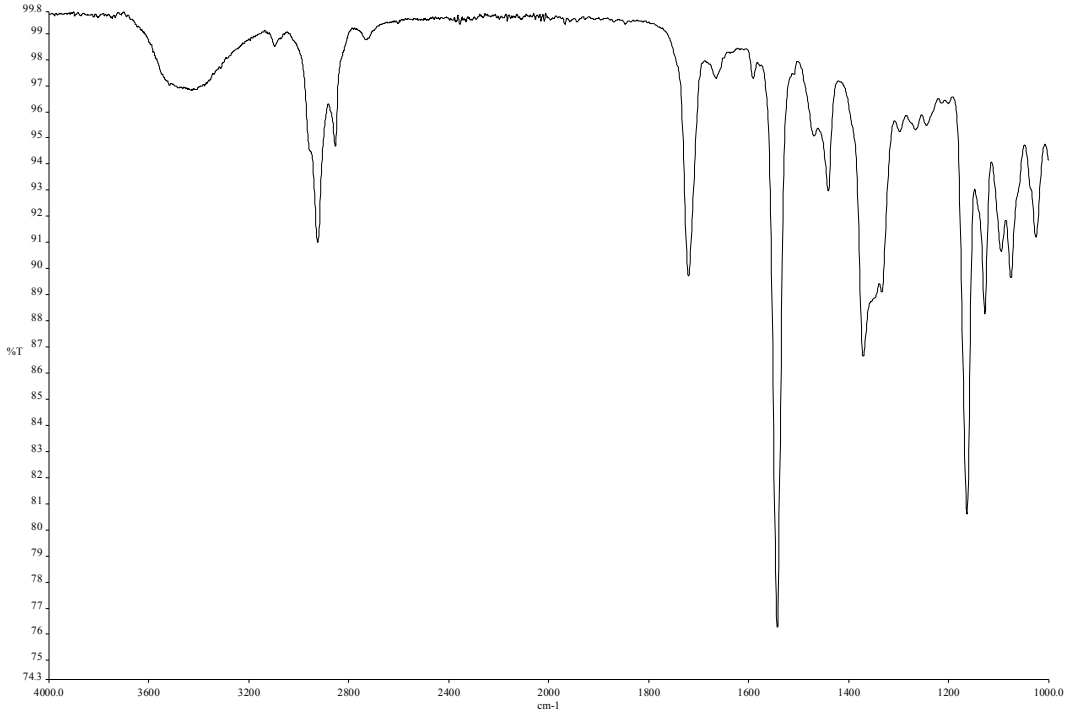

Figure 2.40 Infrared spectrum of compound **2.20**.

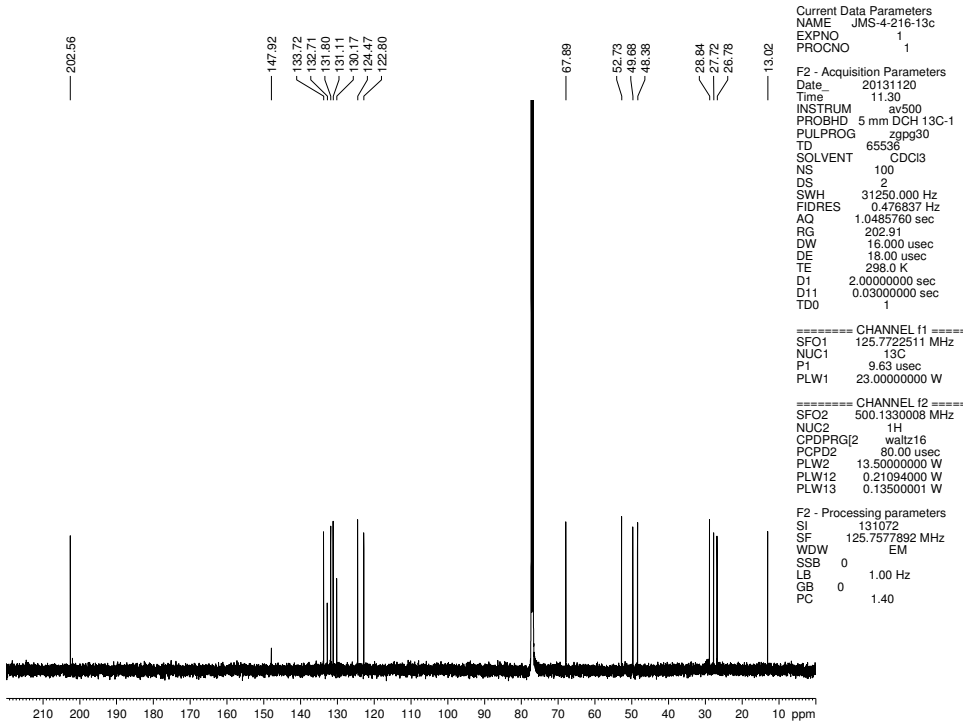

Figure 2.41 ^{13}C NMR (125 MHz, $CDCl_3$) of compound **2.20**.

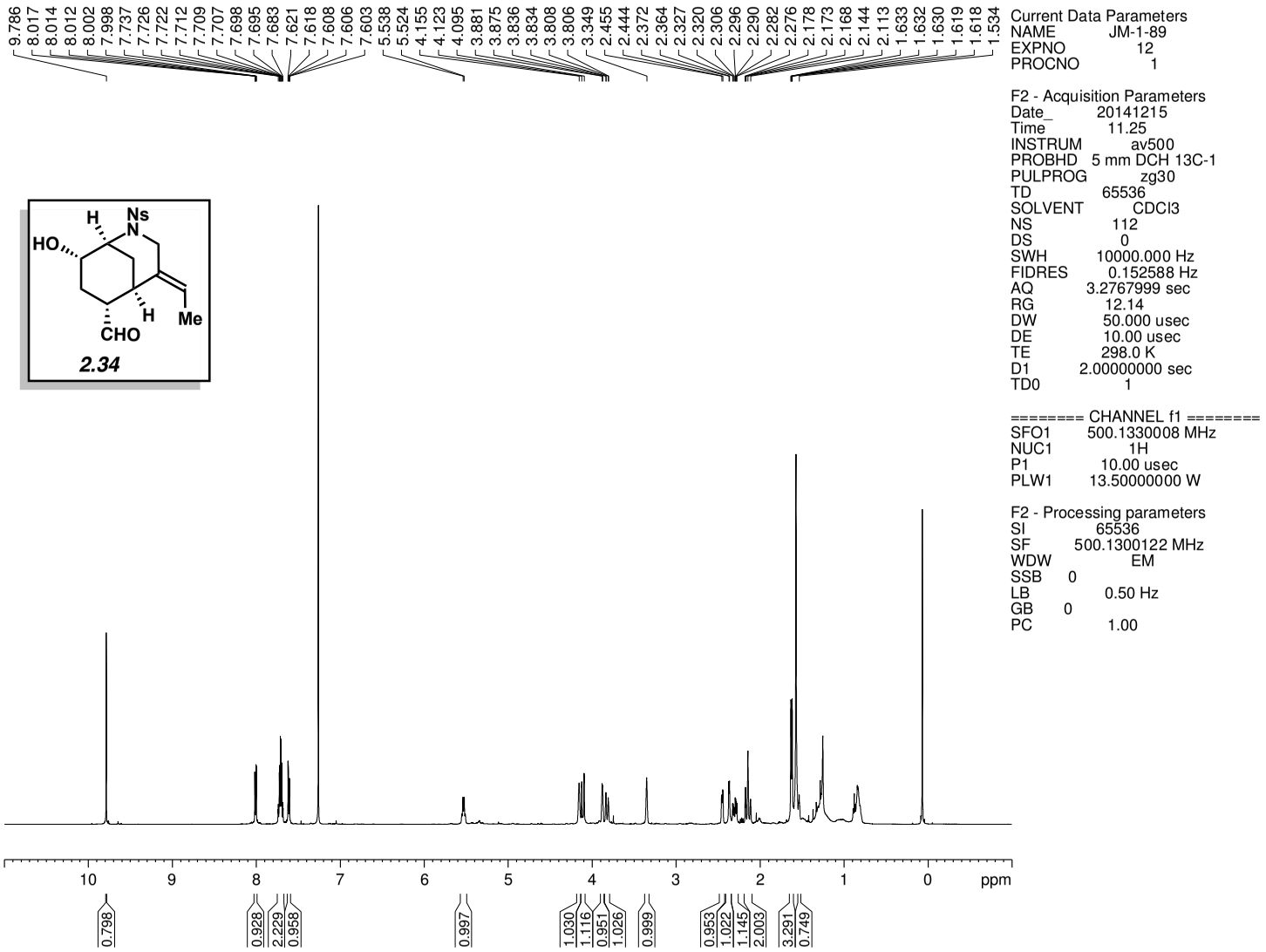

Figure 2.42 ^{1}H NMR (500 MHz, $CDCl_3$) of compound **2.34**.

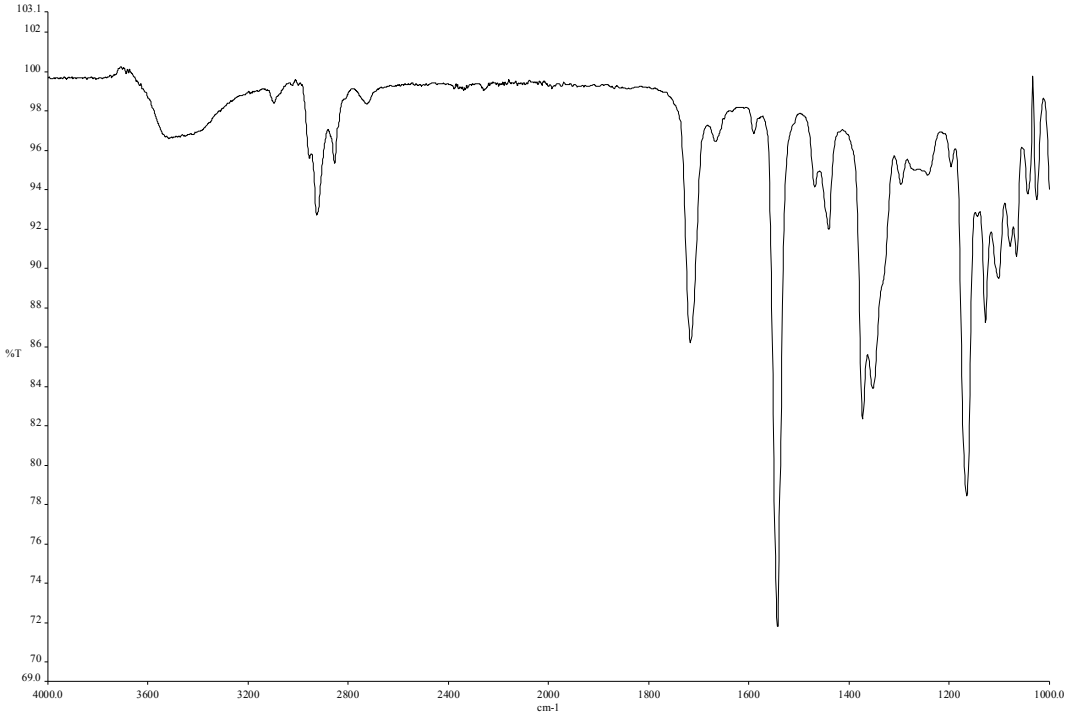

Figure 2.43 Infrared spectrum of compound **2.34**.

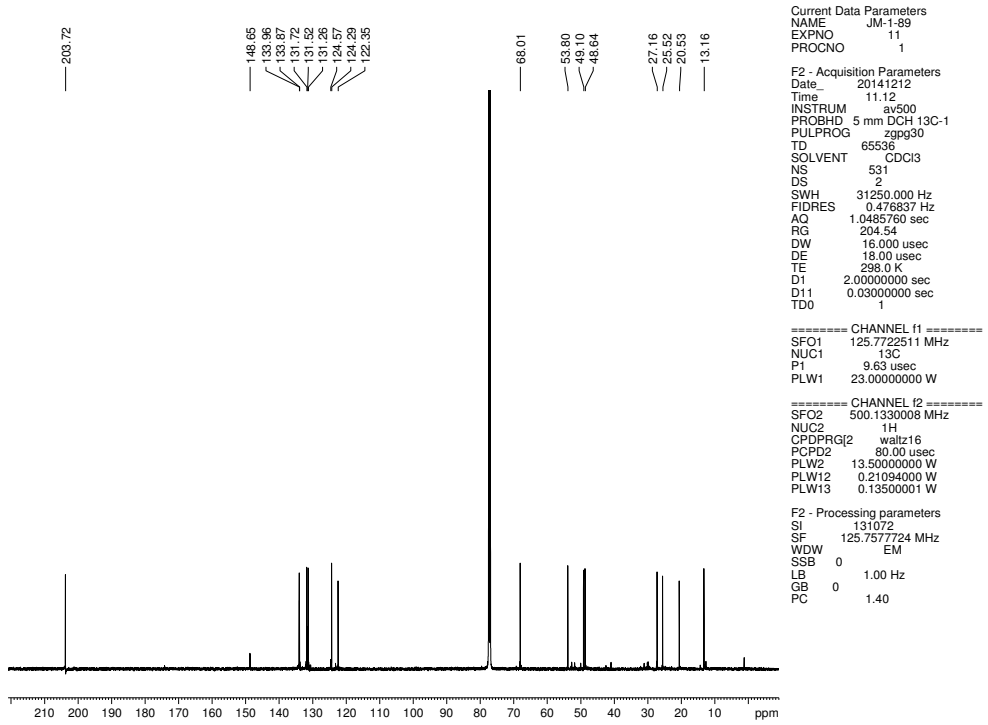

Figure 2.44 ^{13}C NMR (125 MHz, $CDCl_3$) of compound **2.34**.

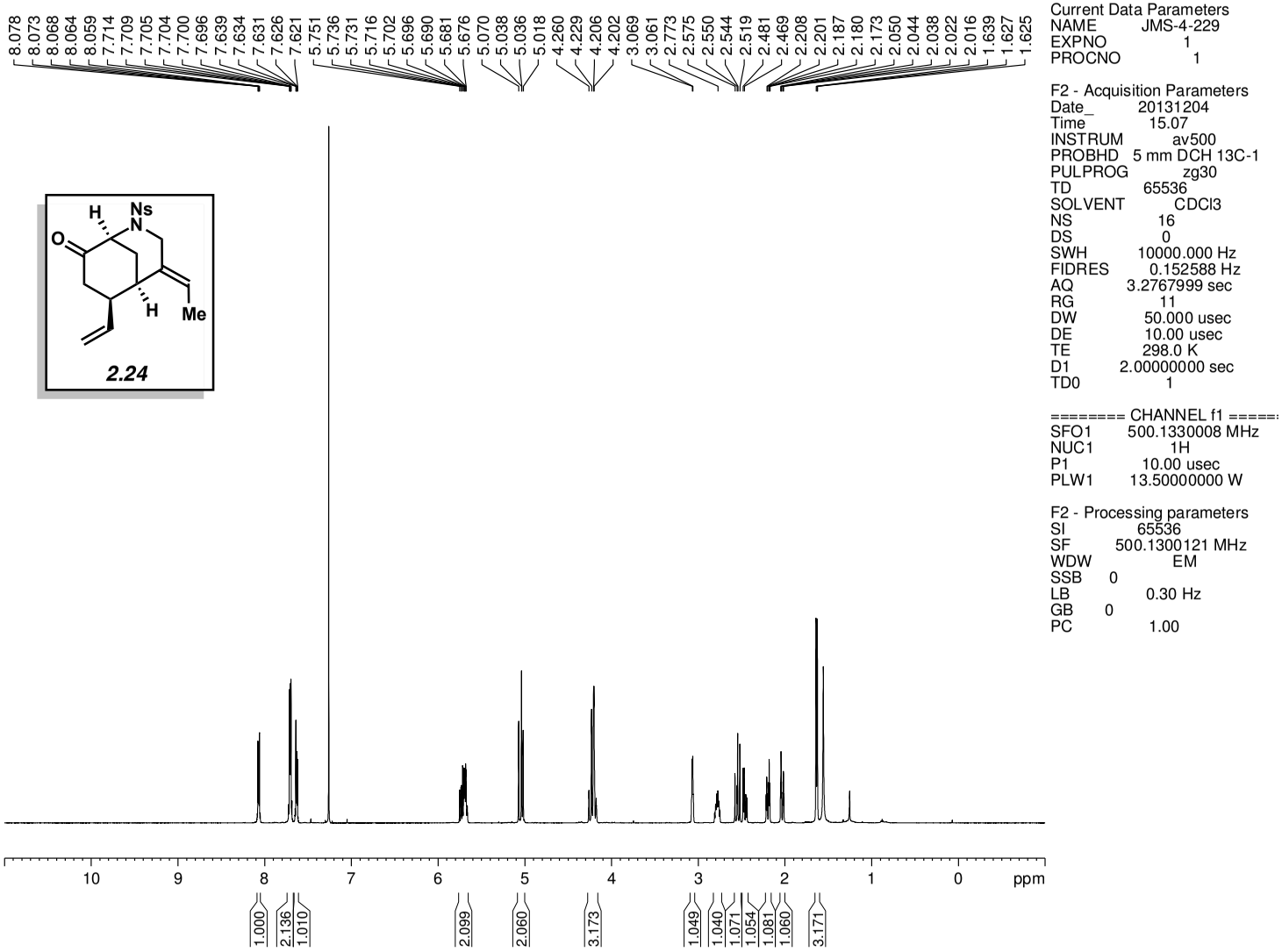

Figure 2.45 ^{1}H NMR (500 MHz, $CDCl_3$) of compound **2.24**.

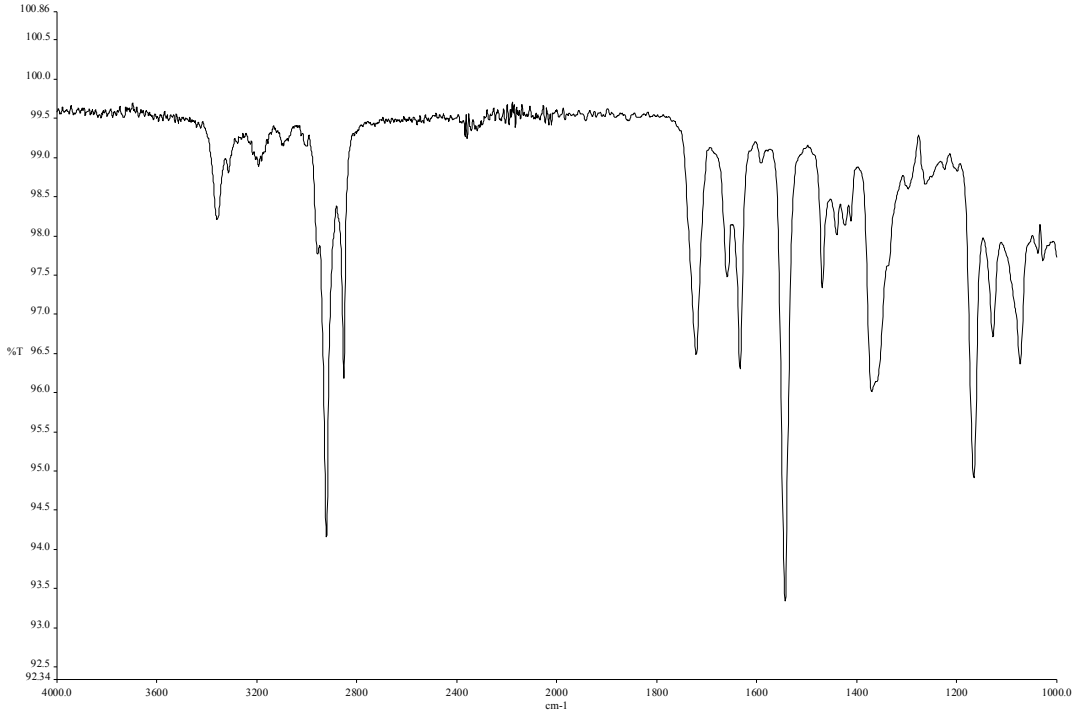

Figure 2.46 Infrared spectrum of compound **2.24**.

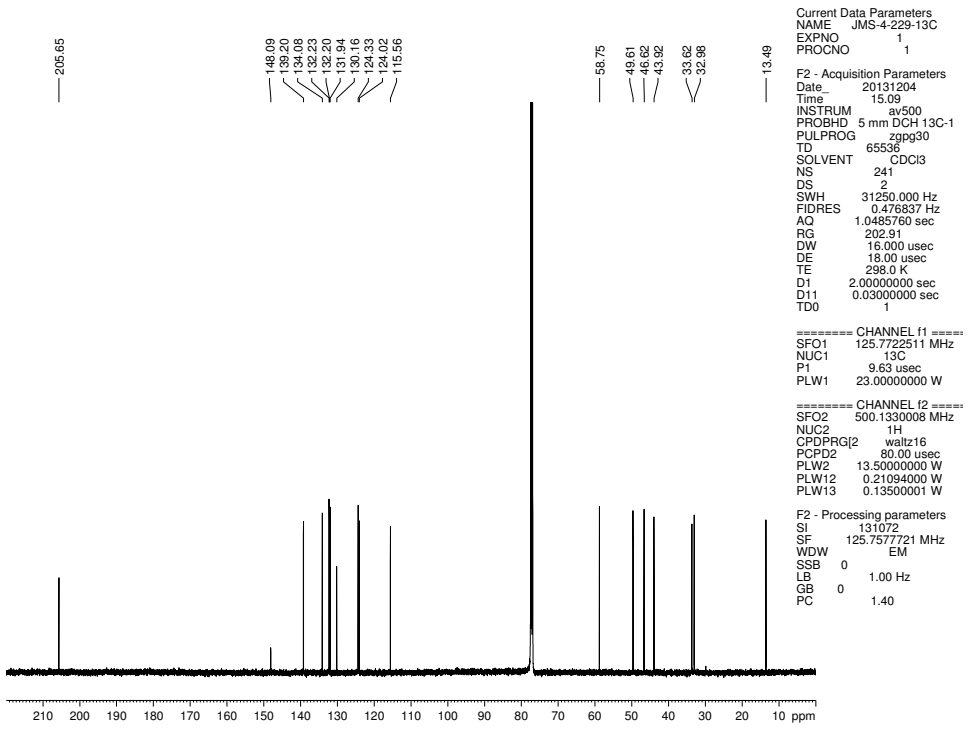

Figure 2.47 ^{13}C NMR (125 MHz, $CDCl_3$) of compound **2.24**.

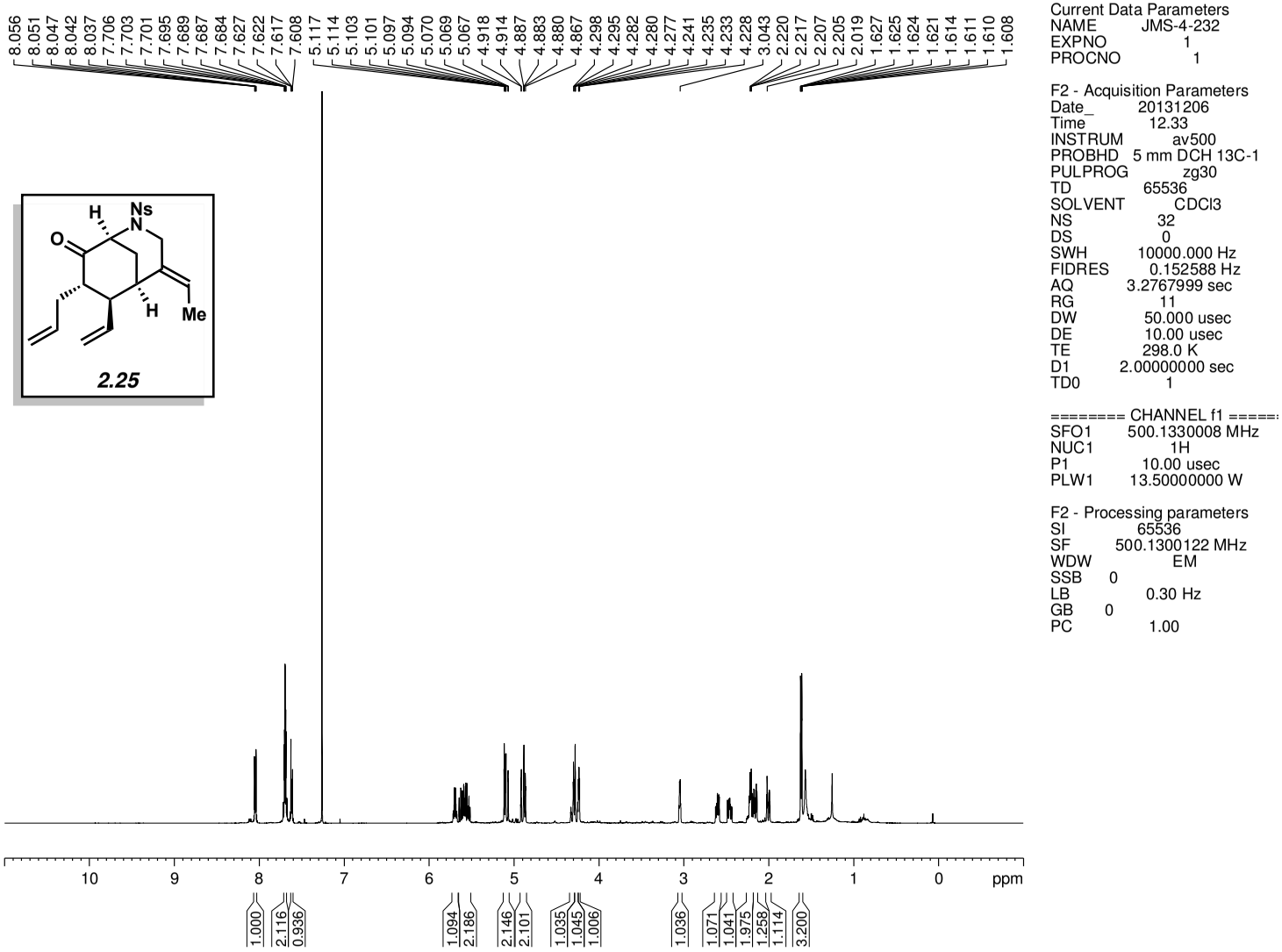

Figure 2.48 ^{1}H NMR (500 MHz, $CDCl_3$) of compound **2.25**.

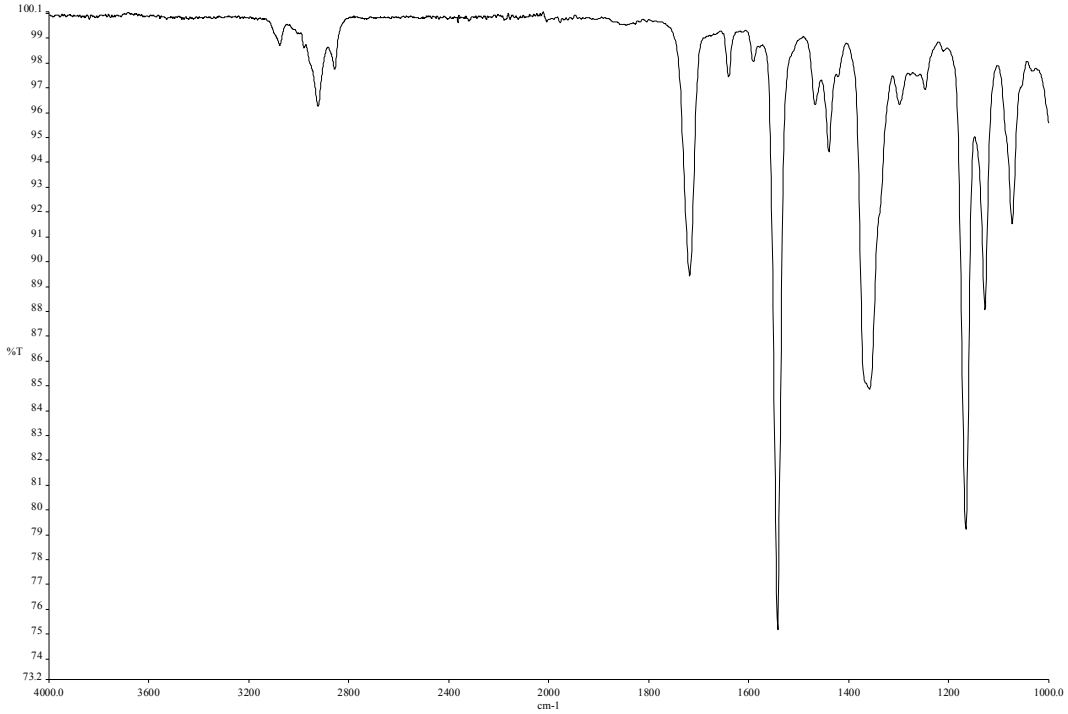

Figure 2.49 Infrared spectrum of compound **2.25**.

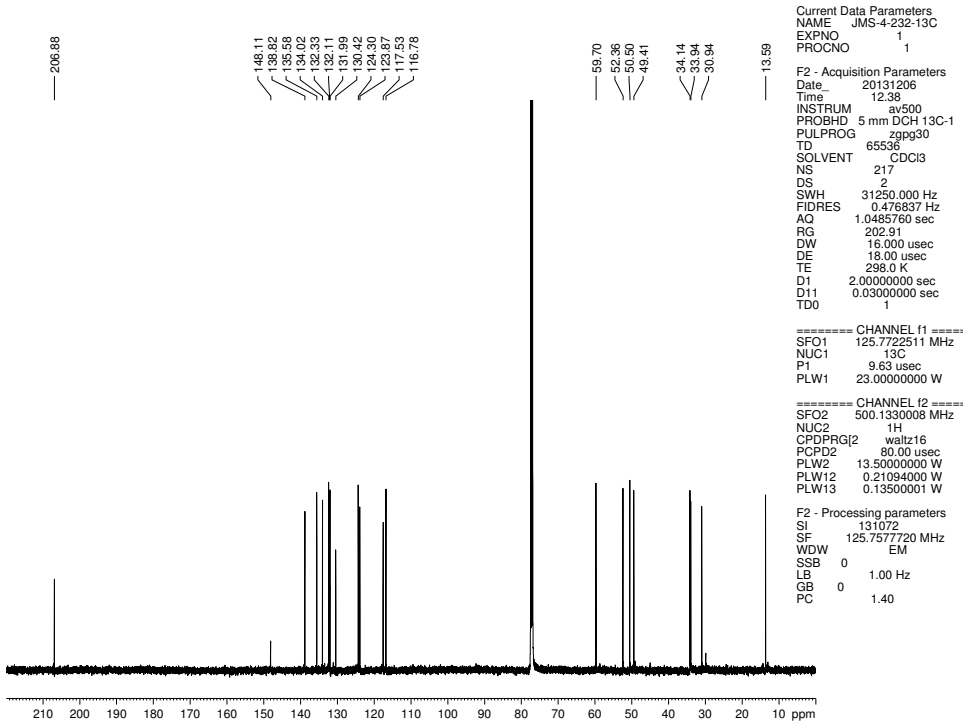

Figure 2.50 ^{13}C NMR (125 MHz, $CDCl_3$) of compound **2.25**.

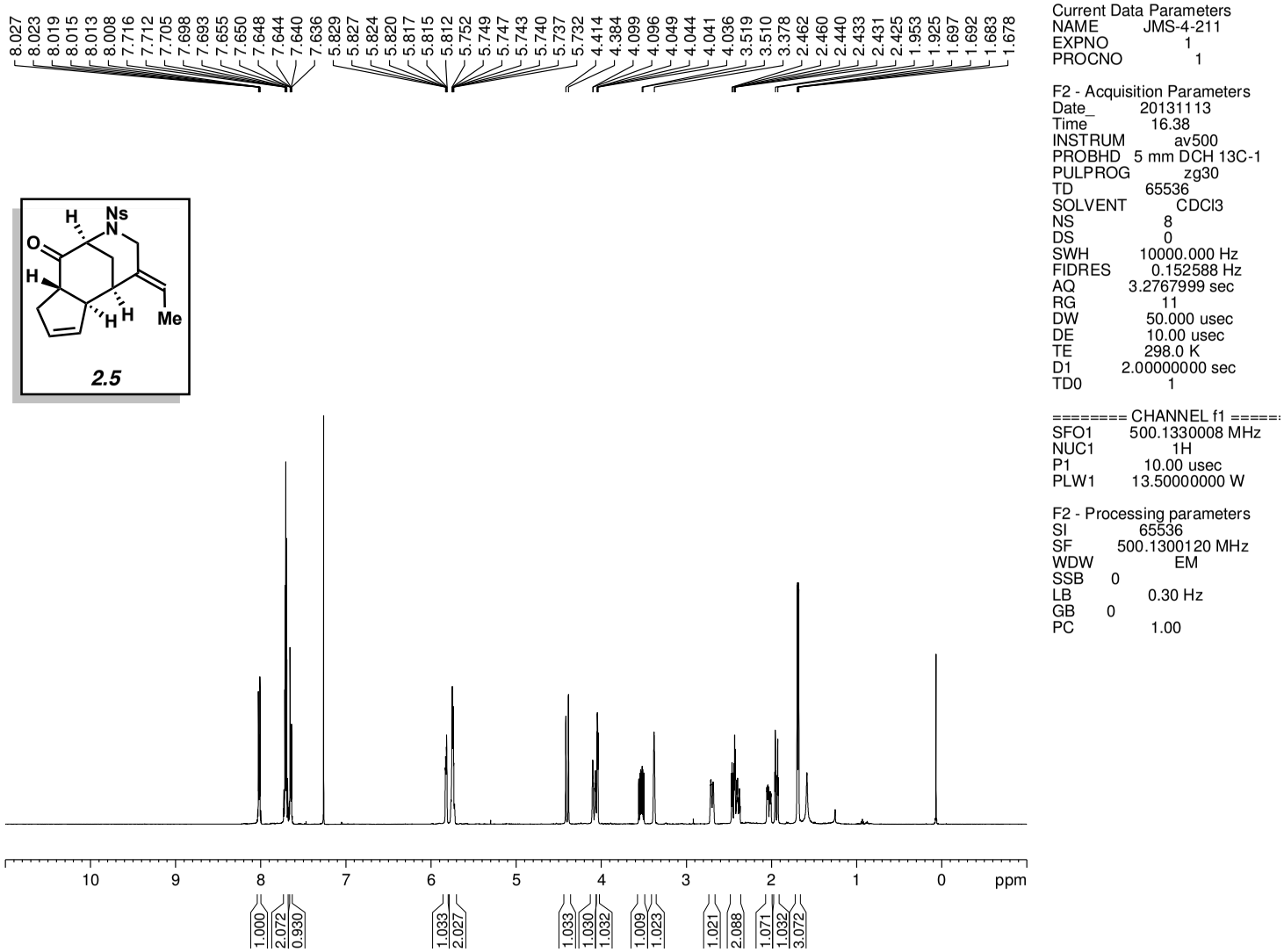

Figure 2.51 ^{1}H NMR (500 MHz, $CDCl_3$) of compound **2.5**.

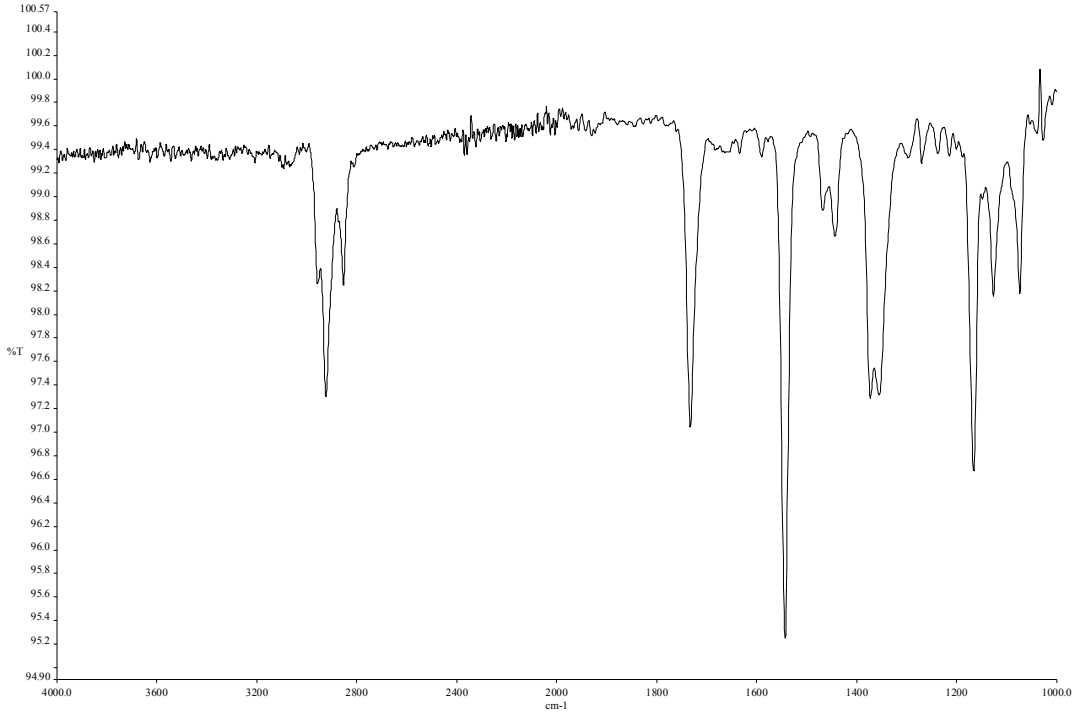

Figure 2.52 Infrared spectrum of compound **2.5**.

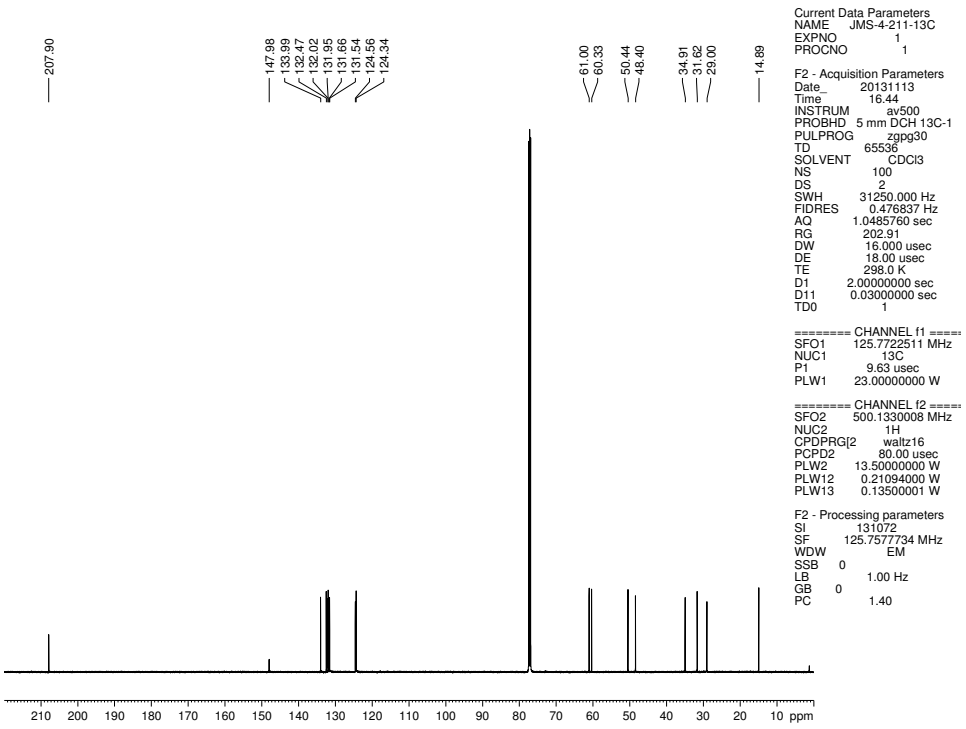

Figure 2.53 ^{13}C NMR (125 MHz, $CDCl_3$) of compound **2.5**.

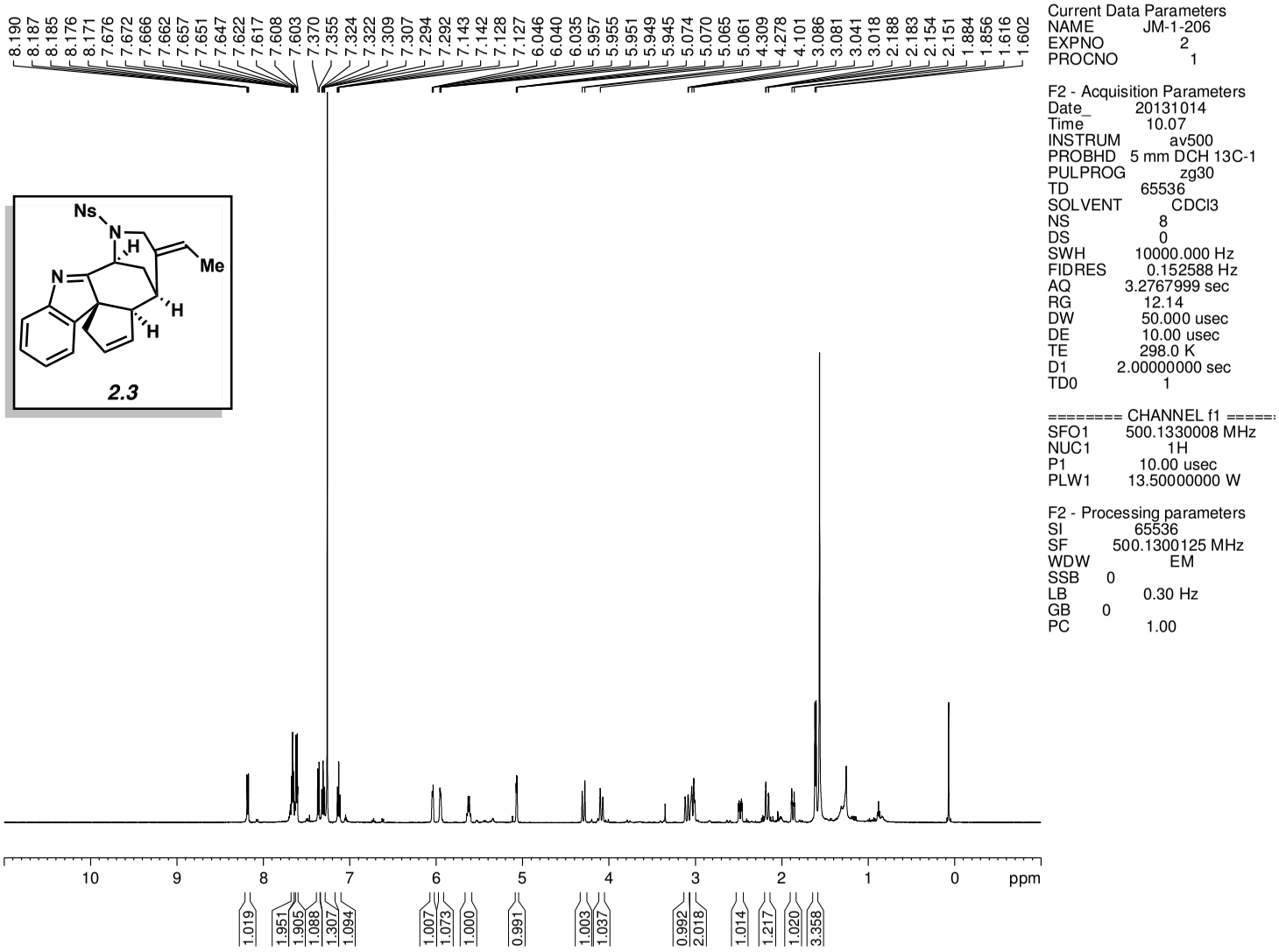

Figure 2.54 ^{1}H NMR (500 MHz, $CDCl_3$) of compound **2.3**.

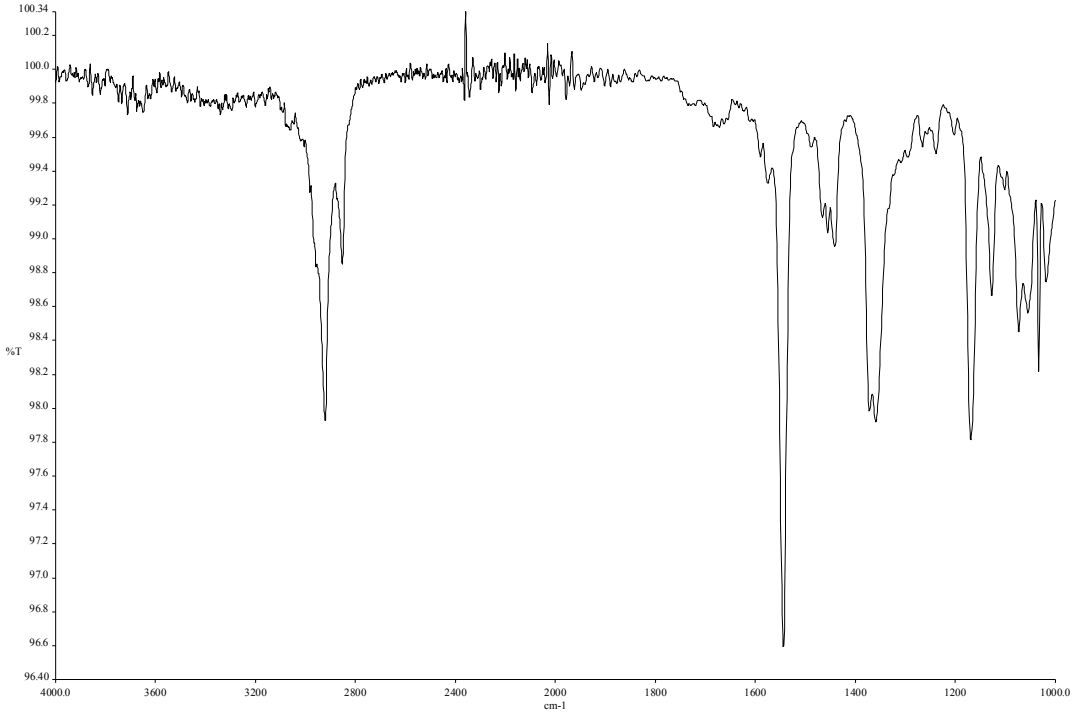

Figure 2.55 Infrared spectrum of compound **2.3**.

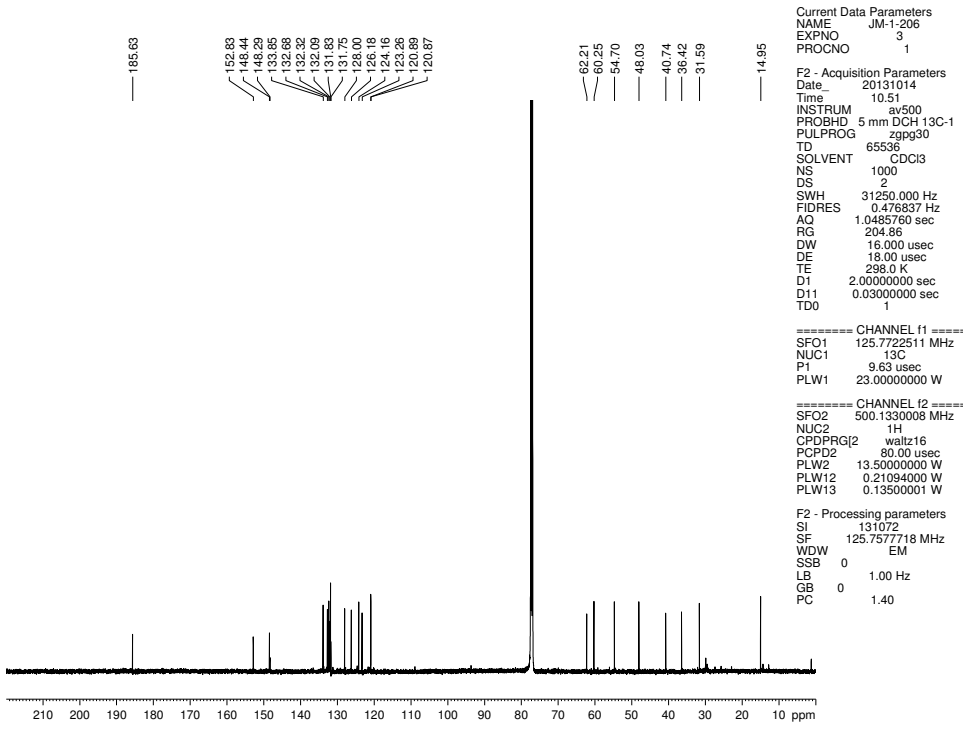

Figure 2.56 13C NMR (125 MHz, CDCl3) of compound **2.3**.

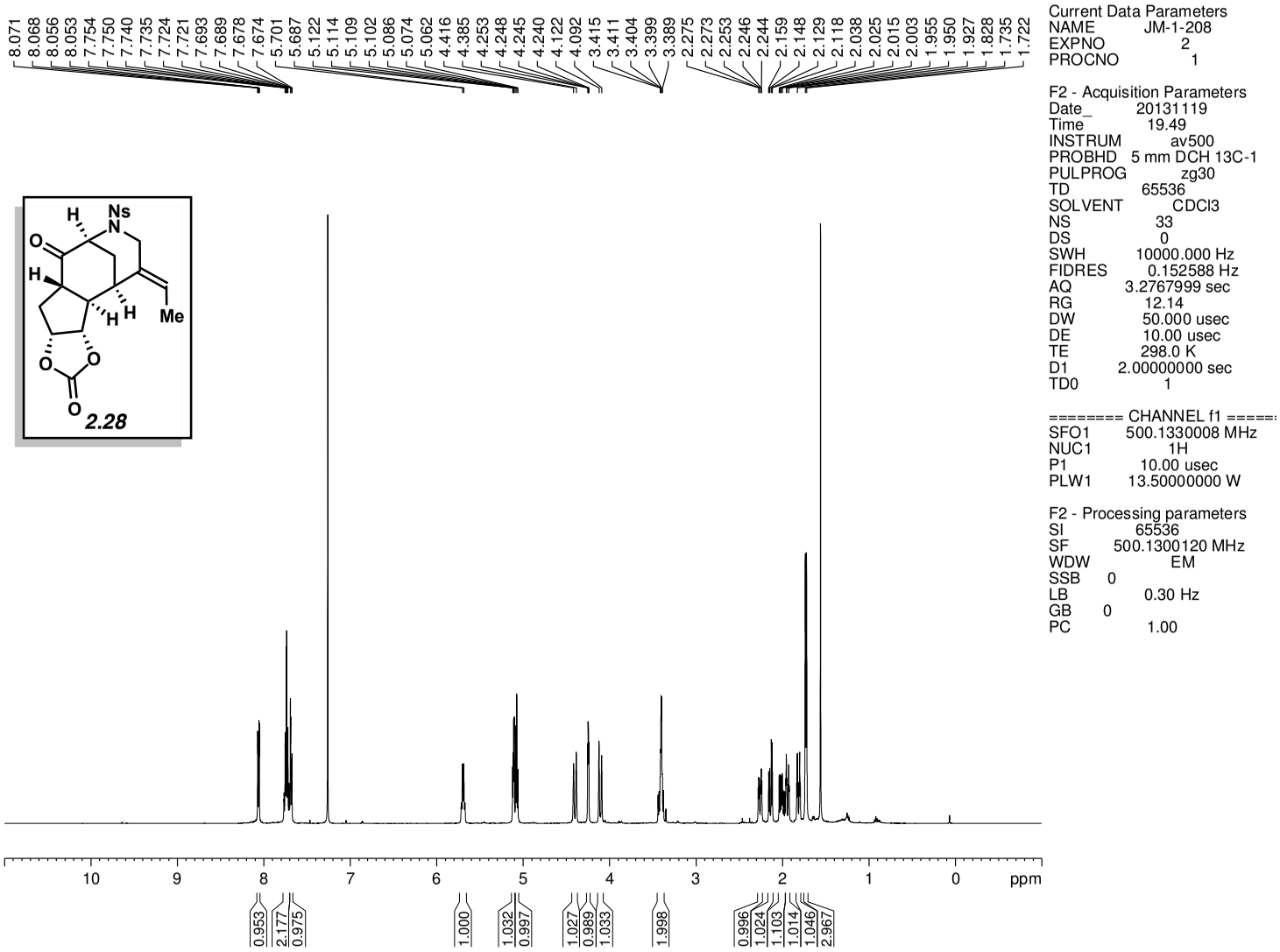

Figure 2.57 ^{1}H NMR (500 MHz, $CDCl_3$) of compound **2.28**.

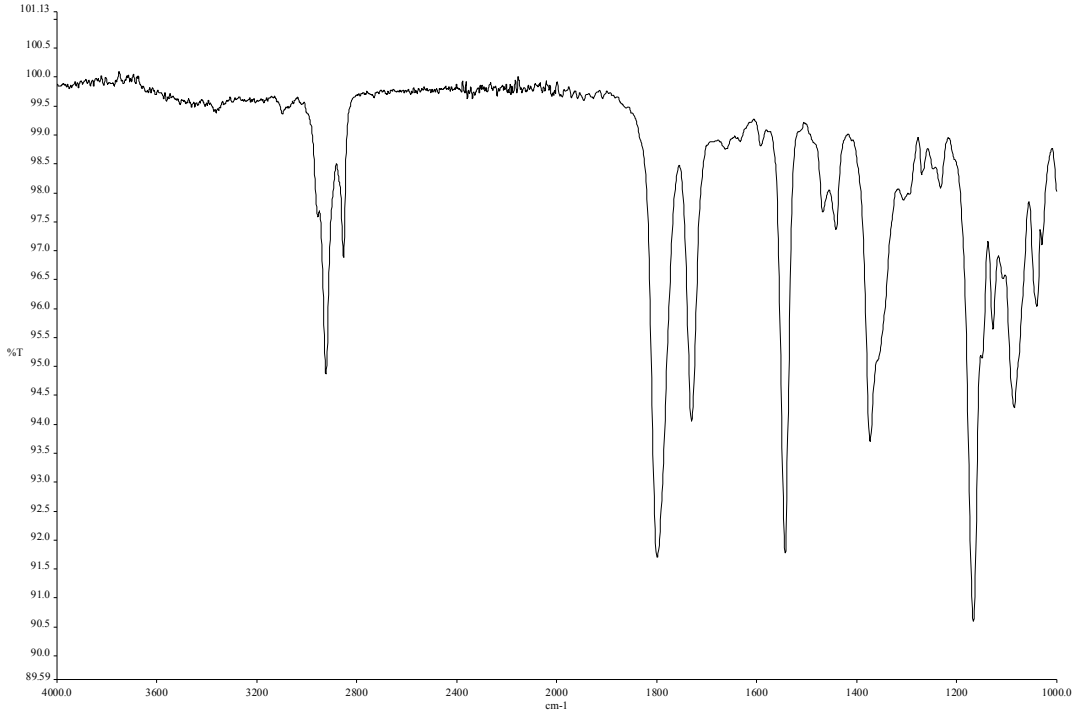

Figure 2.58 Infrared spectrum of compound **2.28**.

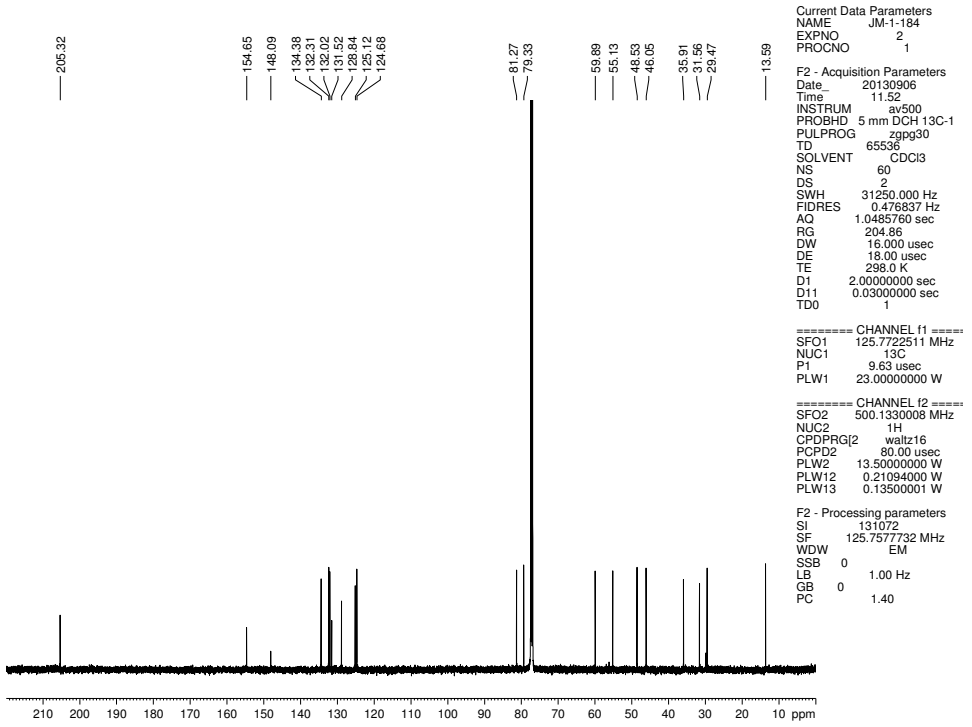

Figure 2.59 ^{13}C NMR (125 MHz, $CDCl_3$) of compound **2.28**.

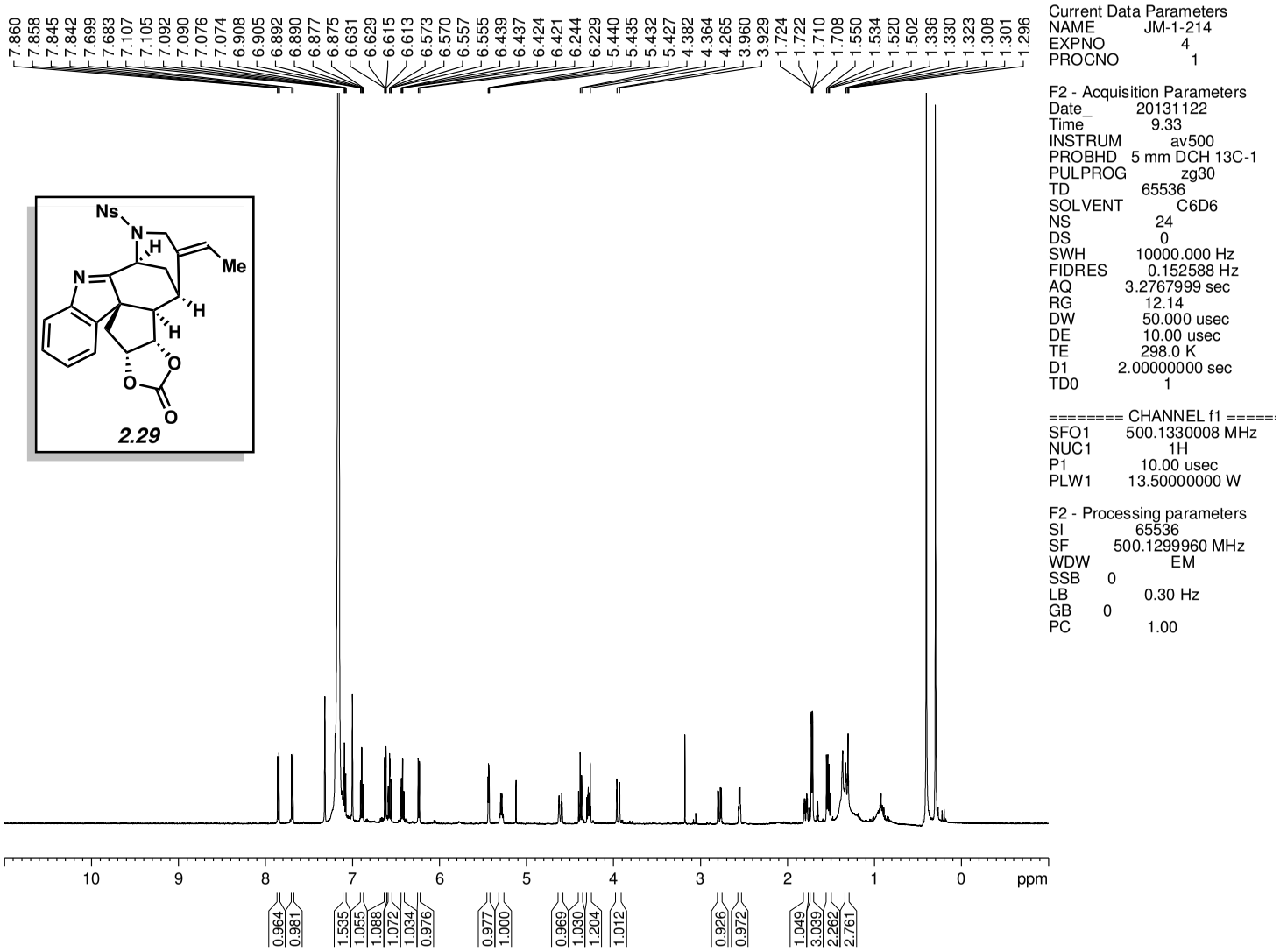

Figure 2.60 ^{1}H NMR (500 MHz, C_6D_6) of compound **2.29**.

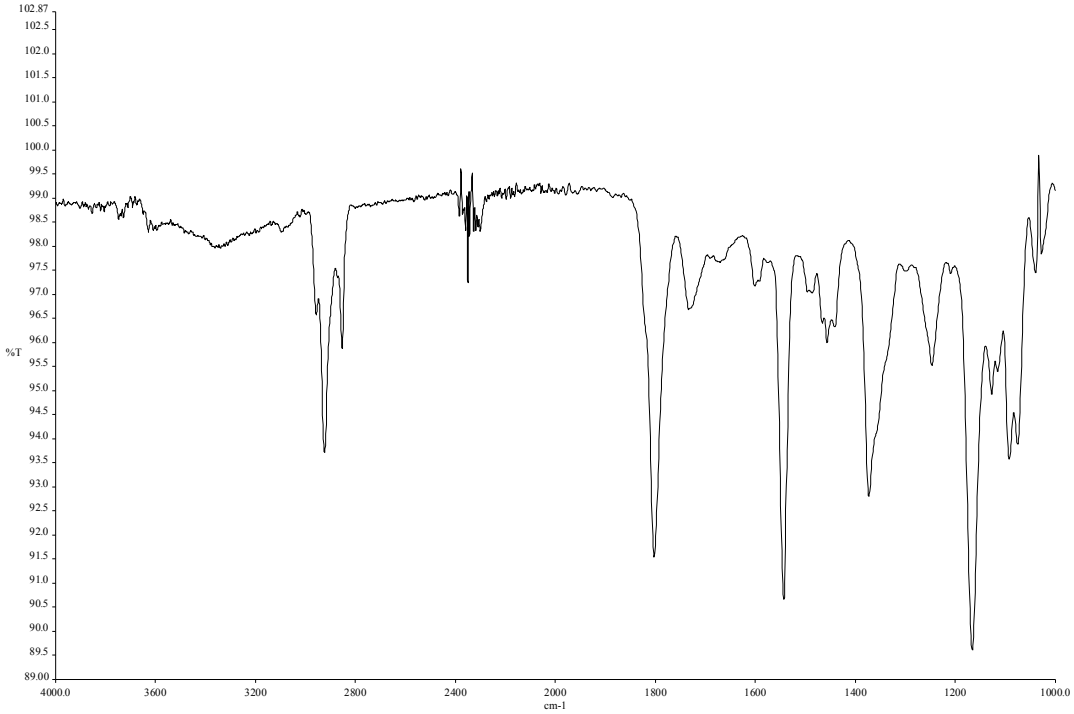

Figure 2.61 Infrared spectrum of compound **2.29**.

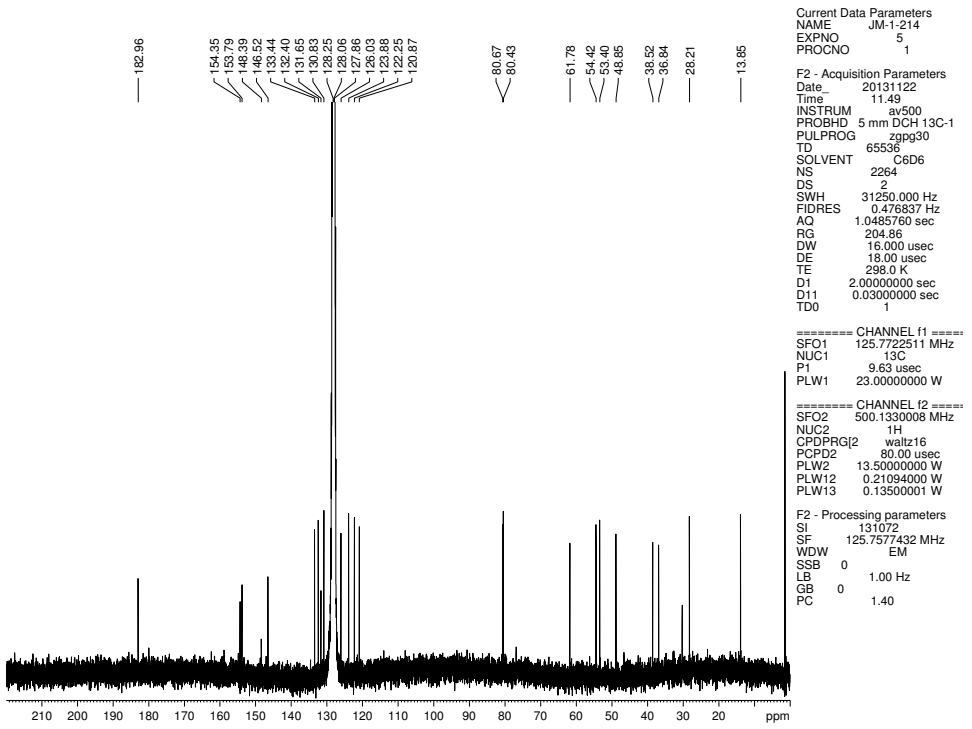

Figure 2.62 ^{13}C NMR (125 MHz, C_6D_6) of compound **2.29**.

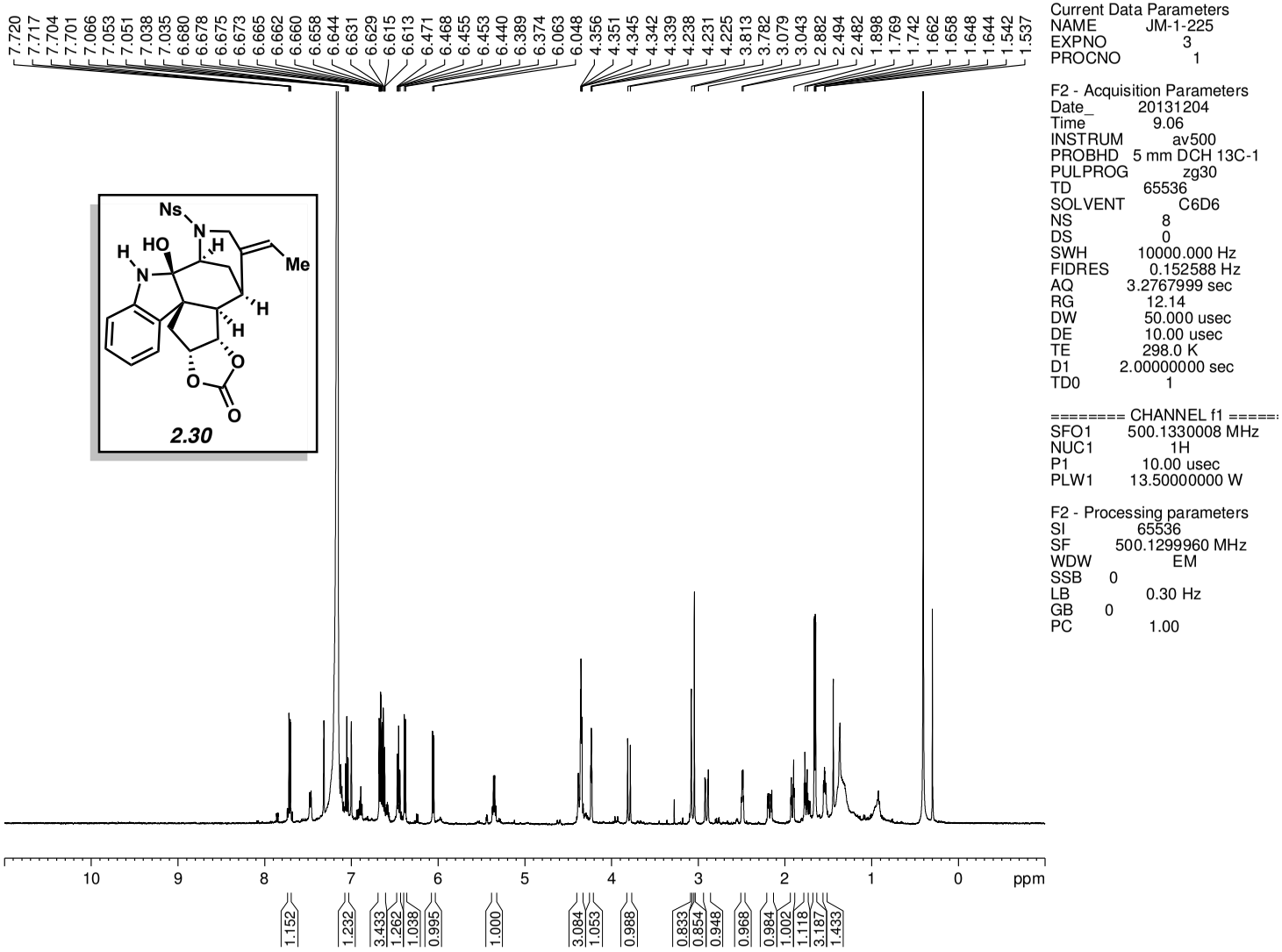

Figure 2.63 ^{1}H NMR (500 MHz, C_6D_6) of compound **2.30**.

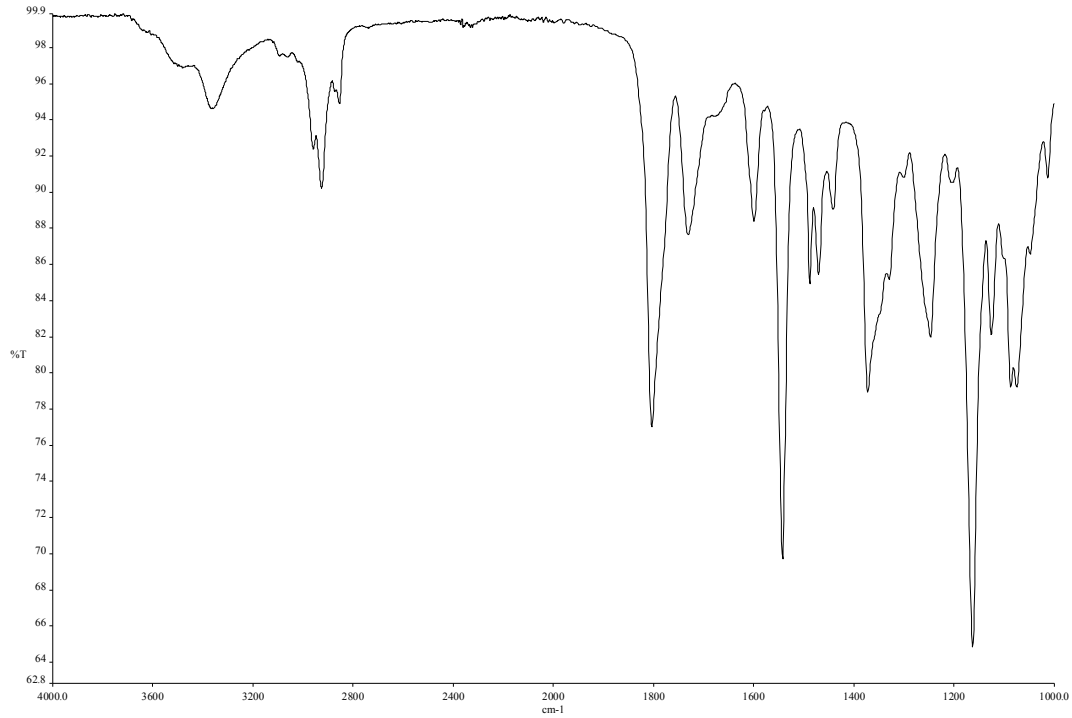

Figure 2.64 Infrared spectrum of compound **2.30**.

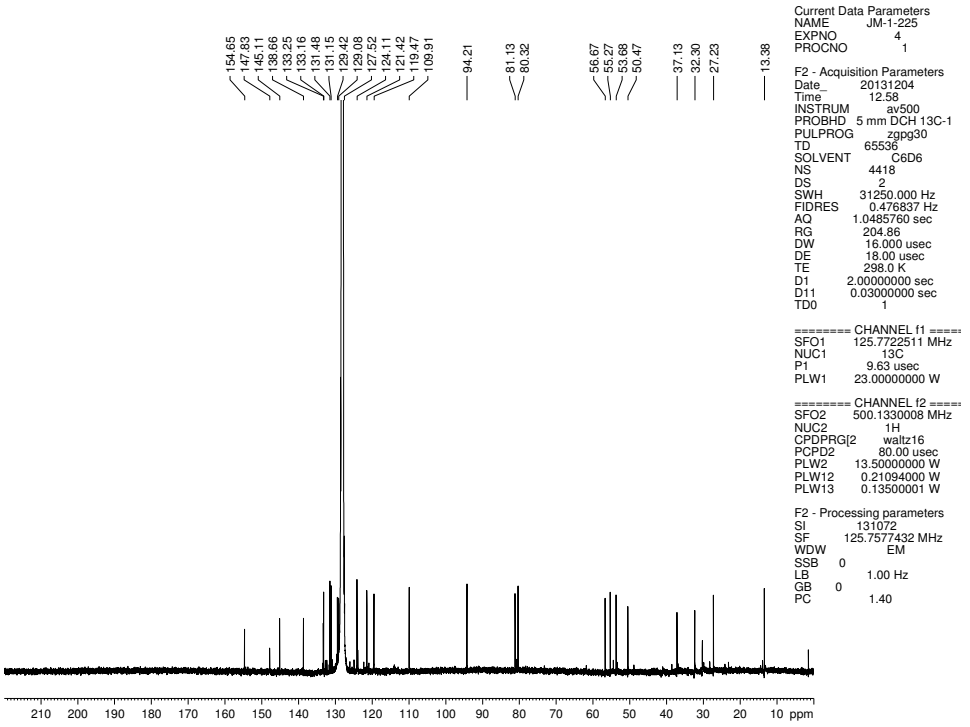

Figure 2.65 ^{13}C NMR (125 MHz, C_6D_6) of compound **2.30**.

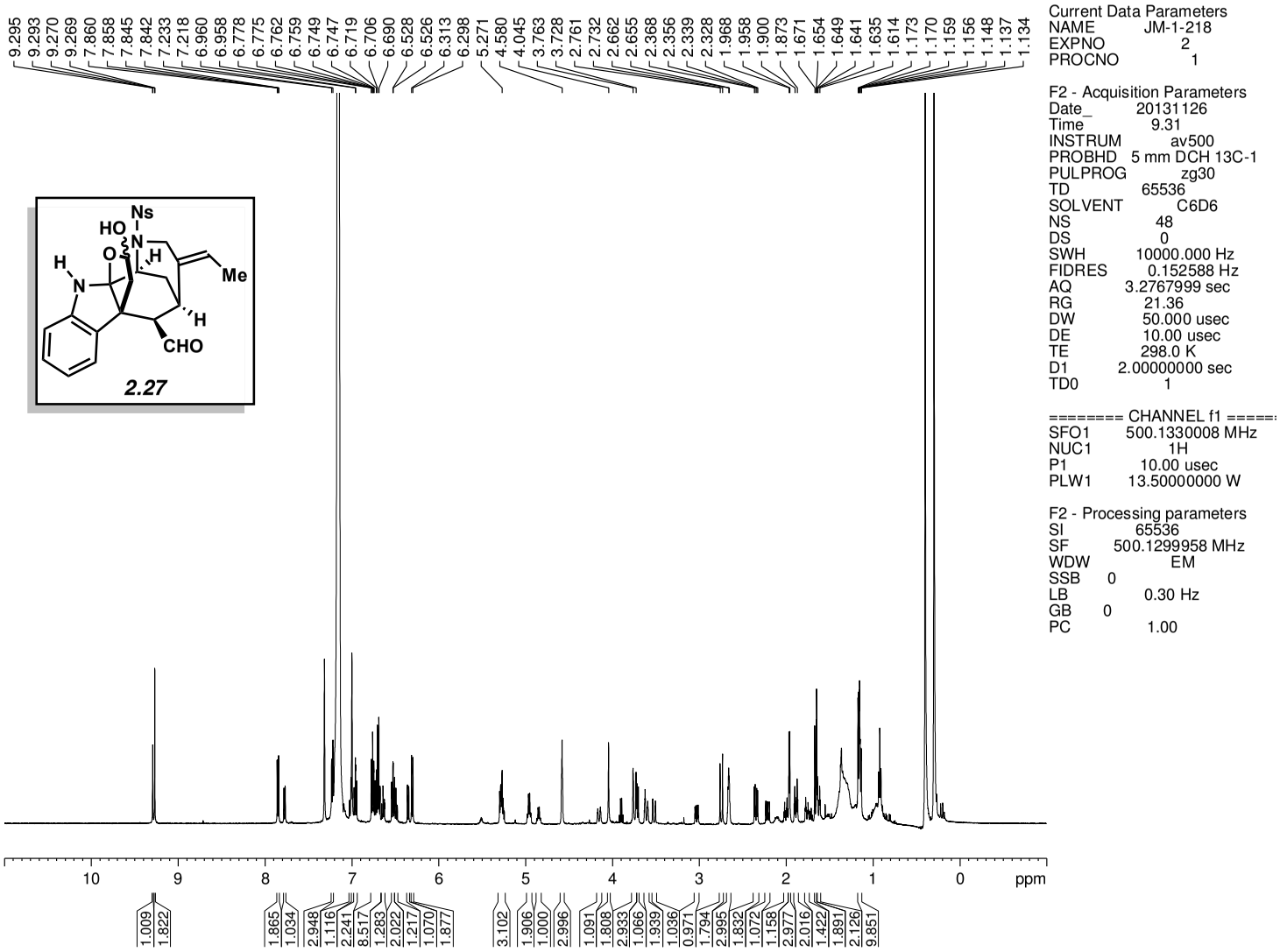

Figure 2.66 ^{1}H NMR (500 MHz, C_6D_6) of compound **2.27**.

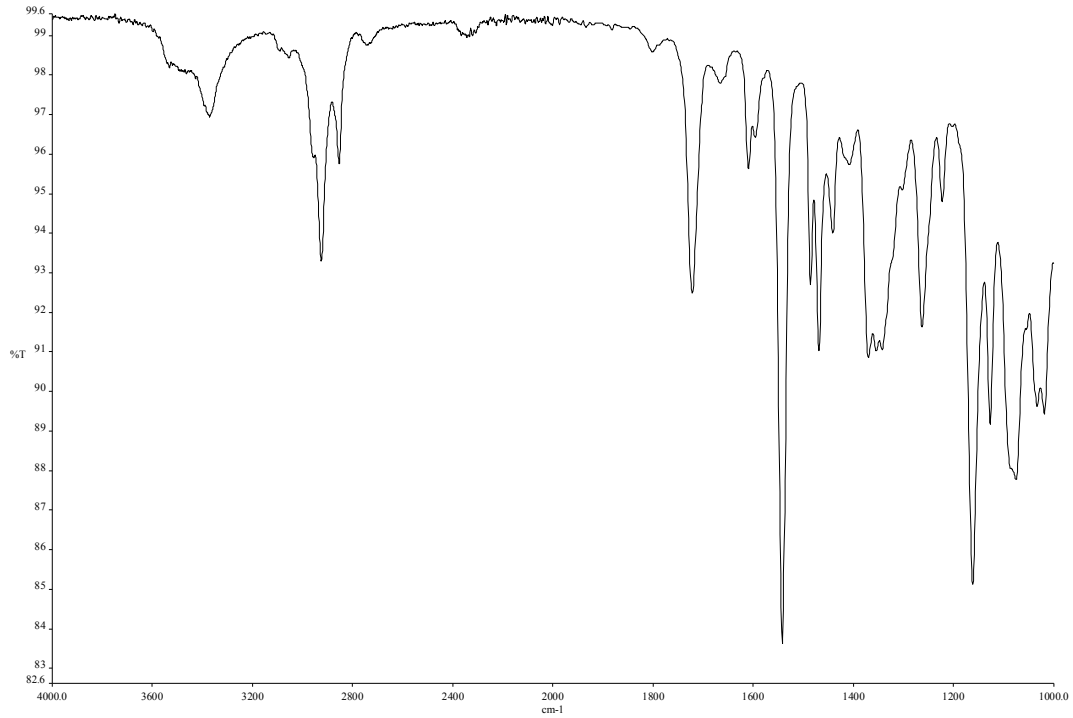

Figure 2.67 Infrared spectrum of compound **2.27**.

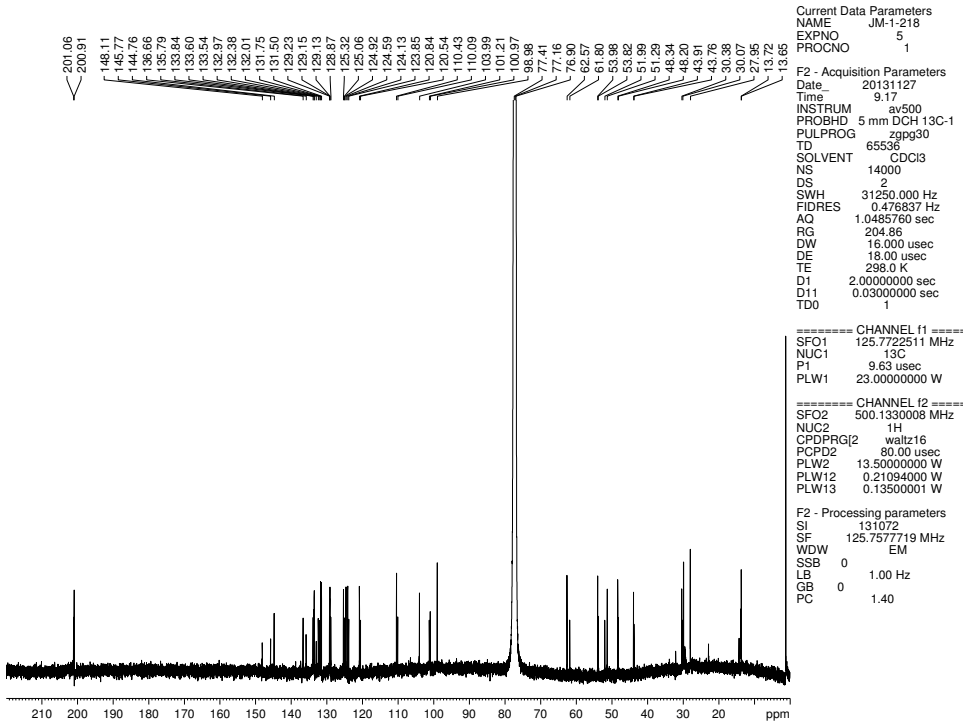

Figure 2.68 ^{13}C NMR (125 MHz, $CDCl_3$) of compound **2.27**.

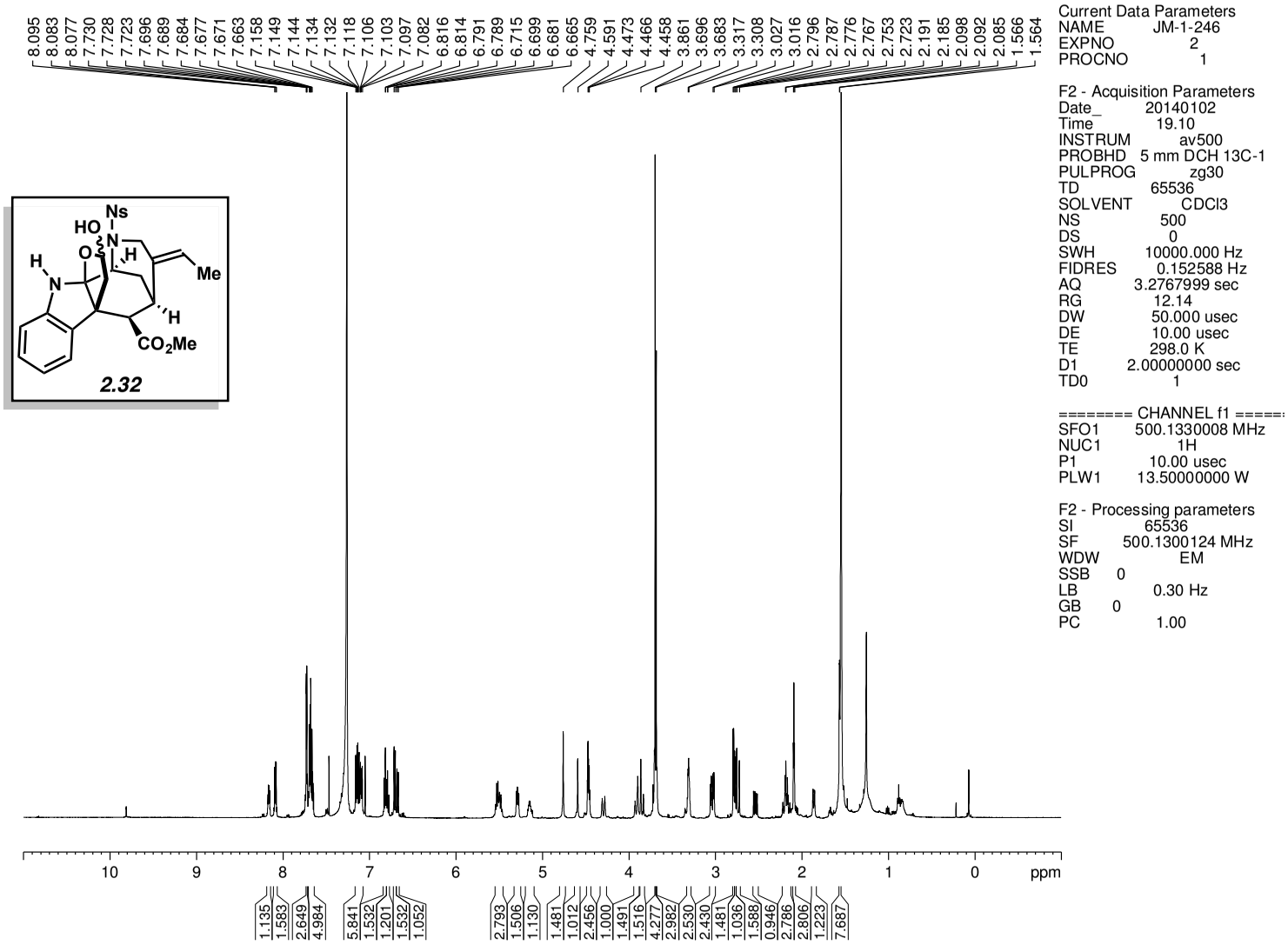

Figure 2.69 ^{1}H NMR (500 MHz, $CDCl_3$) of compound **2.32**.

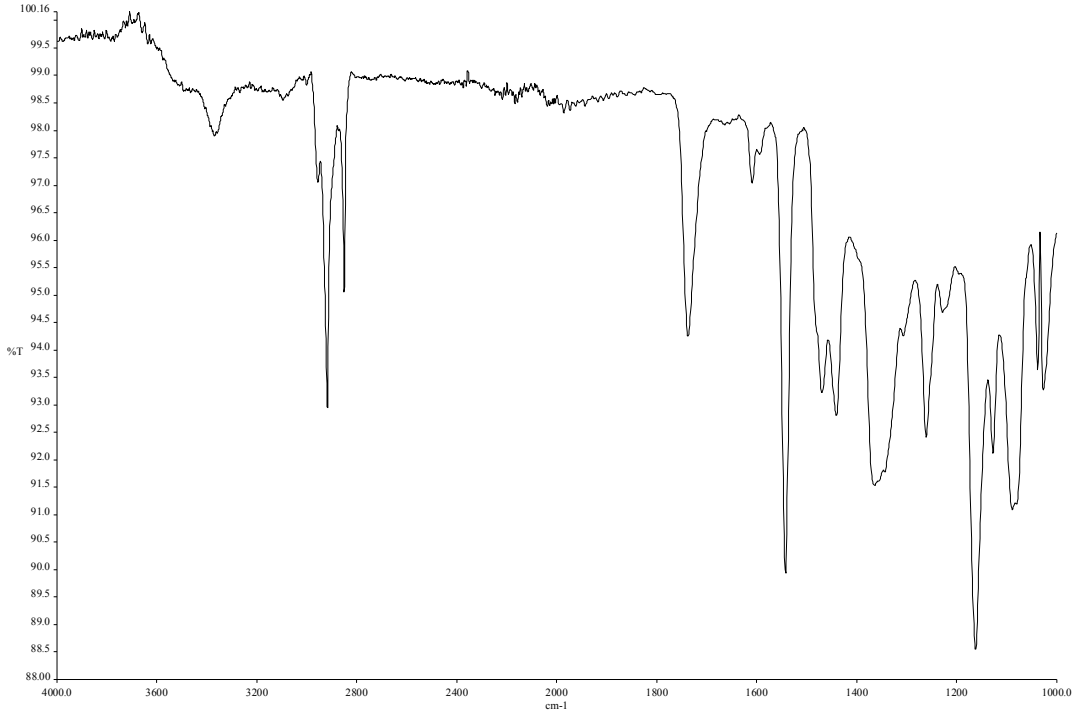

Figure 2.70 Infrared spectrum of compound **2.32**.

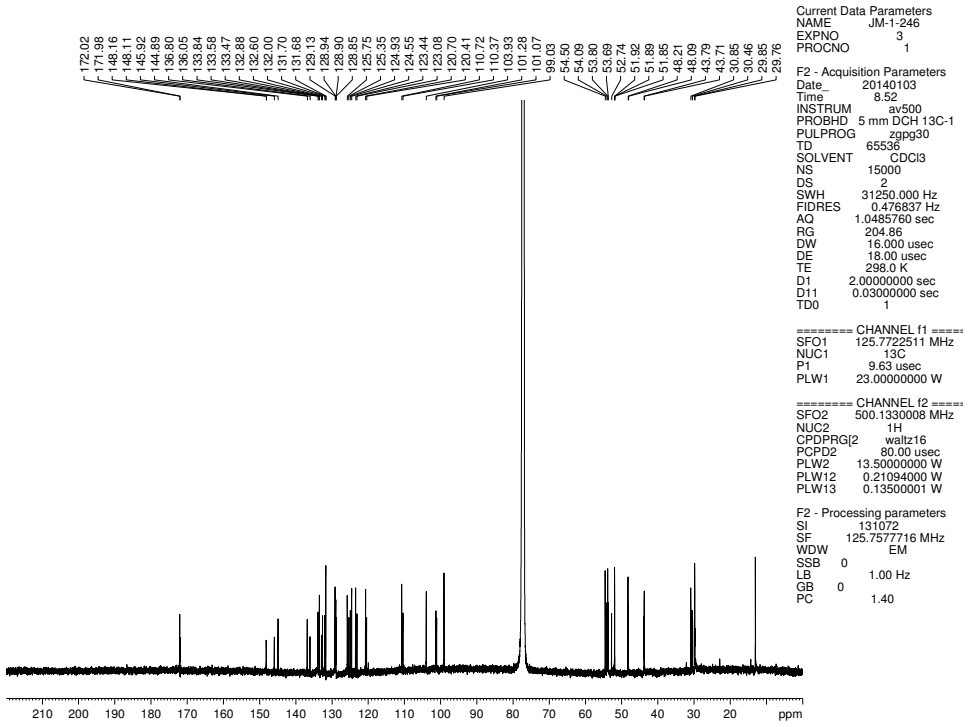

Figure 2.71 ^{13}C NMR (125 MHz, $CDCl_3$) of compound **2.32**.

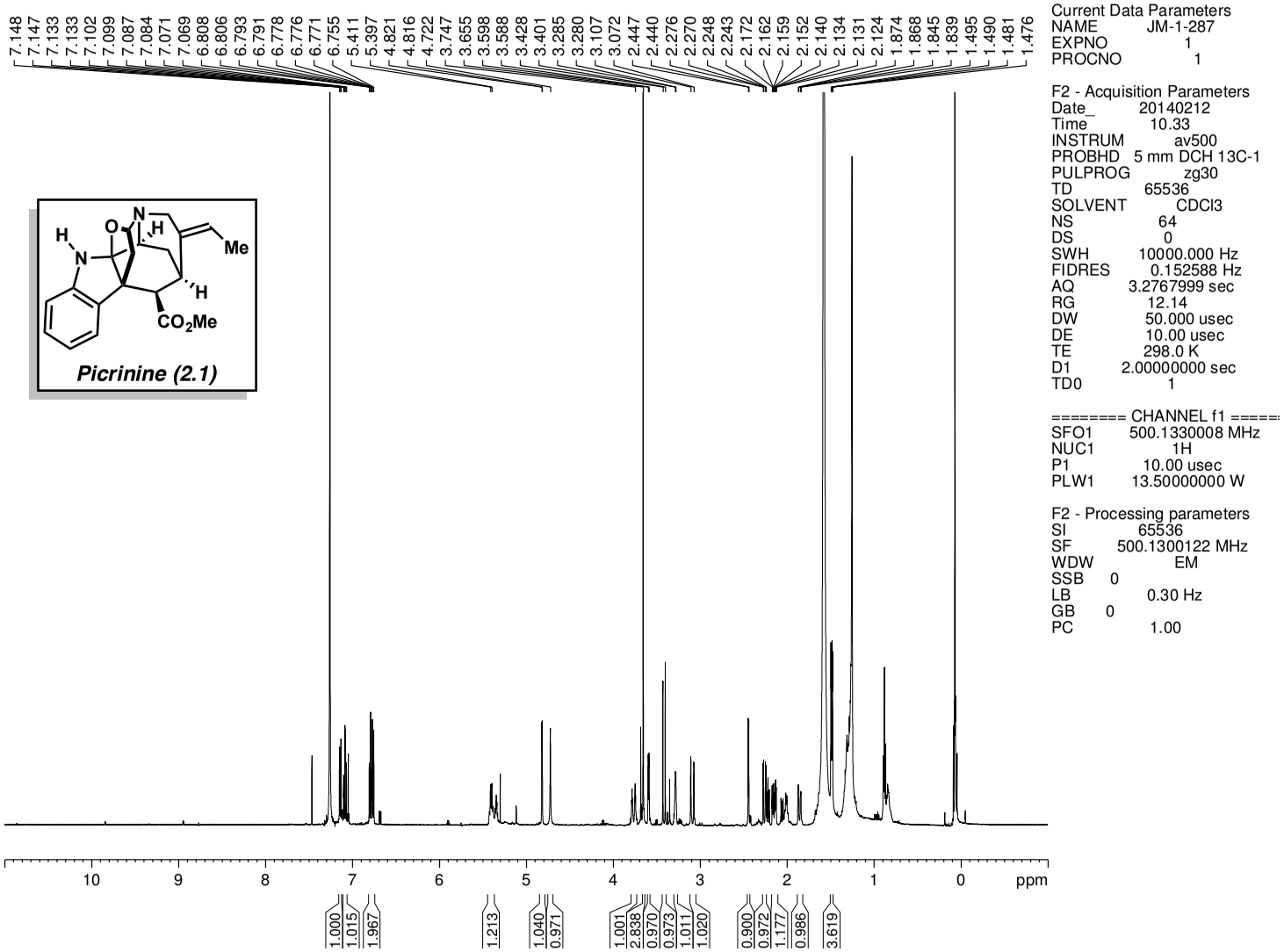

Figure 2.72 ^{1}H NMR (500 MHz, $CDCl_3$) of compound **2.1**.

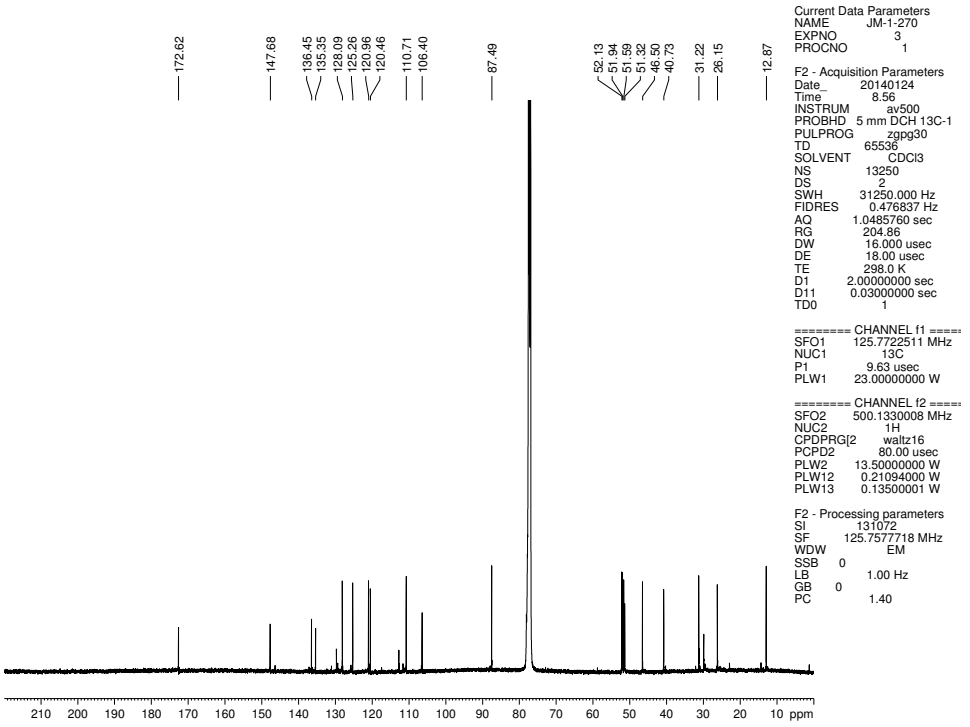

Figure 2.73 ^{13}C NMR (125 MHz, $CDCl_3$) of compound **2.1**.

2.11 Notes and References

(1) Smith, J. M.; Moreno, J.; Boal, B. W.; Garg, N. K. *J. Org. Chem.* **2015**, *80*, 8954–8967.

(2) For an example of an oxidative cleavage cascade, see: Wagnières, O.; Xu, Z.; Wang, Q.; Zhu, J. *J. Am. Chem. Soc.* **2014**, *136*, 15102–15108.

(3) Nagata, H.; Kawamura, M.; Ogasawara, K. *Synthesis* **2000**, *13*, 1825–1834.

(4) Sulfonamide **60** is commercially available from Aurora Fine Chemicals LLC (CAS No. 115462-23-0) or can be readily prepared in two steps from trans-4-aminocyclohexanol•HCl.

(5) Rawal, V. H.; Michoud, C. *Tetrahedron Lett.* **1991**, *32*, 1695–1698.

(6) For related Pd-catalyzed cyclizations, see: (a) Sole, D.; Piedro, E.; Bonjoch, J. *Org. Lett.* **2000**, *2*, 2225−2228. (b) Liao, X.; Zhou, H.; Yu, J.; Cook, J. M. *J. Org. Chem.* **2006**, *71*, 8884−8890.

(c) Dounay, A. B.; Humphreys, P. G.; Overman, L. E.; Wrobleski, A. D. *J. Am. Chem. Soc.* **2008**, *130*, 5368−5377.

(7) Nicolaou, K. C.; Montagnon, T.; Baran, P. S. *Angew. Chem., Int. Ed.* **2002**, *41*, 993−996.

(8) For preparation of the stannane, see: (a) Danheiser, R. L.; Romines, K. R.; Koyama, H.; Gee, S. K.; Johnson, C. R.; Medlich, J. R. *Org. Syn.* **1993**, *71*, 133–139. For use of the reagent, see: (b) Buchanan, G. S.; Cole, K. P.; Tang, Y.; Hsung, R. P. *J. Org. Chem.* **2011**, *76*, 7027–7039.

(9) For the original Dauben oxidation, see: Dauben, W. G.; Michno, D. M. *J. Org. Chem.* **1977**, *42*, 682–685.

(10) Shibuya, M.; Ito, S.; Takahashi, M.; Iwabuchi, Y. *Org Lett.* **2004**, *6*, 4303–4306.

(11) Shibuya, M.; Tomizawa, M.; Iwabuchi, Y. *J. Org. Chem.* **2008**, *73*, 4750–4752.

(12) Nagaoka, H.; Kobayashi, K.; Matsui, T.; Yamada, Y. *Tetrahedron Lett.* **1987**, *28*, 2021–2023.

(13) Zhang, P.; Morken, J. P. *J. Am. Chem. Soc.* **2009**, *131*, 12550–12551.

(14) Campagnole, M.; Delmond, B. *Synth. Commun.* **2007**, *37*, 1077–1090.

(15) Reed, K. L.; Gupton, J. T.; Solarz, T. L. *Synth. Commun.* **1989**, *19*, 3579−3587.

(16) Newton, R. F.; Wadsworth, A. H. *J. Chem. Soc., Perkin Trans. 1* **1982**, 823−830.

(17) For a review, see: (a) Deutsch, C.; Krause, N.; Lipshutz, B. *Chem. Rev.* **2008**, *108*, 2916–2927. For examples, see: (b) Mahoney, W. S.; Brestensky, D. M.; Stryker, J. M. *J. Am. Chem. Soc.* **1988**, *110*, 291–293. (c) Baker, B. A.; Bošković, Ž. V.; Lipshutz, B. H. *Org. Lett.* **2008**, *10*, 289-292. See also reference 3.

(18) Ojima, I.; Kogure, T. *Organometallics* **1982**, *1*, 1390–1399.

(19) Keinan, E.; Gleize, P. A. *Tetrahedron Lett.* **1982**, *23*, 477−480.

(20) For the effect of silyl groups on controlling diastereoselective protonation, see: (a) Bouzide, A. *Org. Lett.* **2002**, *4*, 1347–1350. (b) Rodrigues Jr., M. T.; Gomes, J. C.; Smith, J.; Coelho, F. *Tetrahedron Lett.* **2010**, *51*, 4988–4990.

(21) Hénon, H.; Mauduit, M.; Alexakis, A. *Angew. Chem., Int. Ed.* **2008**, *47*, 9122−9124.

(22) Sabahi, A.; Novikov, A.; Rainier, J. D. *Angew. Chem., Int. Ed.* **2006**, *45*, 4317–4320.

(23) (a) Jabri, S. Y.; Overman, L. E. *J. Org. Chem.* **2013**, *78*, 8766–8788. (b) He, F.; Bo, Y.; Altom, J. D.; Corey, E. J. *J. Am. Chem. Soc.* **1999**, *121*, 6771–6772.

(24) Yang, D.; Zhang, C. *J. Org. Chem.* **2001**, *66*, 4814–4818.

(25) Akbutina, F. A.; Torosyan, S. A.; Vyrypaev, E. M.; Furlei, I. I.; Miftakhov, M. S. *Russ. J. Org. Chem.* **1999**, *35*, 1386–1387.

(26) VanRheenen, V.; Kelly, R. C.; Cha, D. Y. *Tetrahedron Lett*. **1976**, *17*, 1973–1976.

(27) Burk, R. M.; Roof, M. B. *Tetrahedron Lett*. **1993**, *34*, 395–398.

(28) Indolenine **2.29** and hydrate **2.30** readily interconverted in $CDCl_3$ or upon prolonged exposure to silica gel.

(29) For examples of the Fischer indolization being employed in late-stage total synthesis of complex alkaloids, see: (a) Zu, L.; Boal, B. W.; Garg, N. K. *J. Am. Chem. Soc.* **2011**, *133*, 8877−8879. (b) Adams, G. L.; Carroll, P. J.; Smith, A. B., III. *J. Am. Chem. Soc.* **2012**, *134*, 4037−4040. (c) Adams, G. L.; Carroll, P. J.; Smith, A. B., III. *J. Am. Chem. Soc.* **2013**, *135*, 519−528. (d) Ban, Y.; Sato, Y.; Inoue, I.; Nagai, M.; Oishi, T.; Terashima, M.; Yonemitsu, O.; Kanaoka, Y. *Tetrahedron Lett.* **1965**, *6*, 2261−2268. (e) Ueda, H.; Satoh, H.; Matsumoto, K.; Sugimoto, K.; Fukuyama, T.; Tokuyama, H. *Angew. Chem., Int. Ed.* **2009**, *48*, 7600−7603. (f) Satoh, H.; Ueda, H.; Tokuyama, H. *Tetrahedron* **2013**, *69*, 89−95.

(30) Yamashita, M.; Ohta, N.; Shimizu, T.; Matsumoto, K.; Matsuura, Y.; Kawasaki, I.; Tanaka, T.; Maezaki, N.; Ohta, S. *J. Org. Chem.* **2003**, *68*, 1216−1224.

(31) Foos, J.; Steel, F.; Rizvi, S. Q. A.; Fraenkel, G. *J. Org. Chem.* **1979**, *44*, 2522−2529.

(32) (a) For the removal of nosyl groups using a solid-supported thiol reagent, see: Cardullo, F.; Donati, D.; Merlo, G.; Paio, A.; Salaris, M.; Taddei, M. *Synlett* **2005**, 2996−2998. (b) The thiol resin was obtained from SiliCycle Inc. (Product No. R51030B).

(33) (a) For the removal of nosyl groups using a solid-supported thiol reagent, see: Cardullo, F.; Donati, D.; Merlo, G.; Paio, A.; Salaris, M.; Taddei, M. *Synlett* **2005**, 2996−2998. (b) The thiol resin was obtained from SiliCycle Inc. (Product No. R51030B).

(34) Mass spectral analysis of the crude reaction mixture suggests that nosyl cleavage occurred. However, efforts to purify products formed in the reaction were unsuccessful.

(35) Kraus, G. A.; Roth, B. *J. Org. Chem.* **1980**, *45*, 4825−4830.

(36) Although the MetSThiol reagent is typically used as a metal scavenger, this is the first example of this resin being used for the cleavage of a nosyl group.

(37) Ferreira Batista, C. V.; Schripsema, J.; Verpoorte, R.; Rech, S. B.; Henriques, A. T. *Phytochemistry* **1996**, *41*, 969–973.

CHAPTER THREE

Enantioselective Total Syntheses of Akuammiline Alkaloids (+)-Strictamine, (–)-2(*S*)-Cathafoline, and (–)-Aspidophylline A

Adapted from: Jesus Moreno, Elias Picazo, Lucas A. Morrill, Joel M. Smith, and Neil K. Garg. *J. Am. Chem. Soc.* **2016**, *138*, 1162–1165.

3.1 Abstract

The akuammiline alkaloids are a family of natural products that have been widely studied for decades. Although notable synthetic achievements have been made recently, akuammilines that possess a methanoquinolizidine core have evaded synthetic efforts. We report an asymmetric approach to these alkaloids, which has culminated in the first total syntheses of (–)-2(*S*)-cathafoline and the long-standing target (+)-strictamine. Moreover, the first enantioselective total synthesis of aspidophylline A is described.

3.2 Introduction

The akuammiline alkaloids are a family of bioactive natural products that have been studied for over a century.[1] To date, over 30 akuammilines have been isolated, examples of which are shown in Figure 3.1 (**3.1–3.6**). These natural products can be divided into four structural subclasses, with completed total syntheses recently reported in three of these categories. Aspidophylline A (**3.3**), an example of the furoindoline-containing subclass, has been accessed synthetically by our group,[2] Zhu's,[3] and Ma's.[4] In addition, our laboratory has completed the total

synthesis of picrinine (**3.6**), a C5-oxidized akuammiline.[5] With regard to the skeletally-rearranged akuammilines, breakthroughs include total syntheses of vincorine (**3.4**) by Qin,[6] Ma,[7] and MacMillan,[8] and total syntheses of scholarisine A (**3.5**) by Smith[9] and Snyder.[10]

Despite these synthetic triumphs, one structural subclass of the akuammilines has remained inaccessible. Namely, compounds that possess a methanoquinolizidine core have not yet succumbed to total synthesis. We have targeted the total synthesis of two such alkaloids: strictamine (**3.1**) and 2(*S*)-cathafoline (**3.2**), isolated in 1966[11] and 2014,[12] respectively. As a salient feature of their caged methanoquinolizidine cores, each of these natural products also contains a densely-functionalized cyclohexane ring that is part of two conjoined [3.3.1]-azabicycles. Strictamine (**3.1**) possesses an indolenine motif and four stereocenters, whereas 2(*S*)-cathafoline (**3.2**) bears an indoline unit and five contiguous stereocenters. The rich history, structural complexity, and bioactivity[13] of **3.1** have prompted many synthetic efforts beginning with seminal studies by Dolby and Bosch and Bennasar.[14a–d] More recent approaches by the labs of Sakai,[14e] Cook,[14f] Tokuyama,[14g] Matsuo,[14h] and Zhu[14i] have also been put forward. Herein, we describe an enantioselective approach to several akuammilines, including family members that contain the elusive methanoquinolizidine core. These efforts result in the first enantioselective total synthesis of aspidophylline A (**3.3**), in addition to the first enantioselective total syntheses of strictamine (**3.1**) and 2(*S*)-cathafoline (**3.2**).

Figure 3.1 Representative Akuammiline Alkaloids **3.1–3.6**.

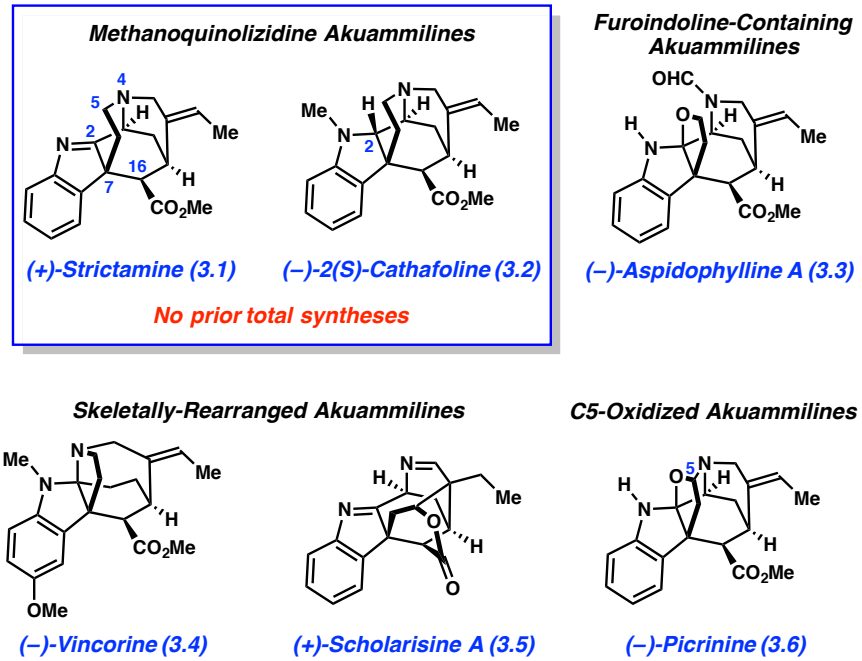

3.3 Retrosynthetic Analysis

Our retrosynthetic analysis for the enantioselective total syntheses of strictamine (**3.1**) and 2(*S*)-cathafoline (**3.2**) is shown in Scheme 3.1. It was envisioned that both natural products could be derived from tetracyclic chloride **3.8**. In the forward sense, late-stage deprotection and cyclization would forge the methanoquinolizidine core (see transition structure **3.7**).[15] In turn, chloride **3.8** would arise from methanolysis and subsequent chlorination of lactone **3.9**. This key late-stage compound would be accessed from phenylhydrazine (**3.11**) and ketolactone **3.12** using an uncommon reductive variant of the interrupted Fischer indolization reaction.[16,17,18] The success of this step would lead to the introduction of two new rings and two stereogenic centers, including the C2 stereocenter seen in 2(*S*)-cathafoline (**3.2**) (via transition structure **3.10**) and the challenging C7 quaternary center common to all akuammilines. Ketolactone **3.12**, which would also be a viable

intermediate toward aspidophylline A (**3.3**), would be prepared from enone **3.13**, the product of a gold-mediated cyclization[19] of enantioenriched silyl enol ether **3.14**.

Scheme 3.1 Retrosynthetic Analysis of Strictamine (**3.1**) and 2(*S*)-Cathafoline (**3.2**).

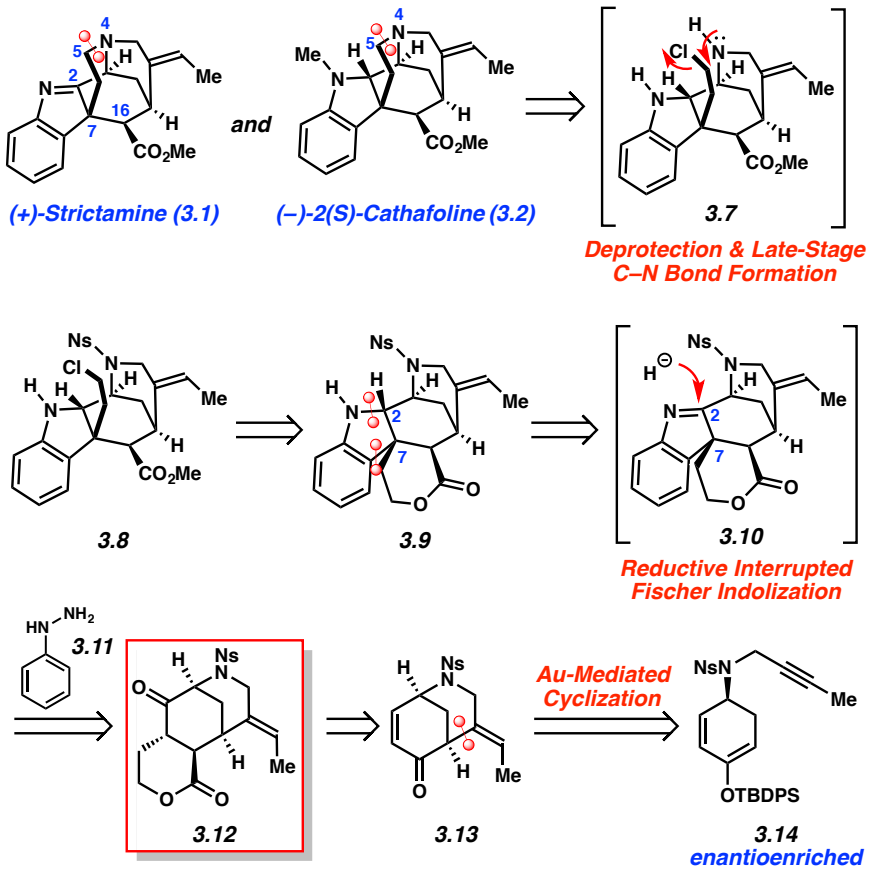

3.4 Robust Synthesis of [3.3.1]-Azabicyclic Core via a Gold-mediated Cyclization en Route to Enal 3.20

Our synthetic studies commenced with the asymmetric construction of the akuammiline [3.3.1]-azabicyclic core and the formation of enal **3.20** (Scheme 3.2). It is worth mentioning that the efforts to render this route robust and enantioselective were driven by my colleagues Joel Smith, Lucas Morrill and Elias Picazo. Beginning with dibenzoate **3.15**, a Trost

desymmetrization[20] was performed. In the event, dibenzoate **3.15** was treated with sulfonamide **3.16** in the presence of a suitable Pd precatalyst and (*R*, *R*)-DACH-phenyl Trost ligand. Direct saponification of the product furnished alcohol **3.17** in 89% yield. Subsequent oxidation delivered enone **3.18**, a crystalline compound that was deemed suitable for X-ray analysis.[21] By virtue of the heavy atom, it was found that the desired C3 stereocenter had been introduced in the Trost desymmetrization step. To attempt the key gold-mediated cyclization, ketone **3.18** was advanced to silyl enol ether **3.14**, which in turn was subjected to a modification of Li's cyclization conditions.[19] This transformation smoothly delivered a 10:1 mixture of isomeric bicyclic adducts **3.13** (96% ee) and **3.19**, even when performed on multigram scale. Although the bicycles were inseparable, exposure of the mixture to a previously established two step epoxidation / Wittig olefination sequence[5] allowed enantioenriched enal **3.20** to be isolated in 49% yield from silyl enol ether **3.14**.

Scheme 3.2 Asymmetric Synthesis of Enal **3.20**.

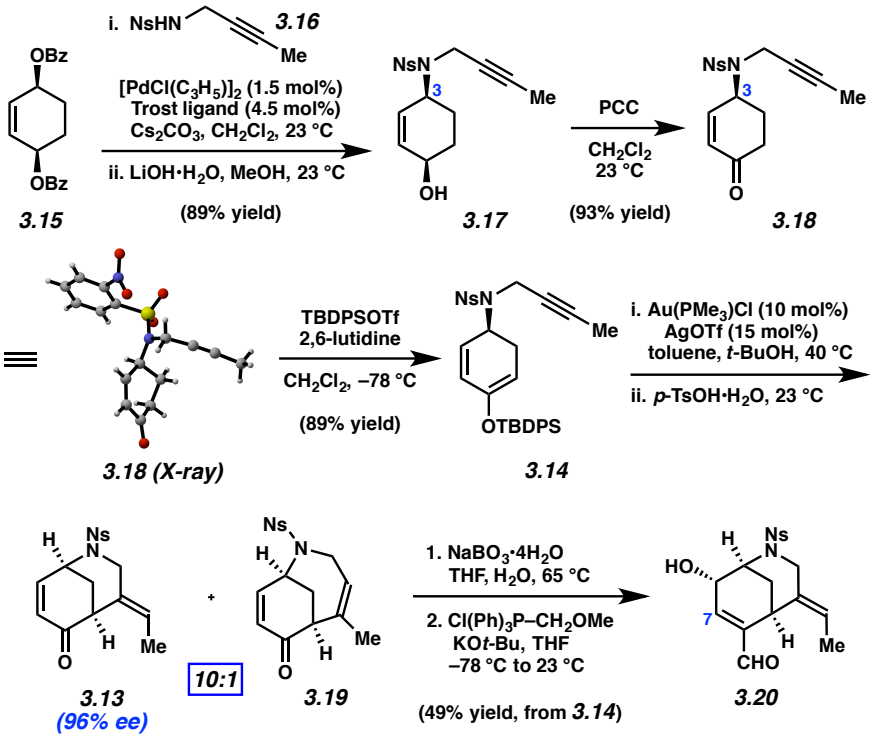

3.5 Access to Common Late-stage Intermediate 3.12 and Enantioselective Synthesis of (–)-Aspidophylline A (3.3)

With enal **3.20** in hand, our next task was to install a C7 alkyl substituent and access ketolactone **3.12** (Scheme 3.3). Toward this endeavor, enal **3.20** was first oxidized by NIS in the presence of potassium carbonate in methanol[22] to provide enoate **3.21**. Next, treatment of enoate **3.21** with ethyl vinyl ether (**3.22**) and NIS furnished an intermediate mixed acetal bearing an iodide,[23] thus setting the stage for a Ueno–Stork cyclization.[24] Exposure of this compound to radical cyclization conditions efficiently delivered C7-alkylated product **3.23** with diastereocontrol about the two newly formed stereocenters. From **3.23**, the desired ketolactone **3.12** could be readily accessed via a sequence involving hydrolysis and reduction (**3.23**→**3.24**), followed by lactonization and alcohol oxidation (**3.24**→**3.12**).[2]

Having accessed ketolactone **3.12** in an enantioenriched form, we opted to pursue the asymmetric total synthesis of aspidophylline A (**3.3**) (Scheme 3.3). As suggested earlier, three prior total syntheses of **3.3** have been reported, all of which deliver racemic material.[2,3,4] Analogous to our earlier efforts,[2] albeit with a nosyl protecting group instead of a tosyl group, ketolactone **3.12** was exposed to phenylhydrazine (**3.11**) and TFA to provide Fischer indolization adduct **3.25**. In the same pot, treatment of **3.25** with K_2CO_3 in methanol furnished furoindoline **3.27**, presumably via transition structure **3.26**. This transformation serves to introduce two new rings, four new bond linkages, and the challenging C7 quaternary stereocenter, all with complete diastereoselectivity. For reasons that shall soon become apparent, it should be noted that no evidence of epimerization at C16 is seen in this complexity-generating transformation. To complete the synthesis of (–)-aspidophylline A (**3.3**), interrupted Fischer indolization[25] adduct **3.27** underwent nosyl cleavage using a solid-supported thiol resin, followed by *N*-formylation.

Scheme 3.3 C7 Functionalization and Second-generation Synthesis of (–)-Aspidophylline A (**3.3**).

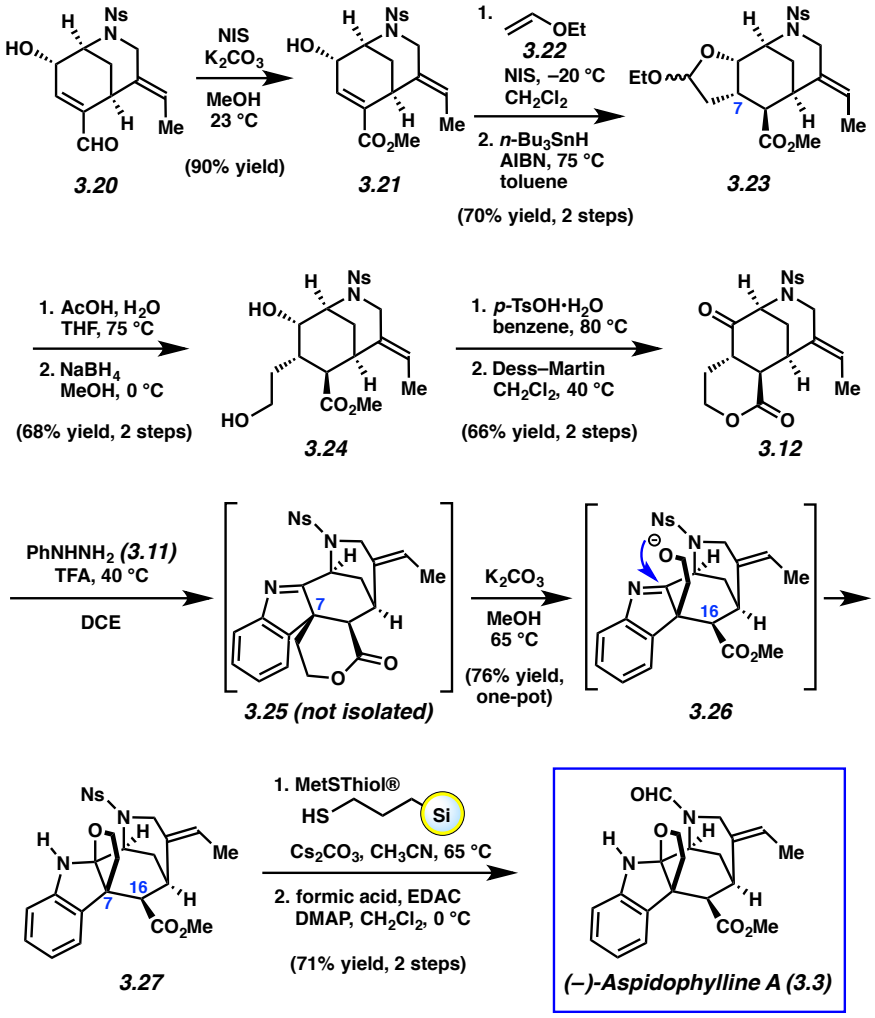

3.6 Reductive Interrupted Fischer Indolization, C16-Epimerization Challenges, and Ultimate Workaround

We next directed our attention to the methanoquinolizidine alkaloids, which have evaded prior synthetic efforts.[14] As shown in Scheme 3.4, Fischer indolization product **3.25** was accessed as demonstrated previously. However, this intermediate was directly intercepted by a hydride nucleophile. Interestingly, this process occurred in high yield and with complete control of

stereochemistry to give the depicted 2*S* diastereomer of product **3.9**. The overall conversion of **3.12** to **3.9** represents an uncommon reductive variant[18] of the interrupted Fischer indolization reaction, and is also one of the most complex examples[26] of this venerable synthetic method. It proceeds by introducing two stereocenters (at C2 and C7) and establishes an intricate pentacyclic framework bearing five contiguous stereocenters.

From product **3.9**, we pursued the seemingly simple conversion to hydroxyester **3.29** (Scheme 3.4). Despite that intermediate **3.25** readily underwent smooth ring-opening (see Scheme 3.3), we were disappointed to find that exposure of its reduced counterpart (**3.9**) to methoxide or two-step hydrolysis/methylation protocols failed to furnish **3.29**. Instead, C16 epimer **3.28** was formed. Exhaustive efforts to overcome this roadblock were undertaken. For example, epimerization under a variety of acidic or basic conditions, attempted lactone opening via amidation,[27] Pd-catalyzed ring-opening,[28] or S_N2 displacements,[29] all proved fruitless. With our best efforts thwarted, we pursued a more stepwise approach. Reduction of **3.9**, followed by selective silylation of the less hindered primary alcohol, proceeded without stereochemical erosion at C16 and gave alcohol **3.30**. Lastly, an oxidation/esterification sequence (**3.30**→**3.31**), with in situ desilylation, provided a reliable means to synthesize the coveted late-stage intermediate **3.29**. Of note, the Dess–Martin oxidation was achieved in the presence of the indoline, a conversion that was not possible when other oxidants were tried.

Scheme 3.4 Alternative Strategy to Access Hydroxyester **3.29**.

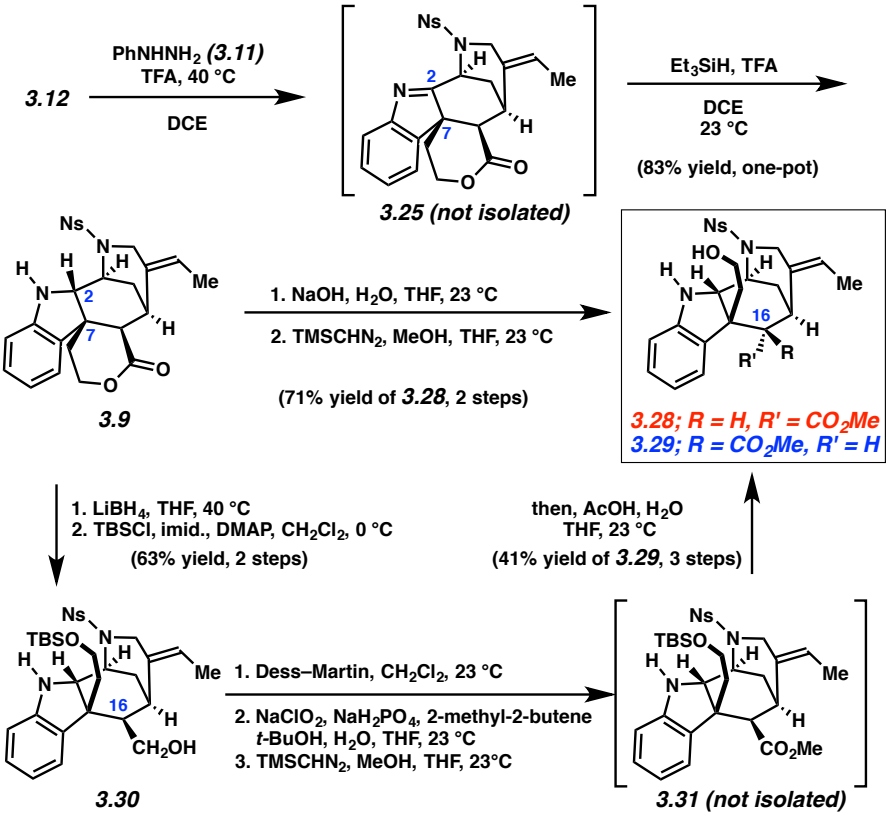

3.7 Divergent Syntheses of (+)-Strictamine and (–)-2(*S*)-Cathafoline

Having accessed alcohol **3.29**, we set our sights on accessing the elusive methanoquinolizidine alkaloids (Scheme 5). Initial efforts to elaborate aminoalcohol **3.29** without using protecting groups were deemed challenging. However, a mesylation / chlorination sequence[30] was found to be viable and delivered aminochloride **3.8** in 77% yield. To our delight, chloride **3.8** could be elaborated to strictamine (**3.1**) and 2(*S*)-cathafoline (**3.2**). The former of the natural products was accessed via oxidation of the indoline with PCC, followed by denosylation. To access 2(*S*)-cathafoline (**3.2**), an *N*-methylation / deprotection sequence was performed. In both cases, the denosylation step proceeded with the desired in situ chloride displacement by the

liberated amine to establish the hexacyclic methanoquinolizidine framework. NMR spectra of synthetic (+)-**3.1** and (–)-**3.2** were found to be in accord with spectra for the natural samples.

Scheme 3.5 Synthetic Endgame to Access **(+)**-Strictamine (**3.1**) and (–)-2(*S*)-Cathafoline (**3.2**).

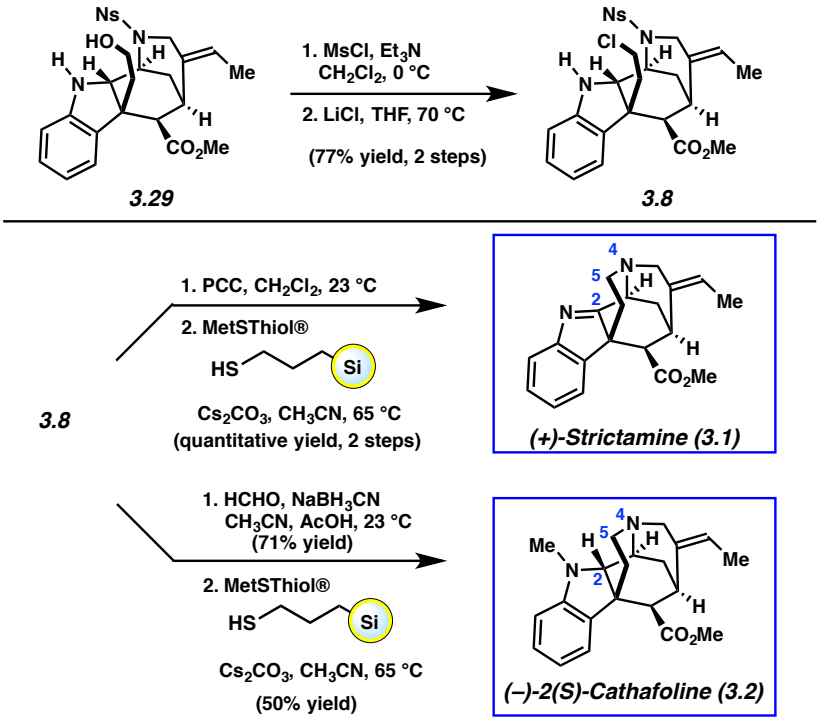

3.8 Conclusion

In summary, we have completed the first total syntheses of two akuammiline natural products that possess a methanoquinolizidine core. Our asymmetric approach to **3.1** and **3.2** features a gold-mediated cyclization to assemble the [3.3.1]-azabicyclic core of the natural products, a reductive interrupted Fischer indolization reaction to introduce the key C7 quaternary stereocenter and access late-stage compounds, and a series of carefully executed late-stage transformations to complete the total syntheses. Moreover, we have also completed the first enantioselective total synthesis of aspidophylline A (**3.3**). These studies constitute new

achievements in the popular area of akuammiline alkaloid synthesis, and provide many lessons that should impact future endeavors in the synthesis of complex molecules.

3.9 Experimental Section

3.9.1 Materials and Methods

Unless stated otherwise, reactions were conducted in flame-dried glassware under an atmosphere of nitrogen using anhydrous solvents (either freshly distilled or passed through activated alumina columns). Dess–Martin periodinane[31] and TBDPSOTf[32] were prepared from known literature procedures. $[Pd(C_3H_5)Cl]_2$ and $Au(PMe_3)Cl$ were obtained from Strem. $Cl(Ph)_3P–CH_2OMe$, KO*t*-Bu, and LiCl were dried *in vacuo* at 100 °C for 12 h prior to use. NIS was recrystallized from dioxane–CCl_4 prior to use. MsCl was distilled from P_2O_5 prior to use. $PhNHNH_2$ (**11**) was purified by flash chromatography (4:1 hexanes:EtOAc) prior to use. Solid supported thiol-resin MetSThiol® was obtained from SiliCycle (Product # R51030B). Unless stated otherwise, reactions were performed at room temperature (approximately 23 °C). Thin-layer chromatography (TLC) was conducted with EMD gel 60 F254 pre-coated plates (0.25 mm) and visualized using a combination of UV, anisaldehyde, $KMnO_4$, and iodine staining. SiliCycle silica gel 60 (particle size 0.040–0.063 mm) and Florisil® (60–100 mesh) was used for flash column chromatography. ^{1}H NMR spectra were recorded on a Bruker spectrometer (500 MHz). Data for ^{1}H spectra are reported as follows: chemical shift (δ ppm), multiplicity, coupling constant (Hz), integration and are referenced to the residual solvent peak 7.26 ppm for $CDCl_3$ and 7.16 ppm for C_6D_6. ^{13}C NMR spectra are reported in terms of chemical shift (at 125 MHz) and are referenced to the residual solvent peak 77.16 ppm for $CDCl_3$, and 128.06 for C_6D_6. IR spectra were recorded on a Perkin-Elmer 100 spectrometer and are reported in terms of frequency absorption (cm^{-1}).

Optical rotations were measured with a Rudolph Autopol III Automatic Polarimeter.[33] Uncorrected melting points were measured using a Mel-Temp II melting point apparatus with a Fluke 50S thermocouple and a Digimelt MPA160 melting point apparatus. High-resolution mass spectra were obtained from the UC Irvine and UCLA Mass Spectrometry Facilities. At UC Irvine, high resolution mass spectra were obtained on a Waters Micromass LCT Premier TOF Mass Spectrometer (Waters) equipped with a ZSpray source for electrospray ionization (ESI) and a time-of-flight (TOF) analyzer. The instrument was controlled by Waters MassLynx 4.0. At UCLA, DART-MS spectra were collected on a Thermo Exactive Plus MSD (Thermo Scientific) equipped with an ID-CUBE ion source and a Vapur Interface (IonSense Inc.). Both the source and MSD were controlled by Excalibur software v. 3.0. The analyte was spotted onto OpenSpot sampling cards (IonSense Inc.) Ionization was accomplished using UHP He (Airgas Inc.) plasma with no additional ionization agents. The mass calibration was carried out using Pierce LTQ Velos ESI (+) and (–) Ion calibration solutions (Thermo Fisher Scientific).

3.9.2 Experimental Procedures

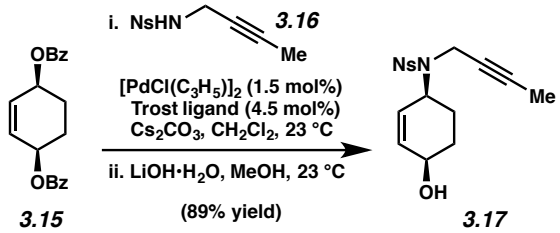

Alcohol 3.17. To a solution of $[Pd(C_3H_5)Cl]_2$ (0.353 g, 0.966 mmol), (*R*, *R*)-DACH-phenyl Trost ligand (2.00 g, 2.90 mmol), and Cs_2CO_3 (24.1 g, 74.0 mmol) in CH_2Cl_2 (380 mL) was added dibenzoate **3.15**[34] (21.7 g, 67.6 mmol) and sulfonamide **3.16**[35] (16.3 g, 64.3 mmol). After stirring for 5 h, $LiOH•H_2O$ (5.40 g, 128.7 mmol) and MeOH (380 mL) were added and the mixture was

stirred for an additional 12 h. The reaction was poured into a 7.0 pH buffer solution (300 mL), diluted with CH_2Cl_2 (300 mL), and the layers were separated. The aqueous layer was extracted with CH_2Cl_2 (4 x 150 mL) and the organic layers were combined, dried with Na_2SO_4, and concentrated under reduced pressure. The resulting residue was purified via flash chromatography (7:3 hexanes:EtOAc) to afford alcohol **3.17** (20.1 g, 89% yield) as a clear oil. Alcohol **3.17**: R_f 0.21 (3:7 hexanes:EtOAc); ^{1}H NMR (500 MHz, $CDCl_3$): δ 8.20–8.15 (m, 1H), 7.71–7.62 (m, 3H), 6.01–5.97 (m, 1H), 5.70 (d, *J* = 10.1, 1H), 4.52–4.47 (m, 1H), 4.15–4.10 (m, 1H), 4.09 (dq, *J* = 18.3, 2.3, 1H), 3.96 (dq, *J* = 18.3, 2.3, 1H), 2.09–2.00 (m, 1H), 1.90 (s, 1H), 1.89–1.84 (m, 1H), 1.83–1.75 (m, 2H) 1.60 (t, J = 2.3, 3H); ^{13}C NMR (125 MHz, $CDCl_3$): δ 148.1, 134.2, 133.6, 133.4, 131.64, 131.56, 131.4, 124.2, 81.1, 74.7, 62.6, 55.8, 34.2, 29.9, 22.9, 3.5; IR (film): 3367, 2946, 1542, 1438, 1371, 1165, 1123, 1071, 1025 cm^{-1}; HRMS–APCI (*m/z*) $[M + H]^+$ calcd for $C_{16}H_{19}N_2O_5S^+$, 351.10092; found, 351.10003; $[\alpha]^{25.1}_D$ –4.0° (c = 1.0, CH_2Cl_2).

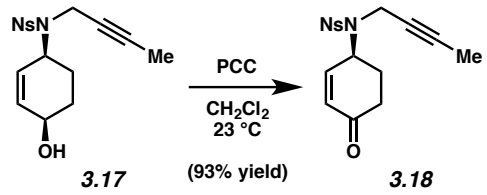

Enone 3.18. To a solution of alcohol **3.17** (22.5 g, 64.2 mmol) in CH_2Cl_2 (583 mL) was added PCC (20.8 g, 96.3 mmol). After stirring for 2.5 h, celite® (16 g) was added followed by Et_2O (80 mL). The mixture was filtered over a pad of celite® (40 g) and basic alumina (20 g), and then washed with EtOAc (750 mL). The filtrate was concentrated under reduced pressure and the resulting residue was purified via flash chromatography (1:9 benzene:EtOAc) to afford enone **3.18** (18.5 g, 93% yield) as a yellow solid. Crystals suitable for X-ray diffraction studies (CCDC 1440684) were obtained by slow mixing of **3.18** in a mixture of EtOAc and heptane. Enone **18**:

mp: 97–99 °C, R_f 0.68 (1:2 hexanes:EtOAc); ^{1}H NMR (500 MHz, $CDCl_3$): δ 8.24–8.20 (m, 1H), 7.77–7.69 (m, 3H), 6.92 (dt, *J* = 10.3, 2.0, 1H), 6.08 (ddd, *J* = 10.3, 2.7, 1.0, 1H), 5.03–4.98 (m, 1H), 4.08–4.04 (m, 2H), 2.61 (dt, *J* = 16.7, 4.1, 1H), 2.57–2.49 (m, 1H), 2.40–2.30 (m, 1H), 2.30–2.24 (m, 1H), 1.61 (t, *J* = 2.4, 3H); ^{13}C NMR (125 MHz, $CDCl_3$): δ 197.5, 150.8, 148.1, 134.0, 133.9, 132.0, 131.8, 131.7, 124.5, 82.3, 73.9, 55.9, 37.1, 34.6, 29.0, 3.5; IR (film): 2922, 1685, 1541, 1439, 1356, 1296, 1251, 1209, 1164, 1125, 1082, 1016 cm^{-1}; HRMS–APCI (*m/z*) $[M + H]^+$ calcd for $C_{16}H_{17}N_2O_5S^+$, 349.08527; found, 349.08457; $[\alpha]^{25.1}_D$ –40.3° (c = 1.0, CH_2Cl_2).

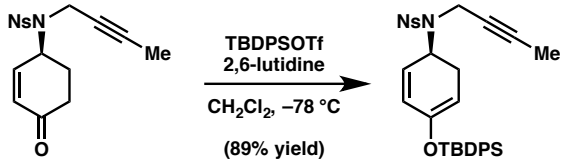

3.18 ***3.14***

Silyl Enol Ether 3.14. To a solution of enone **3.18** (11.0 g, 31.6 mmol) and 2,6-lutidine (4.4 mL, 37.9 mmol) in CH_2Cl_2 (105 mL) at –78 °C was added a freshly prepared solution of TBDPSOTf in CH_2Cl_2[32] (107 mL, 74.7 mmol; 0.7 M solution), by cannula over 20 min. Following the addition, the cooling bath was removed and the reaction was allowed to warm to room temperature. After stirring for 1 h, the reaction was quenched with sat. aq. $NaHCO_3$ (100 mL). The layers were separated and the aqueous layer was extracted with CH_2Cl_2 (3 x 100 mL). The organic layers were combined and rinsed sequentially with 10 wt% citric acid (100 mL), deionized water (100 mL), and sat. aq. NaCl (100 mL). The organic layers were then dried with $MgSO_4$ and concentrated under reduced pressure. The resulting residue was purified via flash chromatography (10:1 → 5:1 hexanes:EtOAc) to afford silyl enol ether **3.14** (16.5 g, 89% yield) as a white solid. Silyl enol ether **3.14**: mp: 101–103 °C, R_f 0.79 (1:1 hexanes:EtOAc); ^{1}H NMR (500 MHz, $CDCl_3$): δ 8.17–8.13 (m, 1H), 7.73–7.68 (m, 4H), 7.67–7.60 (m, 3H), 7.46–7.35 (m, 6H), 6.07 (dt, *J* = 10.1, 2.1, 1H),

5.64 (dd, J = 10.1, 4.8, 1H), 4.66–4.58 (m, 2H), 3.94 (dq, J = 18.3, 2.3, 1H), 3.73 (dq, J = 18.3, 2.3, 1H), 2.49 (ddd, J = 18.6, 10.6, 3.7, 1H), 2.39 (dt, J = 18.6, 5.4, 1H), 1.48 (t, J = 2.3, 3H), 1.03 (s, 9H); ^{13}C NMR (125 MHz, $CDCl_3$): (25 of 26 signals observed) δ 148.1, 146.5, 135.64, 135.58, 134.6, 133.4, 132.93, 132.89, 131.8, 131.4, 130.4, 130.0, 127.88, 127.86, 125.5, 124.1, 102.0, 80.4, 74.9, 50.4, 34.4, 27.8, 26.6, 19.3, 3.5; IR (film): 2927, 2856, 1543, 1428, 1403, 1359, 1236, 1165, 1113, 1070 cm^{-1}; HRMS–APCI (*m/z*) $[M + H]^+$ calcd for $C_{32}H_{35}N_2O_5SiS^+$, 587.20305; found, 587.20078; $[\alpha]^{25.1}_D$ –72.0° (c = 0.10, CH_2Cl_2).

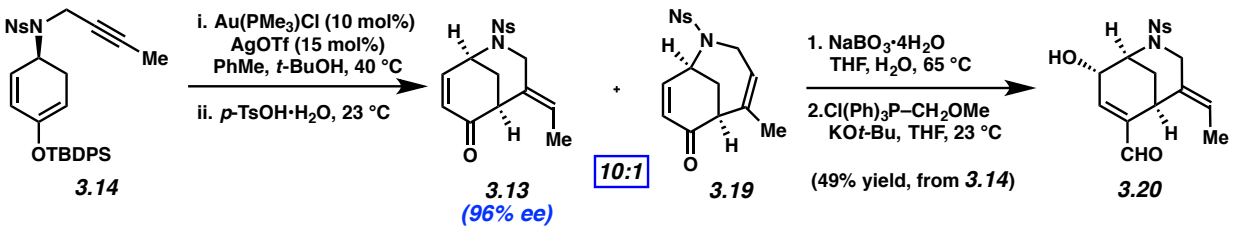

Enal 3.20. To a solution of $Au(PMe_3)Cl$ (91.0 mg, 0.294 mmol) and silyl enol ether **3.14** (1.72 g, 2.94 mmol) in toluene (76 mL) and *t*-BuOH (8 mL) was added AgOTf (113 mg, 0.441 mmol). The reaction was heated to 40 °C. After stirring for 3.5 h, *p*-TsOH•H_2O (559 mg, 2.94 mmol) was added. After stirring for an additional 15 min, the reaction was filtered through celite® (2.5 g) and poured into a mixture of sat. aq. NaCl (25 mL) and sat. aq. $NaHCO_3$ (25 mL). The layers were separated. The aqueous layer was extracted with EtOAc (4 x 20 mL) and the organic layers were combined, dried with $MgSO_4$, and concentrated under reduced pressure. The resulting residue was purified via flash chromatography (3:2 hexanes:EtOAc) to afford an inseparable mixture of isomeric enones **3.13** and **3.19** (1.02 g, 2.94 mmol; 10:1 ratio of **3.13** to **3.19**) as a clear oil. Enones **3.13** and **3.19** were analyzed as a mixture using ^{1}H and ^{13}C NMR spectroscopy. For the preparation of an analytical sample of enone **3.13** used in the determination of enantiomeric excess, see Section

3.9.3 (page 165). Enone **3.13**: R_f 0.48 (1.5:1 hexanes:EtOAc); ^{1}H NMR (500 MHz, $CDCl_3$): δ 8.07 (dd, *J* = 7.4, 1.9, 1H), 7.76–7.66 (m, 3H), 6.86–6.79 (m, 1H), 6.25 (dd, *J* =10.0, 0.8, 1H), 5.58 (qd, *J* = 6.9, 1.4, 1H), 4.74 (quint., *J* = 2.9, 1H), 4.00 (d, *J* = 14.6, 1H), 3.84 (dt, *J* = 14.6, 2.0, 1H), 3.66 (t, *J* = 2.9, 1H), 2.36 (dt, *J* = 13.0, 3.2, 1H), 2.05 (dq, *J* = 13.0, 2.9, 1H), 1.72 (dd, *J* = 6.8, 2.2, 3H); ^{13}C NMR (125 MHz, $CDCl_3$): δ 197.2, 147.9, 142.3, 134.1, 133.1 (2 carbons), 132.1, 130.9, 128.0, 124.8, 124.7, 47.5, 47.1, 44.2, 32.8, 12.9. Enone **3.19**: R_f 0.48 (1.5:1 hexanes:EtOAc); δ 8.11 (dd, *J* = 7.1, 2.2, 1H), 7.76–7.66 (m, 3H), 6.86–6.79 (m, 1H), 6.41 (d, *J* =10.2, 1H), 5.64 dq, *J* = 7.6, 1.3, 1H), 4.86 (t, *J* = 4.9, 1H), 4.04–4.00 (d, 1H), 3.66–3.60 (dt, 1H), 3.10 (dd, *J* = 5.1, 1.5, 1H), 2.41 (dt, *J* = 14.5, 5.2, 1H), 2.30 (dq, *J* = 14.5, 1.9, 1H), 1.88 (t, *J* = 1.7, 3H); ^{13}C NMR (125 MHz, $CDCl_3$): (15 of 16 signals observed) δ 192.5, 143.2, 139.8, 136.5, 134.9, 134.0, 133.4, 132.1, 131.3, 127.8, 124.3, 51.3, 49.4, 42.3, 27.6.

To the mixture of enones **3.13** and **3.19** (1.02 g, 2.94 mmol) in 1:1 THF:H_2O (15 mL) was added $NaBO_3$•$4H_2O$ (1.40 g, 9.11 mmol). The reaction was heated to 65 °C. After stirring for 1 h, the reaction was cooled to room temperature and poured into deionized water (150 mL) and diluted with EtOAc (150 mL). The layers were separated and the aqueous layer was extracted with EtOAc (3 x 150 mL). The organic layers were combined, dried over $MgSO_4$, and evaporated under reduced pressure to afford the corresponding epoxides. The material was used in the subsequent step without further purification.

A round-bottom flask was charged with $Cl(Ph)_3P–CH_2OMe$ (1.56 g, 4.99 mmol) and KO*t*-Bu (560 mg, 4.99 mmol), placed under N_2 pressure, and THF (25 mL) was added. The solution was stirred for 30 min, at which point a solution of the substrate obtained in THF (5 mL) was added dropwise over 1 min. The mixture was stirred for 1 h and quenched with a solution of sat. aq. NH_4Cl (30 mL). The resulting mixture was poured into deionized water (150 mL) and diluted

with EtOAc (150 mL). The layers were separated and the aqueous layer was extracted with EtOAc (3 x 150 mL). The organic layers were combined, dried over $MgSO_4$, and evaporated under reduced pressure. The resulting residue was purified via flash chromatography (99:1 → 2:3 hexanes:EtOAc) to afford enal **20** (542 mg, 49% yield from silyl enol ether **3.14**). Enal **3.20**: $[\alpha]^{23.1}_D$ +160.80° (c = 1.0, CH_2Cl_2). Characterization data for racemic enal **3.20** have been previously reported (see Chapter Two, Section 2.9.2, page 61)[5]

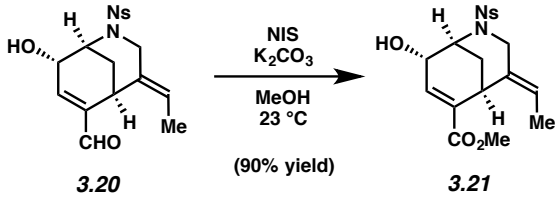

3.20 *3.21*

Enoate 3.21. To a solution of enal **3.20** (9.9 g, 26.2 mmol) in MeOH (262 mL) was added NIS (4.90 g, 21.8 mmol) and K_2CO_3 (3.01 g, 21.8 mmol). Following 1 h of stirring, additional NIS (4.90 g, 21.8 mmol) and K_2CO_3 (3.01 g, 21.8 mmol) were added. After an additional 2 h, NIS (4.90 g, 21.8 mmol) and K_2CO_3 (3.01 g, 21.8 mmol) were added. Following 30 min of additional stirring, the reaction was quenched with aqueous $Na_2S_2O_3$ (300 mL) and diluted with EtOAc (300 mL). The layers were separated and the aqueous layer was extracted with EtOAc (4 x 200 mL). The combined organic layers were dried over Na_2SO_4 and concentrated under reduced pressure to afford the corresponding enoate **3.21** (9.60 g, 90% yield) as a yellow oil. Enoate **3.21**: R_f 0.56 (3:7 hexanes:EtOAc); ^{1}H NMR (500 MHz, $CDCl_3$): (19 of 20 signals observed) δ 8.06–8.02 (m, 1H), 7.73–7.64 (m, 3H), 7.05 (dd, *J* = 4.1, 1.2, 1H), 5.48 (dq, *J* = 6.9, 1H), 4.24 (d, *J* = 4.1, 1H), 4.17 (br s, 1H), 3.93 (t, *J* = 3.1, 1H), 3.85 (d, *J* = 14.1, 1H), 3.74 (s, 3H), 3.67 (dt, *J* = 14.1, 1.8, 1H), 1.96 (dt, *J* = 12.9, 3.1, 1H), 1.76 (dd, *J* = 6.9, 1.8, 3H), 1.74 (dt, *J* = 12.9, 3.1, 1H); ^{13}C NMR (125 MHz, $CDCl_3$): δ 166.2, 147.9, 138.0, 134.3, 133.8, 133.4, 132.1, 130.9, 130.1, 124.6, 123.1, 67.2,

54.3, 52.2, 47.3, 29.6, 27.2, 12.9; IR (film): 3485, 1954, 1716, 1543, 1371, 1163 cm^{-1}; HRMS–APCI (*m/z*) $[M + H]^+$ calc for $C_{18}H_{21}N_2O_7S^+$, 409.10640, found 409.10491; $[\alpha]^{24.9}_D$ +164.60° (c = 1.0, CH_2Cl_2).

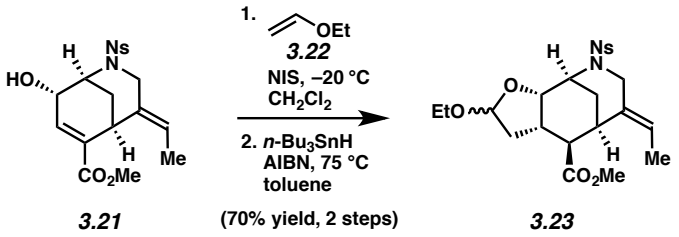

Acetal 3.23. To a solution of enoate **3.21** (0.323 g, 0.637 mmol) in CH_2Cl_2 (3.2 mL) at –20 °C was added NIS (0.860 g, 3.82 mmol). The reaction vessel was wrapped with aluminum foil to shield it from light and the mixture was stirred for 5 min. Ethyl vinyl ether (**3.22**) (0.49 mL, 5.09 mmol) was then added dropwise over 2 min at –20 °C. The reaction was stirred for 3 h, and allowed to warm to room temperature. Next, the reaction was quenched with sat. aq. sodium thiosulfate (20 mL). The resulting mixture was diluted with deionized water (5 mL) and EtOAc (10 mL), and the layers were separated. The aqueous layer was extracted with EtOAc (3 x 10 mL) and the organic layers were combined and dried over $MgSO_4$. Evaporation of the solvent under reduced pressure afforded the corresponding iodoacetal, which was used in the subsequent step without further purification.

To a solution of the the crude iodoacetal in toluene (4.4 mL) was added a solution of AIBN (0.052 g, 0.319 mmol) and *n*-Bu_3SnH (0.34 mL, 1.27 mmol) in toluene (0.67 mL). The mixture was heated to 75 °C. After 1 h, a second identical solution of AIBN and *n*-Bu_3SnH in toluene was added. After one additional hour, a third identical solution of AIBN and *n*-Bu_3SnH in toluene was added. Finally, after 3 additional hour, the resulting yellow solution was cooled to room

temperature, concentrated under reduced pressure, and purified via flash chromatography (3:20 benzene:EtOAc) to afford acetal **3.23** as a 1:1 mixture of diastereomers (213 mg, 70% yield over two steps) as a white solid. Although acetals **3.23** were typically used in the subsequent step as a mixture, analytical samples of each isomer were obtained by preparative thin layer chromatography (9:1 benzene:EtOAc). Acetal **3.23A**: R_f 0.38 (9:1 benzene:EtOAc); ^{1}H NMR (500 MHz, $CDCl_3$): δ 8.10–8.06 (m, 1H), 7.71–7.63 (m, 3H), 5.48 (dq, *J* = 6.9, 1.4, 1H), 5.05 (d, *J* = 5.8, 1H), 4.25 (m, 1H), 4.09 (app. q, *J* = 2.7, 1H), 4.04 (d, *J* = 15.2, 1H), 3.93 (dt, *J* = 15.1, 2.2 1H), 3.73 (q, *J* = 7.1, 1H), 3.64 (s, 3H), 3.40 (q, *J* = 7.1, 1H), 3.36–3.31 (m, 2H), 2.89 (dt, *J* = 13.0, 6.9, 1H), 2.25–2.22 (m, 1H), 2.11 (dt, *J* = 13.0, 2.6, 1H), 1.77 (d, *J* = 13.8, 1H), 1.68–1.64 (m, 1H), 1.55 (dd, *J* = 6.7, 2.1, 3H), 1.19 (t, *J* = 7.1, 3H); ^{13}C NMR (125 MHz, $CDCl_3$): δ 174.0, 147.9, 133.7, 133.6, 132.0, 131.2, 130.9, 124.6, 123.5, 103.2, 80.0, 63.5, 51.8, 50.5, 50.0, 47.4, 40.5, 35.5, 31.2, 27.4, 15.5, 12.4; IR (film): 2919, 1732, 1543, 1439, 1373, 1196 cm^{-1}; HRMS–APCI (*m/z*) $[M + H]^+$ calc for $C_{22}H_{29}N_2O_8S^+$, 481.16391, found 481.16230; $[\alpha]^{28.4}_D$ –9.40° (c = 1.0, CH_2Cl_2). Acetal **3.23B**: R_f 0.28 (9:1 benzene:EtOAc); ^{1}H NMR (500 MHz, $CDCl_3$): δ 8.08–8.05 (m, 1H), 7.72–7.66 (m, 3H), 5.49 (q, *J* = 6.9, 1H), 5.13 (dd, *J* = 5.7, 4.0, 1H), 4.33 (app. q, *J* = 2.8, 1H), 4.11–4.06 (m, 2H), 4.02 (dt, *J* = 15.2, 1.9, 1H), 3.74 (q, *J* = 7.1, 1H), 3.65 (s, 3H), 3.43 (q, *J* = 7.1, 1H), 3.26 (q, *J* = 3.4, 1H), 2.92–2.86 (m, 1H), 2.48 (dd, *J* = 11.5, 4.2, 1H), 2.13–2.09 (m, 1H), 2.06 (dt, *J* = 13.2, 2.9, 1H), 1.86 (dd, *J* = 13.9, 5.9, 1H), 1.64 (dt, *J* = 13.2, 3.6, 1H), 1.52 (dd, *J* = 6.9, 1.8, 3H). 1.16 (t, *J* = 7.1, 3H); ^{13}C NMR (125 MHz, $CDCl_3$): δ 173.34, 148.0, 133.6, 131.9, 131.1, 130.3, 124.6, 123.7, 102.2, 76.08, 63.7, 52.0, 50.0, 49.6, 49.5, 41.5, 37.1, 31.6, 28.2, 15.4, 12.5; IR (film): 2922, 1733, 1544, 1439, 1373 cm^{-1}; HRMS–APCI (*m/z*) $[M + H]^+$ calc for $C_{22}H_{29}N_2O_8S^+$, 481.16391, found 481.16223; $[\alpha]^{28.4}_D$ +16.20° (c = 1.0, CH_2Cl_2).

*The stereochemistry of esters **3.23A** and **3.23B** were verified by NOESY (500 MHz, $CDCl_3$), as the following correlations were observed:*

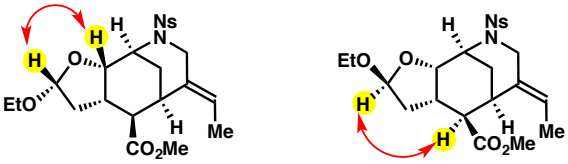

3.23A ***3.23B***

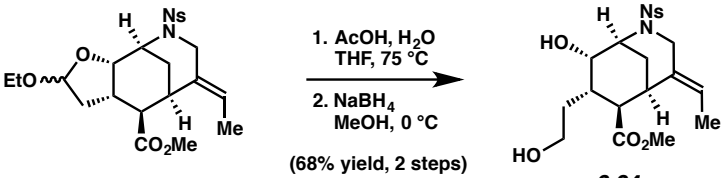

3.23 ***3.24***

Diol 3.24. To a solution of diastereomeric acetals **3.23** (9.15 g, 19.1 mmol) in THF (128 mL) and deionized water (128 mL) was added AcOH (382 mL, 6.69 mmol). The reaction vessel was heated to 75 °C. After stirring for 5 h, the reaction was cooled to room temperature, quenched with sat. aq. sodium bicarbonate (500 mL), and diluted with EtOAc (500 mL). The layers were separated and the aqueous layer was extracted with EtOAc (4 x 300 mL). The organic layers were combined, dried over $MgSO_4$, and concentrated under reduced pressure to afford the corresponding lactol (6.80 g, 15.0 mmol), which was used in the subsequent step without further purification.

To a solution of the lactol (6.80 g, 15.0 mmol) in MeOH (312 mL) at 0 °C was added $NaBH_4$ (1.18 g, 30.0 mmol). After stirring for 1.5 h, the reaction was diluted with EtOAc (300 mL) and then poured into deionized water (300 mL). The layers were separated and the aqueous layer was extracted with EtOAc (4 x 200 mL). The organic layers were combined, dried over $MgSO_4$, and concentrated under reduced pressure. The crude mixture was purified via flash chromatography (1:1 hexanes:EtOAc) to afford diol **3.24** (5.81 g, 68% yield over two steps) as a white solid. Diol **3.24**: mp: 151–154 °C; R_f 0.45 (3:1 EtOAc:hexanes); ^{1}H NMR (500 MHz, $CDCl_3$): δ 8.07–8.03 (m, 1H), 7.72–7.63 (m, 3H), 5.44 (q, J = 6.9, 1H), 4.26 (dt, J = 15.1, 2.3, 1H),

4.19 (app t, J = 3.5, 1H), 4.07 (app q, J = 3.3, 1H), 3.97 (d, J = 15.1, 1H), 3.80–3.71 (m, 2H), 3.62 (s, 3H), 3.40 (br s, 1H), 3.20 (app q, J = 3.4, 1H), 2.80 (dd, J = 12.1, 4.4, 1H), 2.41–2.35 (m, 1H), 2.31 (dt, J = 13.4, 3.1, 1H), 2.03 (br s, 1H), 1.72–1.64 (m, 2H), 1.53–1.49 (m, 4H); ^{13}C NMR (125 MHz, $CDCl_3$): δ 174.1, 148.1, 133.7, 133.1, 131.9, 131.2, 131.1, 124.6, 122.3, 69.2, 61.1, 53.1, 51.8, 50.0, 47.5, 36.8, 32.8, 31.9, 26.5, 12.4; IR (film): 3397, 2951, 1728, 1542, 1162, 1128 cm^{-1}; HRMS–APCI (m/z) $[M + H]^+$ calcd for $C_{20}H_{27}N_2O_8S^+$, 455.14826; found 455.14686; $[\alpha]^{29.2}_D$ +77.00° (c = 1.0, CH_2Cl_2).

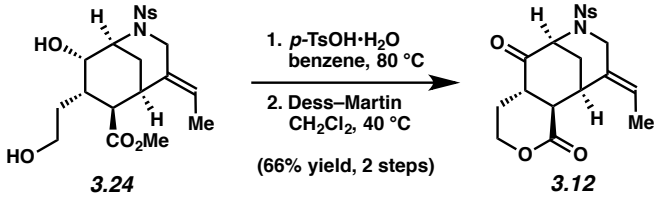

Lactone 3.12. To a solution of diol **3.24** (93.2 mg, 0.205 mmol) in benzene (10.3 mL) was added *p*-TsOH (9.8 mg, 0.051 mmol). The resulting mixture was placed into a preheated heating block at 80 °C. After stirring for 30 min, the reaction was cooled to room temperature, diluted with EtOAc (5 mL), and poured into a mixture of sat. aq. $NaHCO_3$ (50 mL) and deionized water (5 mL). The layers were separated and the aqueous layer was extracted with EtOAc (2 x 10 mL). The organic layers were combined and dried over $MgSO_4$ then concentrated under reduced pressure to afford the corresponding γ-hydroxyl lactone (73.9 mg, 0.174 mmol), which was used subsequently without further purification.

To a solution of the crude γ-hydroxyl lactone (73.9 mg, 0.174 mmol) in CH_2Cl_2 (1.75 mL) was added Dess–Martin periodinane (0.225 g, 0.525 mmol). The resulting mixture was heated to 40 °C. After stirring for 13 h, the reaction was cooled to room temperature and quenched with a 1:1 mixture of sat. aq. sodium thiosulfate (5 mL). The mixture was stirred for 5 min and then

suspended in deionized water (5 mL) and CH_2Cl_2 (5 mL). The resulting layers were separated and the aqueous layer was extracted with CH_2Cl_2 (2 x 10 mL) and the organic layers were combined, dried over $MgSO_4$, and concentrated under reduced pressure. The crude mixture was purified via flash chromatography (3:7 EtOAc:hexanes) to afford lactone **3.12** (57.6 mg, 66% yield over two steps) as a yellow solid. Lactone **3.12**: mp: 199–203 °C; R_f 0.49 (3:7 hexanes:EtOAc); ^{1}H NMR (500 MHz, $CDCl_3$): δ 8.11–8.08 (m, 1H), 7.77–7.67 (m, 3H), 5.72 (q, *J* = 7.0, 1H), 4.43 (ddd, *J* = 11.6, 6.0, 3.8, 1H), 4.39–4.28 (m, 3H), 4.19 (d, *J* = 15.2, 1H), 3.66 (q, *J* = 3.2, 1H), 3.14 (ddd, *J* = 14.4, 10.4, 4.4, 1H), 2.67 (dd, *J* = 14.0, 3.5, 1H), 2.23–2.15 (m, 2H), 2.07–1.98 (m, 2H), 1.83 (dd, *J* = 7.0, 1.4, 3H); ^{13}C NMR (125 MHz, $CDCl_3$): δ 203.2, 168.8, 147.9, 134.3, 132.1, 132.0, 131.7, 127.9, 127.0, 124.6, 68.0, 58.6, 50.6, 49.8, 45.2, 34.2, 28.7, 22.7, 13.5; IR (film): 2917, 1725, 1542, 1370, 1167, 1072 cm^{-1}; HRMS–APCI (*m/z*) $[M + H]^+$ calcd for $C_{19}H_{21}N_2O_7S^+$, 421.10640; found 421.10445; $[\alpha]^{29.3}_D$ +772.00° (c = 0.1, CH_2Cl_2).

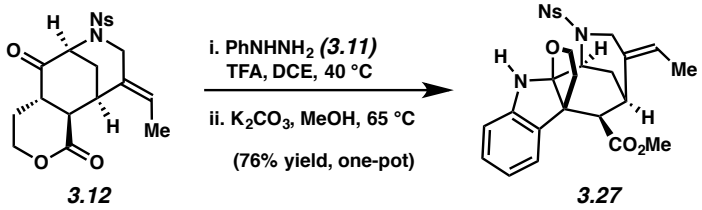

Furoindoline 3.27. To a solution of lactone **3.12** (31.0 mg, 0.0738 mmol) in DCE (3.7 mL) was added TFA (30 µL, 0.369 mmol) and $PhNHNH_2$ (**3.11**) (15 µL, 0.148 mmol). The resulting mixture was degassed via the freeze-pump-thaw method using a –78 °C bath. After warming to room temperature, the reaction vessel was placed into a preheated 40 °C oil bath. Upon stirring for 12 h, the reaction was concentrated under reduced pressure. The resultant residue was suspended in MeOH (3.7 mL) and stirred for 5 min, at which point K_2CO_3 (102 mg, 0.738 mmol) was added. After 1 h of stirring, the reaction was quenched with 1 M HCl (10 mL) and diluted with CH_2Cl_2

(10 mL). The layers were separated and the aqueous layer was extracted with CH_2Cl_2 (4 x 10 mL). The organic layers were combined, dried over $MgSO_4$, and then concentrated under reduced pressure. The crude mixture was purified by flash chromatography (4:1 hexanes:EtOAc → 3:2 hexanes:EtOAc) to afford furoindoline **3.27** (29.4 mg, 76% yield) as a yellow solid. Furoindoline **3.27**: mp: 230–232 °C (Decomp); R_f 0.49 (3:7 hexanes:EtOAc); ^{1}H NMR (500 MHz, $CDCl_3$): δ 8.07–8.03 (m, 1H), 7.70–7.61 (m, 3H), 7.09–7.04 (m, 2H), 6.74 (t, *J* = 7.5, 1H), 6.60 (d, *J* = 7.7, 1H), 5.52 (q, *J* = 6.8, 1H), 4.53 (br. s, 1H), 4.41 (t, *J* = 3.2, 1H), 4.01 (dt, *J* = 14.9, 2.0, 1H), 3.89 (d, *J* = 14.9, 1H), 3.80 (t, *J* = 8.3, 1H), 3.70 (s, 3H), 3.39–3.30 (m, 2H), 2.97 (d, *J* = 4.7, 1H), 2.86–2.78 (m, 1H), 2.48 (dd, *J* =13.6, 5.4, 1H), 2.04 (app. t, *J* =3.6, 2H), 1.57 (dd, *J* = 7.0, 1.8, 3H); ^{13}C NMR (125 MHz, $CDCl_3$): δ 172.3, 148.1, 146.7, 135.9, 134.0, 133.1, 131.5, 131.2, 129.7, 128.5, 125.3, 124.4, 123.2, 119.9, 109.1, 101.8, 68.5, 54.5, 54.11, 54.06, 51.8, 48.6, 36.6, 31.3, 30.1, 12.9; IR (film): 2952, 1737, 1542, 1468, 1371, 1163, 1072 cm^{-1}; HRMS–APCI (*m/z*) $[M + H]^+$ calcd for $C_{26}H_{28}N_3O_7S^+$, 526.16425; found 526.16367; $[\alpha]^{29.5}_D$ +242.00° (c = 0.1, CH_2Cl_2).

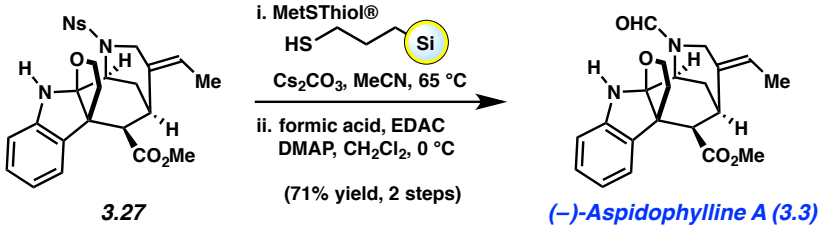

(–)-Aspidophylline A (3.3). To a suspension of furoindoline **3.27** (5.0 mg, 0.00952 mmol) and Cs_2CO_3 (9.4 mg, 0.0283 mmol) in MeCN (0.32 mL) was added SiliaMetS® Thiol (28.4 mg, 0.0381 mmol). The reaction was heated to 65 °C. After stirring for 2 h, the reaction was cooled to room temperature and filtered through a plug of celite® (400 mg, MeCN eluent, 10 mL). The filtrate was concentrated under reduced pressure to afford the corresponding secondary amine, which was used subsequently without further purification.

In a separate vessel, CH_2O_2 (5.4 μL, 0.143 mmol) was added to a solution of DMAP (23 mg, 0.190 mmol) and EDAC•HCl (18 mg, 0.0952 mmol) in CH_2Cl_2 (2.0 mL) at 0 °C. This mixture was stirred at 0 °C for 15 min, at which point, a 200 μL aliquot of this stock solution was added to a solution of the crude denosylated product in CH_2Cl_2 (0.20 mL). After stirring for 1.5 h, the reaction was quenched with sat. aq. $NaHCO_3$ (5 mL) and diluted with CH_2Cl_2 (5 mL). The layers were separated and the aqueous layer was extracted with CH_2Cl_2 (2 x 5 mL). The organic layers were combined, dried over $MgSO_4$, and concentrated under reduced pressure. The crude mixture was purified via flash chromatography (1.5:1 EtOAc:hexanes) to afford (–)-aspidophylline A (**3.3**) (2.5 mg, 71% yield) as a white foam. Spectral data for synthetic **3.3** was consistent with literature reports, our previous synthesis of (–)-aspidophylline A,[2] and a natural sample of (–)-**3.3** obtained from Prof. T.-S. Kam (see comparision ^{1}H NMR spectra and Table 3.1) .(–)-Aspidophylline A was observed as an 8:1 mixture of rotational isomers in $CDCl_3$. (–)-Aspidophylline A **3.3 (major rotational isomer)**: ^{1}H NMR (500 MHz, $CDCl_3$): δ 8.14 (s, 1H), 7.13–7.08 (m, 2H), 6.79 (t, *J* = 7.5, 1H), 6.68 (d, *J* = 7.7, 1H), 5.61 (q, *J* = 7.0, 1H), 4.40 (s, 1H), 4.29 (d, *J* = 17.7, 1H), 4.06 (d, *J* = 17.7, 1H), 3.98–3.92, (m, 1H), 3.90 (s, 1H), 3.70 (s, 1H), 3.56 (dd, *J* = 17.5, 8.0, 1H), 3.41 (d, *J* = 3.7, 1H) 2.83 (d, *J* = 4.5, 1H) 2.72–2.67 (m, 2H), 2.20 (dt, *J* = 13.5, 2.8, 1H), 2.02 (dt, *J* = 13.5, 3.7, 1H), 1.59 (d, *J* = 1.95, 3H); ^{13}C NMR (125 MHz, $CDCl_3$): δ 172.2, 164.6, 146.5, 136.0, 129.3, 128.6, 124.5, 123.2, 120.5, 110.3, 102.3, 69.4, 54.1, 53.9 (2 carbons), 51.8, 44.7, 34.5, 30.8, 30.4, 13.0; IR (film): 3312, 2925, 1739, 1655, 1469, 1158, 1044; HRMS–APCI (*m/z*) $[M + H]^+$ calcd for $C_{21}H_{25}N_2O_4^+$, 369.18088; found 369.17955; reported $[\alpha]^{25.0}_D$ –86.0° (c = 0.09, $CHCl_3$),[36] observed $[\alpha]^{22.1}_D$ –48.0° (c = 0.09, $CHCl_3$).[33]

Table 3.1 Comparison of ^{13}C NMR Data for Natural vs. Synthetic (–)-Aspidophylline A (**3.3**)

Natural (–)-Aspidophylline A (**3.3**) (From Sample Provided by T. S. Kam) ^{13}C NMR, 125 MHz, $CDCl_3$	Synthetic (–)-Aspidophylline A (**3.3**) ^{13}C NMR, 125 MHz, $CDCl_3$
172.2	172.2
164.6	164.6
146.5	146.5
136.0	136.0
129.4	129.3
128.6	128.6
124.4	124.5
123.2	123.2
120.5	120.5
110.3	110.3
102.3	102.3
69.3	69.4
54.1	54.1
53.9	53.9
51.8	51.8
44.7	44.7
34.5	34.5
30.8	30.8
30.4	30.4
13.0	13.0

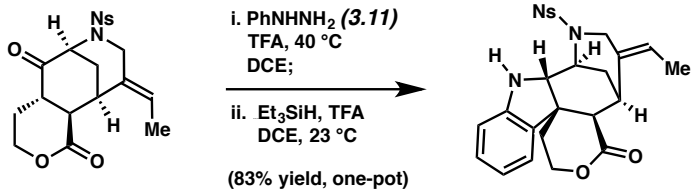

3.12 ***3.9***

Indoline 3.9. To a solution of lactone **3.12** (57.6 mg, 0.137 mmol) in DCE (2.7 mL) was added TFA (55 μL, 0.719 mmol) and $PhNHNH_2$ (**3.11**) (25 μL, 0.251 mmol). The resulting mixture was degassed via the freeze-pump-thaw method using a –78 °C bath. After warming to room temperature, the reaction was backfilled with N_2 for 1 min and heated to 40 °C. After stirring for 14 h, the reaction was cooled to room temperature, at which point additional TFA (0.52 mL, 6.86 mmol) and Et_3SiH (1.0 mL, 6.26 mmol) were added. The reaction was flushed with N_2 for 1 min

and stirred at room temperature. After 1 h of stirring, the reaction was quenched with sat. aq. $NaHCO_3$ (20 mL) and diluted with CH_2Cl_2 (10 mL). The layers were separated and the aqueous layer was extracted with CH_2Cl_2 (2 x 10 mL). The organic layers were combined, dried over $MgSO_4$, and concentrated under reduced pressure. The crude mixture was purified via flash chromatography (3:1 hexanes:EtOAc → 2:1 hexanes:EtOAc) to afford indoline **3.9** (56.3 mg, 83% yield) as a yellow solid. Indoline **3.9**: mp: 135–137 °C; R_f 0.30 (1:1 EtOAc:hexanes); ^{1}H NMR (500 MHz, $CDCl_3$): δ 8.07–8.03 (m, 1H), 7.78–7.70 (m, 2H), 7.68–7.65 (m, 1H), 7.10–7.04 (m, 2H), 6.75 (dt, *J* = 7.5, 0.9, 1H), 6.66 (d, *J* = 7.8, 1H), 5.62 (q, *J* = 7.2, 1H), 4.72–4.64 (m, 1H), 4.61–4.53 (m, 1H), 4.21 (s, 1H), 4.18 (d, *J* = 2.4, 1H), 4.06 (d, *J* = 14.6, 1H), 3.95 (s, 1H), 3.82 (dt, *J* = 14.5, 1.3, 1H), 3.55–3.49 (m, 1H), 3.08 (d, *J* = 6.4, 1H), 2.51–2.43 (m, 1H), 2.11 (dt, *J* = 13.9, 2.8, 1H), 2.07–1.98 (m, 1H), 1.87 (dtd, *J* = 13.9, 3.8, 1.3, 1H), 1.68 (d, *J* = 7.1, 3H); ^{13}C NMR (125 MHz, $CDCl_3$): δ 171.8, 148.4, 147.8, 136.3, 134.1, 132.0 (2 carbons), 131.3, 130.5, 128.8, 126.4, 124.5, 122.9, 119.8, 109.9, 68.3, 66.1, 53.3, 49.6, 48.1, 43.5, 31.8, 29.7, 27.5, 13.7; IR (film): 3360, 2923, 1730, 1543, 1372, 1165 cm^{-1}; HRMS–APCI (*m/z*) $[M + H]^+$ calcd for $C_{25}H_{26}N_3O_6S^+$, 496.15368; found 496.15187; $[\alpha]^{23.3}_D$ –8.00° (c = 0.1, CH_2Cl_2).

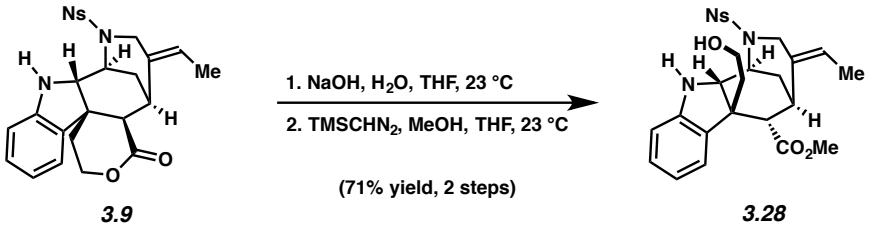

3.9 ***3.28***

Ester 3.28. To a solution of indoline **3.9** (12.9 mg, 0.026 mmol) in THF (1.3 mL) was added an aqueous solution of NaOH (0.5 N, 1.3 mL). After vigorously stirring for 13 h, the reaction mixture was quenched with an aqueous solution of HCl (1 N, 0.7 mL), poured into deionized water (10 mL), and diluted with EtOAc (10 mL). The layers were separated and the aqueous layer was

extracted with EtOAc (2 x 10 mL). The organic layers were combined, dried over $MgSO_4$, and concentrated under reduced pressure to afford the corresponding carboxylic acid, which was used in the subsequent step without further purification.

To a solution of the crude reaction mixture in a 5:3 mixture of THF:MeOH (2.6 mL) was added $TMSCHN_2$ (16 μL of a 2.0 M solution in hexanes, 0.313 mmol). After stirring for 1.5 h, the reaction mixture was poured into deionized water (5 mL) and sat. aq. NaCl (5 mL), and then further diluted with EtOAc (10 mL). The layers were separated and the aqueous layer was extracted with EtOAc (2 x 10 mL). The organic layers were combined, dried over $MgSO_4$ and concentrated under reduced pressure. The crude mixture was purified via preparative thin layer chromatography (3:1 EtOAc:hexanes) to afford ester **3.28** (9.7 mg, 71% yield) as a colorless oil. Ester **3.28**: R_f 0.46 (3:1 EtOAc:hexanes); ^{1}H NMR (500 MHz, $CDCl_3$): (27 of 29 signals observed) δ 8.08–8.01 (m, 1H), 7.77–7.72 (m, 2H), 7.64–7.61 (m, 1H), 7.07–7.02 (m, 2H), 6.73 (t, *J* = 7.5, 1H), 6.68 (d, *J* = 7.9, 1H), 5.53 (q, *J* = 7.0, 1H), 4.25 (br. s, 1H), 4.20 (s, 1H), 4.12 (d, *J* = 13.9, 1H), 3.76 (d, *J* = 14.1, 1H), 3.72–3.62 (m, 1H), 3.56–3.47 (m, 1H), 3.22 (s, 3H), 3.09 (br. s, 1H), 2.95–2.87 (m, 2H), 2.48–2.38 (m, 1H), 2.25–2.15 (m, 1H), 1.72 (d, *J* = 14.3, 1H), 1.67 (d, *J* = 7.0, 3H); ^{13}C NMR (125 MHz, $CDCl_3$): δ 174.0, 149.4, 148.9, 134.9, 134.1, 132.2, 131.8, 131.4, 131.1, 128.7, 124.4, 124.3, 123.0, 119.3, 110.5, 65.1, 59.9, 54.1, 52.6, 51.4, 48.1, 45.8, 43.4, 28.8, 20.3, 13.3; IR (film): 3548, 3365, 2920, 2851, 1732, 1544, 1374, 1165 cm^{-1}; HRMS–APCI (*m/z*) $[M + H]^+$ calcd for $C_{26}H_{30}N_3O_7S^+$, 528.17990; found 528.18111; $[\alpha]^{25.7}_D$ 400.00° (c = 0.1, CH_2Cl_2).

*The stereochemistry of ester **3.28** was verified by NOESY (500 MHz, $CDCl_3$), as the following correlation was observed:*

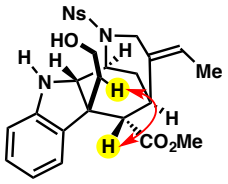

3.28

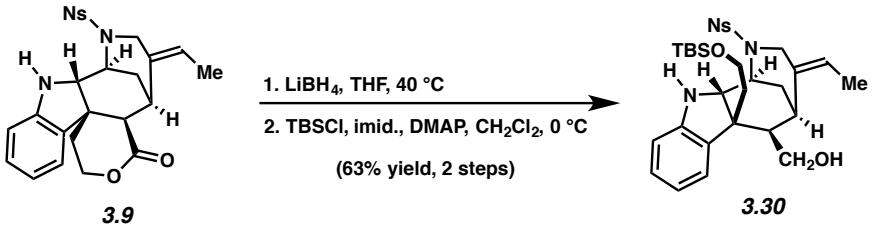

3.9 ***3.30***

Silyl Ether 3.30. To a solution of indoline **3.9** (80.0 mg, 0.162 mmol) in THF (10 mL) was added a solution of $LiBH_4$ (14.5 mg, 0.668 mmol) in THF (2 mL). The reaction was heated to 40 °C. After stirring for 8 h, the reaction was cooled to room temperature, poured into deionized water (20 mL), and diluted with EtOAc (20 mL). The layers were separated and the aqueous layer was extracted with EtOAc (2 x 20 mL). The organic layers were combined, dried over $MgSO_4$ and concentrated under reduced pressure to afford the corresponding diol, which was used in the subsequent step without further purification.

To a solution of the crude reaction mixture in CH_2Cl_2 (4.8 mL) was added imidazole (11.7 mg, 0.172 mmol) and DMAP (17.5 mg, 0.143 mmol). The reaction was flushed with N_2 for 1 min and stirred. After 1 min, TBSCl (31.5 mg, 0.200 mmol) was added. The reaction was flushed with N_2 for 1 min and allowed to stir at rt. After 2.5 h, additional imidazole (11.7 mg, 0.172 mmol), DMAP (17.5 mg, 0.143 mmol), and TBSCl (31.5 mg, 0.200 mmol) were added. The reaction was flushed with N_2 for 1 min and stirred at room temperature. After 30 additional min of stirring, the

reaction was quenched with sat. aq. NH_4Cl (5 mL), poured into deionized water (5 mL), and diluted with CH_2Cl_2 (5 mL). The layers were separated and the aqueous layer was extracted with CH_2Cl_2 (2 x 5 mL). The organic layers were combined, dried over $MgSO_4$, and concentrated under reduced pressure. The crude mixture was purified via flash chromatography (6:1 hexanes:EtOAc → 2:1 hexanes:EtOAc) to afford silyl ether **3.30** (62.1 mg, 63% yield, two steps) as a beige solid. Silyl Ether **3.30**: mp: 150–154 °C; R_f 0.43 (1:1 EtOAc:hexanes); ^{1}H NMR (500 MHz, $CDCl_3$): δ 8.04–8.00 (m, 1H), 7.74–7.69 (m, 2H), 7.64–7.59 (m, 1H), 7.11 (dd, *J* = 7.4, 0.7, 1H), 7.05 (td, *J* = 7.6, 1.2, 1H), 6.74 (td, *J* = 7.4, 1.0, 1H), 6.66 (dd, *J* = 7.8, 0.5, 1H), 5.62 (qd, *J* = 7.0, 1.2, 1H), 4.26 (dt, *J* = 14.9,1.6, 1H), 4.22 (q, *J* = 3.0, 1H), 3.99 (br s, 1H), 3.95–3.86 (m, 3H), 3.70 (ddd, *J* = 19.7, 9.8, 6.2, 1H), 3.60 (ddd, *J* = 20.8, 10.4, 5.9, 1H), 3.36 (ddd, *J* = 20.5, 10.4, 4.3, 1H), 3.18 (d, *J* = 2.6, 1H), 2.35 (td, *J* = 13.6, 2.9, 1H), 2.21–2.13 (m, 1H), 1.84–1.70 (m, 6H), 1.05 (br s, 1H), 0.81 (s, 9H), –0.04 (s, 6H); ^{13}C NMR (125 MHz, $CDCl_3$): δ 149.0, 148.7, 135.7, 133.8, 131.6, 131.51, 131.47, 131.3, 127.9, 124.5, 124.2, 123.5, 118.8, 110.2, 66.1, 60.8, 59.8, 51.7, 51.4, 48.2, 46.4, 33.0, 26.8, 26.7, 26.2, 18.5, 13.8, –5.1; IR (film): 3558, 3371, 2929, 2858, 1545, 1372, 1166, 1084 cm^{-1}; HRMS–APCI (*m/z*) $[M + H]^+$ calcd for $C_{31}H_{44}N_3O_6SSi^+$, 614.27146; found 614.26895; $[\alpha]^{23.2}_D$ –54.0° (c = 0.1, CH_2Cl_2).

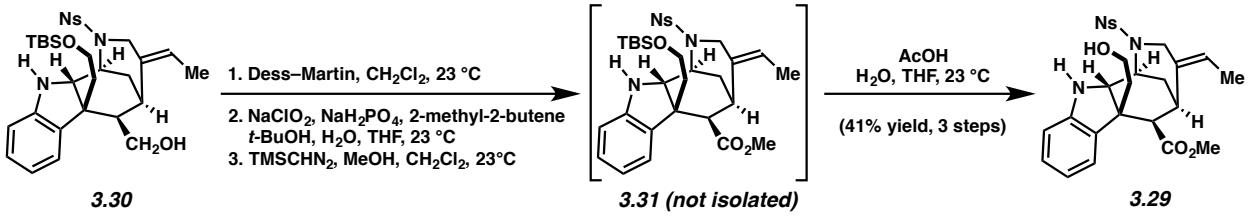

Ester 3.29. To a solution of the silyl ether **3.30** (37.8 mg, 0.0616 mmol) in CH_2Cl_2 (0.61 mL) was added Dess–Martin periodinane (32.5 mg, 0.770 mmol). After stirring for 30 min, the reaction was quenched with sat. aq. $Na_2S_2O_3$ (1 mL). The resulting mixture was stirred for 5 min, at which point

it was poured into deionized water (5 mL), and then diluted with CH_2Cl_2 (10 mL). The resulting layers were separated and the aqueous layer was extracted with CH_2Cl_2 (2 x 10 mL). The organic layers were combined, dried over $MgSO_4$, and concentrated under reduced pressure to afford the corresponding aldehyde, which was used in the subsequent step without further purification.

To a solution of the crude aldehyde in *t*-BuOH (1.5 mL) and 2-methyl-2-butene (1.5 mL of a 2.0 M solution in THF, 3.0 mmol) was added a solution of sodium chlorite (23.2 mg, 0.256 mmol) and monobasic sodium phosphate (36.2 mg, 0.303 mmol) in deionized water (1.5 mL). After stirring vigorously for 12 h, the reaction mixture was poured into deionized water (10 mL) and diluted with EtOAc (10 mL). The layers were separated and the aqueous layer was extracted with EtOAc (2 x 10 mL). The organic layers were combined and dried over $MgSO_4$. Evaporation of the solvent under reduced pressure afforded the corresponding carboxylic acid, which was used in the subsequent step without further purification.

To a solution of the crude carboxylic acid in 5:3 mixture of THF:MeOH (2.5 mL) was added $TMSCHN_2$ (124 μL of a 0.6 M solution in hexanes, 0.313 mmol). After stirring for 10 min, the reaction mixture was concentrated under reduced pressure and redissolved in THF (0.9 mL), deionized water (0.9 mL), and AcOH (2.7 mL). After stirring vigorously for 2 h, the reaction was quenched with sat. aq. $NaHCO_3$ (30 mL) and diluted with EtOAc (20 mL). The layers were separated and the aqueous layer was extracted with EtOAc (2 x 20 mL). The organic layers were combined, dried over $MgSO_4$ and concentrated under reduced pressure. The crude mixture was purified via flash chromatography (1.5:1 EtOAc:hexanes) to afford ester **3.29** (13.4 mg, 41% yield, three steps) as a colorless oil. Ester **3.29**: R_f 0.40 (3:1 EtOAc:hexanes); ^{1}H NMR (500 MHz, $CDCl_3$): (28 of 29 signals observed) δ 8.11–8.01 (m, 1H), 7.77–7.69 (m, 2H), 7.68–7.61 (m, 1H), 7.07 (dd, *J* = 7.5, 0.7, 1H), 7.04 (td, *J* = 7.7, 1.2, 1H), 6.72 (td, *J* = 7.5, 0.9, 1H), 6.66 (d, *J* = 7.7,

1H), 5.55 (q, J = 7.2, 1H), 4.27 (q, J = 2.9, 1H), 4.21 (d, J = 14.6, 1H), 4.11 (br. s, 1H), 4.07 (app. br s, 1H), 3.78 (td, J = 14.5, 1.8, 1H), 3.68–3.60 (m, 1H), 3.59 (s, 3H), 3.56–3.48 (m, 1H), 3.32 (d, J = 3.0, 1H), 3.01 (ddd, J = 5.8, 8.4, 14.4, 1H), 2.90 (d, J = 4.1, 1H), 2.38–2.30 (m, 2H), 1.86 (td, J = 13.7, 1.0, 1H), 1.52 (d, J = 7.1, 3H); ^{13}C NMR (125 MHz, $CDCl_3$): δ 172.4, 148.42, 148.41, 135.0, 134.0, 131.98, 131.89, 131.7, 131.5, 128.2, 124.40, 124.37, 123.9, 119.5, 110.3, 66.5, 60.5, 52.3, 52.0, 51.5, 47.8, 46.6, 34.3, 30.1, 27.7, 13.4; IR (film): 3558, 3365, 2950, 1738, 1543, 1373, 1164 cm^{-1}; HRMS–APCI (*m/z*) $[M + H]^+$ calcd for $C_{26}H_{30}N_3O_7S^+$, 528.17990; found 528.17876; $[\alpha]^{23.1}_D$ –110.00° (c = 0.1, CH_2Cl_2).

*The stereochemistry of ester **3.29** was verified by NOESY (500 MHz, $CDCl_3$), as the following correlation was observed:*

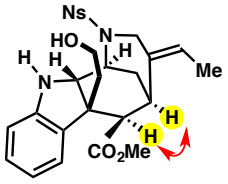

3.29

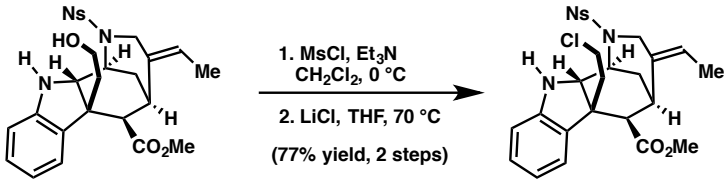

3.29 ***3.8***

Chloride 3.8. To a solution of ester **3.29** (7.5 mg, 0.0142 mmol) in CH_2Cl_2 (0.5 mL) at 0 °C was added Et_3N (1.5 µL, 0.0171 mmol). After stirring for 2 min, MsCl (4 µL, 0.0285 mmol) was added. After stirring the reaction at 0 °C for 2 h, it was filtered through a plug of celite® (CH_2Cl_2 and benzene eluent, 1 mL each). The filtrate was concentrated under reduced pressure to afford the corresponding mesylate, which was used in the subsequent step without further purification.

To a solution of the crude mesylate in THF (0.25 mL) was added a solution of LiCl in THF (0.3 mL of a 0.5 M solution, 0.150 mmol). The reaction was heated to 70 °C. After stirring for 4.5 h, the reaction was cooled to room temperature, poured into sat. aq. $NaHCO_3$ (5 mL), and diluted with EtOAc (5 mL). The layers were separated and the aqueous layer was extracted with EtOAc (2 x 5 mL). The organic layers were combined, dried over $MgSO_4$ and concentrated under reduced pressure. The crude mixture was purified via preparative thin layer chromatography (1:1 EtOAc:hexanes) to afford chloride **3.8** (6 mg, 77% yield, two steps) as a colorless oil. Chloride **3.8**: R_f 0.43 (1:1 EtOAc:hexanes); ^{1}H NMR 8.13–8.03 (m, 1H), 7.77–7.71 (m, 2H), 7.67–7.60 (m, 1H), 7.09 (dd, *J* = 7.6, 0.7, 1H), 7.06 (td, *J* = 7.7, 1.2, 1H), 6.74 (td, *J* = 7.5, 0.9, 1H), 6.66 (d, *J* = 7.5, 1H), 5.60 (q, *J* = 7.0, 1H), 4.29 (q, *J* = 3.0, 1H), 4.23 (d, *J* = 14.6, 1H), 4.04 (br. s, 1H), 3.94 (d, *J* = 2.0, 1H), 3.80 (td, *J* = 1.7, 1.5, 1H), 3.59 (s, 3H), 3.57–3.49 (m, 1H), 3.36–3.29 (m, 2H), 3.29–3.21 (m, 1H), 2.83 (d, *J* = 3.6, 1H), 2.65–2.54 (m, 1H), 2.39 (td, *J* = 13.9, 3.0, 1H), 1.88 (td, *J* = 13.8, 0.8, 1H), 1.52 (d, *J* = 7.2, 3H); ^{13}C NMR (125 MHz, $CDCl_3$): δ 172.1, 148.48, 148.47, 134.07. 134.04, 131.9, 131.7, 131.6, 131.1, 128.4, 124.9, 124.3, 123.8, 119.6, 110.3, 66.0, 51.9, 51.6, 51.5, 47.8, 47.4, 41.8, 34.1, 30.1, 27.4, 13.5; IR (film): 3365, 2924, 1738, 1544, 1466, 1373, 1163 cm^{-1}; HRMS–APCI (*m/z*) $[M + H]^+$ calcd for $C_{26}H_{29}ClN_3O_6S^+$, 546.14601; found 546.14674; $[\alpha]^{23.0}_D$ –46.0° (c = 0.1, CH_2Cl_2).

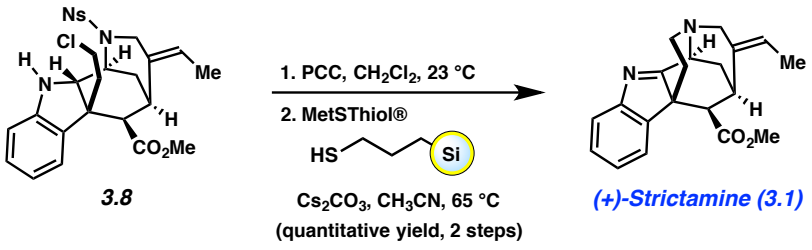

(+)-Strictamine (3.1). To a solution of chloride **3.8** (11.0 mg, 0.0202 mmol) in CH_2Cl_2 (2.0 mL) was added PCC (6.6 mg, 0.0303 mmol). After stirring at room temperature for 30 min, the reaction

was filtered through a plug of celite® (200 mg) and basic alumina (1.50 g) using ethyl acetate (15 mL). The volatiles were removed under reduced pressure to afford the corresponding indolenine (11.0 mg, 0.0202 mmol) as an oil, which was used in the subsequent step without further purification.

To a solution of the crude indolenine (11.0 mg, 0.0202 mmol) and Cs_2CO_3 (18.1 mg, 0.0605 mmol) in MeCN (2.3 mL) was added SiliaMetS® Thiol (52.0 mg, 0.0807 mmol). The reaction was heated to 65 °C. After stirring for 6 h, the reaction was cooled to room temperature, and filtered through a plug of celite® (400 mg). The plug was washed with MeCN (15 mL) and the filtrate was concentrated under reduced pressure. The crude mixture was purified via flash chromatography (19:1 $CHCl_3$:MeOH) to afford (+)-strictamine (**3.1**) (6.5 mg, quantitative yield, two steps) as a colorless oil. Spectral data for synthetic **3.1** were consistent with literature reports[13c,37] and a natural sample provided by T. S. Kam. (+)-Strictamine (**3.1**) (see comparision ^{1}H NMR spectra and Table 3.2): ^{1}H NMR (500 MHz, $CDCl_3$): δ 7.62 (d, *J* = 7.7, 1H), 7.42 (dd, *J* = 7.5, 0.5 1H), 7.34 (td, *J* = 7.6, 1.3, 1H), 7.17 (td, *J* = 7.5, 1.0, 1H), 5.51 (q, *J* = 7.0, 1H), 4.70 (d, *J* = 5.2, 1H), 4.06 (d, *J* = 16.8, 1H), 3.76–3.67 (m, 4H), 3.51 (br. s, 1H), 3.13 (d, *J* = 16.8, 1H), 2.76–2.65 (m, 2H), 2.60 (td, *J* = 14.3, 5.0, 1H), 2.08 (d, *J* = 3.8, 1H), 2.00 (dd, *J* = 14.7, 4.9, 1H), 1.74 (dd, *J* = 13.4, 2.7, 1H) 1.55 (dd, *J* = 7.1, 2.6, 3H); ^{13}C NMR (125 MHz, $CDCl_3$): δ 191.5, 171.8, 155.7, 146.4, 138.4, 128.3, 125.7, 123.6, 121.0, 119.9, 56.3, 55.5, 55.3, 53.8, 52.1, 51.7, 36.2, 33.9, 32.6, 13.1; IR (film): 2924, 2856, 1737, 1448, 1190, 1170, 1041 cm^{-1}; HRMS–APCI (*m/z*) $[M + H]^+$ calcd for $C_{20}H_{23}N_2O_2^+$, 323.17540; found 323.17489; reported $[\alpha]^{24.0}_D$ +103° (c = 0.72, $CHCl_3$)[38], observed $[\alpha]^{26.3}_D$ +68.3° (c = 0.72, $CHCl_3$).[33]

Table 3.2 Comparison of ^{13}C NMR Data for Natural vs. Synthetic (+)-Strictamine (**3.1**)

Natural (+)-Strictamine (**3.1**) (From Gao, et. al. Report)[37b] ^{13}C NMR, 100 MHz, $CDCl_3$	Synthetic (+)-Strictamine (**3.1**) ^{13}C NMR, 125 MHz, $CDCl_3$
191.2	191.5
171.7	171.8
155.5	155.7
146.3	146.4
138.2	138.4
128.1	128.3
125.5	125.7
123.5	123.6
120.9	121.1
119.8	119.9
56.1	56.3
55.3	55.5
55.1	55.3
53.7	53.8
52.0	52.1
51.6	51.7
36.1	36.2
33.7	33.9
32.5	32.6
12.9	13.1

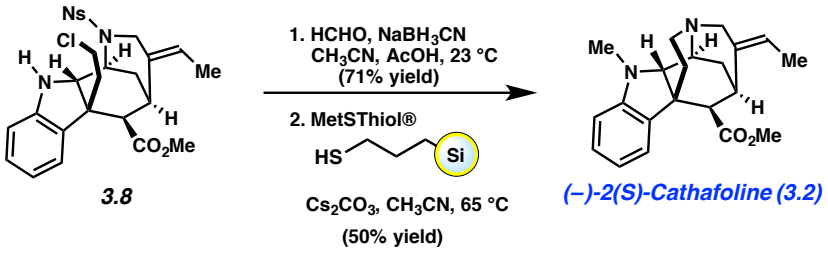

(–)2(*S*)-Cathafoline (3.2). To a solution of chloride **3.8** (8.0 mg, 0.0147 mmol) in MeCN (0.3 mL) was added 37% w/w HCHO in H_2O (3.3 µL, 0.0440 mmol) and AcOH (2.5 µL, 0.0440 mmol). After stirring for 3 min, $NaBH_3CN$ (2.8 mg, 0.0440 mmol) was added. The reaction was flushed with N_2 for 1 min, and stirred at room temperature. After stirring for 1 h, the reaction was quenched with sat. aq. $NaHCO_3$ (5 mL) and diluted with EtOAc (5 mL). The layers were separated and the

aqueous layer was extracted with EtOAc (2 x 5 mL). The organic layers were combined, dried over $MgSO_4$ and concentrated under reduced pressure to afford the corresponding *N*-methyl indoline (5.7 mg, 71% yield), which was used in the subsequent step without further purification.

To a vial containing the crude *N*-methyl indoline intermediate (5.7 mg, 0.0102 mmol), and a stir bar were added Cs_2CO_3 (19 mg, 0.0306 mmol) and SiliaMetS® Thiol (29 mg, 0.0408 mmol). The reaction was flushed with Ar for 1 min, evacuated for 1 min, and carefully backfilled with Ar. MeCN (0.5 mL) was added, and the reaction was degassed with Ar for 10 min, at which point the reaction was heated to 65 °C. After stirring for 2 h, additional Cs_2CO_3 (19 mg, 0.0306 mmol) and SiliaMetS® Thiol (29 mg, 0.0408 mmol) were added. The reaction was flushed with Ar for 1 min, and reheated to 65 °C. After stirring for an addition 1.5 h, the reaction was cooled to room temperature, filtered through a plug of celite® (MeCN eluent, 10 mL), and the filtrate was concentrated under reduced pressure. The crude mixture was purified via flash chromatography using florisil® as the stationary phase (99:1 $CHCl_3$:MeOH → 19:1 $CHCl_3$:MeOH) to afford (–)-2(*S*)-cathafoline **(3.2)** (1.7 mg, 50% yield) as a colorless oil. ^{1}H NMR spectral data for (–)-**3.2** (in $CDCl_3$) was consistent with literature reports[12] and a natural sample provided by T. S. Kam (see comparision ^{1}H NMR). Due to the compound's relative instability, the ^{13}C spectrum was acquired in C_6D_6, which matched a natural sample provided by T. S. Kam (see comparison ^{13}C NMR and Table 3.3). (–)-2(*S*)-Cathafoline (**3.2**): ^{1}H NMR (500 MHz, $CDCl_3$): δ 7.15–7.08 (m, 2H), 6.75 (td, J = 7.4, 0.9, 1H), 6.63 (d, J = 7.8, 1H), 5.38 (q, J = 7.5, 1H), 3.99–3.90 (m, 2H), 3.53 (s, 3H), 3.43 (td, J = 12.7, 6.4, 1H), 3.38 (br s, 1H), 3.36–3.26 (m, 2H), 2.96 (d, J = 16.3, 1H), 2.71 (d, J = 4.0, 1H), 2.68 (s, 3H), 2.55 (dd, J = 14.6, 7.4, 1H), 2.11 (dd, J = 13.8, 2.3, 1H), 2.05 (dd, J = 14.4, 6.2, 1H), 2.01–1.95 (m, 1H), 1.45 (dd, J = 6.9, 2.1 3H); ^{13}C NMR (125 MHz, C_6D_6): (20 of 21 signals observed) δ 172.7, 153.3, 140.4, 139.0, 123.8, 119.9, 118.5, 109.5, 71.0, 57.0, 50.44, 50.43, 48.9,

47.0, 43.7, 33.8, 33.2, 30.0. 25.8, 13.1; IR (film): 2921, 2852, 1738, 1464, 1165, 1123, 1038 cm^{-1}; HRMS–APCI (*m/z*) $[M + H]^+$ calcd for $C_{21}H_{27}N_2O_2^+$, 339.20660; found 339.20725; observed for natural sample $[\alpha]^{25.0}_D$ –28.0° (c = 0.1, CH_2Cl_2), observed for synthetic sample $[\alpha]^{25.2}_D$ –78.00° (c = 0.1, CH_2Cl_2).[12]

Table 3.3 Comparison of ^{13}C NMR Data for Natural vs. Synthetic (–)-2(*S*)-Cathafoline (**3.2**)

Natural (–)-2(*S*)-Cathafoline (**3.2**) (From Sample Provided by T. S. Kam) ^{13}C NMR, 125 MHz, C_6D_6	Synthetic (–)-2(*S*)-Cathafoline (**3.2**) ^{13}C NMR, 125 MHz, C_6D_6
172.7	172.7
153.3	153.3
140.4	140.4
138.9	139.0
123.8	123.8
119.9	119.9
118.6	118.5
109.5	109.5
70.9	71.0
57.0	57.0
50.44	50.44
50.41	50.43
48.9	48.9
47.0	47.0
43.7	43.7
33.8	33.8
33.2	33.2
39.9	30.0
25.7	25.8
13.1	13.1

3.9.3 Determination of Enantiomeric Excess and Absolute Stereochemistry

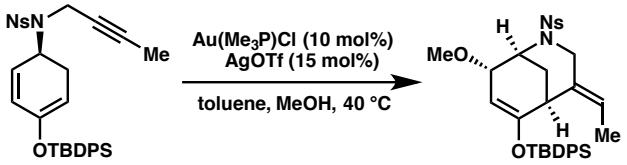

3.14 *3.32*

Silyl Enol Ether 3.32. To a solution of $Au(PMe_3)Cl$ (5.3 mg, 0.0171 mmol) and enol ether **3.14** (100.0 mg, 0.171 mmol) in toluene (4.4 mL) and MeOH (0.5 mL) was added AgOTf (6.6 mg, 0.0256 mmol). The reaction was heated to 40 °C. After stirring for 3.5 h, the reaction was poured into sat. aq. $NaHCO_3$ (40 mL). The layers were separated and the aqueous layer was extracted with EtOAc (3 x 25 mL). The organic layers were combined and dried over $MgSO_4$. An aliquot of the resulting residue was purified via preparative thin layer chromatography (1:1 hexanes:EtOAc) to afford Michael adduct **3.32** (4.5 mg) as a brown oil. Silyl enol ether **3.32**: R_f 0.85 (1:1 hexanes:EtOAc); ^{1}H NMR (500 MHz, $CDCl_3$): δ 8.03–7.99 (m, 1H), 7.74–6.89 (m, 2H), 7.67–7.60 (m, 5H), 7.46–7.34 (m, 6H), 5.54 (qd, *J* = 6.9, 1.0, 1H), 4.74 (d, *J* = 4.6, 1H), 3.99 (app. br s, 1H), 3.78 (d, *J* = 14.2, 1H), 3.59 (dt, *J* = 14.2, 1.7, 1H), 3.44 (dt, *J* = 4.6, 0.9, 1H), 3.37 (t, *J* = 3.0, 1H), 3.07 (s, 3H), 2.06 (dt, *J* = 12.5, 3.3, 1H), 1.73 (dd, *J* = 6.9, 1.8, 3H), 1.55 (dt, *J* = 12.5, 2.8, 1H), 0.99 (s, 9H); ^{13}C NMR (125 MHz, $CDCl_3$): (26 of 27 signals observed) δ 154.5, 148.0, 135.62, 135.57, 133.9, 133.5, 132.5, 132.0, 131.8, 131.3, 131.0, 130.3, 130.1, 127.93, 127.88, 124.5, 122.1, 104.4, 56.5, 50.7, 47.9, 36.0, 27.9, 26.6, 19.3, 13.1; IR (film): 2932, 2859, 1712, 1656, 1543, 1360, 1164, 1073 cm^{-1}; HRMS–APCI (*m/z*) $[M + H]^+$ calcd for $C_{33}H_{39}N_2O_6SSi^+$, 619.22198; found, 619.25150; $[\alpha]^{26.2}_D$ 46.4° (c = 1.0, CH_2Cl_2).

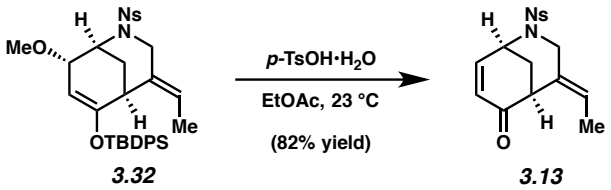

3.32 *3.13*

Enone 3.13. To a solution of enol ether **3.32 (**149 mg, 0.241 mmol) in EtOAc (10 mL) was added *p*-TsOH•H_2O (46 mg, 0.241 mmol). After stirring at room temperature for 1 h, the reaction was poured into sat. aq. $NaHCO_3$ (40 mL). The layers were separated and the aqueous layer was extracted with EtOAc (3 x 50 mL). The organic layers were combined and dried over $MgSO_4$. The resulting residue was purified via flash chromatography (7:3 hexanes:EtOAc) to afford enone **3.13** (68.6 mg, 82% yield) as a clear oil. Enone **3.13** $[\alpha]^{25.1}_{D}$ –22.0° (c = 0.10, CH_2Cl_2). Characterization data for racemic enone **3.13** has previously been reported (see Chapter Two, Section 2.9.2, page 56).[5a]

The enantiomeric excess of synthetic enone **3.13** (Section 3.9.2, page 143) was determined using SFC. The chiral SFC assay was performed on a Daicel ChiralPak OD–H column at 35 °C with a 12% *i*-PrOH isocratic solvent system and a flow rate of 2 mL/min. The retention times of the two enantiomers of **3.13** were 7.59 (minor) and 8.34 (major), respectively. The enantiomeric ratio (er) was found to be 2:98.

Figure 3.2 Chiral SFC Trace of (±)-**3.13**.

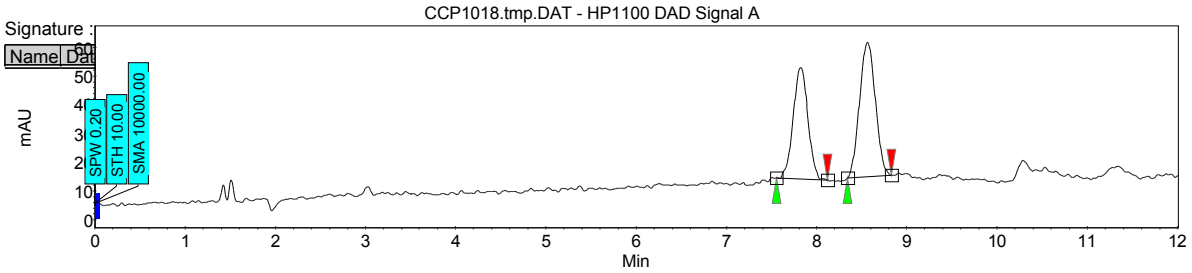

Index	Name	Start	Time	End	RT Offset	Quantity	Height	Area	Area
		[Min]	[Min]	[Min]	[Min]	[% Area]	[µV]	[µV.Min]	[%]
1	UNKNOWN	7.56	7.82	8.12	0.00	44.06	38.7	7.5	44.055
2	UNKNOWN	8.35	8.57	8.83	0.00	55.94	46.6	9.5	55.945
Total						100.00	85.3	16.9	100.000

Figure 3.3 Chiral SFC Trace of Enantioenriched **3.13**.

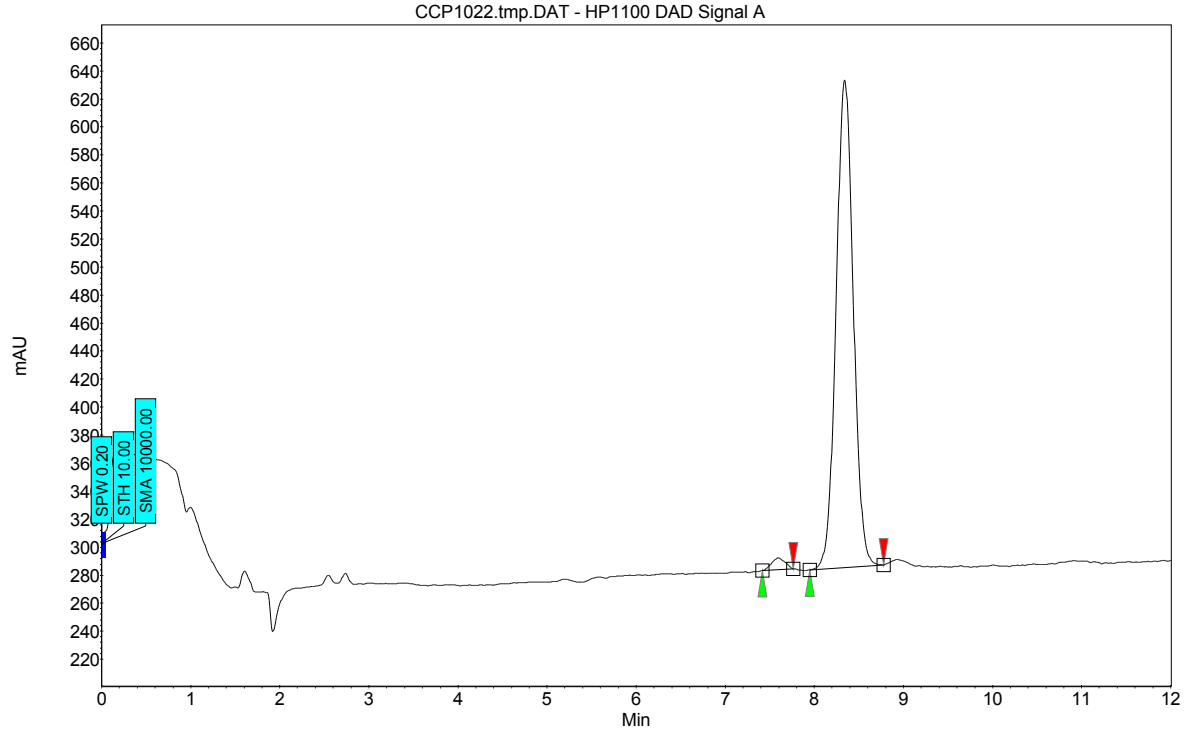

Index	Name	Start	Time	End	RT Offset	Quantity	Height	Area	Area
		[Min]	[Min]	[Min]	[Min]	[% Area]	[µV]	[µV.Min]	[%]
1	UNKNOWN	7.42	7.59	7.77	0.00	1.83	8.4	1.5	1.830
2	UNKNOWN	7.95	8.34	8.78	0.00	98.17	348.0	78.0	98.170
Total						100.00	356.4	79.4	100.000

3.10 Spectra Relevant to Chapter Three:

Enantioselective Total Syntheses of Akuammiline Alkaloids (+)-Strictamine, (–)-2(*S*)-Cathafoline, and (–)-Aspidophylline A

Adapted from: Jesus Moreno, Elias Picazo, Lucas A. Morrill, Joel M. Smith, and Neil K. Garg. *J. Am. Chem. Soc.* **2016**, *138*, 1162–1165.

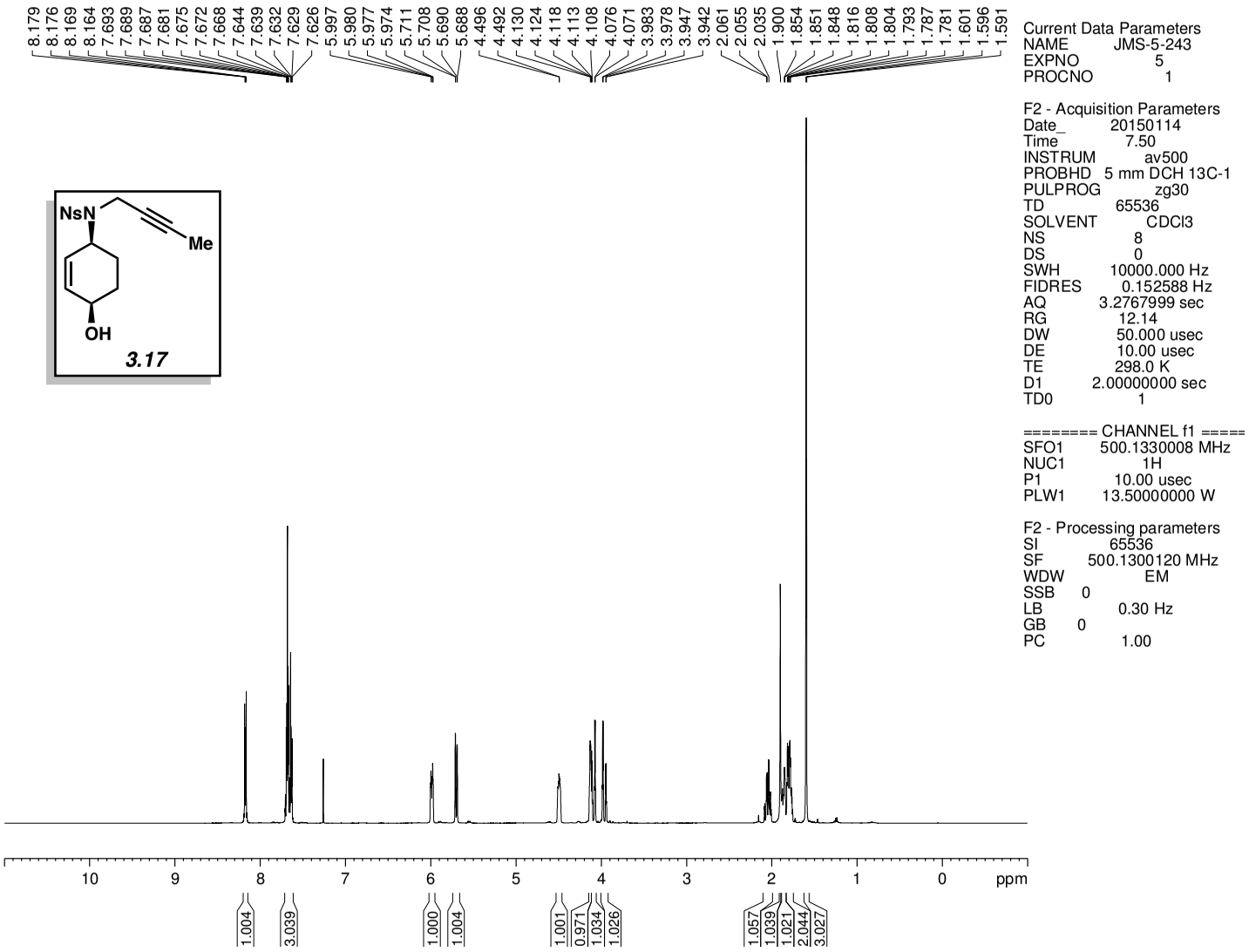

Figure 3.4 ^{1}H NMR (500 MHz, $CDCl_3$) of compound **3.17**.

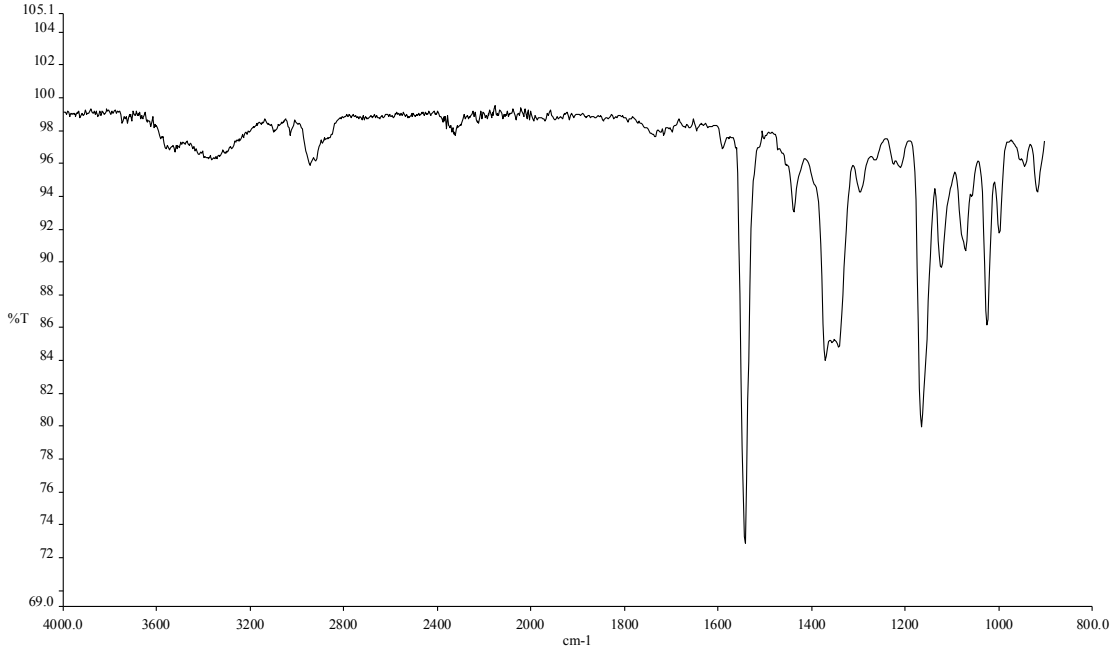

Figure 3.5 Infrared spectrum of compound **3.17**.

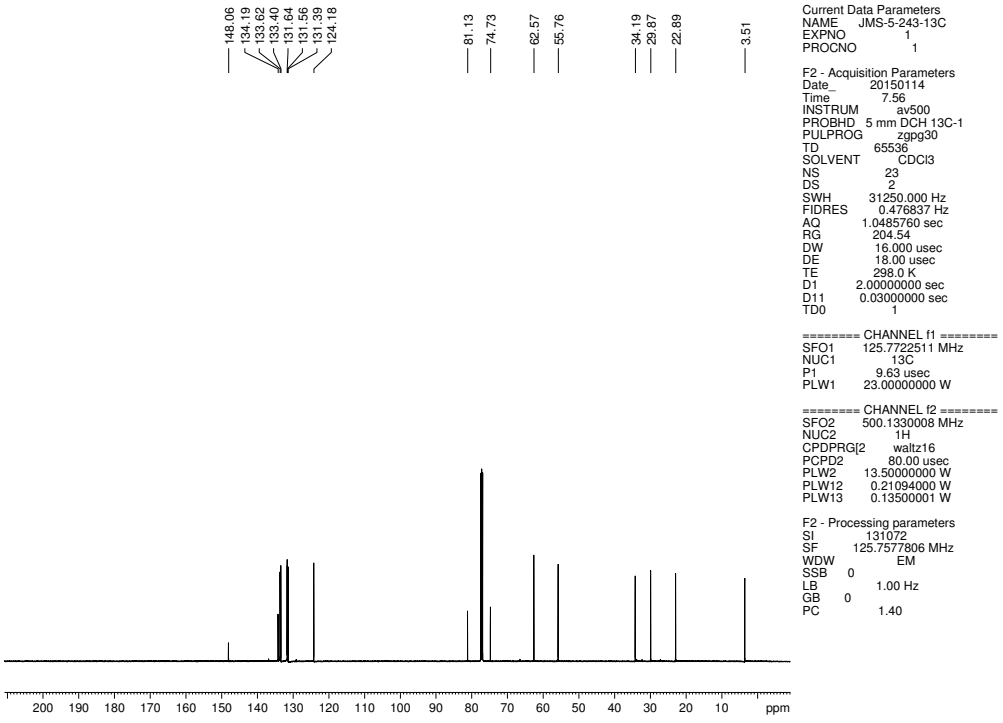

Figure 3.6 ^{13}C NMR (125 MHz, $CDCl_3$) of compound **3.17**.

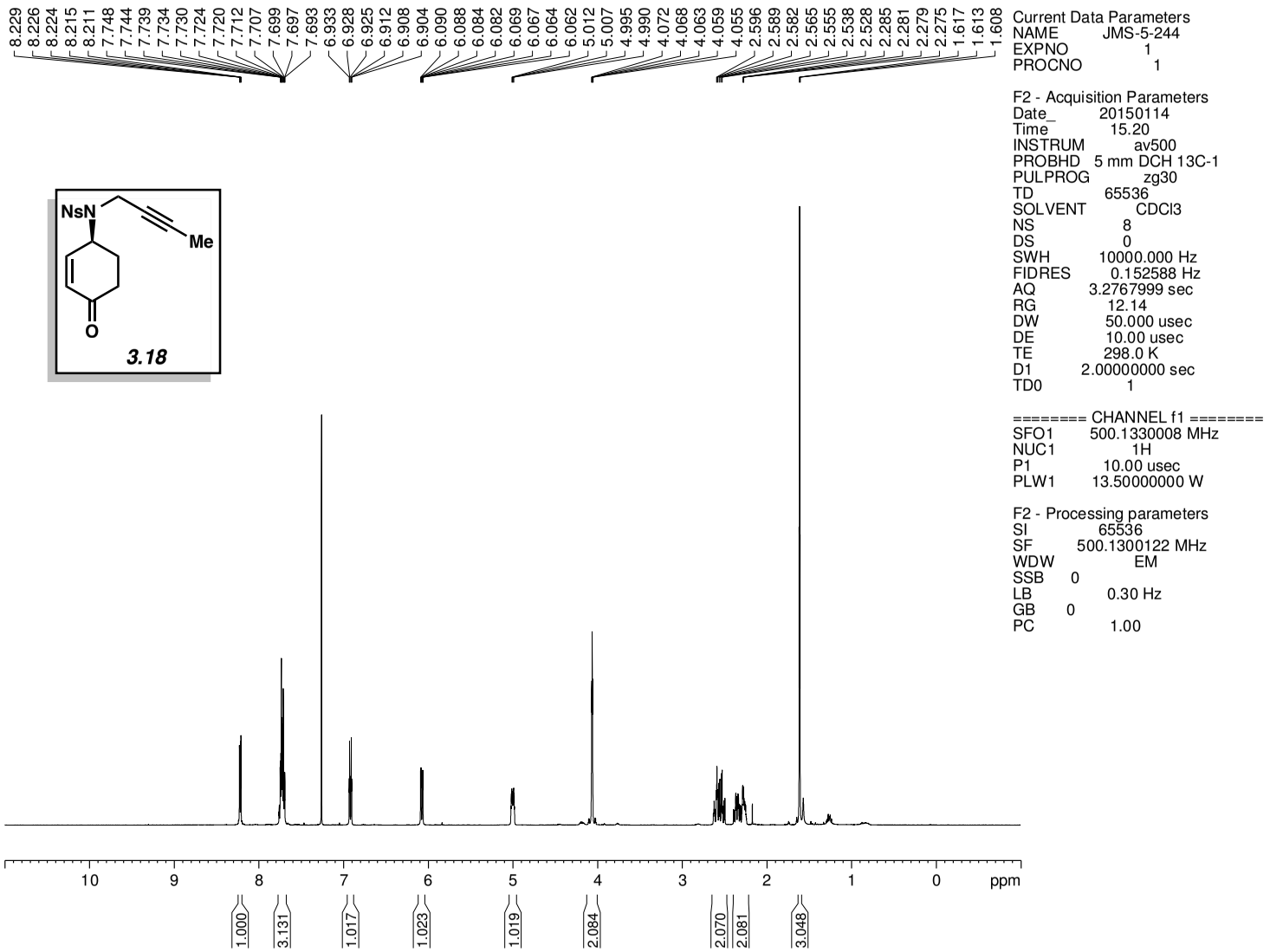

Figure 3.7 ^{1}H NMR (500 MHz, $CDCl_3$) of compound **3.18**.

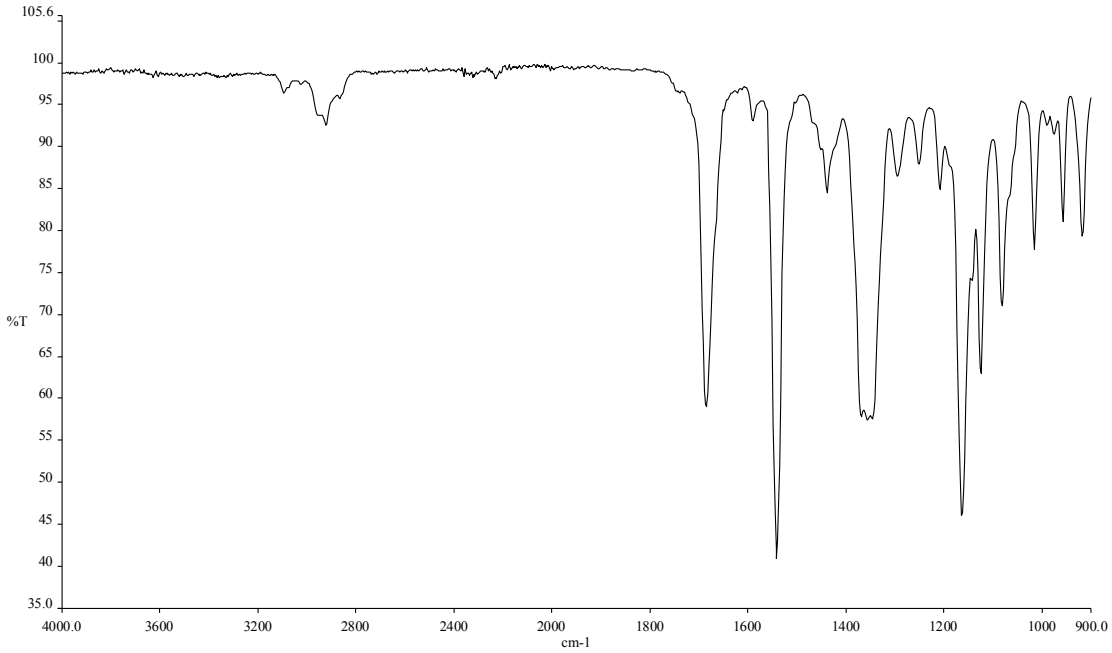

Figure 3.8 Infrared spectrum of compound **3.18**.

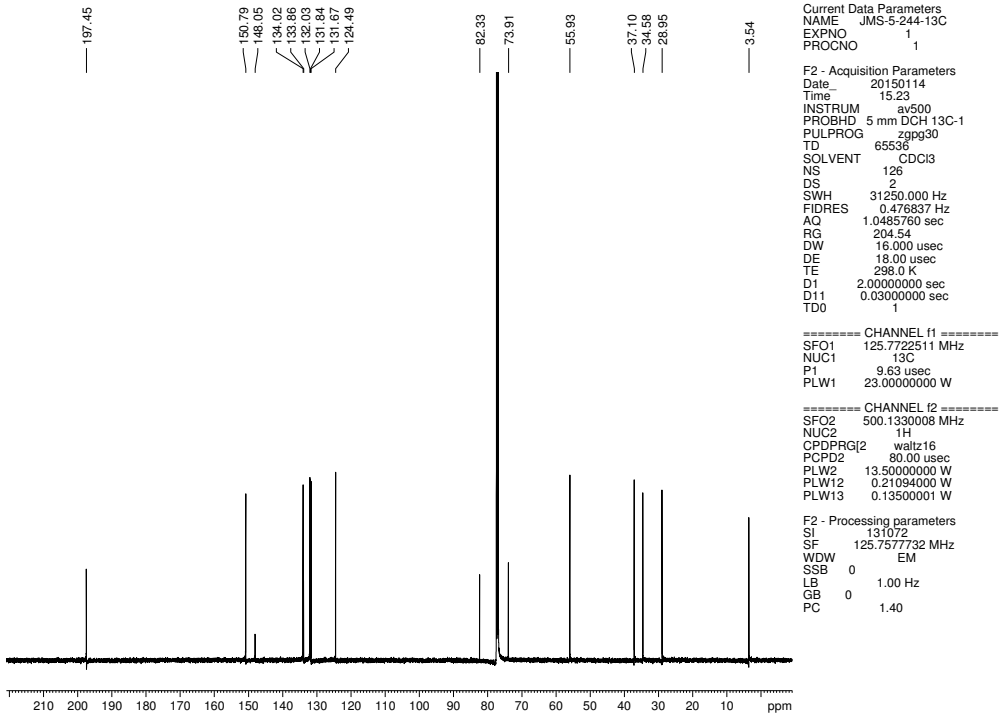

Figure 3.9 ^{13}C NMR (125 MHz, $CDCl_3$) of compound **3.18**.

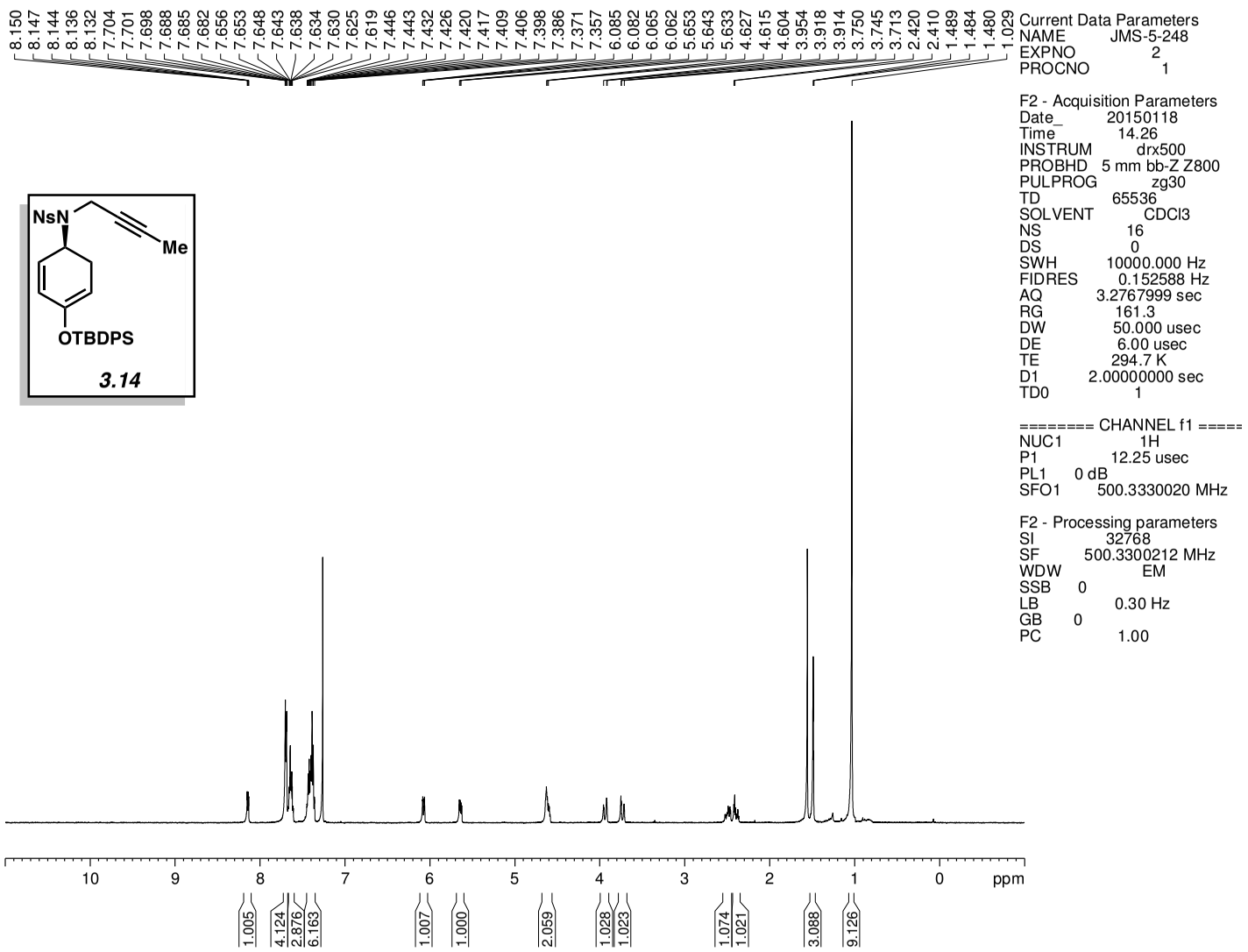

Figure 3.10 ^{1}H NMR (500 MHz, $CDCl_3$) of compound **3.14**.

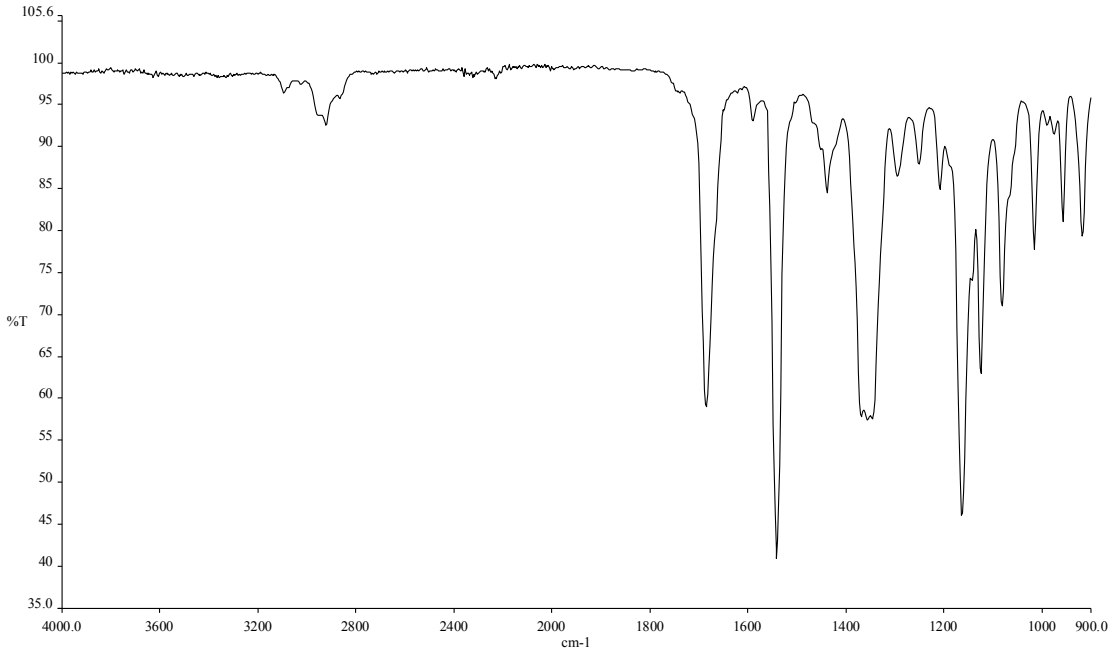

Figure 3.11 Infrared spectrum of compound **3.14**.

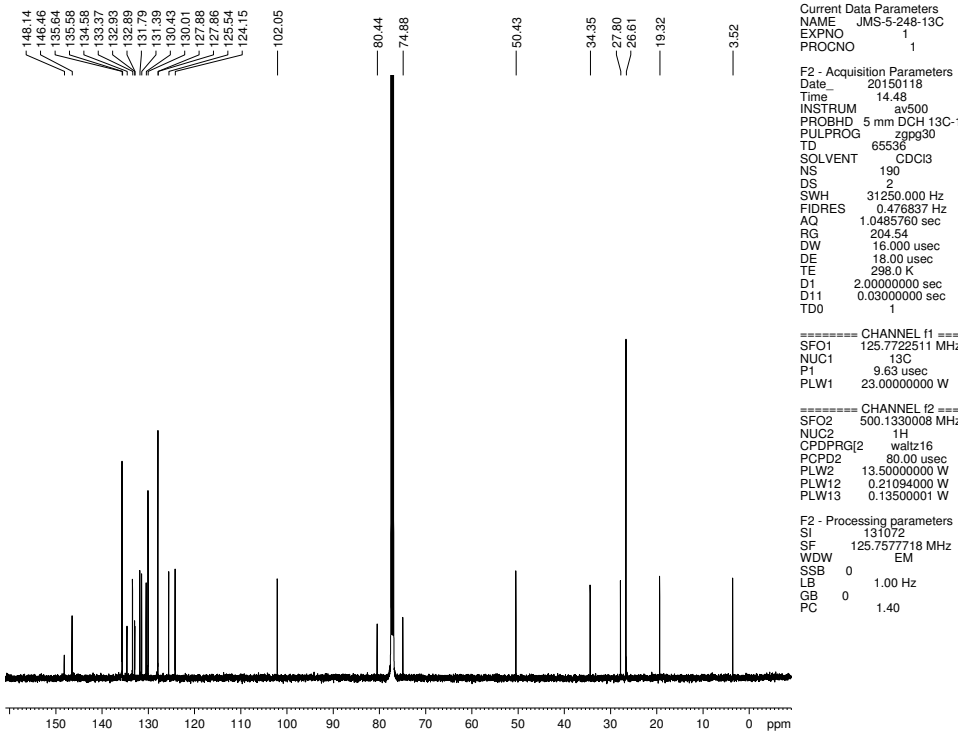

Figure 3.12 ^{13}C NMR (125 MHz, $CDCl_3$) of compound **3.14**.

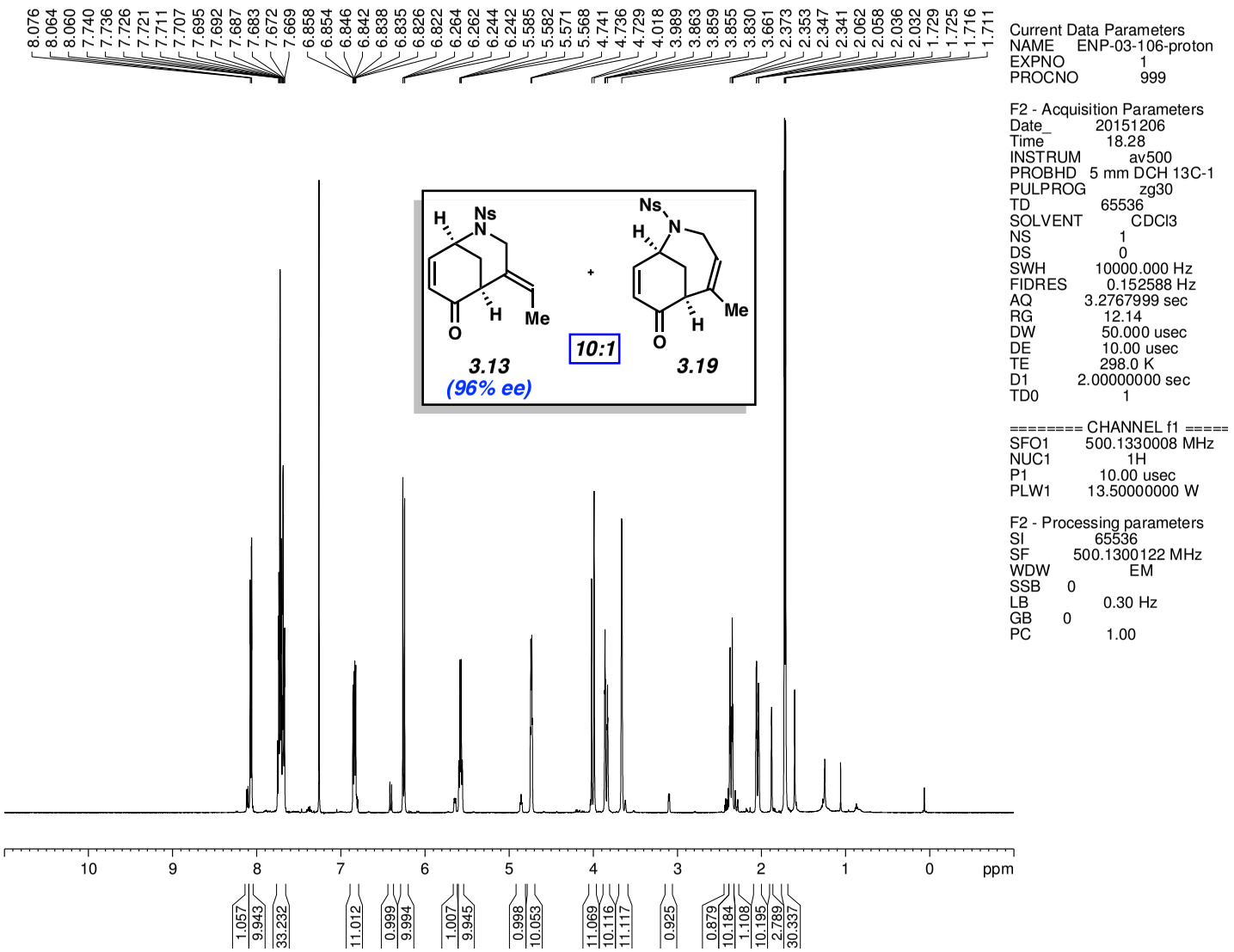

Figure 3.13 ^{1}H NMR (500 MHz, $CDCl_3$) of compounds **3.13** and **3.19**.

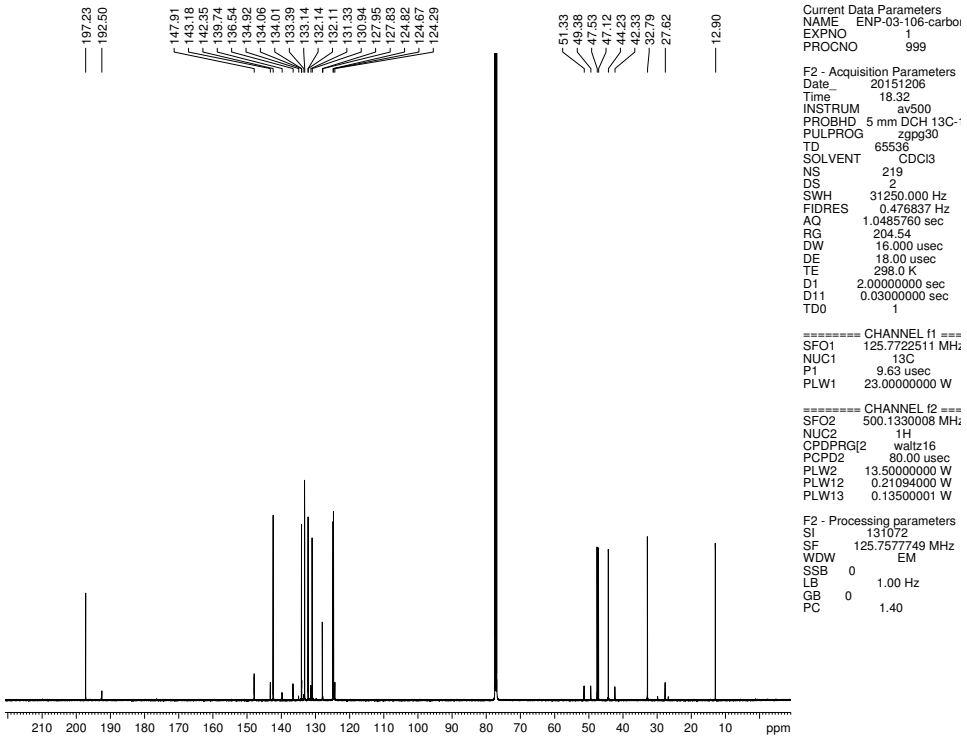

Figure 3.14 ^{13}C NMR (125 MHz, $CDCl_3$) of compounds **3.13** and **3.19**.

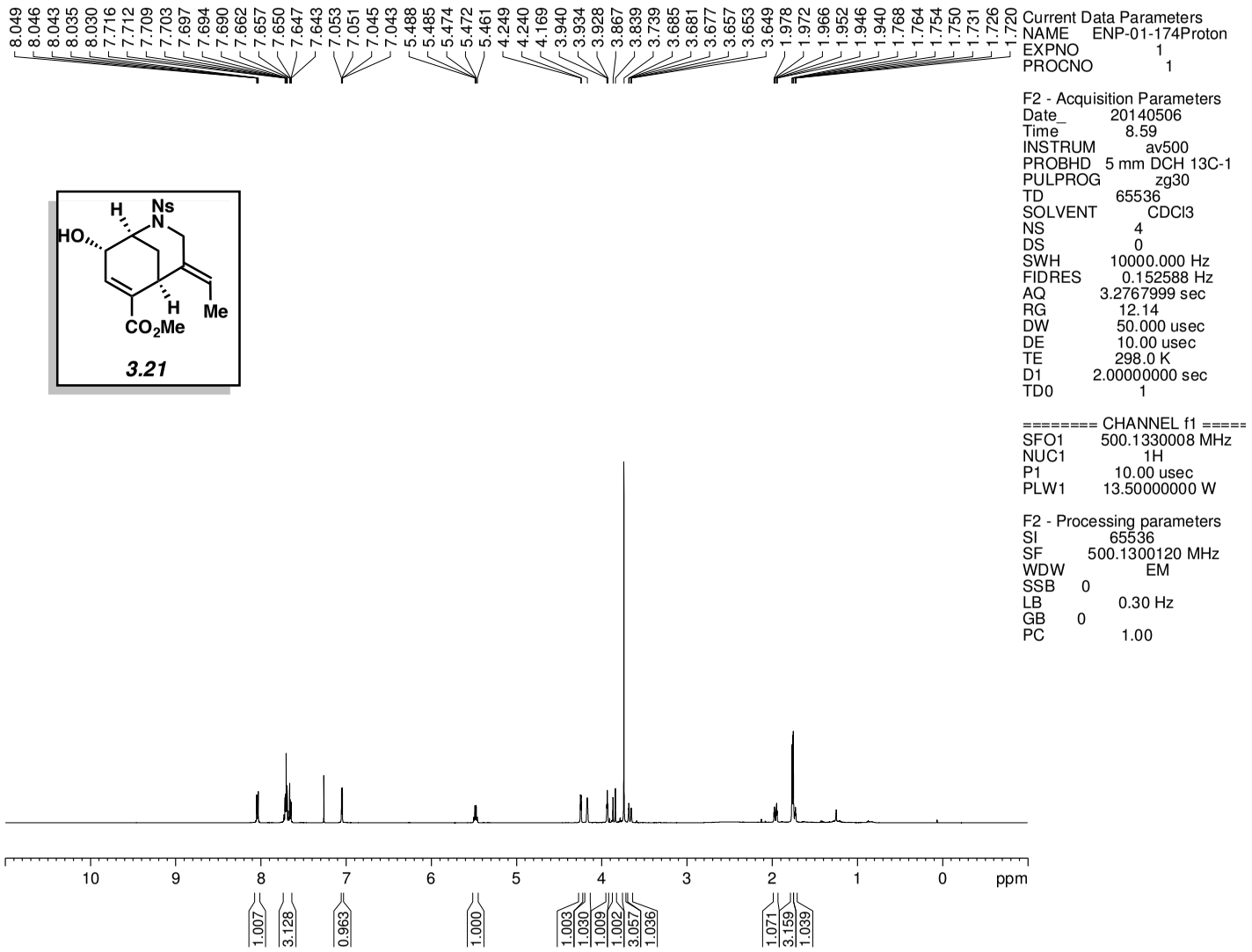

Figure 3.15 ^{1}H NMR (500 MHz, $CDCl_3$) of compound **3.21**.

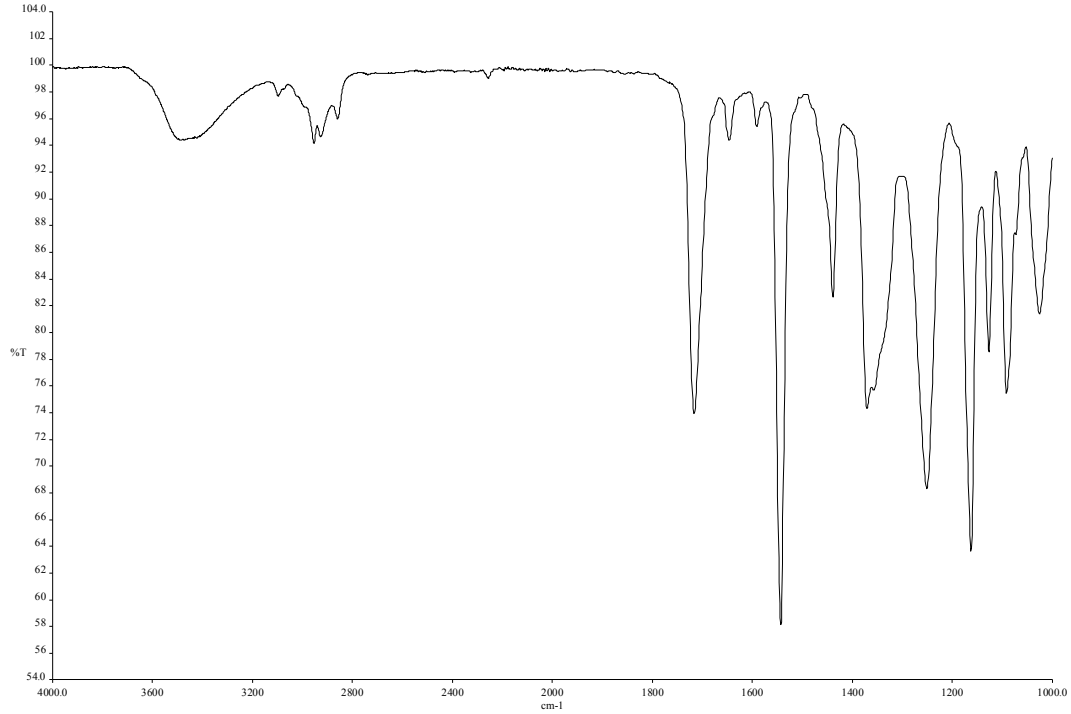

Figure 3.16 Infrared spectrum of compound **3.21**.

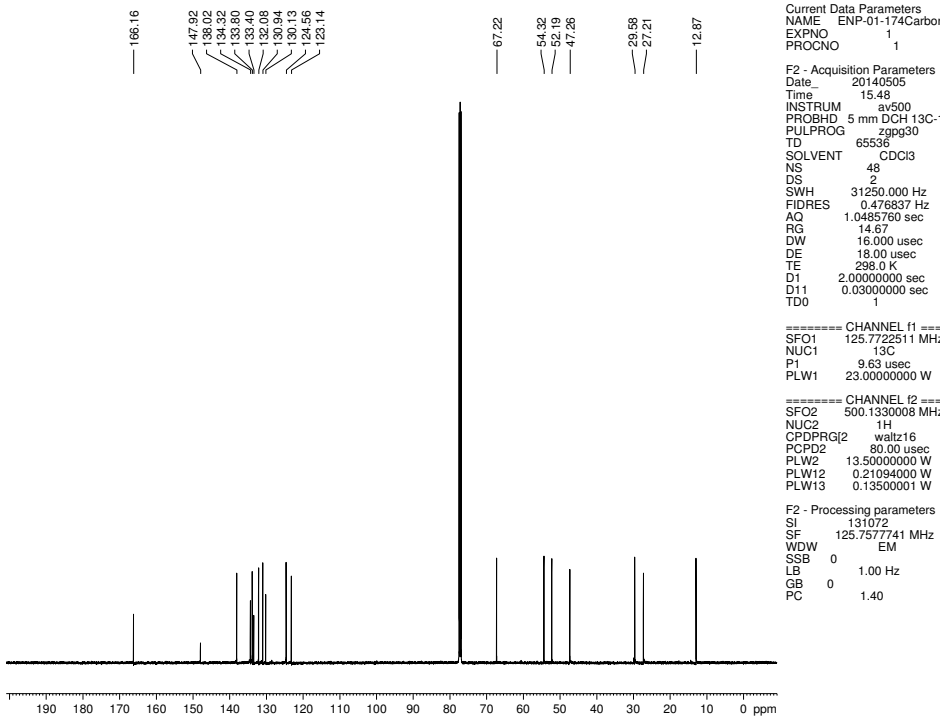

Figure 3.17 ^{13}C NMR (125 MHz, $CDCl_3$) of compound **3.21**.

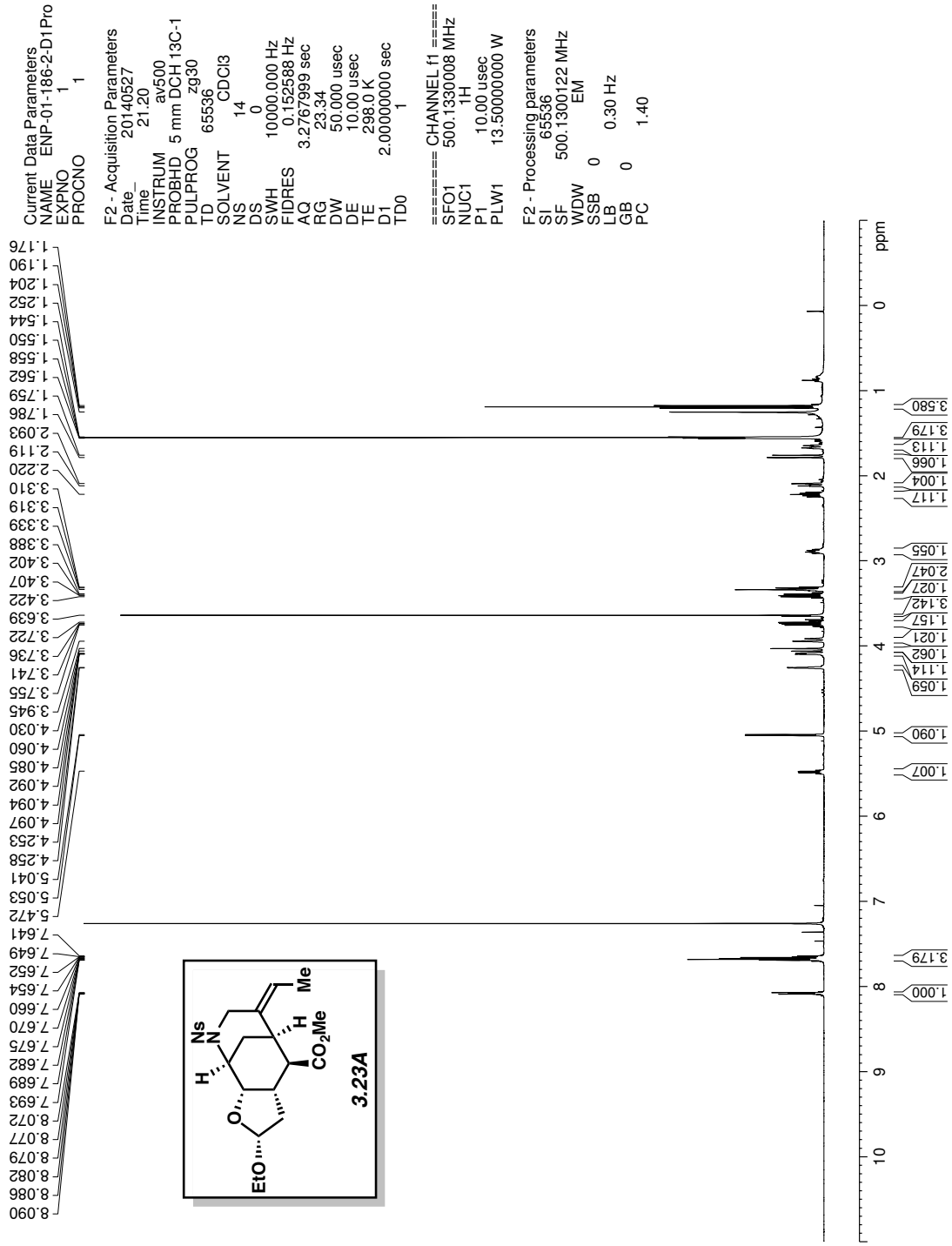

Figure 3.18 ^{1}H NMR (500 MHz, $CDCl_3$) of compound **3.23A**.

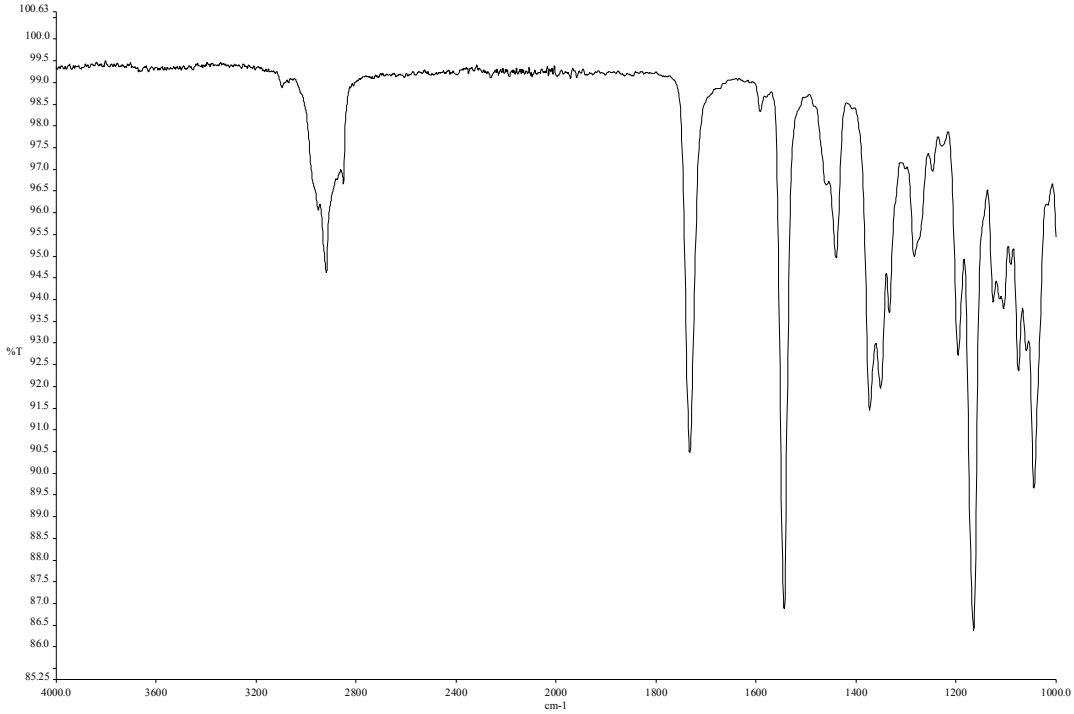

Figure 3.19 Infrared spectrum of compound **3.23A**.

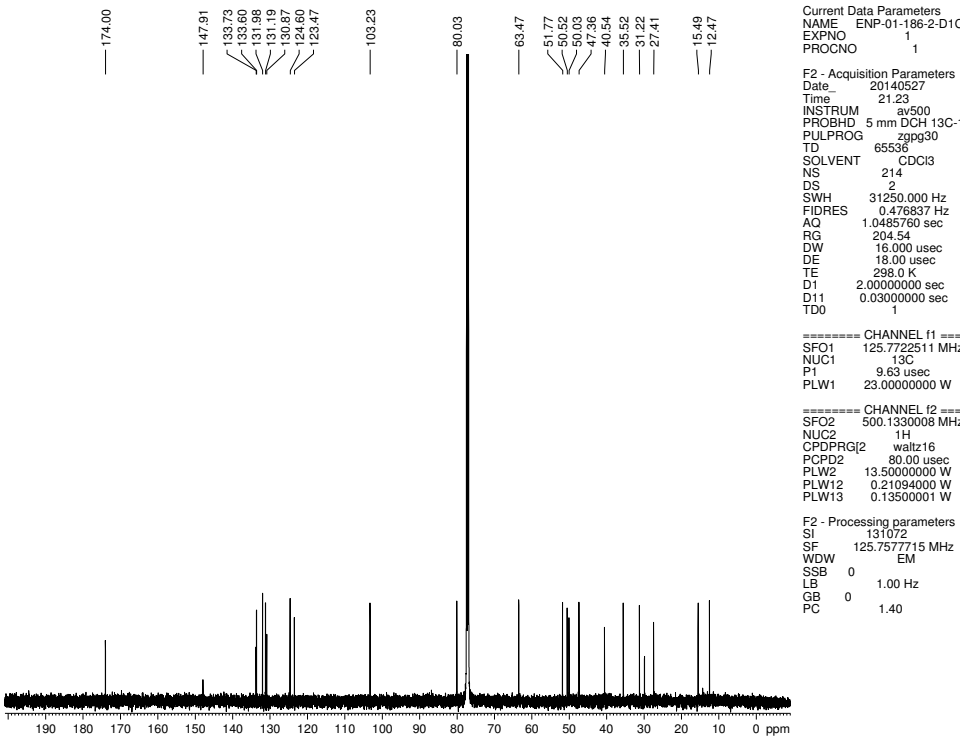

Figure 3.20 ^{13}C NMR (125 MHz, $CDCl_3$) of compound **3.23A**.

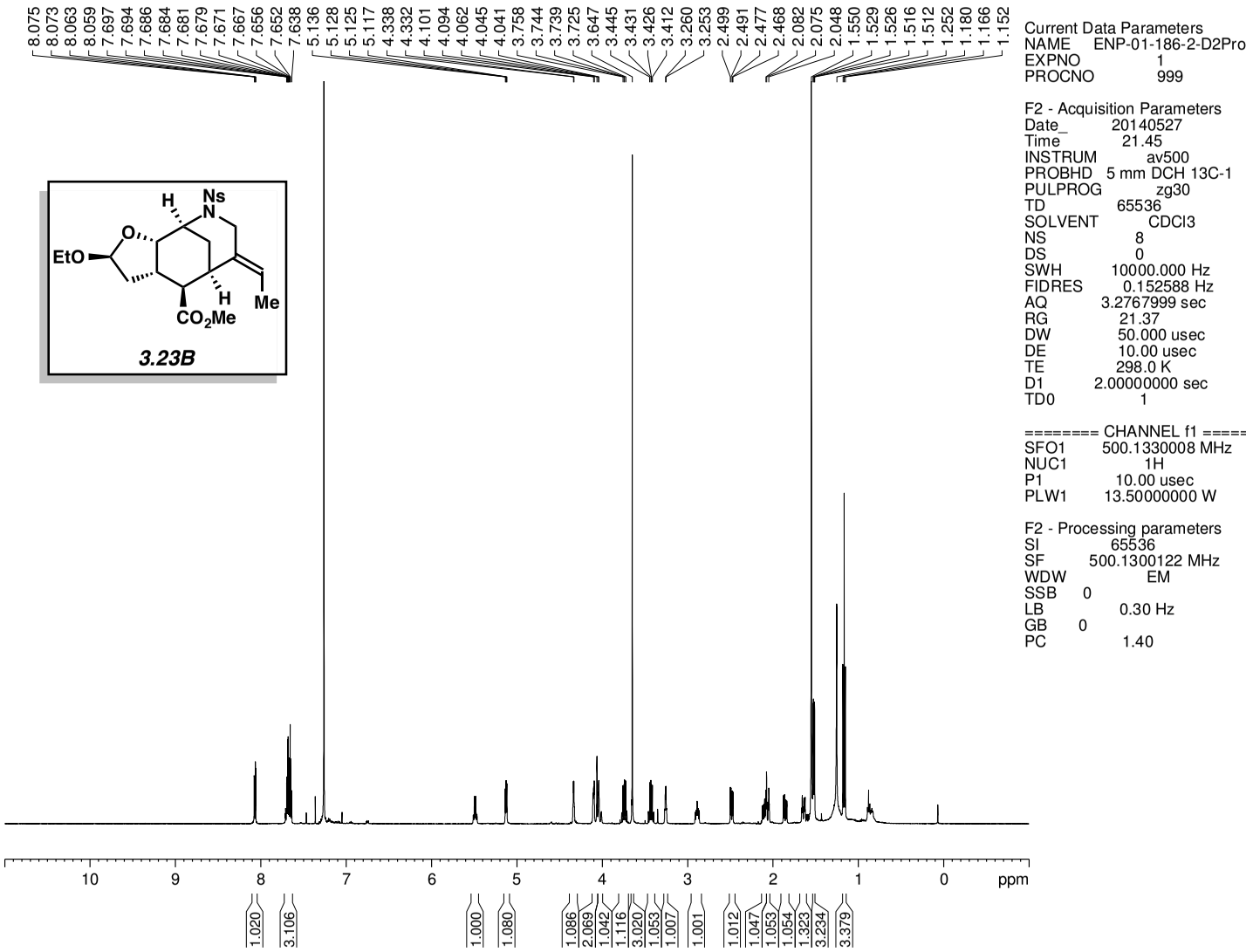

Figure 3.21 ^{1}H NMR (500 MHz, $CDCl_3$) of compound **3.23B**.

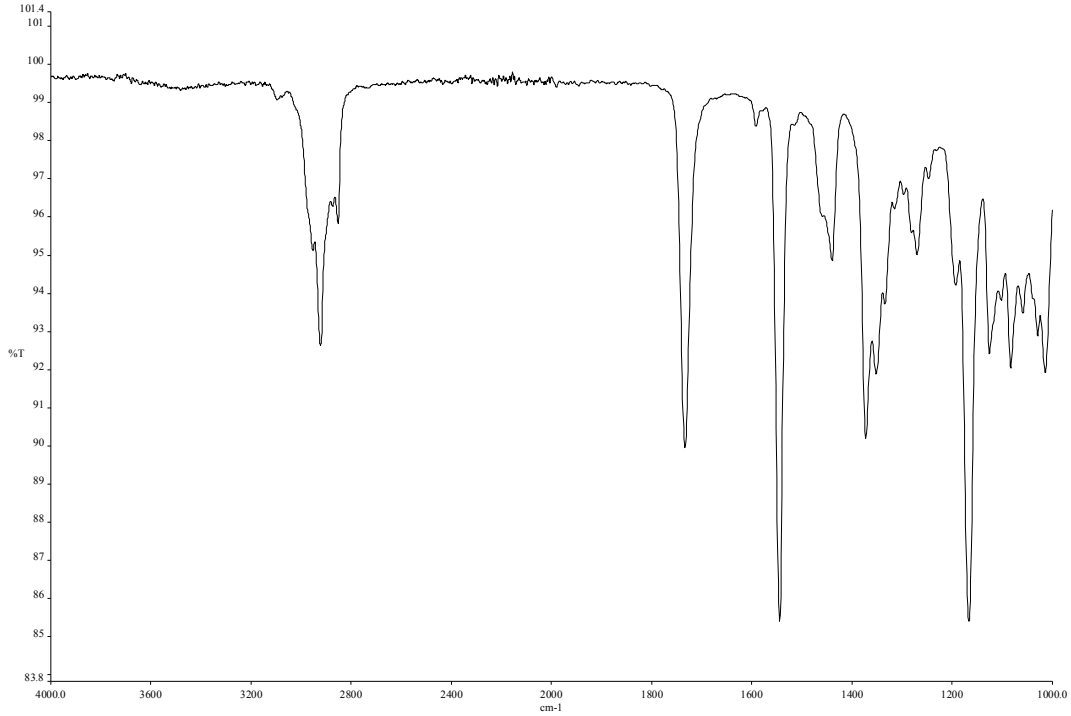

Figure 3.22 Infrared spectrum of compound **3.23B**.

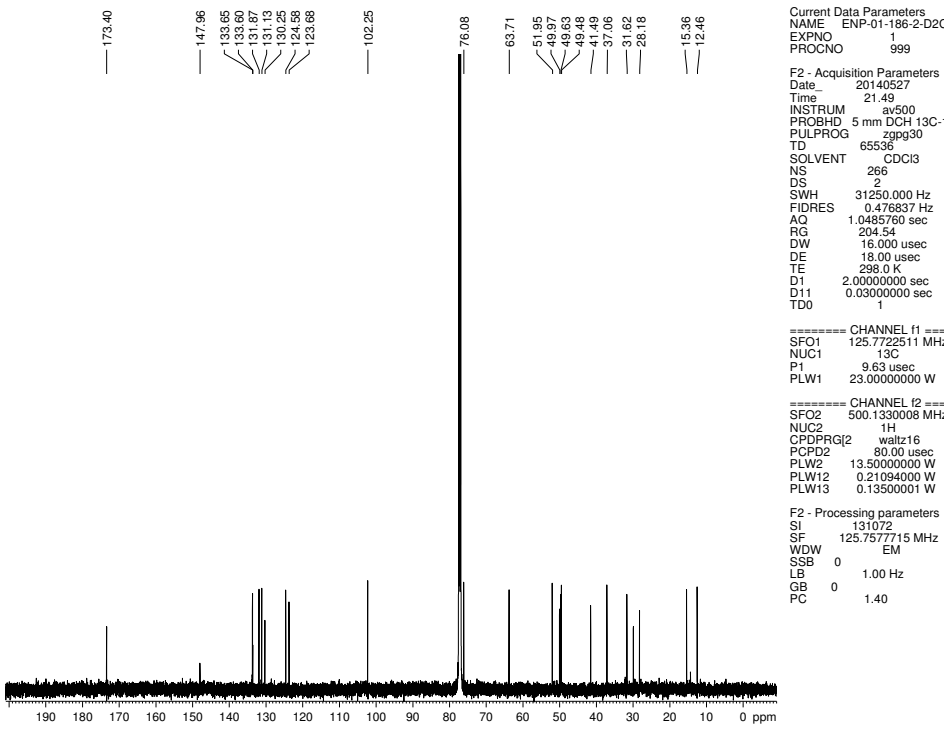

Figure 3.23 ^{13}C NMR (125 MHz, $CDCl_3$) of compound **3.23B**.

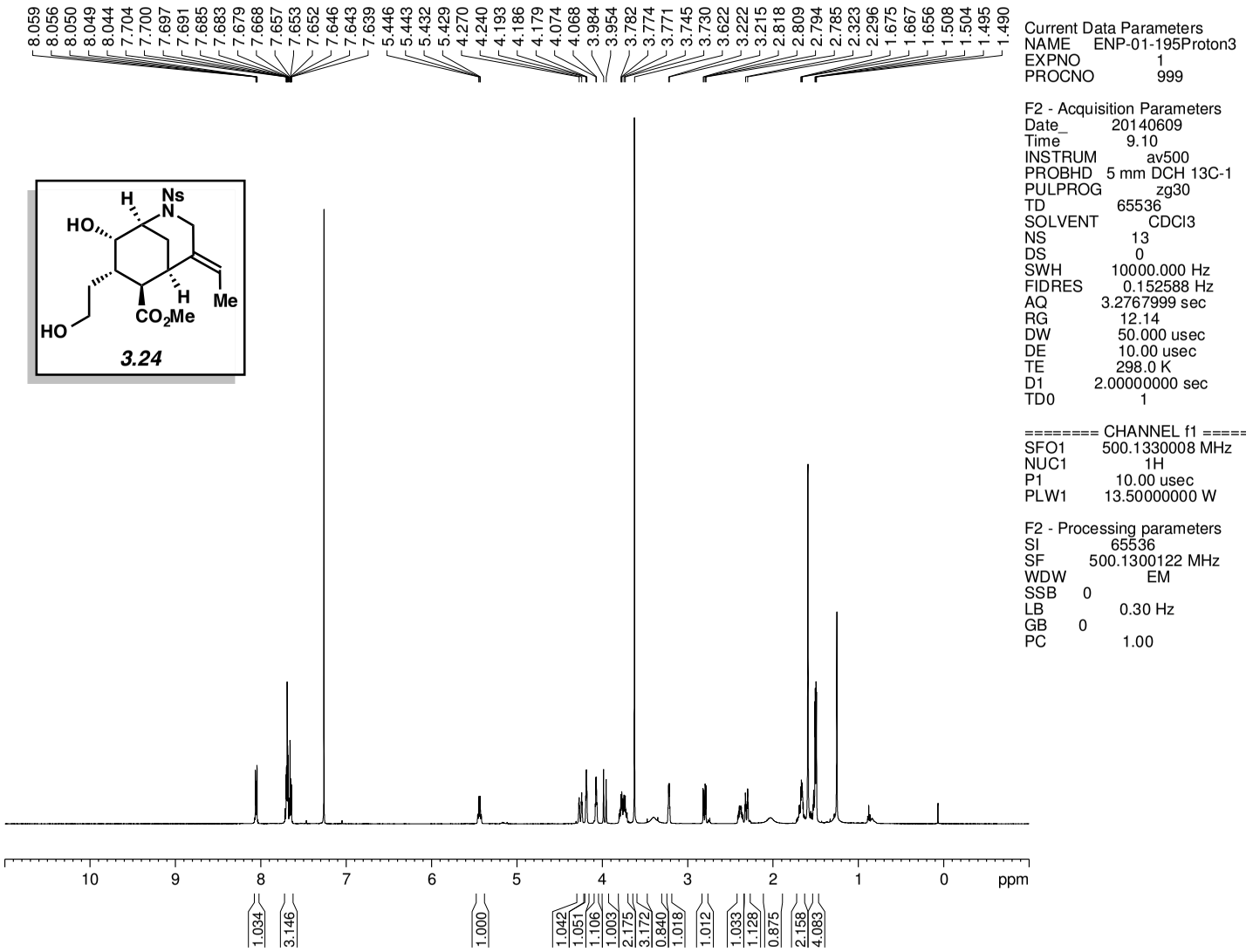

Figure 3.24 ^{1}H NMR (500 MHz, $CDCl_3$) of compound **3.24**.

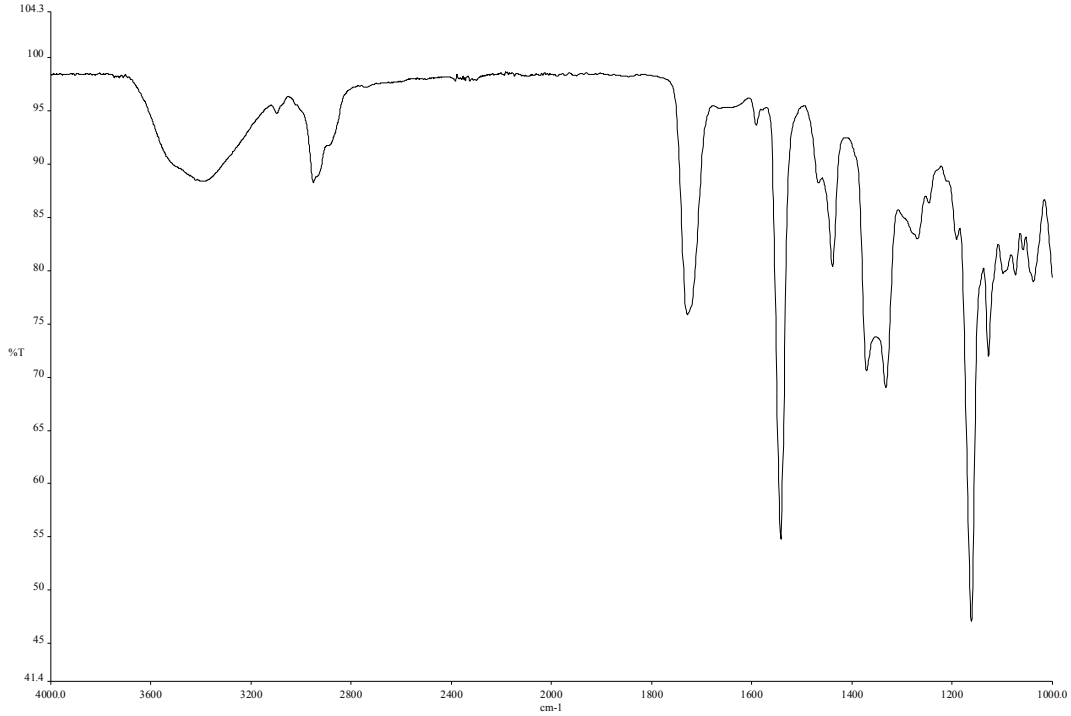

Figure 3.25 Infrared spectrum of compound **3.24**.

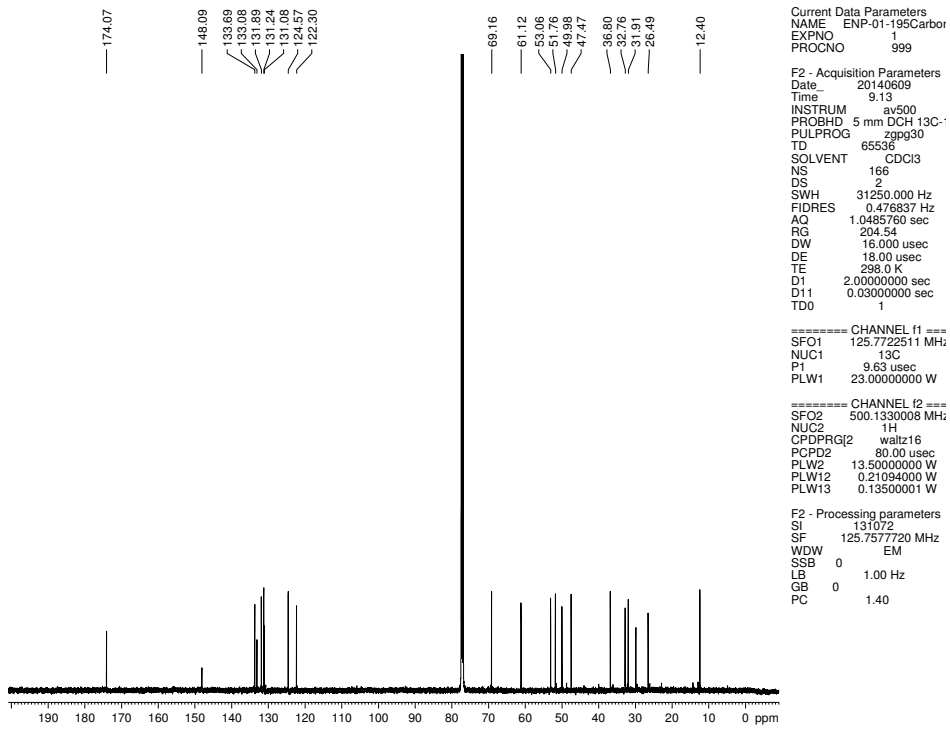

Figure 3.26 ^{13}C NMR (125 MHz, $CDCl_3$) of compound **3.24**.

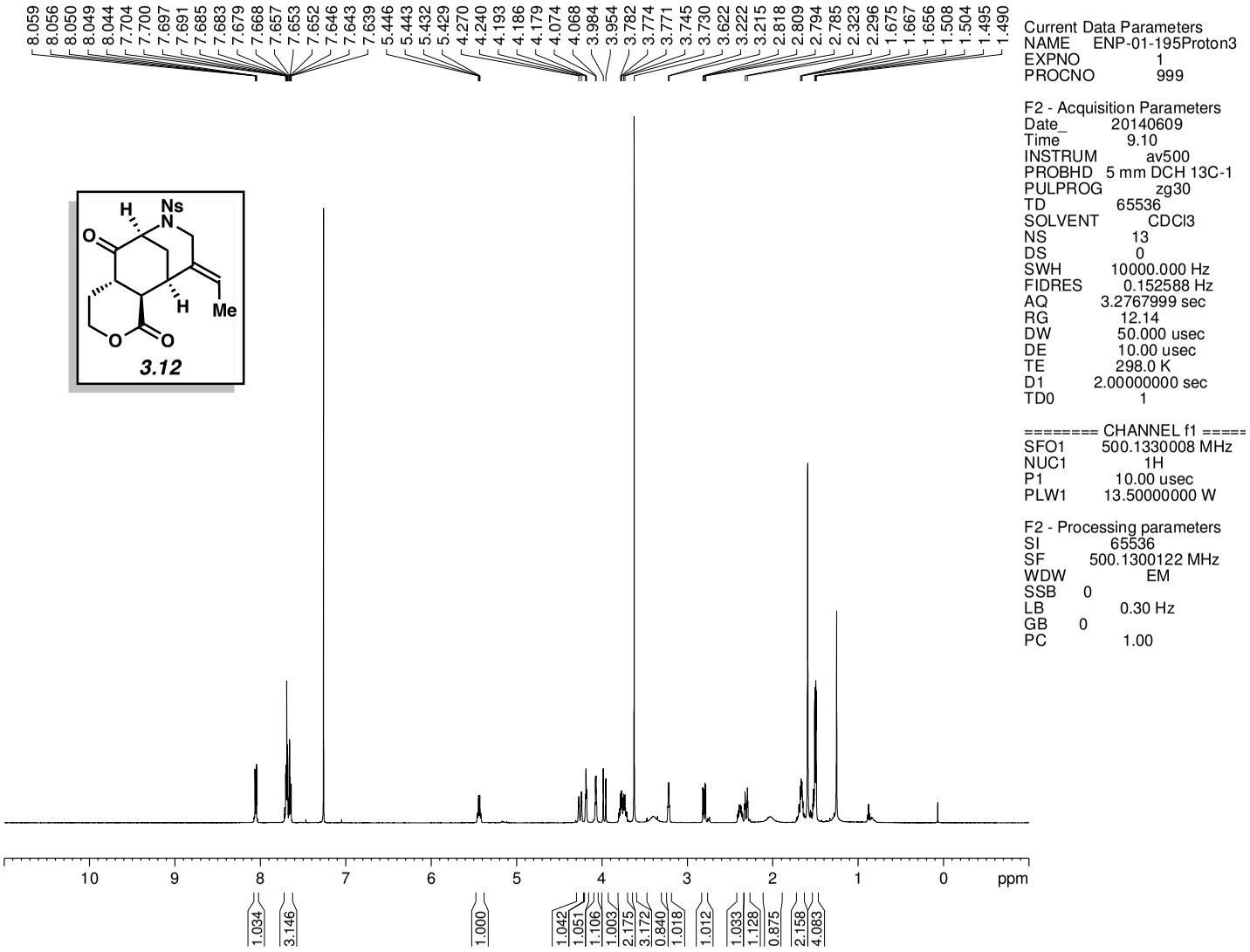

Figure 3.27 ^{1}H NMR (500 MHz, $CDCl_3$) of compound **3.12**.

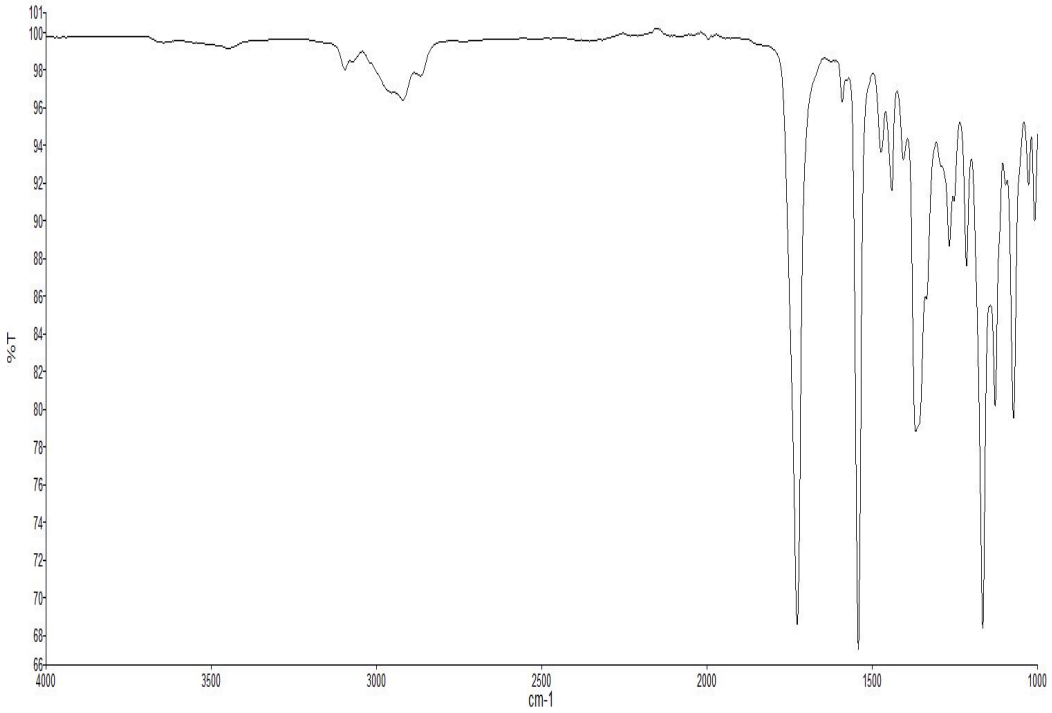

Figure 3.28 Infrared spectrum of compound **3.12**.

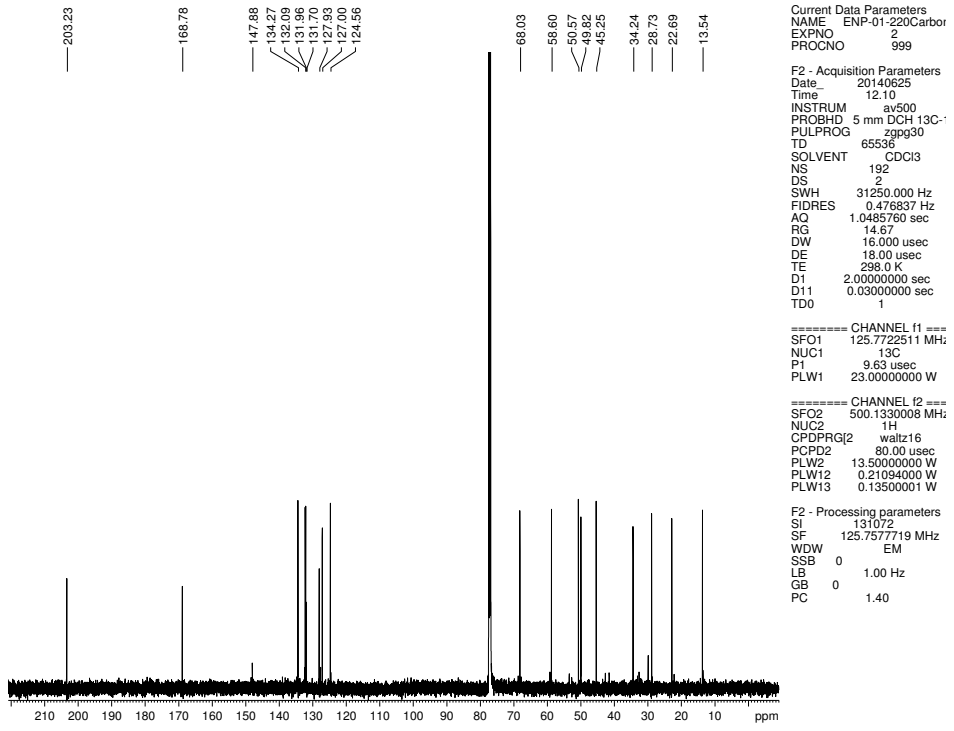

Figure 3.29 ^{13}C NMR (125 MHz, $CDCl_3$) of compound **3.12**.

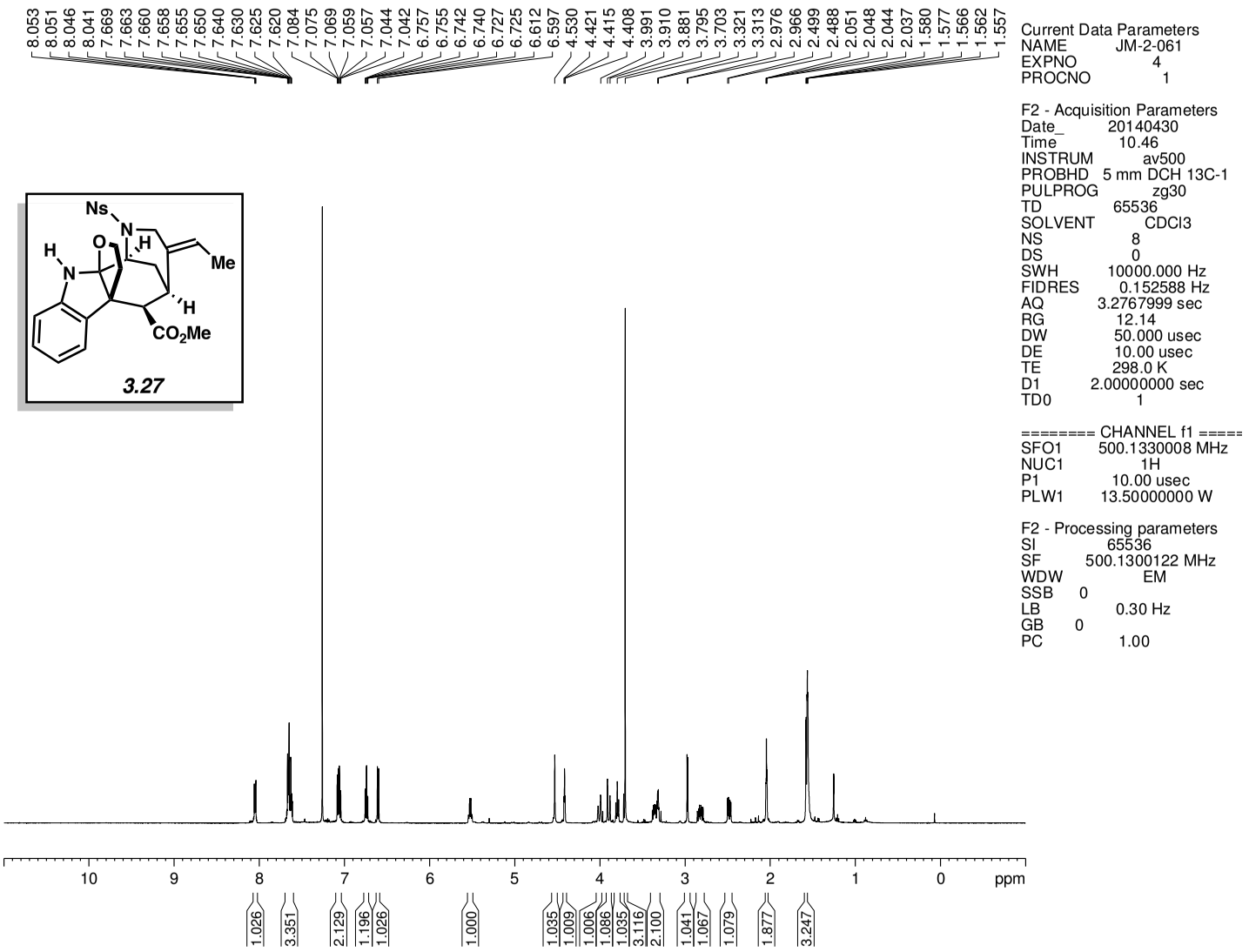

Figure 3.30 ^{1}H NMR (500 MHz, $CDCl_3$) of compound **3.27**.

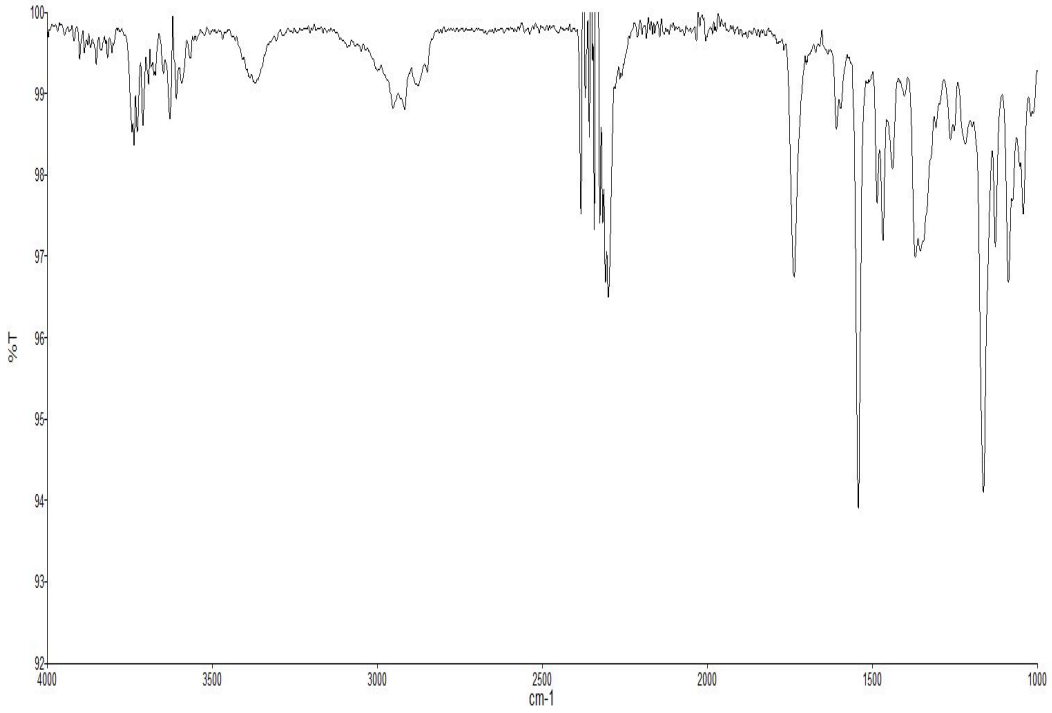

Figure 3.31 Infrared spectrum of compound **3.27**.

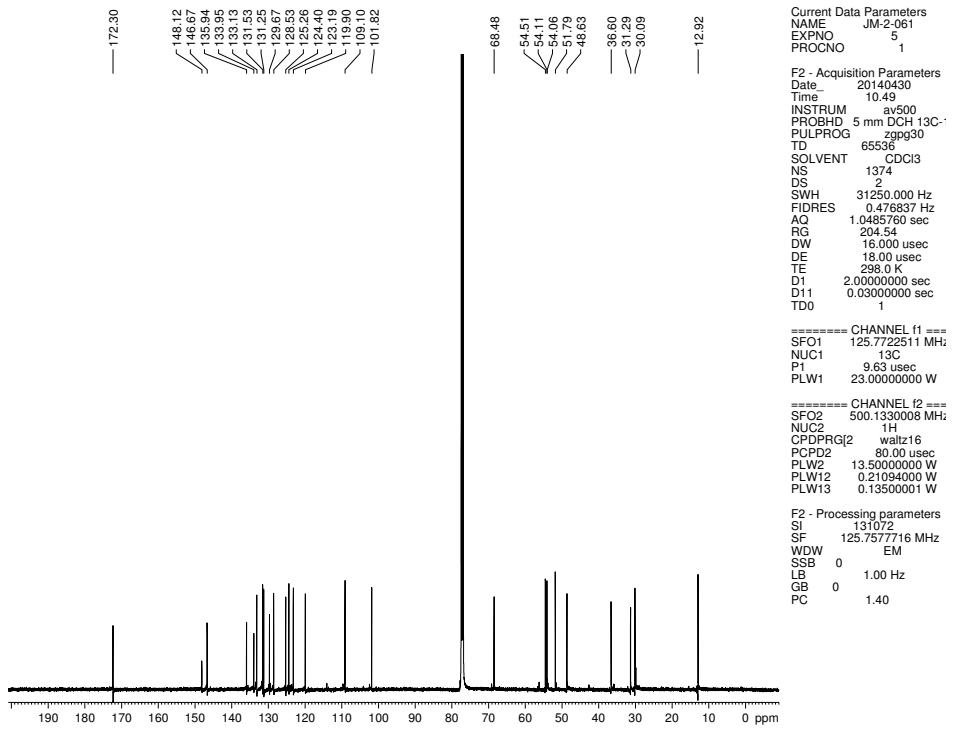

Figure 3.32 ^{13}C NMR (125 MHz, $CDCl_3$) of compound **3.27**.

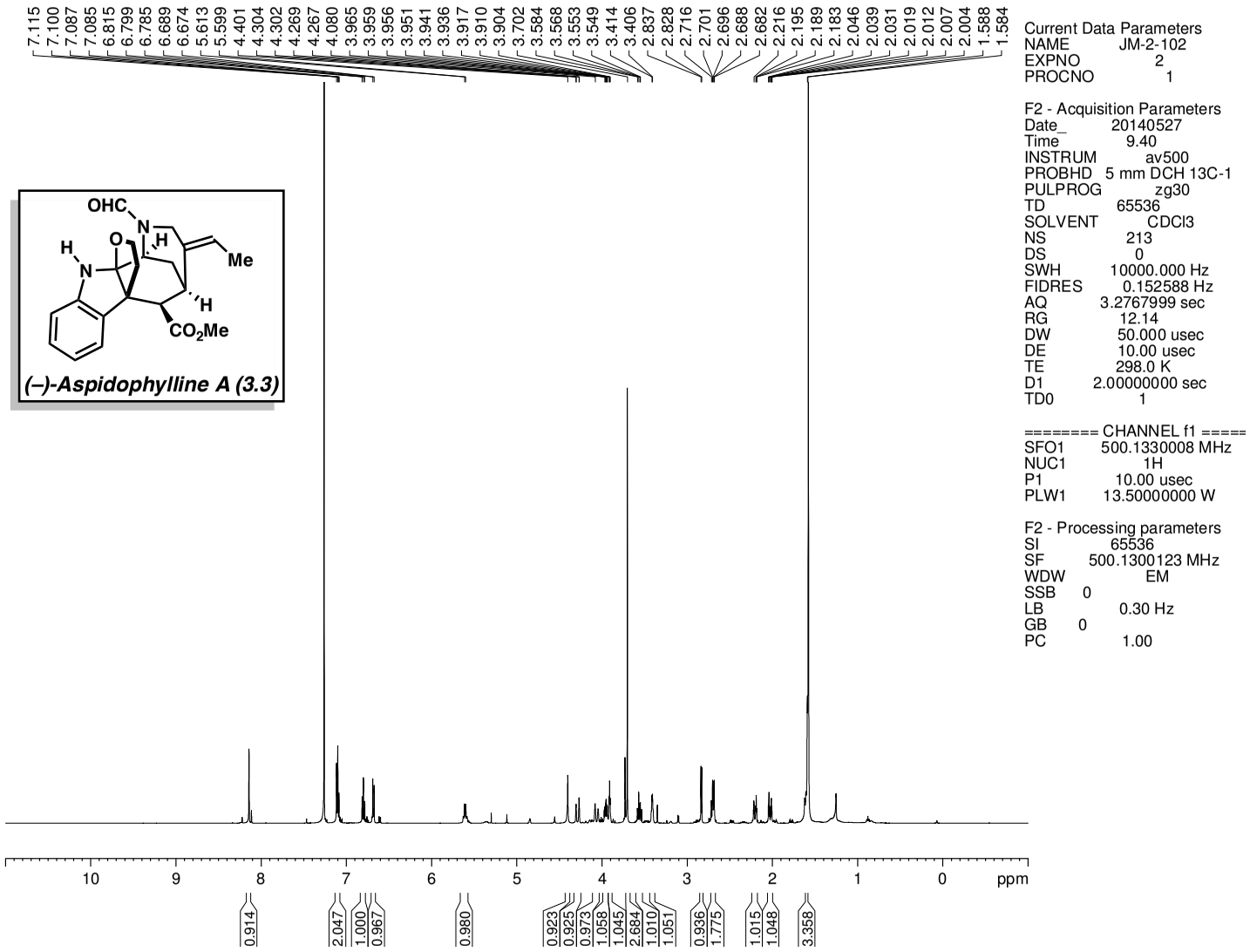

Figure 3.33 ^{1}H NMR (500 MHz, $CDCl_3$) of compound **3.3**.

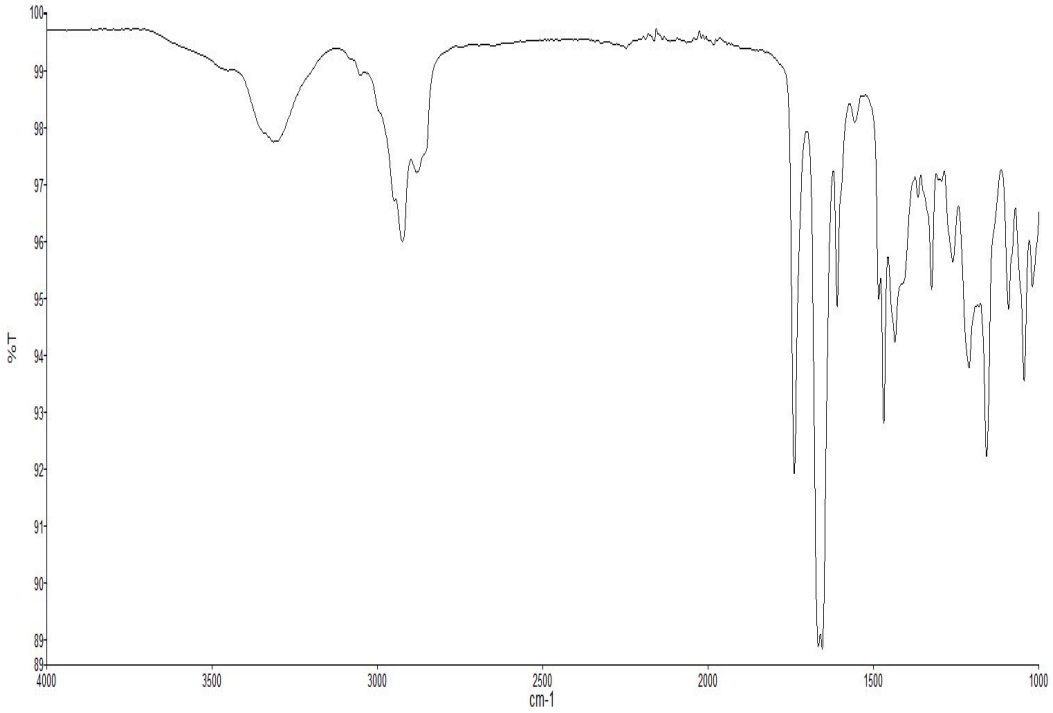

Figure 3.34 Infrared spectrum of compound **3.3**.

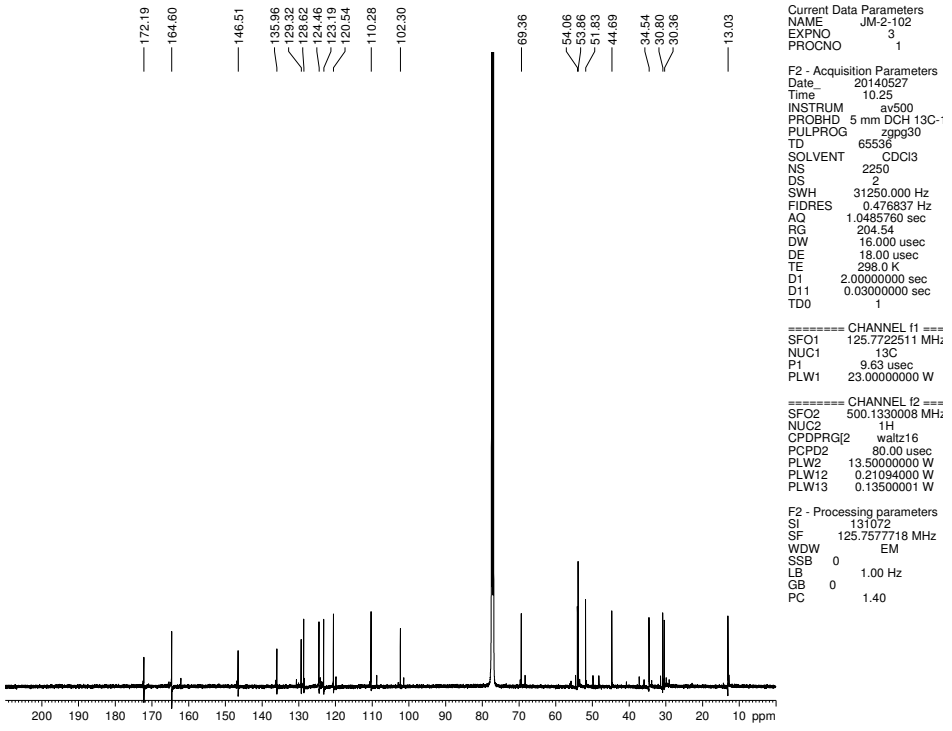

Figure 3.35 ^{13}C NMR (125 MHz, $CDCl_3$) of compound **3.3**.

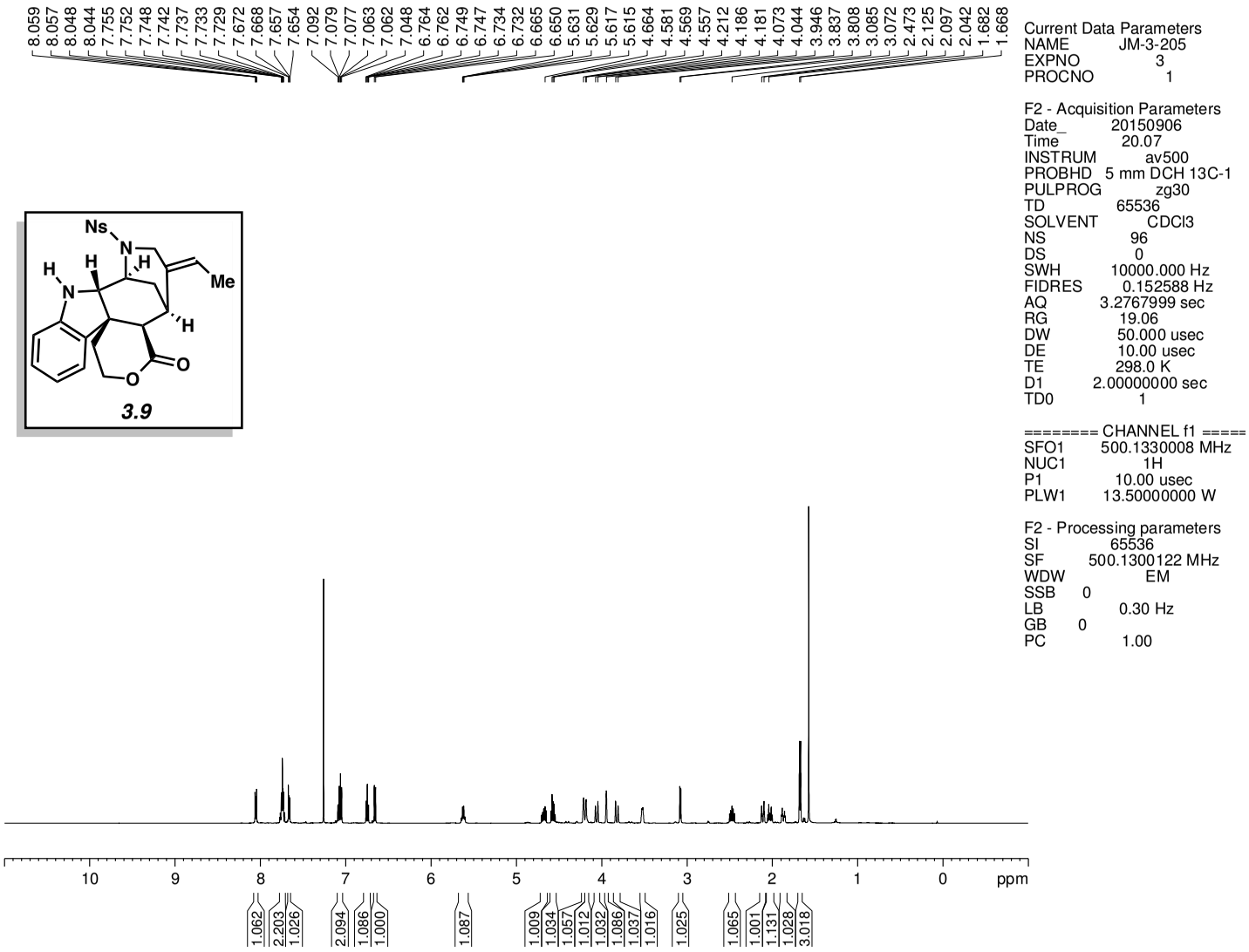

Figure 3.36 ^{1}H NMR (500 MHz, $CDCl_3$) of compound **3.9**.

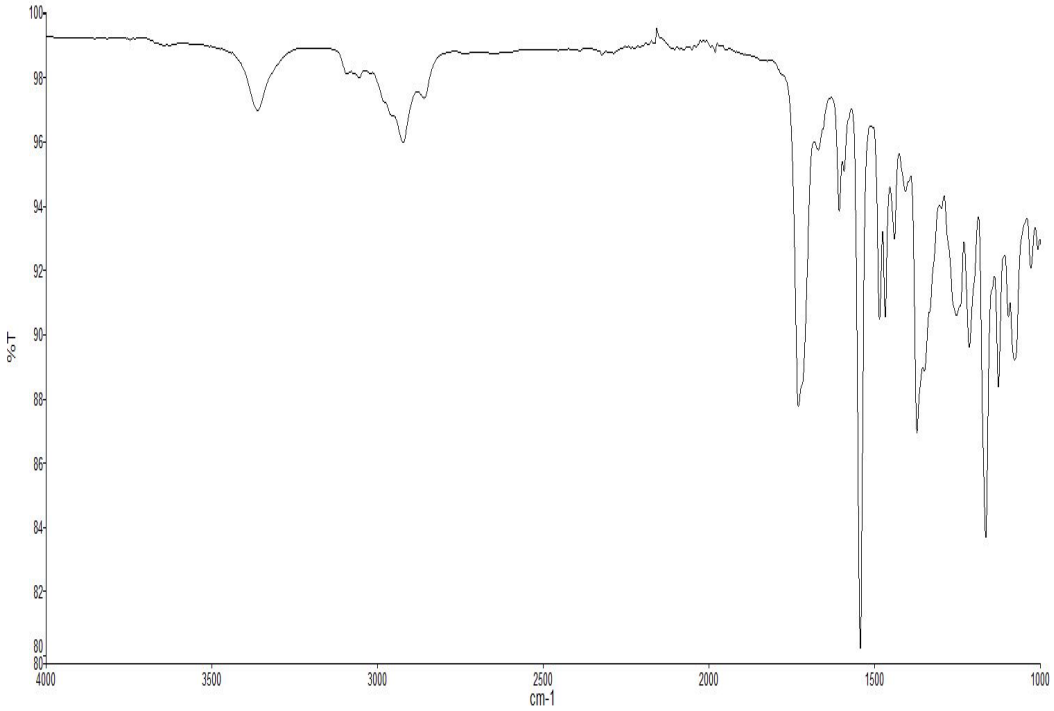

Figure 3.37 Infrared spectrum of compound **3.9**.

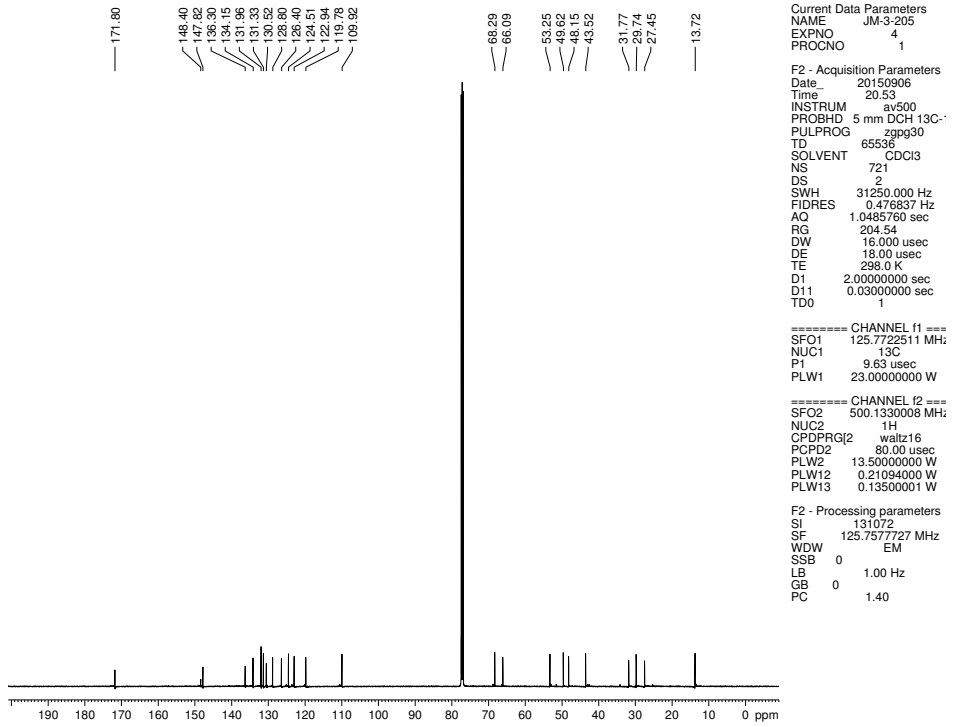

Figure 3.38 ^{13}C NMR (125 MHz, $CDCl_3$) of compound **3.9**.

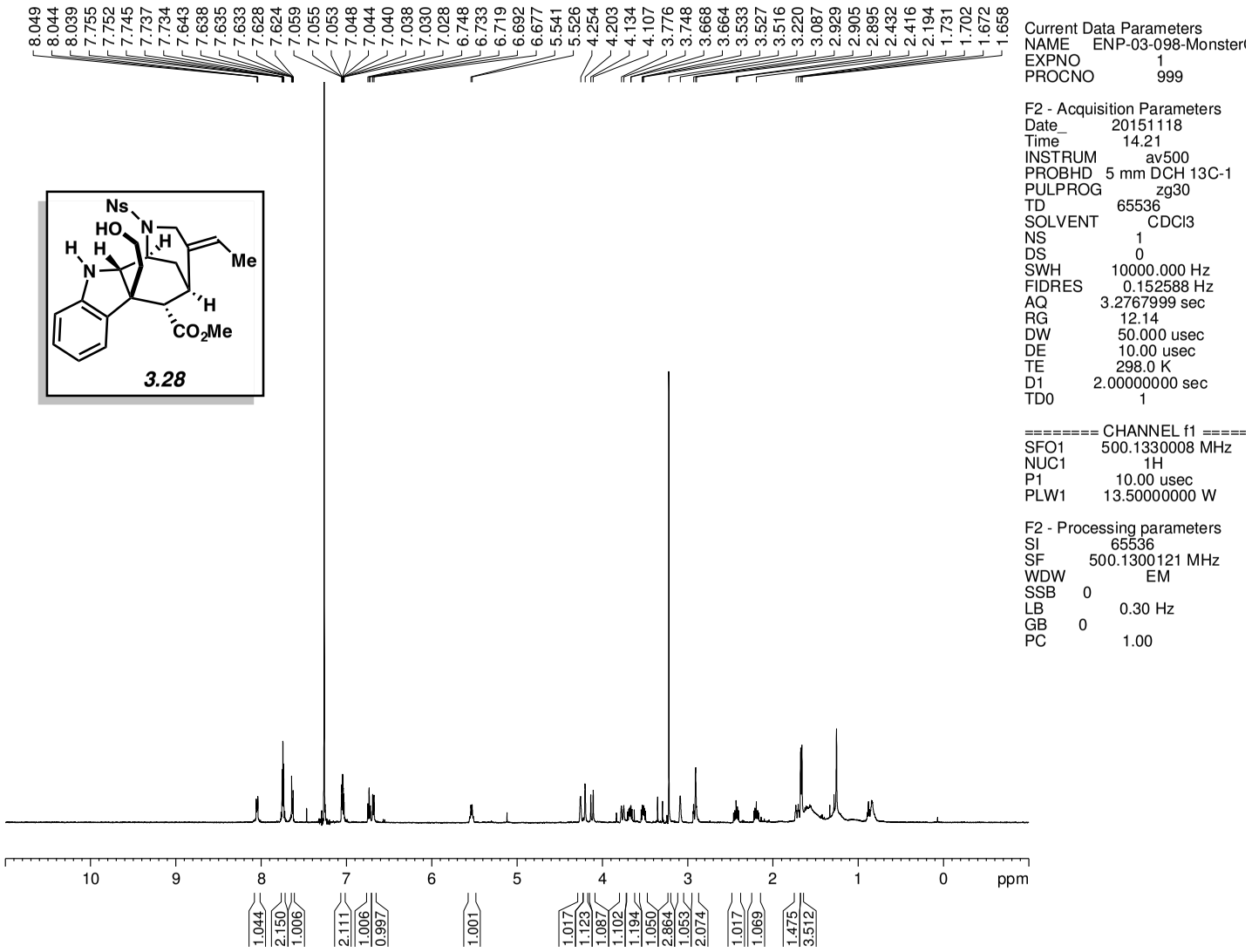

Figure 3.39 ^{1}H NMR (500 MHz, $CDCl_3$) of compound **3.28**.

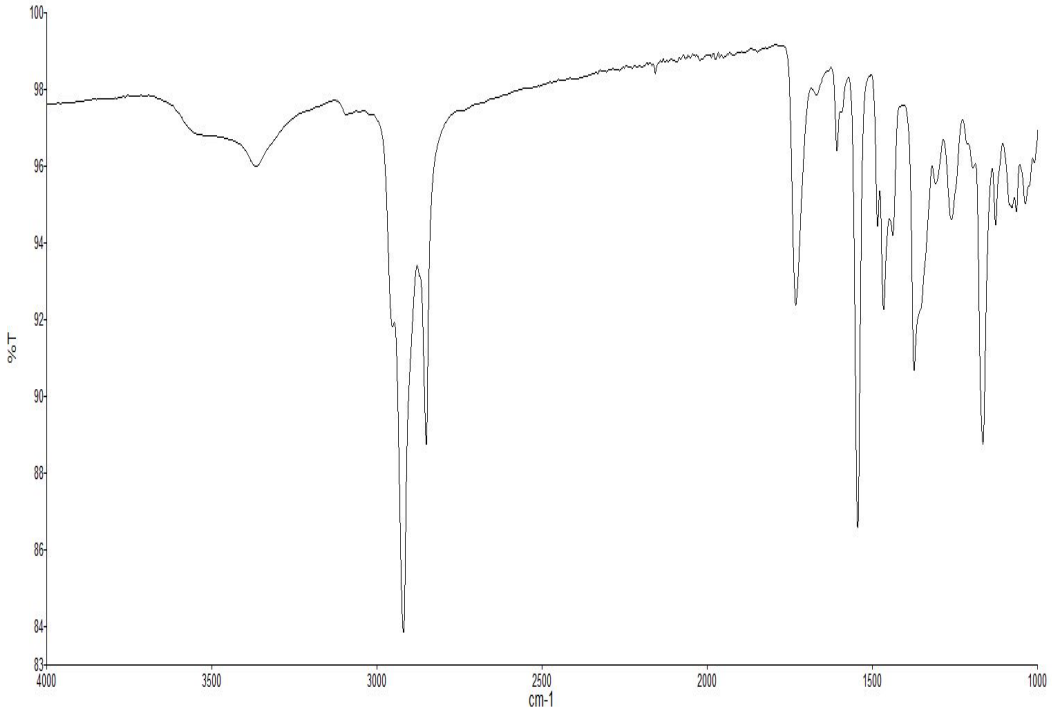

Figure 3.40 Infrared spectrum of compound **3.28**.

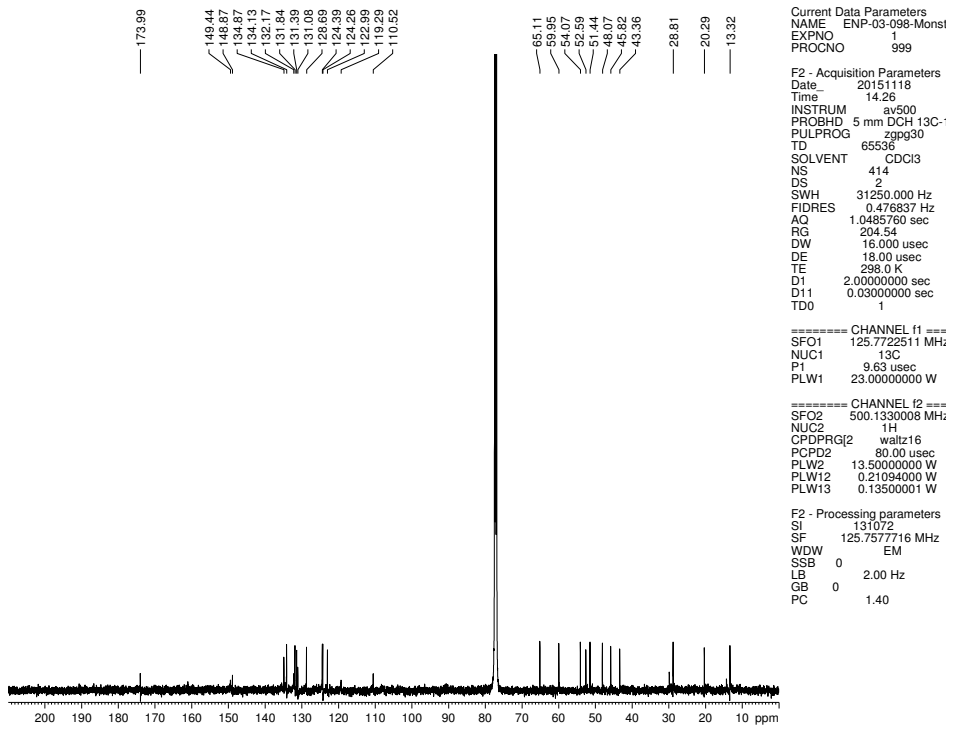

Figure 3.41 ^{13}C NMR (125 MHz, $CDCl_3$) of compound **3.28**.

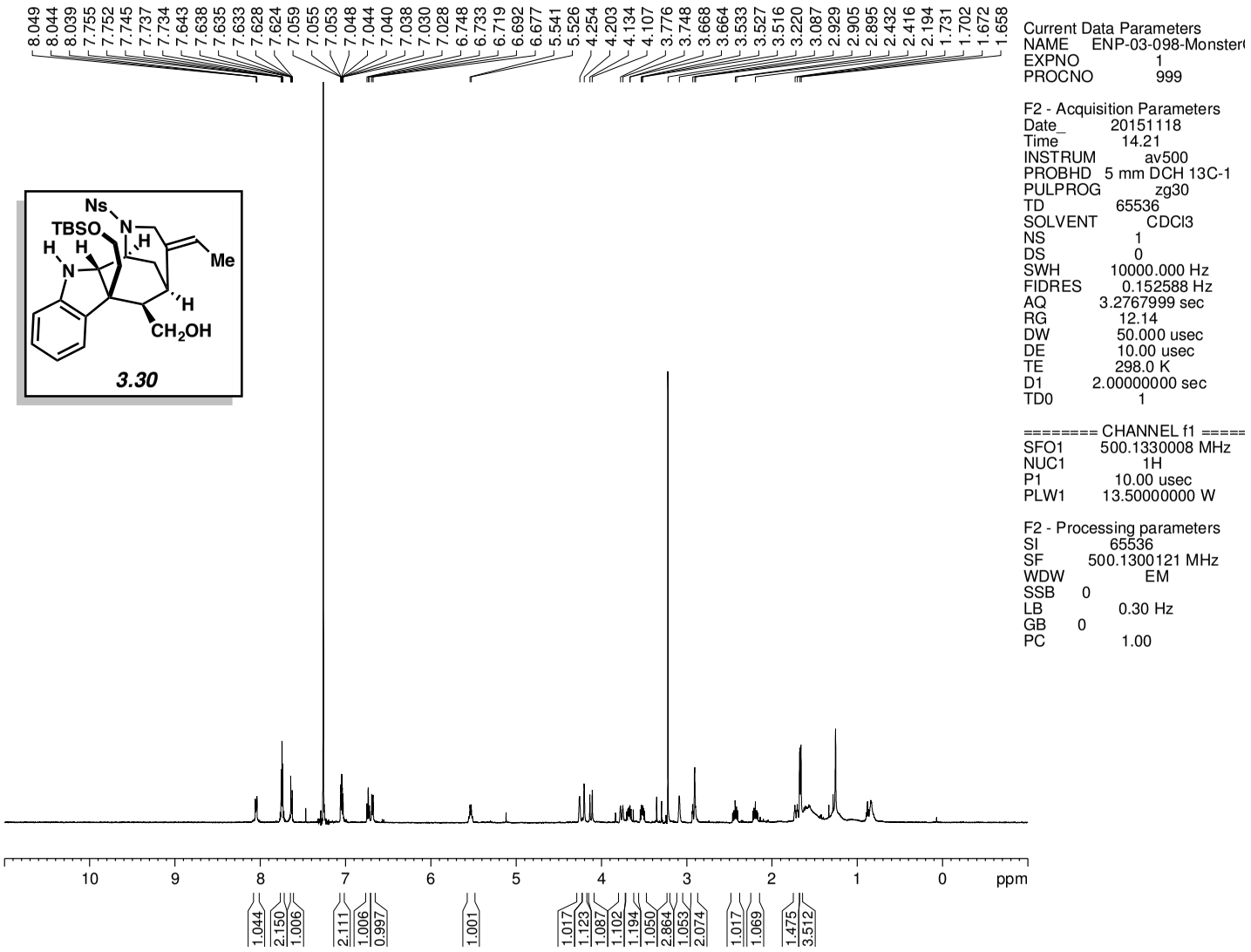

Figure 3.42 ^{1}H NMR (500 MHz, $CDCl_3$) of compound **3.30**.

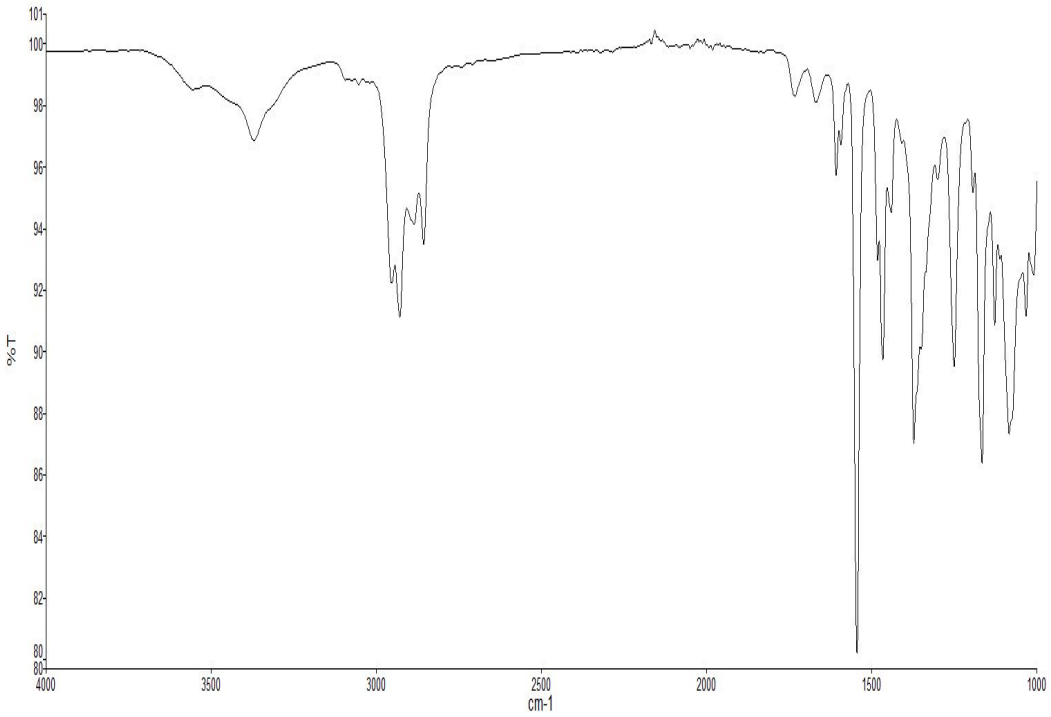

Figure 3.43 Infrared spectrum of compound **3.30**.

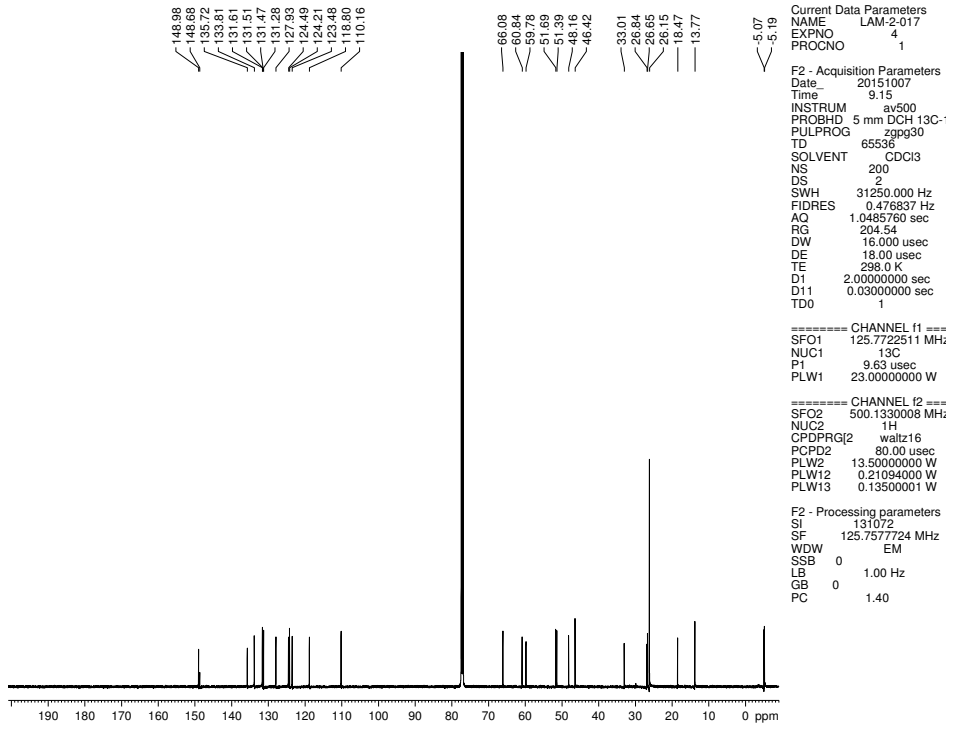

Figure 3.44 ^{13}C NMR (125 MHz, $CDCl_3$) of compound **3.30**.

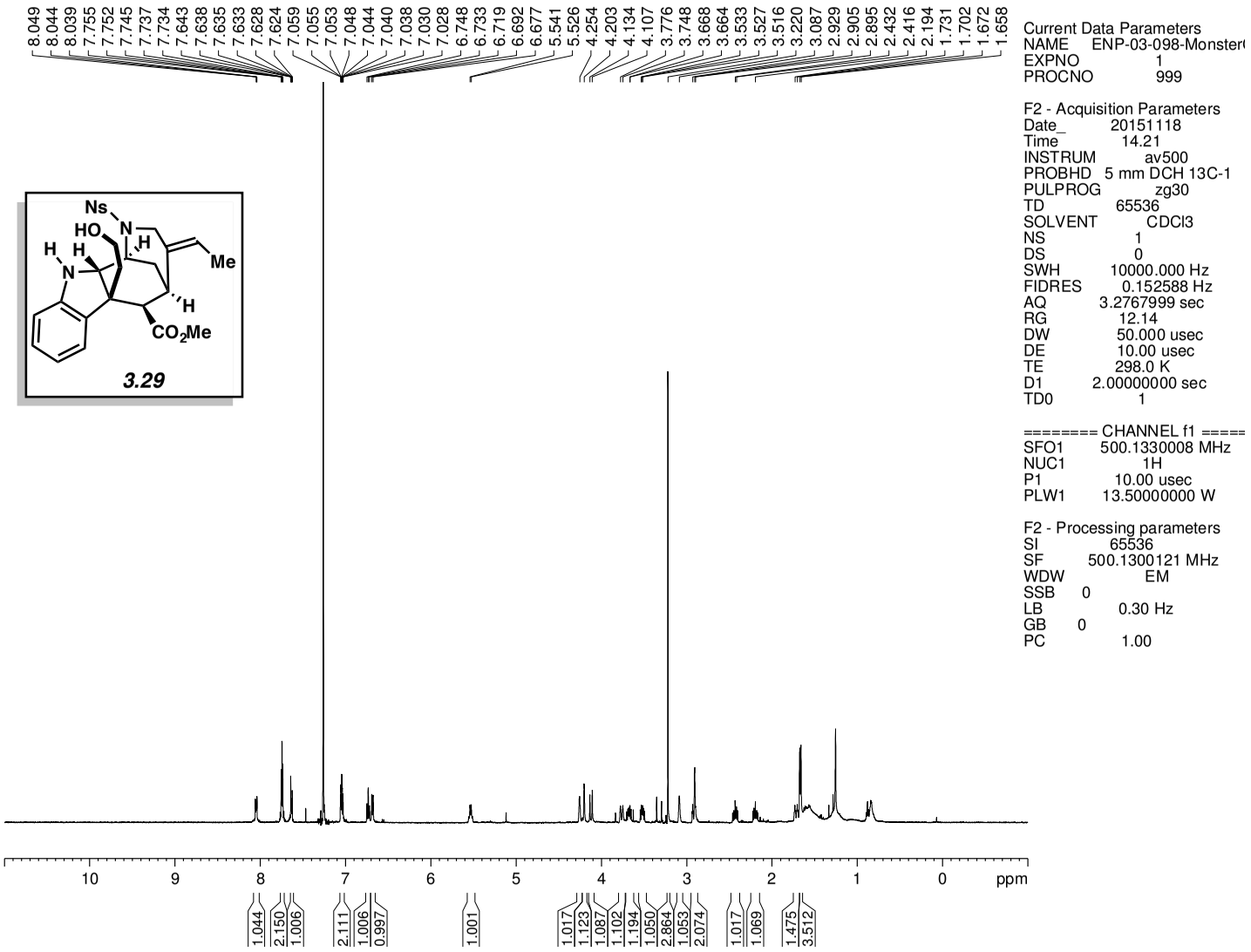

Figure 3.45 ^{1}H NMR (500 MHz, $CDCl_3$) of compound **3.29**.

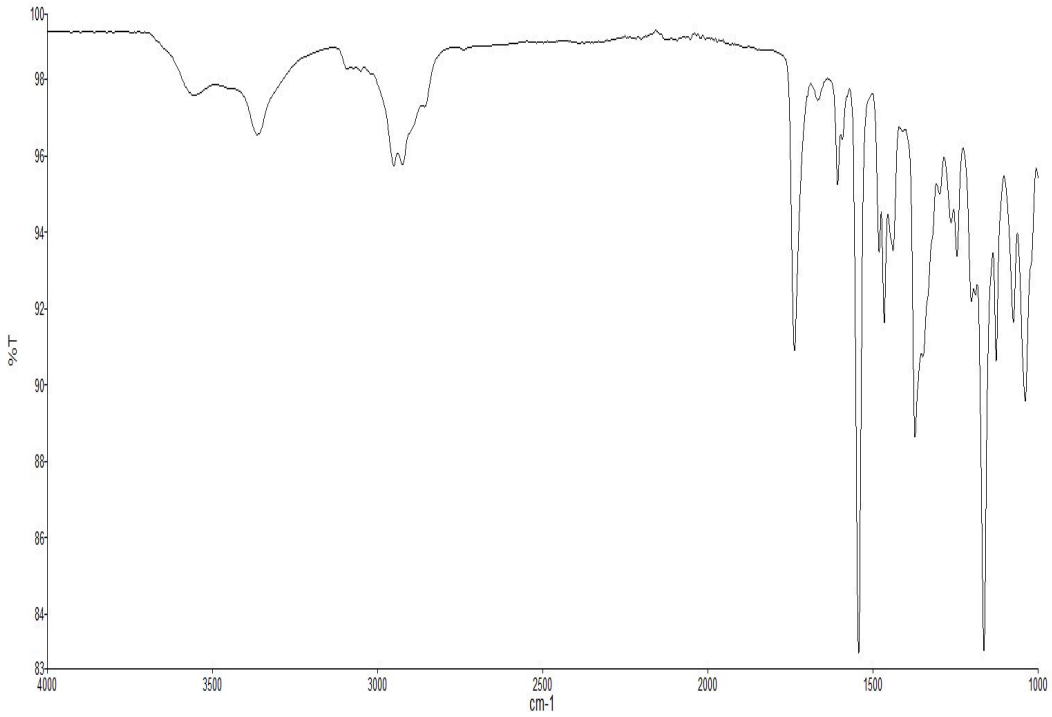

Figure 3.46 Infrared spectrum of compound **3.29**.

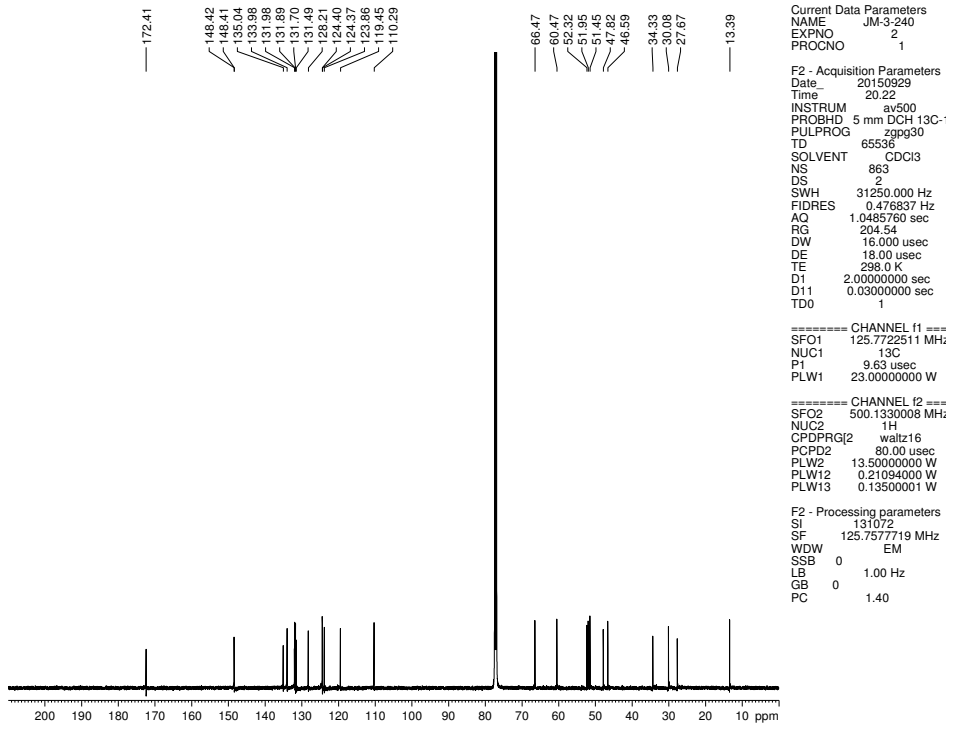

Figure 3.47 ^{13}C NMR (125 MHz, $CDCl_3$) of compound **3.29**.

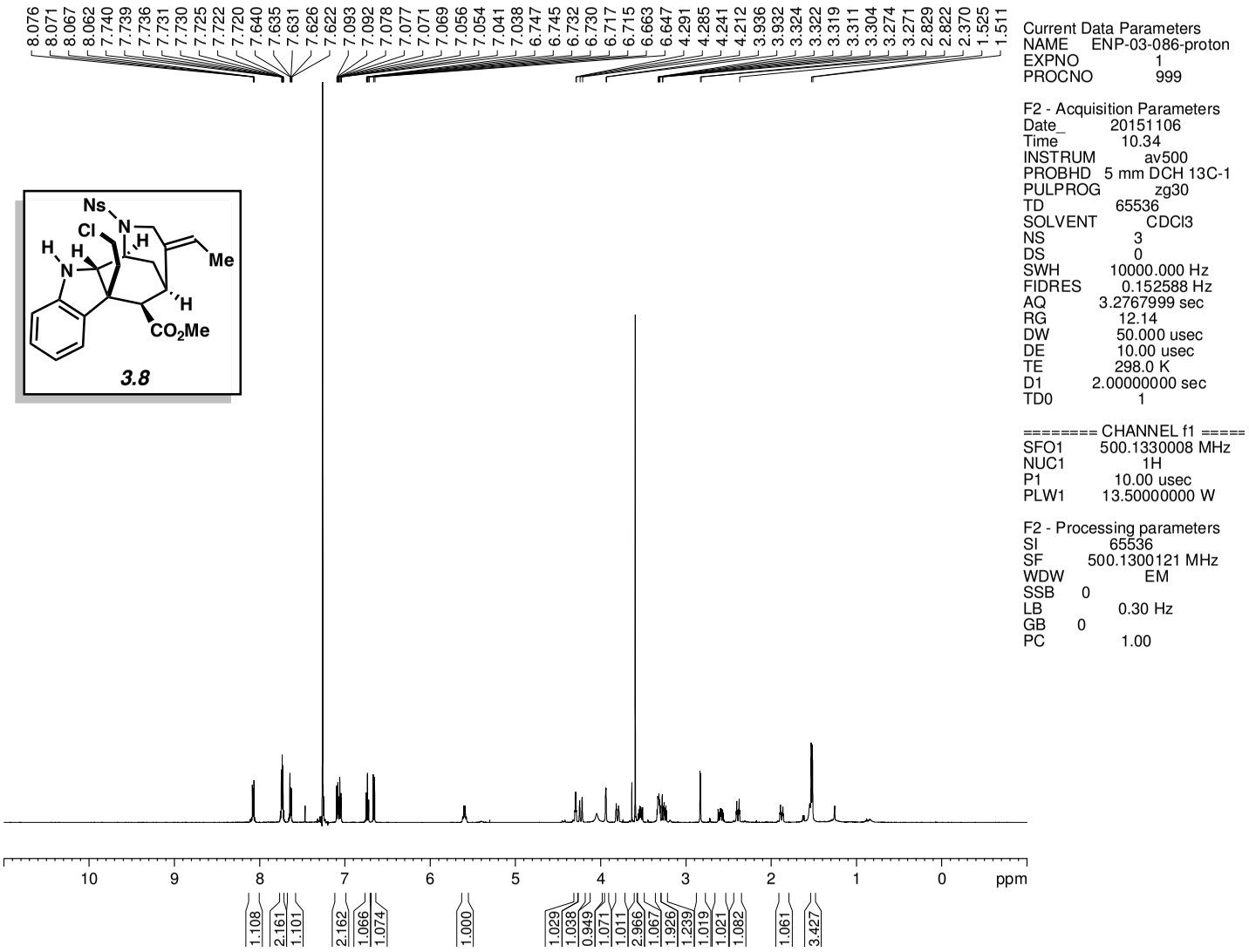

Figure 3.48 ^{1}H NMR (500 MHz, $CDCl_3$) of compound **3.8**.

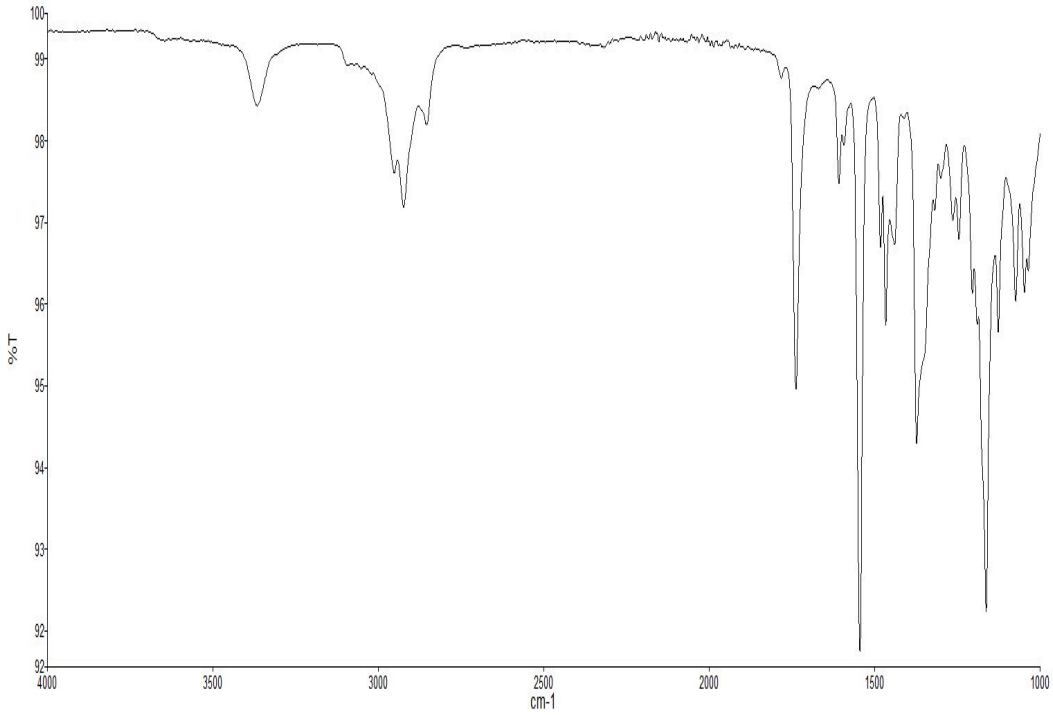

Figure 3.49 Infrared spectrum of compound **3.8**.

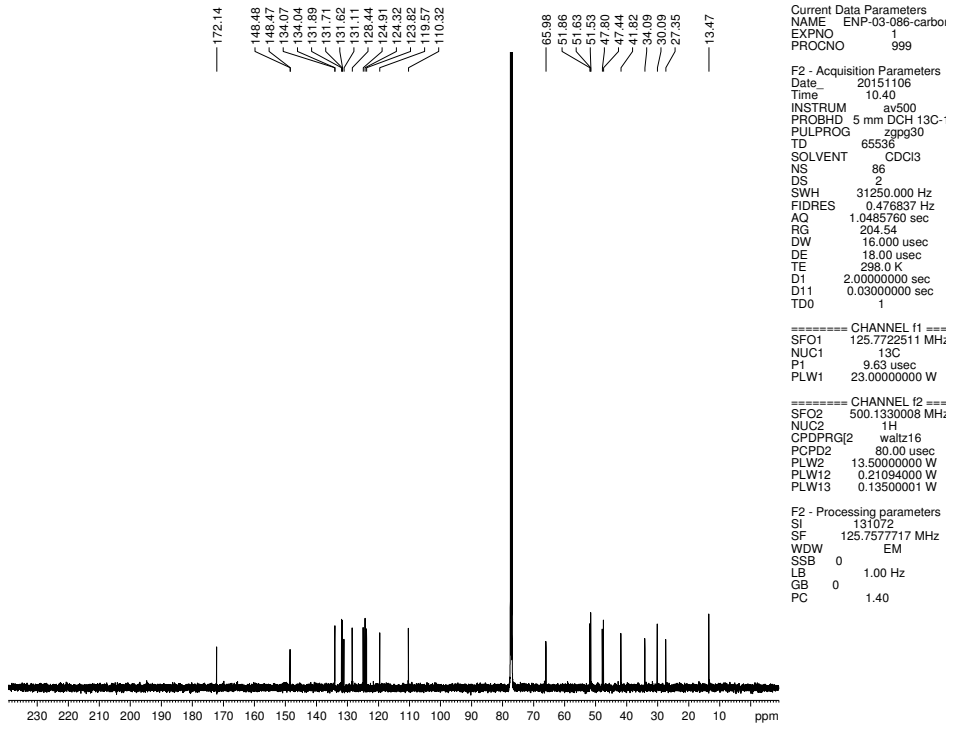

Figure 3.50 ^{13}C NMR (125 MHz, $CDCl_3$) of compound **3.8**.

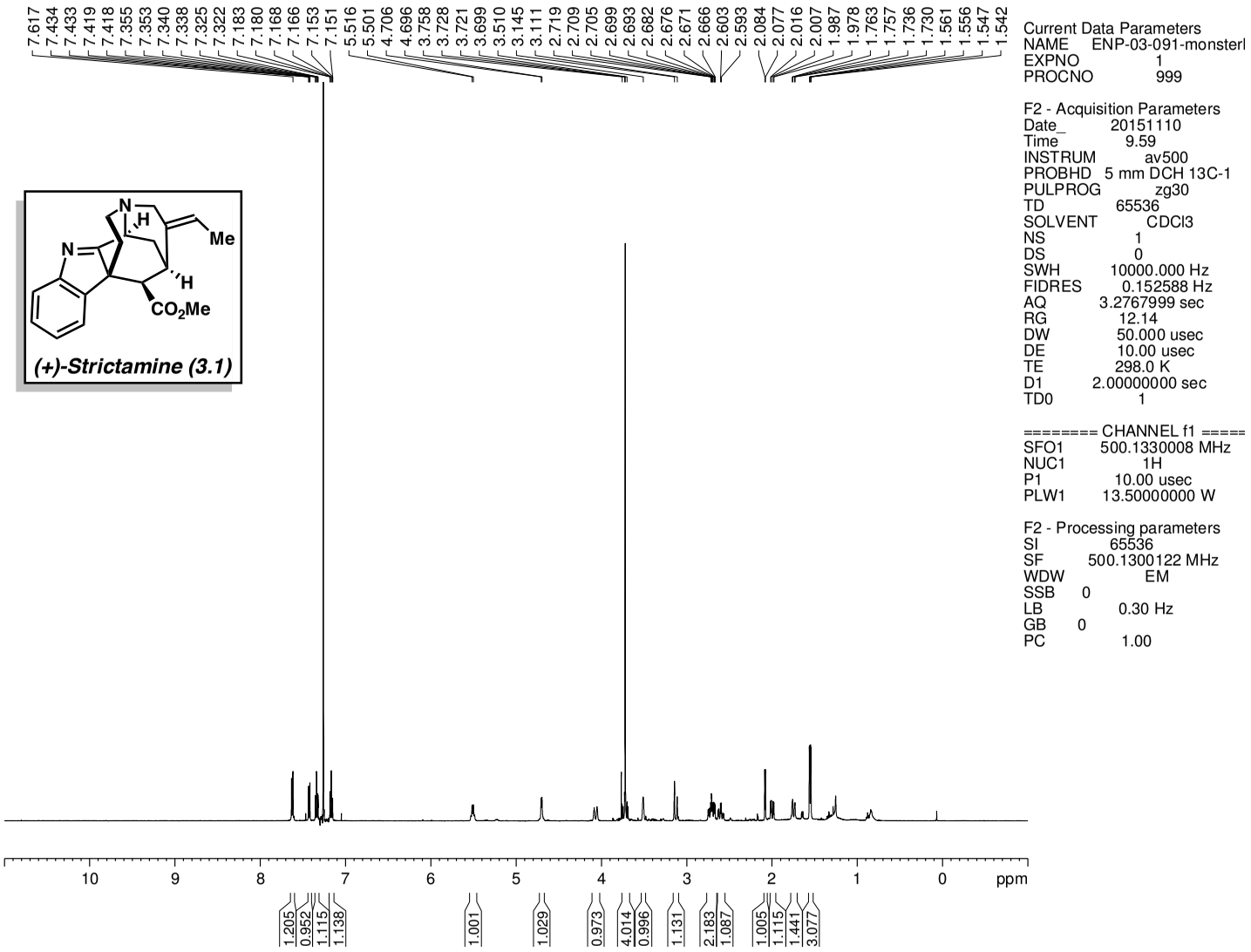

Figure 3.51 ^{1}H NMR (500 MHz, $CDCl_3$) of compound **3.1**.

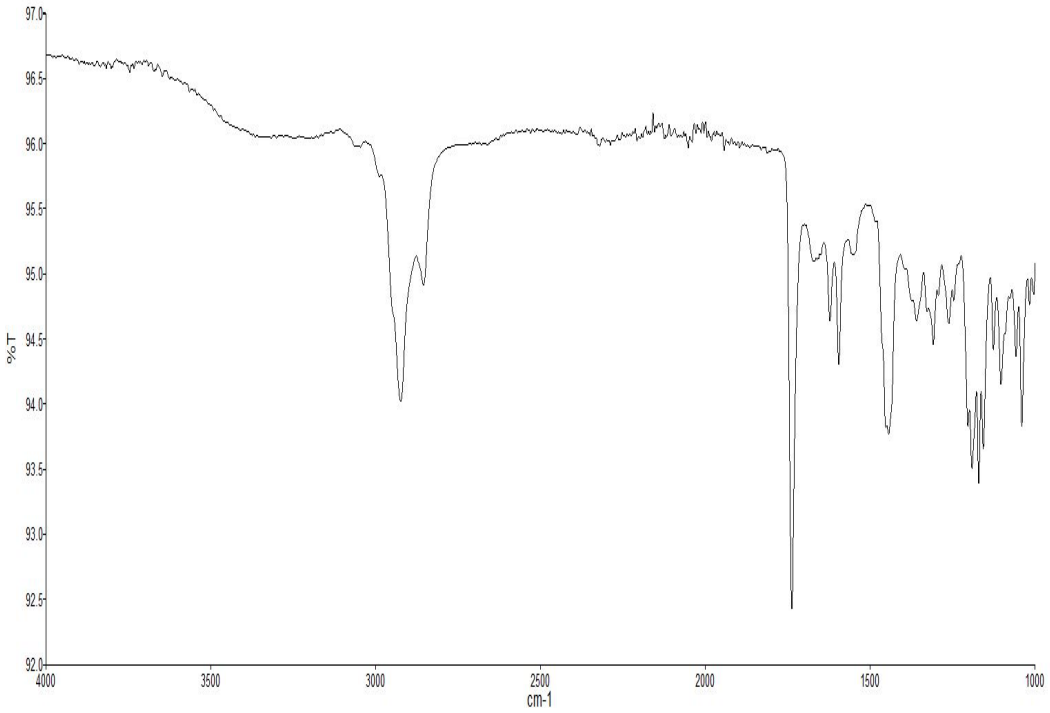

Figure 3.52 Infrared spectrum of compound **3.1**.

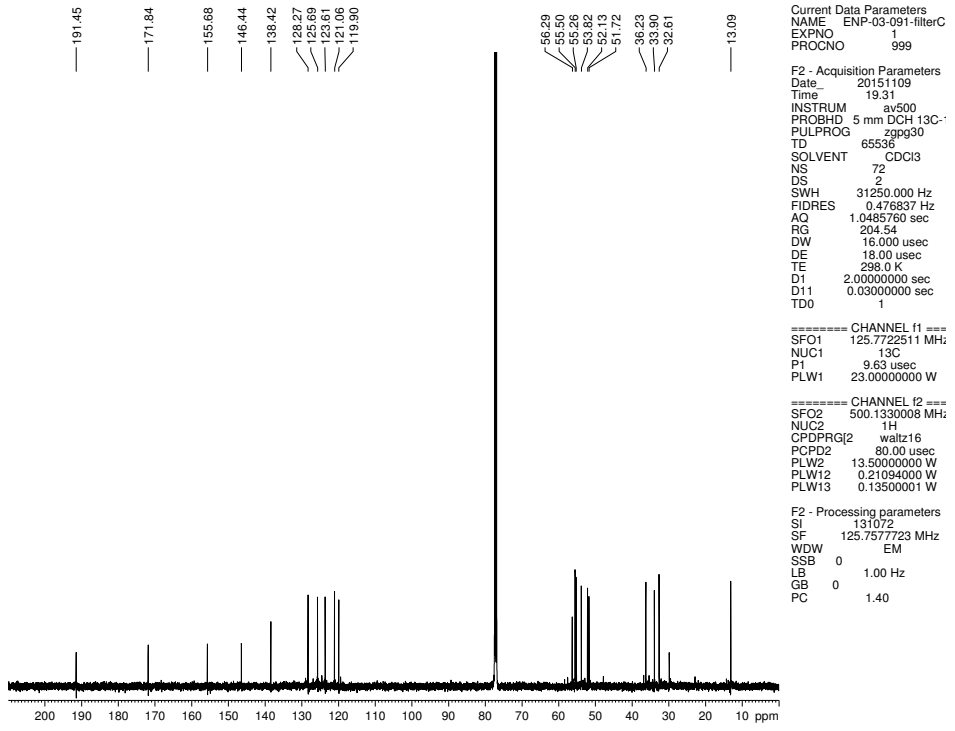

Figure 3.53 ^{13}C NMR (125 MHz, $CDCl_3$) of compound **3.1**.

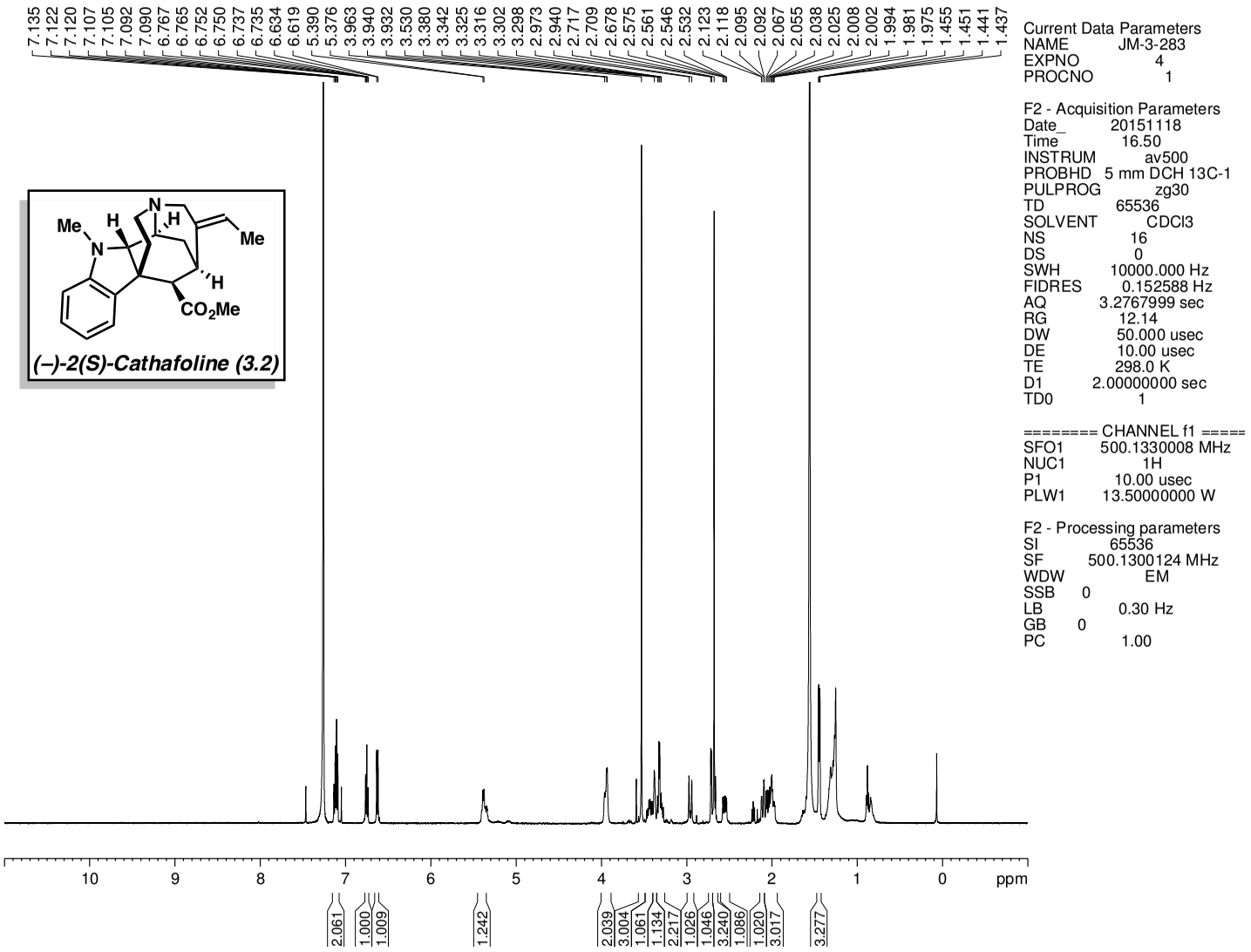

Figure 3.54 ^{1}H NMR (500 MHz, $CDCl_3$) of compound **3.2**.

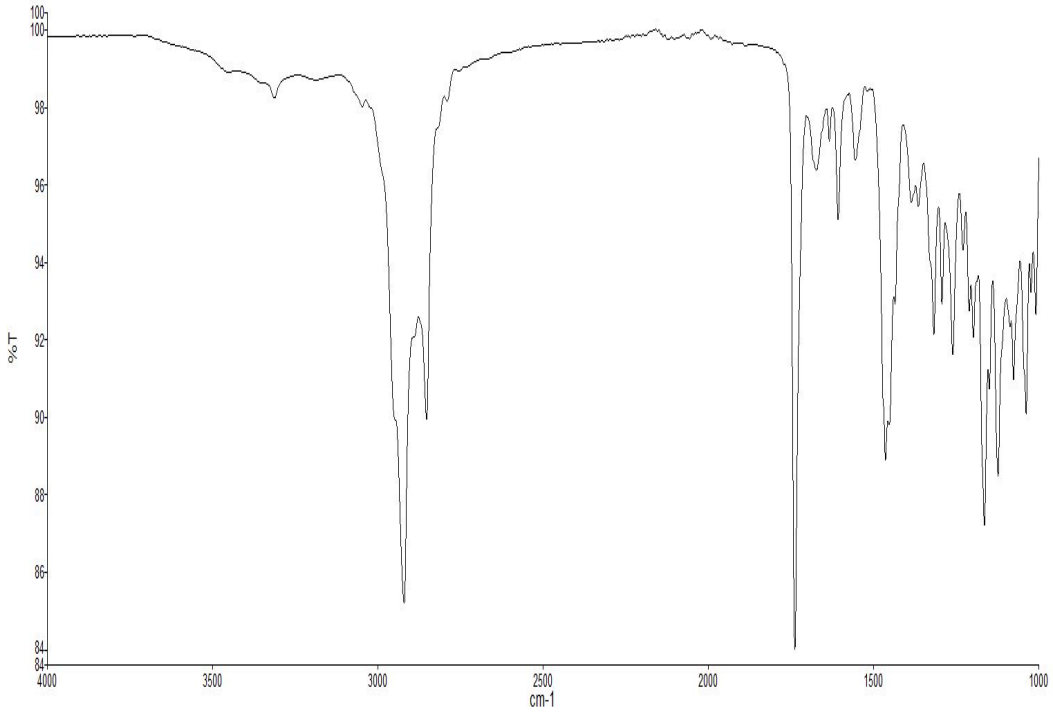

Figure 3.55 Infrared spectrum of compound **3.2**.

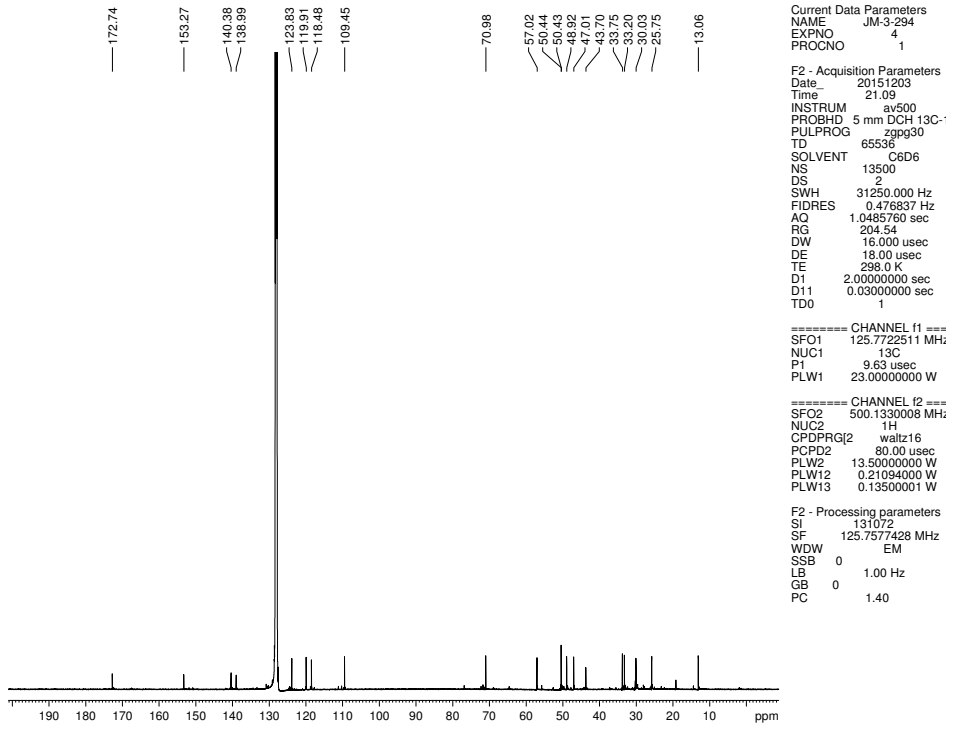

Figure 3.56 ^{13}C NMR (125 MHz, $CDCl_3$) of compound **3.2**.

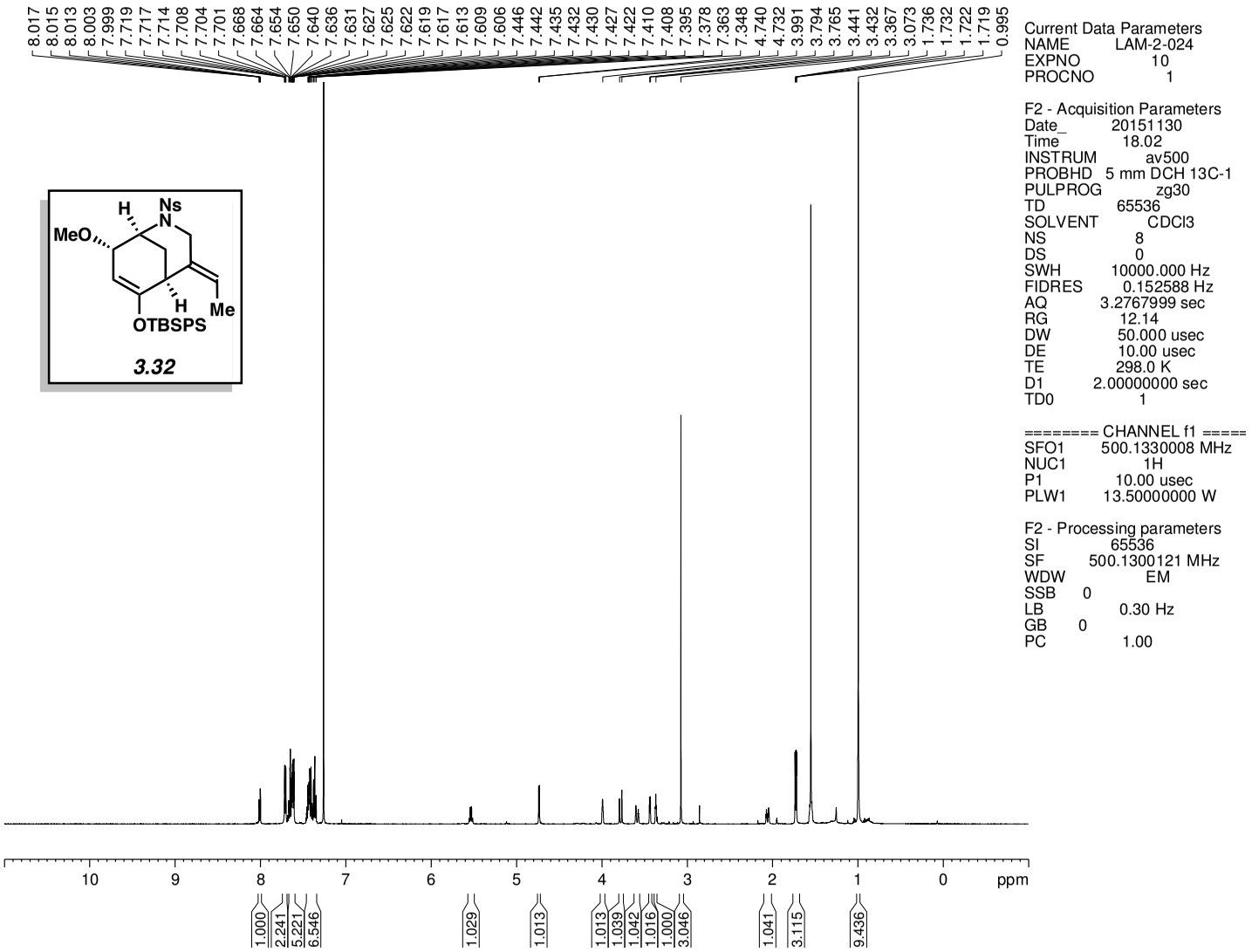

Figure 3.57 ^{1}H NMR (500 MHz, $CDCl_3$) of compound **3.32**.

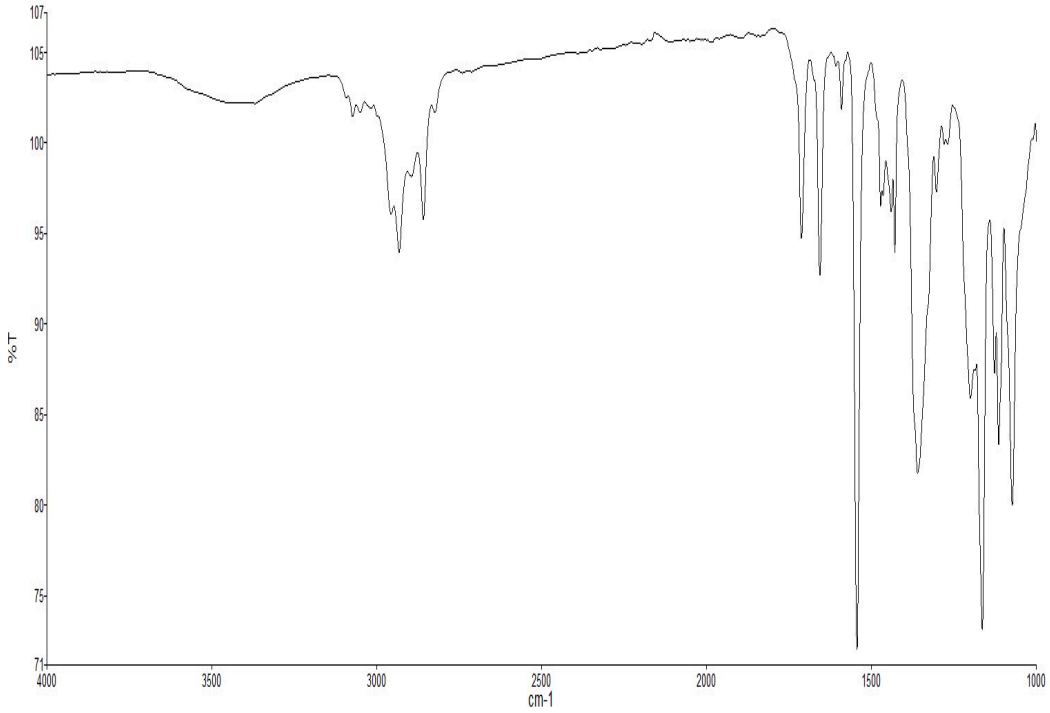

Figure 3.58 Infrared spectrum of compound **3.32**.

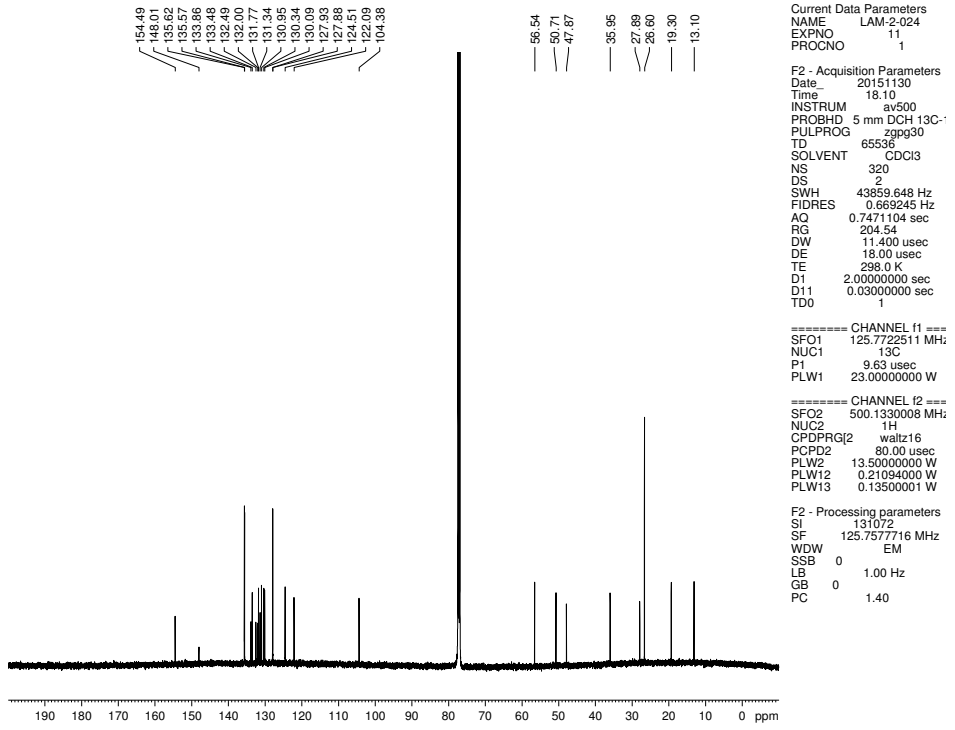

Figure 3.59 ^{13}C NMR (125 MHz, $CDCl_3$) of compound **3.32**.

3.11 Notes and References

(1) For reviews on akuammiline alkaloids, see: (a) Ramírez, A.; García–Rubio, S. *Curr. Med. Chem.* **2003**, *10*, 1891–1915. (b) Eckermann, R.; Gaich, T. *Synthesis* **2013**, *45*, 2813–2823. (c) Smith, J. M.; Moreno, J.; Boal, B. W.; Garg, N. K. *Angew. Chem., Int. Ed.* **2015**, *54*, 400–412.

(2) Zu, L.; Boal, B. W.; Garg, N. K. *J. Am. Chem. Soc.* **2011**, *133*, 8877–8879.

(3) Ren, W.; Wang, Q.; Zhu, J. *Angew. Chem., Int. Ed*. **2014**, *53*, 1818–1821.

(4) Teng, M.; Zi, W.; Ma, D. *Angew. Chem., Int. Ed*. **2014**, *53*, 1814–1817.

(5) (a) Smith, J. M.; Moreno, J.; Boal, B. W.; Garg, N. K. *J. Am. Chem. Soc.* **2014**, *136*, 4504–4507. (b) Smith, J. M.; Moreno, J.; Boal, B. W.; Garg, N. K. *J. Org. Chem.* **2015**, *80*, 8954–8967.

(6) (a) Zhang, M.; Huang, X.; Shen, L.; Qin, Y. *J. Am. Chem. Soc.* **2009**, *131*, 6013–6020. (b) Zhang, D.; Song, H.; Qin, Y. *Acc. Chem. Res.* **2011**, *44*, 447–457.

(7) Zi, W.; Xie, W.; Ma, D. *J. Am. Chem. Soc.* **2012**, *134*, 9126–9129.

(8) Horning, B. D.; MacMillan, D. W. C. *J. Am. Chem. Soc.* **2013**, *135*, 6442–6445.

(9) (a) Adams, G. L.; Carroll, P. J.; Smith, A. B., III. *J. Am. Chem. Soc.* **2012**, *134*, 4037–4040. (b) Adams, G. L.; Carroll, P. J.; Smith, A. B., III. *J. Am. Chem. Soc.* **2013**, *135*, 519–528.

(10) Smith, M. W.; Snyder, S. A. *J. Am. Chem. Soc.* **2013**, *135*, 12964–12967.

(11) For the initial isolation of strictamine, see: (a) Schnoes, H. K.; Biemann, K.; Mokrý, J.; Kompis, I.; Chatterjee, A.; Ganguli, G. *J. Org. Chem.* **1966**, *31*, 1641–1642. For the X-ray structure of strictamine, see: (b) Ahmad, Y.; Fatima, K.; Occolowitz, J. L.; Solheim, B. A.; Clardy, J.; Garnick, R. L.; Le Quesne, P. W. *J. Am. Chem. Soc.* **1977**, *99*, 1943–1946.

(12) Lim, S.-H.; Low, Y.-Y.; Sinniah, S. K.; Yong, K.-T.; Sim, K.-S.; Kam, T.-S. *Phytochemistry* **2014**, *98*, 204–215.

(13) (a) Bhattacharya, S. K.; Bose, R.; Dutta, S. C.; Ray, A. B.; Guha, S. R. *Indian J. Exp. Bio.* **1979**, *17*, 598–600. (b) Hou, Y.; Cao, X.; Wang, L.; Cheng, B.; Dong, L.; Luo, X.; Bai, G.; Giao, W. *J. Chromatogr. B* **2012**, *908*, 98–104. (c) Zhang, L.; Zhang, C.-J.; Zhang, D.-B.; Wen, J.; Zhao, X.-W.; Li, Y.; Gao, K. *Tetrahedron Lett.* **2014**, *55*, 1815–1817. (d) Liu, L.; Chen, Y.-Y.; Qin, X.-J.; Wang, G.; Jin, Q.; Liu, Y.-P.; Luo, X.-D. *Fitoterapia* **2015**, *105*, 160–164.

(14) For previous synthetic studies on strictamine or related methanoquinolizidine akuammilines, see: (a) Dolby, L. J.; Esfandiabi, Z. *J. Org. Chem.* **1972**, *37*, 43–46. (b) Dolby, L. J.; Nelson, S. J. *J. Org. Chem.* **1973**, *38*, 2882–2887. (c) Bennasar, M.-L.; Zulaica, E.; López, M.; Bosch, J. *Tetrahedron Lett.* **1988**, *29*, 2361–2364. (d) Bennasar, M.-L.; Zulaica, E.; Ramírez, A.; Bosch, J. *J. Org. Chem.* **1996**, *61*, 1239–1251. (e) Koike, T.; Takayama, H.; Sakai, S.-I. *Chem. Pharm. Bull.* **1991**, *39*, 1677–1681. (f) Edwankar, R. V.; Edwankar, C. R.; Namjoshi, O. A.; Deschamps, J. R.; Cook, J. M. *J. Nat. Prod.* **2012**, *75*, 181–188. (g) Komatsu, Y.; Yoshida, K.; Ueda, H.; Tokuyama, H. *Tetrahedron Lett.* **2013**, *54*, 377–380. (h) Kawano, M.; Kiuchi, T.; Negishi, S.; Tanaka, H.; Hoshikawa, T.; Matsuo, J.; Ishibashi, H. *Angew. Chem., Int. Ed.* **2013**, *52*, 906–910. (i) Ren, W.; Tappin, N.; Wang, Q.; Zhu, J. *Synlett* **2013**, *24*, 1941–1944.

(15) It was envisioned that the deprotection/cyclization could be followed by either oxidation or *N*-methylation as suggested schematically. However, the order of operations could also be reversed.

(16) For the classic Fischer indole synthesis, see: (a) Fischer, E.; Jourdan, F. *Ber.* **1883**, *16*, 2241–2245. (b) Fischer, E.; Hess, O. *Ber.* **1884**, *17*, 559–568.

(17) For the use of the Fischer indolization reaction in akuammiline alkaloid synthesis, see references 2 and 5.

(18) For the reductive interrupted Fischer indolization reaction, see: Maligres, P. E.; Houpis, I.; Rossen, K.; Molina, A.; Sager, J.; Upadhyay, V.; Wells, K. M.; Reamer, R. A.; Lynch, J. E.; Askin, D.; Volante, R. P.; Reider, P. J. *Tetrahedron* **1997**, *53*, 10983–10992.

(19) (a) Lu, Z.; Li, Y.; Deng, J.; Li, A. *Nat. Chem*. **2013**, *5*, 679–683. (b) Xiong, X.; Li, Y.; Lu, Z.; Wan, M.; Deng, J.; Wu, S.; Shao, H.; Li, A. *Chem. Commun*. **2014**, *50*, 5294–5297.

(20) For a review on catalytic asymmetric allylic alkylation employing heteroatom nucleophiles, see: Trost, B. M.; Zhang, T.; Sieber, J. D. *Chem. Sci.* **2010**, *1*, 427–440.

(21) For the crystallographic data of **3.18**, refer to CCDC number 1440684.

(22) McDonald, C.; Holcomb, H.; Kennedy, K.; Kirkpatrick, E.; Leathers, T.; Vanemon, P. *J. Org. Chem.* **1989**, *54*, 1213–1215.

(23) Bian, M.; Wang, Z.; Xiong, X.; Sun, Y.; Matera, C.; Nicolaou, K. C.; Li, A. *J. Am. Chem. Soc.* **2012**, *134*, 8078–8081.

(24) Salom-Roig, X. J.; Dénès, F.; Renaud, P. *Synthesis* **2004**, 1903–1928.

(25) For methodology studies, see: (a) Boal, B. W.; Schammel, A. W.; Garg, N. K. *Org. Lett.* **2009**, *11*, 3458–3461. (b) Schammel, A. W.; Boal, B. W.; Zu, L.; Mesganaw, T.; Garg, N. K. *Tetrahedron* **2010**, *66*, 4687–4695.

(26) For the Fischer indolization in late-stage total synthesis of complex alkaloids, see references 2, 5, and 9, in addition to the following: (a) Ueda, H.; Satoh, H.; Matsumoto, K.; Sugimoto, K.; Fukuyama, T.; Tokuyama, H. *Angew. Chem., Int. Ed.* **2009**, *48*, 7600−7603. (b) Satoh, H.; Ueda, H.; Tokuyama, H. *Tetrahedron* **2013**, *69*, 89−95.

(27) (a) Basha, A.; Lipton, M.; Weinreb, S. M. *Tetrahedron Lett.* **1977**, *18*, 4171–4174. (b) Shimizu, T.; Osako, K.; Nakata, T. *Tetrahedron Lett.* **1997**, *38*, 2685–2688.

(28) Iwata, A.; Oshita, J.; Tang, H.; Kunai, A. *J. Org. Chem.* **2002**, *67*, 3927–3929.

(29) (a) Liotta, D.; Sunay, U.; Santiesteban, H.; Markiewicz, W. *J. Org. Chem.* **1981**, *46*, 2605–2610. (b) McMurry, J. *Org. React.* **1976**, *24*, 187–224.

(30) Wang, H.; Reisman, S. E. *Angew. Chem., Int. Ed.* **2014**, *53*, 6206–6210.

(31) Niu, C.; Pettersson, T.; Miller, M. J. *J. Org. Chem.* **1996**, *61*, 1014–1022.

(32) Uyanik, M.; Ishihara, K.; Yamamoto, H. *Org. Lett.* **2006**, *8*, 5649–5652.

(33) The signs of specific rotations matched for synthetic and natural samples, however, the magnitude of the rotations was not consistent. This can be attributed to the presence of minor impurities, user error, or variations in spectrometers. For a pertinent discussion regarding the variability of specific rotations, see: Gawley, R. E. *J. Org. Chem.* **2006**, *71*, 2411–2416.

(34) Trost, B. M.; Masters, J. T.; Lumb, J.-P.; Fateen, D. *Chem. Sci.* **2014**, *5*, 1354–1360.

(35) Kaneda, K.; Honda, T. *Tetrahedron* **2008**, *64*, 11589–11593.

(36) Subramanian, G.; Hiraku, O.; Hayashi, M.; Koyano, T.; Komiyama, K.; Kam, T.-S. *J. Nat. Prod.* **2007**, *70*, 1783–1789.

(37) Atta-ur-Rahman; Habib-ur-Rehman. *Planta Med.* **1986**, *52*, 230–231.

(38) Mokrý, J; Kompiš, I.; Spiteller, G. *Collect. Czech. Chem. Commun*. **1967**, *32*, 2523–2531.

CHAPTER FOUR

Mizoroki–Heck Cyclizations of Amide Derivatives for the Introduction of Quaternary Centers

Adapted from: Jose M. Medina, Jesus Moreno, Sophie Racine, Shuaijing Du, and Neil K. Garg. *Angew. Chem, Int. Ed.* [Online early access]. DOI: 10.1002/anie.201703174R1.

4.1 Abstract

We report the non-decarbonylative Mizoroki–Heck reactions of amide derivatives. The transformation relies on the use of nickel catalysis and proceeds using sterically hindered tri- and tetrasubstituted olefins to give products containing quaternary centers. The resulting polycyclic or spirocyclic products can be obtained in good yields. Moreover, a diastereoselective variant of this methodology demonstrates its value for accessing adducts bearing vicinal, highly substituted sp^3 stereocenters. Our results demonstrate that amide derivatives can be used as building blocks for the assembly of complex scaffolds.

4.2 Introduction

The introduction of quaternary carbon centers remains a popular topic in modern chemical synthesis.[1] Such motifs are often difficult to access due to the steric challenge associated with constructing a fully substituted carbon center. One attractive means to install quaternary centers is via the intramolecular Mizoroki–Heck reaction.[2] Most notably, the Pd-catalyzed Mizoroki–Heck cyclization of *aryl* halides and triflates has been the subject of intense investigation for decades

and has been utilized to assemble many sterically demanding scaffolds. On the other hand, the corresponding Mizoroki–Heck cyclization of *acyl* electrophiles to furnish ketone products bearing quaternary carbons has not been reported.

Considering the aforementioned deficiency concerning the Mizoroki–Heck cyclization of acyl electrophiles, we pursued the transformation shown in Figure 4.1. In the presence of an appropriate nickel catalyst, imide **4.1**, derived from the corresponding secondary amide upon Boc-activation, would be converted to cyclized products **4.2**, bearing the desired quaternary centers. Mechanistically, the conversion would proceed by a sequence akin to classical Mizoroki–Heck chemistry involving oxidative addition (**4.1**→**4.3**), olefin coordination and insertion (**4.3**→**4.4**), followed by β-hydride elimination[3] (**4.4**→**4.2**). It should be noted that amide derivatives have recently been employed in Pd- and Ni-catalyzed couplings for carbon–heteroatom[4] and carbon–carbon[5,6,7] bond formation, although never for the synthesis of quaternary centers.[8] Moreover, precedent for the desired olefin insertion is available from Stambuli's Pd-catalyzed Mizoroki–Heck cyclization of benzoic anhydrides, albeit without quaternary stereocenter formation,[9,10] and Pd-catalyzed carbonylative Mizoroki–Heck reactions of aryl halides and triflates.[11] Herein, we describe the development and scope of the Ni-catalyzed Mizoroki–Heck cyclization of amide derivatives.[12] The transformation provides a new means to build complex scaffolds using non-precious metal catalysis.[13]

Figure 4.1 Designed nickel-catalyzed Heck reaction of amide derivatives to forge quaternary centers.

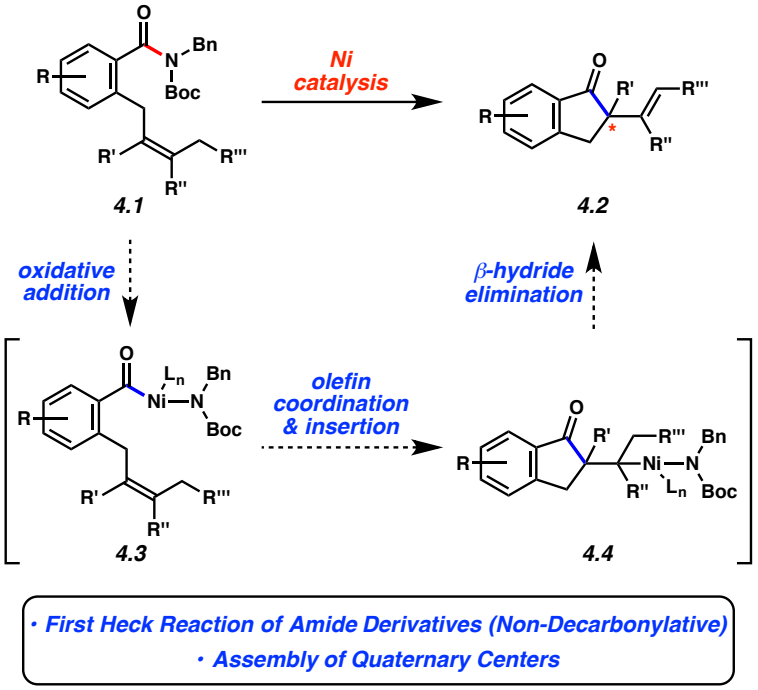

4.3 Evaluation of Reaction Conditions

After some initial experimentation, we arrived at **4.5** as a suitable test substrate (Table 4.1).[14] This substrate contains the *N*-Bn,Boc imide-type motif,[15] which we have previously found to be reactive using Ni/SIPr (**4.7**) combinations,[4,5] in addition to a sterically encumbered tetrasubstituted olefin. The Mizoroki–Heck cyclization of **4.5** was attempted under a variety of reaction conditions,[16] with a selection of key results using $Ni(cod)_2$, NHC ligands, and toluene as solvent at 100 °C depicted. Unfortunately, attempts to conduct the desired cyclization using SIPr•HCl (**4.7**) in the presence of NaO*t*Bu were unsuccessful (entry 1). However, by switching to NHC precursor **4.8** the Mizoroki–Heck product **4.6** was obtained, albeit in modest yield (entry 2). Further improvements were seen when benzimidazolium salt **4.9** was employed,[17] which gave rise to the desired product **4.6** in 76% yield (entry 3). We also probed the Ni to ligand ratio and found

that employing a 1:1 ratio of $Ni(cod)_2$ to **4.9** (rather than a 1:2 ratio), led to diminished yields (entry 4). Efforts to optimize the Ni loading were also undertaken. Although using 10 mol% $Ni(cod)_2$ gave the desired product (entry 5), the use of 15 mol% $Ni(cod)_2$ gave excellent yields (entry 6) and was found more generally effective across a range of substrates studied subsequently. During the course of our studies, we also evaluated a series of additives used previously in Ni-catalyzed couplings.[18] These efforts demonstrated that the reaction temperature could be lowered to 60 °C, provided that *t*-amyl alcohol was employed as the additive, to deliver product **4.6** in 95% yield (entry 7).[19] It should be noted that: (a) Ni-catalyzed Mizoroki–Heck reactions to form quaternary centers are rare,[20] (b) there are no prior examples of Ni-catalyzed Mizoroki–Heck reactions involving tetrasubstituted olefins in the literature,[21] and (c) decarbonylation products were not observed during reaction development.

Table 4.1 Evaluation of ligand effects and reaction conditions for the conversion of **4.5** to Mizoroki–Heck cyclization product **4.6**, bearing a quaternary center.[a]

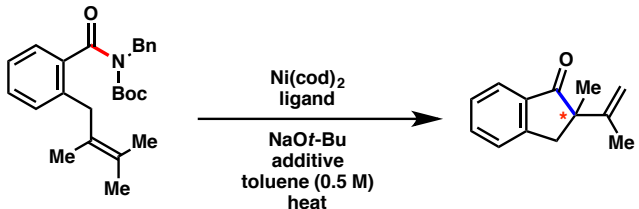

4.5 *4.6*

Entry	*Ni(cod)$_2$ (loading)*	*Ligand (loading)*	*Additive*	*Temp.*	*Yield*[b]
1	20 mol%	***4.7*** (40 mol%)	none	100 °C	0%
2	20 mol%	***4.8*** (40 mol%)	none	100 °C	24%
3	20 mol%	***4.9*** (40 mol%)	none	100 °C	76%
4	20 mol%	***4.9*** (20 mol%)	none	100 °C	67%
5	10 mol%	***4.9*** (20 mol%)	none	100 °C	51%
6	15 mol%	***4.9*** (30 mol%)	none	100 °C	91%
7	15 mol%	***4.9*** (30 mol%)	*t*-amyl alcohol[c]	60 °C	95%

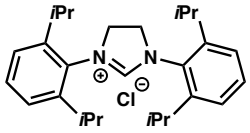

SIPr·HCl (4.7)

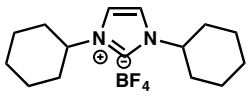

ICy·HBF$_4$ (4.8)

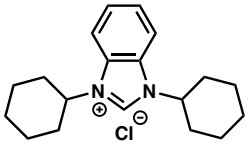

Benz-ICy·HCl (4.9)

[a] Conditions unless otherwise stated: **4.5** (1.0 equiv, 0.1 mmol), Ni(cod)$_2$ (mol% as shown), **4.7**–**4.9** (mol% as shown), toluene (0.5 M), NaO*t*-Bu (1.1x ligand loading) heated at the specified temperature for 24 h in a sealed vial. [b] Yields reflect an average of two experiments and were determined by ^{1}H NMR analysis using hexamethylbenzene as an internal standard. [c] 3.0 equiv of *t*-amyl alcohol was used.

4.4 Evaluation of Substrate Scope

Having identified conditions to achieve the nickel-catalyzed cyclization, we evaluated the scope with respect to the tethered alkene (Table 4.2).[22,23] It was found that a trisubstituted olefin[24] analog of our parent substrate could be employed to furnish terminal olefin product **4.10** in 71% yield (entry 1). We also examined substrates in which the trisubstituted olefin was embedded in a ring. Using both 5- and 6-membered ring substrates, the desired Mizoroki–Heck cyclization proceeded smoothly to give the corresponding spirocyclic products, **4.11** and **4.12**, respectively,

as mixtures of olefin isomers (entries 2 and 3).[25] Returning to the more challenging tetrasubstituted olefins, a series of substrates bearing exocyclic olefins were prepared and evaluated. Whereas utilization of a substrate containing a 5-membered ring led to product **4.13** in 51% yield (entry 4), the use of 6- and 7-membered ring-containing substrates furnished products **4.14** and **4.15**, respectively, in good yields (entries 5 and 6). Lastly, two heterocyclic substrates were examined. We were delighted to find that our methodology proved tolerant of a tetrahydropyran and a protected piperidine, thus giving rise to tricycles **4.16** and **4.17**, respectively, in excellent yields (entries 7 and 8).

Table 4.2 Heck cyclization of a variety of tri- and tetrasubstituted olefin substrates.

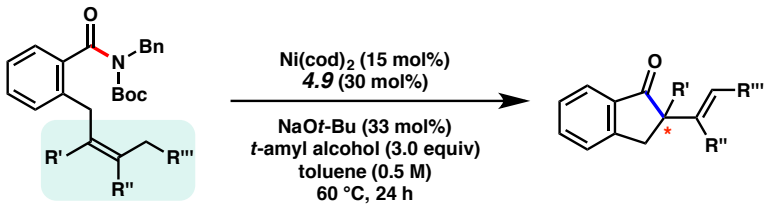

Entry	Alkene	Product	Yield[a]
1	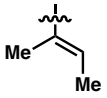	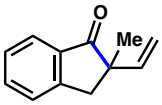 4.10	71%[b]
2		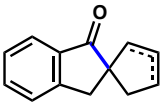 4.11	92%[b]
3	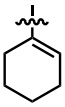	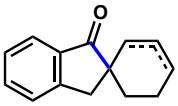 4.12	75%[b]
4	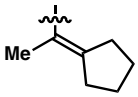	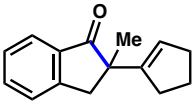 4.13	51%
5	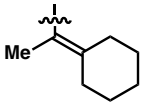	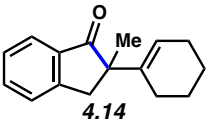 4.14	96%
6	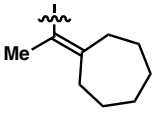	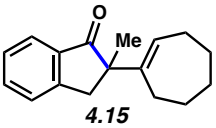 4.15	80%
7	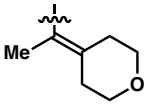	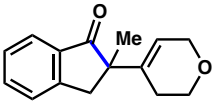 4.16	91%
8	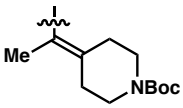	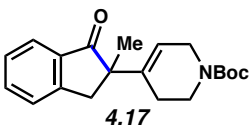 4.17	93%

[a] Yields shown reflect the average of two isolation experiments. [b] Reaction performed at 100 °C in the absence of *t*-amyl alcohol.

As shown in Figure 4.2, the methodology is also tolerant of substituents on the arene. For example, use of substrates containing the fluoride or trifluoromethyl group, both of which are critical in medicinal chemistry,[26] gave rise to products **4.18** and **4.19**, respectively. The methoxy group was also well tolerated, as shown by the formation of **4.20** and **4.21**. As demonstrated by the synthesis of **4.22** and **4.23**, substrates bearing a methyl group could also be utilized. In the latter case, it is notable that the presence of a methyl group ortho to the tethered alkene did not hinder reactivity.

Figure 4.2 Substituents on the arene motif.[a]

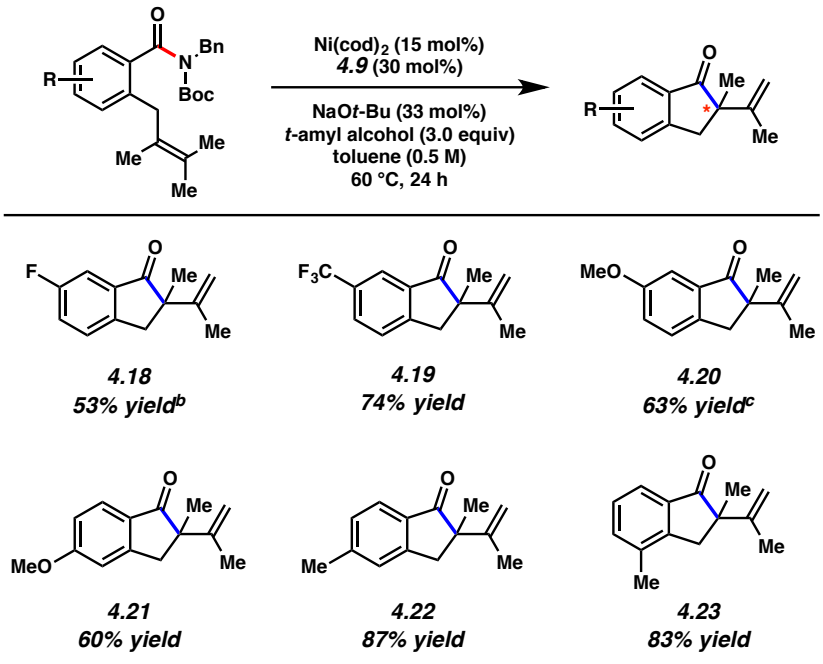

[a] Yields shown reflect the average of two isolation experiments. [b] Yield determined by ^{1}H NMR analysis using hexamethylbenzene as an external standard. [c] Reaction performed at 100 °C in the absence of *t*-amyl alcohol.

4.5 Diastereoselecitve Application to Build Vicinal sp^3 stereocenters

As a further test, we questioned if this methodology could be performed in a diastereoselective sense (Figure 4.3). Trisubstituted olefin **4.24**,[27] which bears an allylic methyl

group, was treated under our optimal reaction conditions. This reaction delivered ketone **4.25** in 80% yield, as a 92:8 ratio of diastereomers. Of note, **4.25** contains vicinal sp^3 stereocenters, both of which are highly substituted. Prior transition metal-catalyzed methods for the synthesis of 2-vinylindanones[22] have not been demonstrated for the construction of such complexity. The diastereoselectivity seen in the conversion of **4.24** to **4.25** can be rationalized by considering the two competing olefin insertion transition states, **TS1** and **TS2**. In both cases, the olefin insertion event is thought to occur via a standard 4-centered transition state, which, in turn, prompts allylic strain arguments.[28] In **TS1**, A(1,3) strain between the two highlighted hydrogens is minimal and the methyl group rests in a pseudo-equatorial disposition. As such, **TS1** is favorable and leads to the major diastereomer of **4.25** shown, with the methyl groups residing in a cis fashion. On the other hand, the minor diastereomer of **4.25** (not depicted) is thought to arise from **TS2**, which displays a less favorable A(1,3) interaction between the highlighted hydrogen and methyl substituents.

Figure 4.3 Diastereoselective Heck cyclization for the introduction of vicinal sp^3 stereocenters.[a]

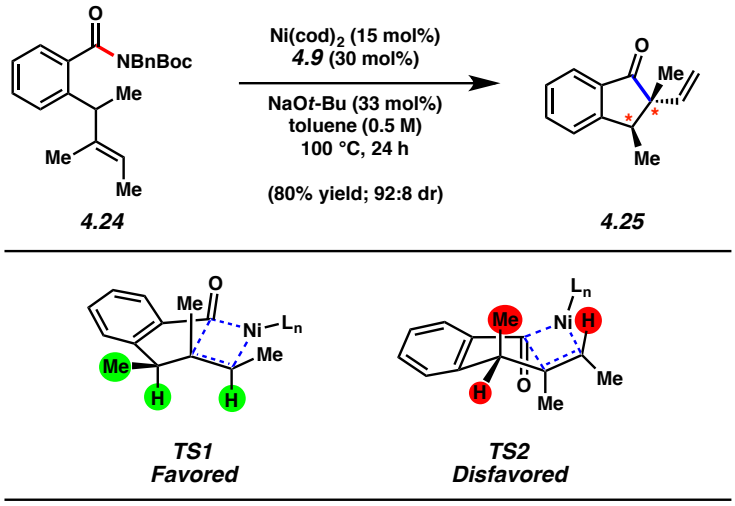

[a] Yields shown reflect the average of two isolation experiments.

4.6 Conclusion

We have developed the Mizoroki–Heck cyclization of amide derivatives to access ketones containing quaternary centers. The transformation is tolerant of variation on both the alkene and aryl moieties, and most notably, proceeds using sterically hindered tetrasubstituted olefins. As a result, polycyclic, spirocyclic, and heteroatom-containing products can be synthesized using this methodology. Moreover, we have demonstrated that a diastereoselective Mizoroki–Heck cyclization proceeds for the controlled formation of an adduct bearing vicinal, highly substituted sp^3 stereocenters. In addition to providing a rare Ni-catalyzed Mizoroki–Heck cyclization methodology for accessing quaternary centers and the first Mizoroki–Heck cyclizations of amide derivatives, our results demonstrate that amides, despite once being viewed as unreactive, can be used as building blocks for the preparation of complex scaffolds.

4.7 Experimental Section

4.7.1 Materials and Methods

Unless stated otherwise, reactions were conducted in flame-dried glassware under an atmosphere of nitrogen and commercially obtained reagents were used as received. Non-commercially available substrates were synthesized following protocols specified in Section 4.7.2.1. Prior to use, toluene was purified by distillation and taken through three freeze-pump-thaw cycles. 2-Halobenzoic acids derivatives **4.31, 4.33, 4.35** were obtained from Combi-Blocks; **4.29** and **4.26** were obtained from Oakwood; **4.37** was obtained from AstaTech; and **4.41** was obtained from Ark Pharm. $Ni(cod)_2$ and Benz-ICy•HCl (**4.9**) were obtained from Strem Chemicals. Reductive coupling ligands **4.60**[14c] and **4.66**[14d] were prepared from known literature procedures. Reaction temperatures were controlled using an IKAmag temperature modulator, and unless stated

otherwise, reactions were performed at room temperature (approximately 23 °C). Thin-layer chromatography (TLC) was conducted with EMD gel 60 F254 pre-coated plates (0.25 mm for analytical chromatography and 0.50 mm for preparative chromatography) and visualized using a combination of UV, anisaldehyde, iodine, and potassium permanganate staining techniques. Silicycle Siliaflash P60 (particle size 0.040–0.063 mm) was used for flash column chromatography. ^{1}H NMR spectra were recorded on Bruker spectrometers (at 400 and 500 MHz) and are referenced to the residual solvent peak 7.26 ppm for $CDCl_3$. Data for ^{1}H NMR spectra are reported as follows: chemical shift (δ ppm), multiplicity, coupling constant (Hz), integration.^{13}C NMR spectra were recorded on Bruker spectrometers (at 125 MHz) and are referenced to the residual solvent peak 77.16 ppm for $CDCl_3$. Data for ^{13}C NMR are reported as follows: chemical shift (δ ppm), multiplicity, and coupling constant (Hz). ^{19}F NMR spectra were recorded on Bruker spectrometers (at 376 MHz) and are reported in terms of chemical shift in $CDCl_3$. IR spectra were recorded on a Perkin-Elmer 100 spectrometer and are reported in terms of frequency absorption (cm^{-1}). High-resolution mass spectra were obtained from the UC Irvine and UCLA Mass Spectrometry Facilities. At UC Irvine, high resolution mass spectra were obtained on a Waters Micromass LCT Premier TOF Mass Spectrometer (Waters) equipped with a ZSpray source for electrospray ionization (ESI) and a time-of-flight (TOF) analyzer. The instrument was controlled by Waters MassLynx 4.0. At UCLA, DART-MS spectra were collected on a Thermo Exactive Plus MSD (Thermo Scientific) equipped with an ID-CUBE ion source and a Vapur Interface (IonSense Inc.). Both the source and MSD were controlled by Excalibur software v. 3.0. The analyte was spotted onto OpenSpot sampling cards (IonSense Inc.) Ionization was accomplished using UHP He (Airgas Inc.) plasma with no additional ionization agents. The mass calibration was

carried out using Pierce LTQ Velos ESI (+) and (–) Ion calibration solutions (Thermo Fisher Scientific).

4.7.2 Experimental Procedures

4.7.2.1 Syntheses of Heck Cyclization Substrates

4.7.2.1.1 Scalable Synthesis of Imide 4.5 for Reaction Discovery

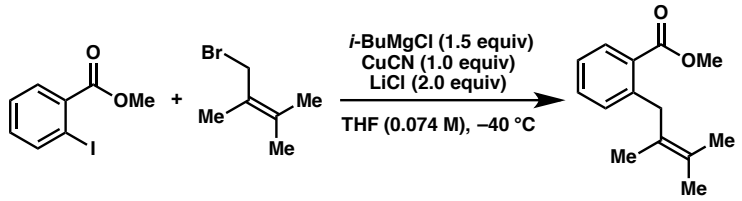

4.26 *4.27* (31% yield) *4.28*

Ester 4.28. Following a modification of the general procedure reported by Querolle and co-workers,[29] a flask containing a stir bar was charged with CuCN (1.03 g, 11.5 mmol, 1.0 equiv) and LiCl (971 mg, 22.9 mmol, 2.0 equiv) in the glovebox. The flask was removed from the glovebox, and the solids were suspended in THF (39 mL). The resulting mixture was stirred vigorously until a completely dissolved solution of CuCN•2LiCl was formed. In a separate flask containing a solution of methyl-2-iodobenzoate (**4.26**) (3.02 g, 11.45 mmol, 1.0 equiv) in THF (115 mL) at –40 °C was added *i*-BuMgCl (8.6 mL of a 2.0 M solution in THF, 17.2 mmol, 1.5 equiv) dropwise over 1 min. After this mixture was stirred at –40 °C for 1 h, the solution of CuCN•2LiCl was added via cannula. The combined mixture stirred at –40 °C for an additional 15 min, at which point bromide **4.27** (4.65 g, 28.6 mmol, 2.5 equiv) was added dropwise over 1 min. After stirring at –40 °C for an additional hour, the reaction was poured into 9:1 sat. aq. NH_4Cl:NH_4OH (150 mL). The layers were separated and the aqueous layer was extracted with EtOAc (3 x 100 mL). The organic

layers were combined, dried over $MgSO_4$, and concentrated under reduced pressure. The crude mixture was purified via flash chromatography (4:1 Benzene:Hexanes) to afford ester **4.28** (767 mg, 31% yield) as a colorless oil. Ester **4.28**: R_f 0.63 (3:1 Hexanes:EtOAc); ^{1}H NMR (500 MHz, $CDCl_3$): δ 7.83 (dd, *J* = 7.7, 1.3, 1H), 7.40 (td, *J* = 7.5, 1.5, 1H), 7.23 (t, *J* = 7.5, 1H), 7.20 (d, *J* = 7.7, 1H), 3.89 (s, 3H), 3.78 (s, 2H) 1.76 (s, 3H), 1.71 (s, 3H), 1.57 (s, 3H); ^{13}C NMR (125 MHz, $CDCl_3$): δ 168.7, 142.1, 131.9, 130.6, 130.3, 129.2, 127.1, 125.73, 125.66, 52.0, 37.7, 20.73, 20.69, 18.6; IR (film): 2916, 1720, 1433, 1262, 1246, 1121, 1076 cm^{-1}; HRMS–APCI (m/z) $[M + H]^+$ calcd for $C_{14}H_{19}O_7^+$, 219.13796; found 219.13784.

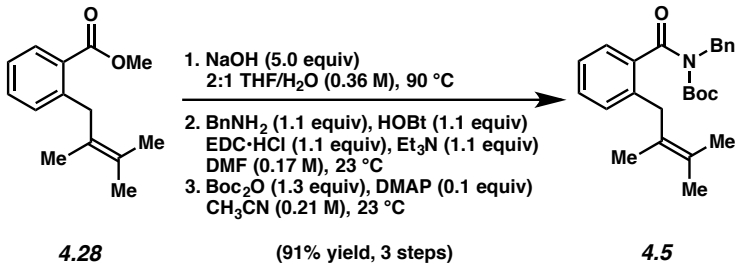

4.28 (91% yield, 3 steps) *4.5*

Imide 4.5. To a solution of ester **4.28** (767 mg, 3.51 mmol, 1.0 equiv) in THF (6.6 mL) was added a solution of NaOH (703 mg, 17.6 mmol, 5.0 equiv) in H_2O (3.3 mL). The reaction was heated to 90 °C and stirred for 12 h. After cooling to room temperature, the reaction mixture was poured into deionized water (25 mL) and diluted with EtOAc (25 mL). The layers were separated and the aqueous layer was acidified to pH ~4 with 1 N HCl (15 mL) and extracted with EtOAc (3 x 25 mL). The organic layers were combined, washed with deionized water (300 mL), dried over $MgSO_4$, and concentrated under reduced pressure to afford the corresponding carboxylic acid, which was used in the subsequent step without further purification.

To a solution of the crude carboxylic acid, HOBt (591 mg, 3.86 mmol, 1.1 equiv from **4.28**), and EDC•HCl (740 mg, 3.86 mmol, 1.1 equiv from **4.28**) in DMF (21 mL) was added

$BnNH_2$ (0.42 mL, 3.86 mmol, 1.1 equiv from **4.28**) and Et_3N (0.5 mL, 3.86 mmol, 1.1 equiv from **4.28**). After stirring for 7 h, the reaction mixture was poured into deionized water (100 mL) and diluted with EtOAc (50 mL). The layers were separated and the aqueous layer was extracted with EtOAc (2 x 50 mL). The organic layers were combined, washed with deionized water (100 mL), dried over $MgSO_4$, and concentrated under reduced pressure to afford the corresponding amide, which was used in the subsequent step without further purification.

To a solution of the crude amide in CH_3CN (17 mL) was added DMAP (43 mg, 0.351 mmol, 0.1 equiv from **4.28**) and Boc_2O (996 mg, 4.56 mmol, 1.3 equiv from **4.28**). After stirring for 7 h, the reaction mixture was concentrated under reduced pressure and purified by flash chromatography (99:1 Hexanes:EtOAc) to yield imide **4.5** (1.26 g, 91% yield, three steps) as a white solid. Imide **4.5**: mp: 65–67 °C; R_f 0.60 (3:1 Hexanes:EtOAc); ^{1}H NMR (500 MHz, $CDCl_3$): δ 7.43 (d, J = 7.9, 2H), 7.34 (d, J = 7.4, 2H), 7.31–7.25 (m, 2H), 7.16 (t, J = 7.4, 1H), 7.11 (d, J = 7.9, 2H), 5.03 (s, 2H), 3.43 (s, 2H), 1.75 (s, 3H), 1.70 (s, 3H), 1.58 (s, 3H), 1.11 (s, 9H); ^{13}C NMR (125 MHz, $CDCl_3$): δ 172.6, 153.0, 138.7, 138.0, 137.7, 129.5, 128.6, 128.40, 128.36, 127.5, 127.2, 125.9, 125.44, 125.37, 83.4, 48.0, 36.8, 27.5, 20.76, 20.75, 18.8; IR (film): 2981, 2922, 1728, 1670, 1368, 1333, 1229, 1138 cm^{-1}; HRMS–APCI (m/z) $[M + H]^+$ calcd for $C_{25}H_{32}NO_3^+$, 394.23767; found 394.23462.

4.7.2.1.2 Syntheses of Halo-Imide Reductive Coupling Partners

Representative Procedure (synthesis of imide 4.30 is used as an example).

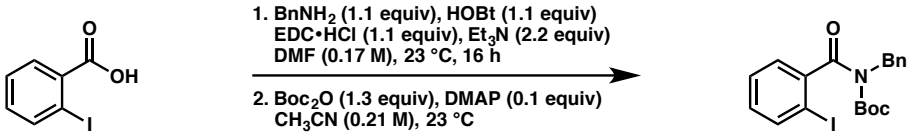

4.29 (93% yield, 2 steps) *4.30*

Iodo-imide 4.30. To a mixture of 2-iodo-benzoic acid (**4.29**) (10.0 g, 40.4 mmol, 1.0 equiv), EDC•HCl (8.5 g, 44 mmol, 1.1 equiv), HOBt (6.0 g, 44 mmol, 1.1 equiv) and Et_3N (6.2 mL, 88 mmol, 2.2 equiv) in DMF (238 mL) was added $BnNH_2$ (5.0 mL, 44 mmol, 1.1 equiv). The resulting mixture was stirred for 16 h, and then diluted with deionized water (100 mL). The layers were separated and the aqueous layer was extracted with EtOAc (3 x 100 mL). The combined organic layers were washed with 0.1 N HCl (100 mL), sat. aq. $NaHCO_3$ (100 mL), and brine (100 mL), dried over Na_2SO_4, and filtered. Concentration under reduced pressure afforded the crude amide, which was used in the subsequent step without further purification.

To the vessel containing the crude amide was added DMAP (0.5 g, 4 mmol, 0.1 equiv from **4.29**), followed by acetonitrile (192 mL). Boc_2O (11.5 g, 52.5 mmol, 1.3 equiv from **4.29**) was added in one portion and the reaction vessel was flushed with N_2. The reaction mixture was allowed to stir for 16 h. The reaction was concentrated under reduced pressure and the resulting crude residue was purified by flash chromatography (9:1 Hexanes:EtOAc) to yield iodo-imide **4.30** (16.4 g, 93% yield, two steps) as a white solid. Iodo-imide **4.30**: mp: 100–101 ºC; R_f 0.54 (4:1 Hexanes:EtOAc); ^{1}H NMR (500 MHz, $CDCl_3$): δ 7.79 (d, J = 8.0, 1H), 7.47 (d, J = 8.0, 2H), 7.37–7.32 (m, 3H), 7.30–7.27 (m, 1H), 7.18–7.15 (m, 1H), 7.10–7.05 (m, 1H), 5.05 (s, 2H), 1.14 (s, 9H); ^{13}C NMR (125 MHz, $CDCl_3$): δ 171.7, 152.1, 144.6, 139.2, 137.5, 130.3, 128.6, 128.5, 127.9,

127.6, 127.0, 91.7, 83.9, 48.0, 27.6; IR (film): 2979, 1731, 1668, 1228, 741 cm^{-1}; HRMS–APCI (m/z) $[M + H]^+$ calcd for $C_{19}H_{21}INO_3^+$, 438.05606; found 438.05536.

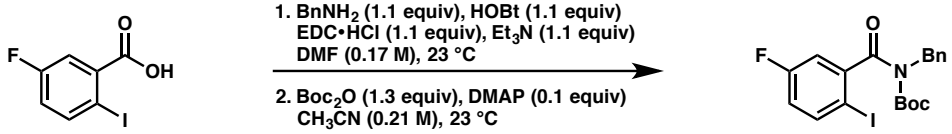

4.31 (72% yield, 2 steps) *4.32*

Iodo-imide 4.32. Following the representative procedure with 2-iodo-5-fluorobenzoic acid (**4.31**) (2.0 g, 7.52 mmol), purification by flash chromatography (99:1 Pentane:Et_2O → 19:1 Pentane:Et_2O) afforded iodo-imide **4.32** (2.46 g, 72% yield, two steps) as a white solid. Iodo-imide **4.32**: mp: 61–63 °C; R_f 0.60 (3:1 Hexanes:EtOAc); ^1H NMR (500 MHz, $CDCl_3$): δ 7.72 (dd, J = 8.7, 5.2, 1H), 7.46 (d, J = 7.3, 2H), 7.34 (tt, J = 7.1, 1.4, 2H), 7.28 (tt, J = 7.3, 1.4, 1H), 6.93 (dd, J = 8.5, 3.1, 1H), 6.83 (dt, J = 8.5, 3.1, 1H), 5.04 (s, 2H), 1.20 (s, 9H); ^{13}C NMR (125 MHz, $CDCl_3$): δ 170.3 (d, J = 2.2), 162.7 (d, J = 246), 151.8, 146.2 (d, J = 7.2), 140.6 (d, J = 7.7), 137.2, 128.63, 128.56, 127.7, 117.7 (d, J = 22), 114.7 (d, J = 24), 84.6 (d, J = 3.6), 84.3, 48.0, 27.6; ^{19}F NMR (376 MHz, $CDCl_3$): δ –113.7, (s, 1F); IR (film): 2981, 1736, 1671, 1369, 1350, 1331, 1232, 1149 cm^{-1}; HRMS–APCI (m/z) $[M + H]^+$ calcd for $C_{19}H_{20}FINO_3^+$ 456.04664; found 456.04664.

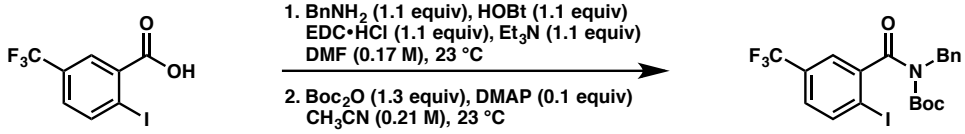

4.33 (88% yield, 2 steps) *4.34*

Iodo-imide 4.34. Following the representative procedure with 2-iodo-5-(trifluoromethyl)benzoic acid (**4.33**) (1.98 g, 6.27 mmol), purification by flash chromatography (99:1 Pentane:Et_2O → 19:1 Pentane:Et_2O) afforded iodo-imide **4.34** (2.79 g, 88% yield, two steps) as an off-white solid. Iodo-

imide **4.34**: mp: 60–62 °C; R_f 0.70 (3:1 Hexanes:EtOAc); ^{1}H NMR (500 MHz, $CDCl_3$): δ 7.93 (d, J = 8.3, 1H), 7.48 (d, J = 7.3, 2H), 7.41 (d, J = 2.0, 1H), 7.35 (tt, J = 7.6, 1.5, 2H), 7.33–7.28 (m, 2H), 5.07 (s, 2H), 1.15 (s, 9H); ^{13}C NMR (125 MHz, $CDCl_3$): δ 170.4, 151.7, 145.5, 139.8, 137.1, 130.8 (q, J = 33), 128.7, 128.6, 127.8, 126.5 (q, J = 3.6), 123.68 (q, J = 273), 123.67 (q, J = 3.8), 95.8, 84.4, 48.0, 27.5; ^{19}F NMR (376 MHz, $CDCl_3$): δ –63.0, (s, 3F); IR (film): 2982, 1737, 1669, 1317, 1225, 1126, 1079 cm^{-1}; HRMS–APCI (m/z) $[M + H]^+$ calcd for $C_{20}H_{20}F_3INO_3^+$ 506.04345; found 506.04387.

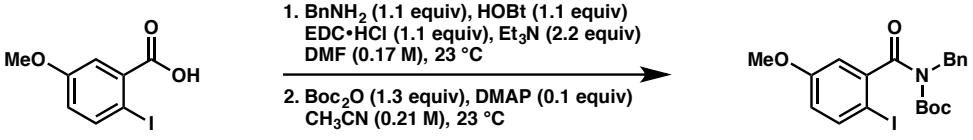

4.35 (87% yield, 2 steps) *4.36*

Iodo-imide 4.36. Following the representative procedure with 2-iodo-5-methoxybenzoic acid (**4.35**) (1.0 g, 3.6 mmol), 2-iodo-imide **4.36** (1.5 g, 87% yield, two steps) was obtained as a colorless oil. Iodo-imide **4.36**: R_f 0.24 (4:1 Hexanes:EtOAc); ^{1}H NMR (400 MHz, $CDCl_3$): δ 7.62 (d, J = 8.8, 1H), 7.48–7.45 (m, 2H), 7.36–7.32 (m, 2H), 7.30–7.26 (m, 1H), 6.73 (d, J = 3.1, 1H), 6.66 (dd, J = 8.7, 3.1, 1H), 5.04 (s, 2H), 3.76, (s, 3H), 1.17 (s, 9H); ^{13}C NMR (125 MHz, $CDCl_3$): δ 171.3, 159.6, 151.9, 145.1, 139.7, 137.3, 128.5, 128.4, 127.4, 116.8, 112.8, 83.7, 80.0, 55.5, 47.9, 27.4; IR (film): 2979, 1735, 1466, 1144, 848, 699 cm^{-1}; HRMS–APCI (m/z) $[M + H]^+$ calcd for $C_{20}H_{23}INO_4^+$, 468.06663; found 468.06671.

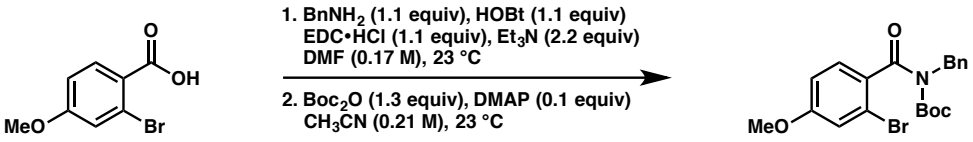

4.37 **(quantitative yield, 2 steps)** ***4.38***

Bromo-imide 4.38. Following the representative procedure with 2-bromo-4-methoxybenzoic acid (**4.37**) (0.46 g, 2.0 mmol), 2-bromo-imide **4.38** (0.86 g, quantitative yield, two steps) was obtained as a yellow oil. Bromo-imide **4.38**: R_f 0.25 (9:1 Hexanes:EtOAc); ^{1}H NMR (500 MHz, $CDCl_3$): δ 7.46–7.44 (m, 2H), 7.35–7.31 (m, 2H), 7.32–7.29 (m, 1H), 7.22 (d, J = 8.7, 1H), 7.07 (d, J = 2.5, 1H), 6.86 (dd, J = 8.7, 2.5, 1H), 5.02 (s, 2H), 3.81, (s, 3H), 1.19 (s, 9H); ^{13}C NMR (125 MHz, $CDCl_3$): δ 170.5, 160.8, 152.5, 137.7, 132.7, 129.3, 128.5 (4 carbons), 127.5, 119.8, 118.1, 113.2, 83.5, 55.8, 48.2, 27.6; IR (film): 2979, 1731, 1599, 1227, 848, 558 cm^{-1}; HRMS–APCI (m/z) [M + H]$^+$ calcd for $C_{20}H_{23}BrNO_4^+$, 420.08050; found 420.08082.

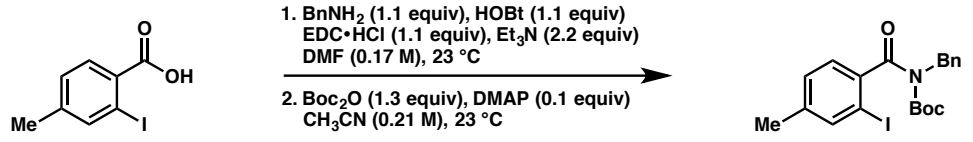

4.39 **(92% yield, 2 steps)** ***4.40***

Iodo-imide 4.40. Following the representative procedure with 2-iodo-4-methylbenzoic acid (**4.39**) (2.0 g, 7.6 mmol), iodo-imide **4.40** (3.3 g, 92% yield, two steps) was obtained as a colorless oil. Iodo-imide **4.40**: R_f 0.34 (9:1 Hexanes:EtOAc); ^{1}H NMR (500 MHz, $CDCl_3$): δ 7.65 (d, J = 7.8, 1H), 7.48–7.45 (m, 2H), 7.35–7.31 (m, 2H), 7.29–7.25 (m, 1H), 7.00 (d, J = 2.1, 1H), 6.89 (ddd, J = 8.1, 2.1, 0.8, 1H), 5.04 (s, 2H), 2.29 (s, 3H), 1.15 (s, 9H); ^{13}C NMR (125 MHz, $CDCl_3$): δ 171.7, 152.1, 144.2, 138.8, 138.0, 137.4, 131.2, 128.5, 128.4, 127.8, 127.4, 87.4, 83.6, 47.9, 27.4, 20.8; IR (film): 2979, 1731, 1668, 1141, 848, 698 cm^{-1}; HRMS–APCI (m/z) [M + H]$^+$ calcd for $C_{20}H_{23}INO_3^+$, 452.07171; found 452.07080.

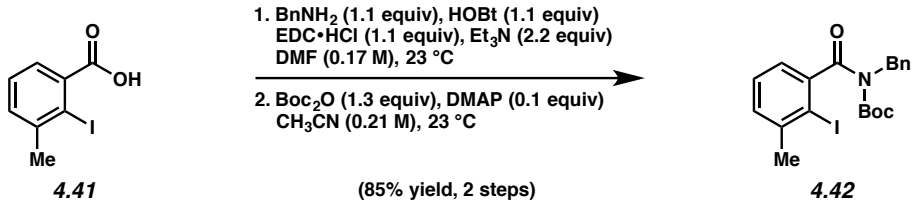

Iodo-imide 4.42. Following the representative procedure with 2-iodo-3-methylbenzoic acid (**4.41**) (3.0 g, 12 mmol), iodo-imide **4.42** (4.4 g, 85% yield, two steps) was obtained as a white solid. Iodo-imide **4.42**: mp: 87–89 ºC; R_f 0.62 (4:1 Hexanes:EtOAc); ^{1}H NMR (500 MHz, $CDCl_3$): δ 7.48 (d, J = 7.8, 2H), 7.36–7.32 (m, 2H), 7.29–7.26 (m, 1H), 7.24–7.20 (m, 2H), 6.90 (dd, J = 6.7, 2.4, 1H), 5.07 (s, 2H), 2.46 (s, 3H), 1.11 (s, 9H); ^{13}C NMR (125 MHz, $CDCl_3$): δ 171.9, 152.0, 145.7, 142.2, 137.4, 129.5, 128.42, 128.36, 127.9, 127.4, 123.7, 98.5, 83.6, 47.7, 28.8, 27.4; IR (film): 2979, 1732, 1338, 1145, 849, 699 cm^{-1}; HRMS–APCI (m/z) $[M + H]^+$ calcd for $C_{20}H_{23}INO_3^+$, 452.07171; found 452.07177.

4.7.2.1.3 Syntheses of Carbonate Reductive Coupling Partners

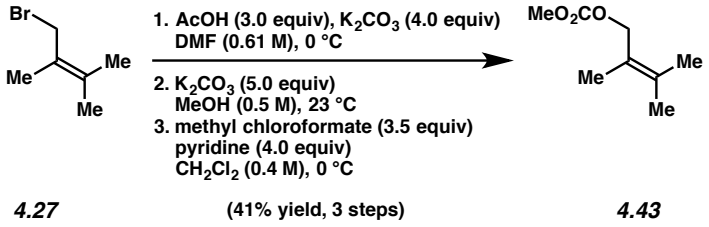

Carbonate 4.43. To a suspension of K_2CO_3 (39.0 g, 0.282 mol, 4.0 equiv) in DMF (116 mL) was added AcOH (12 mL, 0.212 mol, 3.0 equiv). The mixture was cooled to 0 °C. After stirring for 5 min, bromide **4.27**[30] (11.5 g, 0.0705 mol, 1.0 equiv) was added. After stirring vigorously at 0 °C for 2 h, the reaction mixture was poured into deionized water (300 mL) and diluted with Et_2O (150 mL). The layers were separated and the aqueous layer was extracted with Et_2O (2 x 150 mL). The

organic layers were combined, washed with deionized water (300 mL), dried over $MgSO_4$, and concentrated under reduced pressure (~100 mbar, at room temperature) to afford the corresponding acetate, which was used in the subsequent step without further purification.

To a solution of the crude acetate in MeOH (141 mL) was added K_2CO_3 (48.7 g, 0.353 mol, 4.0 equiv from **4.27**). After stirring vigorously for 12 h, the reaction mixture was poured into deionized water (300 mL) and diluted with Et_2O (150 mL). The layers were separated and the aqueous layer was extracted with Et_2O (2 x 150 mL). The organic layers were combined, washed with deionized water (300 mL), dried over $MgSO_4$, and concentrated under reduced pressure (~100 mbar, at room temperature) to afford the corresponding alcohol, which was used in the subsequent step without further purification.

To a solution of the crude alcohol in CH_2Cl_2 (176 mL) was added pyridine (17.0 mL, 0.212 mol, 3.0 equiv from **4.27**). The reaction was cooled to 0 °C. After stirring for 5 min, methyl chloroformate (11 mL, 0.141 mol, 2.0 equiv from **4.27**) was added dropwise over 1 min. The reaction was stirred for 6 h, and allowed to warm to room temperature, at which point additional pyridine (8.50 mL, 0.141 mol, 1.0 equiv from **4.27**) and methyl chloroformate (5.5 ml, 0.106 mol, 1.5 equiv from **4.27**) was added. After stirring for an additional 12 h, the reaction mixture was poured into brine (200 mL) and diluted with Et_2O (150 mL). The layers were separated and the aqueous layer was extracted with Et_2O (2 x 150 mL). The organic layers were combined, washed with 1 N HCl (300 mL), dried over $MgSO_4$, and concentrated under reduced pressure (~100 mbar, at room temperature). The crude mixture was purified via flash chromatography (99:1 Pentane:Et_2O → 15:1 Pentane:Et_2O) to afford carbonate **4.43** (4.62 g, 41% yield, three steps) as a colorless oil. Carbonate **4.43**: R_f 0.61 (3:1 Hexanes:EtOAc); ^{1}H NMR (500 MHz, $CDCl_3$): δ 4.63 (s, 2H), 3.74 (s, 3H), 1.75–1.73 (m, 3H), 1.70–1.68 (m, 3H), 1.67 (s, 3H); ^{13}C NMR (125 MHz,

$CDCl_3$): δ 156.1, 132.8, 122.4, 69.3, 54.7, 20.9, 20.3, 16.7; IR (film): 2988, 2919, 1744, 1442, 1246 cm^{-1}; HRMS–ESI (m/z) $[M + Na]^+$ calcd for $C_8H_{14}NaO_3^+$, 181.0841; found 181.0843.

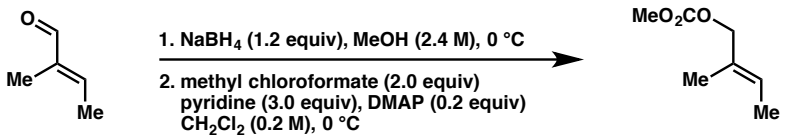

4.44 **(80% yield, 2 steps)** ***4.45***

Carbonate 4.45. To a solution of tiglic aldehyde (**4.44**) (3.0 g, 36 mmol, 1.0 equiv) in MeOH (15 mL) at 0 °C was added $NaBH_4$ (1.6 g, 43 mmol, 1.2 equiv) in 10 portions over 5 min at 0 °C. After 3 h of stirring at room temperature, the mixture was poured into deionized water (50 mL) and diluted with CH_2Cl_2 (50 mL). The layers were separated and the aqueous layer was extracted with CH_2Cl_2 (2 x 50 mL). The organic layers were combined, washed with brine (50 mL), dried over $MgSO_4$, and concentrated under reduced pressure to afford the corresponding alcohol, which was used in the subsequent step without further purification.

To a solution of the crude alcohol in CH_2Cl_2 (180 mL) was added pyridine (2.57 mL, 31.9 mmol, 3.0 equiv from **4.44**) and DMAP (0.86 g, 7.1 mmol, 0.2 equiv). The reaction was cooled to 0 °C. After stirring for 5 min, methyl chloroformate (0.87 mL, 11.3 mmol, 2.0 equiv from **4.44**) was added dropwise over 20 min. The reaction was allowed to warm to room temperature. After stirring for 1 h, the reaction mixture was poured into brine (50 mL) and diluted with CH_2Cl_2 (50 mL). The layers were separated and the aqueous layer was extracted with CH_2Cl_2 (2 x 50 mL). The organic layers were combined, washed with 1 N HCl (50 mL), dried over $MgSO_4$, and concentrated under reduced pressure. The crude mixture was purified via flash chromatography (9:1 Pentane:Et_2O) to afford carbonate **4.45** (4.6 g, 80% yield, two steps) as a colorless oil. Carbonate **4.45**: R_f 0.61 (4:1 Hexanes:EtOAc); ^1H NMR (500 MHz, $CDCl_3$): δ 5.59 (q, J = 7.0,

1H), 4.51 (s, 2H), 3.77 (s, 3H), 1.67 (s, 3H), 1.63 (d, J = 7.0, 3H); ^{13}C NMR (125 MHz, $CDCl_3$): δ 156.0, 130.4, 125.2, 74.0, 54.8, 13.7, 13.4; IR (film): 2957, 1745, 1442, 1250, 935, 792 cm^{-1}; HRMS–ESI (m/z) $[M + Na]^+$ calcd for $C_8H_{14}O_3Na$ 181.0843; found 181.0841.

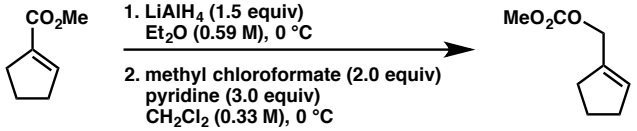

4.46 **(50% yield, 2 steps)** ***4.47***

Carbonate 4.47. To a solution of methyl ester **4.46** (1.26 g, 10.0 mmol, 1.0 equiv) in Et_2O (17 mL) at 0 °C was added $LiAlH_4$ (570 mg, 15.0 mmol, 1.5 equiv) at 0 °C. After stirring for 4 h, deionized water (3 mL) was added dropwise over 5 min at 0 °C. The resulting heterogeneous mixture was filtered through a plug of celite® (50 mL of Et_2O eluent) and the filtrate was diluted with deionized water (50 mL). The layers were separated and the aqueous layer was extracted with Et_2O (3 x 50 mL). The organic layers were combined, dried over $MgSO_4$, and concentrated under reduced pressure (~100 mbar, at room temperature) to afford the corresponding alcohol, which was used in the subsequent step without further purification.

To a solution of the crude alcohol in CH_2Cl_2 (30 mL) was added pyridine (2.50 mL, 30.0 mmol, 3.0 equiv from **4.46**). The reaction was cooled to 0 °C. After stirring for 5 min, methyl chloroformate (1.55 mL, 20.0 mmol, 2.0 equiv from **4.46**) was added dropwise over 1 min. The reaction was allowed to warm to room temperature. After stirring for 15 h, the reaction mixture was poured into brine (150 mL) and diluted with CH_2Cl_2 (50 mL). The layers were separated and the aqueous layer was extracted with CH_2Cl_2 (3 x 50 mL). The organic layers were combined, washed with 1 N HCl (50 mL), dried over $MgSO_4$, and concentrated under reduced pressure (~100 mbar, at room temperature). The crude mixture was purified via flash chromatography (98:2

Hexanes:Et_2O) to afford carbonate **4.47** (792 mg, 50% yield, two steps) as a colorless oil. Carbonate **4.47**: R_f 0.48 (9:1 Hexanes:EtOAc); ^{1}H NMR (500 MHz, $CDCl_3$): δ 5.72 (s, 1H), 4.69 (s, 2H), 3.79 (s, 3H), 2.38–2.31 (m, 4H), 1.92 (quint, J =7.7, 2H); ^{13}C NMR (125 MHz, $CDCl_3$): δ 156.0, 138.6, 129.6, 66.9, 54.9, 32.9, 32.6, 23.4; IR (film): 2960, 2918, 2848, 1750, 1447, 1263, 949 cm^{-1}; HRMS–ESI (m/z) $[M + Na]^+$ calcd for $C_8H_{12}O_3Na$, 179.0684; found 179.0677.

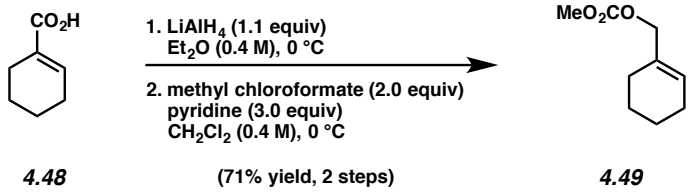

Carbonate 4.49. To a solution of carboxylic acid **4.48** (2.00 g, 16.5 mmol, 1.0 equiv) in Et_2O (40 mL) at 0 °C was added $LiAlH_4$ (18.2 mL of a 1.0 M solution in Et_2O, 18.2 mmol, 1.1 equiv) dropwise over 5 min at 0 °C. After stirring for 15 min, deionized water (5 mL) was added dropwise at 0 °C. The resulting heterogeneous mixture was filtered through a plug of celite® (25 mL of Et_2O eluent) and the filtrate was diluted with deionized water (50 mL). The layers were separated and the aqueous layer was extracted with Et_2O (2 x 50 mL). The organic layers were combined, dried over $MgSO_4$, and concentrated under reduced pressure (~100 mbar, at room temperature) to afford the corresponding alcohol, which was used in the subsequent step without further purification.

To a solution of the crude alcohol in CH_2Cl_2 (40 mL) was added pyridine (2.55 mL, 49.5 mmol, 3.0 equiv from **4.48**). The reaction was cooled to 0 °C. After stirring for 5 min, methyl chloroformate (2.6 mL, 33.0 mmol, 2.0 equiv from **4.48**) was added dropwise over 1 min. The reaction was allowed to warm to room temperature. After stirring for 4 h, the reaction mixture was poured into brine (50 mL) and diluted with CH_2Cl_2 (50 mL). The layers were separated and the aqueous layer was extracted with CH_2Cl_2 (2 x 50 mL). The organic layers were combined, washed

with 1 N HCl (50 mL), dried over $MgSO_4$, and concentrated under reduced pressure (~100 mbar, at room temperature). The crude mixture was purified via flash chromatography (99:1 Pentane:Et_2O → 49:1 Pentane:Et_2O) to afford carbonate **4.49** (2.00 g, 71% yield, two steps) as a colorless oil. Carbonate **4.49**: R_f 0.86 (1:1 Hexanes:EtOAc); ^1H NMR (500 MHz, $CDCl_3$): δ 5.78 (m, 1H), 4.49 (s, 2H), 3.78 (s, 3H), 2.02 (m, 4H), 1.64 (m, 2H), 1.57 (m, 2H); ^{13}C NMR (125 MHz, $CDCl_3$): δ 156.0, 132.5, 127.5, 72.7, 54.8, 25.9, 25.1, 22.4, 22.2; IR (film): 2930, 1744, 1441, 1250 cm^{-1}; HRMS–ESI (m/z) $[M + Na]^+$ calcd for $C_9H_{14}NaO_3^+$, 193.0841; found 193.0839.

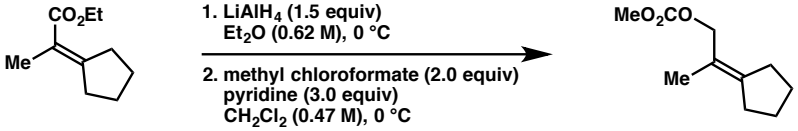

4.50 **(61% yield, 2 steps)** ***4.51***

Carbonate 4.51. To a solution of known ester **4.50**[31] (3.15 g, 18.7 mmol, 1.0 equiv) in Et_2O (30 mL) at 0 °C was added $LiAlH_4$ (1.07 g, 28.1 mmol, 1.5 equiv) at 0 °C. After stirring for 4 h, deionized water (3 mL) was added dropwise over 5 min at 0 °C. The resulting heterogeneous mixture was filtered through a plug of celite® (25 mL of Et_2O eluent) and the filtrate was diluted with deionized water (25 mL). The layers were separated and the aqueous layer was extracted with Et_2O (2 x 50 mL). The organic layers were combined, dried over $MgSO_4$, and concentrated under reduced pressure (~100 mbar, at room temperature) to afford the corresponding alcohol, which was used in the subsequent step without further purification.

To a solution of the crude alcohol in CH_2Cl_2 (40 mL) was added pyridine (4.65 mL, 56.1 mmol, 3.0 equiv from **4.50**). The reaction was cooled to 0 °C. After stirring for 5 min, methyl chloroformate (2.9 mL, 37.4 mmol, 2.0 equiv from **4.50**) was added dropwise over 1 min. The reaction was allowed to warm to room temperature. After stirring for 15 h, the reaction mixture

was poured into brine (100 mL) and diluted with Et_2O (50 mL). The layers were separated and the aqueous layer was extracted with Et_2O (3 x 50 mL). The organic layers were combined, washed with 1 N HCl (25 mL), dried over $MgSO_4$, and concentrated under reduced pressure. The crude mixture was purified via flash chromatography (95:5 Hexanes:Et_2O) to afford carbonate **4.51** (2.09 g, 61% yield, two steps) as a colorless oil. Carbonate **4.51**: R_f 0.45 (9:1 Hexanes:EtOAc); ^{1}H NMR (500 MHz, $CDCl_3$): δ 4.63 (s, 2H), 3.78 (s, 3H), 2.33 (s, 2H), 2.22 (s, 2H), 1.70–1.63 (m, 7H); ^{13}C NMR (125 MHz, $CDCl_3$): δ 156.2, 145.0, 119.6, 70.6, 54.8, 31.3, 30.4, 27.0, 26.4, 17.2; IR (film): 2956, 2867, 1748, 1442, 1373, 1256, 942 cm^{-1}; HRMS–APCI (m/z) $[M + H]^+$ calcd for $C_{10}H_{17}O_3^+$, 185.11722; found 185.11700.

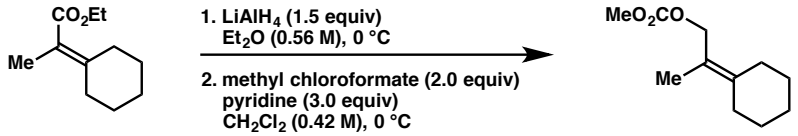

Carbonate 4.53. To a solution of known ester **4.52**[3] (3.08 g, 16.9 mmol, 1.0 equiv) in Et_2O (30 mL) at 0 °C was added $LiAlH_4$ (965 mg, 25.4 mmol, 1.5 equiv). After stirring for 1 h, deionized water (3 mL) was added dropwise over 5 min at 0 °C. The resulting heterogeneous mixture was filtered through a plug of celite® (25 mL of Et_2O eluent) and the filtrate was diluted with deionized water (25 mL). The layers were separated and the aqueous layer was extracted with Et_2O (2 x 50 mL). The organic layers were combined, dried over $MgSO_4$, and concentrated under reduced pressure (~100 mbar, at room temperature) to afford the corresponding alcohol, which was used in the subsequent step without further purification.

To a solution of the crude alcohol in CH_2Cl_2 (40 mL) was added pyridine (4.21 mL, 50.7 mmol, 3.0 equiv from **4.52**). The reaction was cooled to 0 °C. After stirring for 5 min, methyl

chloroformate (2.6 mL, 33.8 mmol, 2.0 equiv from **4.52**) was added dropwise over 1 min. The reaction was allowed to warm to room temperature. After stirring for 15 h, the reaction mixture was poured into brine (100 mL) and diluted with Et_2O (50 mL). The layers were separated and the aqueous layer was extracted with Et_2O (3 x 50 mL). The organic layers were combined, washed with 1 N HCl (25 mL), dried over $MgSO_4$, and concentrated under reduced pressure. The crude mixture was purified via flash chromatography (95:5 Hexanes:Et_2O) to afford carbonate **4.53** (1.83 g, 54% yield, two steps) as a colorless oil. Carbonate **4.53**: R_f 0.45 (9:1 Hexanes:EtOAc); ^{1}H NMR (500 MHz, $CDCl_3$): δ 4.68 (s, 2H), 3.77 (s, 3H), 2.28–2.22 (m, 2H), 2.21–2.15 (m, 2H), 1.73 (s, 3H), 1.60–1.48 (m, 6H); ^{13}C NMR (125 MHz, $CDCl_3$): δ 156.2, 141.4, 119.1, 69.0, 54.8, 31.0, 30.7, 28.4, 27.9, 26.8, 16.5; IR (film): 2925, 2854, 1744, 1443, 1373, 1247, 937 cm^{-1}; HRMS–APCI (m/z) $[M + H]^+$ calcd for $C_{11}H_{19}O_3^+$, 199.13287; found 199.13247.

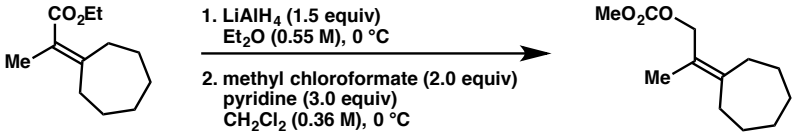

4.54 **(64% yield, 2 steps)** ***4.55***

Carbonate 4.55. To a solution of known ester **4.54**[32] (2.15 g, 10.9 mmol, 1.0 equiv) in Et_2O (20 mL) at 0 °C was added $LiAlH_4$ (626 mg, 16.4 mmol, 1.5 equiv). After stirring for 1 h, deionized water (3 mL) was added dropwise over 5 min at 0 °C. The resulting heterogeneous mixture was filtered through a plug of celite® (25 mL of Et_2O eluent) and the filtrate was diluted with deionized water (25 mL). The layers were separated and the aqueous layer was extracted with Et_2O (2 x 50 mL). The organic layers were combined, dried over $MgSO_4$, and concentrated under reduced pressure (~100 mbar, at room temperature) to afford the corresponding alcohol, which was used in the subsequent step without further purification.

To a solution of the crude alcohol in CH_2Cl_2 (30 mL) was added pyridine (2.80 mL, 32.9 mmol, 3.0 equiv from **4.54**). The reaction was cooled to 0 °C. After stirring for 5 min, methyl chloroformate (1.7 mL, 21.9 mmol, 2.0 equiv from **4.54**) was added dropwise over 1 min. The reaction was allowed to warm to room temperature. After stirring for 15 h, the reaction mixture was poured into brine (100 mL) and diluted with Et_2O (50 mL). The layers were separated and the aqueous layer was extracted with Et_2O (3 x 50 mL). The organic layers were combined, washed with 1 N HCl (25 mL), dried over $MgSO_4$, and concentrated under reduced pressure. The crude mixture was purified via flash chromatography (95:5 Hexanes:Et_2O) to afford carbonate **4.55** (1.49 g, 64% yield, two steps) as a colorless oil. Carbonate **4.55**: R_f 0.52 (9:1 Hexanes:EtOAc); ^{1}H NMR (500 MHz, $CDCl_3$): δ 4.67 (s, 2H), 3.77 (s, 3H), 2.33 (t, J = 6.0, 2H), 2.26 (t, J = 6.0, 2H), 1.71 (s, 3H), 1.60–1.53 (m, 4H), 1.51–1.44 (m, 4H); ^{13}C NMR (125 MHz, $CDCl_3$): δ 156.1, 142.2, 122.4, 69.1, 54.6, 32.3, 31.2, 28.9, 28.6, 28.2, 26.8, 16.4; IR (film): 2922, 2854, 1748, 1443, 1374, 1256, 936 cm^{-1}; HRMS–ESI (m/z) $[M + Na]^+$ calcd for $C_{12}H_{20}O_3Na^+$, 235.1310; found 235.1301.

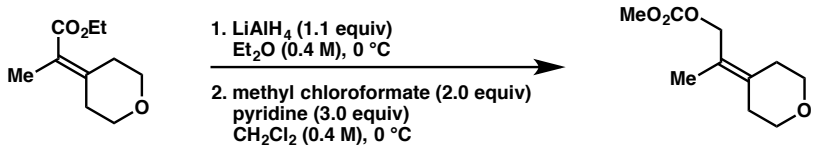

4.56 (71% yield, 2 steps) *4.57*

Carbonate 4.57. To a solution of ester **4.56**[33] (1.47 g, 8.0 mmol, 1.0 equiv) in Et_2O (20 mL) at 0 °C was added $LiAlH_4$ (8.8 mL of a 1.0 M solution in Et_2O, 8.8 mmol, 1.1 equiv) dropwise over 5 min. After stirring for 1 h, deionized water (1 mL) was added dropwise over 5 min at 0 °C. The resulting heterogeneous mixture was filtered through a plug of celite® (25 mL of Et_2O eluent) and the filtrate was diluted with deionized water (25 mL). The layers were separated and the aqueous layer was extracted with Et_2O (2 x 50 mL). The organic layers were combined, dried over $MgSO_4$,

and concentrated under reduced pressure (~100 mbar, at room temperature) to afford the corresponding alcohol, which was used in the subsequent step without further purification.

To a solution of the crude alcohol in CH_2Cl_2 (20 mL) was added pyridine (1.93 mL, 24.0 mmol, 3.0 equiv from **4.56**). The reaction was cooled to 0 °C. After stirring for 5 min, methyl chloroformate (1.24 mL, 16.0 mmol, 2.0 equiv from **4.56**) was added dropwise over 1 min. The reaction was allowed to warm to room temperature. After stirring for 12 h, the reaction mixture was poured into brine (25 mL) and diluted with Et_2O (25 mL). The layers were separated and the aqueous layer was extracted with Et_2O (2 x 50 mL). The organic layers were combined, washed with 1 N HCl (25 mL), dried over $MgSO_4$, and concentrated under reduced pressure. The crude mixture was purified via flash chromatography (9:1 Hexanes:EtOAc → 5:1 Hexanes:EtOAc) to afford carbonate **4.57** (1.14 g, 71% yield, two steps) as a colorless oil. Carbonate **4.57**: R_f 0.73 (1:1 Hexanes:EtOAc); ^{1}H NMR (500 MHz, $CDCl_3$): δ 4.66 (s, 2H), 3.78 (s, 3H), 3.67 (app ddd, J = 13.2, 7.7, 5.5, 4H), 2.39 (t, J = 5.5, 2H), 2.32 (t, J = 5.5, 2H) 1.75 (s, 3H); ^{13}C NMR (125 MHz, $CDCl_3$): δ 156.1, 135.6, 121.5, 68.9–68.2 (2 carbons), 54.9, 31.3 & 31.1 (1 carbon), 16.3; IR (film): 2958, 2847, 1743, 1442, 1251 cm^{-1}; HRMS–APCI (m/z) $[M + H]^+$ calcd for $C_{10}H_{17}O_7^+$, 201.11214; found 201.11059.

*Note: The data for carbonate **4.57** represents empirically observed chemical shifts from the ^{13}C NMR spectrum, presumably due to the oxygen-containing heterocycle.*

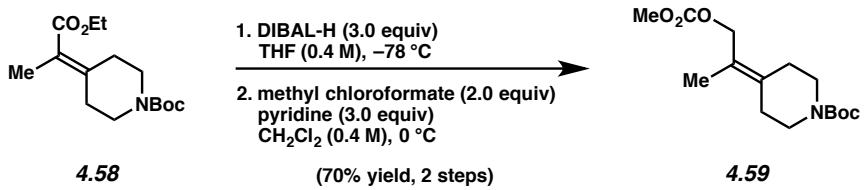

4.58 (70% yield, 2 steps) *4.59*

Carbonate 4.59. To a solution of ester **4.58**[34] (1.60 g, 5.65 mmol, 1.0 equiv) in THF (14 mL) at 0 °C was added DIBAL-H (11.3 mL of a 1.0 M solution in THF, 11.3 mmol, 2.0 equiv) dropwise over 5 min. The reaction was stirred for 3 h, and allowed to warm to room temperature, at which point additional DIBAL-H (5.65 mL of a 1.0 M solution in THF, 5.65 mmol, 1.0 equiv) was added. After stirring for an additional hour, the reaction mixture was poured into water (50 mL) and diluted with Et_2O (50 mL). The resulting heterogeneous mixture was filtered through a plug of celite® (100 mL of Et_2O eluent). The layers of the resulting filtrate were separated and the aqueous layer was extracted with Et_2O (1 x 50 mL). The organic layers were combined, dried over $MgSO_4$, and concentrated under reduced pressure to afford the corresponding alcohol, which was used in the subsequent step without further purification.

To a solution of the crude alcohol in CH_2Cl_2 (14 mL) was added pyridine (2.57 mL, 31.9 mmol, 3.0 equiv from **4.58**). The reaction was cooled to 0 °C. After stirring for 5 min, methyl chloroformate (0.87 mL, 11.3 mmol, 2.0 equiv from **4.58**) was added dropwise over 1 min. The reaction was allowed to warm to room temperature. After stirring for 1 h, the reaction mixture was poured into brine (50 mL) and diluted with CH_2Cl_2 (50 mL). The layers were separated and the aqueous layer was extracted with CH_2Cl_2 (2 x 50 mL). The organic layers were combined, washed with 1 N HCl (50 mL), dried over $MgSO_4$, and concentrated under reduced pressure. The crude mixture was purified via flash chromatography (9:1 Hexanes:EtOAc) to afford carbonate **4.59** (1.18 g, 70% yield, two steps) as a colorless oil. Carbonate **4.59**: R_f 0.78 (1:1 Hexanes:EtOAc); ^1H NMR (500 MHz, $CDCl_3$): δ 4.66 (s, 2H), 3.77 (s, 3H), 3.40 (app q, J = 6.8, 4H), 2.35 (t, J = 5.6,

2H), 2.28 (t, J = 5.6, 2H) 1.75 (s, 3H), 1.45 (s, 9H); ^{13}C NMR (125 MHz, $CDCl_3$): δ 156.0, 154.9, 136.2, 122.3, 79.6, 68.3, 54.9, 29.9, 29.5, 28.6, 16.5; IR (film): 2974, 1745, 1691, 1441, 1420, 1365, 1250, 1228, 1164 cm^{-1}; HRMS–APCI (m/z) $[M + H]^+$ calcd for $C_{15}H_{26}NO_5^+$, 300.18055; found 300.17829.

4.7.2.1.4 Reductive Cross Coupling of Imides and Carbonates

Representative Procedure (synthesis of imide 4.5 is used as an example).

Reductive couplings were performed using a modification of the procedure reported by Gong and co-workers for the coupling of aryl bromides with substituted allylic acetates.[14c]

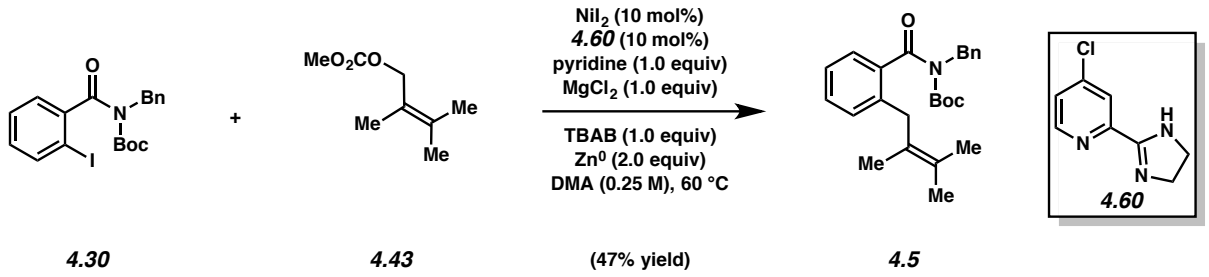

Imide 4.5. A scintillation vial containing imide **4.30** (219 mg, 0.50 mmol, 1.0 equiv), ligand **4.60** (9.1 mg, 0.050 mmol, 10 mol%), and a magnetic stir bar was sequentially charged with NiI_2 (15.6 mg, 0.050 mmol, 10 mol%), $MgCl_2$ (47.6 mg, 0.50 mmol, 1.0 equiv), TBAB (161 mg, 0.50 mmol, 1.0 equiv) and Zn^0 (65.4 mg, 1.0 mmol, 2.0 equiv) in the glovebox. The vial was removed from the glovebox, at which point DMA (2.0 mL), pyridine (40 μL, 0.5 mmol, 1.0 equiv), and carbonate **4.43** (158 mg, 1.0 mmol, 2.0 equiv) were added. The vial was quickly sealed with a teflon-lined screw cap, and stirred at 60 °C for 14 h. After cooling to room temperature, the mixture was passed through a column of silica gel and flushed (5:2 Hexanes:EtOAc) until TLC indicated the desired product had eluted. The volatiles were removed under reduced pressure and the crude mixture was

further purified by flash chromatography (99:1 Hexanes:EtOAc) to yield imide **4.5** (92 mg, 47% yield) as a white solid. Spectral data matched what is reported in Section 4.7.2.1.1.

Any modifications of the conditions shown in the representative procedures above are specified in the following schemes.

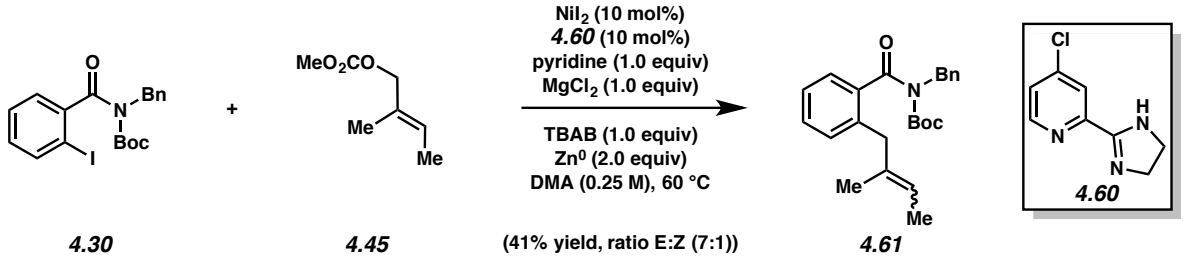

Imide 4.61. Following the representative procedure with iodo-imide **4.30** (218 mg, 0.5 mmol, 1.0 equiv), purification by flash chromatography (9:1 Hexanes:EtOAc) yielded **4.61** as an inseparable mixture of olefin isomers (79 mg, 41% yield, 7:1 isomer ratio E:Z) and as a colorless oil. Configurational isomers of imide **4.61** were analyzed as a mixture: **4.61** (**Major (*E*)-isomer**): ^{1}H NMR (500 MHz, $CDCl_3$): δ 7.45–7.41 (m, 2H), 7.36–7.32 (m, 2H), 7.31–7.26 (m, 1H), 7.21–7.12 (m, 2H), 5.24 (q, J = 6.8, 1H), 5.01 (s, 2H), 3.34 (s, 2H), 1.57 (d, J = 6.8, 3H), 1.53 (s, 3H), 1.10 (s, 9H); ^{13}C NMR (125 MHz, $CDCl_3$): δ 172.5, 153.0, 138.6, 138.1, 137.5, 134.2, 130.0, 129.4, 127.5, 126.4, 125.8, 121.7, 83.4, 48.1, 42.8, 27.6, 16.0, 13.7; **4.61** (**Minor (*Z*)-isomer**): ^{1}H NMR (500 MHz, $CDCl_3$): (20 of 29 signals observed) δ 5.45 (q, J = 6.8, 1H), 5.07–5.03 (m, 1H), 4.90–4.85 (m, 1H), 3.41 (s, 2H), 1.63 (d, J = 6.8, 3H), 1.61 (s, 3H), 1.11 (s, 9H); ^{13}C NMR (125 MHz, $CDCl_3$): δ 172.6, 153.1, 138.7, 138.0, 137.0, 133.8, 129.7, 129.6, 127.6, 126.1, 125.7, 121.9, 83.5, 48.1, 34.2, 27.7, 23.8, 13.8; Imide **4.61** (**mixture**): R_f 0.62 (4:1 Hexanes:EtOAc) IR (film): 2979, 1726, 1669, 1228, 1137, 739 cm^{-1}; HRMS–APCI (m/z) $[M + H]^+$ calcd for $C_{24}H_{29}NO_3$ 380.22202; found 380.22186.

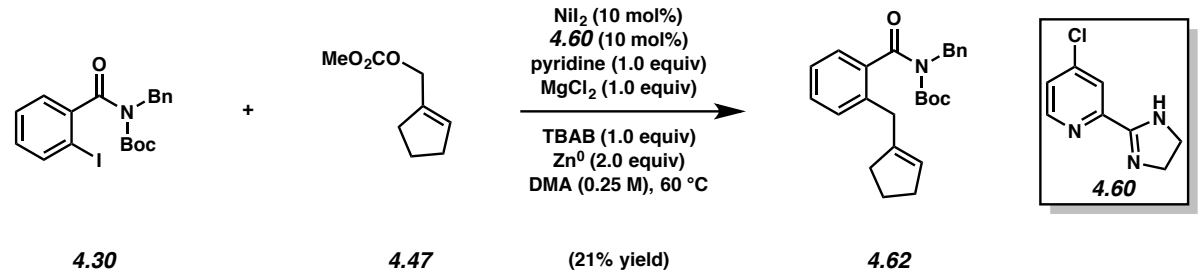

4.30 *4.47* (21% yield) *4.62*

Imide 4.62. Following the representative procedure with iodo-imide **4.30** (874 mg, 2.0 mmol, 1.0 equiv), imide **4.62** (165 mg, 21% yield) was obtained as a colorless oil. Imide **4.62**: R_f 0.48 (9:1 Hexanes:EtOAc); ^{1}H NMR (500 MHz, $CDCl_3$): δ 7.43 (d, J = 7.4, 2H), 7.35–7.24 (m, 4H), 7.22–7.13 (m, 3H), 5.32 (s, 1H), 5.01 (s, 2H), 3.45 (s, 2H), 2.32–2.24 (m, 2H), 2.20–2.14 (m, 2H), 1.83 (quint, J = 7.7, 2H), 1.10 (s, 9H); ^{13}C NMR (125 MHz, $CDCl_3$): δ 172.4, 152.9, 142.6, 138.2, 138.0, 137.3, 130.1, 129.4, 128.5, 128.4, 127.5, 126.7, 126.4, 125.7, 83.3, 48.1, 35.1, 34.9, 32.6, 27.5, 23.6; IR (film): 2933, 1728, 1671, 1369, 1334, 1229, 1139 cm^{-1}; HRMS–APCI (m/z) $[M + H]^+$ calcd for $C_{25}H_{30}NO_3^+$, 392.22202; found 392.21992.

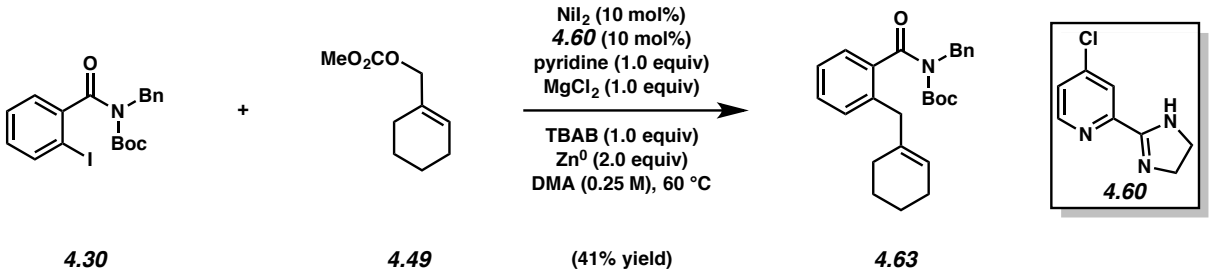

4.30 *4.49* (41% yield) *4.63*

Imide 4.63. Following the representative procedure with iodo-imide **4.30** (1.09 g, 2.5 mmol, 1.0 equiv), imide **4.63** (417 mg, 41% yield) was obtained as a colorless oil. Imide **4.63**: R_f 0.66 (3:1 Hexanes:EtOAc); ^{1}H NMR (500 MHz, $CDCl_3$): δ 7.43 (d, J = 7.1, 2H), 7.33 (t, J = 7.6, 2H), 7.31–7.24 (m, 2H), 7.23–7.13 (m, 3H), 5.43 (m, 1H), 5.01 (s, 2H), 3.31 (s, 2H), 1.98 (s, 2H), 1.83 (s, 2H), 1.55 (m, 4H), 1.11 (s, 9H); ^{13}C NMR (125 MHz, $CDCl_3$): δ 172.5, 152.9, 138.4, 138.0, 137.4, 136.2, 129.9, 129.4, 128.6, 128.4, 127.5, 126.4, 125.7, 124.2, 83.3, 48.1, 41.4, 28.3, 27.5, 25.5,

23.0, 22.4; IR (film): 2929, 1728, 1671, 1334, 1230, 1140 cm^{-1}; HRMS–APCI (m/z) $[M + H]^+$ calcd for $C_{26}H_{32}NO_3^+$, 406.23767; found 406.23493.

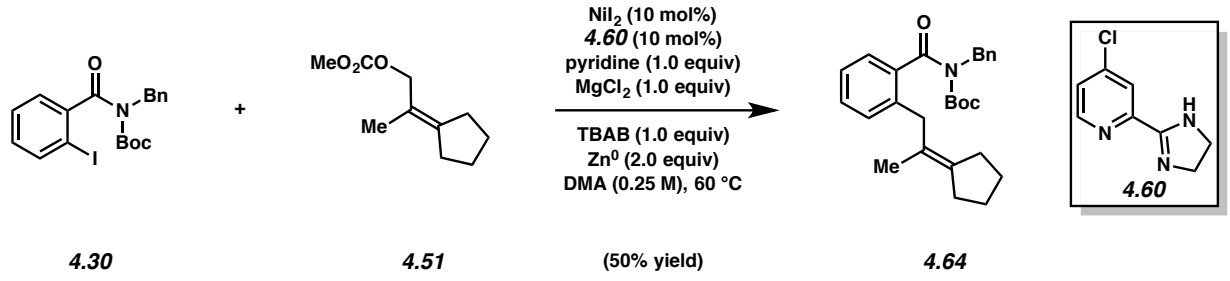

Imide 4.64. Following the representative procedure with iodo-imide **4.30** (874 mg, 2.0 mmol), imide **4.64** (418 mg, 50% yield) was obtained as a colorless oil. Imide **4.64**: R_f 0.45 (9:1 Hexanes:EtOAc); ^{1}H NMR (500 MHz, $CDCl_3$): δ 7.44 (d, J = 7.7, 2H), 7.33 (t, J = 7.2, 2H), 7.31–7.25 (m, 2H), 7.18–7.10 (m, 3H), 5.03 (s, 2H), 3.39 (s, 2H), 2.25 (m, 4H), 1.67 (m, 4H), 1.55 (m, 3H), 1.10 (s, 9H); ^{13}C NMR (125 MHz, $CDCl_3$): δ 172.6, 153.0, 139.7, 138.7, 138.0, 137.5, 129.5, 128.59, 128.57, 128.4, 127.5, 126.1, 125.5, 122.9, 83.4, 48.0, 38.1, 31.0, 30.9, 27.5, 27.2, 27.0, 19.3 ; IR (film): 2938, 1729, 1672, 1335, 1229, 1139 cm^{-1}; HRMS–APCI (m/z) $[M + H]^+$ calcd for $C_{27}H_{34}NO_3^+$, 420.25332; found 420.25300.

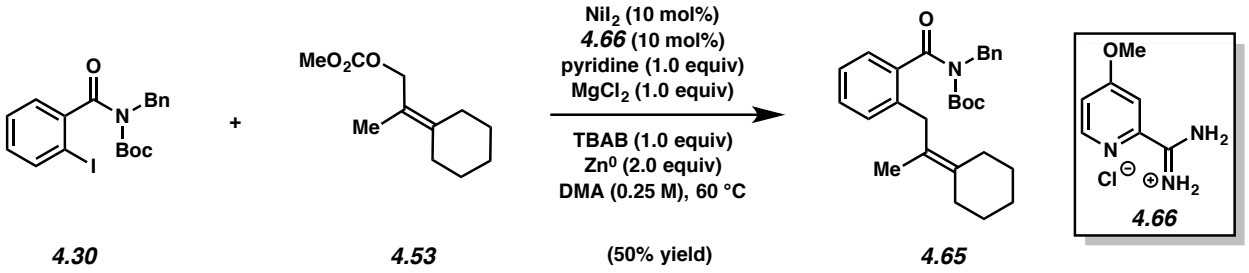

Imide 4.65. Following the representative procedure with iodo-imide **4.30** (0.44 g, 1.0 mmol, 1.0 equiv), imide **4.65** (0.22 g, 50% yield) was obtained as a colorless oil. Imide **4.65**: R_f 0.45 (9:1 Hexanes:EtOAc); ^{1}H NMR (500 MHz, $CDCl_3$): δ 7.45–7.42 (m, 2H), 7.46–7.43 (m, 2H), 7.36–

7.32 (m, 2H), 7.18–7.10 (m, 3H), 5.04 (s, 2H), 3.44 (s, 2H), 2.25 (t, J = 5.8, 2H), 2.17 (t, J = 5.8, 2H), 1.60 (s, 3H), 1.59–1.54 (m, 4H), 1.52–1.46 (m, 2H), 1.10 (s, 9H); ^{13}C NMR (125 MHz, $CDCl_3$): δ 172.6, 153.0, 138.7, 138.0, 137.8, 135.9, 129.5, 128.6, 128.4, 128.3, 127.5, 125.9, 125.4, 121.8, 83.4, 48.0, 36.2, 30.84, 30.78, 28.5, 28.3, 27.5, 27.1, 18.4; IR (film): 2922, 1728, 1368, 1137, 740, 672 cm^{-1}; HRMS–APCI (m/z) $[M + H]^+$ calcd for $C_{28}H_{36}NO_3^+$, 434.26897; found 434.26866.

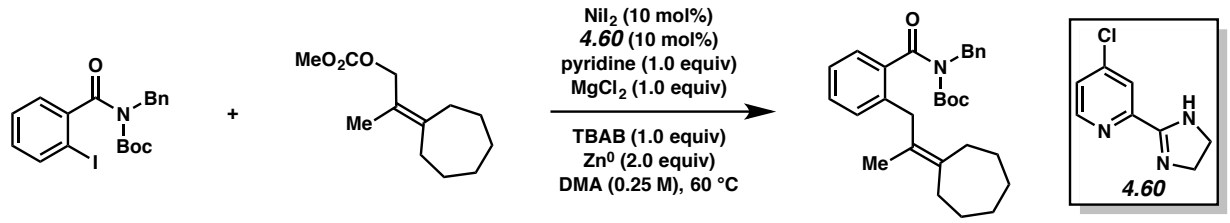

4.30 ***4.55*** **(19% yield)** ***4.67***

Imide 4.67. Following the representative procedure with iodo-imide **4.30** (874 mg, 2.0 mmol, 1.0 equiv), purification by flash chromatography (199:1 Hexanes:EtOAc) yielded imide **4.67** (172 mg, 19% yield) was obtained as a colorless oil. Imide **4.67**: R_f 0.50 (9:1 Hexanes:EtOAc); ^{1}H NMR (500 MHz, $CDCl_3$): δ 7.44 (d, J = 7.8, 2H), 7.33 (t, J = 7.2, 2H), 7.31–7.25 (m, 2H), 7.18–7.10 (m, 3H), 5.04 (s, 2H), 3.42 (s, 2H), 2.31 (t, J = 5.9, 2H), 2.25 (t, J = 5.9, 2H), 1.65–1.59 (m, 2H), 1.58 (s, 3H), 1.57–1.47 (m, 6H), 1.11 (s, 9H); ^{13}C NMR (125 MHz, $CDCl_3$): δ 172.6, 153.0, 138.7, 138.0, 137.7, 137.0, 129.5, 128.6, 128.4, 128.2, 127.5, 126.0, 125.4, 125.3, 83.4, 48.0, 36.4, 32.0, 31.8, 29.4, 29.0, 28.1, 27.8, 27.5, 18.6; IR (film): 2921, 1730, 1673, 1335, 1229, 1138 cm^{-1}; HRMS–APCI (m/z) $[M + H]^+$ calcd for $C_{29}H_{38}NO_3^+$, 448.28462; found 448.28241.

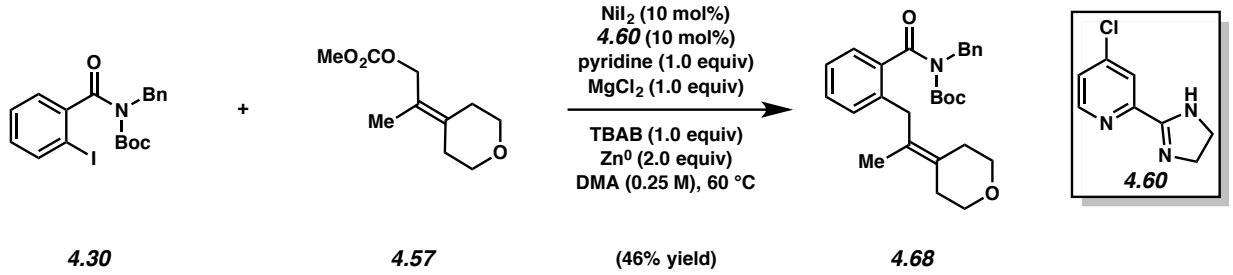

4.30 *4.57* (46% yield) *4.68*

Imide 4.68. After following the representative procedure with iodo-imide **4.30** (1.16 g, 2.66 mmol, 1.0 equiv), the crude reaction mixture was vigorously stirred with 1:1 1 N NaOH/THF (26 mL) solution for 4 h to remove residual carbonate **4.57**. Purification by flash chromatography (49:1 Hexanes:EtOAc → 9:1 Hexanes:EtOAc) afforded imide **4.68** (536 mg, 46% yield) as a colorless oil. Imide **4.68**: R_f 0.49 (3:1 Hexanes:EtOAc); ^{1}H NMR (500 MHz, $CDCl_3$): δ 7.43 (d, *J* = 7.7, 2H), 7.34 (t, *J* = 7.7, 2H), 7.29 (dt, *J* = 7.7, 1.3, 2H), 7.17 (t, *J* = 7.7, 1H), 7.13 (t, *J* = 8.0, 2H), 5.03 (s, 2H), 3.71 (d, *J* = 5.5, 2H), 3.64 (d, *J* = 5.5, 2H), 3.45 (s, 2H), 2.38 (d, *J* = 5.5, 2H), 2.30 (d, *J* = 5.5, 2H), 1.63 (s, 3H), 1.11 (s, 9H); ^{13}C NMR (125 MHz, $CDCl_3$): δ 172.5, 153.0, 138.6, 137.9, 137.3, 130.3, 129.6, 128.6, 128.4, 128.2, 127.6, 126.0, 125.6, 124.5, 83.5, 69.2 & 69.1 (1 carbon), 48.1, 35.9, 31.3 & 31.2 (1 carbon), 27.6, 18.3; IR (film): 2962, 2845, 1728, 1669, 1369, 1333, 1228, 1137, 1101 cm^{-1}; HRMS–APCI (m/z) $[M + H]^+$ calcd for $C_{27}H_{34}NO_4^+$, 436.24824; found 436.24824.

*Note: The data for imide **4.68** represents empirically observed chemical shifts from the ^{13}C NMR spectrum, presumably due to the oxygen-containing heterocycle.*

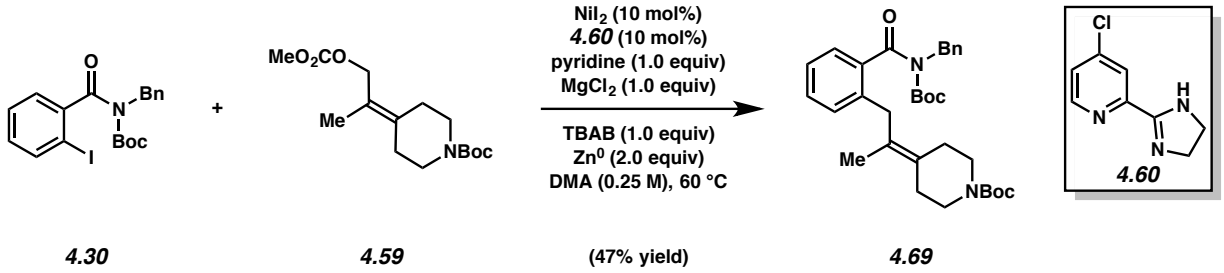

4.30 *4.59* (47% yield) *4.69*

Imide 4.69. After following the representative procedure with iodo-imide **4.30** (1.08 g, 2.47 mmol, 1.0 equiv), the crude reaction mixture was vigorously stirred with 2:1 1 N NaOH/THF (30 mL) solution for 22 h to remove residual carbonate **4.59**. Purification by flash chromatography (199:1 Benzene:EtOAc → 24:1 Benzene:EtOAc) afforded imide **4.69** (622 mg, 47% yield) as a colorless oil. Imide **4.69**: R_f 0.49 (3:1 Hexanes:EtOAc); ^{1}H NMR (500 MHz, $CDCl_3$): δ 7.44 (d, J = 7.9, 2H), 7.34 (tt, J = 7.6, 1.4, 2H), 7.32–7.27 (m, 2H), 7.16 (td, J = 7.6, 1.0, 1H), 7.11 (td, J = 7.4, 1.3, 2H), 5.03 (s, 2H), 3.45 (s, 4H), 3.37 (s, 2H), 2.34 (t, J = 5.6, 2H), 2.27 (s, 2H), 1.63 (s, 3H), 1.47 (s, 9H) 1.11 (s, 9H); ^{13}C NMR (125 MHz, $CDCl_3$): δ 172.5, 155.1, 153.0, 138.6, 137.9, 137.2, 130.9, 129.6, 128.6, 128.4, 128.2, 127.6, 126.0, 125.7, 125.3, 83.5, 79.5, 48.1, 45.0 & 44.4 (1 carbon), 36.2, 29.8 & 29.7 (1 carbon), 28.6, 27.6, 18.5; IR (film): 2976, 1730, 1692, 1672, 1367, 1231, 1164, 1141 cm^{-1}; HRMS–APCI (m/z) $[M + H]^+$ calcd for $C_{32}H_{43}N_2O_5^+$, 535.31665; found 535.31392.

Note: The data for imide **4.69** *represents empirically observed chemical shifts from the ^{13}C NMR spectrum, presumably due to the nitrogen-containing heterocycle.*

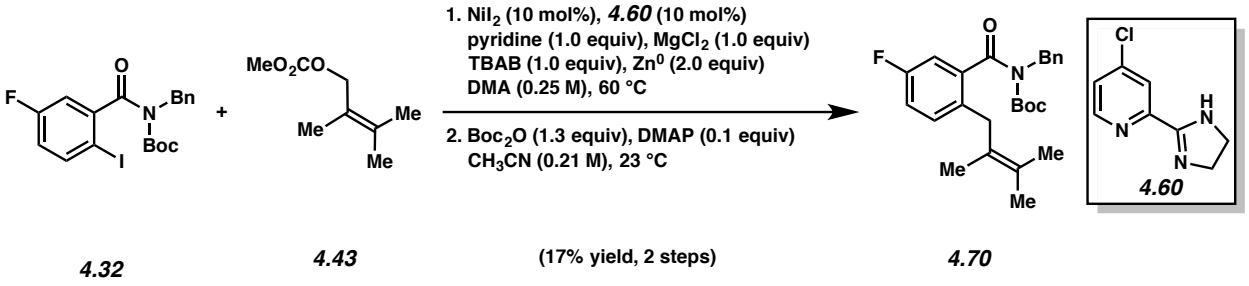

Imide 4.70. Following the representative procedure with iodo-imide **4.32** (1.82g, 4.0 mmol) led to appreciable amounts of des-Boc coupled product. As such, the mixture was re-subjected to the general conditions used to install a boc group described in the synthesis of **4.5** (Section 4.7.2.1.1). Purification by flash chromatography (99:1 Pentane:Et_2O → 49:1 Pentane:Et_2O) afforded imide **4.70** (275 mg, 17% yield, two steps) as an off-white oil. Imide **4.70**: R_f 0.64 (3:1 Hexanes:EtOAc); ^{1}H NMR (500 MHz, $CDCl_3$): δ 7.42 (d, J = 7.8, 2H), 7.34 (tt, J = 7.2, 1.4, 2H), 7.28 (tt, J = 7.4, 1.4, 1H), 7.06 (dd, J = 8.6, 5.6, 1H), 6.98 (dt, J = 8.4, 2.7, 1H), 6.84 (dd, J = 8.6, 2.7, 1H) 5.02 (s, 2H), 3.34 (s, 2H), 1.74 (s, 3H), 1.68 (s, 3H), 1.56 (s, 3H), 1.16 (s, 9H); ^{13}C NMR (125 MHz, $CDCl_3$): δ 171.2 (d, J = 2.4), 160.7 (d, J = 246), 152.6, 139.9 (d, J = 6.8), 137.7, 133.0 (d, J = 3.3), 130.0 (d, J = 7.6), 128.6, 128.3, 127.6, 127.5, 125.2, 116.1 (d, J = 21), 113.0 (d, J = 23), 83.8, 48.0, 36.1, 27.6, 20.8, 20.7, 18.7; ^{19}F NMR (376 MHz, $CDCl_3$): δ –117.9, (s, 1F); IR (film): 2982, 2920, 1734, 1673, 1369, 1331, 1229, 1149 cm^{-1}; HRMS–APCI (m/z) $[M + H]^+$ calcd for $C_{25}H_{31}FNO_3^+$, 412.22825; found 412.22781.

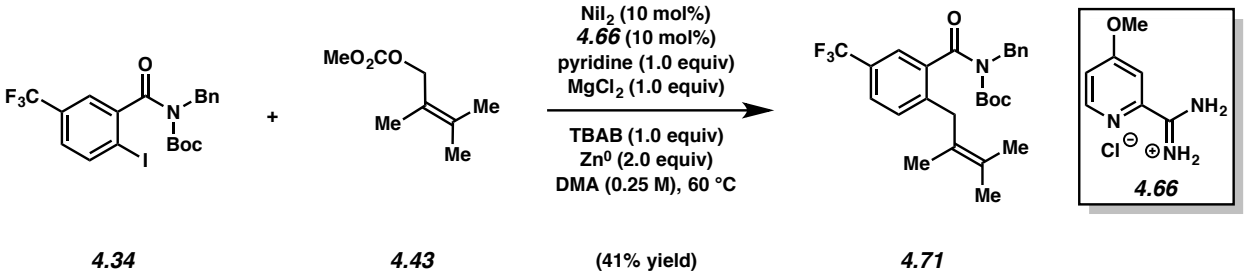

4.34 *4.43* (41% yield) *4.71*

Imide 4.71. Following the representative procedure with iodo-imide **4.34** (455 mg, 0.9 mmol), purification by flash chromatography (199:1 Benzene:EtOAc) yielded imide **4.71** (169 mg, 41% yield) as a yellow oil. Imide **4.71**: R_f 0.75 (3:1 Hexanes:EtOAc); ^{1}H NMR (500 MHz, $CDCl_3$): δ 7.54 (dd, *J* = 8.2, 1.4, 1H), 7.43 (d, *J* = 8.0, 2H), 7.37 (d, *J* = 1.5, 1H), 7.35 (tt, *J* = 7.8, 1.4, 2H), 7.29 (tt, *J* = 7.4, 1.3, 1H), 7.24 (d, *J* = 8.1, 1H) 5.05 (s, 2H), 3.44 (s, 2H), 1.76 (s, 3H), 1.69 (s, 3H), 1.58 (s, 3H), 1.12 (s, 9H); ^{13}C NMR (125 MHz, $CDCl_3$): δ 171.2, 152.4, 141.7, 139.3, 137.6, 128.9, 128.7, 128.4 128.3, 128.2, 127.7, 125.9 (q, *J* = 3.7), 124.4, 124.1 (q, *J* = 274), 122.8 (q, *J* = 3.7), 84.0, 48.1, 36.9, 27.5, 20.78, 20.75, 18.9; ^{19}F NMR (376 MHz, $CDCl_3$): δ –62.4, (s, 3F); IR (film): 2983, 1736, 1672, 1318, 1141, 1123 cm^{-1}; HRMS–APCI (m/z) $[M + H]^+$ calcd for $C_{26}H_{31}F_3NO_3^+$, 462.22505; found 462.22240.

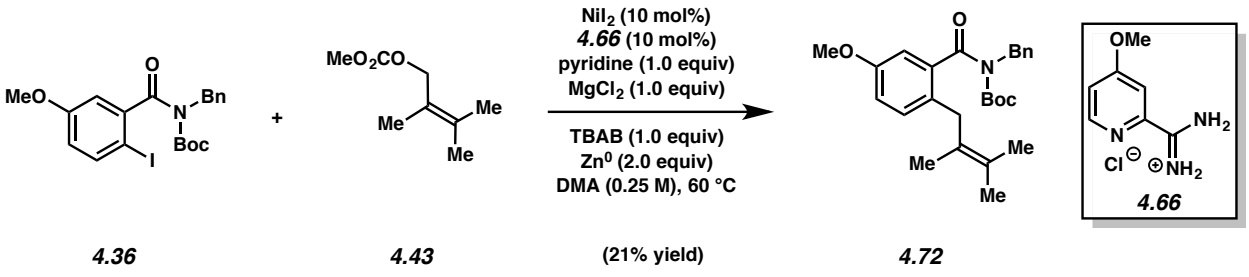

4.36 *4.43* (21% yield) *4.72*

Imide 4.72. Following the representative procedure with iodo-imide **4.36** (0.42 g, 0.9 mmol), purification by flash chromatography (99:1 Hexanes:EtOAc) yielded imide **4.72** (79 mg, 21% yield) as a colorless oil. Imide **4.72**: R_f 0.52 (4:1 Hexanes:EtOAc); ^{1}H NMR (500 MHz, $CDCl_3$): δ 7.45–7.42 (m, 2H), 7.36–7.31 (m, 2H), 7.29–7.25 (m, 1H), 7.00 (d, *J* = 8.6, 1H), 6.84 (dd, *J* =

8.6, 2.8, 1H), 6.66 (d, J = 2.8, 1H), 5.02 (s, 2H), 3.74 (s, 3H), 3.33 (s, 2H), 1.73 (s, 3H), 1.69 (s, 3H), 1.56 (s, 3H), 1.13 (s, 9H); ^{13}C NMR (125 MHz, $CDCl_3$): δ 172.4, 157.5, 153.0, 139.4, 138.0, 129.60, 129.57, 128.7, 128.5, 127.6, 127.0, 125.8, 115.3, 111.5, 83.5, 55.6, 48.1, 36.0, 27.7, 20.84, 20.81, 18.8; IR (film): 2980, 1730, 1672, 1142, 1039, 851 cm^{-1}; HRMS–APCI (m/z) $[M + H]^+$ calcd for $C_{26}H_{34}NO_4^+$, 424.24824; found 424.24803.

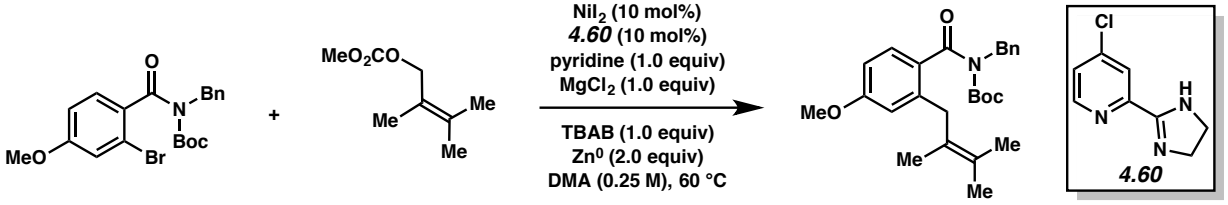

Imide 4.73: Following the representative procedure with bromo-imide **4.38** (0.84 g, 2.0 mmol), purification by flash chromatography (98:2 Hexanes:EtOAc) yielded imide **4.73** (0.24 g, 28% yield) as a colorless oil. Imide **4.73**: R_f 0.40 (9:1 Hexanes:EtOAc); ^{1}H NMR (500 MHz, $CDCl_3$): δ 7.44–7.42 (m, 2H), 7.35–7.32 (m, 2H), 7.28–7.24 (m, 1H), 7.13–7.10 (m, 1H), 6.69–6.66 (m, 2H), 5.00 (s, 2H), 3.78 (s, 3H), 3.47 (s, 2H), 1.75 (s, 3H), 1.70 (s, 3H), 1.59 (s, 3H), 1.15 (s, 9H); ^{13}C NMR (125 MHz, $CDCl_3$): (20 of 21 signals observed) δ 172.5, 160.9, 153.3, 140.7, 138.1, 131.0, 128.6, 128.34, 128.30, 127.4, 125.3, 114.7, 109.7, 83.0, 55.4, 48.4, 37.0, 27.7, 20.8, 18.9; IR (film): 2979, 1726, 1328, 1227, 966, 626 cm^{-1}; HRMS–APCI (m/z) $[M + H]^+$ calcd for $C_{26}H_{34}NO_4^+$, 424.24824; found 424.24858.

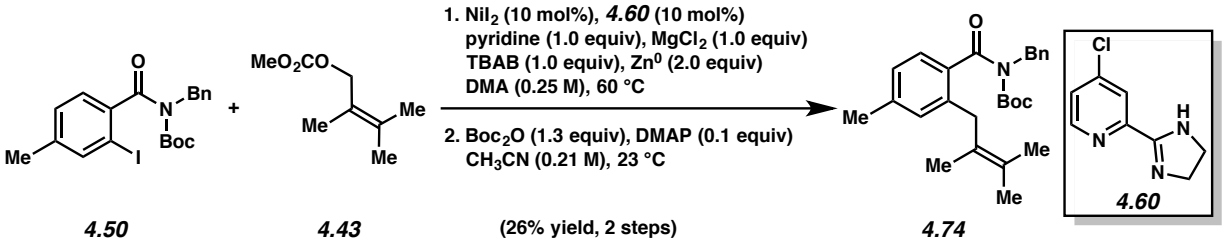

Imide 4.74. Following the representative procedure with iodo-imide **4.50** (2.1 g, 4.5 mmol) led to appreciable amounts of des-Boc coupled product. As such, the mixture was re-subjected to the general conditions used to install a boc group described in the synthesis of **4.5** (Section 4.7.2.1.1). Purification by flash chromatography (9:1 Hexanes:EtOAc) afforded imide **4.74** (0.48 g, 26% yield, two steps) as a colorless oil. Imide **4.74**: R_f 0.51 (9:1 Hexanes:EtOAc); ^{1}H NMR (500 MHz, $CDCl_3$): δ 7.42–7.39 (m, 2H), 7.33–7.29 (m, 2H), 7.27–7.22 (m, 1H), 7.01 (d, J = 7.7, 1H), 6.94 (d, J = 7.7, 1H), 6.88 (s, 1H), 5.00 (s, 2H), 3.41 (s, 2H), 2.30 (s, 3H), 1.73 (s, 3H), 1.69 (s, 3H), 1.56 (s, 3H), 1.11 (s, 9H); ^{13}C NMR (125 MHz, $CDCl_3$): δ 172.6, 153.0, 139.4, 137.9, 137.7, 135.5, 129.0, 128.4, 128.1, 127.2, 126.7, 126.1, 125.9, 125.4, 83.0, 47.9, 36.6, 27.4, 21.5, 20.6, 18.6; IR (film): 2980, 1728, 1670, 1229, 1142, 969 cm^{-1}; HRMS–APCI (m/z) $[M + H]^+$ calcd for $C_{26}H_{33}NO_3^+$, 408.25332; found 408.25332.

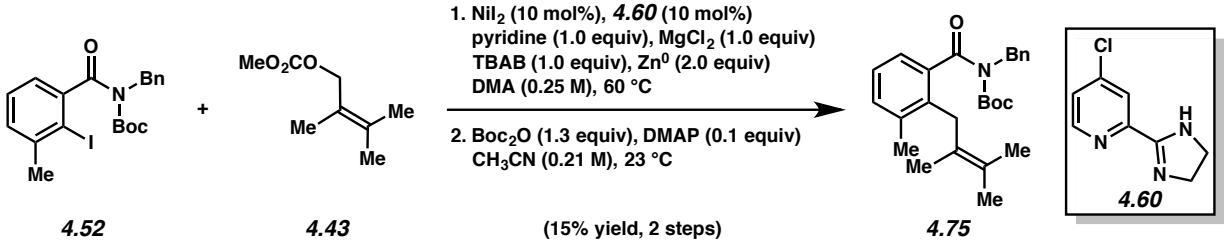

Imide 4.75. Following the representative procedure with iodo-imide **4.52** (0.93 g, 2.0 mmol, 1.0 equiv) led to appreciable amounts of des-Boc coupled product. As such, the mixture was re-subjected to the general conditions used to install a boc group described in the synthesis of **4.5** (Section 4.7.2.1.1). Purification by flash chromatography (9:1 Hexanes:EtOAc) afforded imide

4.75 (102 mg, 15% yield, two steps) as a colorless oil. Imide **4.75**: R_f 0.57 (4:1 Hexanes:EtOAc); ^{1}H NMR (500 MHz, $CDCl_3$): δ 7.42–7.39 (m, 2H), 7.34–7.30 (m, 2H), 7.28–7.24 (m, 1H), 7.13 (d, *J* = 8.0, 1H), 7.06 (t, *J* = 8.0, 1H), 6.95 (d, *J* = 8.0, 1H), 5.00 (s, 2H), 3.43 (br s, 2H), 2.21 (s, 3H), 1.74 (s, 3H), 1.67 (s, 3H), 1.39 (s, 3H), 1.10 (s, 9H); ^{13}C NMR (125 MHz, $CDCl_3$): δ 173.1, 153.0, 139.6, 138.3, 138.2, 136.5, 131.2, 128.6, 128.4, 127.5, 125.7, 125.3, 125.1, 123.8, 83.8, 48.0, 34.8, 27.6, 21.1, 20.7, 19.8, 16.9; IR (film): 2979, 1729, 1674, 1368, 1144, 698 cm^{-1}; HRMS–APCI (m/z) $[M + H]^+$ calcd for $C_{26}H_{34}NO_3^+$, 408.25332; found 408.25311.

4.7.3 Initial Evaluation of Ligand Effects and Reaction Conditions

Representative Procedure for the Nickel-Catalyzed Heck Cyclization of Imides

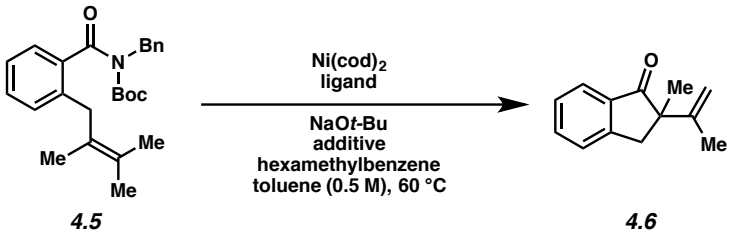

4.5 *4.6*

Indanone 4.6 (Table 4.1). A dram vial containing imide **4.5** (39.3 mg, 0.10 mmol, 1.0 equiv), hexamethylbenzene, and a magnetic stir bar was sequentially charged with the appropriate ligand, $Ni(cod)_2$, and NaO*t*-Bu in a glovebox. Subsequently, toluene (0.20 mL) and the additive (when applicable) were added. The vial was sealed with a Teflon-lined screw cap, removed from the glove box, wrapped with Teflon tape, and stirred at the appropriate temperature for 24 h. After cooling to room temperature, the mixture was diluted with Hexanes (1.0 mL) and filtered through a plug of silica gel (10 mL of EtOAc eluent). The volatiles were removed under reduced pressure, and the yield was determined by ^{1}H NMR analysis with hexamethylbenzene as the internal standard.

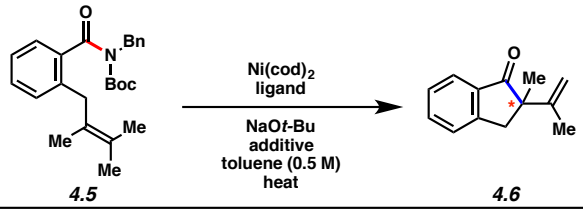

Entry	$Ni(cod)_2$ (loading)	Ligand (loading)	Additive	Temp.	Yield[b]
1	20 mol%	*4.7* (40 mol%)	none	100 °C	0%
2	20 mol%	*4.8* (40 mol%)	none	100 °C	24%
3	20 mol%	*4.9* (40 mol%)	none	100 °C	76%
4	20 mol%	*4.9* (20 mol%)	none	100 °C	67%
5	10 mol%	*4.9* (20 mol%)	none	100 °C	51%
6	15 mol%	*4.9* (30 mol%)	none	100 °C	91%
7	15 mol%	*4.9* (30 mol%)	*t*-amyl alcohol[c]	60 °C	95%

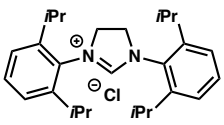

SIPr·HCl (4.7)

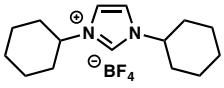

ICy·HBF$_4$ (4.8)

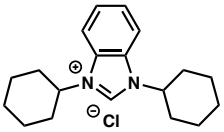

Benz-ICy·HCl (4.9)

4.7.4 Scope of Methodology

Representative Procedure for the Nickel-Catalyzed Heck Cyclization of Imides (synthesis of indanone 4.6 is used as an example).

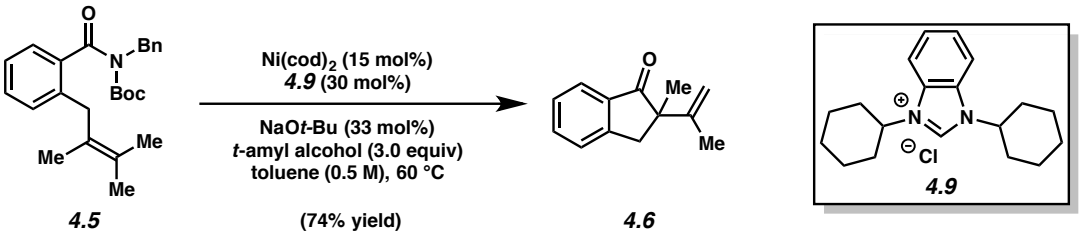

Indanone 4.6 (Table 4.2). A dram vial containing imide **4.5** (39.3 mg, 0.10 mmol, 1.0 equiv) and a magnetic stir bar was sequentially charged with **4.9** (9.6 mg, 0.030 mmol, 30 mol%), $Ni(cod)_2$ (4.1 mg, 0.015 mmol, 15 mol%), and NaO*t*-Bu (3.2 mg, 0.033 mmol, 33 mol%) in a glovebox. Subsequently, toluene (0.20 mL) and then *t*-amyl alcohol (32 µL, 0.30 mmol, 3.0 equiv) were added. The vial was sealed with a Teflon-lined screw cap, removed from the glovebox, and stirred

at 60 °C for 24 h. After cooling to room temperature, the mixture was diluted with hexanes (1.0 mL) and filtered through a plug of silica gel (10 mL of EtOAc eluent). The volatiles were removed under reduced pressure. ^{1}H NMR analysis of the crude reaction mixture indicated a 95% yield (average of two experiments) of ketone **4.6** relative to a hexamethylbenzene external standard. Purification by preparative thin-layer chromatography (3:1 Hexanes:EtOAc) afforded indanone **4.6** (74% yield, average of two experiments) as a colorless oil. The diminished isolated yields of **4.6** can be attributed to the volatility of the neat compound. Indanone **4.6**: R_f 0.59 (3:1 Hexanes:EtOAc); ^{1}H NMR (500 MHz, $CDCl_3$): δ 7.78 (d, J = 7.7, 1H), 7.61 (td, J = 7.5, 1.1, 1H), 7.45 (dt, J = 7.7, 0.9, 1H), 7.38 (td, J = 7.5, 0.7, 1H), 4.95 (m, 2H), 3.33 (d, J = 17.4, 1H), 2.95 (d, J = 17.4, 1H), 1.65 (s, 3H), 1.38 (s, 3H); ^{13}C NMR (125 MHz, $CDCl_3$): δ 209.2, 152.7, 145.9, 135.9, 135.0, 127.6, 126.5, 124.6, 112.1, 54.5, 41.3, 22.7, 19.9; IR (film): 2966, 2928, 1710, 1604, 1464, 1277 cm^{-1}; HRMS–APCI (m/z) $[M + H]^+$ calcd for $C_{13}H_{15}O$, 187.11174; found 187.11130. *Any modifications of the conditions shown in the representative procedure above are specified in the following schemes, which depict all of the results shown in Table 4.2 and Figure 4.2.*

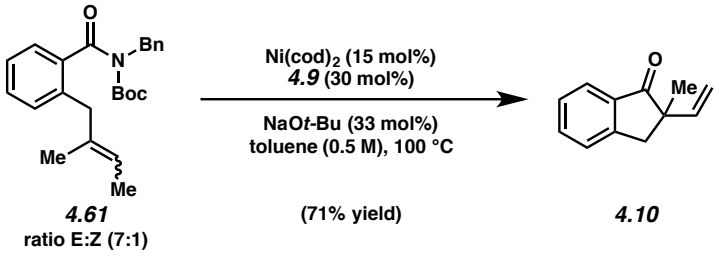

Indanone 4.10 (Table 4.2). Purification by preparative thin-layer chromatography (9:1 Hexanes:EtOAc) afforded indanone **4.10** (71% yield, average of two experiments) as a colorless oil. Indanone **4.10**: R_f 0.59 (4:1 Hexanes:EtOAc); ^{1}H NMR (500 MHz, $CDCl_3$): δ 7.77 (d, J = 7.8, 1H), 7.60 (td, J = 7.5, 1.2, 1H), 7.45 (dt, J = 7.7, 0.9, 1H), 7.38 (t, J = 7.8, 1H), 5.95 (dd, J = 7.5,

10.6, 1H), 5.20–5.11 (m, 2H), 3.32 (d, J = 17.0, 1H), 3.02 (d, J = 17.0, 1H), 1.37 (s, 3H); ^{13}C NMR (125 MHz, $CDCl_3$): δ 208.0, 152.0, 140.6, 135.2, 134.9, 127.5, 126.4, 124.6, 113.9, 52.3, 40.7, 23.2; IR (film): 2966, 1714, 1465, 1279, 738 cm^{-1}; HRMS–APCI (m/z) $[M + H]^+$ calcd for $C_{12}H_{13}O^+$, 173.09609; found 173.09618.

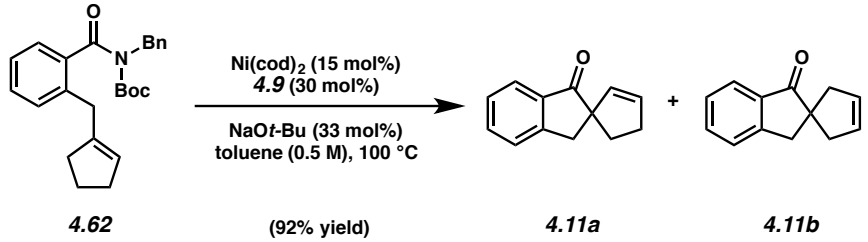

Indanone 4.11 (Table 4.2). Purification by preparative thin-layer chromatography (95:5 Benzene:CH_3CN) afforded indanones **4.11a** and **4.11b** (92% combined yield, average of two experiments) as a ~1:1 mixture of olefin isomers. Iterative purification by preparative thin-layer chromatography (Benzene) afforded analytical samples of indanones **4.11a** and **4.11b** as colorless oils. Spectral data match those previously reported.[35]

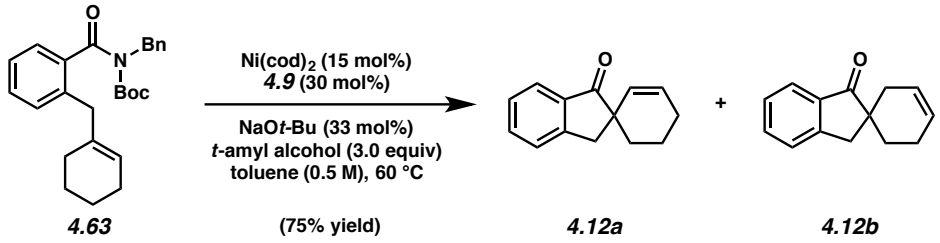

Indanone 4.12 (Table 4.2). Purification by preparative thin-layer chromatography (19:1 Benzene:CH_3CN) afforded indanones **4.12a** and **4.12b** (75% combined yield, average of two experiments) as a ~1:1 mixture of olefin isomers. Iterative purification by preparative thin-layer chromatography (Benzene) afforded analytical samples of **4.12a** and **4.12b** as colorless oils. Indanone **4.12a**: R_f 0.47 (benzene); ^{1}H NMR (500 MHz, $CDCl_3$): δ 7.77 (d, J = 7.6, 1H) 7.59 (td,

J = 7.6, 1.1, 1H), 7.43 (d, J = 7.6, 1H), 7.37 (t, J = 7.6, 1H), 6.00 (ddd, J = 7.5, 4.2, 3.3, 1H), 5.45 (d, J = 9.9, 1H), 3.14 (d, J = 17.1, 1H), 3.07 (d, J = 17.1, 1H), 2.22–2.13 (m, 1H), 2.13–2.04 (m, 1H), 2.04–1.96 (m, 1H), 1.90 (td, J = 11.6, 2.7, 1H), 1.69–1.57 (m, 2H); ^{13}C NMR (125 MHz, $CDCl_3$): δ 210.1, 152.6, 135.9, 135.0, 130.2, 128.3, 127.7, 126.7, 124.7, 51.4, 42.6, 32.8, 24.6, 19.5; IR (film): 3019, 2930, 1712, 1605, 1464, 1282 cm^{-1}; HRMS–APCI (m/z) $[M + H]^+$ calcd for $C_{14}H_{15}O^+$, 199.11174; found 199.11026. Indanone **4.12b**: R_f 0.50 (benzene); ^{1}H NMR (500 MHz, $CDCl_3$): δ 7.77 (d, J = 7.7, 1H) 7.59 (td, J = 7.6, 0.9, 1H), 7.44 (d, J = 7.5, 1H), 7.38 (t, J = 7.5, 1H), 5.79 (m, 2H), 3.06 (d, J = 17.3, 1H), 2.93 (d, J = 17.3, 1H), 2.48 (dquint J = 17.7, 2.5, 1H), 2.30–2.14 (m, 2H), 1.91 (ddd, J = 17.5, 11.1, 6.6, 1H), 1.79 (dt, J = 17.7, 2.5, 1H), 1.50 (dt, J = 17.5, 2.7, 1H); ^{13}C NMR (125 MHz, $CDCl_3$): δ 211.3, 153.0, 136.0, 135.0, 127.6, 126.81, 126.76, 125.3, 124.5, 48.5, 39.2, 34.1, 28.7, 22.8; IR (film): 3026, 2925, 2840, 1712, 1608, 1284 cm^{-1}; HRMS–APCI (m/z) $[M + H]^+$ calcd for $C_{14}H_{15}O^+$, 199.11174; found 199.11028.

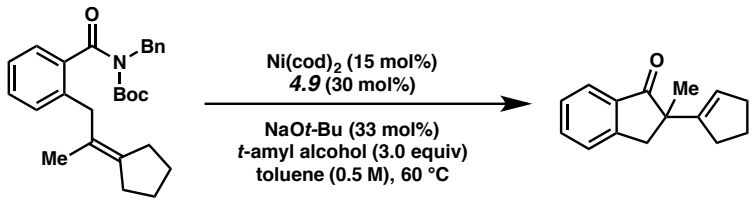

4.64 **(51% yield)** ***4.13***

Indanone 4.13 (Table 4.2). Purification by preparative thin-layer chromatography (97:3 Benzene:CH_3CN) afforded indanone **4.13** (51% yield, average of two experiments) as a colorless oil. Indanone **4.13**: R_f 0.25 (9:1 Hexane:EtOAc); ^{1}H NMR (500 MHz, $CDCl_3$): δ 7.77 (d, J = 7.7, 1H), 7.60 (dt, J = 7.5, 1.2, 1H), 7.44 (td, J = 7.7, 0.9, 1H), 7.37 (dt, J = 7.5, 0.9, 1H), 5.57 (quint, J = 2.2, 1H), 3.32 (d, J = 17.2, 1H), 2.97 (d, J = 17.2, 1H), 2.34–2.20 (m, 3H), 2.15–2.06 (m, 1H), 1.88–1.78 (m, 2H), 1.41 (s, 3H); ^{13}C NMR (125 MHz, $CDCl_3$): δ 208.9, 152.7, 145.5, 135.8, 135.0,

127.6, 126.6, 125.7, 124.7, 51.6, 41.4, 32.4, 32.2, 23.6, 22.9; IR (film): 2956, 2929, 2846, 1713, 1608, 1464, 1280 cm^{-1}; HRMS–APCI (m/z) $[M + H]^+$ calcd for $C_{15}H_{17}O^+$, 213.12739; found 213.12580.

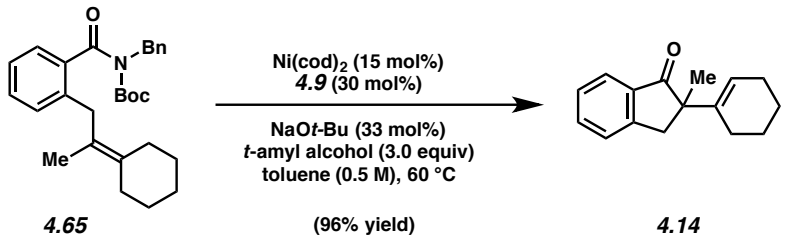

Indanone 4.14 (Table 4.2). Purification by preparative thin-layer chromatography (9:1 Benzene:CH_3CN) afforded indanone **4.14** (96% yield, average of two experiments) as a colorless oil. Indanone **4.14**: R_f 0.48 (9:1 Hexanes:EtOAc); ^1H NMR (500 MHz, $CDCl_3$): δ 7.76 (d, J = 7.6, 1H), 7.59 (td, J = 7.6, 1.2, 1H), 7.43 (dt, J = 7.6, 0.9, 1H), 7.39–7.34 (m, 1H), 5.65 (d, J = 17.6, 1H), 3.29 (d, J = 17.4, 1H), 2.91 (d, J = 17.4, 1H), 2.13–1.99 (m, 2H), 1.92–1.83 (m, 1H), 1.79–1.70 (m, 1H), 1.63–1.50 (m, 4H), 1.33 (s, 3H); ^{13}C NMR (125 MHz, $CDCl_3$): δ 210.2, 153.1, 138.5, 136.3, 134.9, 127.5, 126.6, 124.5, 122.4, 54.6, 41.7, 25.5 (two carbons), 23.1, 22.32, 22.28; IR (film): 2928, 1712, 1464, 1153, 736 cm^{-1}; HRMS–APCI (m/z) $[M + H]^+$ calcd for $C_{16}H_{19}O^+$, 227.14304; found 227.14236.

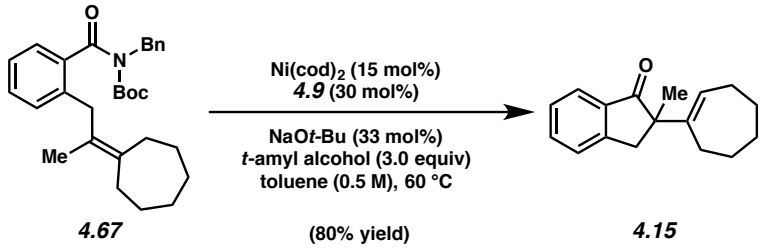

Indanone 4.15 (Table 4.2). Purification by preparative thin-layer chromatography (97:3 Benzene:CH_3CN) afforded indanone **4.15** (80% yield, average of two experiments) as a colorless

oil. Indanone **4.15**: R_f 0.48 (9:1 Hexane:EtOAc); ^{1}H NMR (500 MHz, $CDCl_3$): δ 7.78 (d, *J* = 7.7, 1H), 7.60 (dt, *J* = 7.5, 1.2, 1H), 7.44 (td, *J* = 7.7, 0.9, 1H), 7.37 (dt, *J* = 7.5, 0.9, 1H), 5.86 (t, *J* = 6.8, 1H), 3.26 (d, *J* = 17.4, 1H), 2.89 (d, *J* = 17.4, 1H), 2.22–2.10 (m, 2H), 1.98 (ddd, *J* = 14.9, 9.5, 1.7, 1H), 1.89 (ddd, *J* = 14.9, 8.9, 1.7, 1H), 1.78–1.64 (m, 2H), 1.55–1.45 (m, 2H) 1.45–1.30 (m, 2H), 1.29 (s, 3H); ^{13}C NMR (125 MHz, $CDCl_3$): δ 210.0, 153.1, 145.0, 136.4, 134.9. 127.5, 127.4, 126.7, 124.6, 55.9, 40.9, 33.0, 31.1, 28.5, 27.4, 26.9, 22.7; IR (film): 2920, 2947, 1710, 1607, 1463, 1440, 1750 cm^{-1}; HRMS–APCI (m/z) $[M + H]^+$ calcd for $C_{17}H_{21}O^+$, 241.15869; found 241.15748.

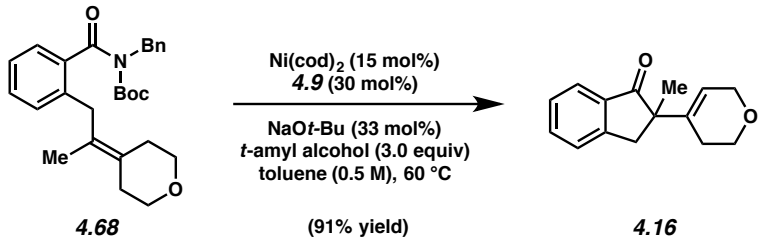

Indanone 4.16 (Table 4.2). Purification by preparative thin-layer chromatography (2:1 Hexanes:EtOAc) afforded indanone **4.16** (91% yield, average of two experiments) as a colorless oil. Indanone **4.16**: R_f 0.34 (3:1 Hexanes:EtOAc); ^{1}H NMR (400 MHz, $CDCl_3$): δ 7.77 (d, *J* = 7.8, 1H), 7.61 (td, *J* = 7.6, 1.3, 1H), 7.45 (dt, *J* = 7.8, 1.0, 1H), 7.39 (t, *J* = 7.6, 1H), 5.65 (app sext, *J* = 1.4, 1H), 4.19 (app tquint, *J* = 16.4, 2.6, 2H), 3.73 (td, *J* = 5.0, 1.1, 2H), 3.34 (d, *J* = 17.3, 1H), 2.95 (d, *J* = 17.3, 1H), 2.12 (m, 1H), 1.86 (m, 1H), 1.37 (s, 3H); ^{13}C NMR (125 MHz, $CDCl_3$): δ 209.0, 152.8, 136.4, 136.0, 135.2, 127.8, 126.6, 124.7, 121.4, 65.9, 64.3, 54.0, 41.0, 25.6, 22.1; IR (film): 2961, 2927, 2850, 1709, 1606, 1464, 1277, 1127 cm^{-1}; HRMS–APCI (m/z) $[M + H]^+$ calcd for $C_{15}H_{17}O_2^+$, 229.12231; found 229.12094.

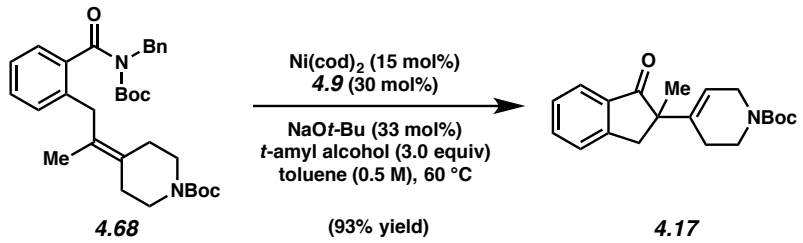

4.68 (93% yield) *4.17*

Indanone 4.17 (Table 4.2). Purification by preparative thin-layer chromatography (2:1 Hexanes:EtOAc) afforded indanone **4.17** (93% yield, average of two experiments) as a colorless oil. Indanone **4.17**: R_f 0.37 (3:1 Hexanes:EtOAc); ^{1}H NMR (400 MHz, $CDCl_3$): δ 7.77 (d *J* = 7.6, 1H) 7.61 (td, *J* = 7.6, 1.1, 1H), 7.45 (d, *J* = 7.7, 1H), 7.39 (t, *J* = 7.7, 1H), 5.61 (br s, 1H), 3.93 (s, 2H), 3.43 (t, *J* = 4.7, 2H), 3.30 (d, *J* = 17.4, 1H), 2.95 (d, *J* = 17.4, 1H), 2.06 (m, 1H), 1.87 (m, 1H), 1.45 (s, 9H), 1.36 (s, 3H); ^{13}C NMR (125 MHz, $CDCl_3$): δ 209.1, 154.9, 152.7, 137.5, 135.9, 135.2, 127.8, 126.6, 124.7, 119.6, 79.7, 54.1, 43.5, 41.0, 39.7, 28.6, 25.7, 22.3; IR (film): 2975, 2931, 1695, 1419, 1365, 1241, 1171 cm^{-1}; HRMS–ESI (m/z) $[M + Na]^+$ calcd for $C_{20}H_{25}NNaO_3^+$, 350.1732; found 350.1736.

*Note: The data for indanone **4.17** represents empirically observed chemical shifts from the ^{13}C NMR spectrum, presumably due to the nitrogen-containing heterocycle.*

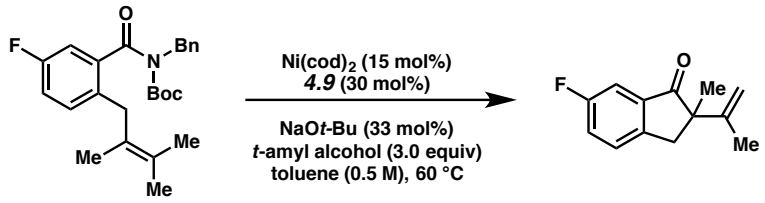

4.70 (53% yield by ^{1}H NMR analysis) *4.18*

Indanone 4.18 (Figure 4.2). ^{1}H NMR analysis of the crude reaction mixture indicated a 53% yield (average of two experiments) of ketone **4.18** relative to a hexamethylbenzene external standard. Purification by preparative thin-layer chromatography (97:3 Benzene: CH_3CN) afforded an analytical sample of **4.18** as an off-white oil. Diminished isolated yields (i.e. <50%) for **4.18** were

observed and can be attributed to the volatility of the neat compound. Indanone **4.18**: R_f 0.59 (3:1 Hexanes:EtOAc); ^{1}H NMR (500 MHz, $CDCl_3$): δ 7.44–7.39 (m, 2H), 7.32 (td, *J* = 8.6, 2.4, 1H), 4.94 (m, 2H), 3.29 (d, *J* = 17.8, 1H), 2.91 (d, *J* = 17.8, 1H), 1.65 (q, *J* = 0.7, 3H), 1.38 (s, 3H); ^{13}C NMR (125 MHz, $CDCl_3$): δ 208.3 (d, *J* = 2.6), 162.5 (d, *J* = 248), 148.1 (d, *J* = 2.1), 145.6, 137.7 (d, *J* = 7.0), 128.0 (d, *J* = 7.9), 122.8 (d, *J* = 24), 112.4, 110.4 (d, *J* = 22), 55.7, 40.8, 22.7, 20.0; ^{19}F NMR (376 MHz, $CDCl_3$): δ –114.3 (s, 1F); IR (film): 2970, 2929, 1712, 1484, 1447, 1263 cm^{-1}; HRMS–APCI (m/z) $[M + H]^+$ calcd for $C_{13}H_{14}FO^+$, 205.10232; found 205.10239.

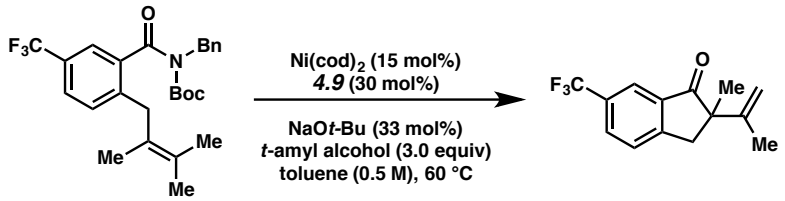

Indanone 4.19 (Figure 4.2). Purification by preparative thin-layer chromatography (4:1 Hexanes:EtOAc) afforded indanone **4.19** (74% yield, average of two experiments) as a yellow oil. Indanone **4.19**: R_f 0.69 (3:1 Hexanes:EtOAc); ^{1}H NMR (500 MHz, $CDCl_3$): δ 8.05 (s, 1H), 7.32 (dd, *J* = 7.9, 1.3, 1H), 7.59 (d, *J* = 7.9, 1H), 4.97 (quint, *J* = 1.1, 1H), 4.95 (s, 1H), 3.40 (d, *J* = 18.0, 1H), 3.02 (d, *J* = 18.0, 1H), 1.67 (q, *J* = 0.7, 3H), 1.40 (s, 3H); ^{13}C NMR (125 MHz, $CDCl_3$): δ 207.9, 156.0, 145.2, 136.4, 131.5 (q, *J* = 3.5), 130.6 (q, *J* = 33), 127.3, 123.9 (q, *J* = 273), 122.0 (d, *J* = 3.9), 112.8, 55.2, 41.4, 22.7, 20.0; ^{19}F NMR (376 MHz, $CDCl_3$): δ –62.5 (s, 3F); IR (film): 2972, 2936, 1722, 1625, 1332, 1257, 1184, 1128 cm^{-1}; HRMS–APCI (m/z) $[M + H]^+$ calcd for $C_{14}H_{14}F_3O^+$, 255.09913; found 255.09744.

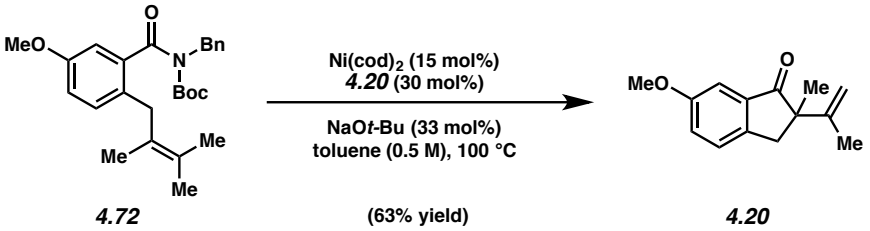

4.72 (63% yield) *4.20*

Indanone 4.20 (Figure 4.2). Purification by preparative thin-layer chromatography (99:1 Benzene:CH_3CN) afforded indanone **4.20** (63% yield, average of two experiments) as a white crystalline solid. Indanone **4.20**: mp: 41–43 ºC; R_f 0.32 (10:1 Hexanes:EtOAc); ^{1}H NMR (500 MHz, $CDCl_3$): δ 7.33 (d, J = 8.0, 1H), 7.23–7.18 (m, 2H), 4.95 (m, 2H), 3.84 (s, 3H), 3.24 (d, J = 17.4, 1H), 2.87 (d, J = 17.4, 1H), 1.64 (s, 3H), 1.37 (s, 3H); ^{13}C NMR (125 MHz, $CDCl_3$): δ 209.2, 159.5, 145.9, 145.5, 137.0, 127.2, 124.5, 112.0, 105.5, 55.6, 40.6, 22.7, 19.8; IR (film): 2964, 1707, 1275, 1280, 894 cm^{-1}; HRMS–APCI (m/z) $[M + H]^+$ calcd for $C_{14}H_{18}O_2^+$, 217.12231; found 217.12123.

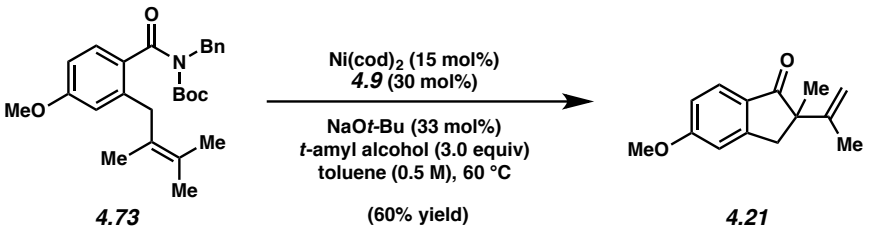

4.73 (60% yield) *4.21*

Indanone 4.21 (Figure 4.2). Purification by preparative thin-layer chromatography (9:1 Hexanes:Et_3N) afforded indanone **4.21** (60% yield, average of two experiments). Spectral data match those previously reported.[11b]

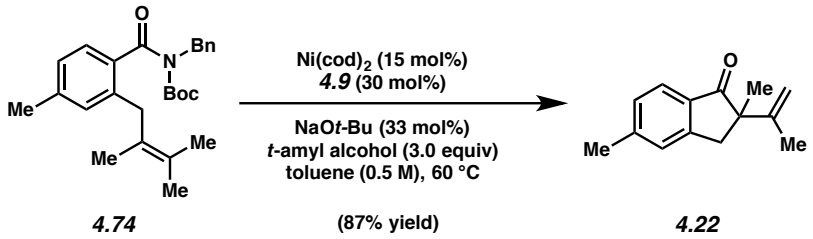

Indanone 4.22 (Figure 4.2). Purification by preparative thin-layer chromatography (9:1 Hexanes:EtOAc) afforded indanone **4.22** (87% yield, average of two experiments) as a colorless oil. Indanone **4.22**: R_f 0.43 (9:1 Hexanes:EtOAc); ^{1}H NMR (500 MHz, $CDCl_3$): δ 7.67 (d, J = 7.8, 1H), 7.25–7.23 (m, 1H), 7.20–7.18 (m, 1H), 4.95–4.93 (m, 2H), 3.27 (d, J = 17.6, 1H), 2.89 (d, J = 17.4, 1H), 2.44 (s, 3H), 1.63 (s, 3H), 1.36 (s, 3H); ^{13}C NMR (125 MHz, $CDCl_3$): δ 208.8, 153.3, 146.3, 146.1, 133.7, 128.9, 126.9, 124.5, 112.0, 54.7, 41.2, 22.8, 22.2, 19.9; IR (film): 2965, 1705, 1608, 1322, 585 cm^{-1}; HRMS–APCI (m/z) $[M + H]^+$ calcd for $C_{14}H_{17}O^+$, 201.12739; found 201.12719.

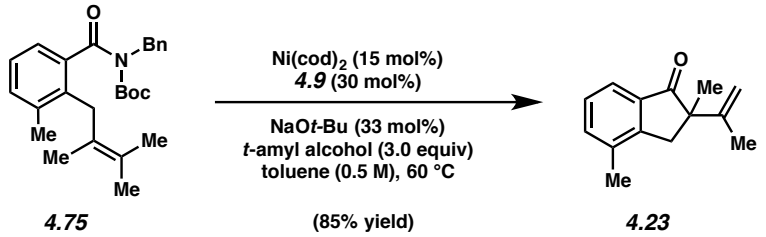

Indanone 23 (Figure 4.2). Purification by preparative thin-layer chromatography (9:1 Hexanes:EtOAc) afforded indanone **23** (85% yield, average of two experiments) as a colorless oil. Indanone **23**: R_f 0.38 (10:1 Hexanes:EtOAc); ^{1}H NMR (500 MHz, $CDCl_3$): δ 7.63 (d, J = 7.4, 1H), 7.43 (d, J = 7.4, 1H), 7.31 (t, J = 7.4, 1H), 4.97–4.94 (m, 2H), 3.21 (d, J = 17.5, 1H), 2.84 (d, J = 17.4, 1H), 2.35 (s, 3H), 1.65 (s, 3H), 1.39 (s, 3H); ^{13}C NMR (125 MHz, $CDCl_3$): δ 209.5, 151.6, 146.0, 135.67, 135.66, 135.4, 127.8, 122.0, 112.0, 54.5, 40.3, 22.8, 19.9, 17.8; IR (film): 2966, 1708, 1591, 1268, 893 cm^{-1}; HRMS–APCI (m/z) $[M + H]^+$ calcd for $C_{14}H_{17}O^+$, 201.12739; found 201.12701.

4.7.5 Diastereoselective Heck Cyclization

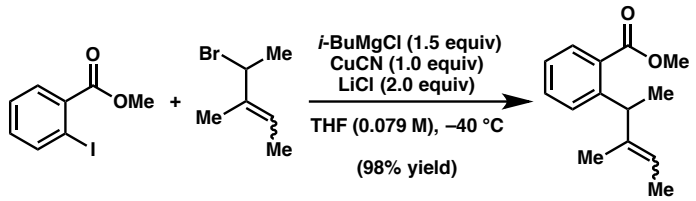

4.26 *4.76* ***4.77***
ratio E:Z (4:1)

Ester 4.77. Following a modification of the general procedure reported by Querolle and co-workers,[29] a flask containing a stir bar was charged CuCN (680 mg, 7.50 mmol, 1.0 equiv) and LiCl (650 mg, 15.0 mmol, 2.0 equiv) in the glovebox. The flask was removed from the glovebox, and the solids were suspended in THF (25 mL). The resulting mixture was stirred vigorously until a completely dissolved solution of CuCN•2LiCl was formed. In a separate flask containing a solution of methyl-2-iodobenzoate (**4.26**) (1.97 g, 7.50 mmol, 1.0 equiv) in THF (70 mL) at –40 °C was added *i*-BuMgCl (5.60 mL of a 2.0 M solution in THF, 11.3 mmol, 1.5 equiv) dropwise over 1 min at –40 °C. After this mixture was stirred at –40 °C for 1 h, the solution of CuCN•2LiCl was added via cannula. The combined mixture was stirred at –40 °C for an additional 15 min, at which point known bromide **4.76**[36] (2.43 g, 15.0 mmol, 2.0 equiv) was added dropwise over 1 min. After stirring at –40 °C for an additional hour, the reaction was poured into 9:1 sat. aq. NH_4Cl:NH_4OH (100 mL). The layers were separated and the aqueous layer was extracted with EtOAc (3 x 75 mL). The organic layers were combined, dried over $MgSO_4$, and concentrated under reduced pressure. The crude mixture was purified via flash chromatography (97:3 Hexanes:EtOAc) to afford ester **4.77** (1.61 g, 98% yield) as an inseparable mixture of olefin isomers and as a colorless oil (4:1 mixture of alkene isomers). Configurational isomers of ester **4.77** were analyzed as a mixture. **4.77** (**Major (*E*)-isomer**): ^{1}H NMR (500 MHz, $CDCl_3$): δ 7.71 (dd, *J* = 7.7, 1.5, 1H), 7.40 (dt, *J* = 7.8, 1.6, 1H), 7.30 (dd, *J* = 8.0, 1.24, 1H), 7.22 (dt, *J* = 7.7, 1.6,

1H), 5.38 (tq, J = 6.7, 1.6, 1H), 4.23 (q, J = 7.1, 1H), 3.88 (s, 3H), 1.63 (dt, J = 6.8, 1.2, 3H), 1.45 (br s, 3H), 1.33 (d, J = 7.0, 3H); **4.77** (**Major (*Z*)-isomer**): δ 7.60 (dd, J = 7.8, 1.3, 1H), 7.45–7.38 (m, 2H), 7.23 (dt, J = 7.6, 1.7, 1H), 5.25 (tq, J = 6.9, 0.8, 1H), 4.78 (q, J = 7.2, 1H), 3.84 (s, 3H), 1.61 (q, J = 1.5, 3H), 1.40 (quint, J = 1.5, 3H), 1.35 (d, J = 7.3, 3H); Ester **4.77** (**mixture**): R_f 0.55 (9:1 Hexanes:EtOAc); ^{13}C NMR (125 MHz, $CDCl_3$): (27 of 28 signals observed) δ 169.4, 169.1, 146.9, 145.1, 139.3, 138.9, 131.7, 131.6, 131.1, 130.9, 129.8, 129.4, 127.8, 127.6, 125.8, 120.3, 118.3, 52.3, 52.1, 42.7, 35.3, 20.3, 20.2, 18.3, 16.0, 13.6, 13.3; IR (film): 2968, 1721, 1601, 1576, 1485, 1446, 1371 cm^{-1}; HRMS–APCI (m/z) $[M + H]^+$ calcd for $C_{14}H_{19}O_2^+$, 219.13796; found 219.13794.

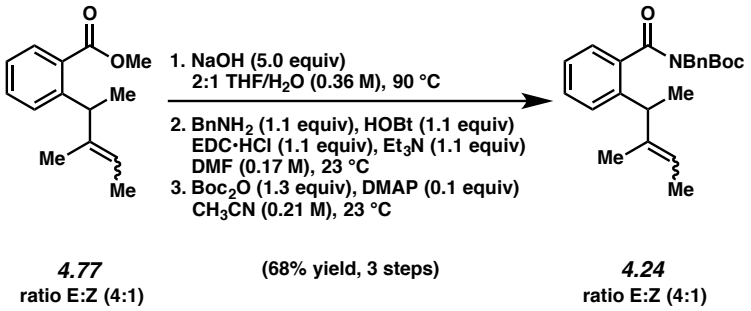

Imide 4.24. To a solution of ester **4.77** (1.61 g, 7.40 mmol, 1.0 equiv) in THF (35 mL) was added a solution of NaOH (1.48 g, 37.0 mmol, 5.0 equiv) in H_2O (35 mL). The reaction was heated to 90 °C and stirred for 12 h. After cooling to room temperature, the reaction mixture was poured into deionized water (25 mL) and diluted with EtOAc (25 mL). The layers were separated and the aqueous layer was acidified to pH ~2 with 1 N HCl (100 mL) and extracted with EtOAc (3 x 50 mL). The organic layers were combined, washed with deionized water (300 mL), dried over $MgSO_4$, and concentrated under reduced pressure to afford the corresponding carboxylic acid, which was used in the subsequent step without further purification.

To a solution of the crude carboxylic acid, HOBt (1.08 g, 7.80 mmol, 1.1 equiv from **4.77**), and EDC•HCl (1.53 g, 7.80 mmol, 1.1 equiv from **4.77**) in DMF (40 mL) was added $BnNH_2$ (0.90 mL, 7.80 mmol, 1.1 equiv from **4.77**) and Et_3N (1.17 mL, 7.80 mmol, 1.1 equiv from **4.77**). After stirring for 15 h, the reaction mixture was poured into deionized water (300 mL) and diluted with EtOAc (50 mL). The layers were separated and the aqueous layer was extracted with EtOAc (3 x 50 mL). The organic layers were combined, washed with deionized water (100 mL), dried over $MgSO_4$, and concentrated under reduced pressure to afford the corresponding amide, which was used in the subsequent step without further purification.

To a solution of the crude amide in CH_3CN (45 mL) was added DMAP (82 mg, 0.65 mmol, 0.1 equiv from **4.77**) and Boc_2O (1.85 g, 8.50 mmol, 1.3 equiv from **4.77**). After stirring for 15 h, the reaction mixture was concentrated under reduced pressure and purified by flash chromatography (99:1 Hexanes:EtOAc) to yield imide **4.24** (1.97 g, 68% yield, three steps) as an inseparable mixture of olefin isomers and as a colorless oil (4:1 mixture of alkene isomers). Configurational isomers of imide **4.24** were analyzed as a mixture **4.24** (**Major (*E*)-isomer**): ^{1}H NMR (500 MHz, $CDCl_3$): δ 7.43 (d, *J* = 7.5, 2H), 7.37–7.31 (m, 3H), 7.29–7.22 (m, 2H), 7.16 (dt, *J* = 7.7, 1.4, 1H), 7.12–7.08 (m, 1H), 5.36 (tq, *J* = 6.8, 1.3, 1H), 5.06 (s, 2H), 3.67 (q, *J* = 6.9, 1H), 1.60 (d, *J* = 6.7, 3H), 1.48 (s, 3H), 1.30 (d, *J* = 7.0, 3H), 1.13 (s, 9H); **4.24** (**Major (*Z*)-isomer**) δ 7.45–7.37 (m, 2H), 7.37–7.31 (m, 3H), 7.29–7.22 (m, 2H), 7.18 (dt, *J* = 7.5, 1.3, 1H), 7.12–7.08 (m, 1H), 5.22 (br s, 1H), 4.99 (br s, 2H), 4.34 (br s, 1H), 1.57 (d, *J* = 6.9, 3H), 1.53 (t, *J* = 1.4, 3H), 1.34 (d, *J* = 7.2, 3H), 1.11 (s, 9H); Imide **4.24** (**mixture**): R_f 0.52 (9:1 Hexanes:EtOAc); ^{13}C NMR (125 MHz, $CDCl_3$): δ 172.4, 152.8, 142.8, 141.3, 138.9, 138.6, 138.1, 138.04, 138.02, 129.4, 129.0, 128.5, 128.3, 127.5, 127.4, 126.3, 126.2, 125.4, 120.0, 118.6, 83.5, 48.0, 43.2, 27.7, 27.6,

20.2, 18.7, 15.5, 13.5, 13.3; IR (film): 2973, 1728, 1670, 1456, 1369, 1335, 1228 cm^{-1}; HRMS–APCI (m/z) $[M + H]^+$ calcd for $C_{25}H_{32}NO_3^+$, 394.23767; found 394.23814.

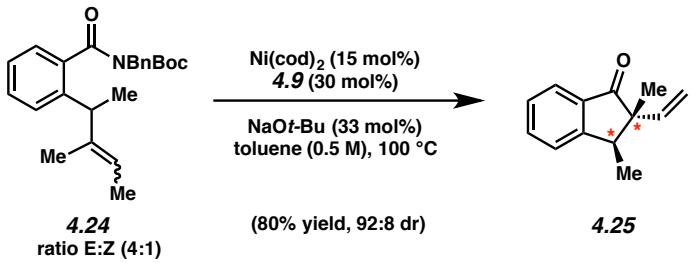

Indanone 4.25 (Figure 4.3). Following the representative procedure described in Section 4.7.4, purification by preparative thin-layer chromatography (98:2 Benzene:CH_3CN) afforded indanone **4.25** (80% yield, 92:8 dr, average of two experiments) as a colorless oil. Indanone **4.25**: R_f 0.48 (9:1 Hexane:EtOAc); ^{1}H NMR (500 MHz, $CDCl_3$): δ 7.75 (d, J = 7.7, 1H), 7.62 (dt, J = 7.7, 1.2, 1H), 7.49 (dd, J = 7.8, 0.9, 1H), 7.38 (tt, J = 7.5, 0.9, 1H), 5.94 (dd, J = 17.4, 10.6, 1H), 5.23–5.15 (m, 2H), 3.40 (q, J = 7.5, 1H), 1.32 (d, J = 7.4, 3H), 1.19 (s, 3H); ^{13}C NMR (125 MHz, $CDCl_3$): δ 208.4, 157.2, 141.0, 135.1, 134.5, 127.8, 125.1, 124.5, 114.6, 56.2, 43.1, 18.5, 15.1; IR (film): 2972, 1712, 1606, 1466, 1328, 1285, 1226 cm^{-1}; HRMS–APCI (m/z) $[M + H]^+$ calcd for $C_{13}H_{15}O^+$, 187.11174; found 187.11180.

*The stereochemistry of indanone **4.25** was verified by NOESY (500 MHz, $CDCl_3$), as the following correlation was observed:*

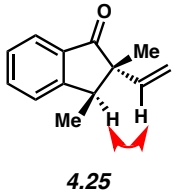

4.25

4.8 Spectra Relevant to Chapter Four:

Mizoroki–Heck Cyclizations of Amide Derivatives for the Introduction of Quaternary Centers

Adapted from: Jose M. Medina, Jesus Moreno, Sophie Racine, Shuaijing Du, and Neil K. Garg. *Angew. Chem, Int. Ed. Soc.* [Online early access]. DOI: 10.1002/anie.201703174R1.

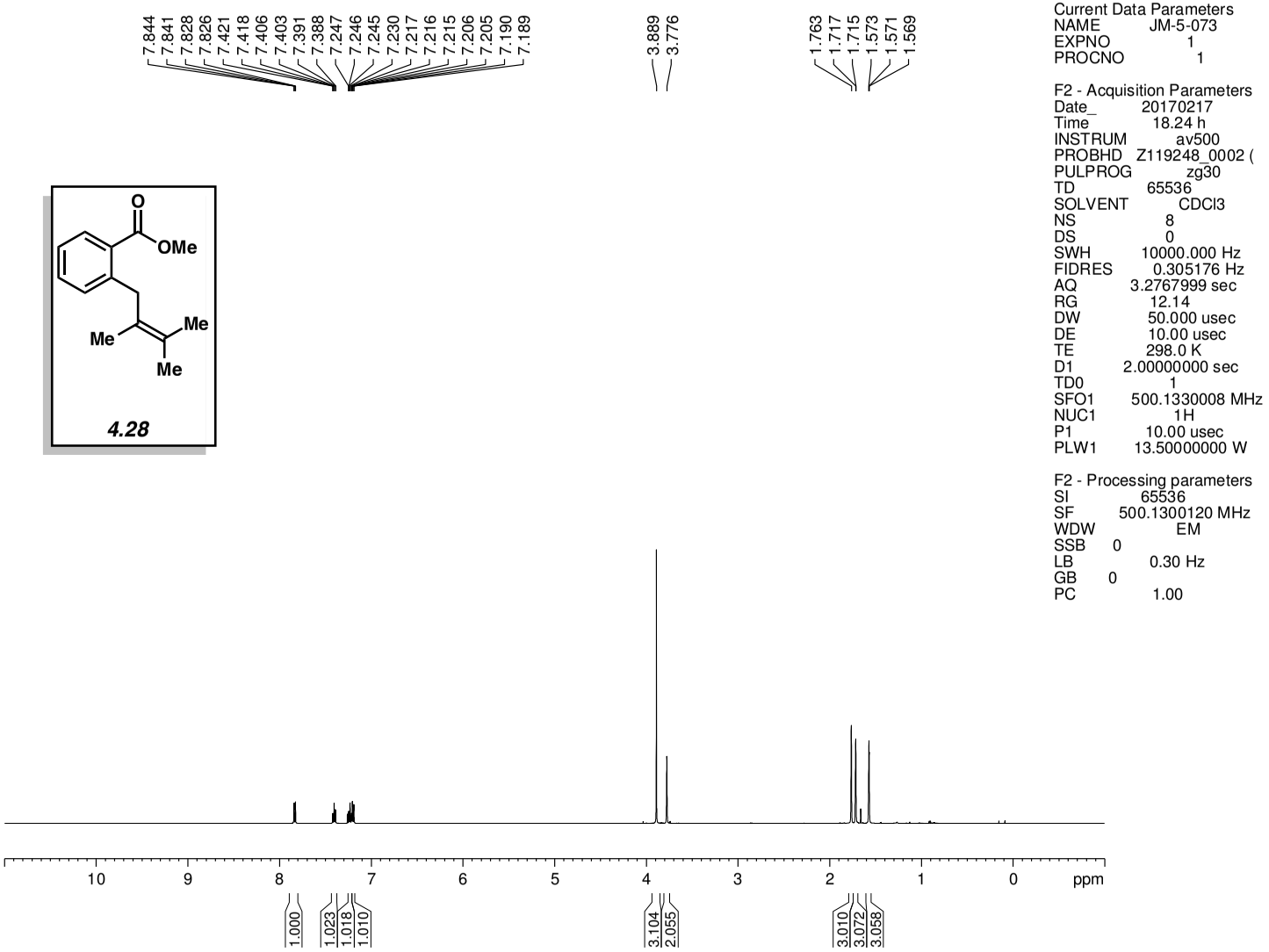

Figure 4.4 ^{1}H NMR (500 MHz, $CDCl_3$) of compound **4.28**.

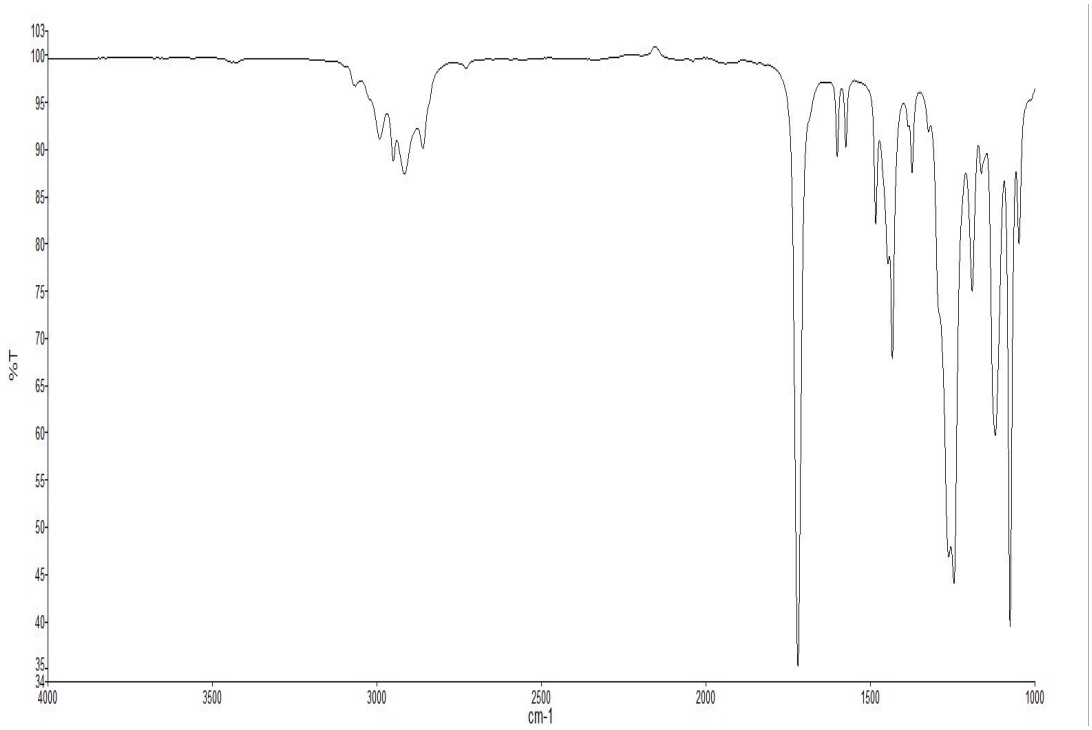

Figure 4.5 Infrared spectrum of compound **4.28**.

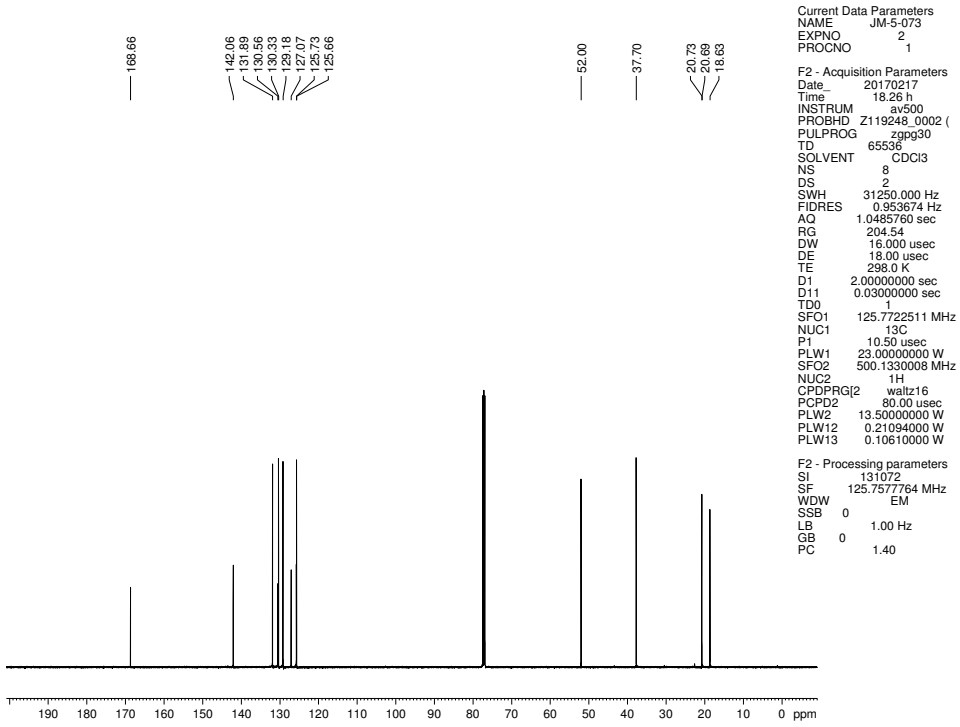

Figure 4.6 ^{13}C NMR (125 MHz, $CDCl_3$) of compound **4.28**.

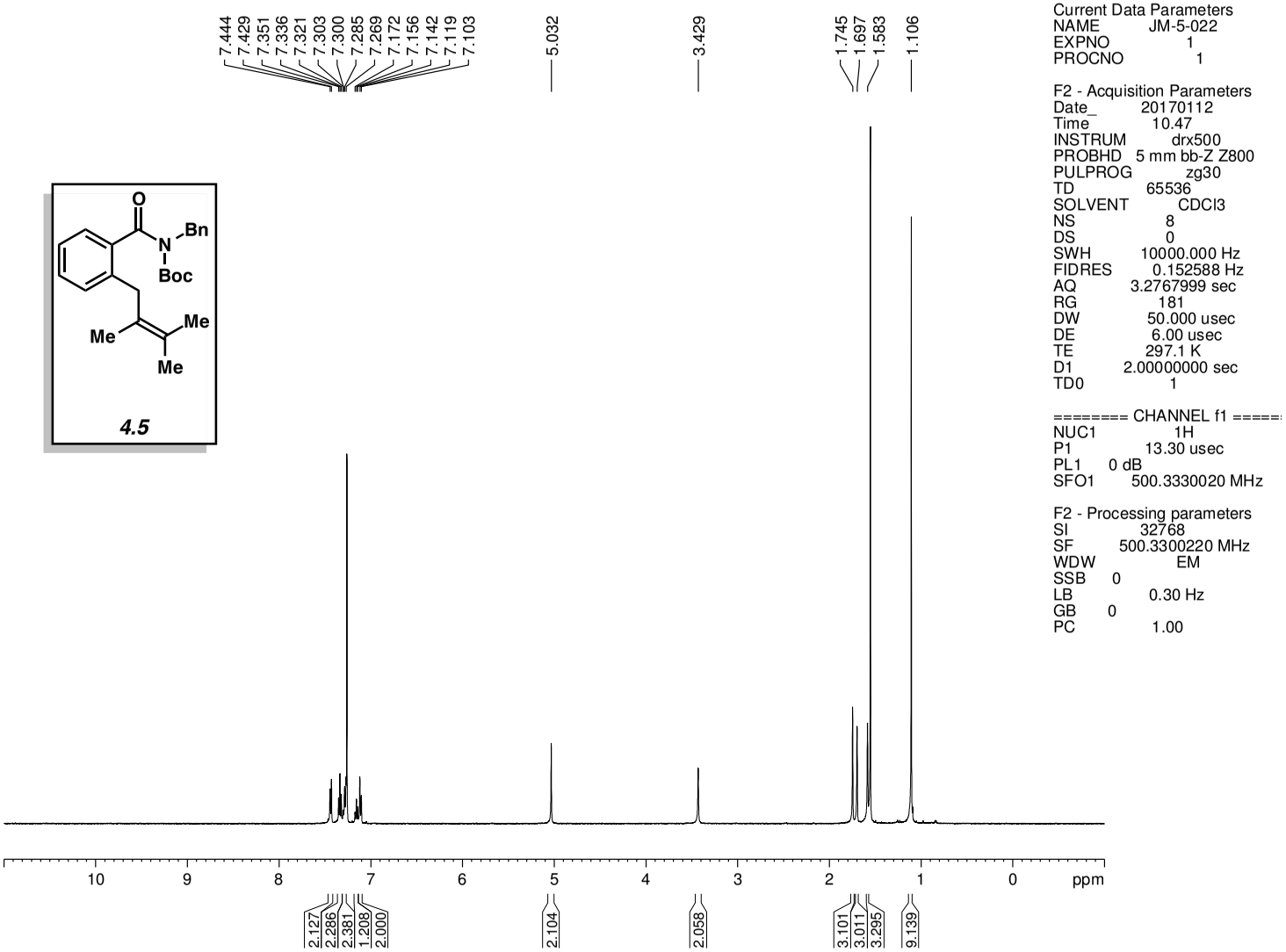

Figure 4.7 ^{1}H NMR (500 MHz, $CDCl_3$) of compound **4.5**.

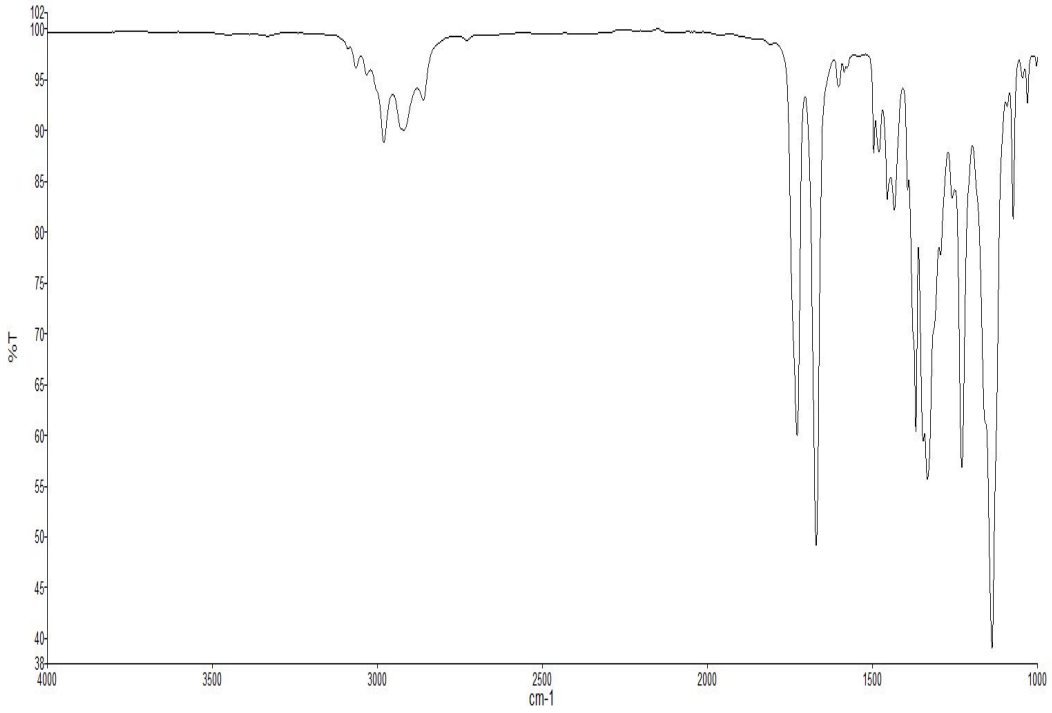

Figure 4.8 Infrared spectrum of compound **4.5**.

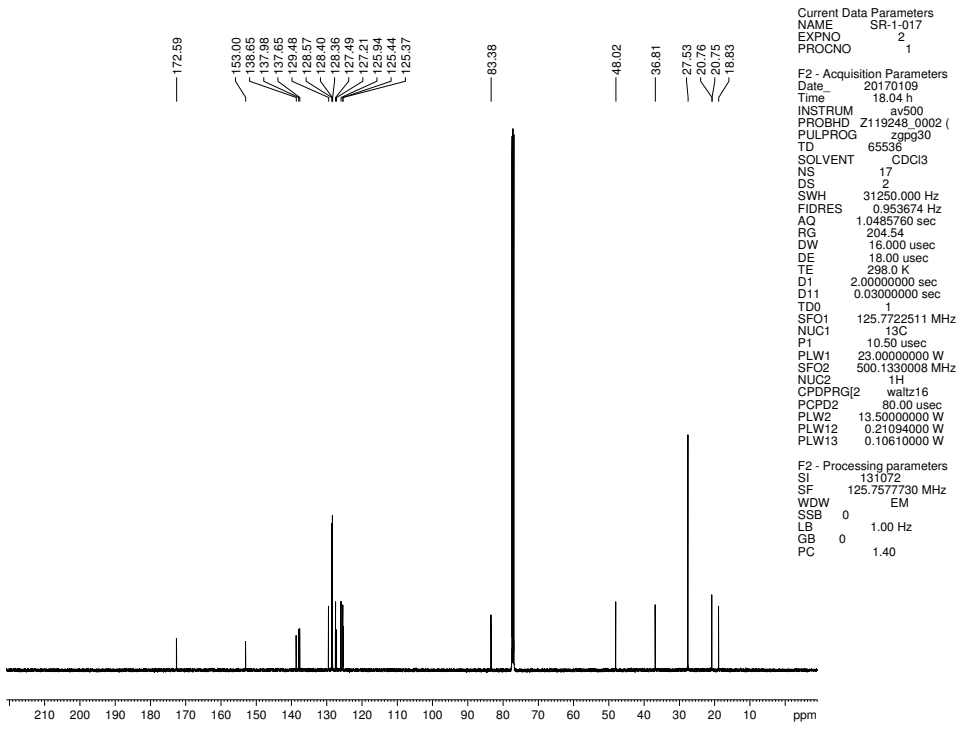

Figure 4.9 ^{13}C NMR (125 MHz, $CDCl_3$) of compound **4.5**.

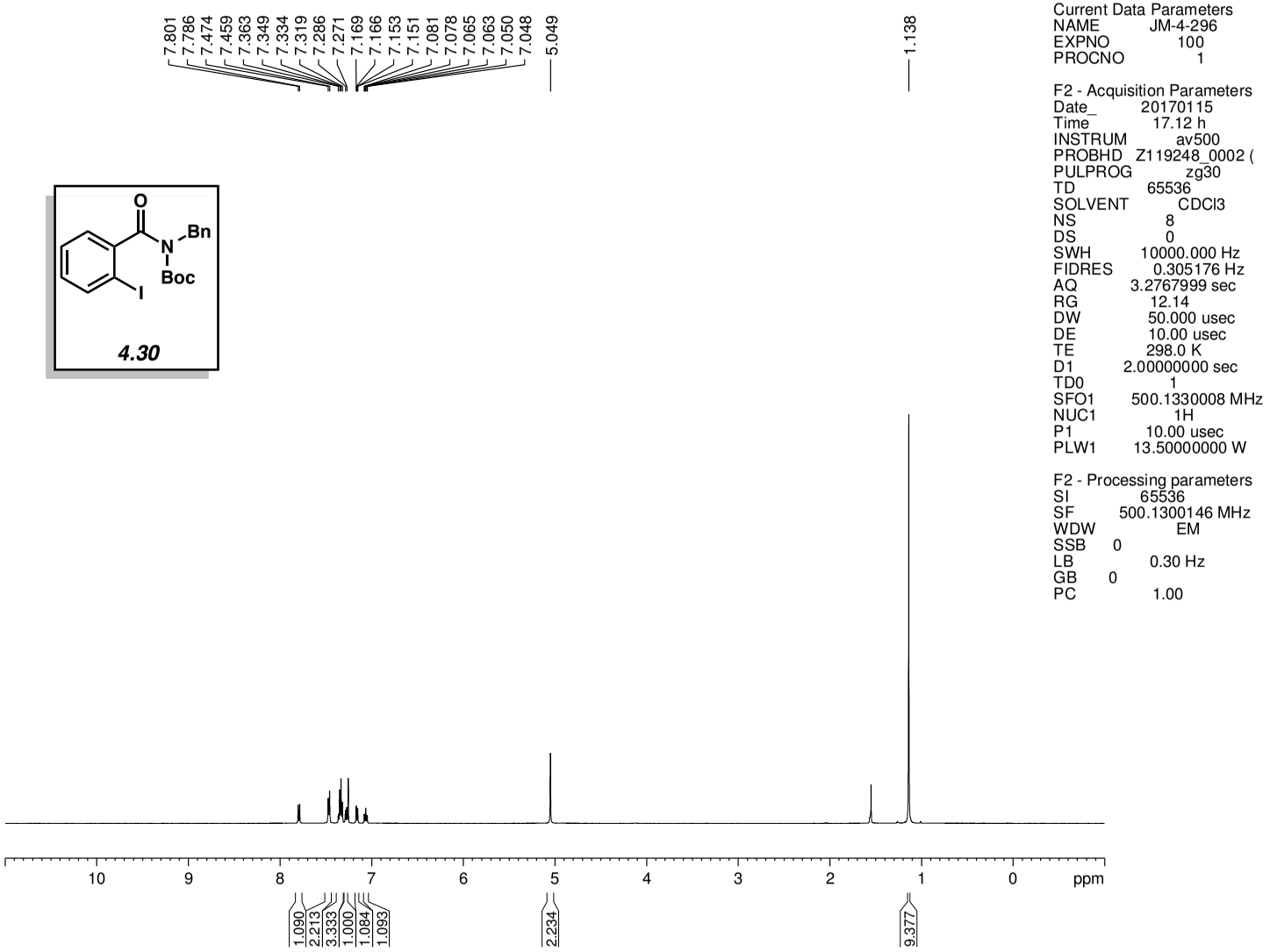

Figure 4.10 ^{1}H NMR (500 MHz, $CDCl_3$) of compound **4.30**.

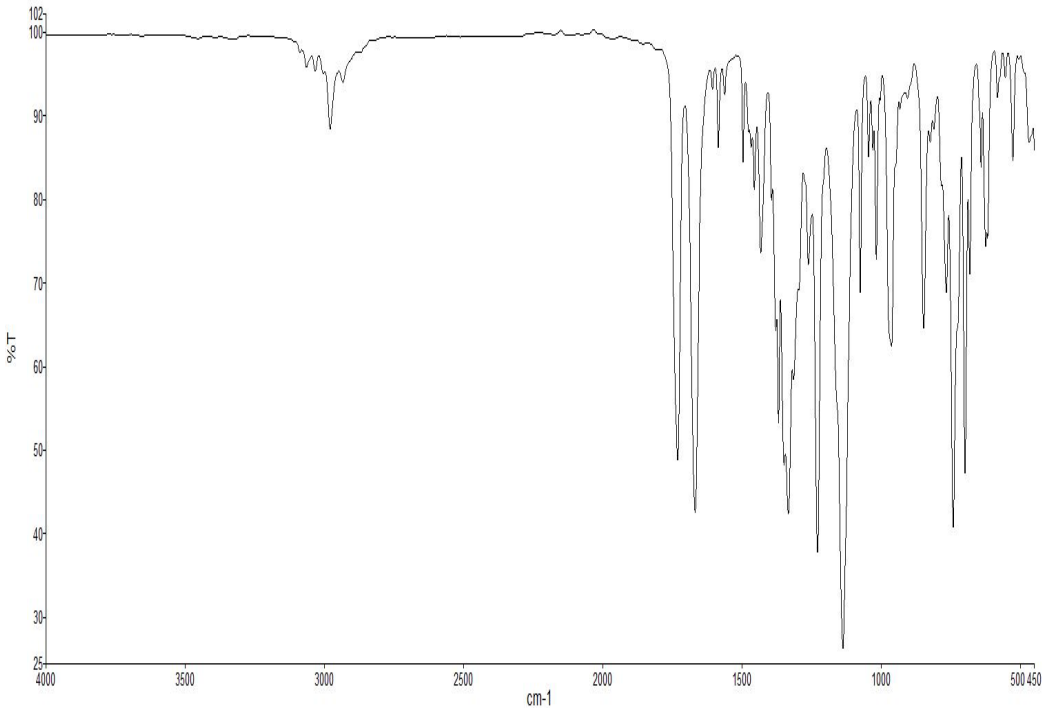

Figure 4.11 Infrared spectrum of compound **4.30**.

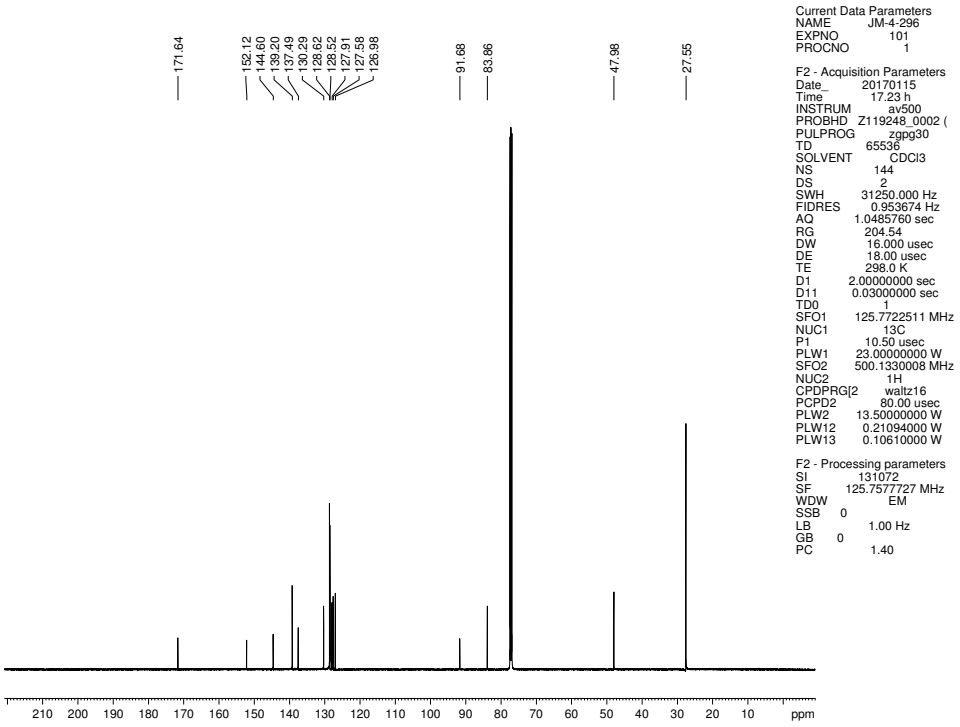

Figure 4.12 ^{13}C NMR (125 MHz, $CDCl_3$) of compound **4.30**.

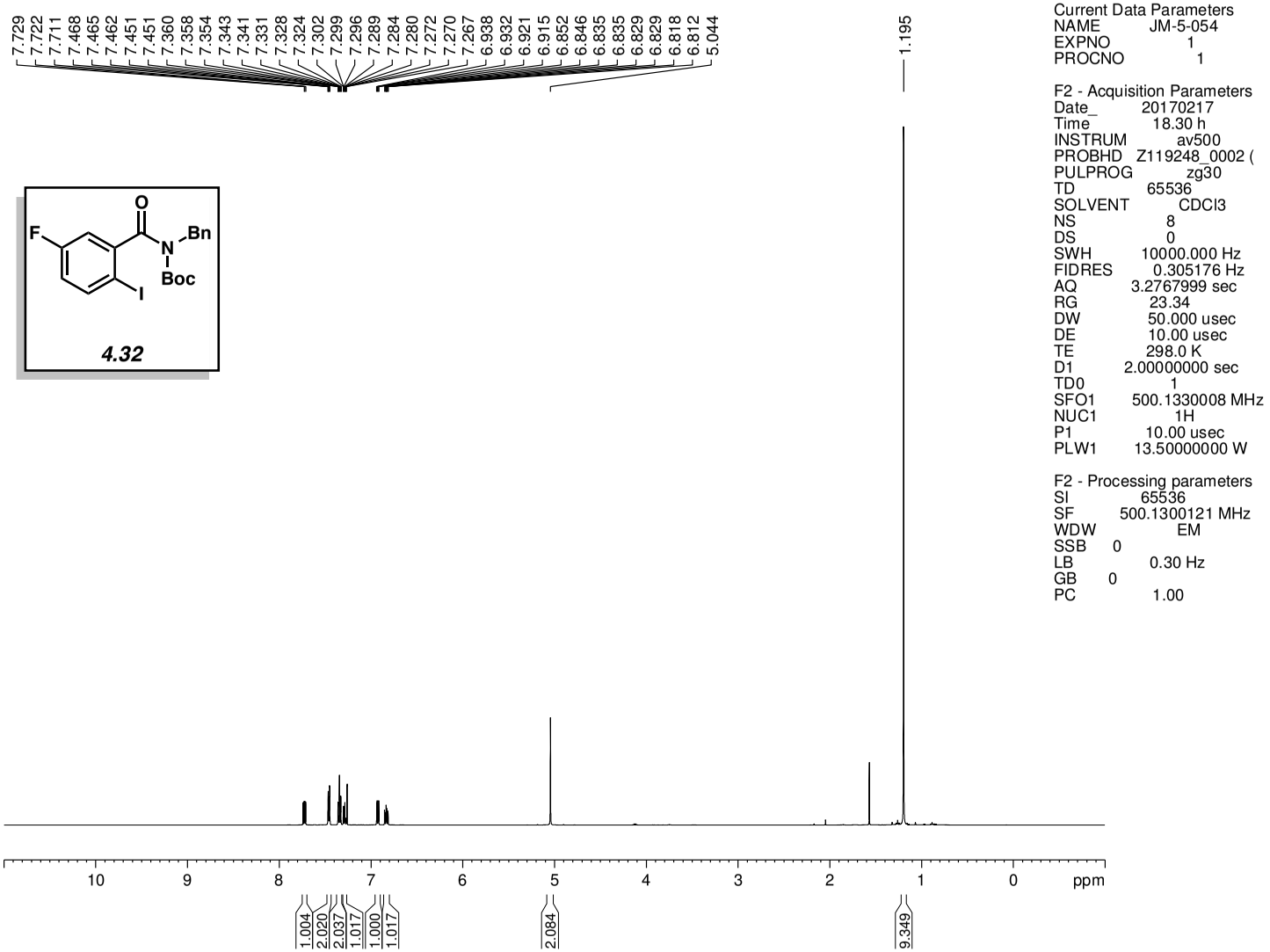

Figure 4.13 ^{1}H NMR (500 MHz, $CDCl_3$) of compound **4.32**.

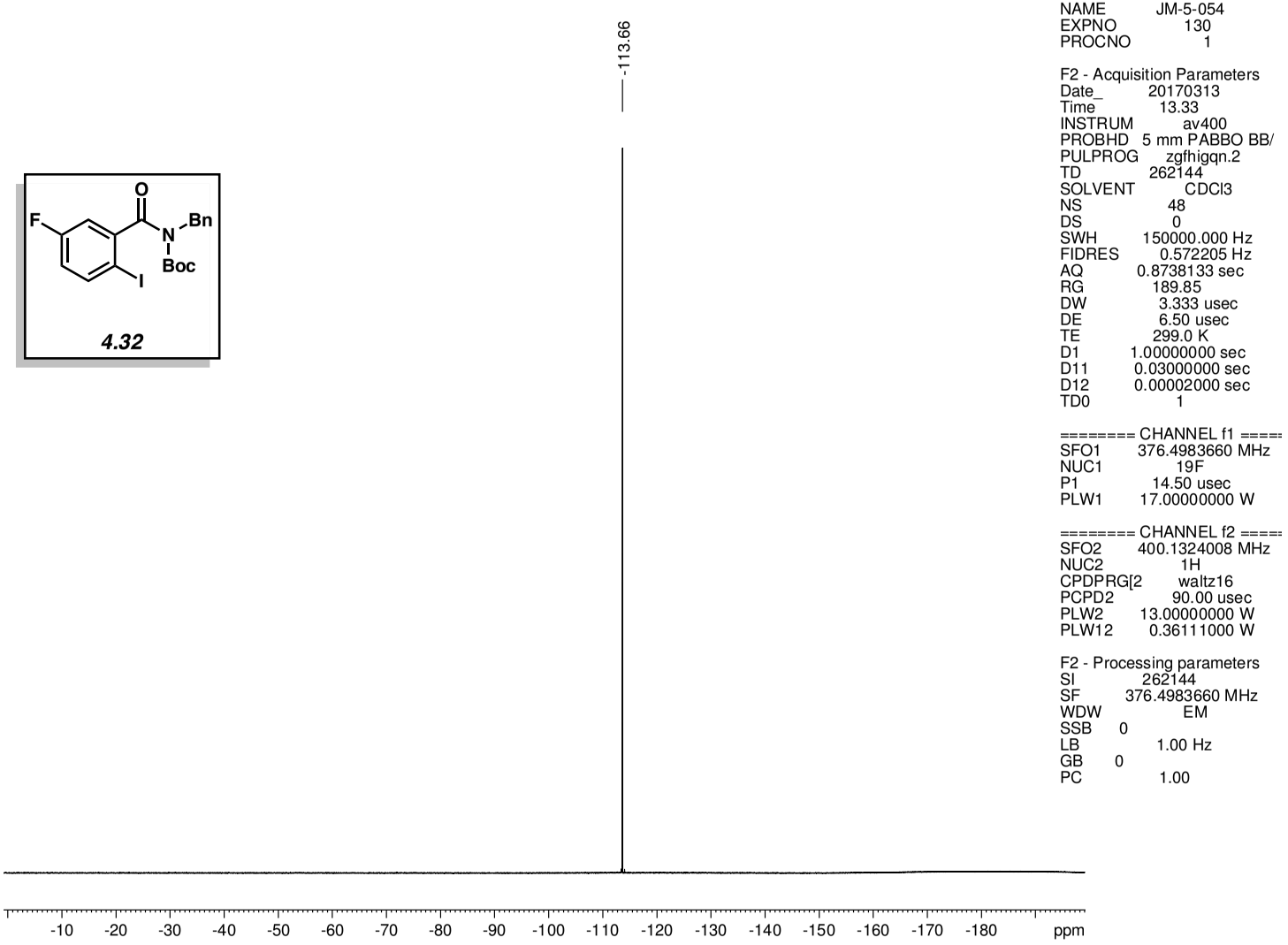

Figure 4.14 ^{19}F NMR (376 MHz, $CDCl_3$) of compound **4.32**.

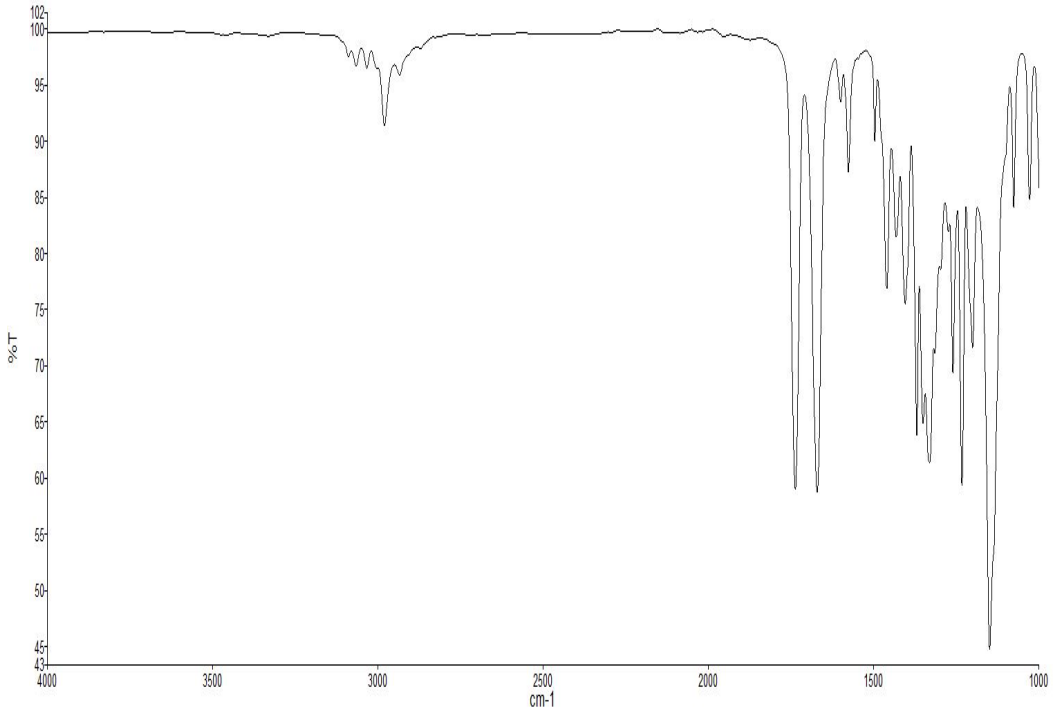

Figure 4.15 Infrared spectrum of compound **4.32**.

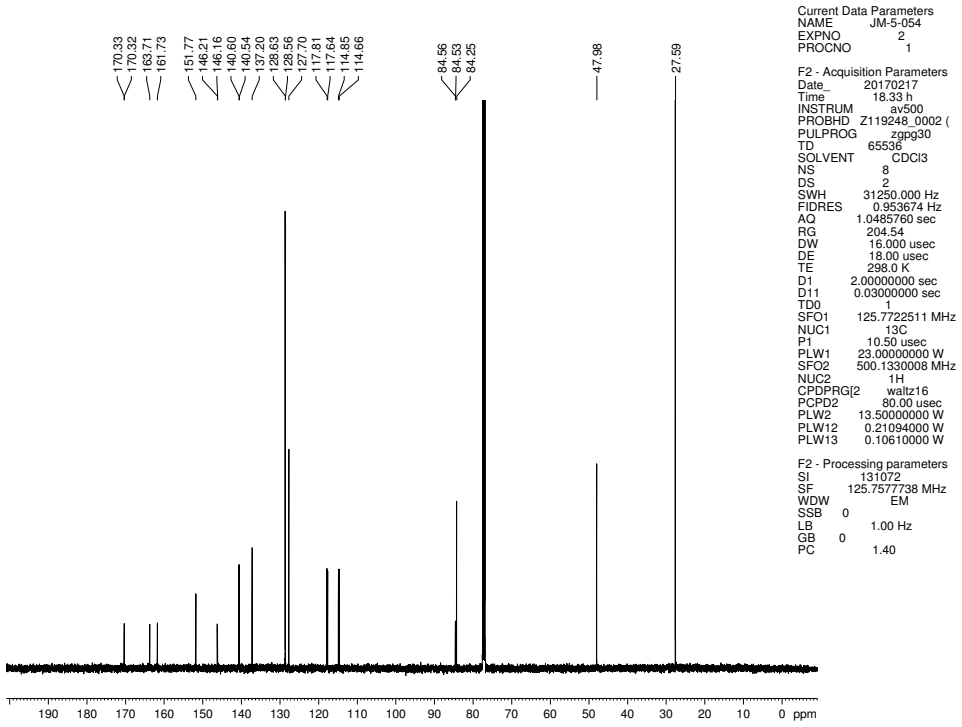

Figure 4.16 ^{13}C NMR (125 MHz, $CDCl_3$) of compound **4.32**.

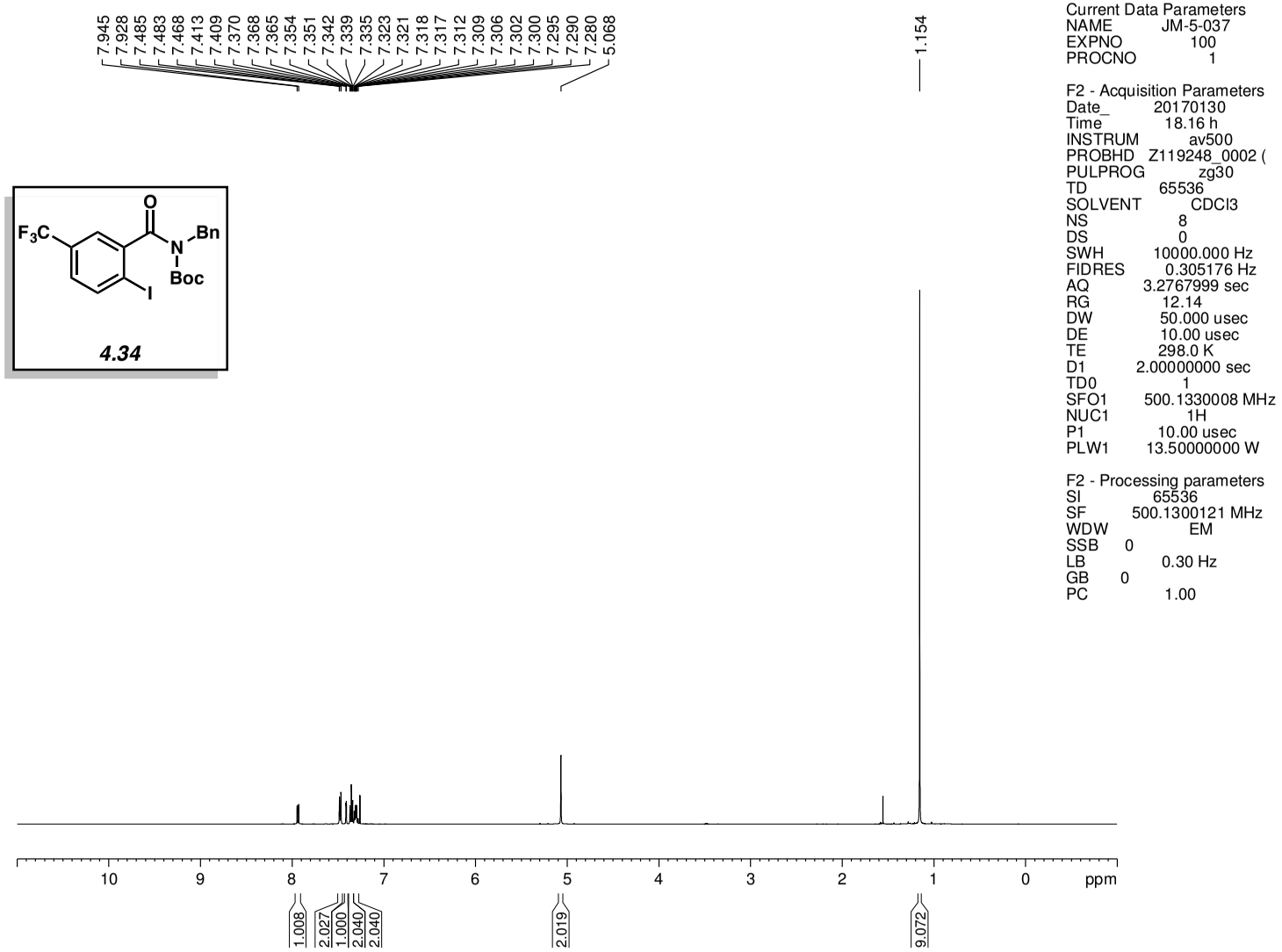

Figure 4.17 ^{1}H NMR (500 MHz, $CDCl_3$) of compound **4.34**.

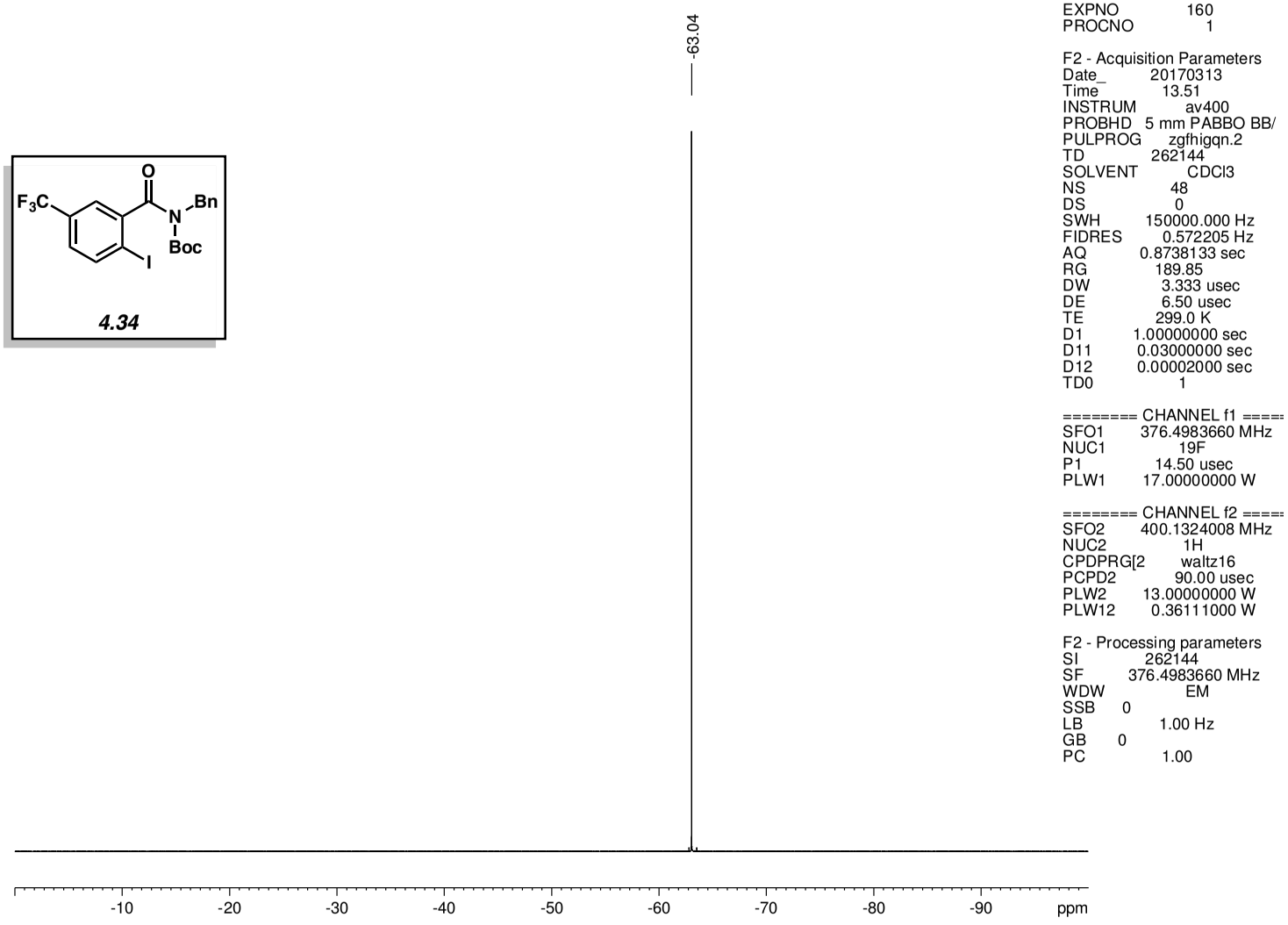

Figure 4.18 ^{19}F NMR (376 MHz, $CDCl_3$) of compound **4.34**.

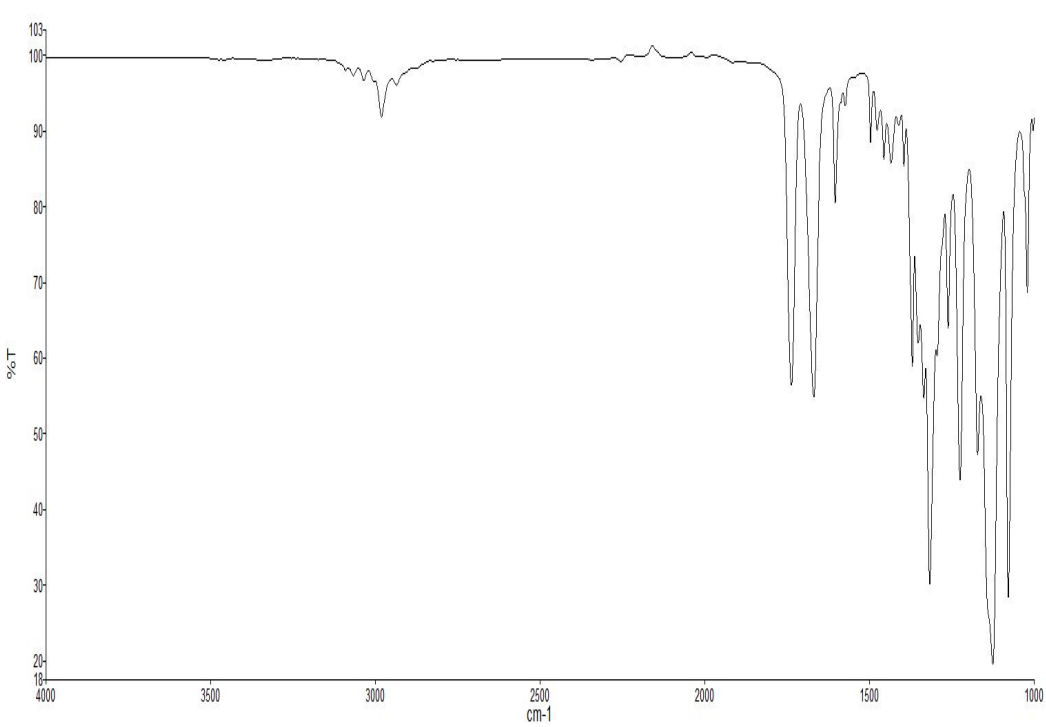

Figure 4.19 Infrared spectrum of compound **4.34**.

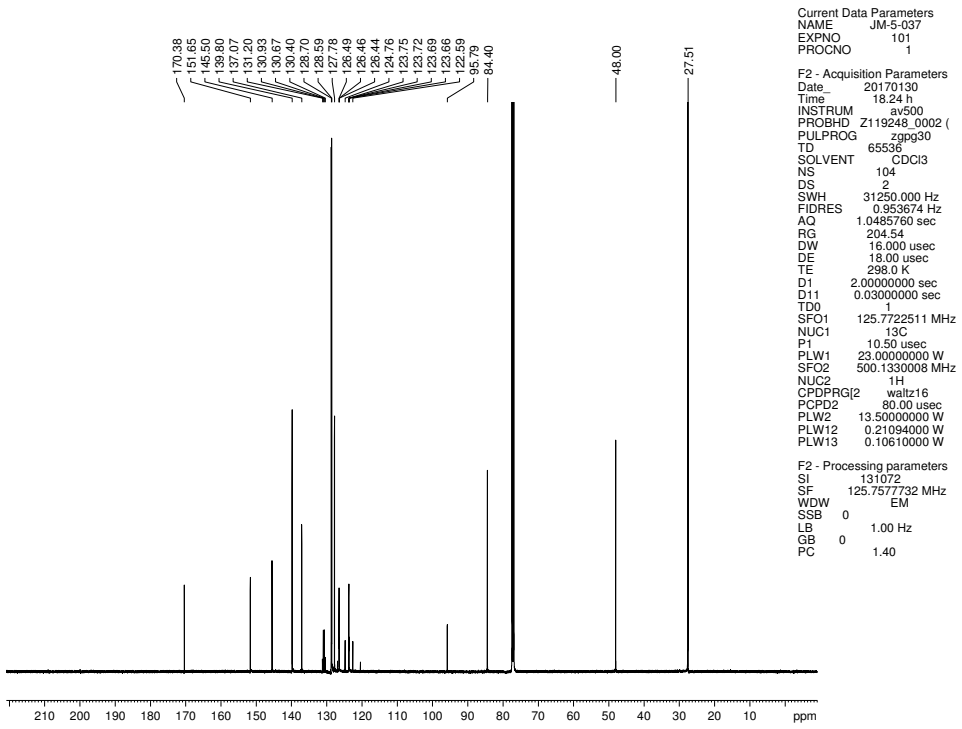

Figure 4.20 ^{13}C NMR (125 MHz, $CDCl_3$) of compound **4.34**.

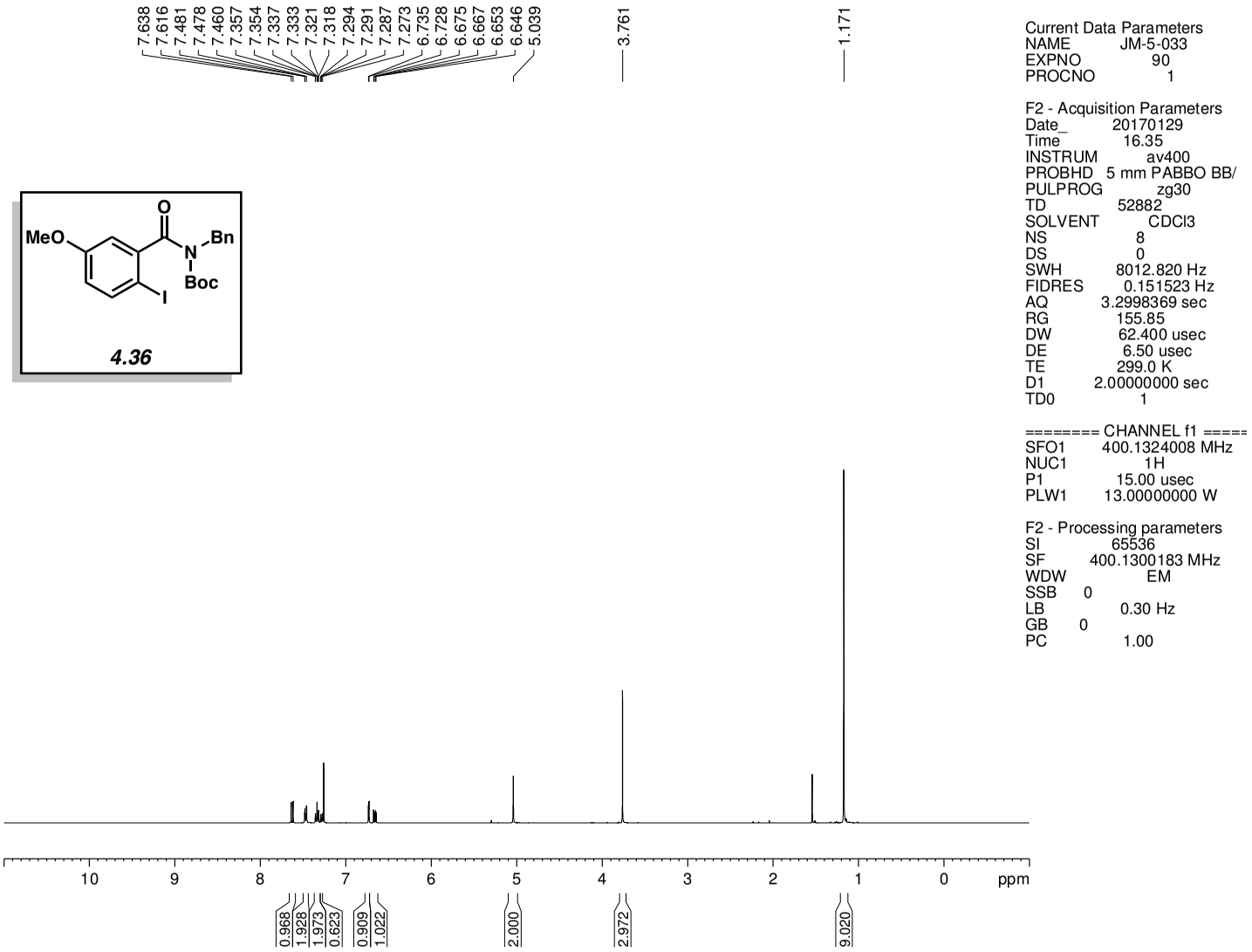

Figure 4.21 ^{1}H NMR (500 MHz, $CDCl_3$) of compound **4.36**.

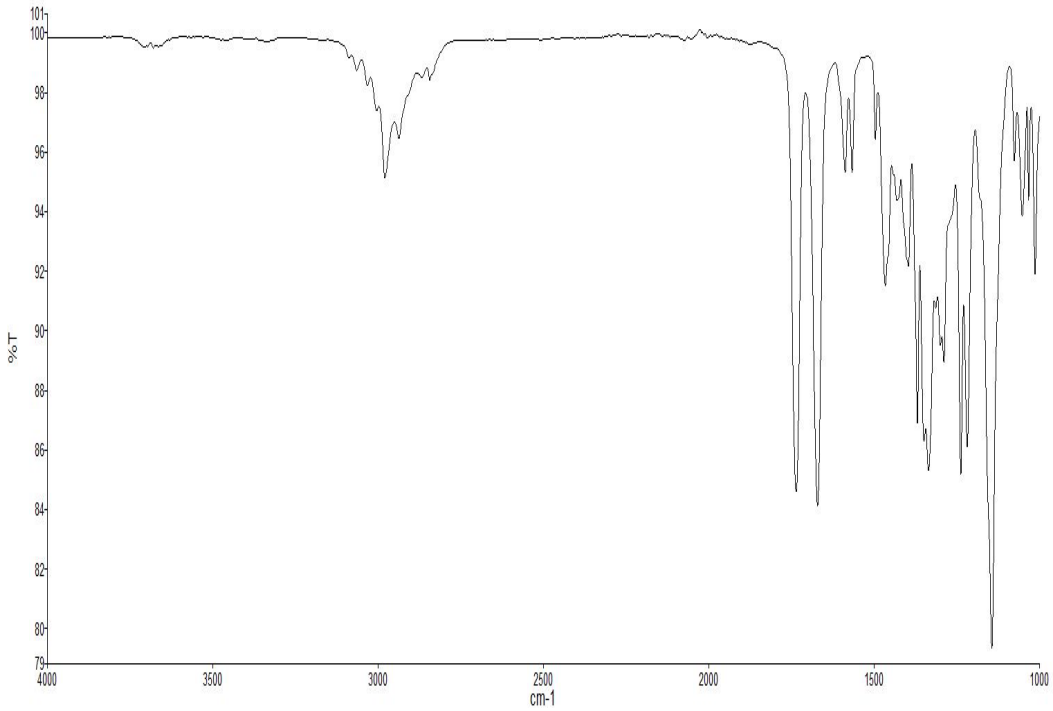

Figure 4.22 Infrared spectrum of compound **4.36**.

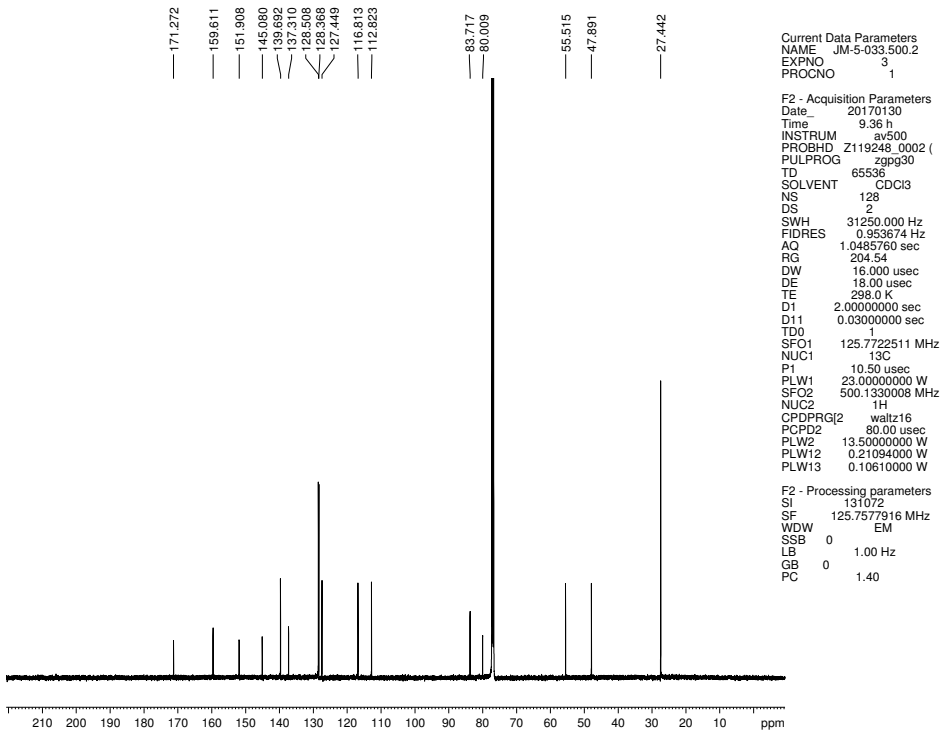

Figure 4.23 ^{13}C NMR (125 MHz, $CDCl_3$) of compound **4.36**.

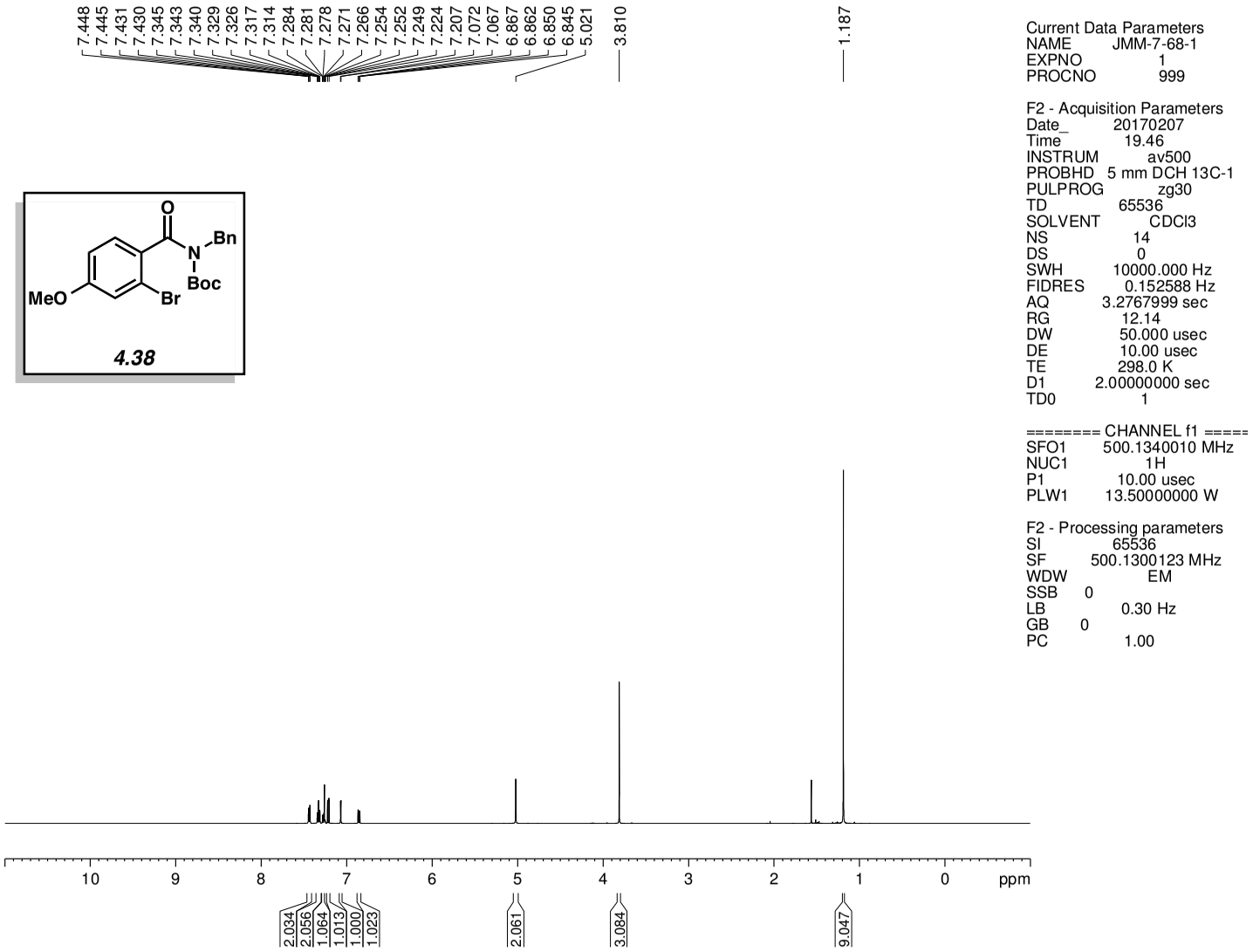

Figure 4.24 ^{1}H NMR (500 MHz, $CDCl_3$) of compound **4.38**.

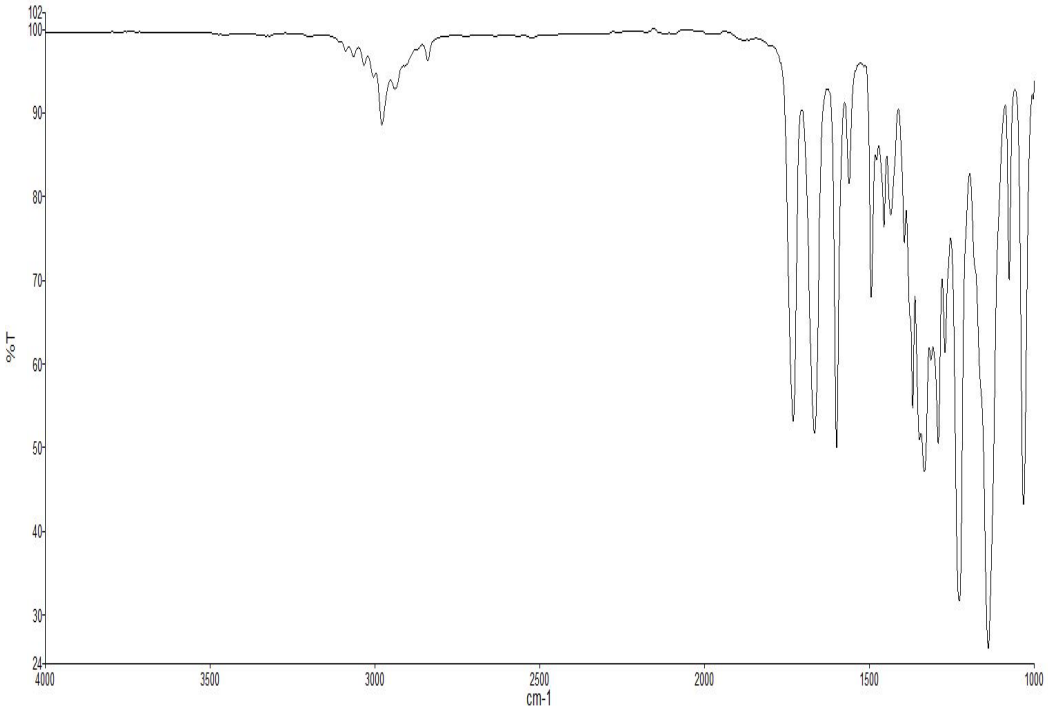

Figure 4.25 Infrared spectrum of compound **4.38**.

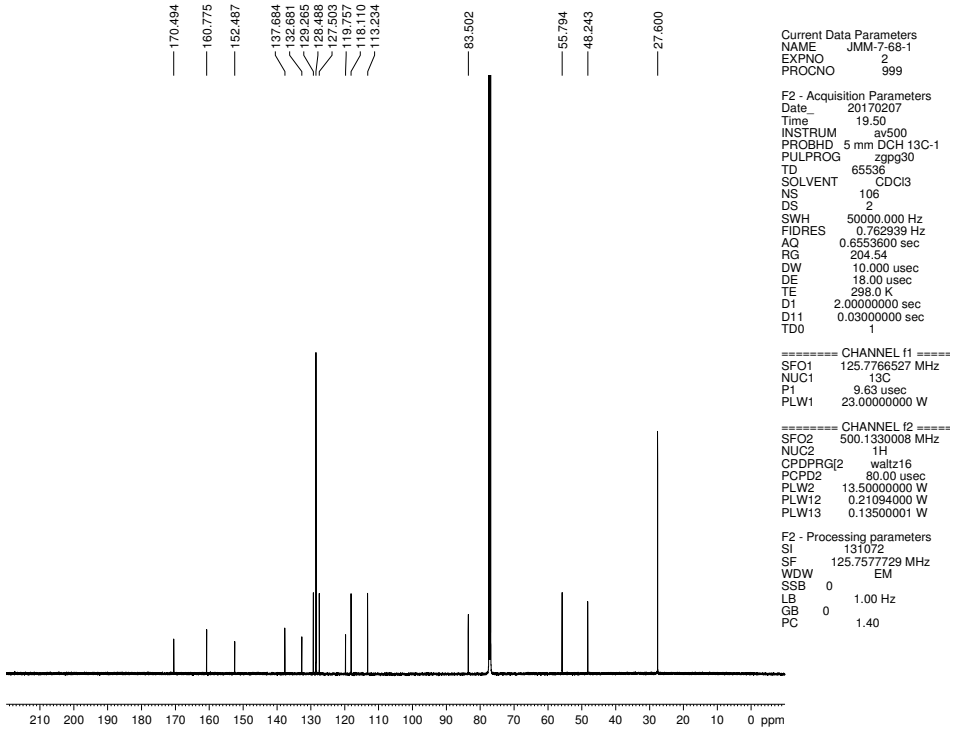

Figure 4.26 ^{13}C NMR (125 MHz, $CDCl_3$) of compound **4.38**.

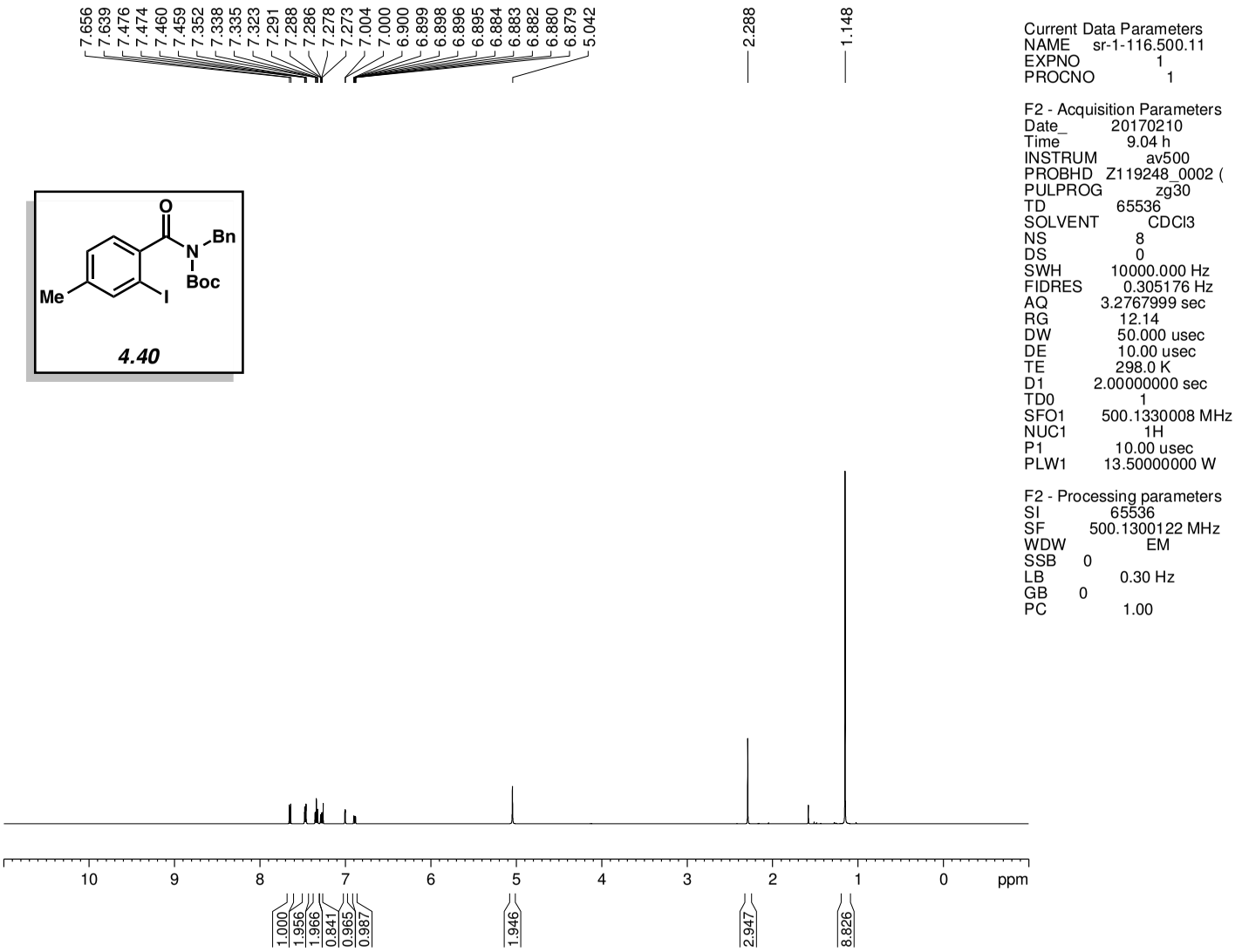

Figure 4.27 ^{1}H NMR (500 MHz, $CDCl_3$) of compound **4.40**.

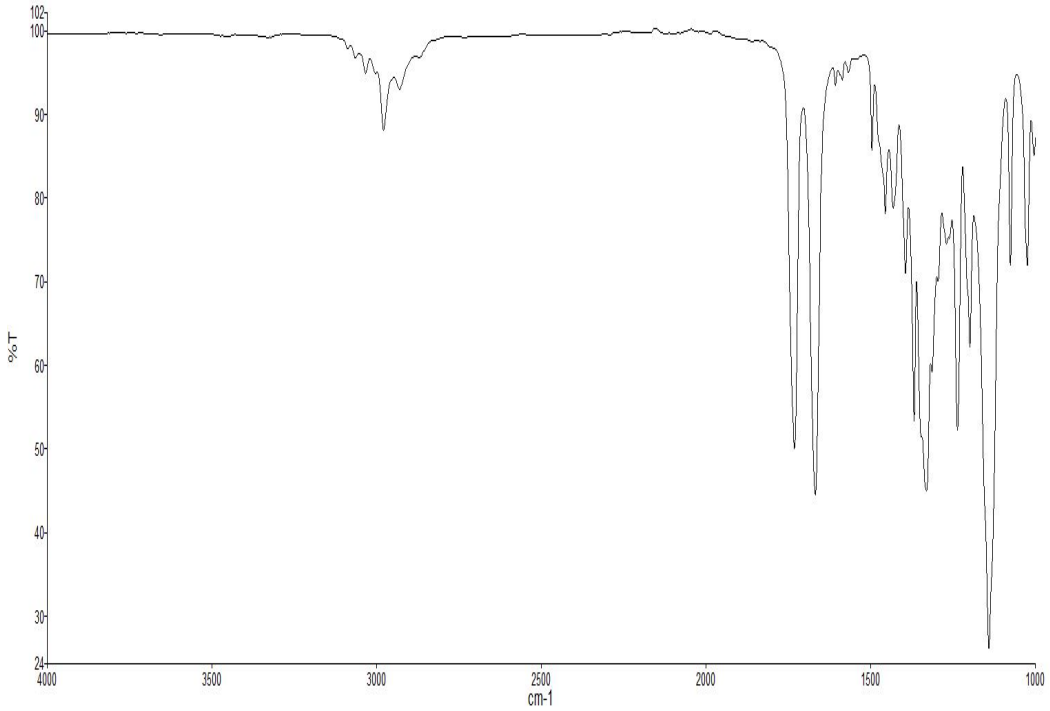

Figure 4.28 Infrared spectrum of compound **4.40**.

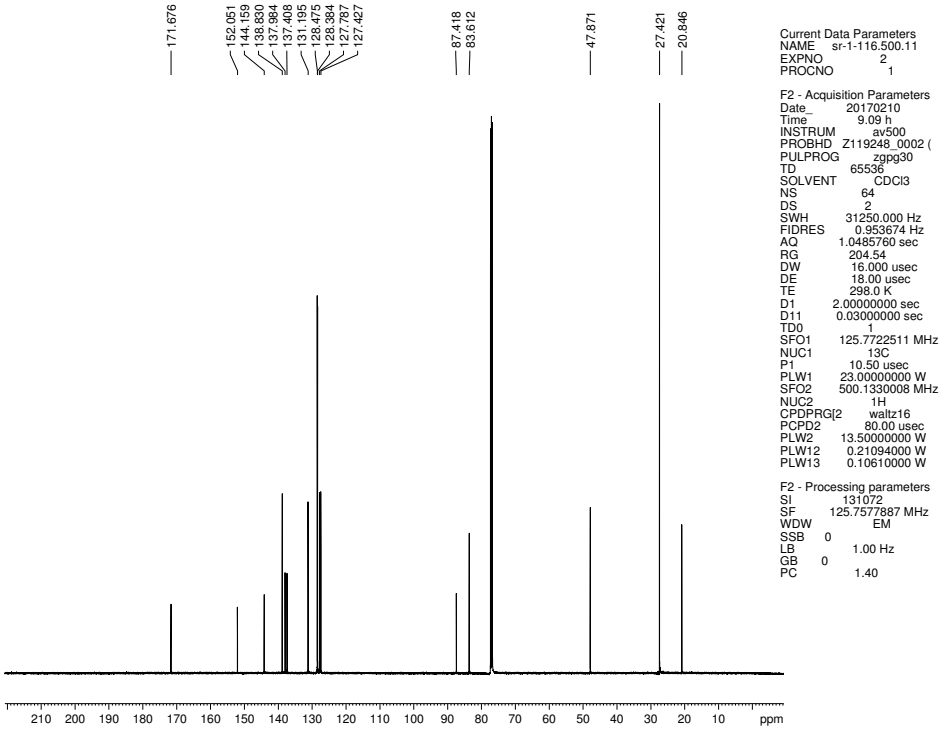

Figure 4.29 ^{13}C NMR (125 MHz, $CDCl_3$) of compound **4.40**.

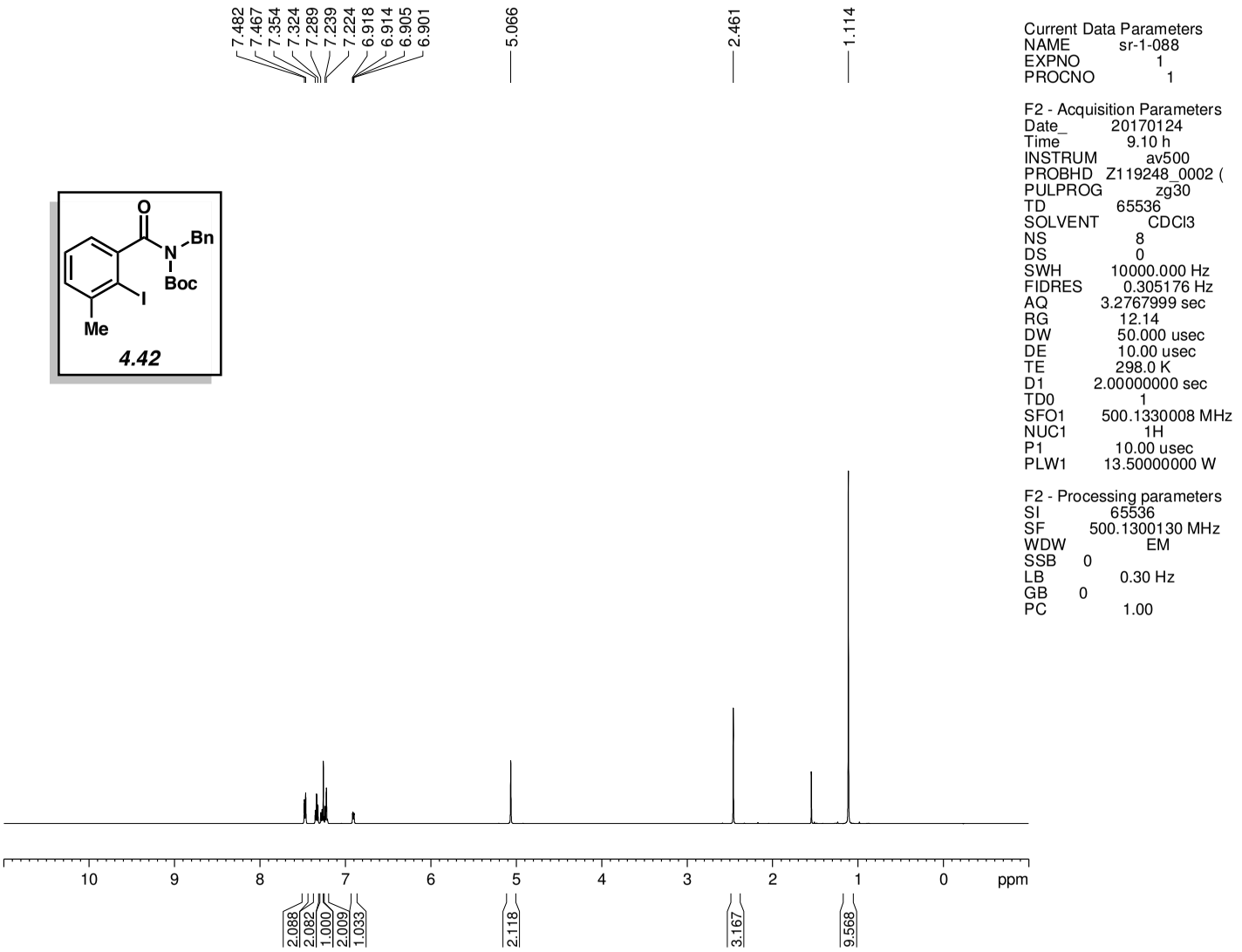

Figure 4.30 ^{1}H NMR (500 MHz, $CDCl_3$) of compound **4.42**.

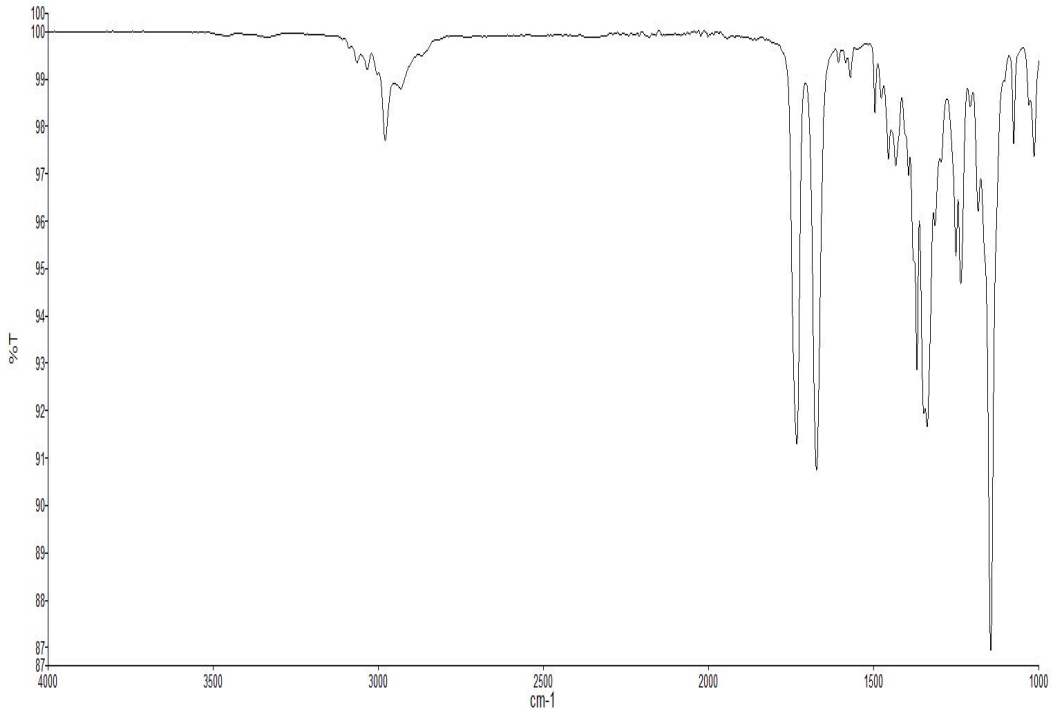

Figure 4.31 Infrared spectrum of compound **4.42**.

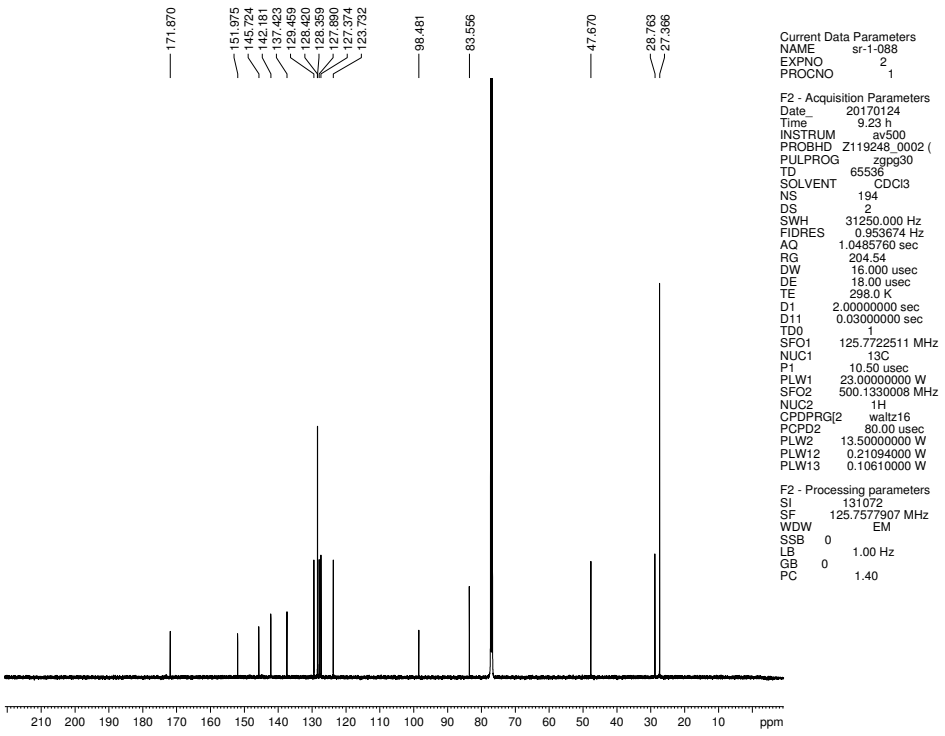

Figure 4.32 ^{13}C NMR (125 MHz, $CDCl_3$) of compound **4.42**.

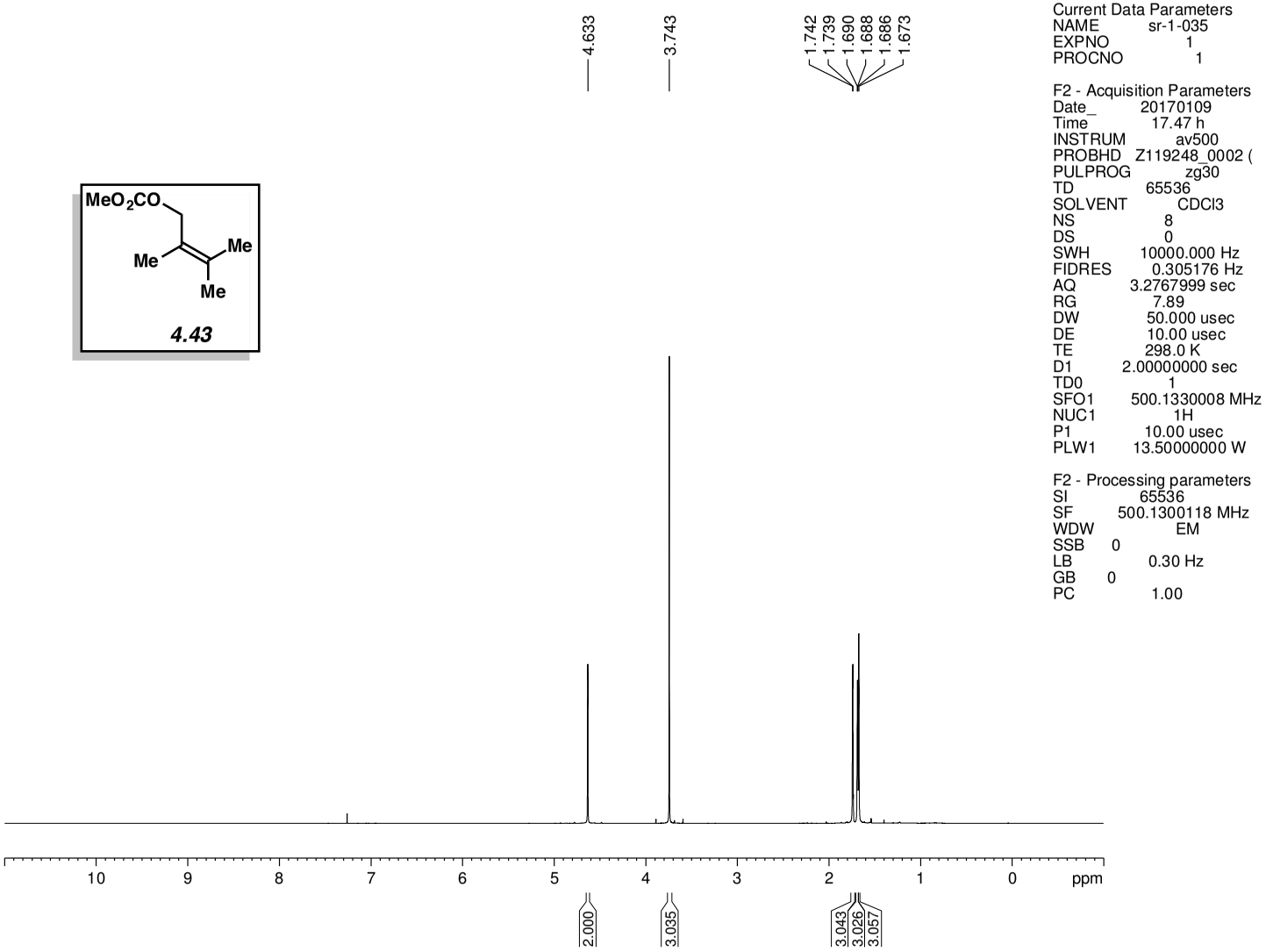

Figure 4.33 ^{1}H NMR (500 MHz, $CDCl_3$) of compound **4.43**.

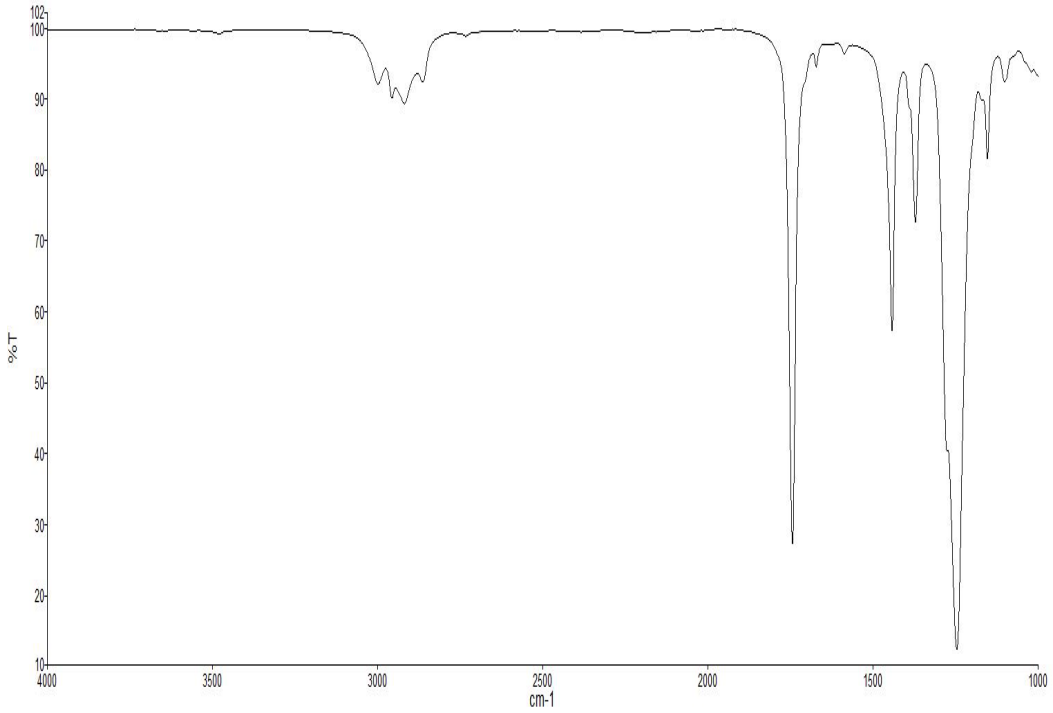

Figure 4.34 Infrared spectrum of compound **4.43**.

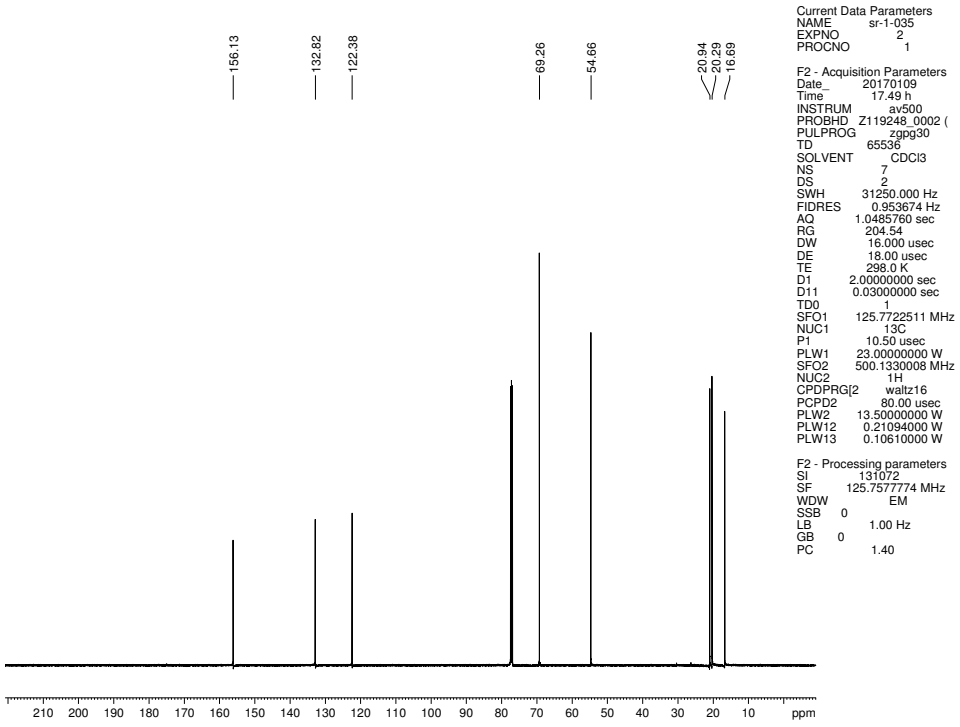

Figure 4.35 ^{13}C NMR (125 MHz, $CDCl_3$) of compound **4.43**.

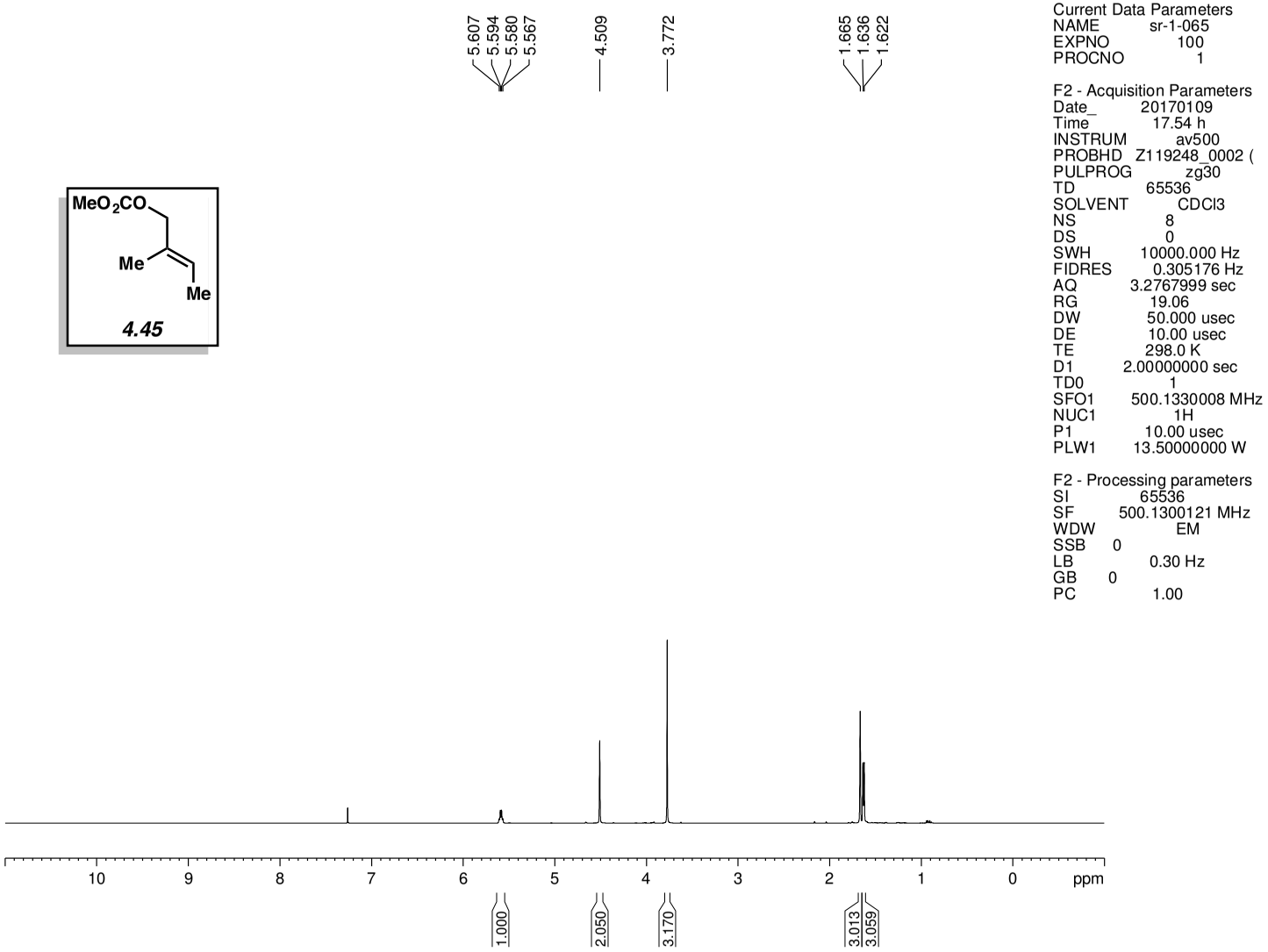

Figure 4.36 ^{1}H NMR (500 MHz, $CDCl_3$) of compound **4.45**.

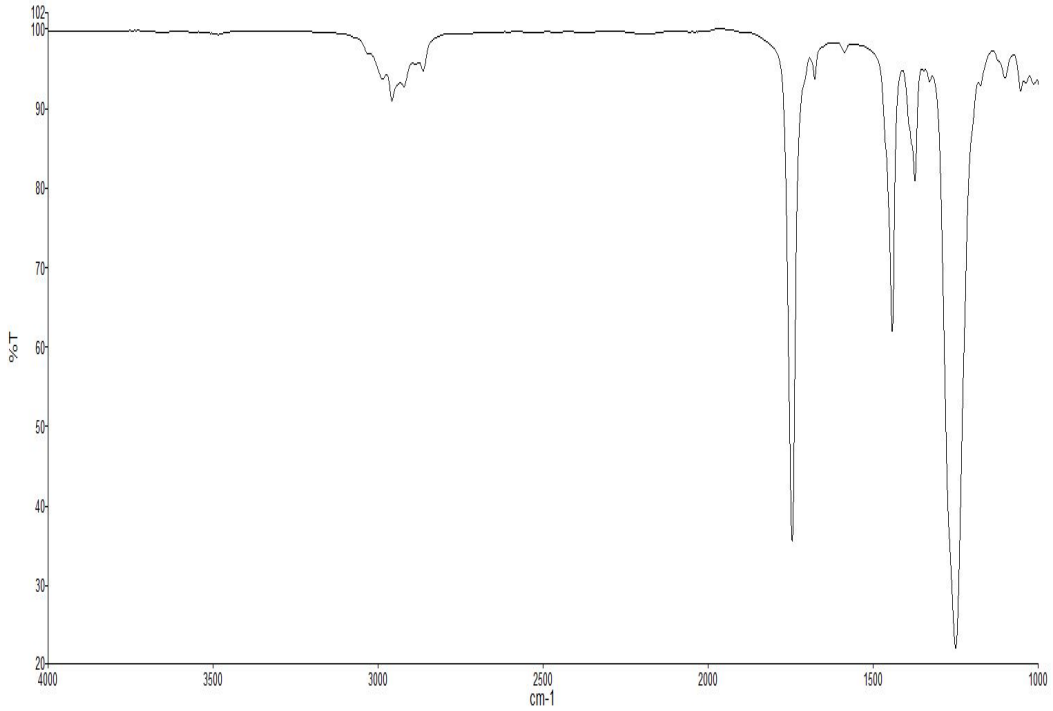

Figure 4.37 Infrared spectrum of compound **4.45**.

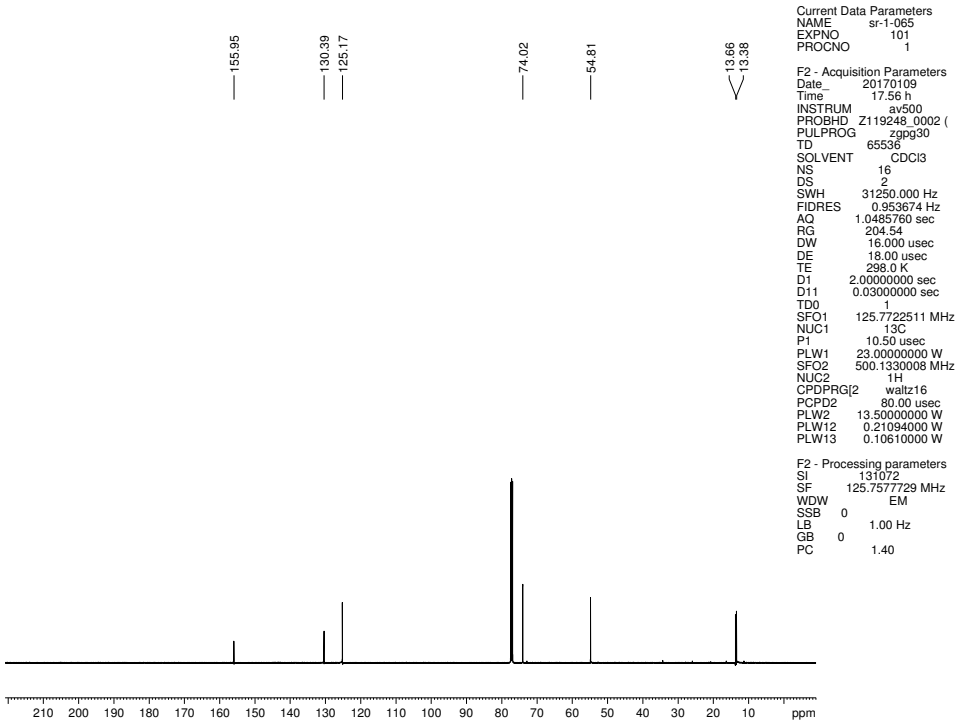

Figure 4.38 ^{13}C NMR (125 MHz, $CDCl_3$) of compound **4.45**.

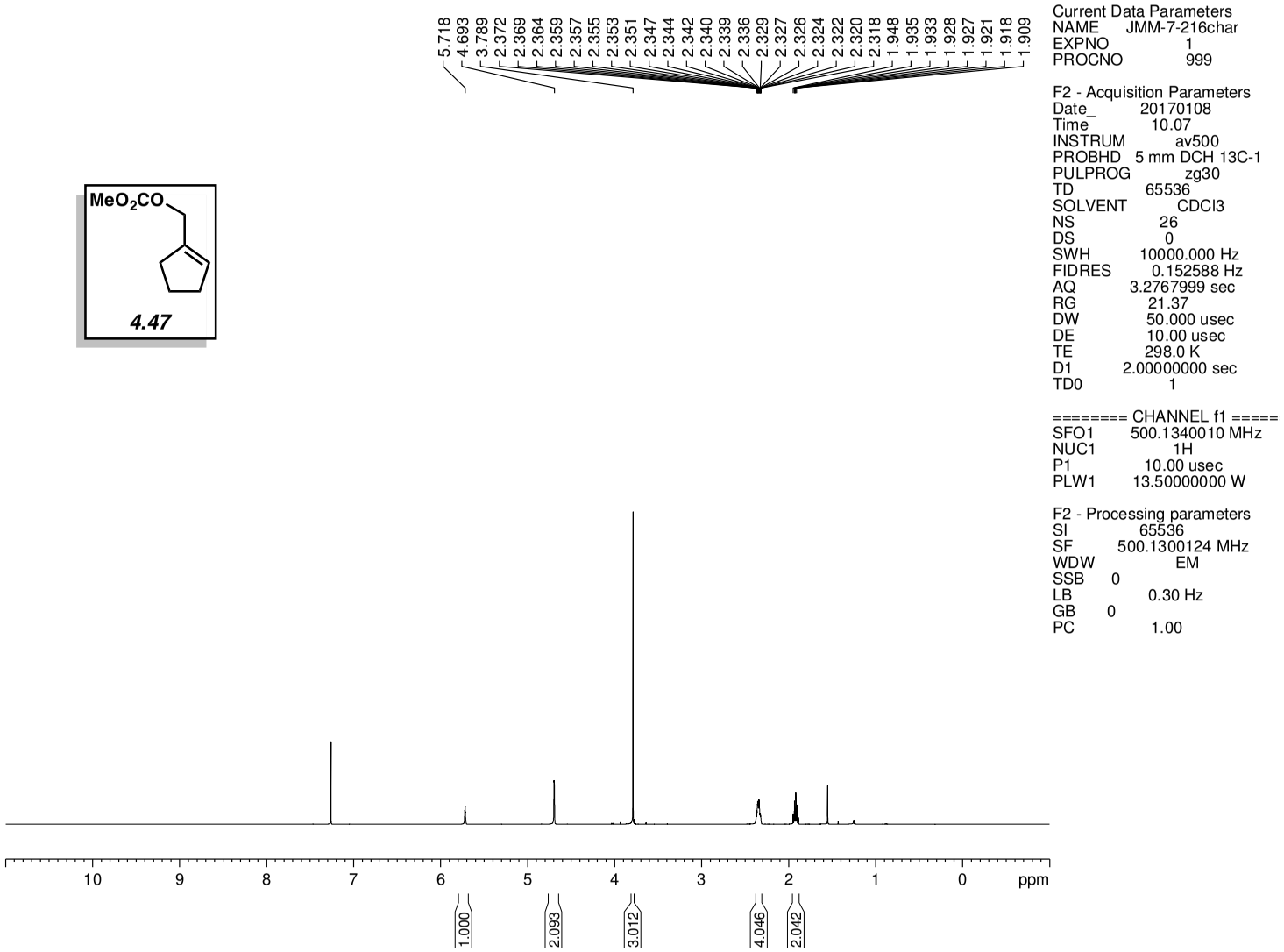

Figure 4.39 ^{1}H NMR (500 MHz, $CDCl_3$) of compound **4.47**.

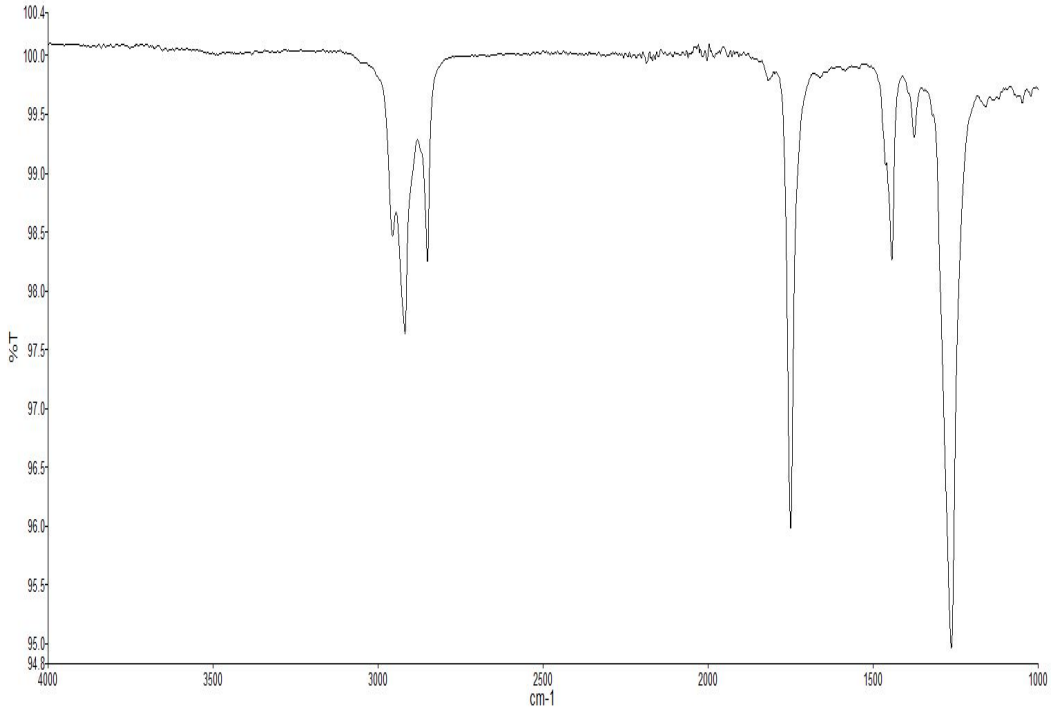

Figure 4.40 Infrared spectrum of compound **4.47**.

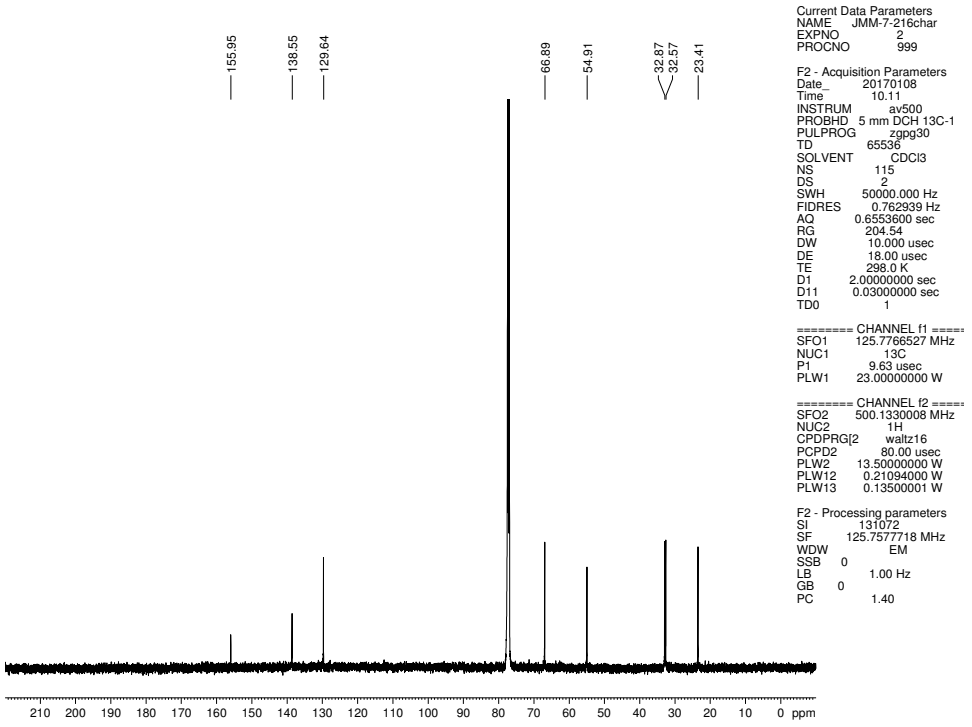

Figure 4.41 ^{13}C NMR (125 MHz, $CDCl_3$) of compound **4.47**.

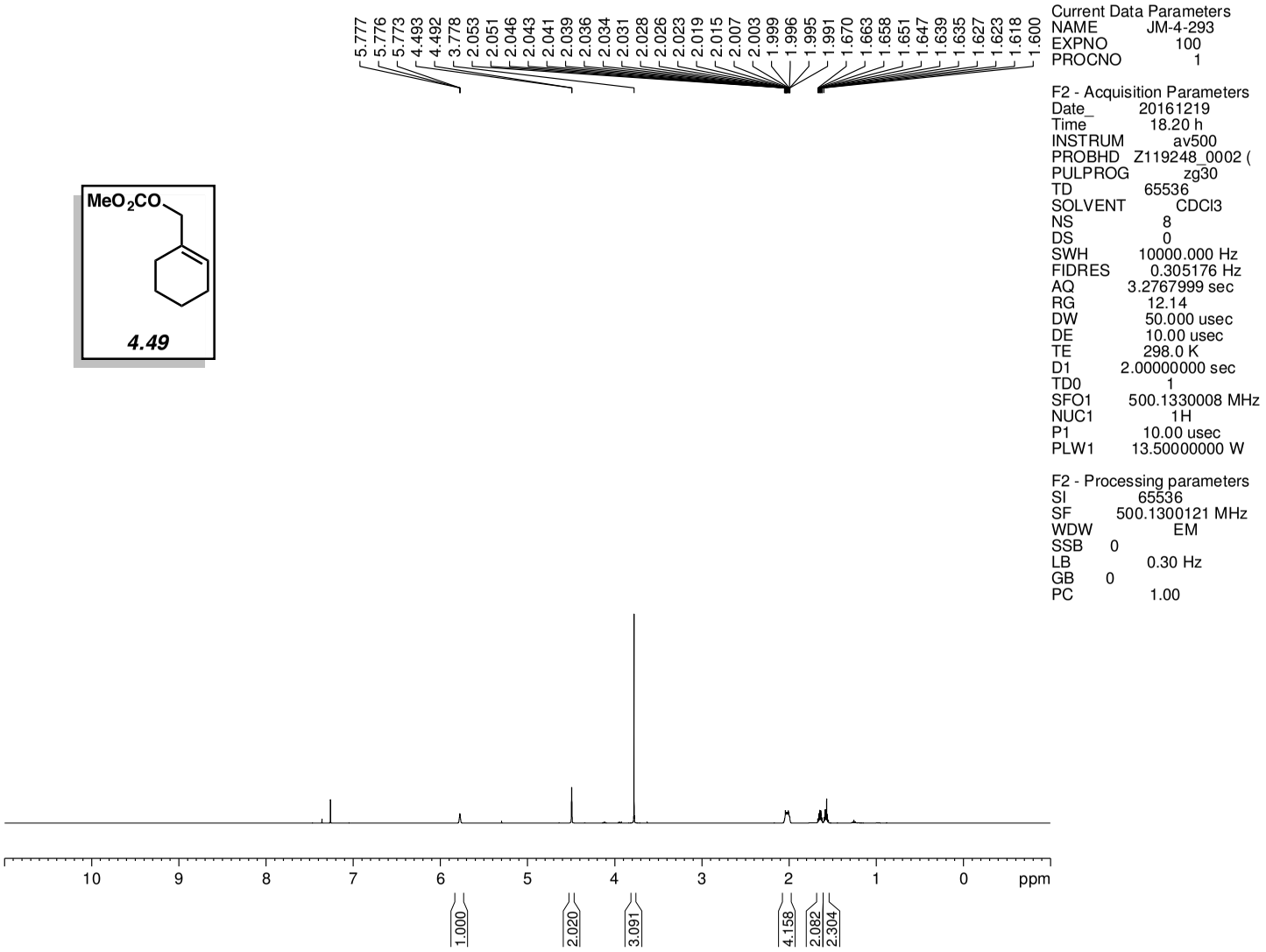

Figure 4.42 ^{1}H NMR (500 MHz, $CDCl_3$) of compound **4.49**.

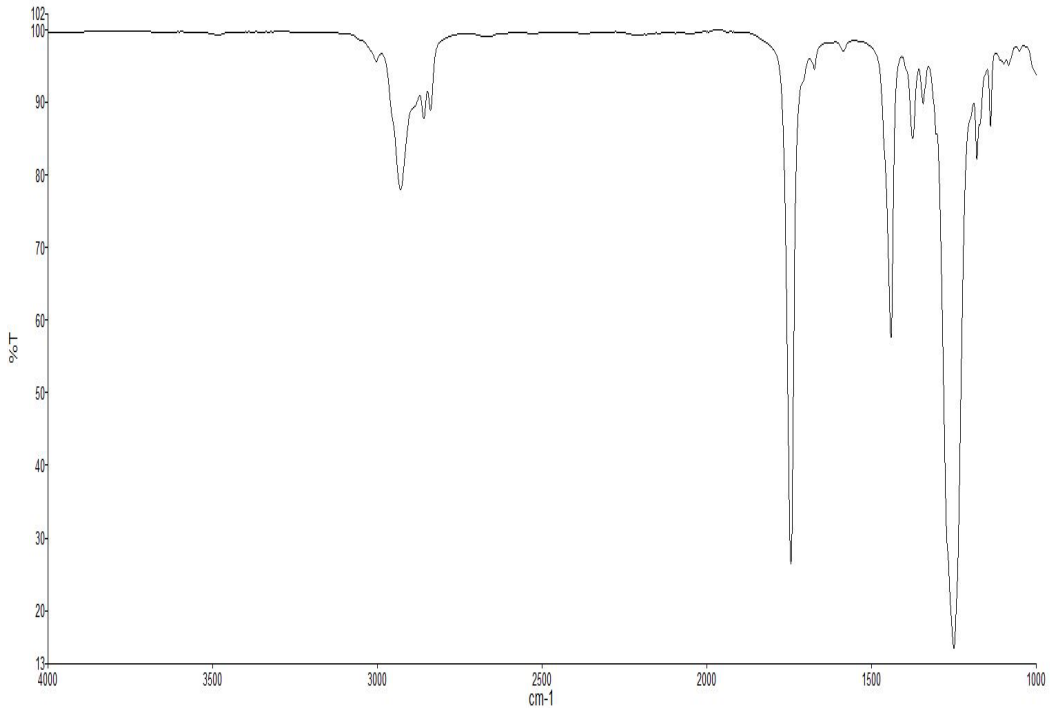

Figure 4.43 Infrared spectrum of compound **4.49**.

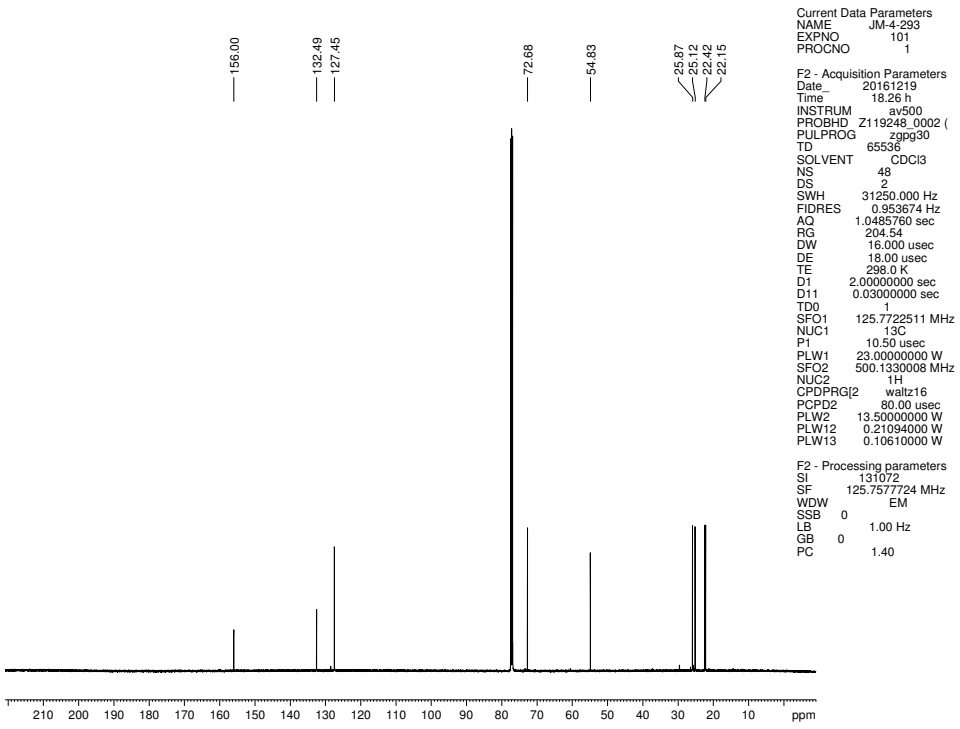

Figure 4.44 ^{13}C NMR (125 MHz, $CDCl_3$) of compound **4.49**.

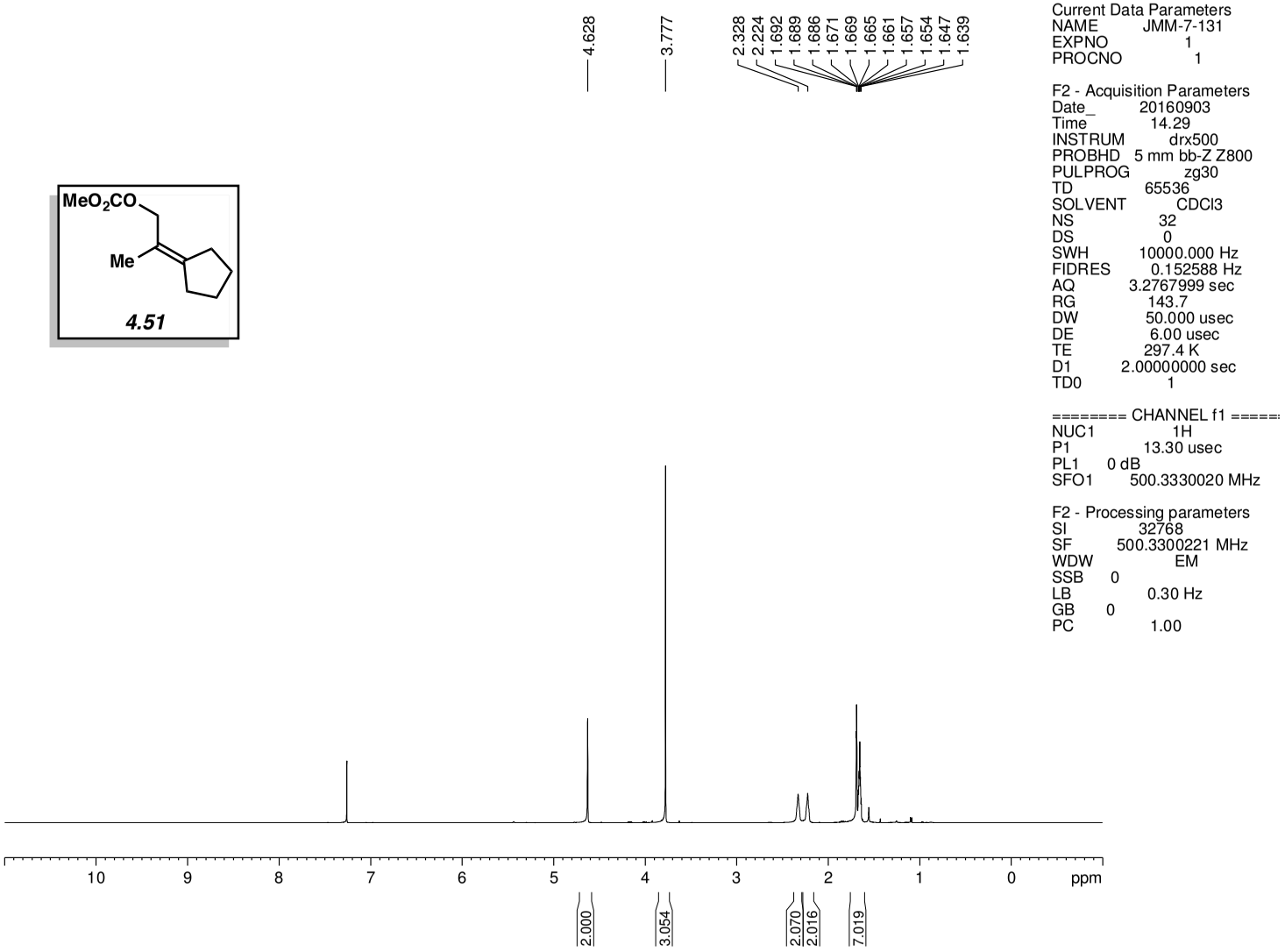

Figure 4.45 ^{1}H NMR (500 MHz, $CDCl_3$) of compound **4.51**.

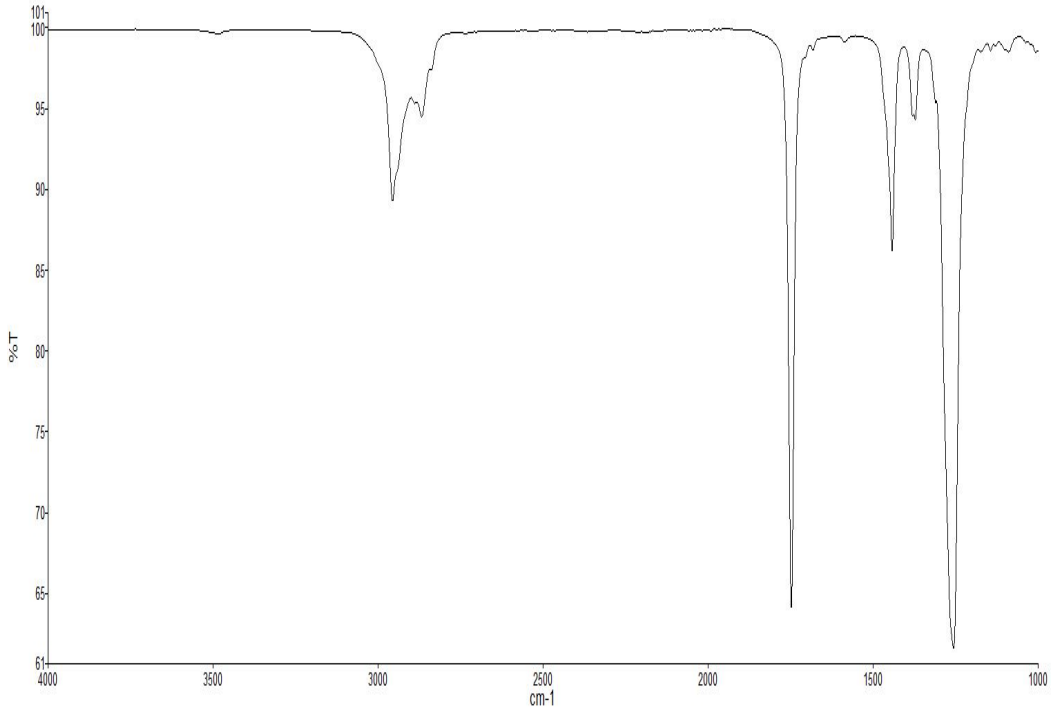

Figure 4.46 Infrared spectrum of compound **4.51**.

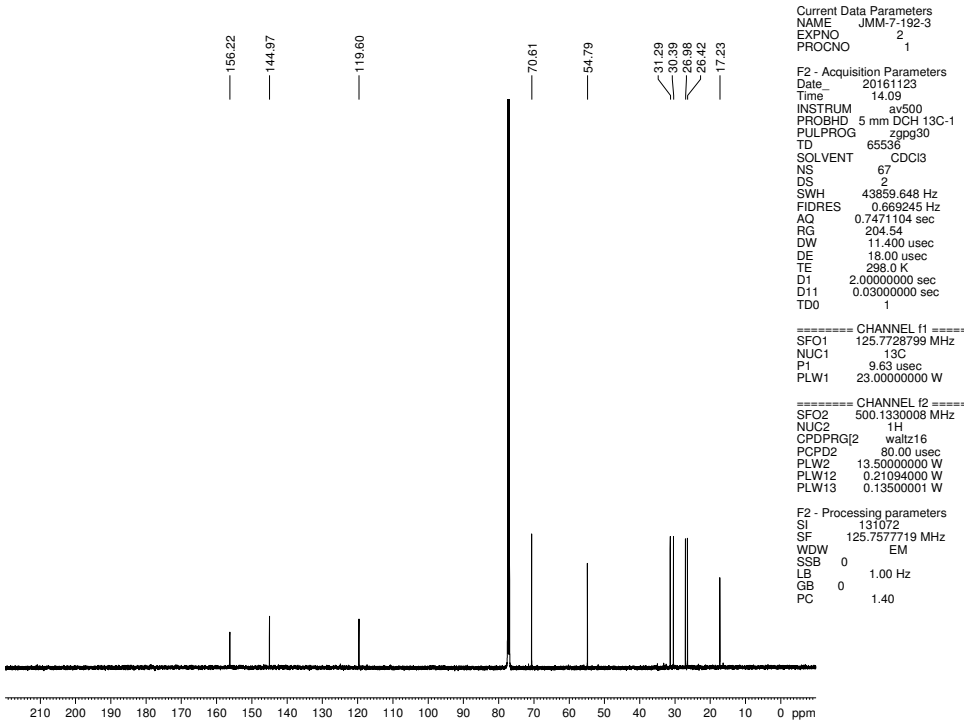

Figure 4.47 ^{13}C NMR (125 MHz, $CDCl_3$) of compound **4.51**.

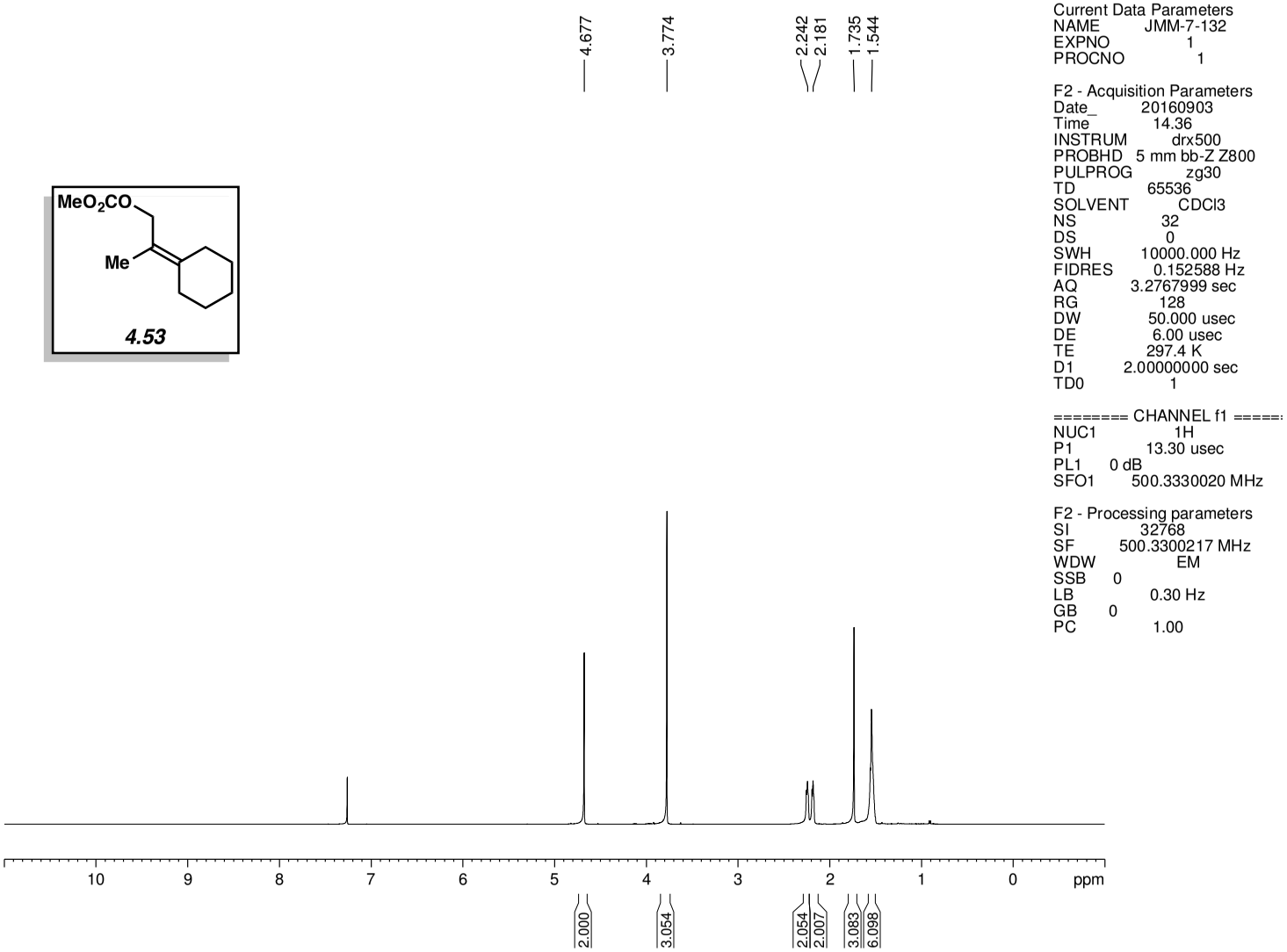

Figure 4.48 ^{1}H NMR (500 MHz, $CDCl_3$) of compound **4.53**.

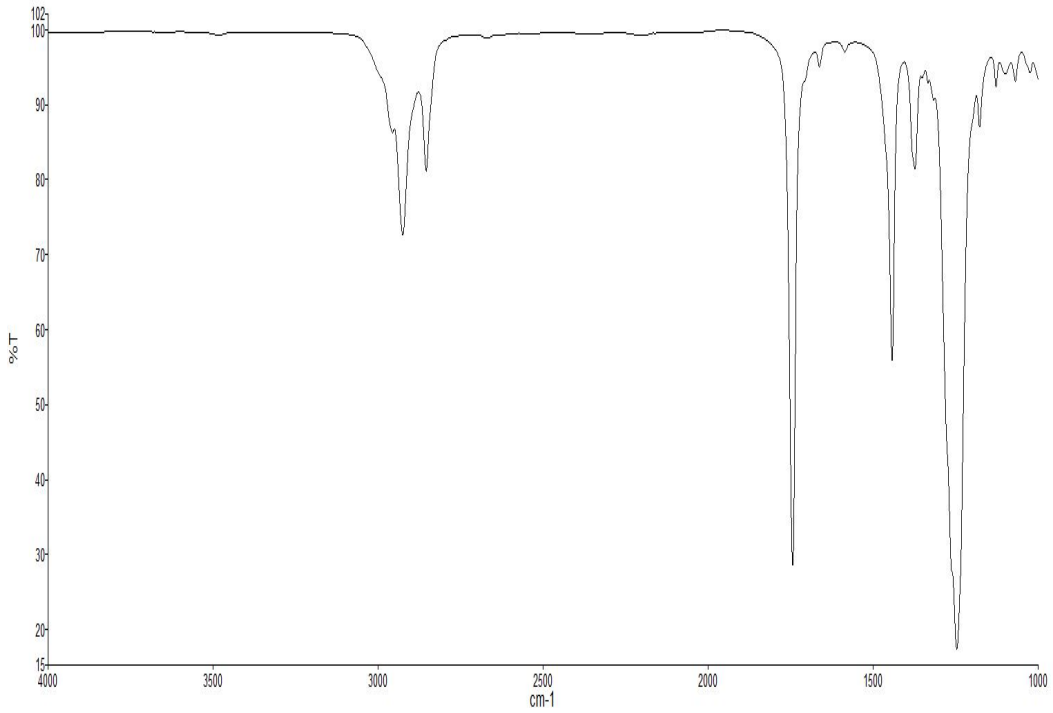

Figure 4.49 Infrared spectrum of compound **4.53**.

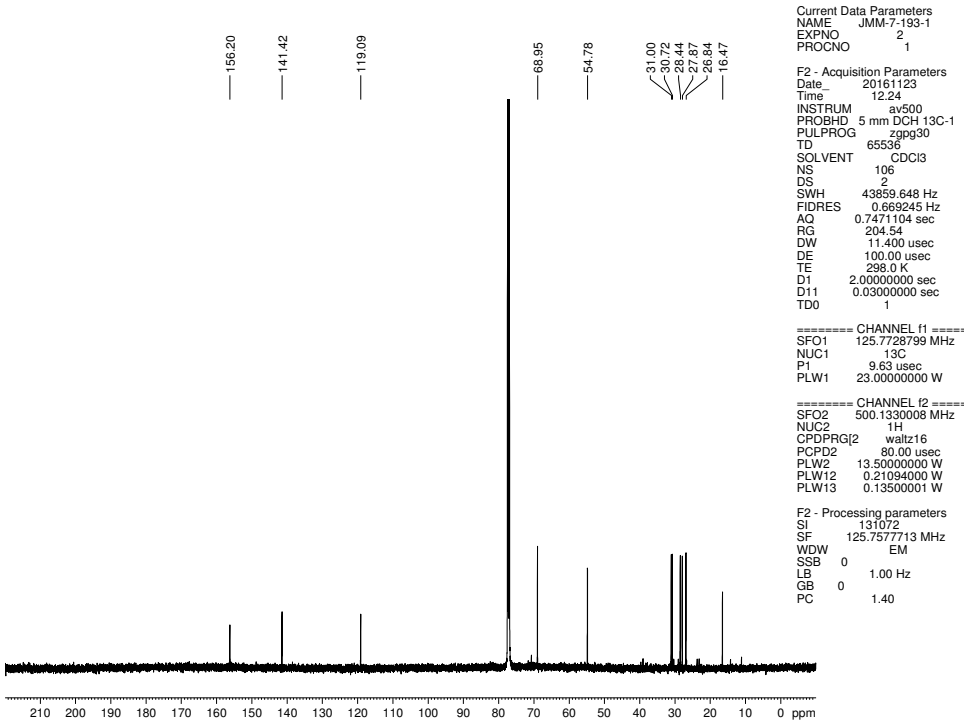

Figure 4.50 ^{13}C NMR (125 MHz, $CDCl_3$) of compound **4.53**.

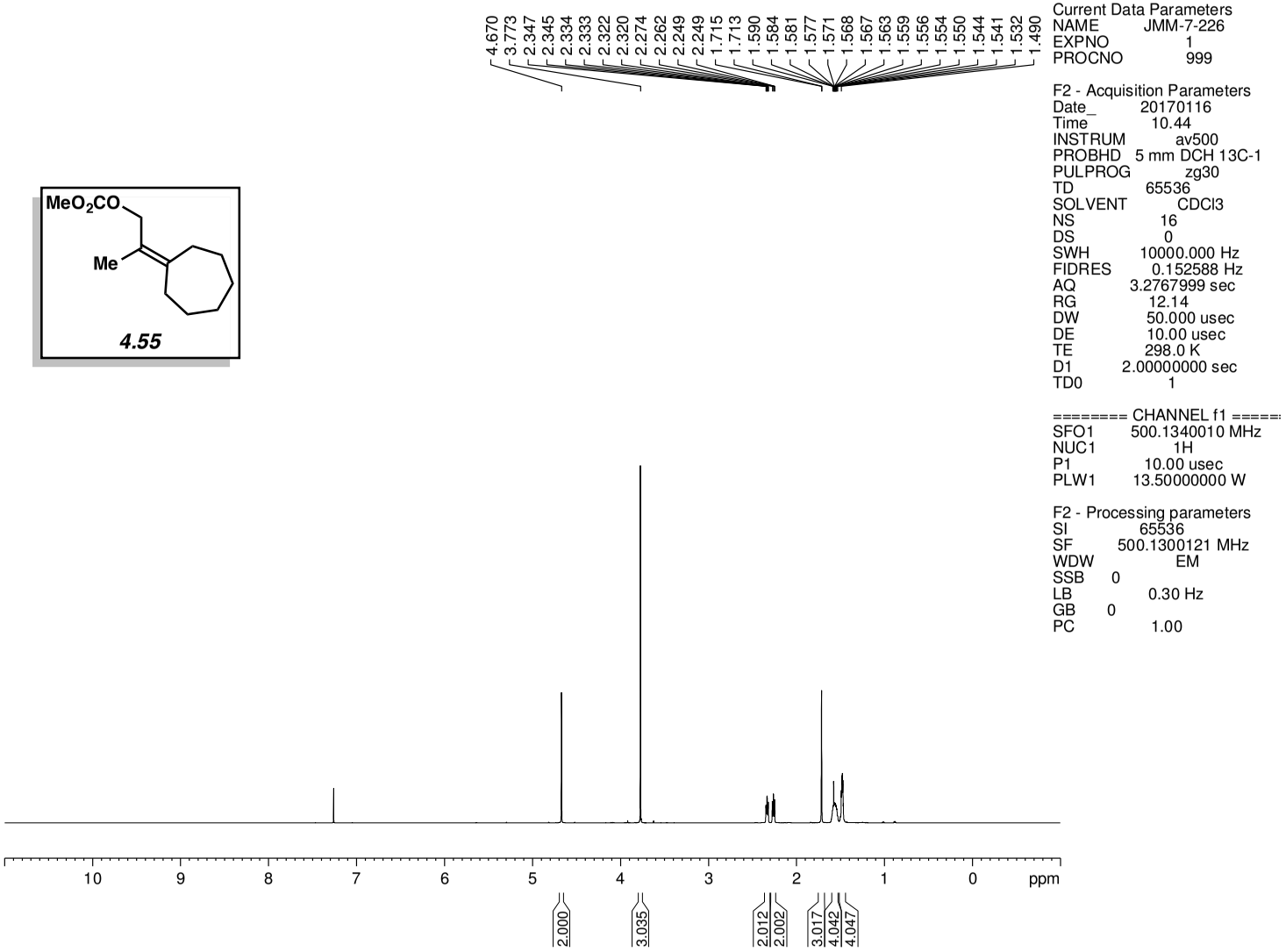

Figure 4.51 ^{1}H NMR (500 MHz, $CDCl_3$) of compound **4.55**.

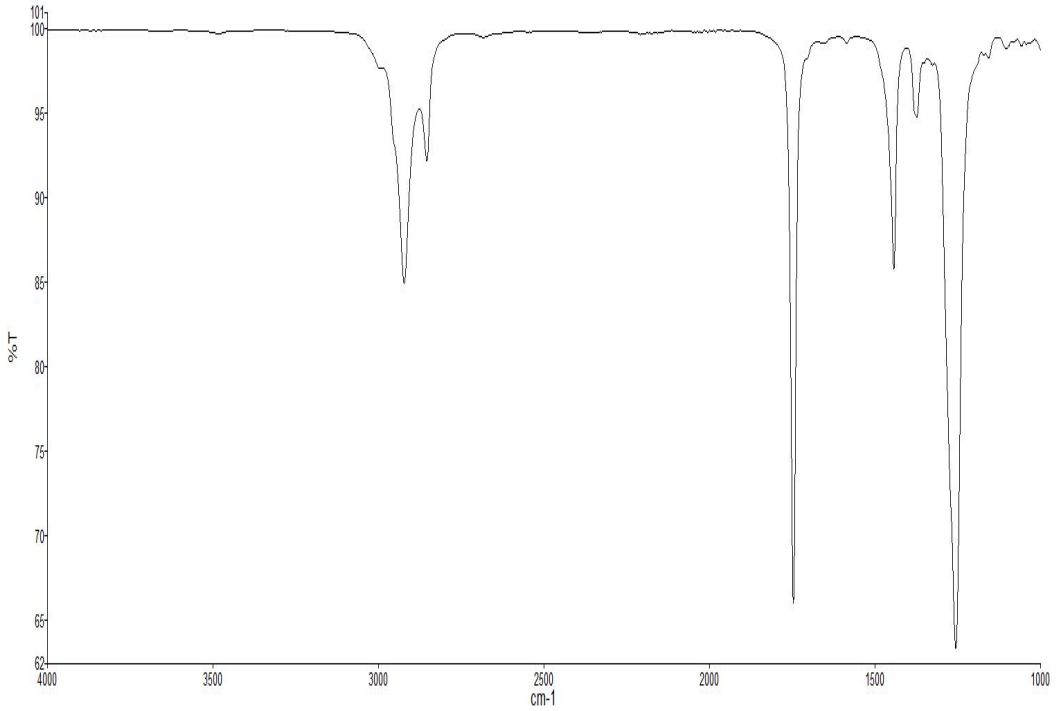

Figure 4.52 Infrared spectrum of compound **4.55**.

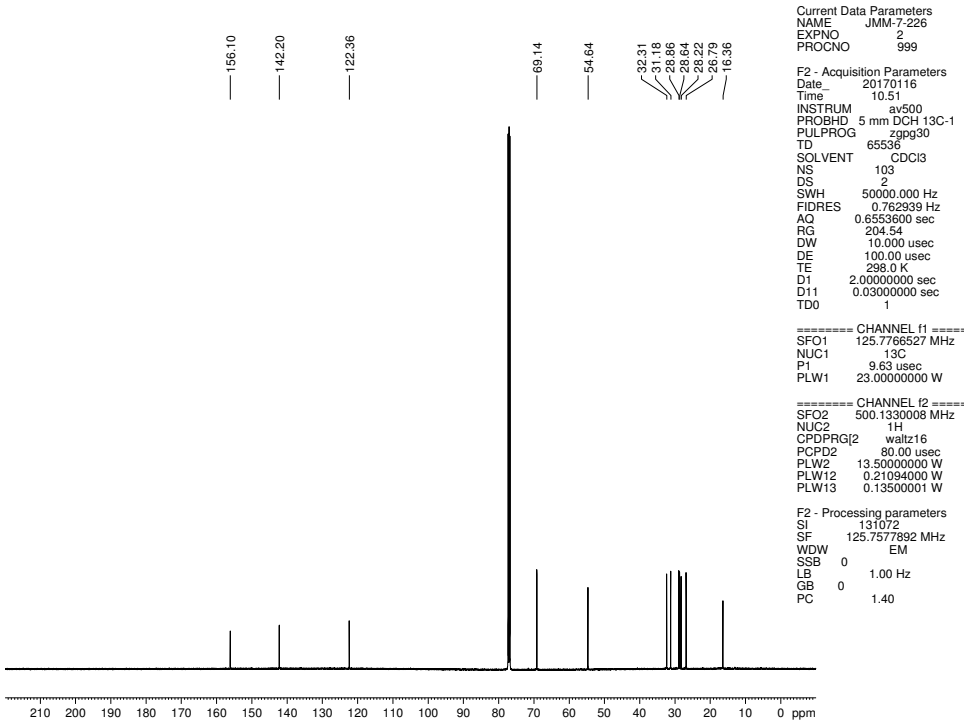

Figure 4.53 ^{13}C NMR (125 MHz, $CDCl_3$) of compound **4.55**.

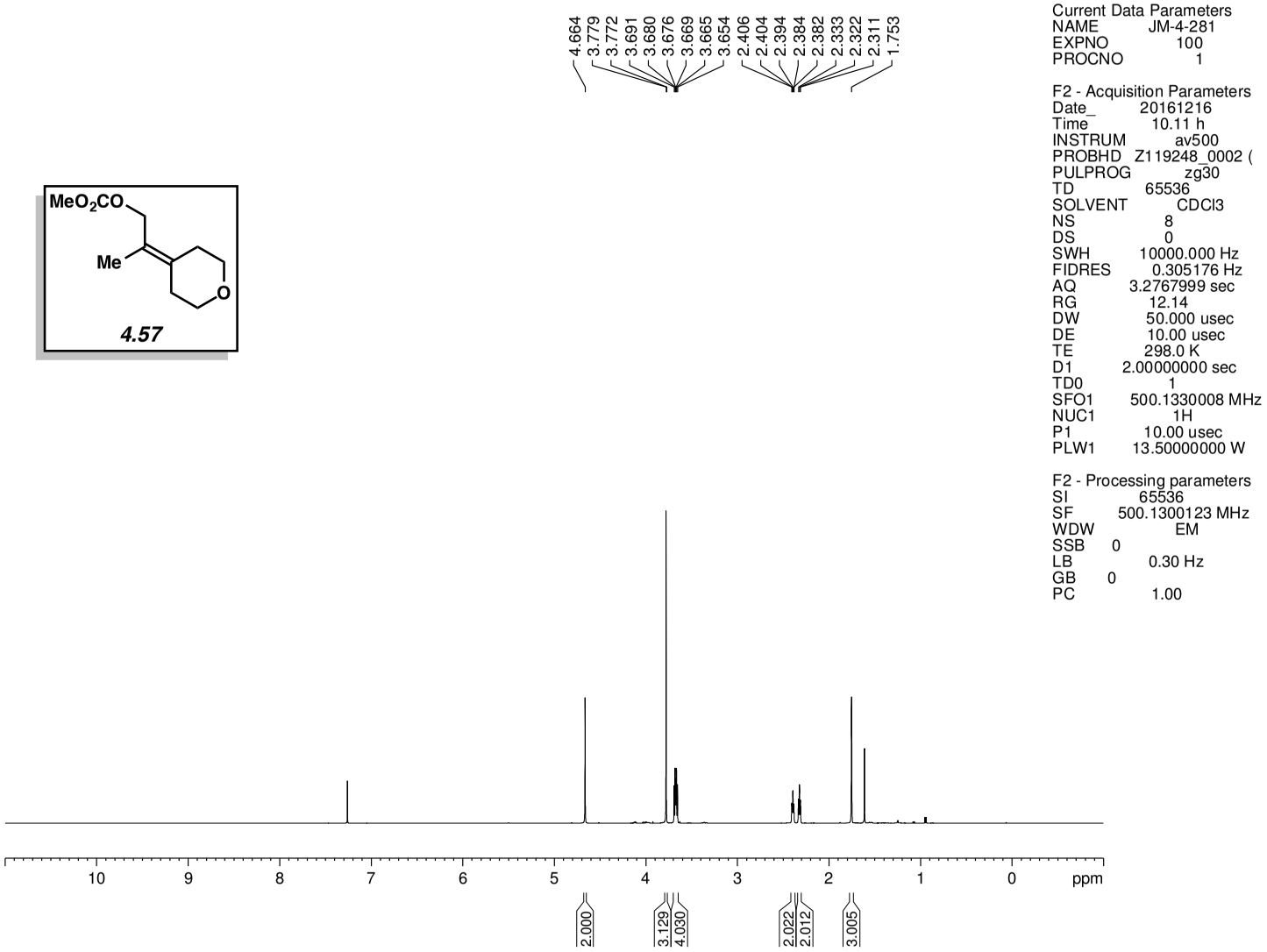

Figure 4.54 ^{1}H NMR (500 MHz, $CDCl_3$) of compound **4.57**.

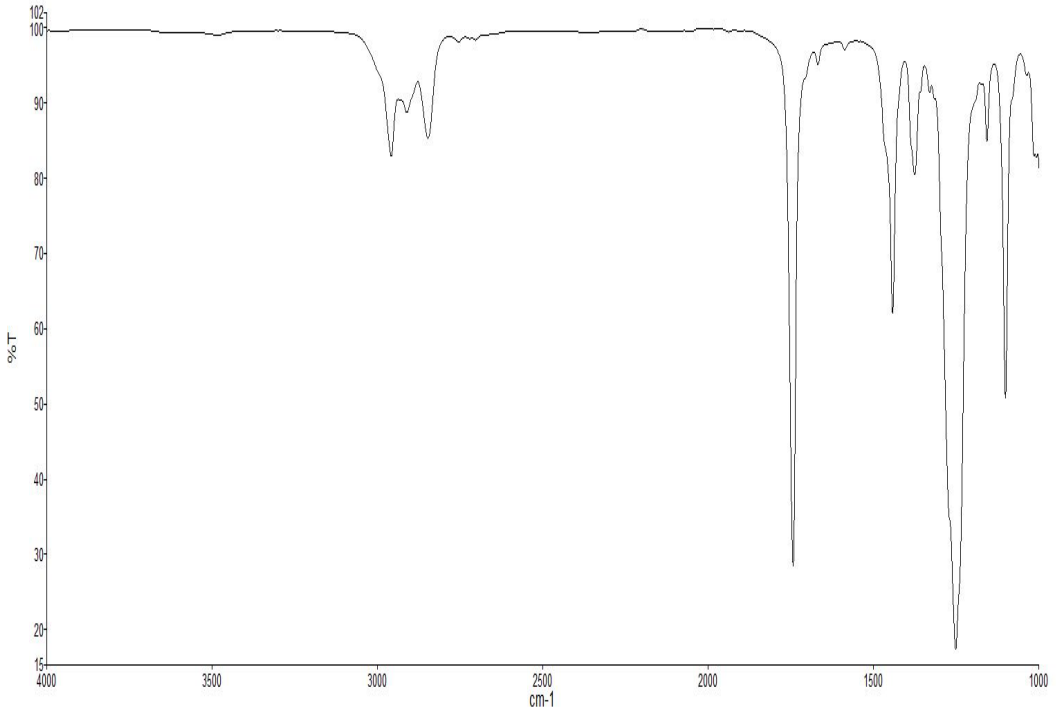

Figure 4.55 Infrared spectrum of compound **4.57**.

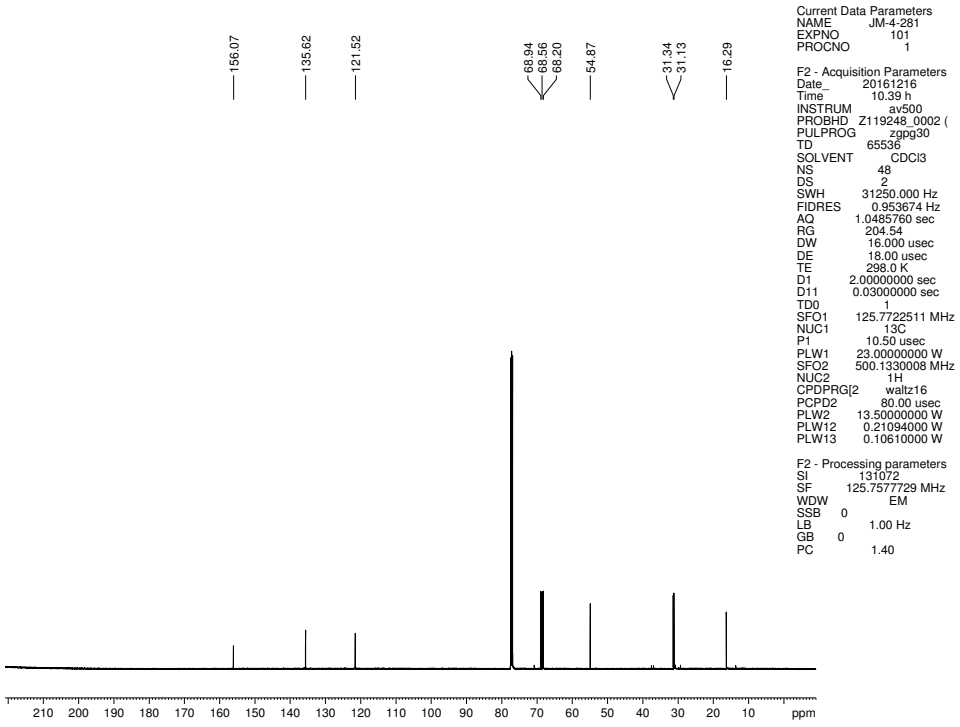

Figure 4.56 ^{13}C NMR (125 MHz, $CDCl_3$) of compound **4.57**.

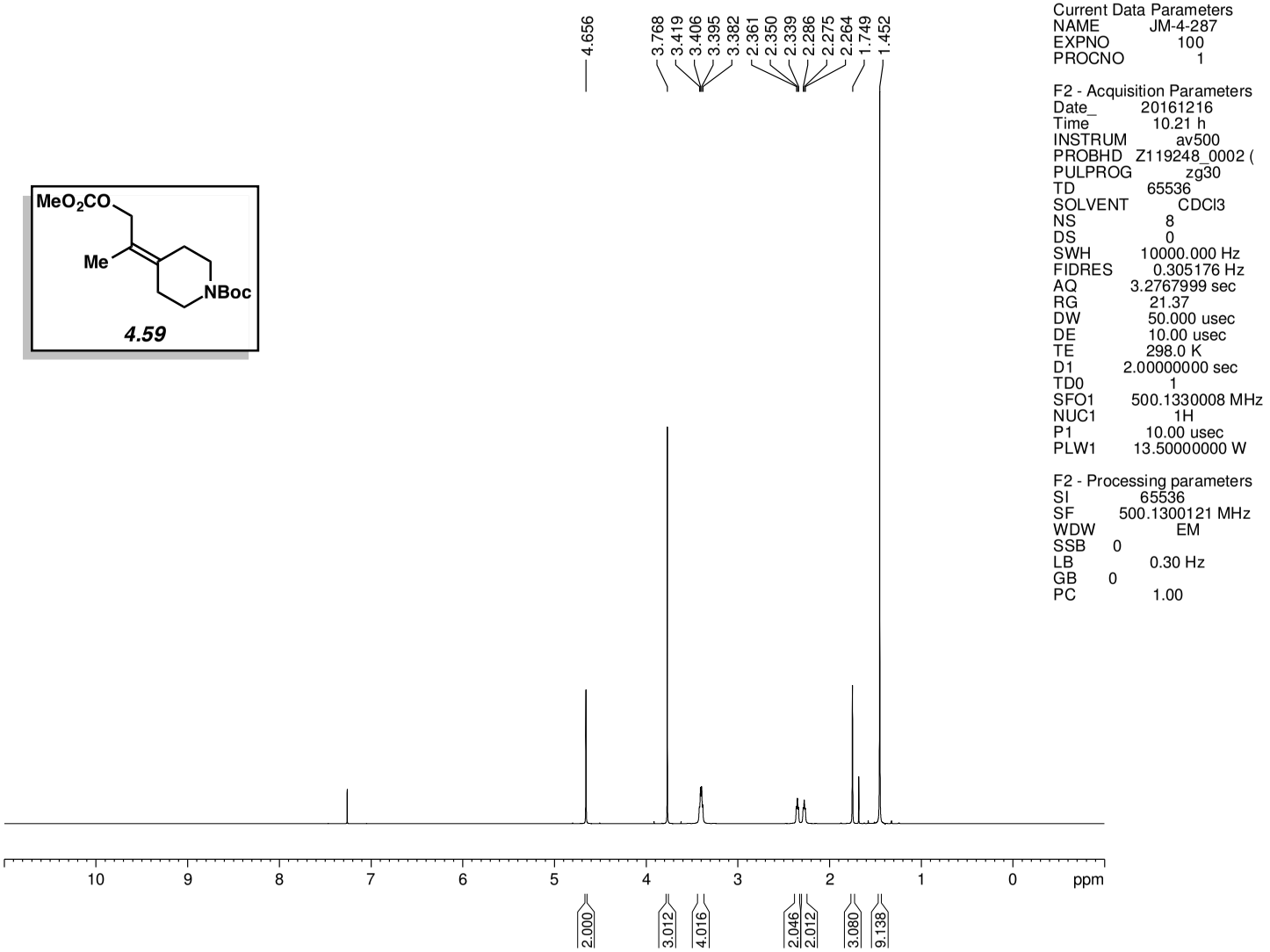

Figure 4.57 ^{1}H NMR (500 MHz, $CDCl_3$) of compound **4.59**.

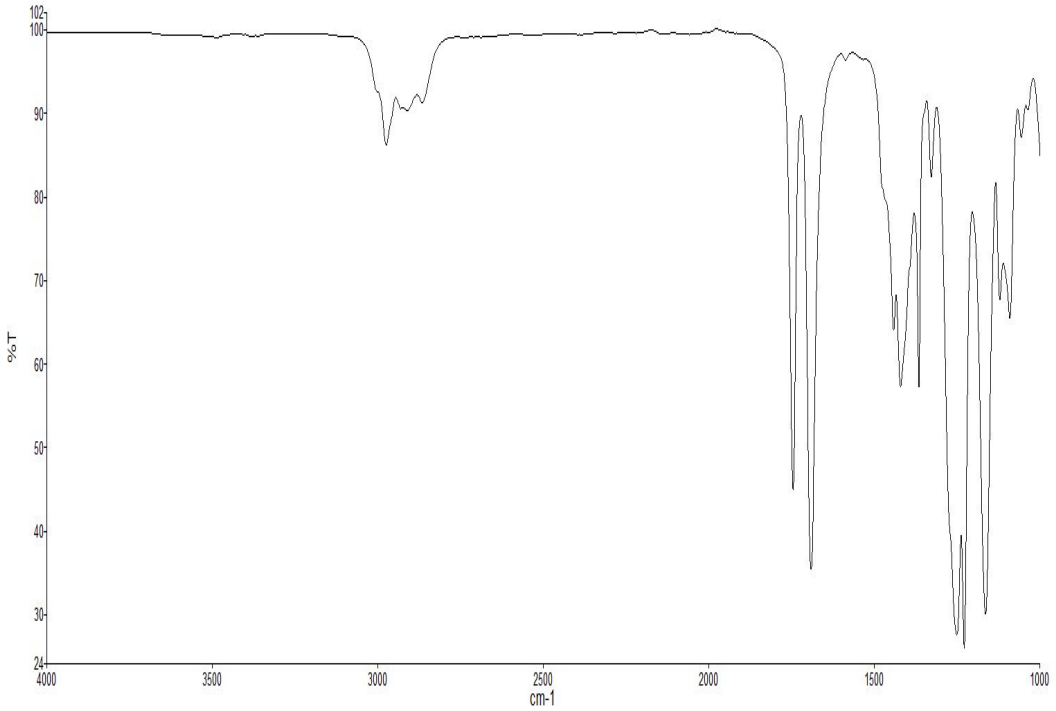

Figure 4.58 Infrared spectrum of compound **4.59**.

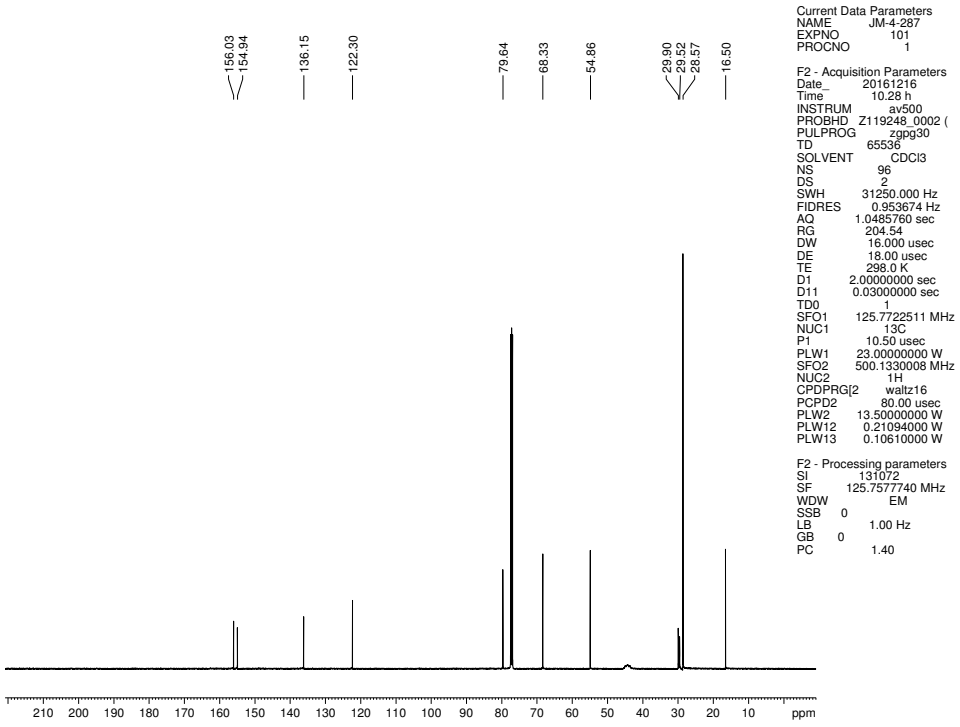

Figure 4.59 ^{13}C NMR (125 MHz, $CDCl_3$) of compound **4.59**.

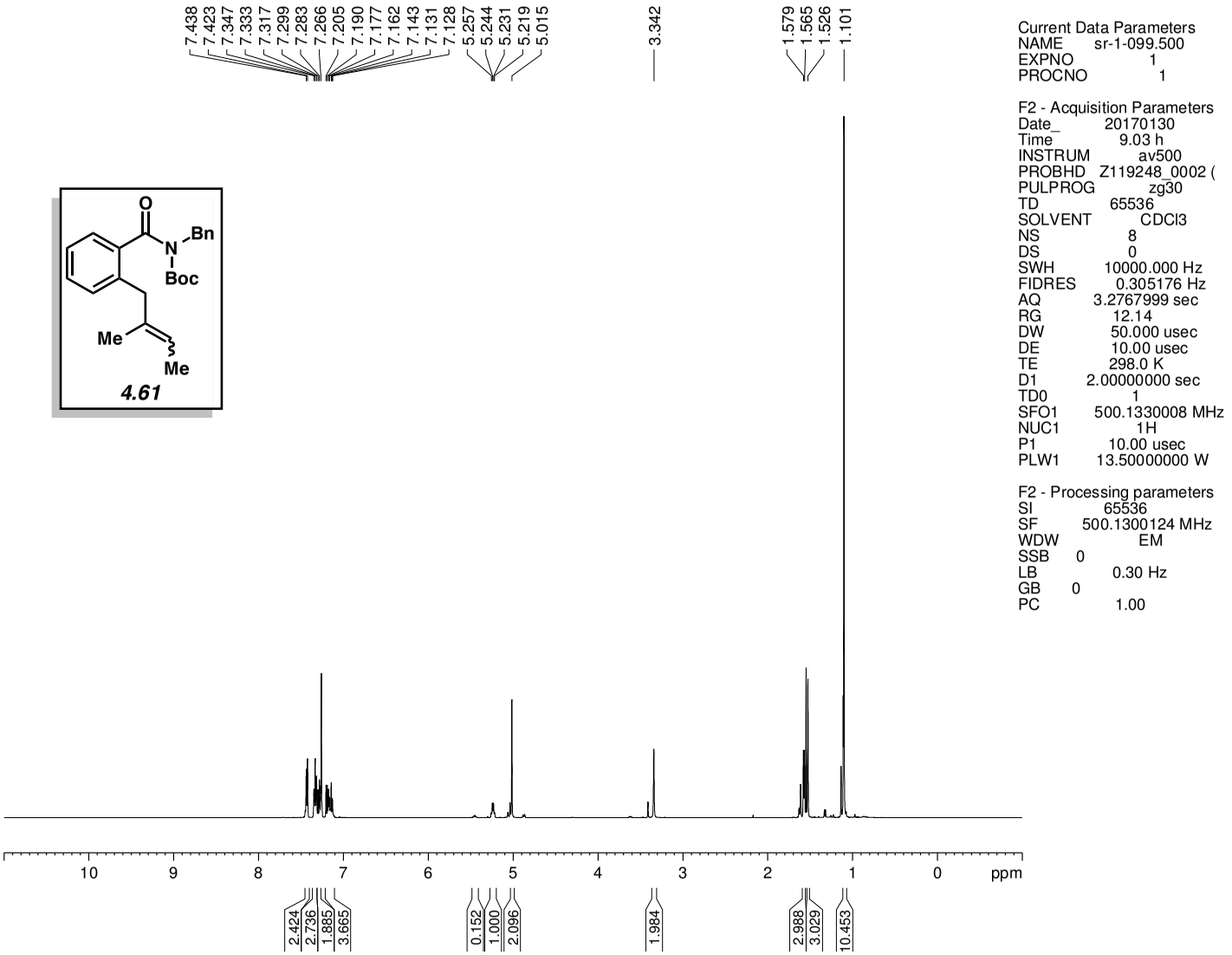

Figure 4.60 ^{1}H NMR (500 MHz, $CDCl_3$) of compound **4.61**.

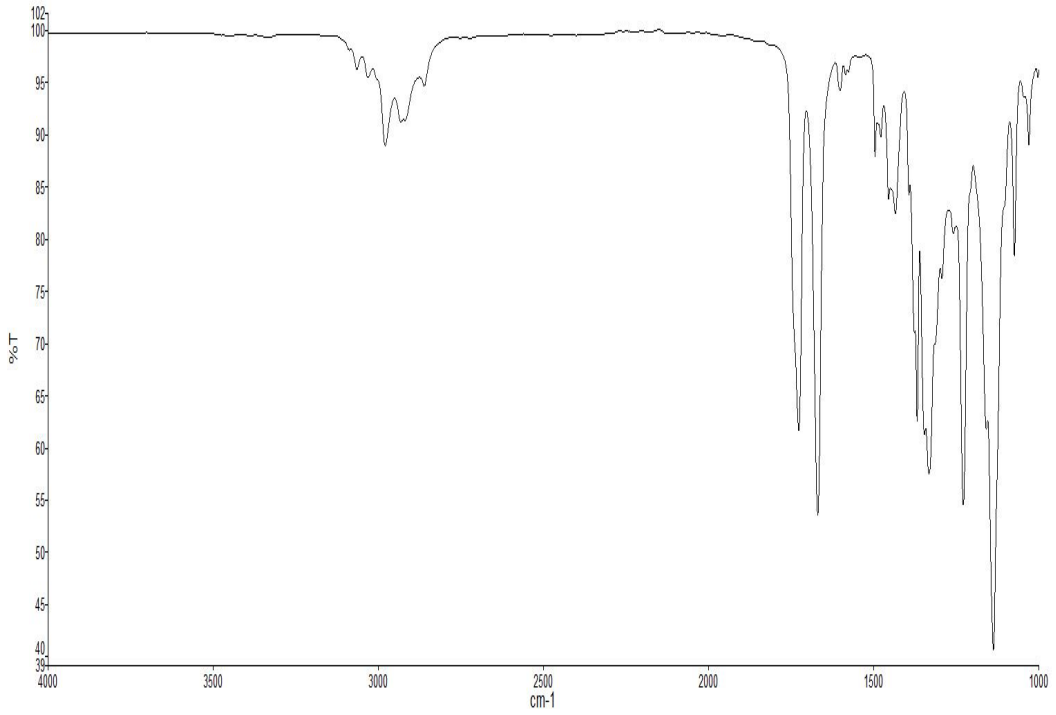

Figure 4.61 Infrared spectrum of compound **4.61**.

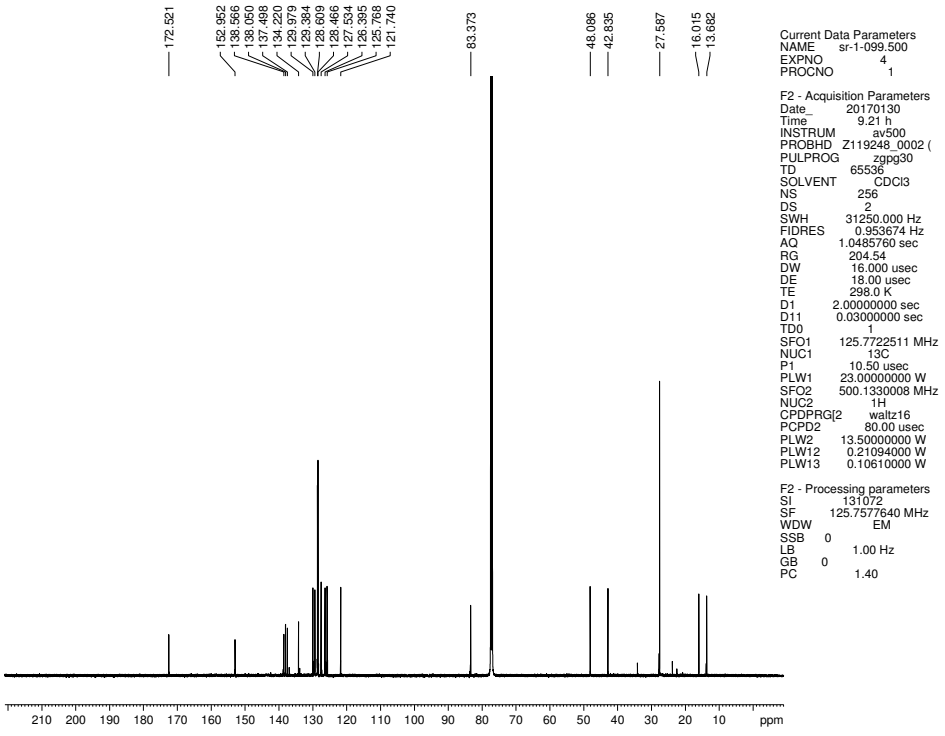

Figure 4.62 ^{13}C NMR (125 MHz, $CDCl_3$) of compound **4.61**.

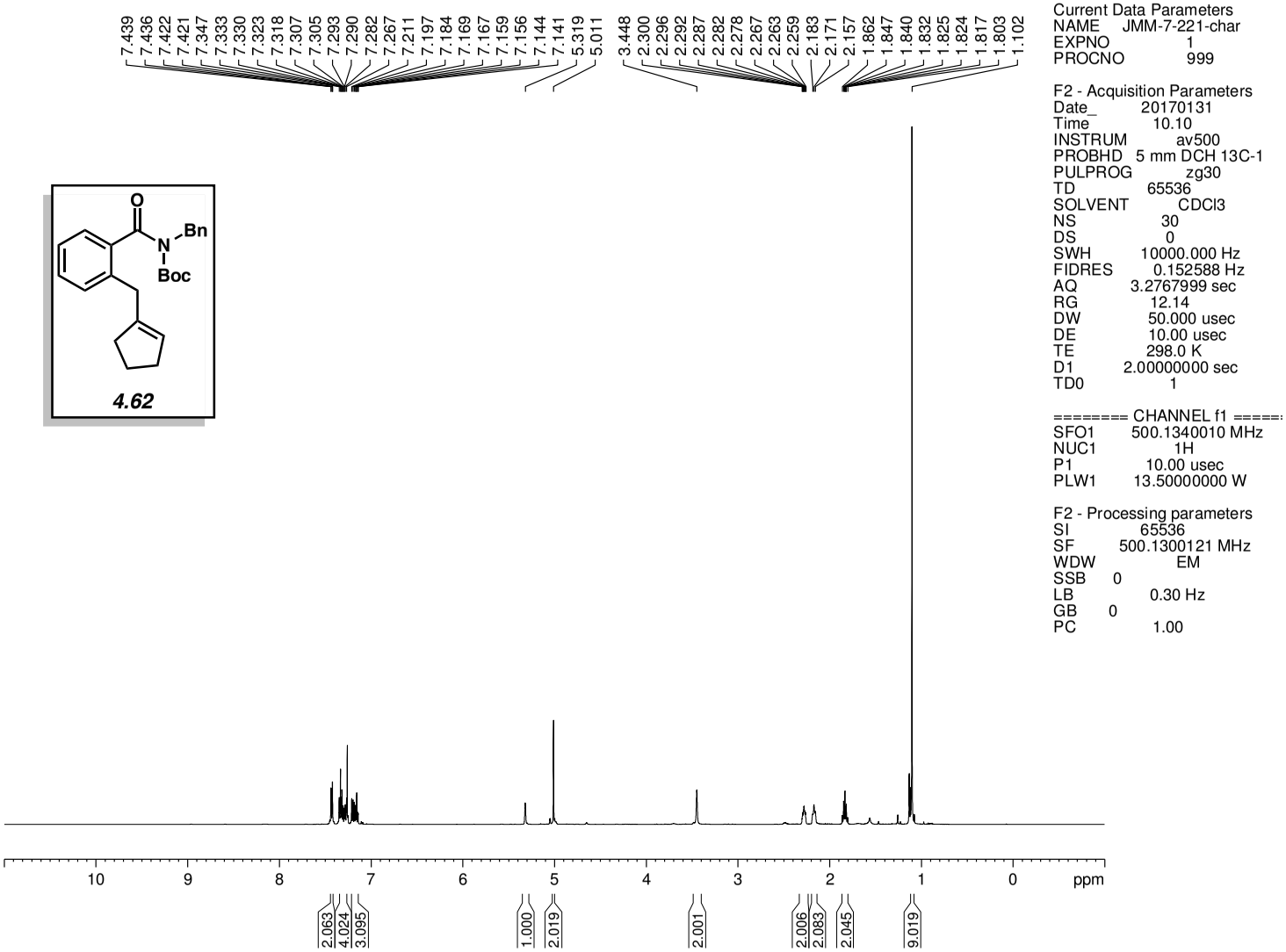

Figure 4.63 ^{1}H NMR (500 MHz, $CDCl_3$) of compound **4.62**.

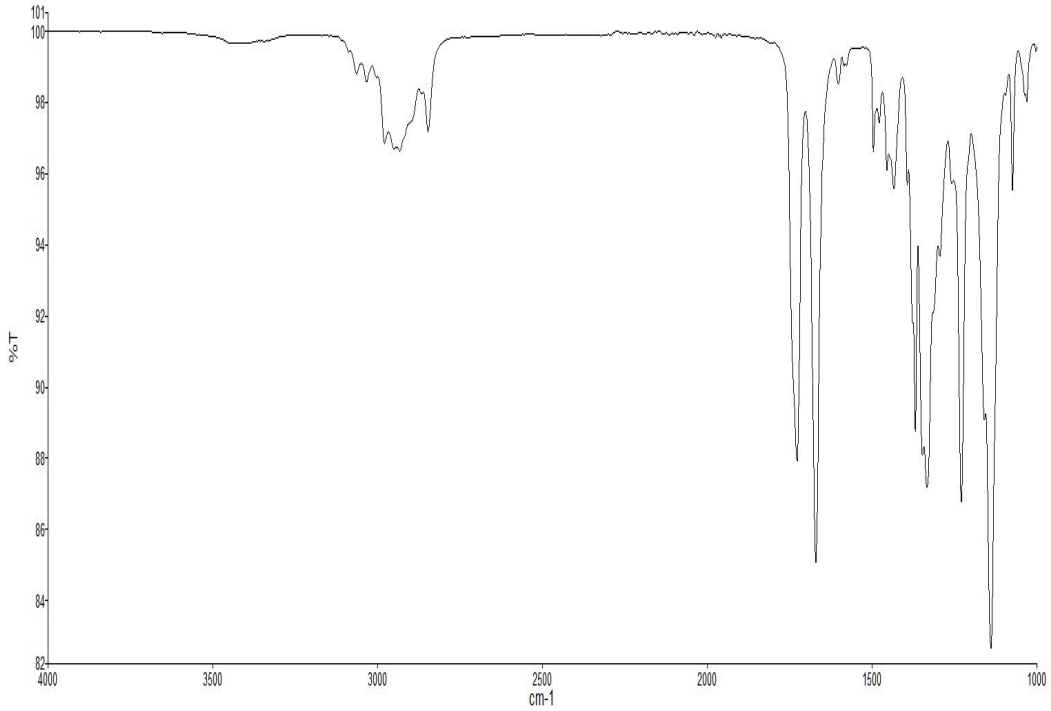

Figure 4.64 Infrared spectrum of compound **4.62**.

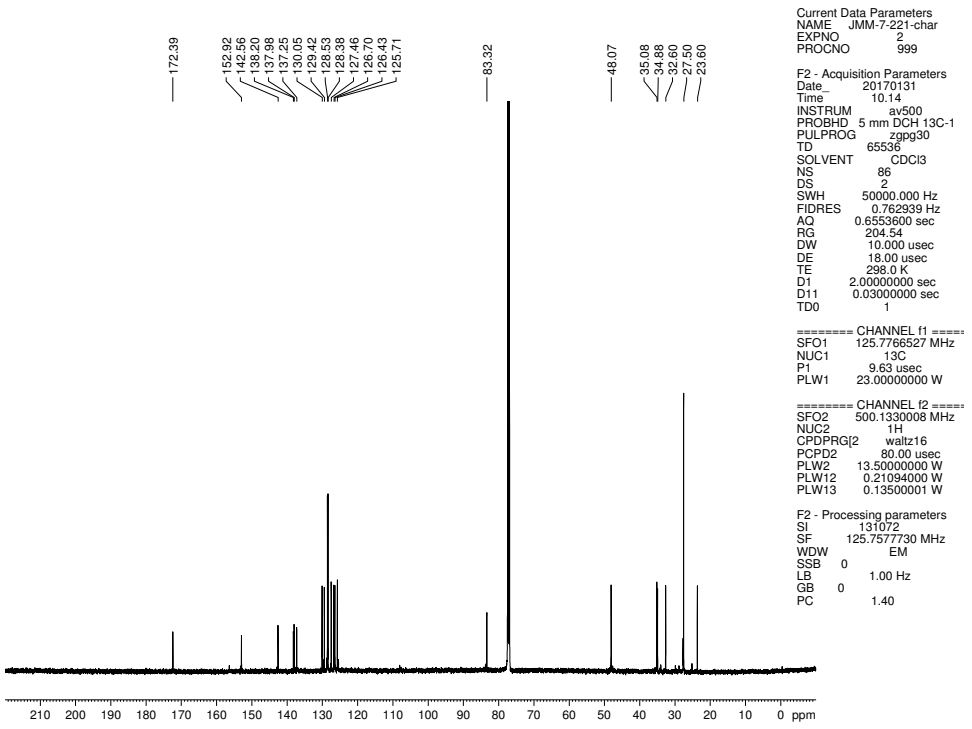

Figure 4.65 ^{13}C NMR (125 MHz, $CDCl_3$) of compound **4.62**.

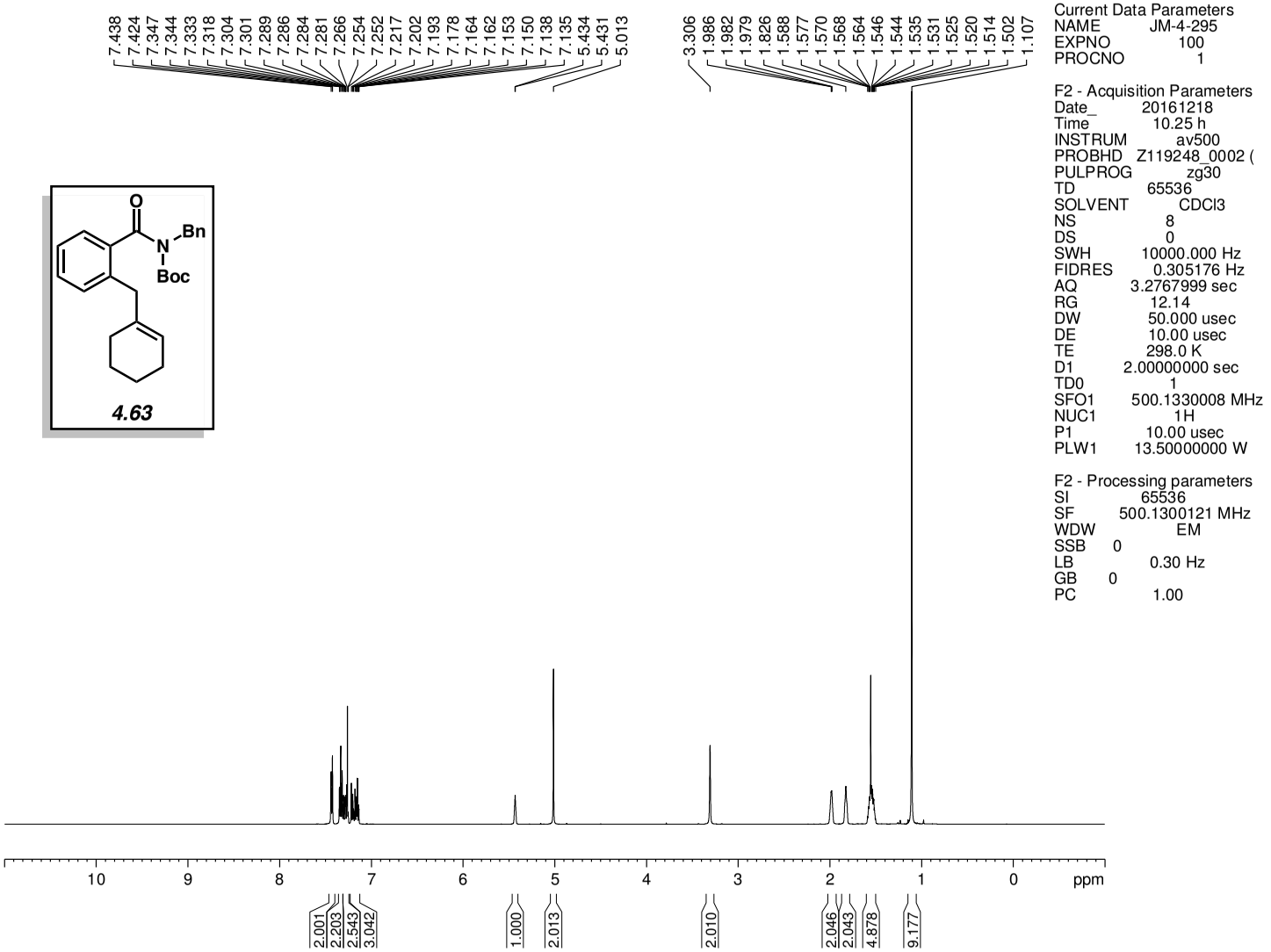

Figure 4.66 ^{1}H NMR (500 MHz, $CDCl_3$) of compound **4.63**.

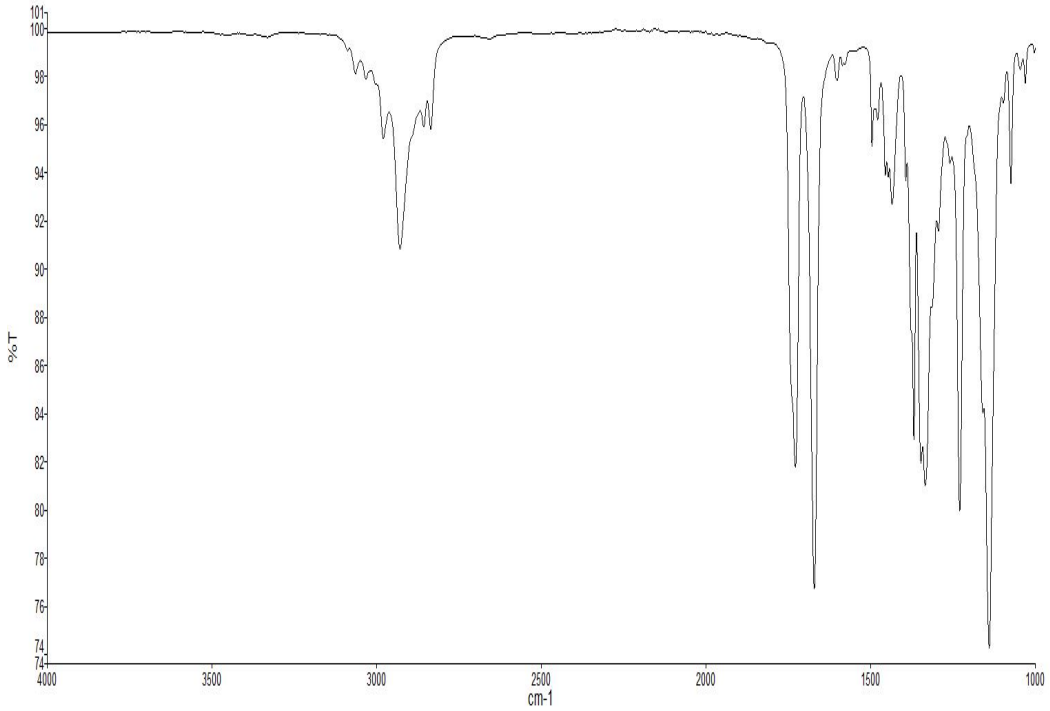

Figure 4.67 Infrared spectrum of compound **4.63**.

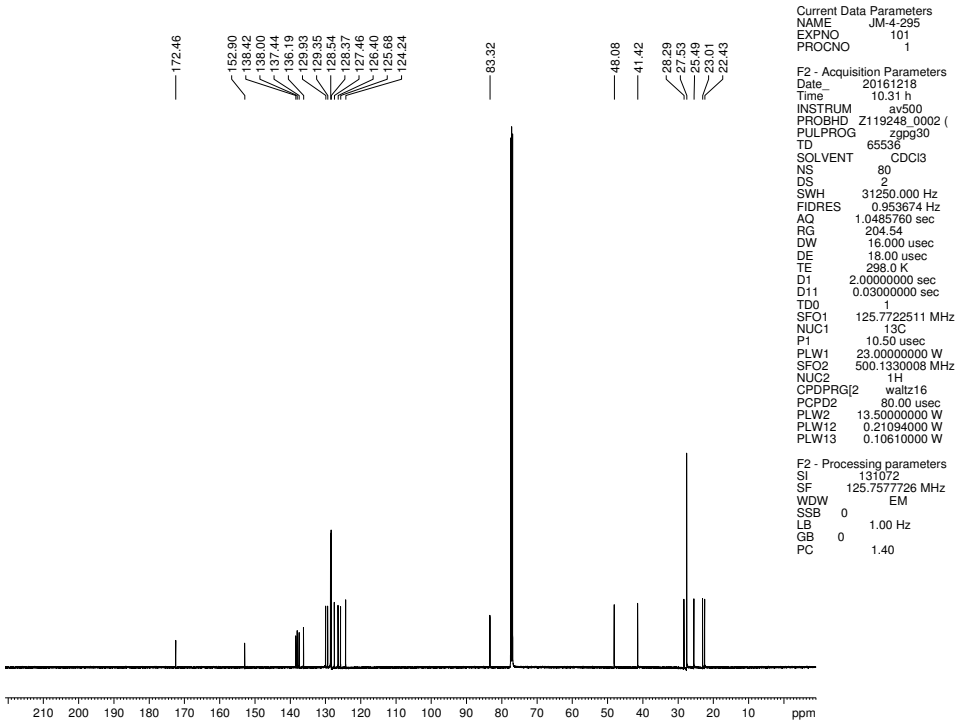

Figure 4.68 ^{13}C NMR (125 MHz, $CDCl_3$) of compound **4.63**.

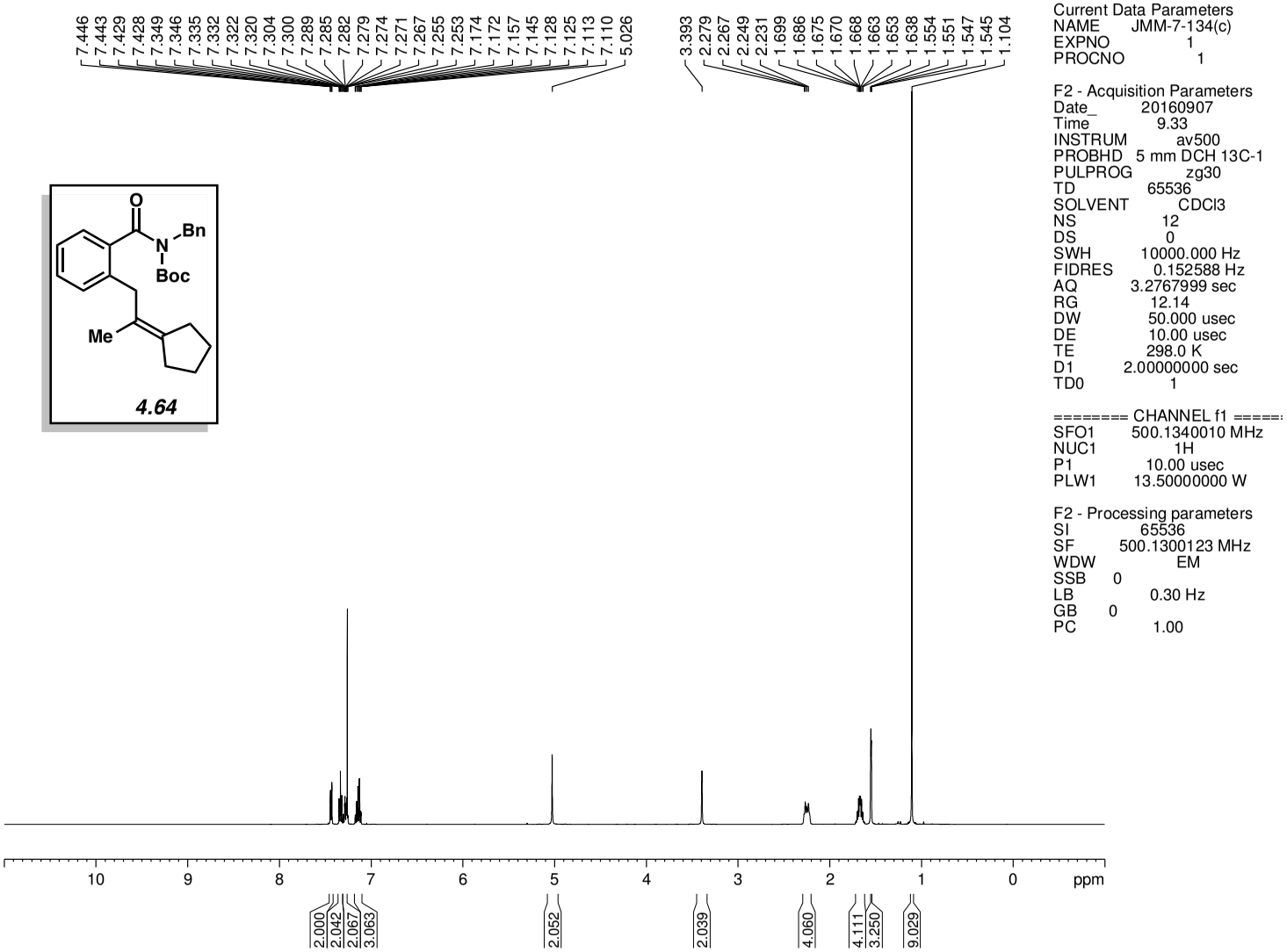

Figure 4.69 ^{1}H NMR (500 MHz, $CDCl_3$) of compound **4.64**.

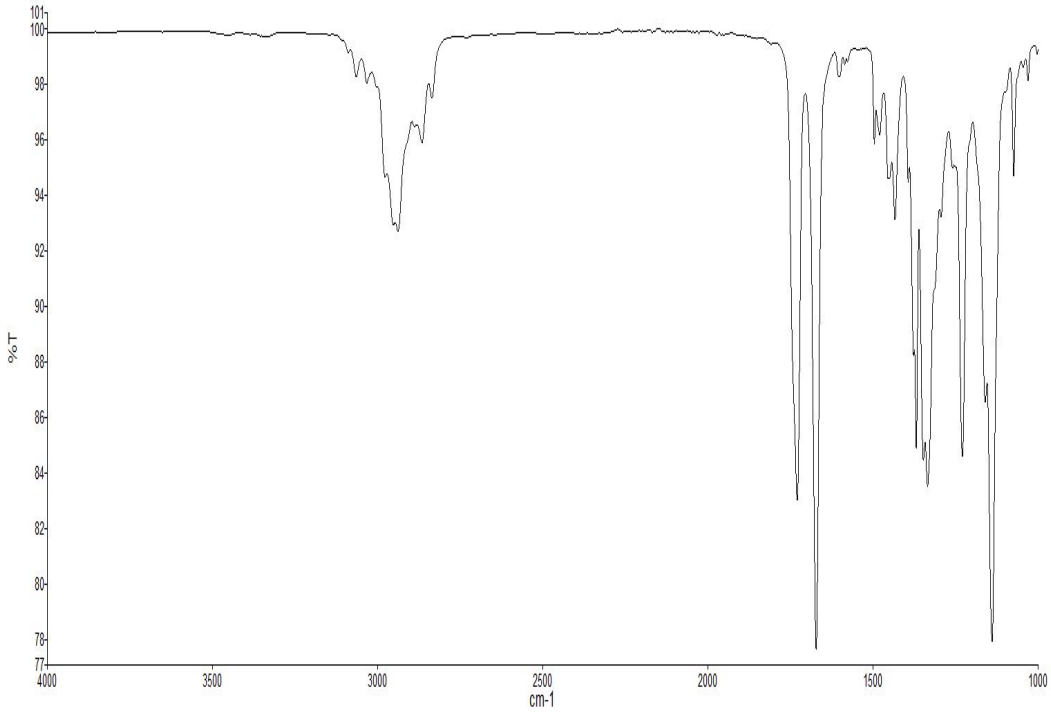

Figure 4.70 Infrared spectrum of compound **4.64**.

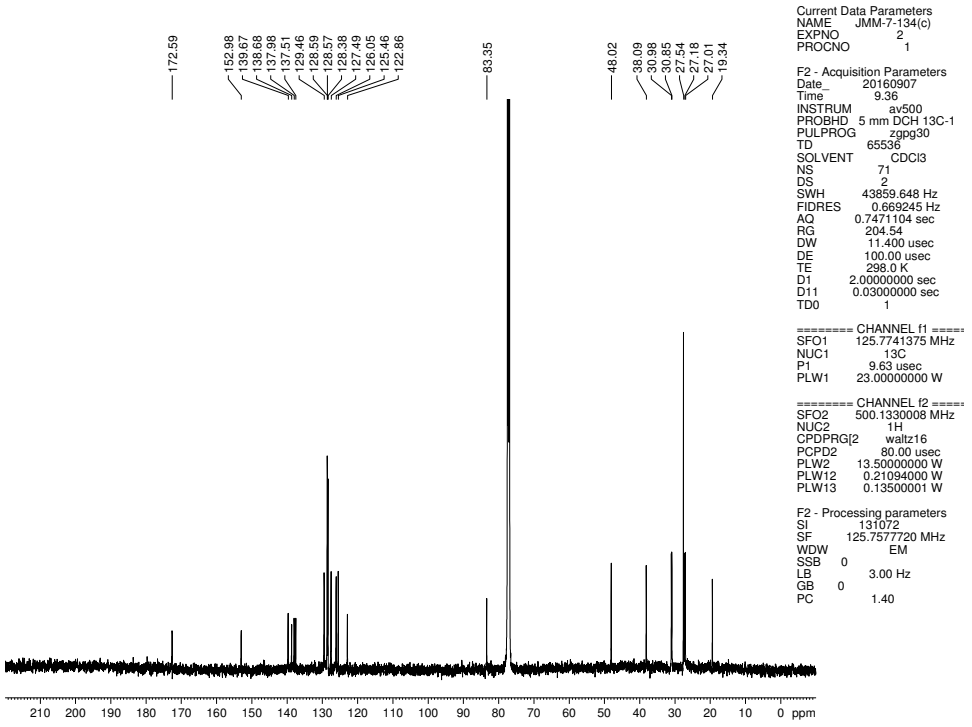

Figure 4.71 ^{13}C NMR (125 MHz, $CDCl_3$) of compound **4.64**.

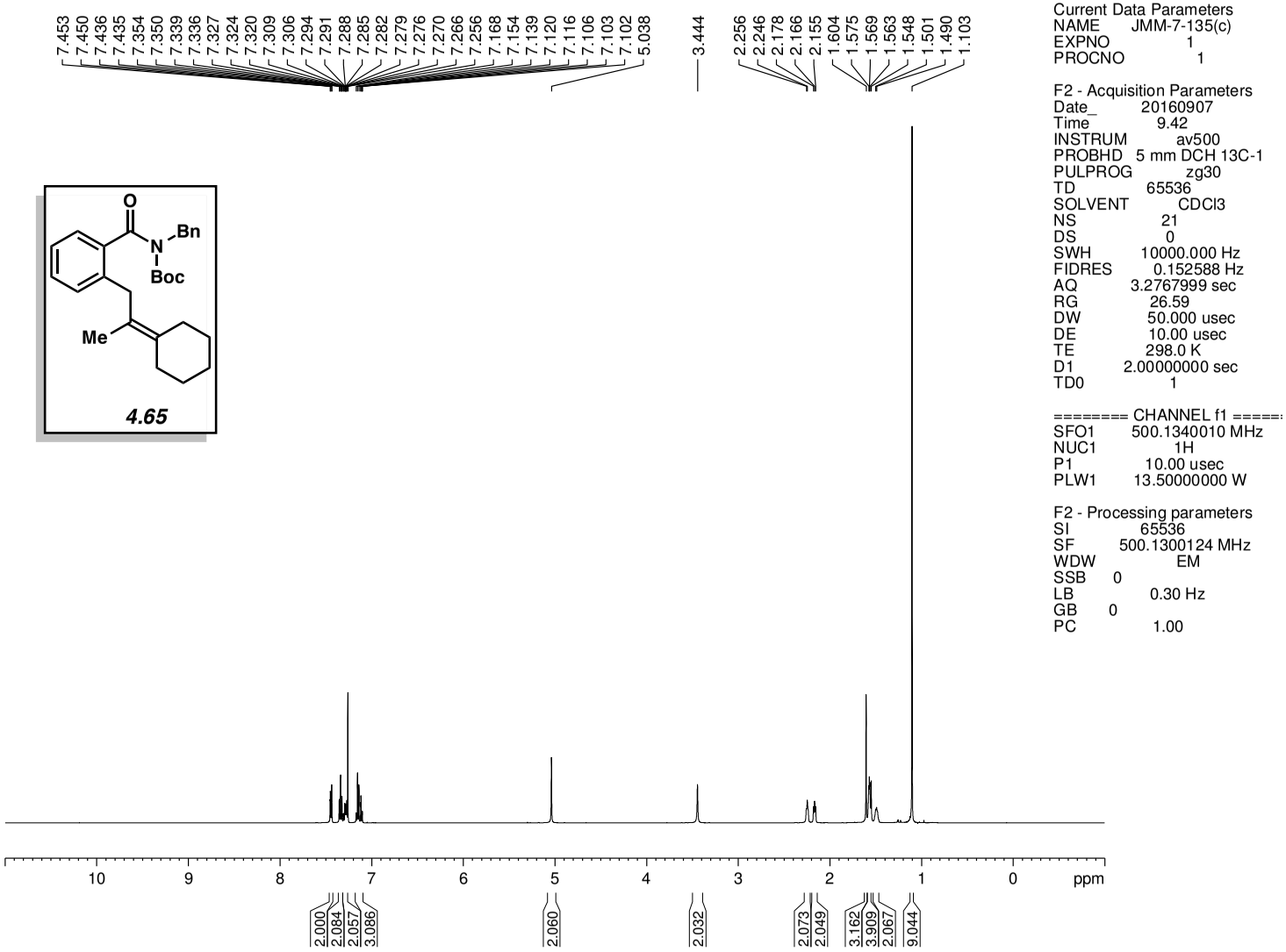

Figure 4.72 ^{1}H NMR (500 MHz, $CDCl_3$) of compound **4.65**.

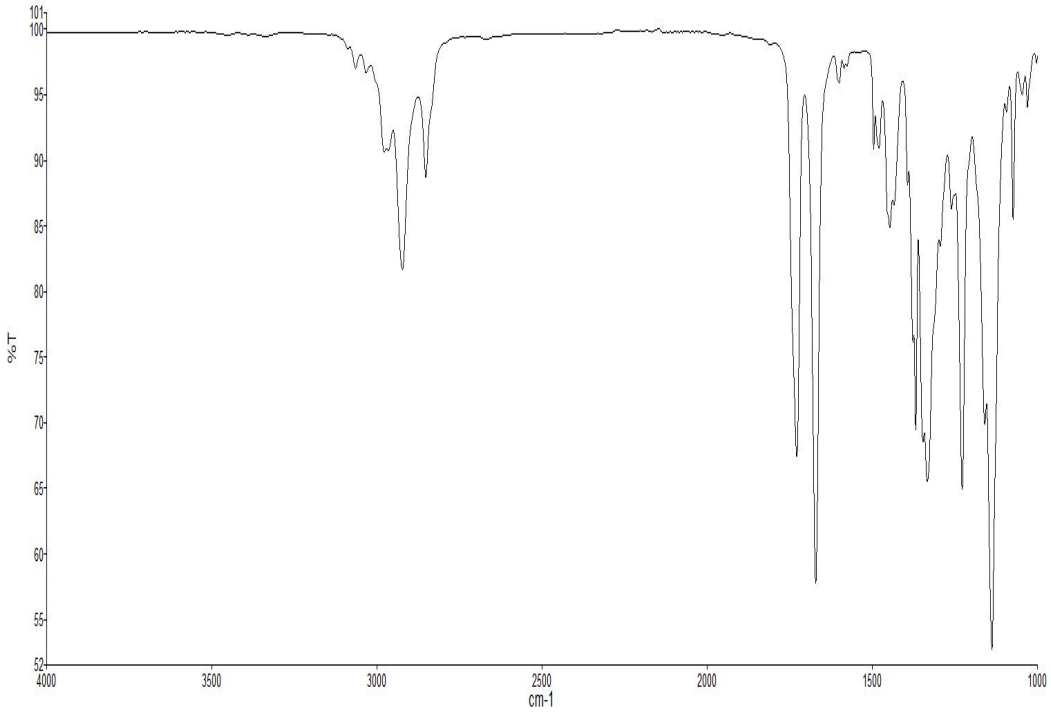

Figure 4.73 Infrared spectrum of compound **4.65**.

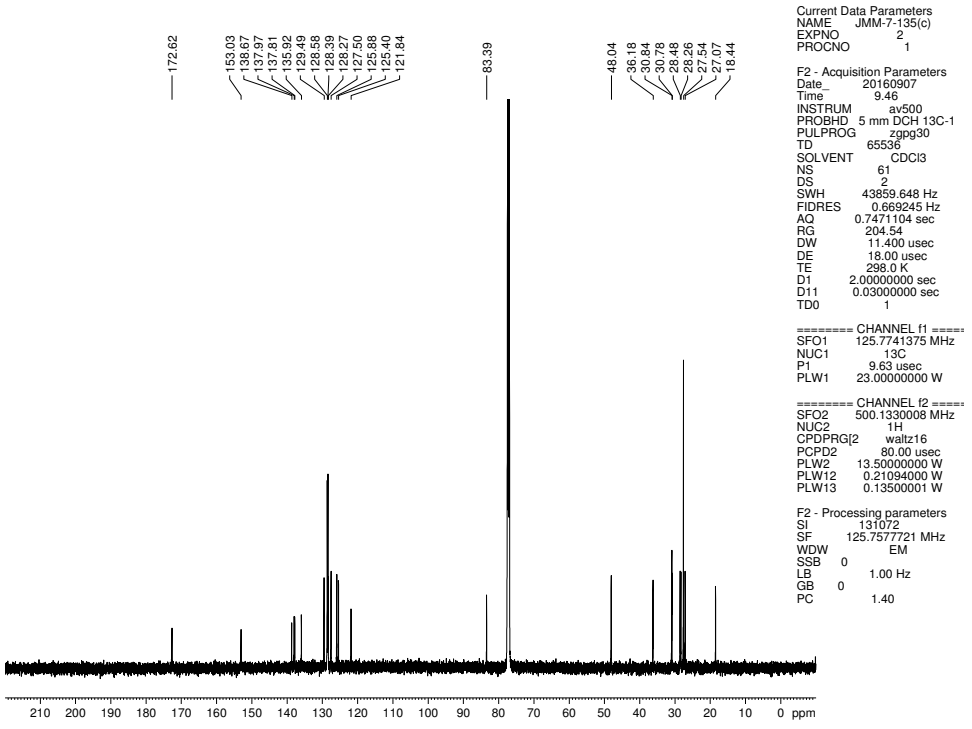

Figure 4.74 ^{13}C NMR (125 MHz, $CDCl_3$) of compound **4.65**.

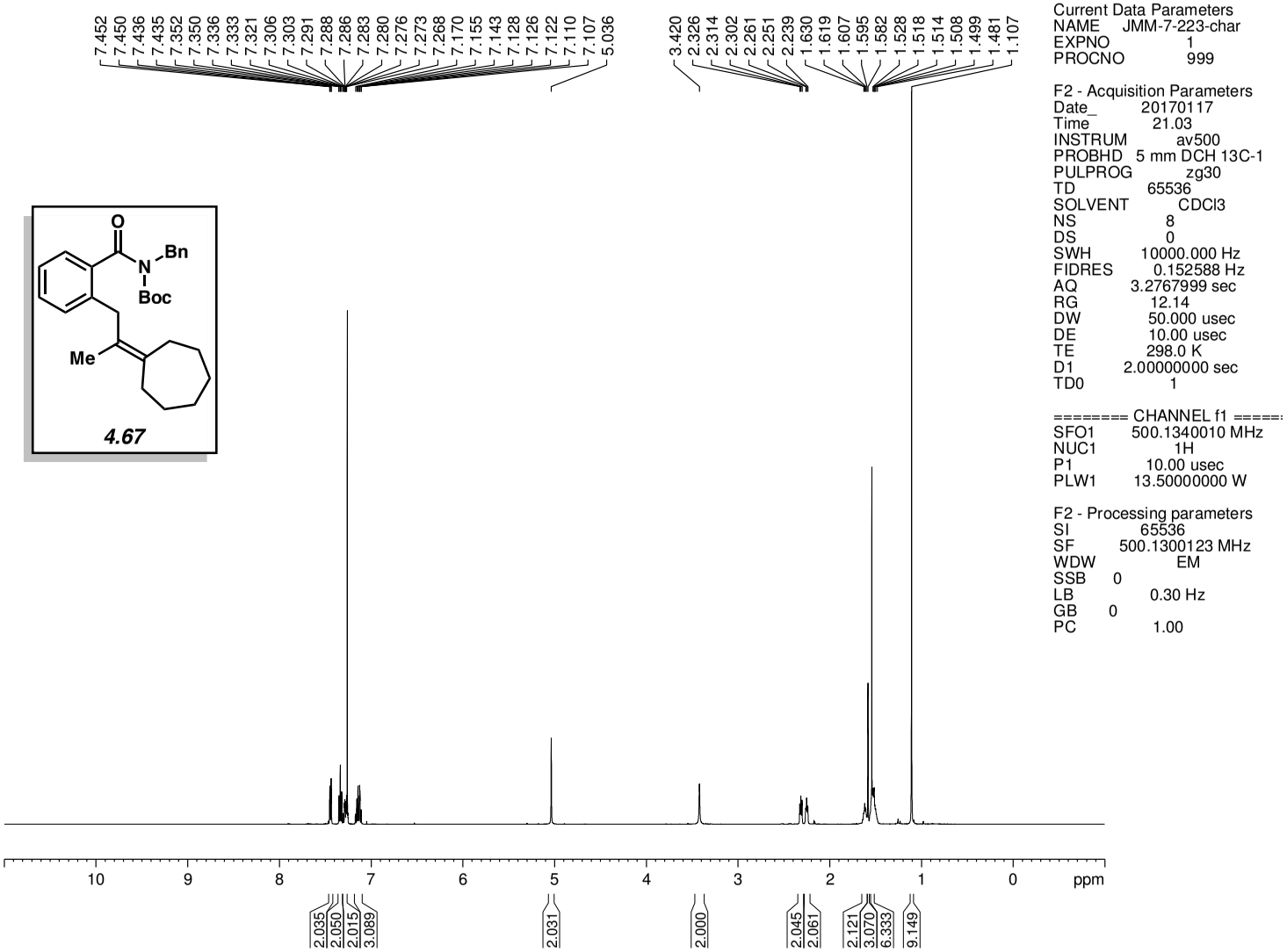

Figure 4.75 ^{1}H NMR (500 MHz, $CDCl_3$) of compound **4.67**.

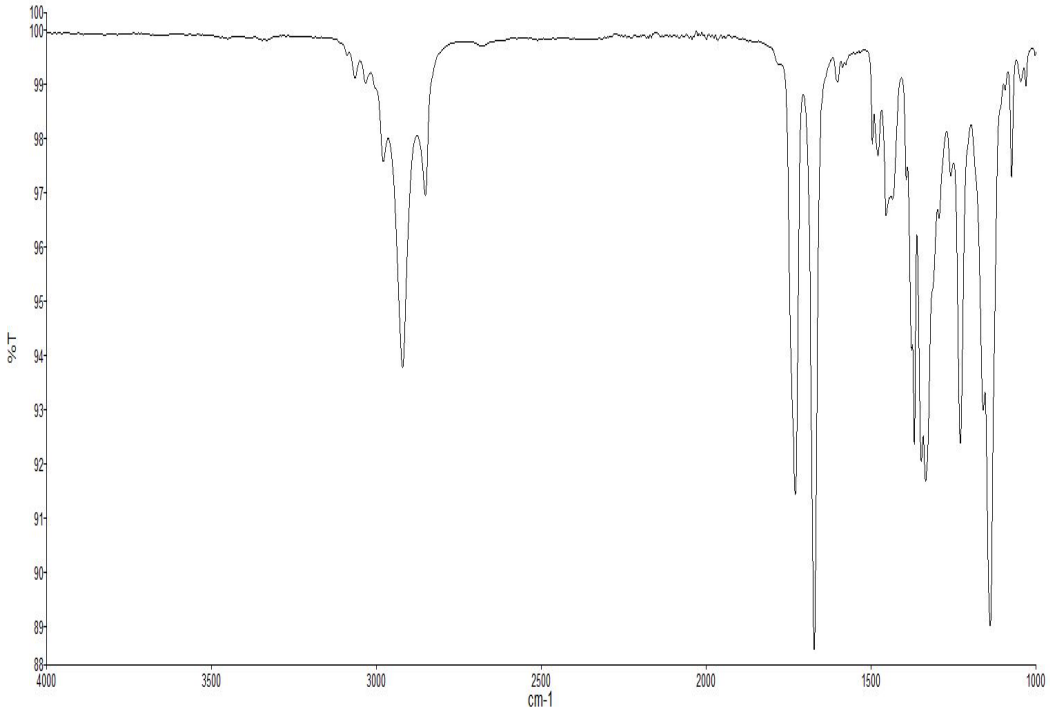

Figure 4.76 Infrared spectrum of compound **4.67**.

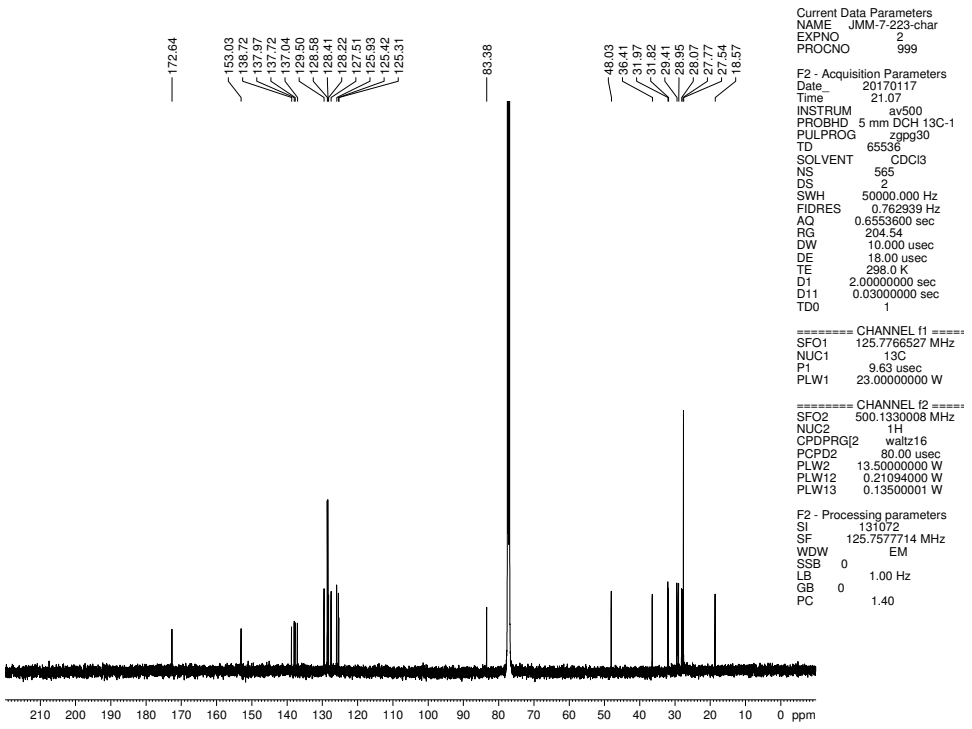

Figure 4.77 ^{13}C NMR (125 MHz, $CDCl_3$) of compound **4.67**.

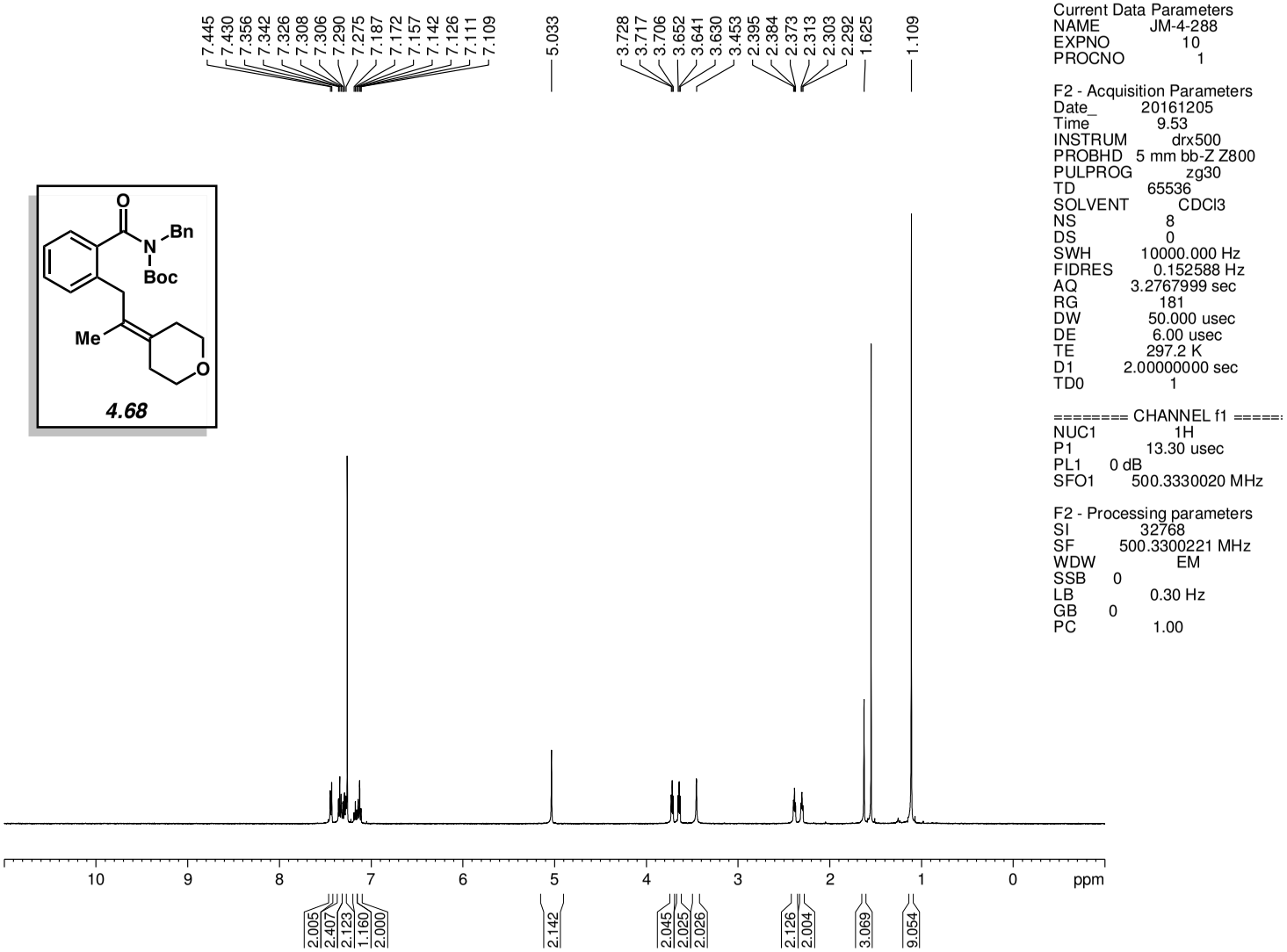

Figure 4.78 ^{1}H NMR (500 MHz, $CDCl_3$) of compound **4.68**.

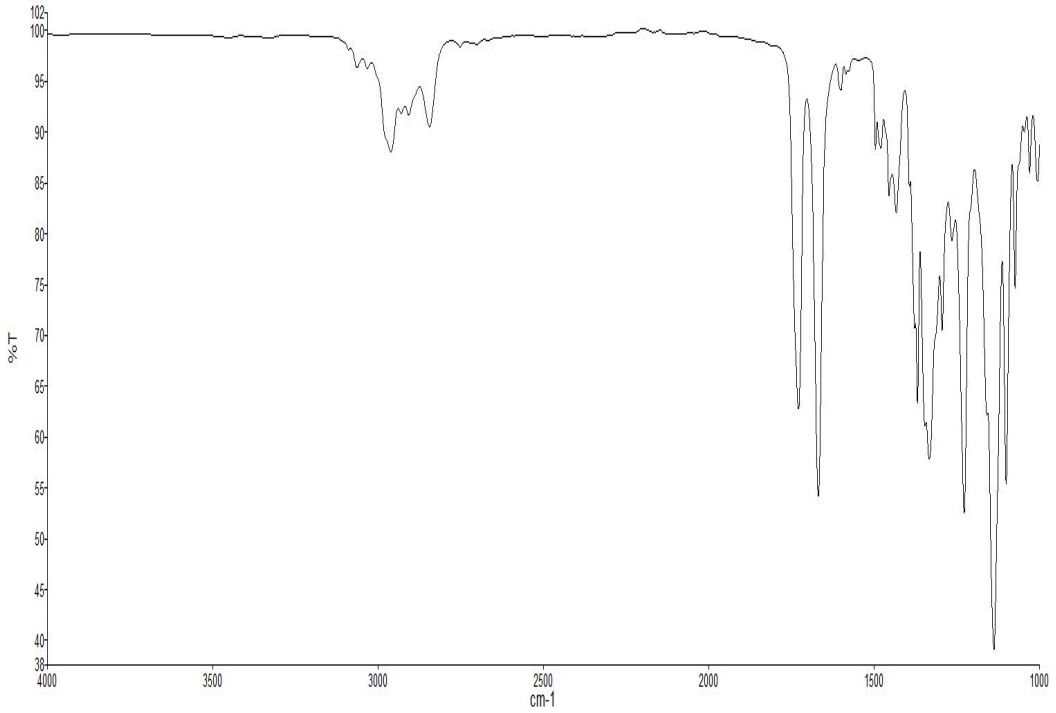

Figure 4.79 Infrared spectrum of compound **4.68**.

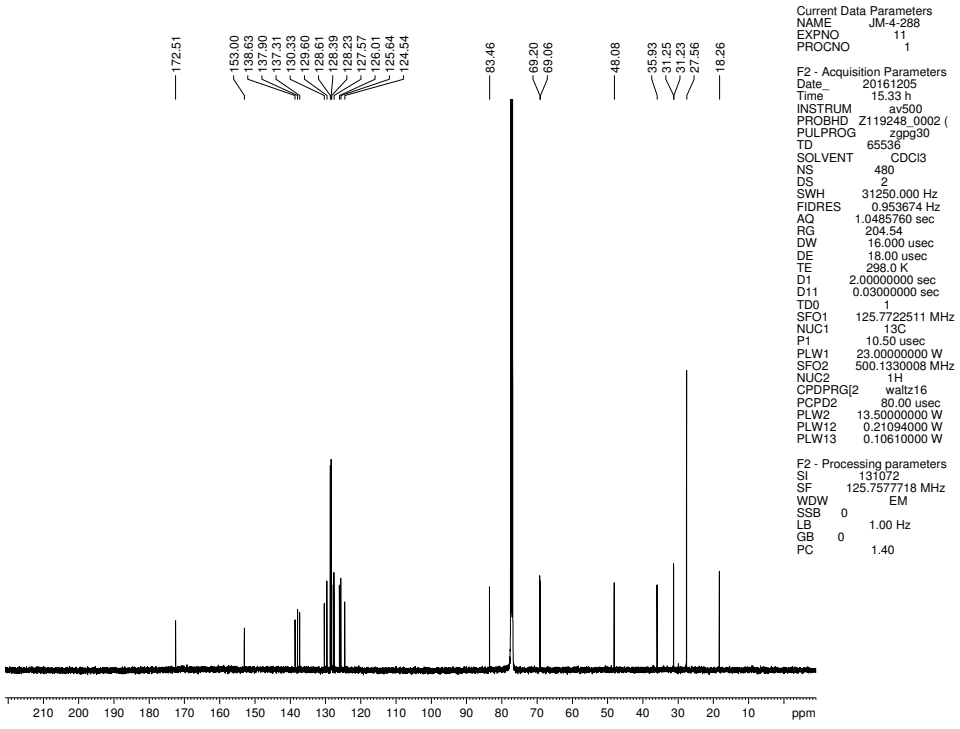

Figure 4.80 ^{13}C NMR (125 MHz, $CDCl_3$) of compound **4.68**.

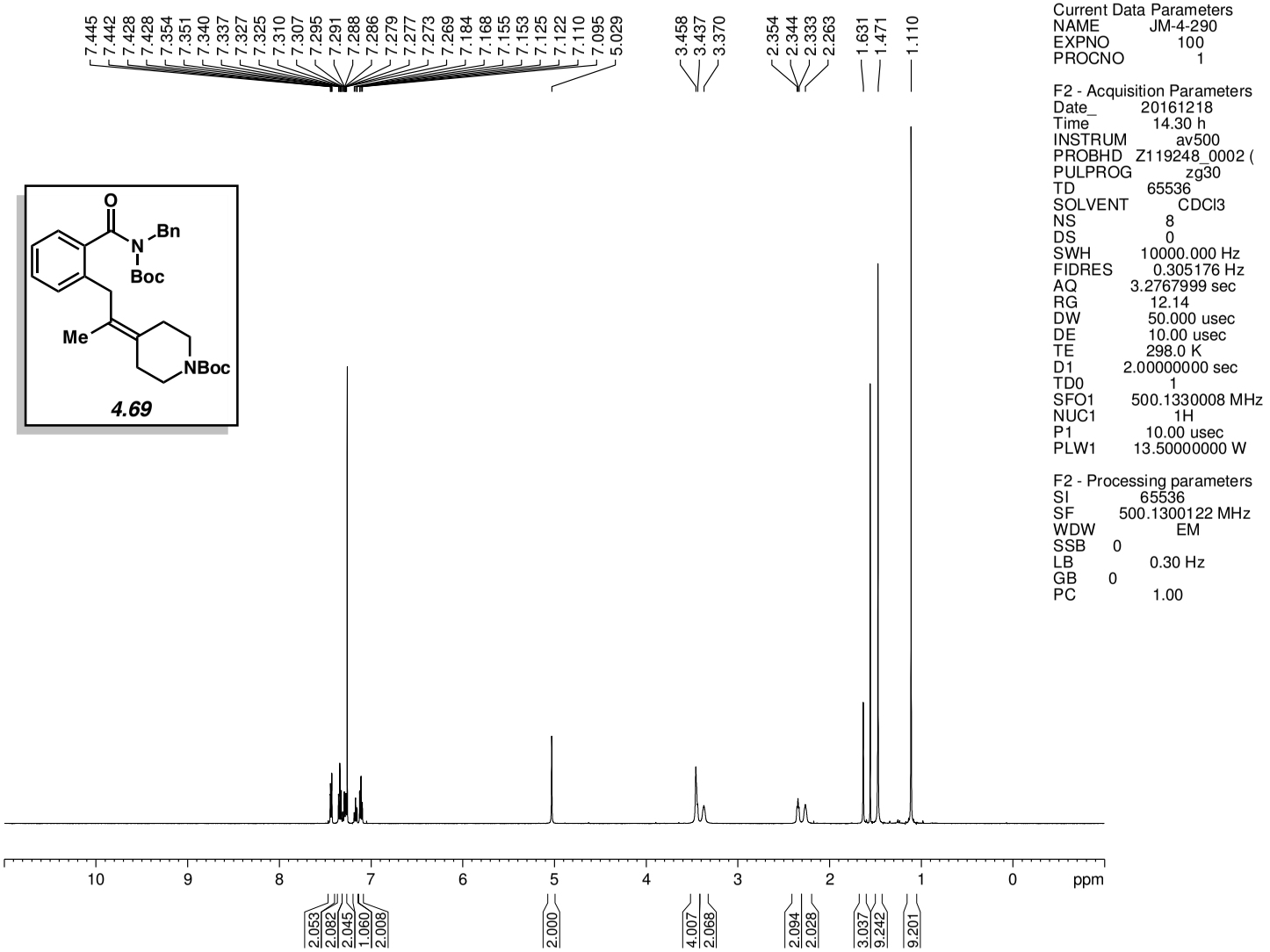

Figure 4.81 ^{1}H NMR (500 MHz, $CDCl_3$) of compound **4.69**.

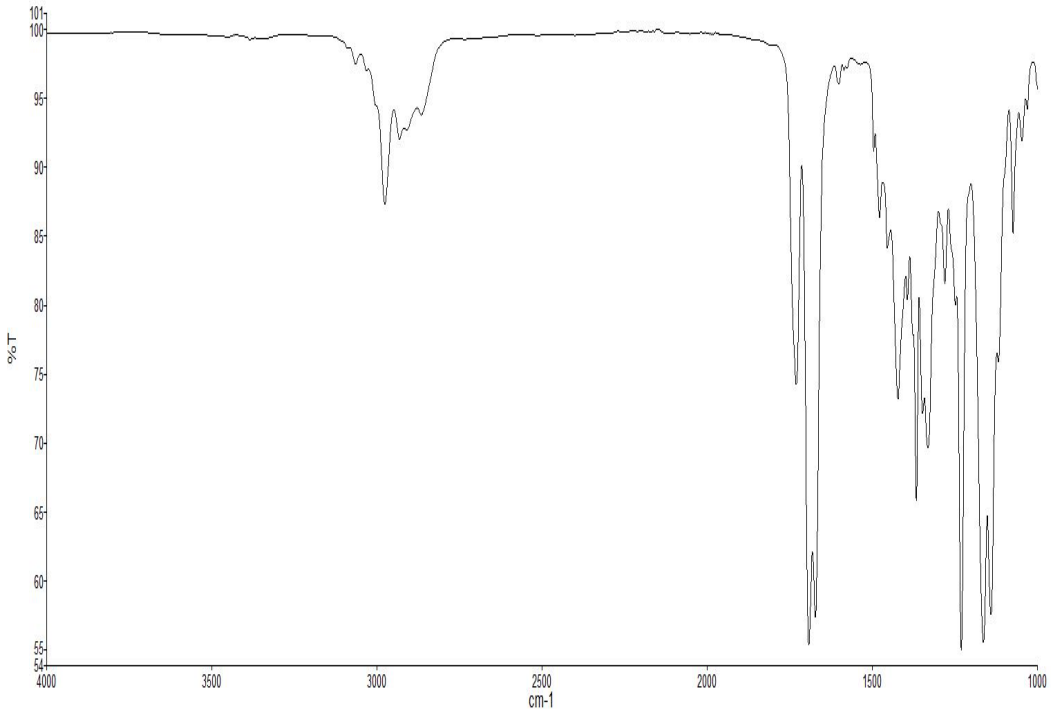

Figure 4.82 Infrared spectrum of compound **4.69**.

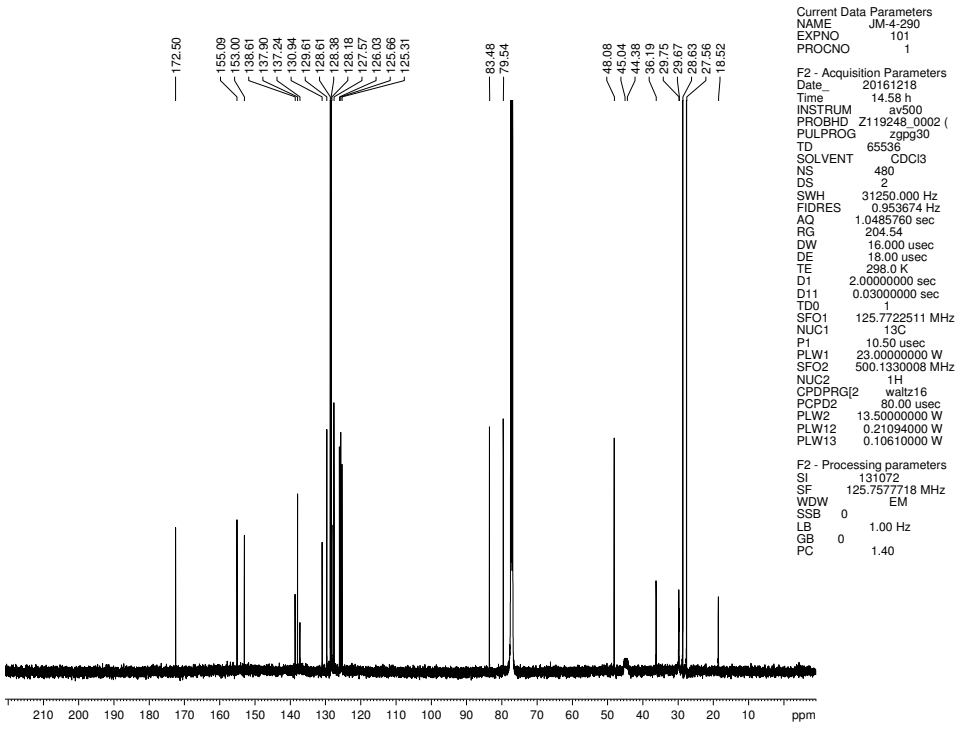

Figure 4.83 ^{13}C NMR (125 MHz, $CDCl_3$) of compound **4.69**.

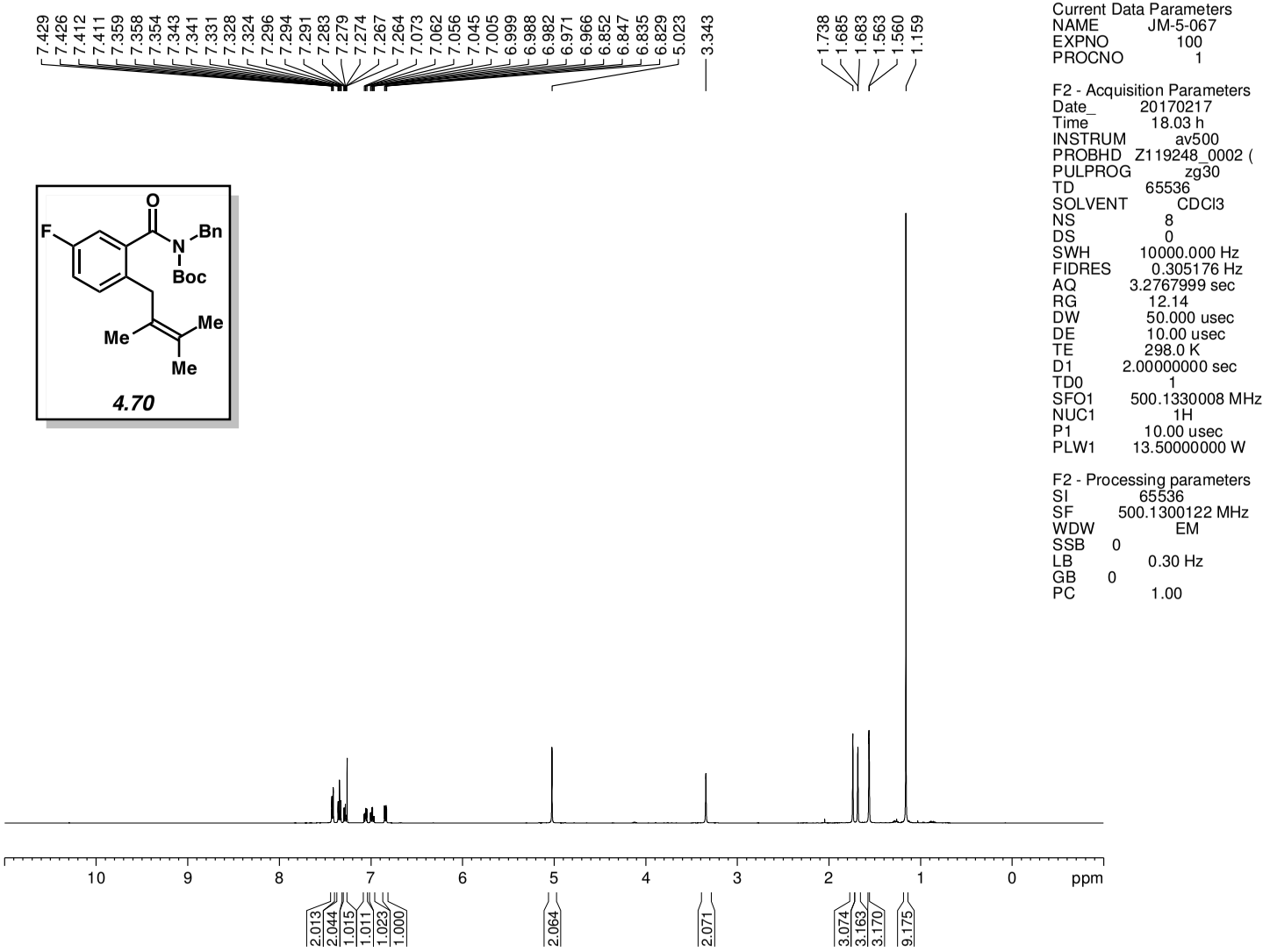

Current Data Parameters
NAME JM-5-067
EXPNO 100
PROCNO 1

F2 - Acquisition Parameters
Date_ 20170217
Time 18.03 h
INSTRUM av500
PROBHD Z119248_0002 (
PULPROG zg30
TD 65536
SOLVENT CDCl3
NS 8
DS 0
SWH 10000.000 Hz
FIDRES 0.305176 Hz
AQ 3.2767999 sec
RG 12.14
DW 50.000 usec
DE 10.00 usec
TE 298.0 K
D1 2.00000000 sec
TD0 1
SFO1 500.1330008 MHz
NUC1 1H
P1 10.00 usec
PLW1 13.50000000 W

F2 - Processing parameters
SI 65536
SF 500.1300122 MHz
WDW EM
SSB 0
LB 0.30 Hz
GB 0
PC 1.00

Figure 4.84 ^{1}H NMR (500 MHz, $CDCl_3$) of compound **4.70**.

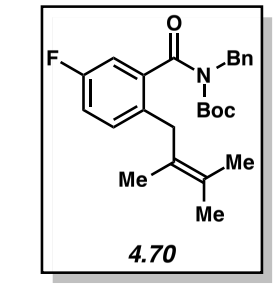

Figure 4.85 ^{19}F NMR (376 MHz, $CDCl_3$) of compound **4.70**.

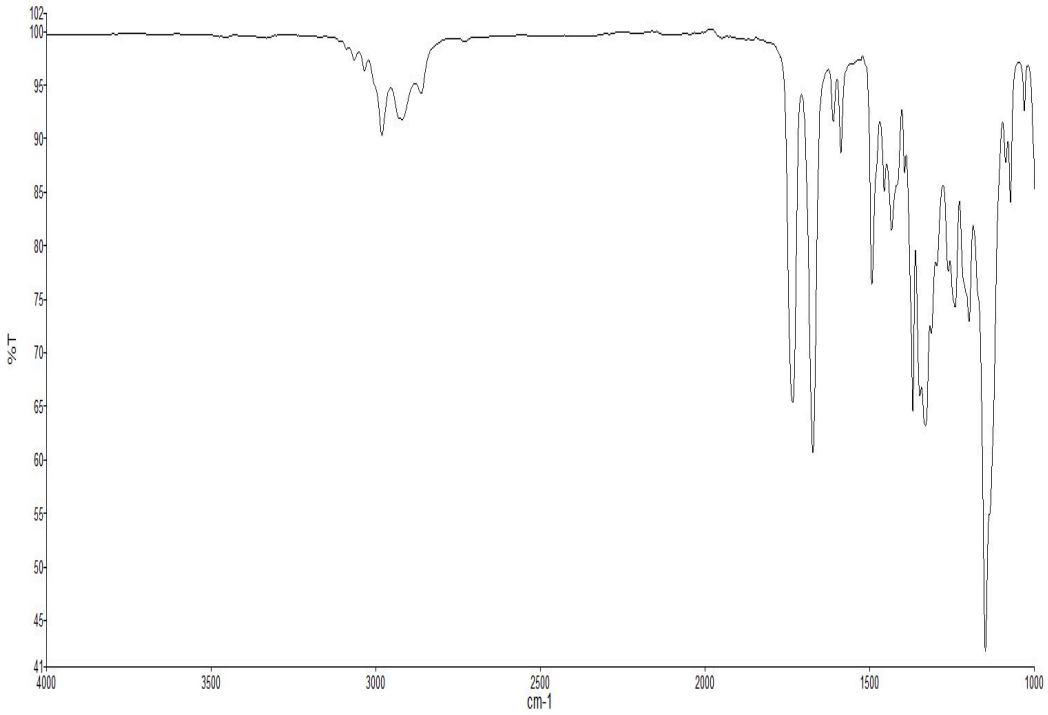

Figure 4.86 Infrared spectrum of compound **4.70**.

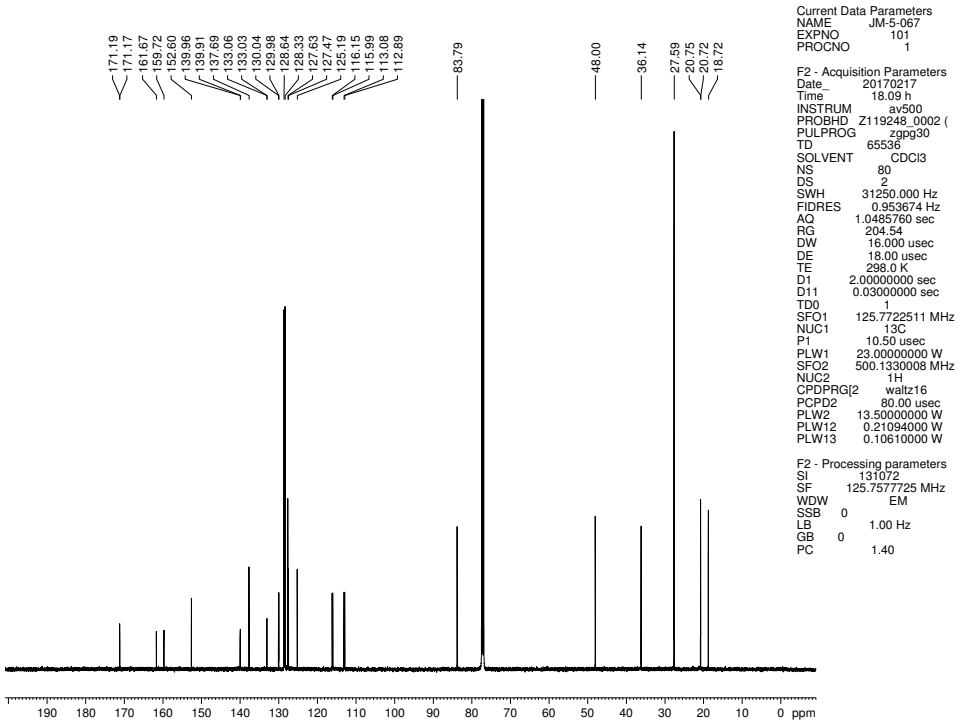

Figure 4.87 ^{13}C NMR (125 MHz, $CDCl_3$) of compound **4.70**.

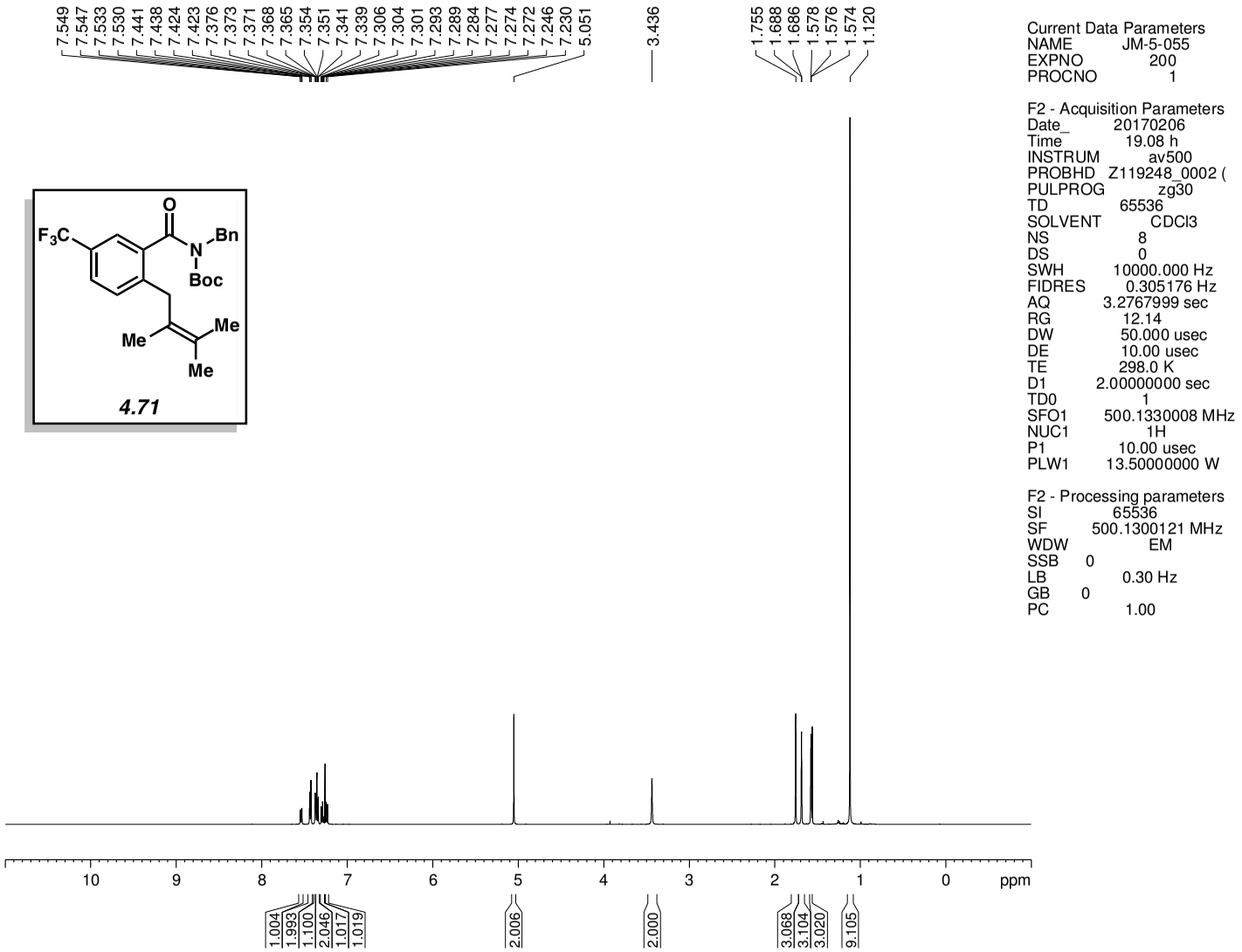

Figure 4.88 ^{1}H NMR (500 MHz, $CDCl_3$) of compound **4.71**.

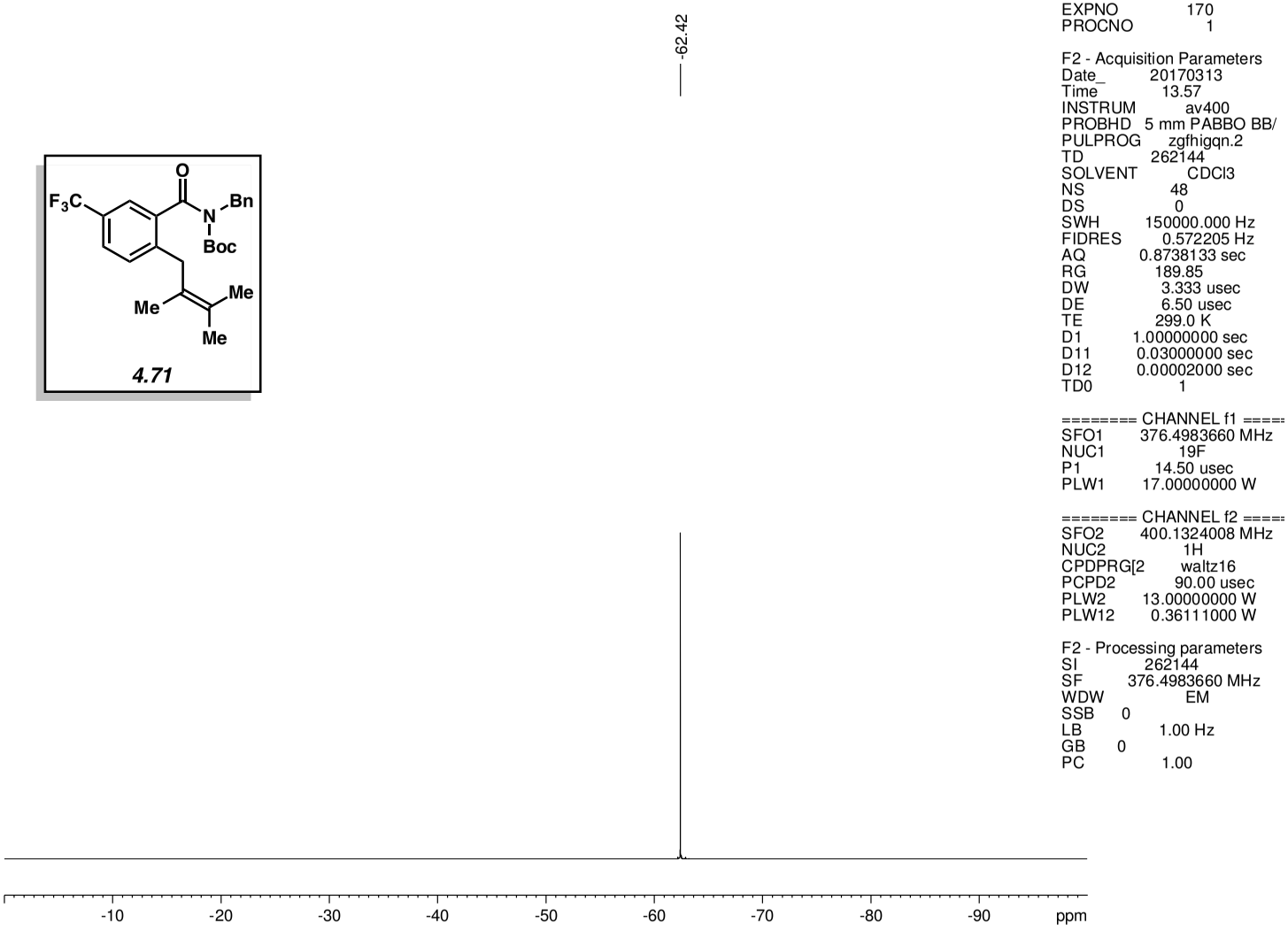

Figure 4.89 ^{19}F NMR (376 MHz, $CDCl_3$) of compound **4.71**.

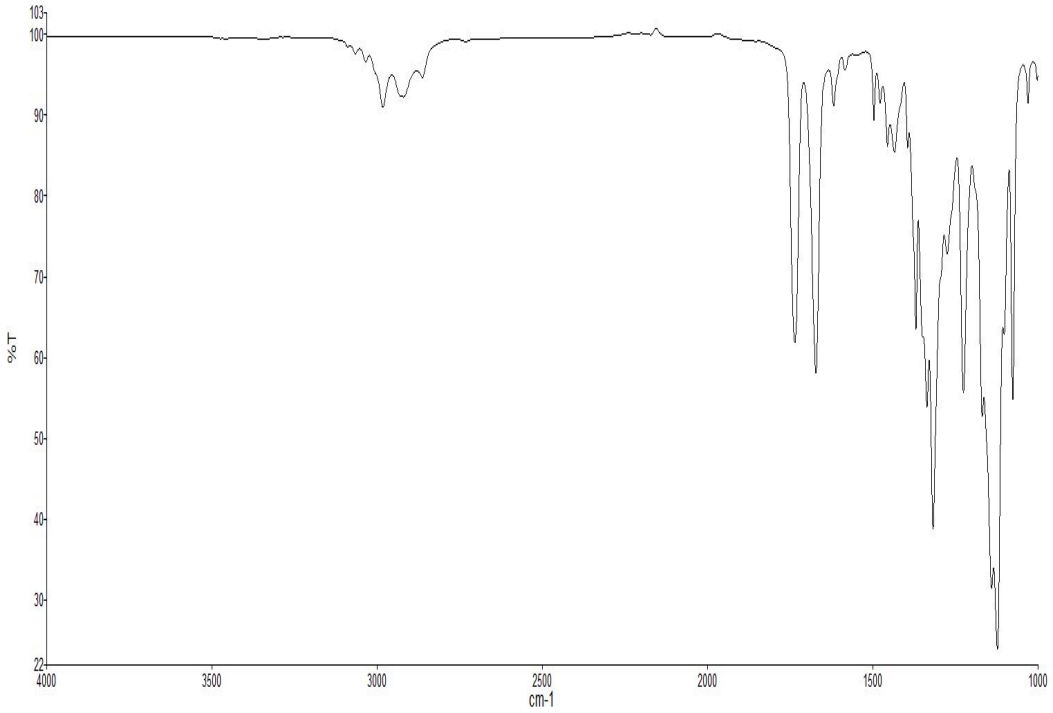

Figure 4.90 Infrared spectrum of compound **4.71**.

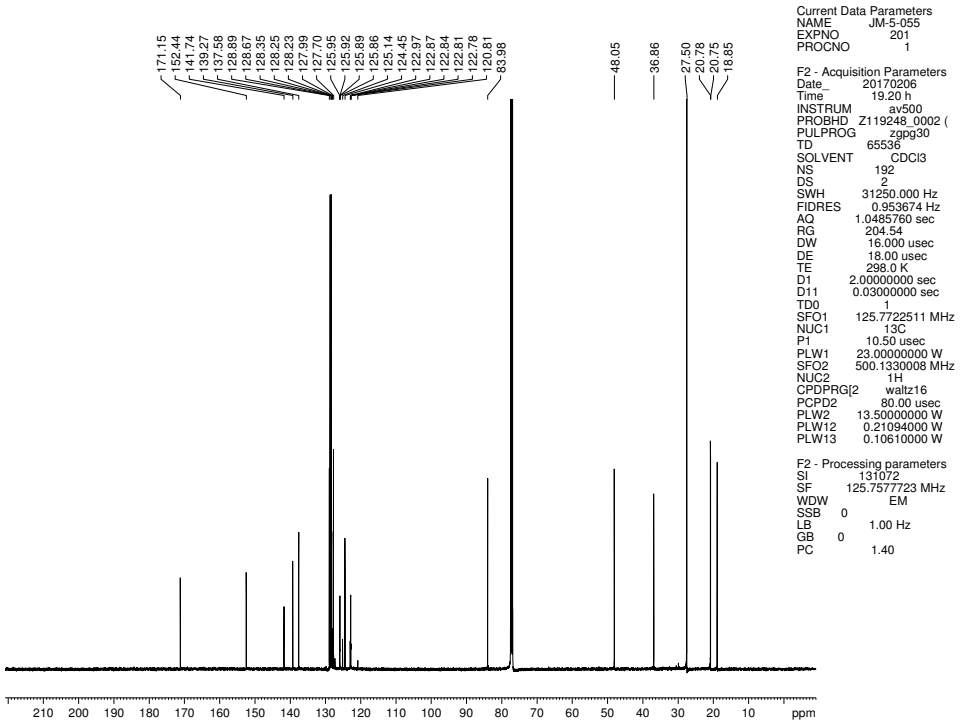

Figure 4.91 ^{13}C NMR (125 MHz, $CDCl_3$) of compound **4.71**.

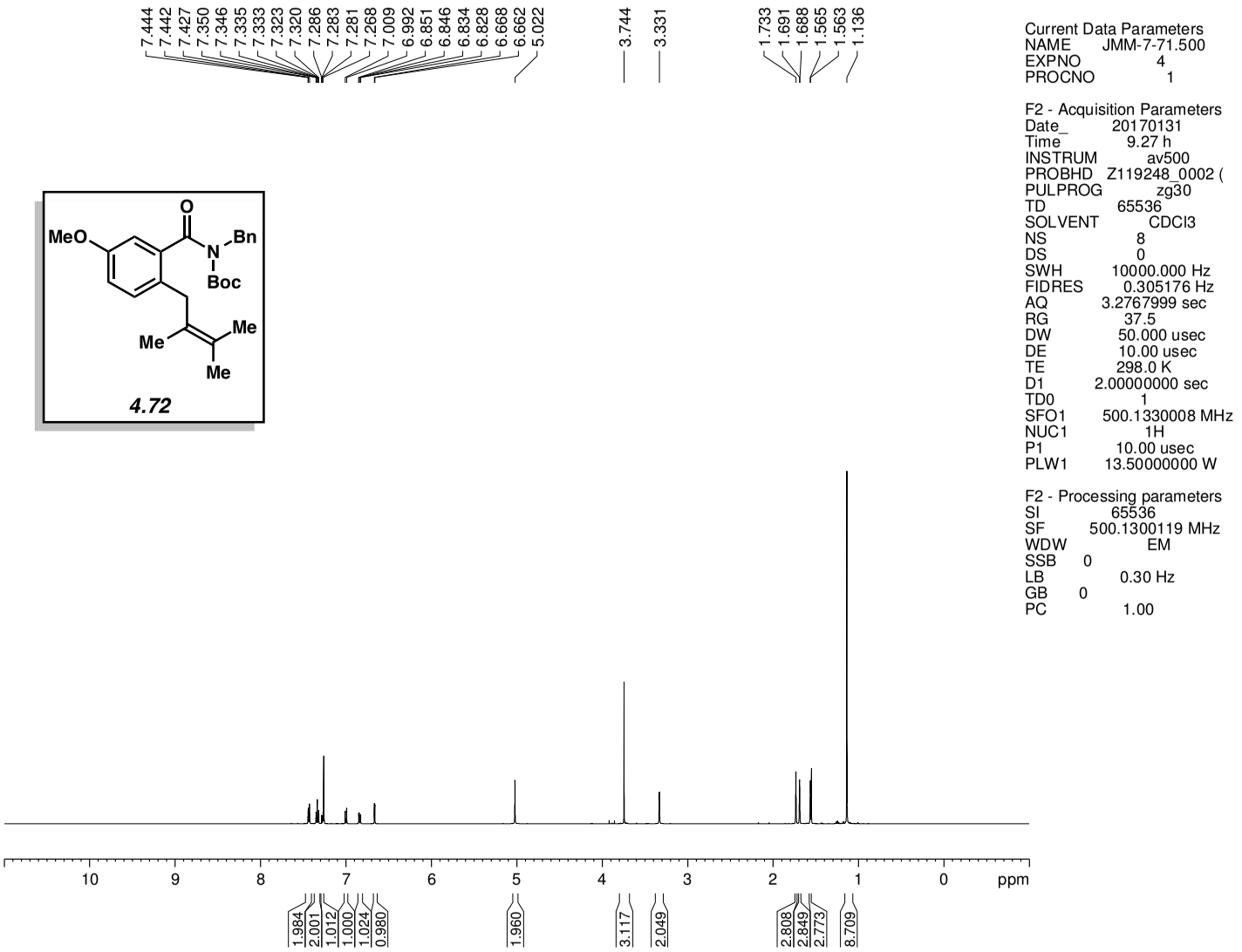

Figure 4.92 ^{1}H NMR (500 MHz, $CDCl_3$) of compound **4.72**.

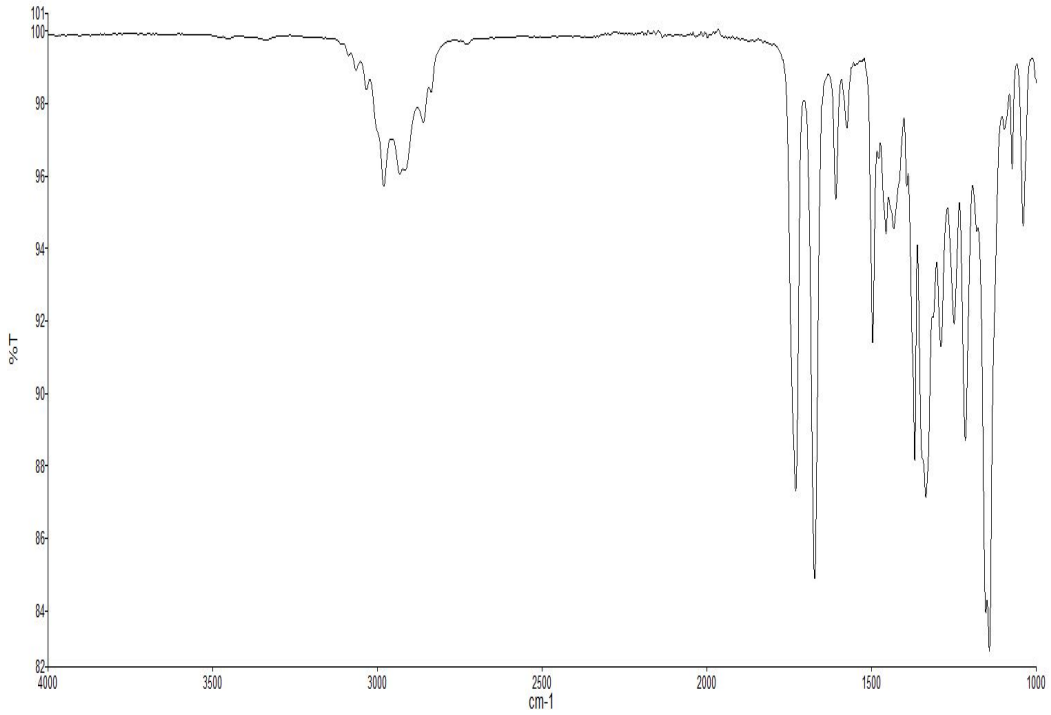

Figure 4.93 Infrared spectrum of compound **4.72**.

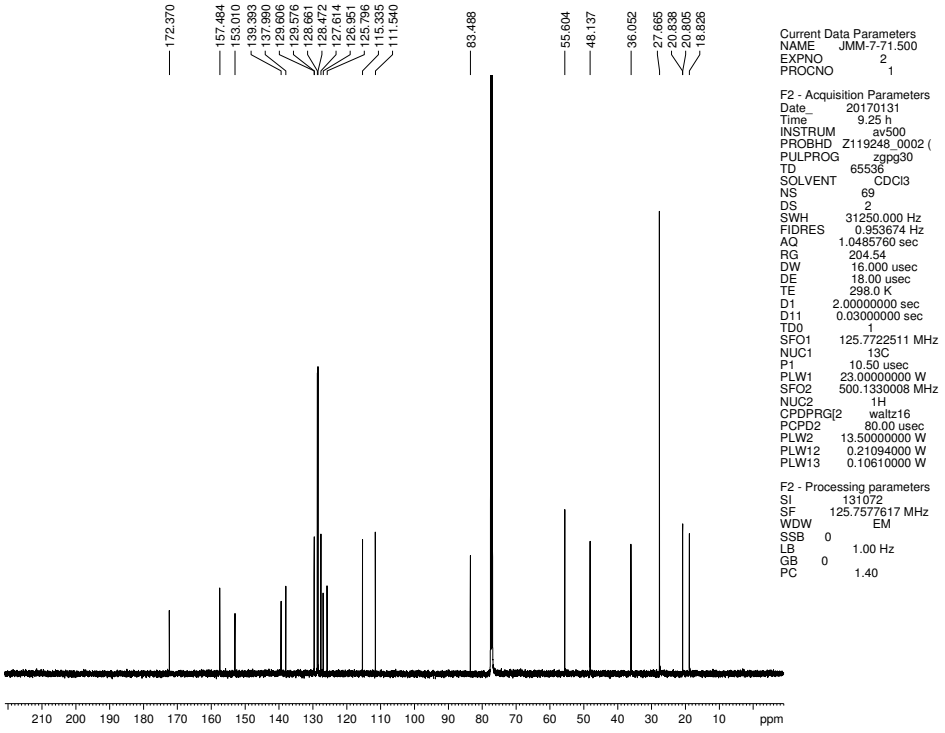

Figure 4.94 ^{13}C NMR (125 MHz, $CDCl_3$) of compound **4.72**.

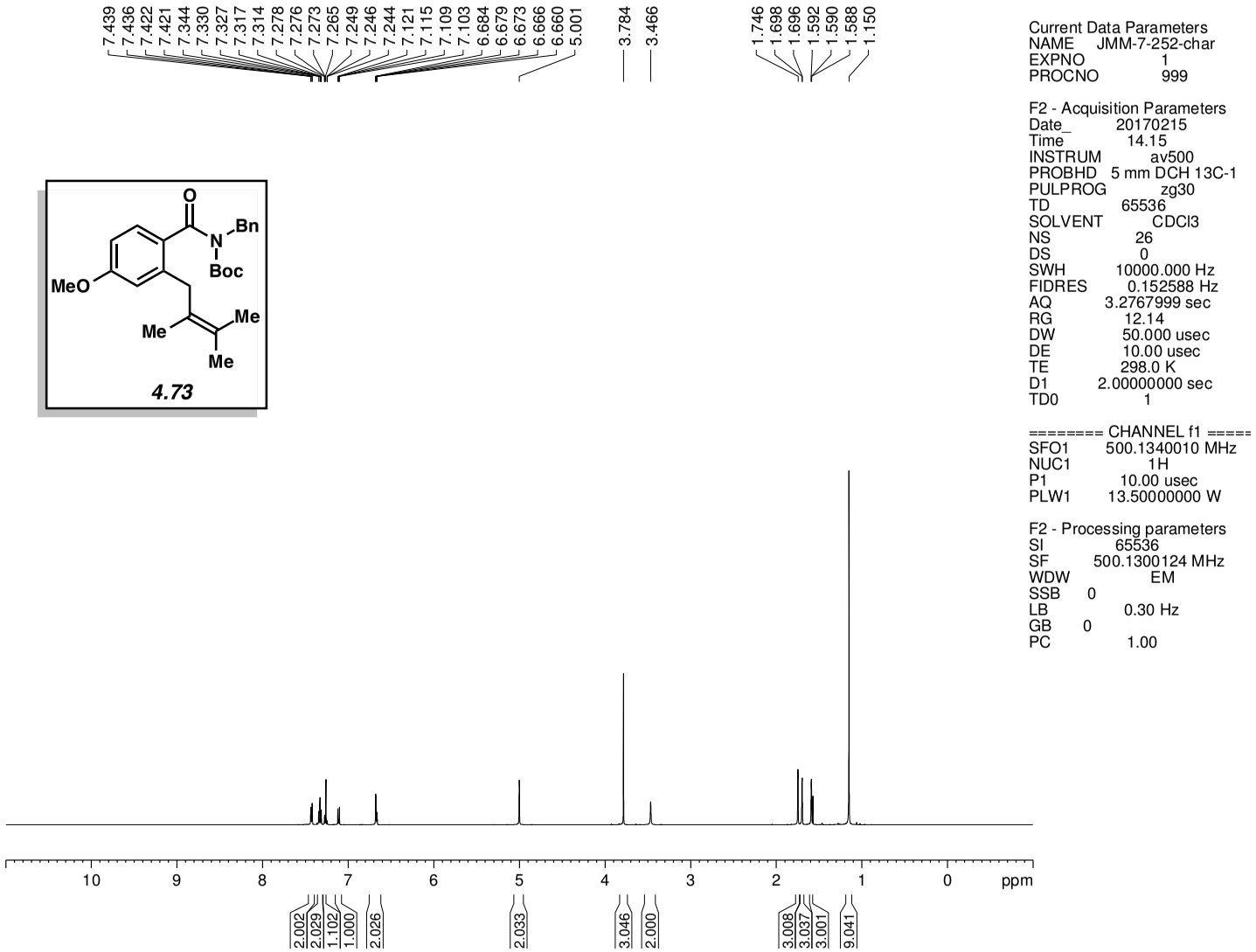

Figure 4.95 ^{1}H NMR (500 MHz, $CDCl_3$) of compound **4.73**.

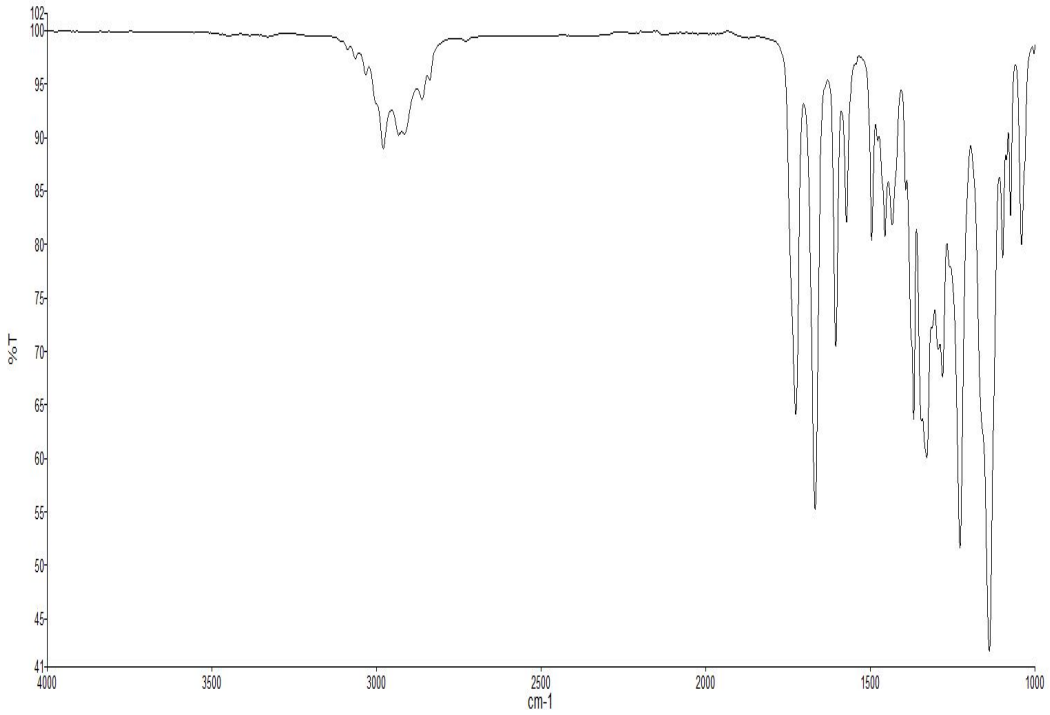

Figure 4.96 Infrared spectrum of compound **4.73**.

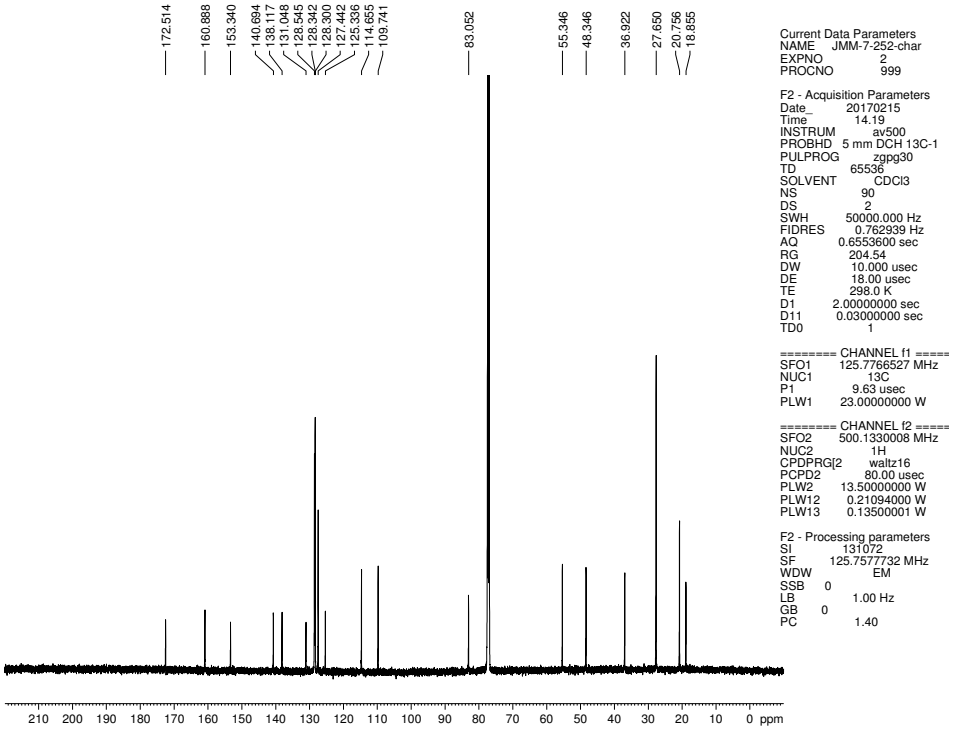

Figure 4.97 ^{13}C NMR (125 MHz, $CDCl_3$) of compound **4.73**.

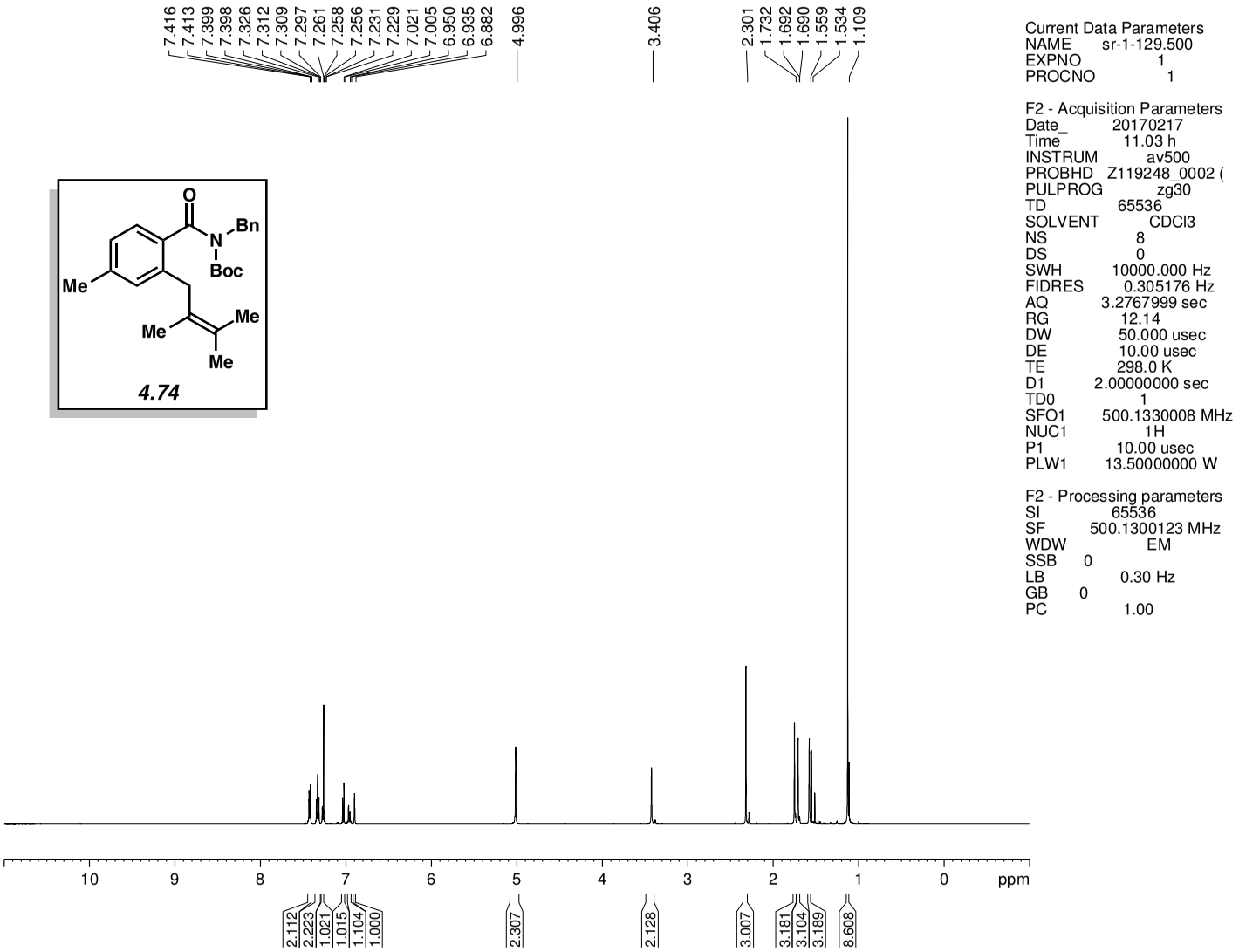

Figure 4.98 ^{1}H NMR (500 MHz, $CDCl_3$) of compound **4.74**.

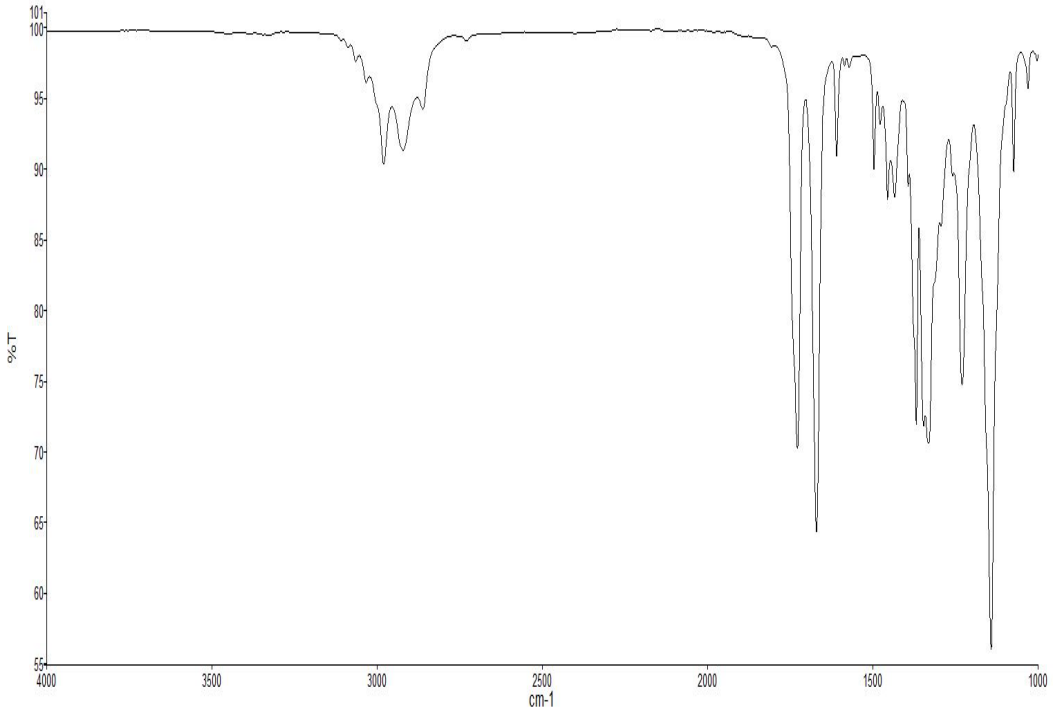

Figure 4.99 Infrared spectrum of compound **4.74**.

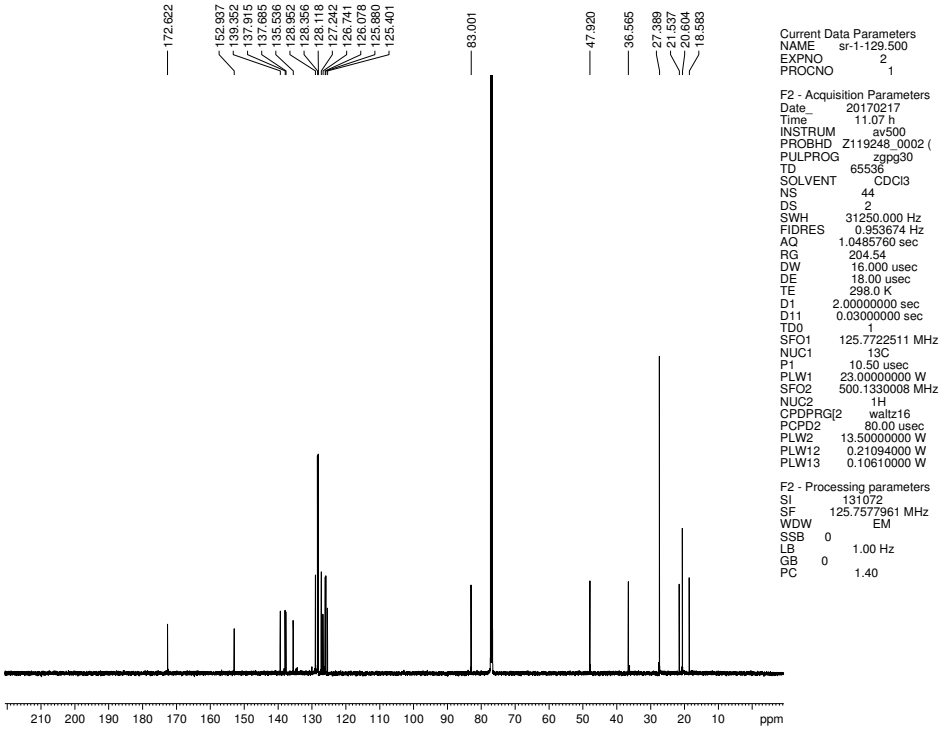

Figure 4.100 ^{13}C NMR (125 MHz, $CDCl_3$) of compound **4.74**.

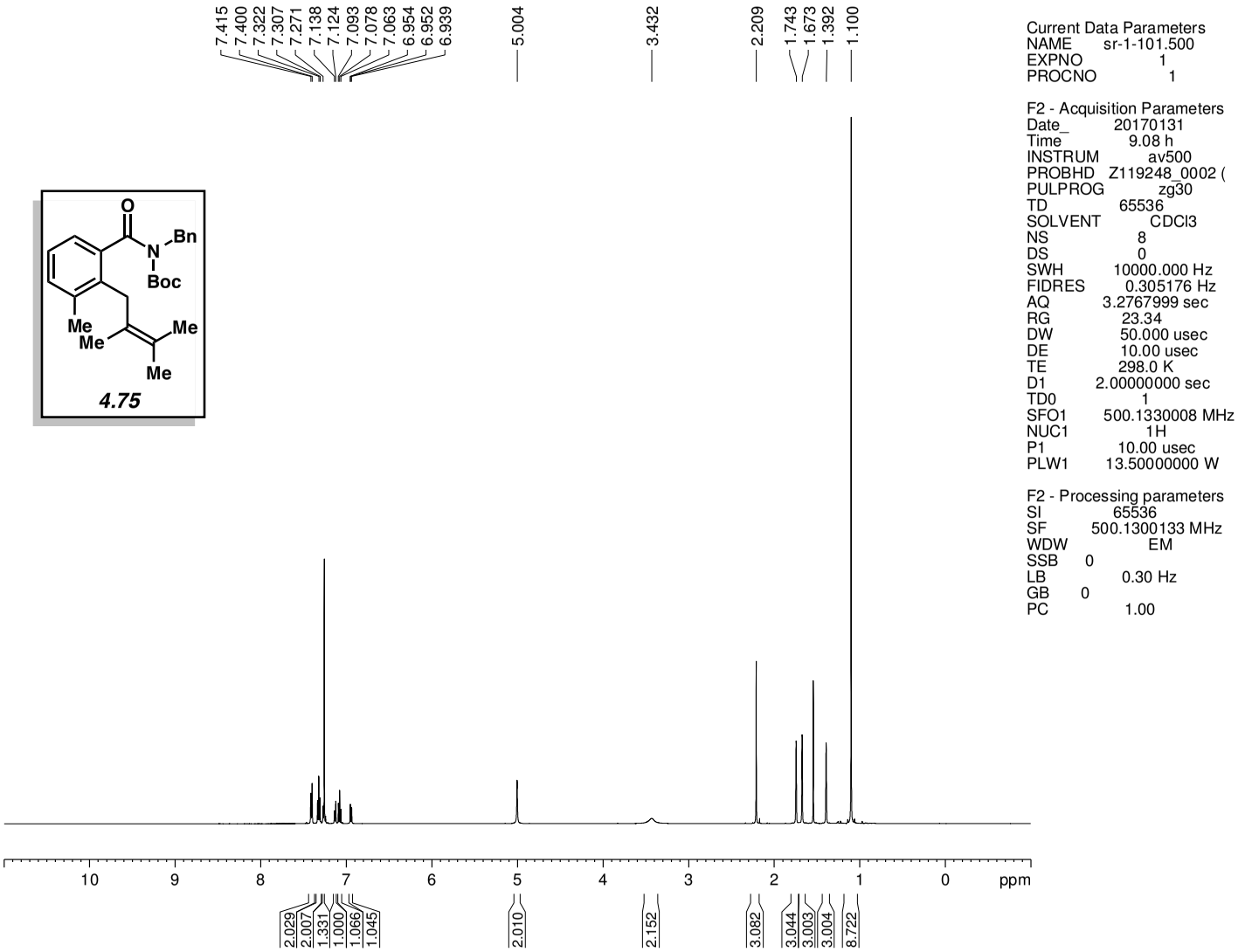

Figure 4.101 ^{1}H NMR (500 MHz, $CDCl_3$) of compound **4.75**.

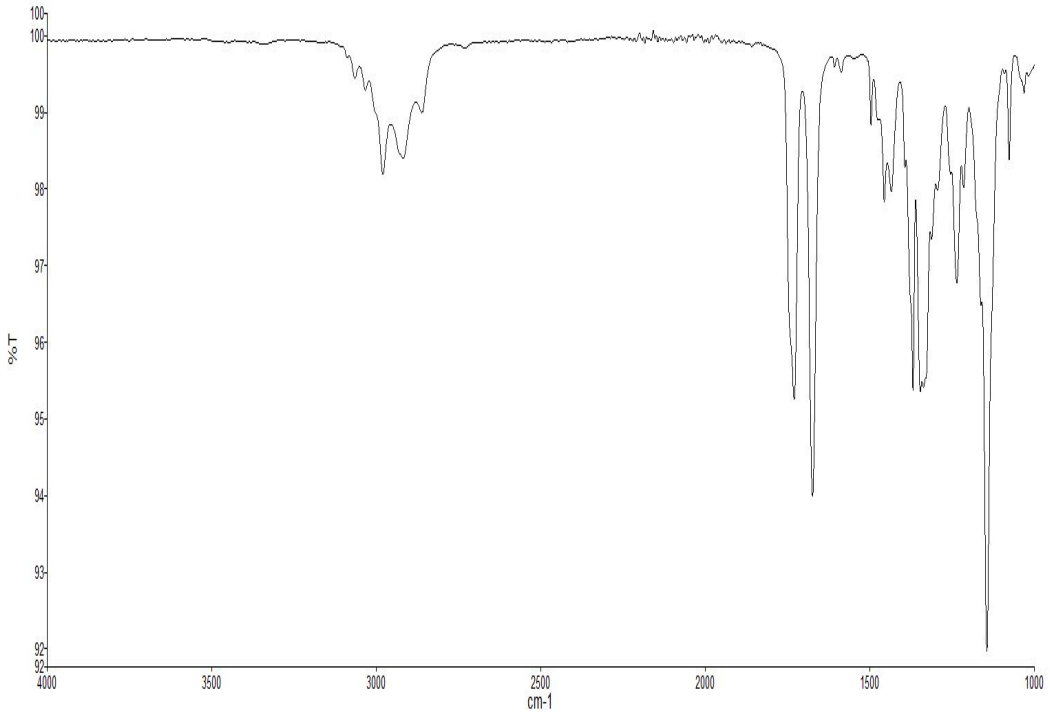

Figure 4.102 Infrared spectrum of compound **4.75**.

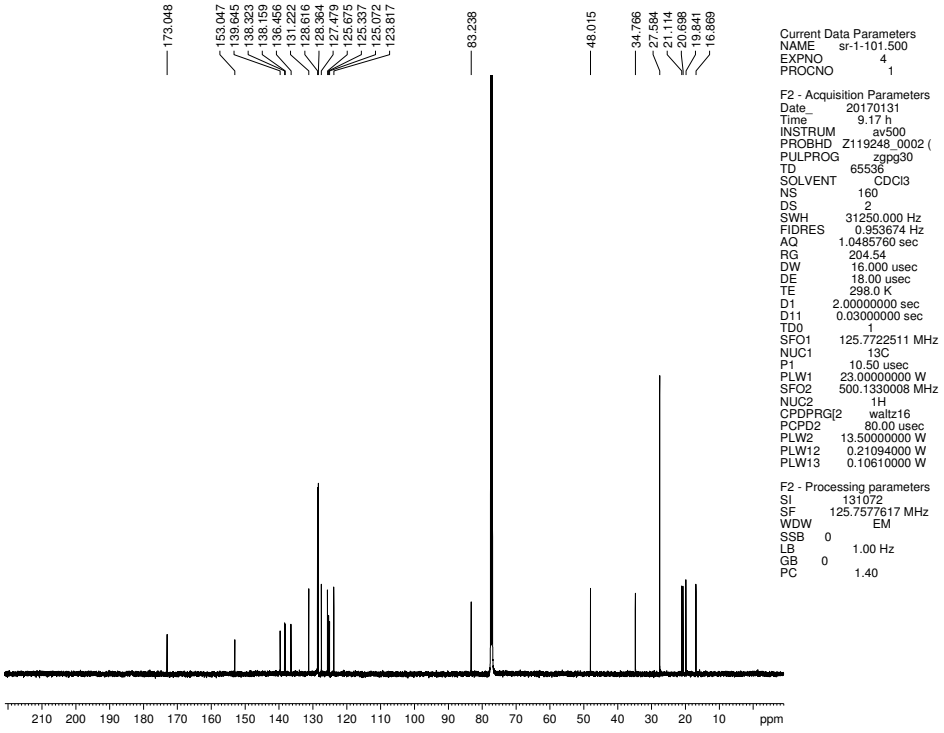

Figure 4.103 ^{13}C NMR (125 MHz, $CDCl_3$) of compound **4.75**.

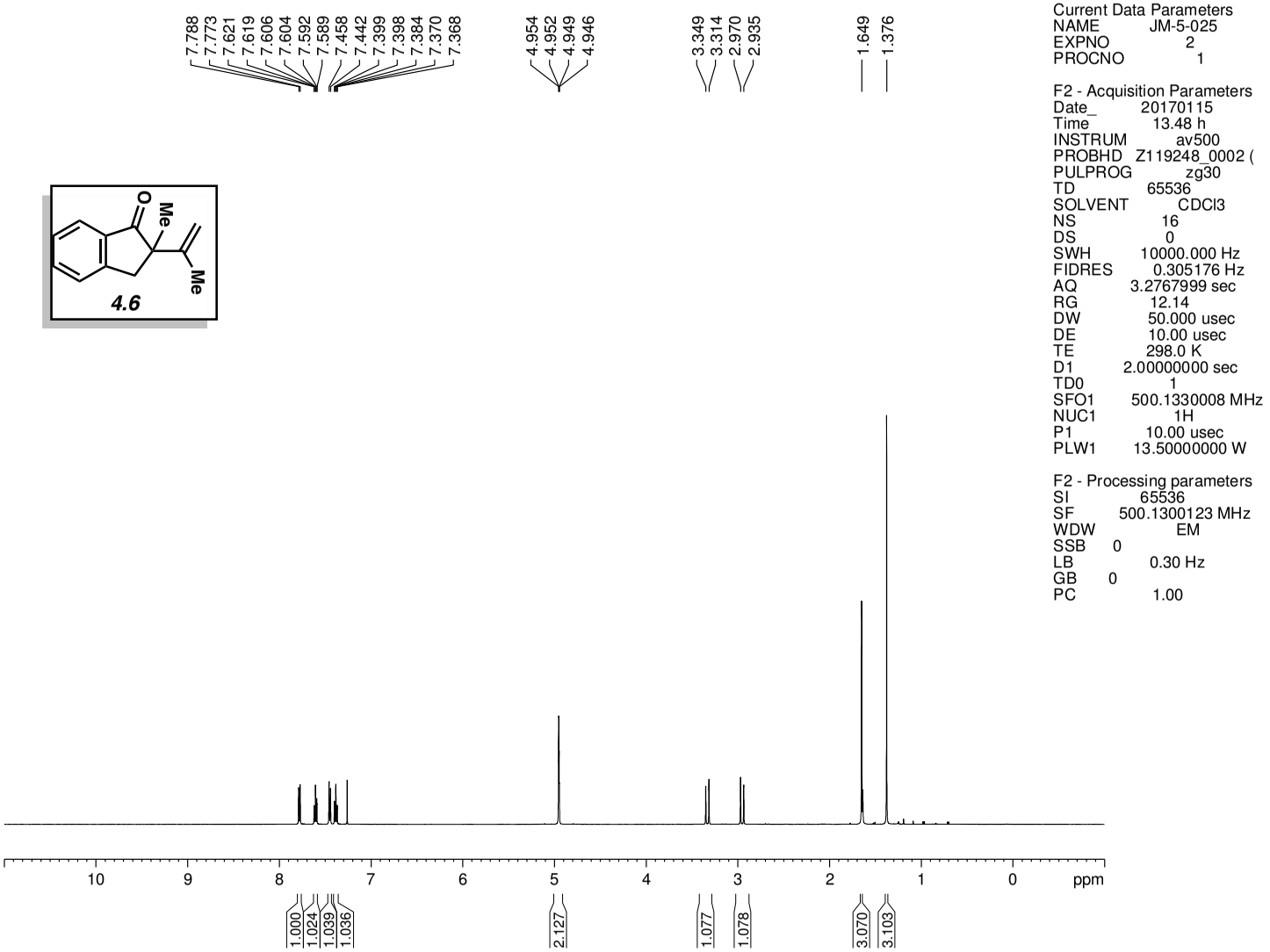

Figure 4.104 ^{1}H NMR (500 MHz, $CDCl_3$) of compound **4.6**.

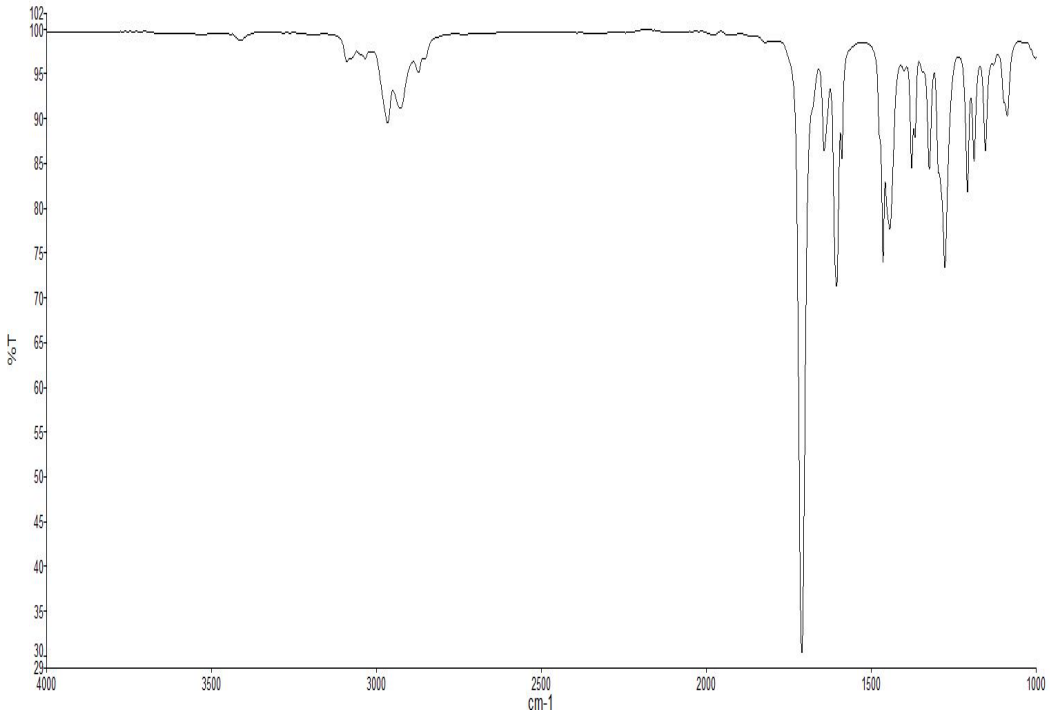

Figure 4.105 Infrared spectrum of compound **4.6**.

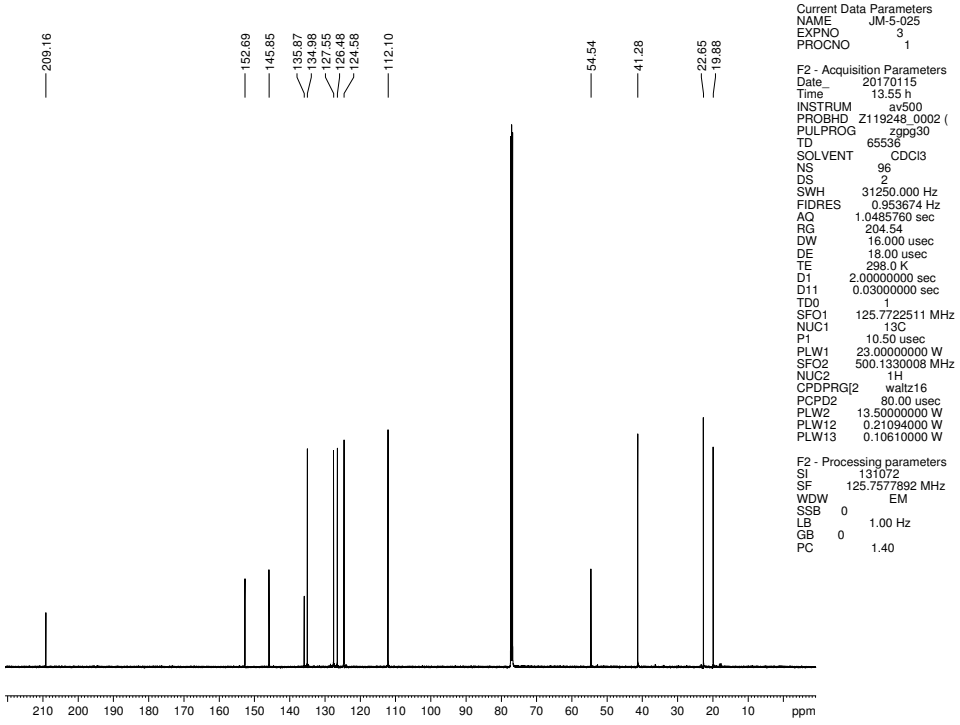

Figure 4.106 ^{13}C NMR (125 MHz, $CDCl_3$) of compound **4.6**.

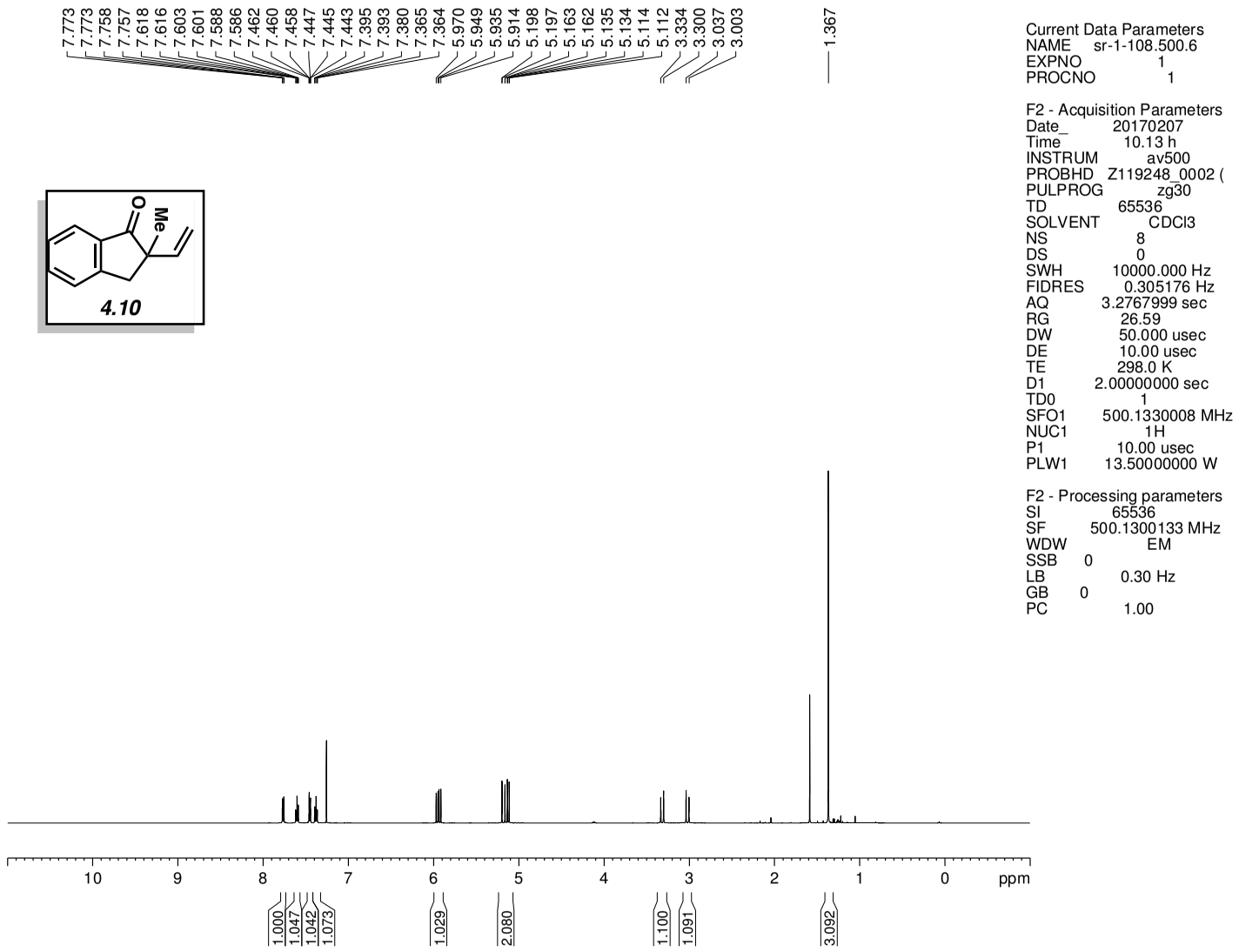

Figure 4.107 ^{1}H NMR (500 MHz, $CDCl_3$) of compound **4.10**.

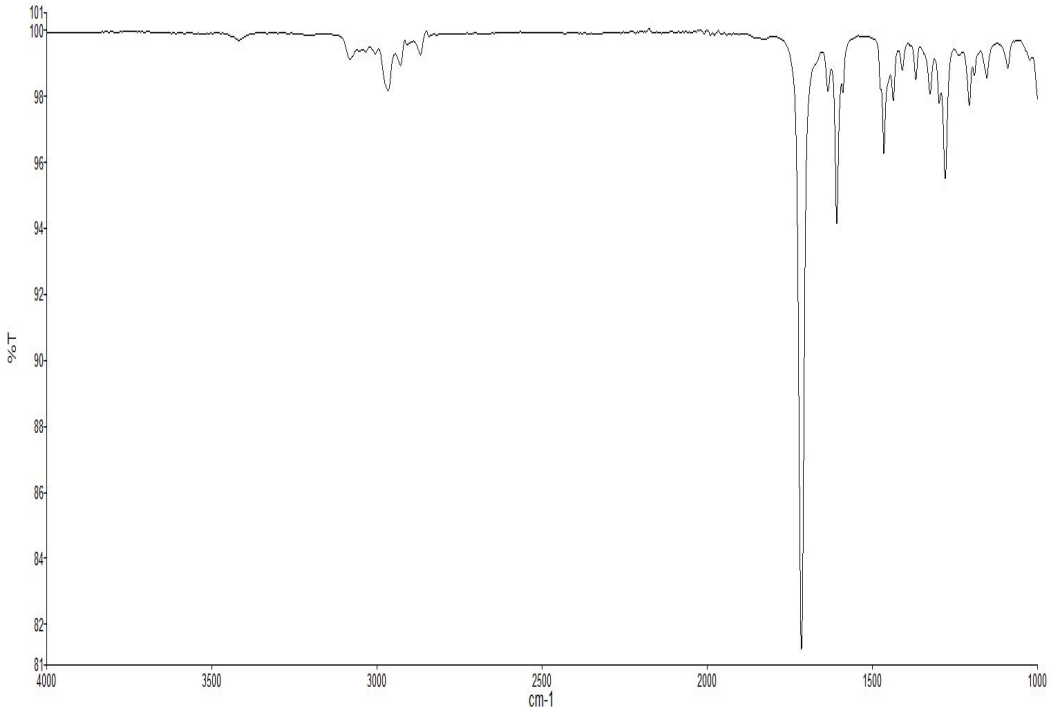

Figure 4.108 Infrared spectrum of compound **4.10**.

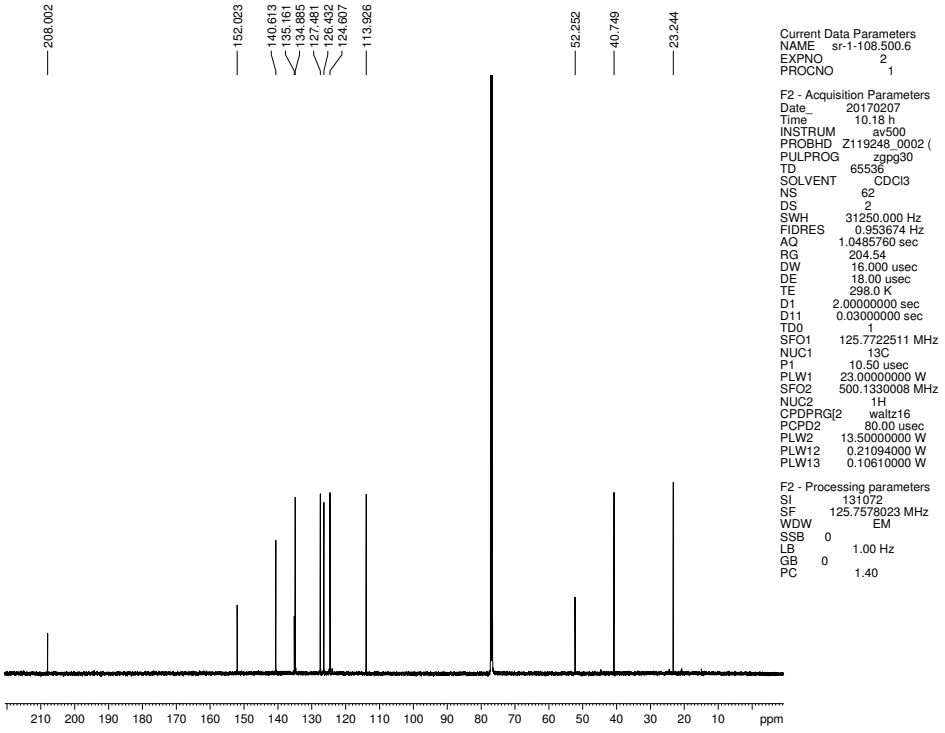

Figure 4.109 ^{13}C NMR (125 MHz, $CDCl_3$) of compound **4.10**.

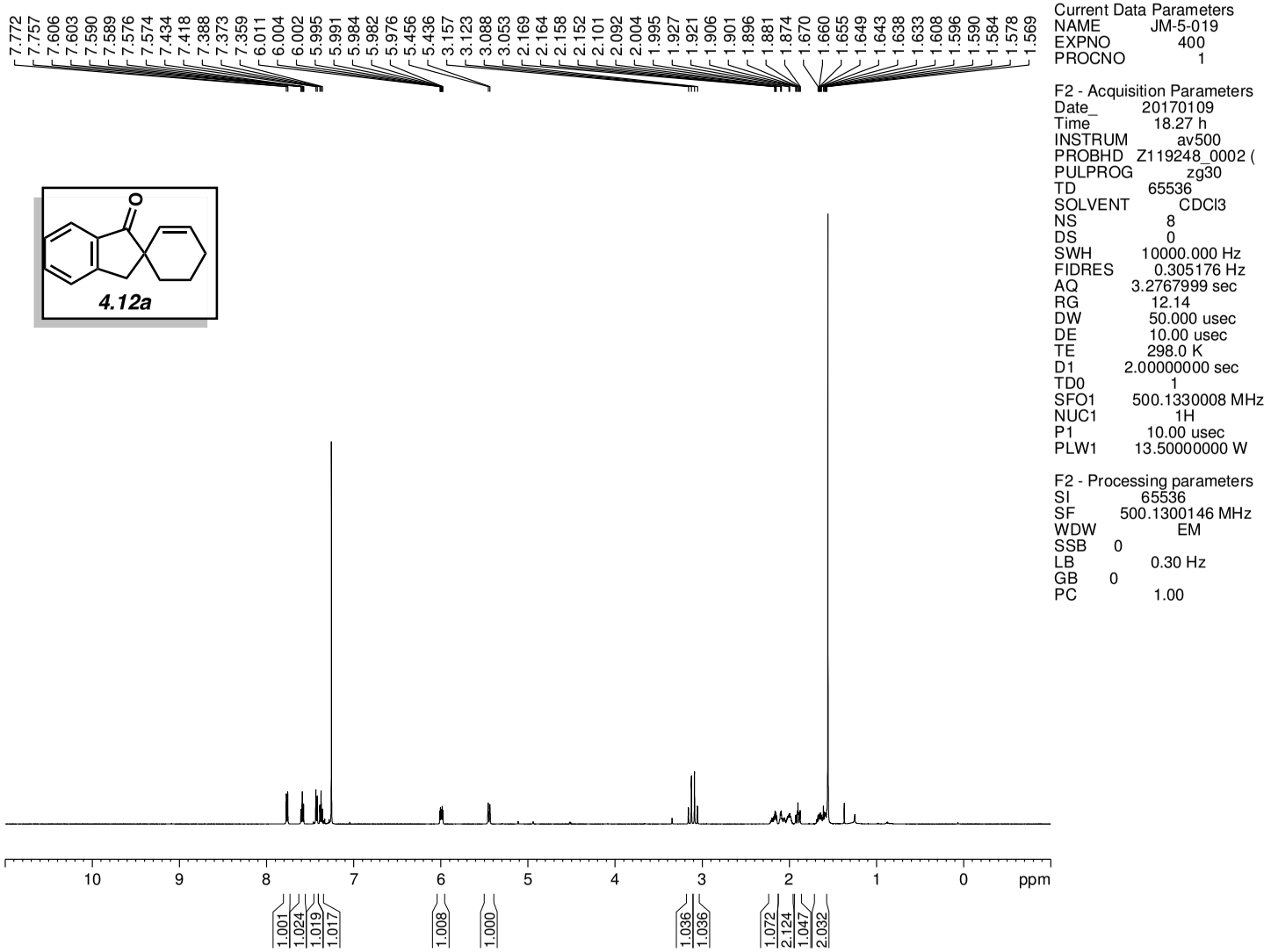

Figure 4.110 ^{1}H NMR (500 MHz, $CDCl_3$) of compound **4.12a**.

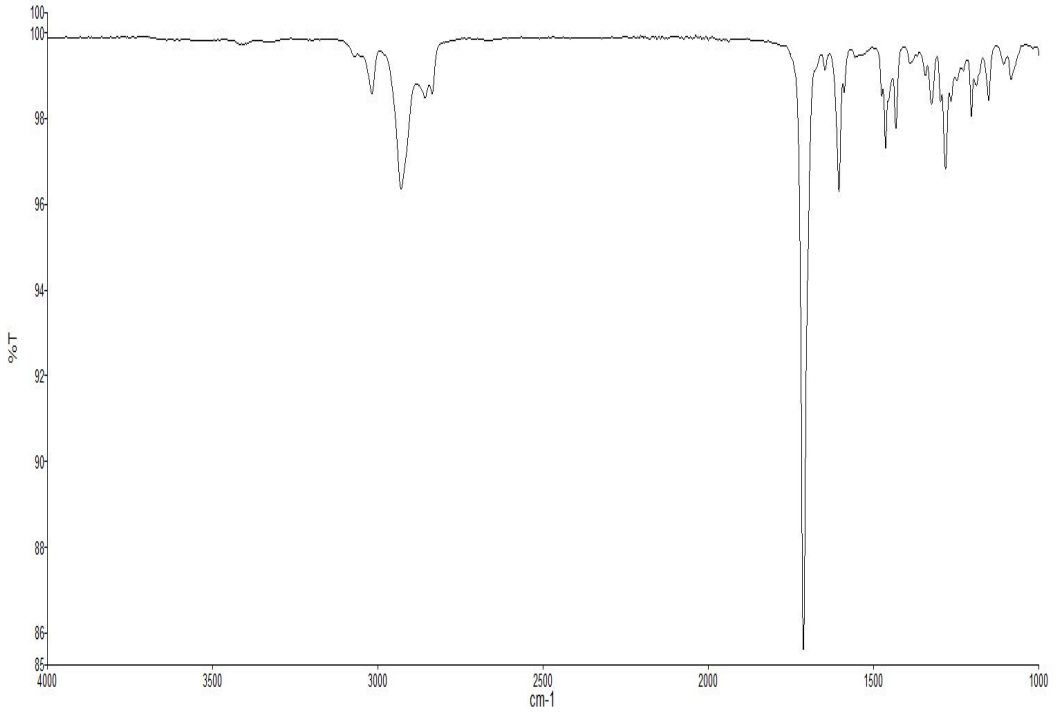

Figure 4.111 Infrared spectrum of compound **4.12a**.

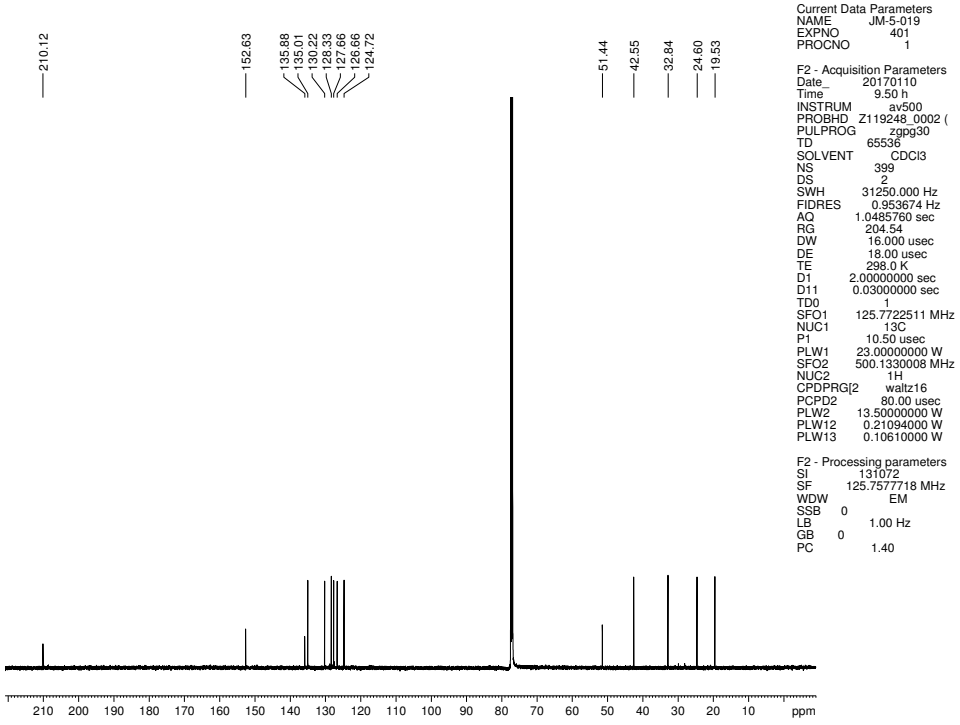

Figure 4.112 ^{13}C NMR (125 MHz, $CDCl_3$) of compound **4.12a**.

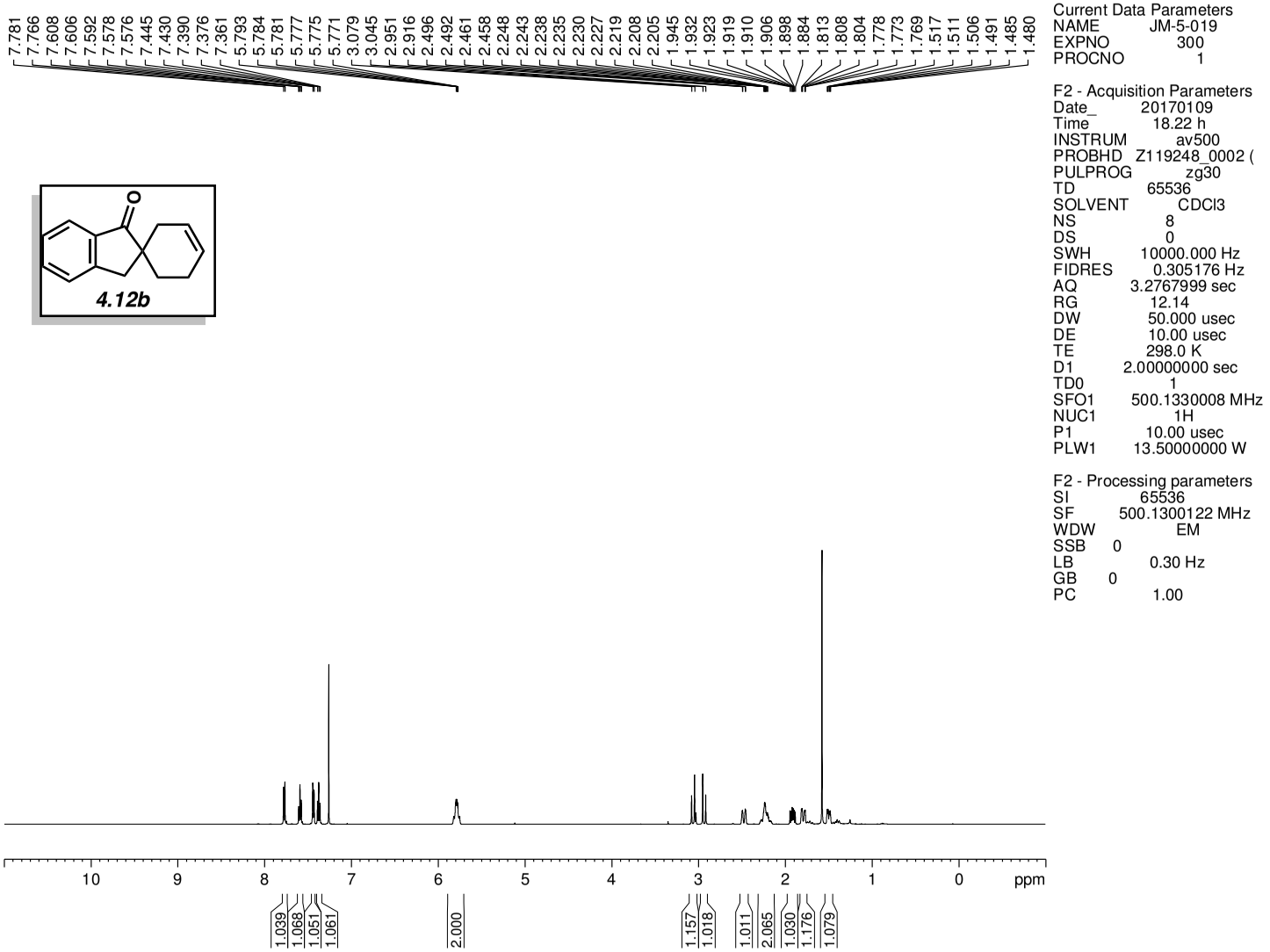

Figure 4.113 ^{1}H NMR (500 MHz, $CDCl_3$) of compound **4.12b**.

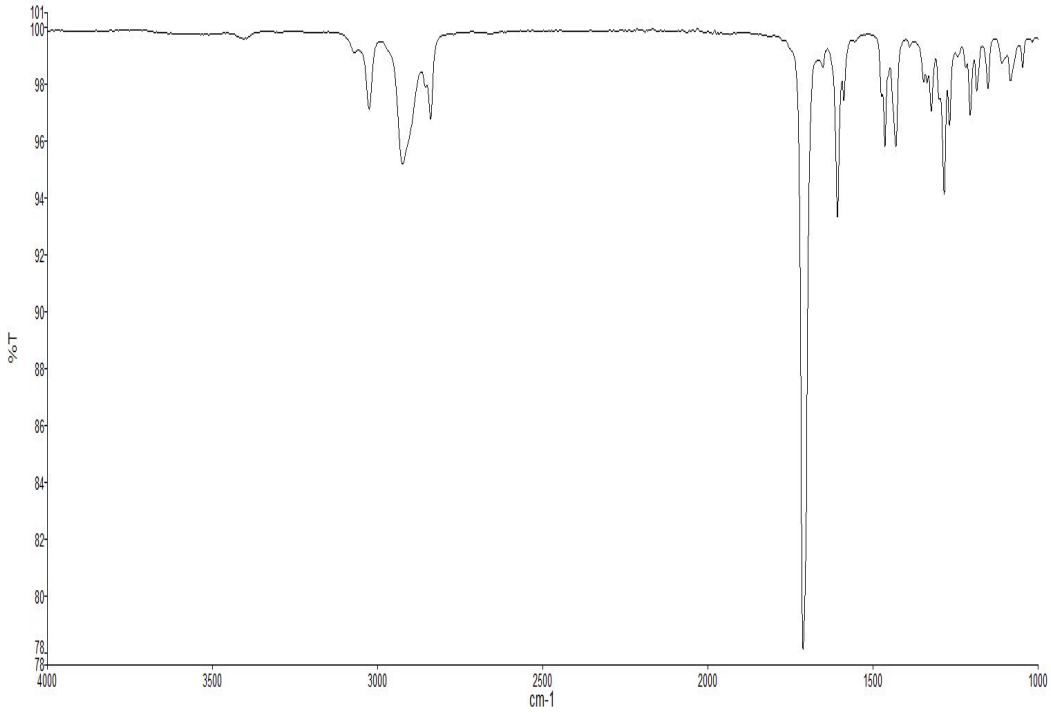

Figure 4.114 Infrared spectrum of compound **4.12b**.

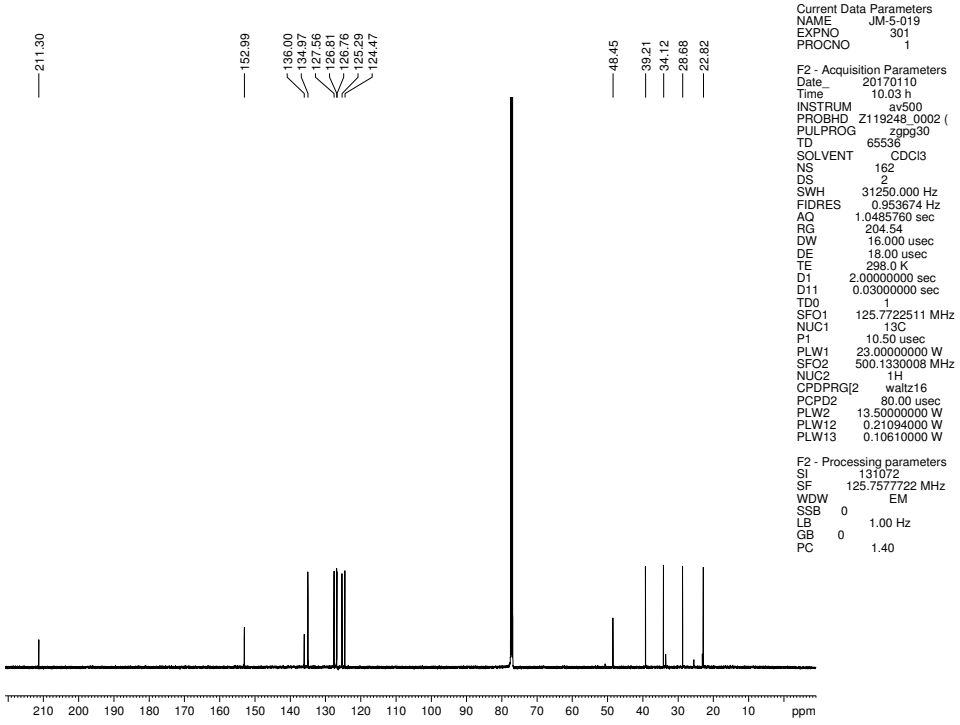

Figure 4.115 ^{13}C NMR (125 MHz, $CDCl_3$) of compound **4.12b**.

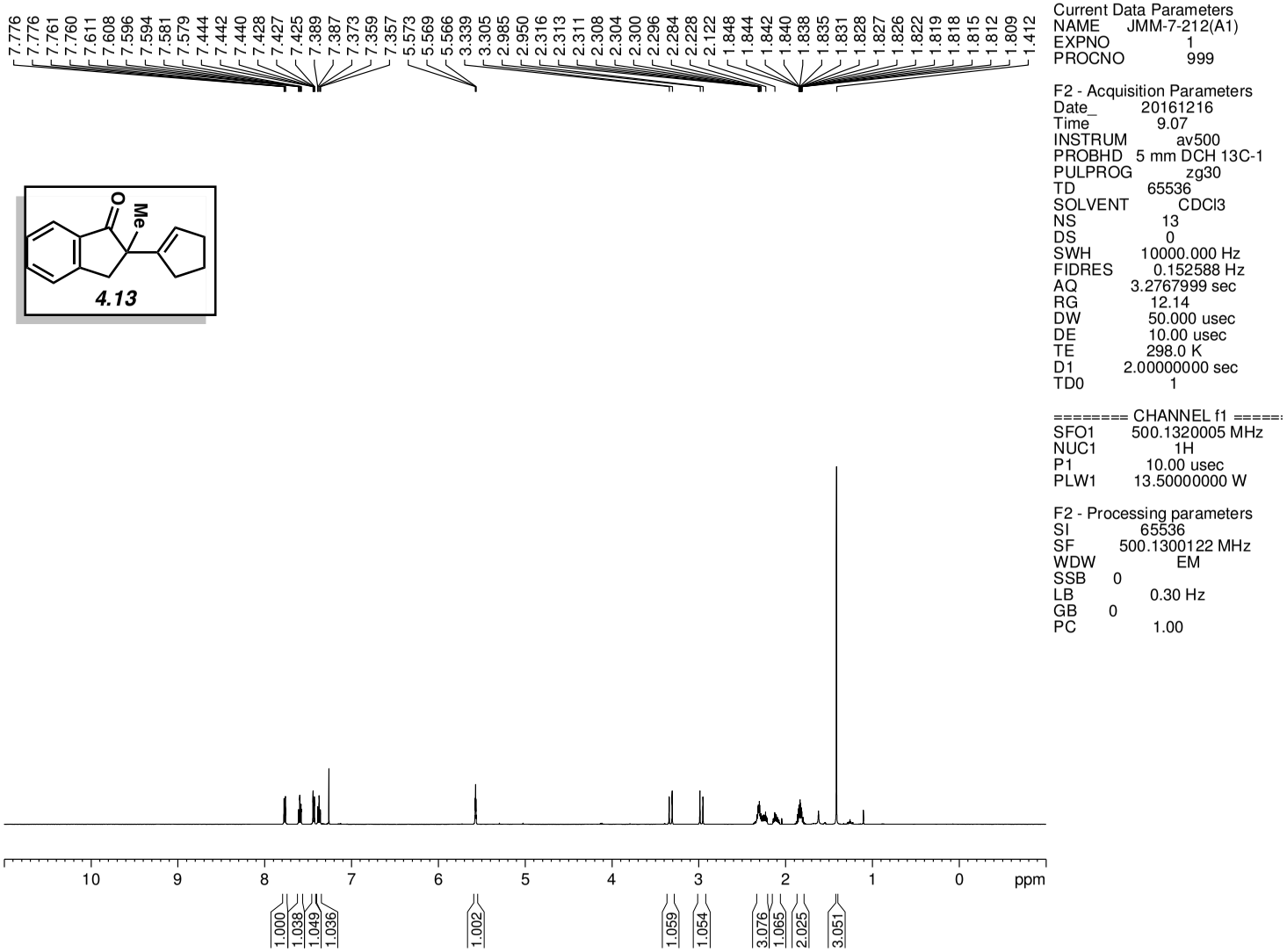

Figure 4.116 ^{1}H NMR (500 MHz, $CDCl_3$) of compound **4.13**.

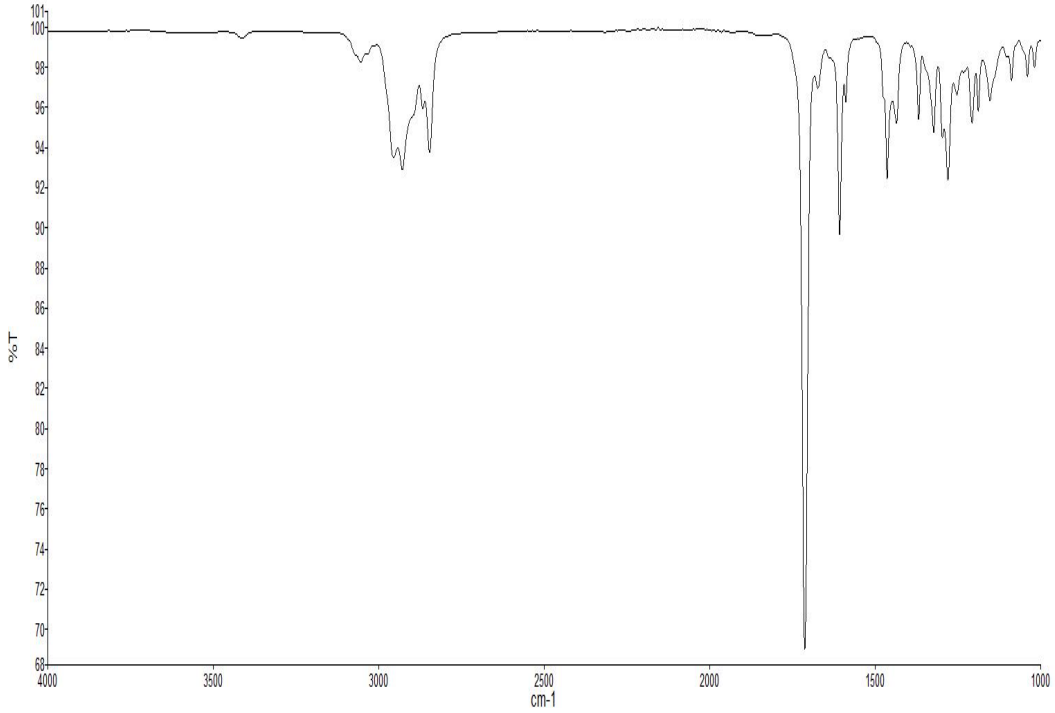

Figure 4.117 Infrared spectrum of compound **4.13**.

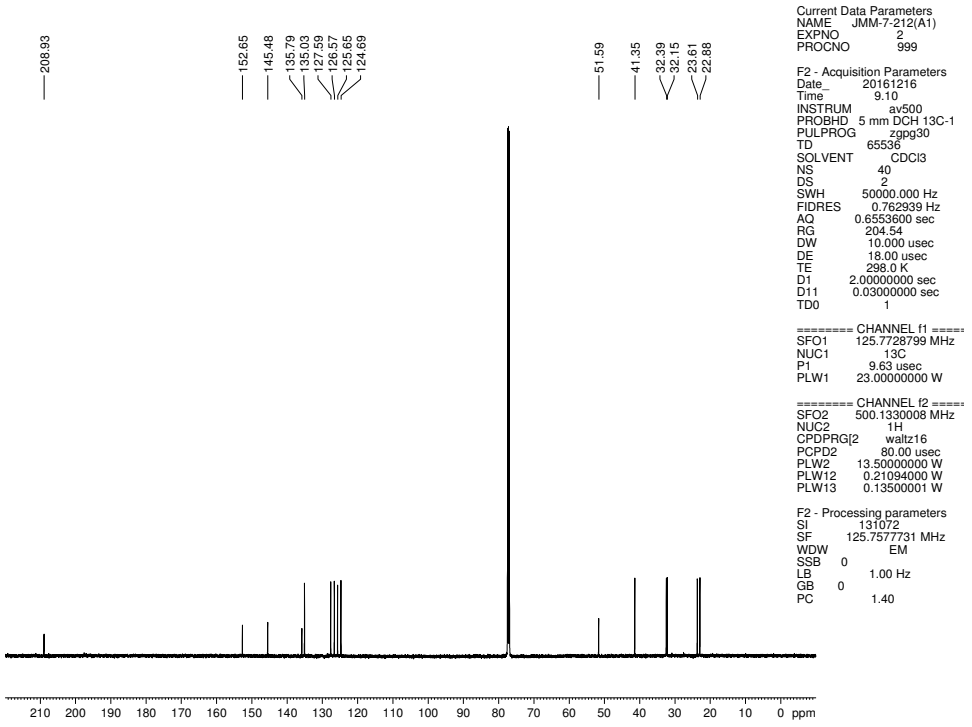

Figure 4.118 ^{13}C NMR (125 MHz, $CDCl_3$) of compound **4.13**.

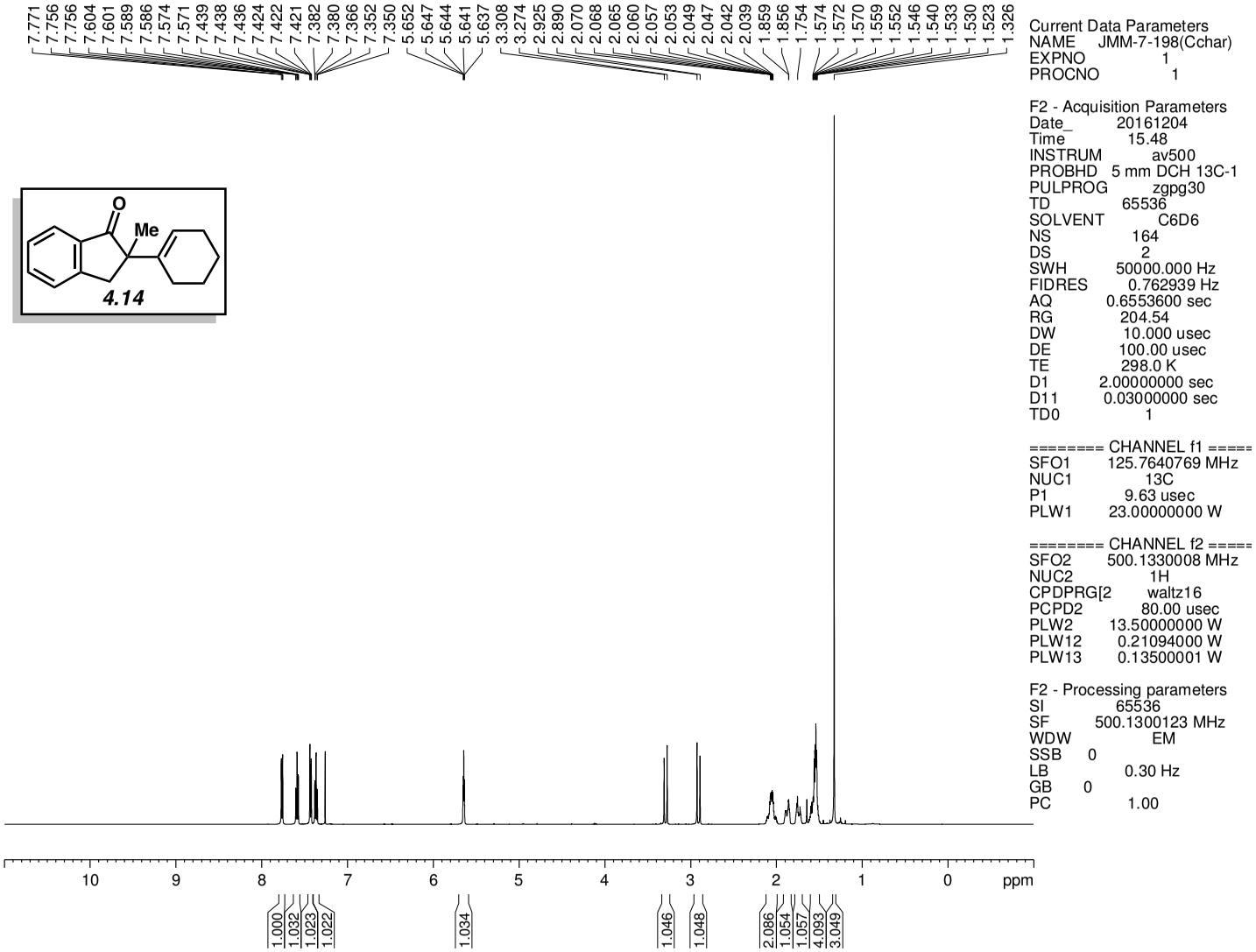

Figure 4.119 ^{1}H NMR (500 MHz, $CDCl_3$) of compound **4.14**.

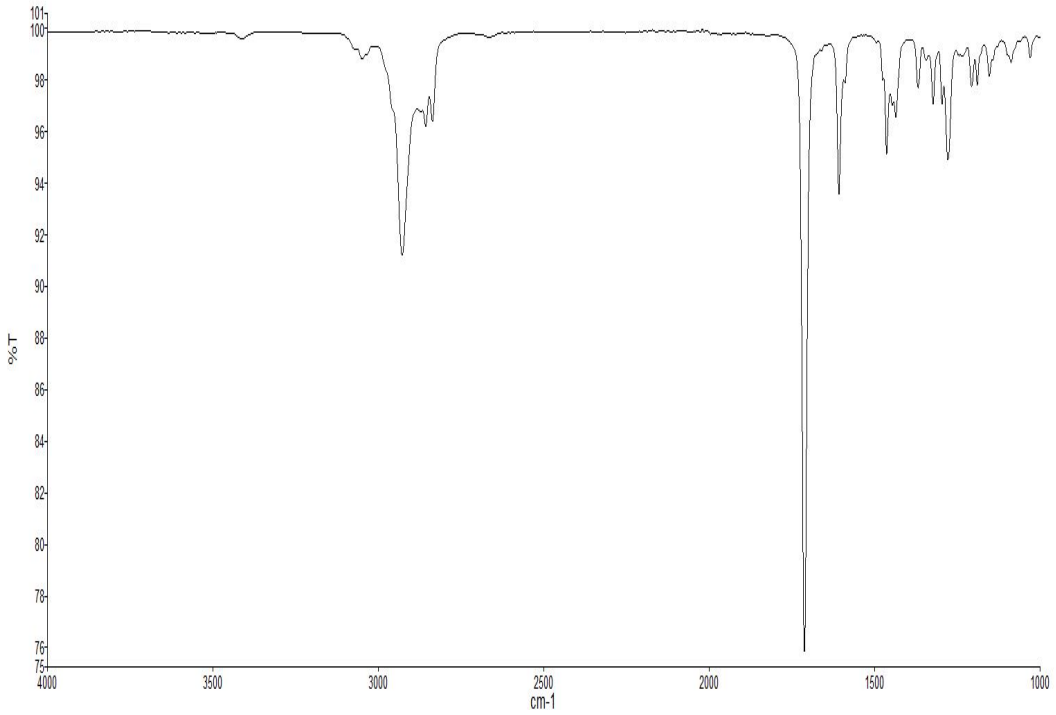

Figure 4.120 Infrared spectrum of compound **4.14**.

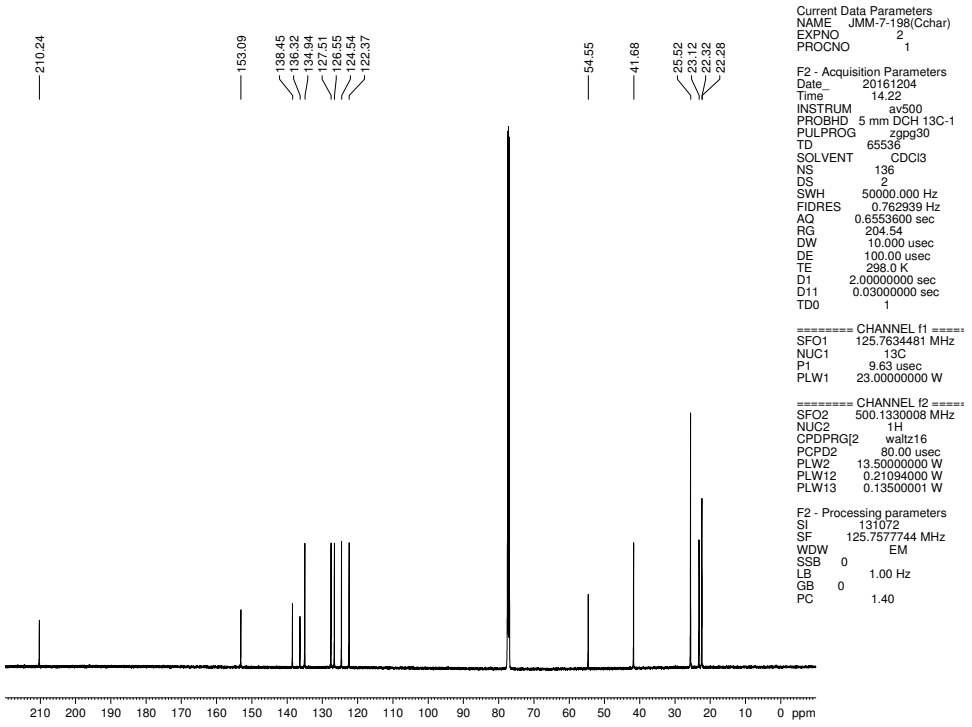

Figure 4.121 ^{13}C NMR (125 MHz, $CDCl_3$) of compound **4.14**.

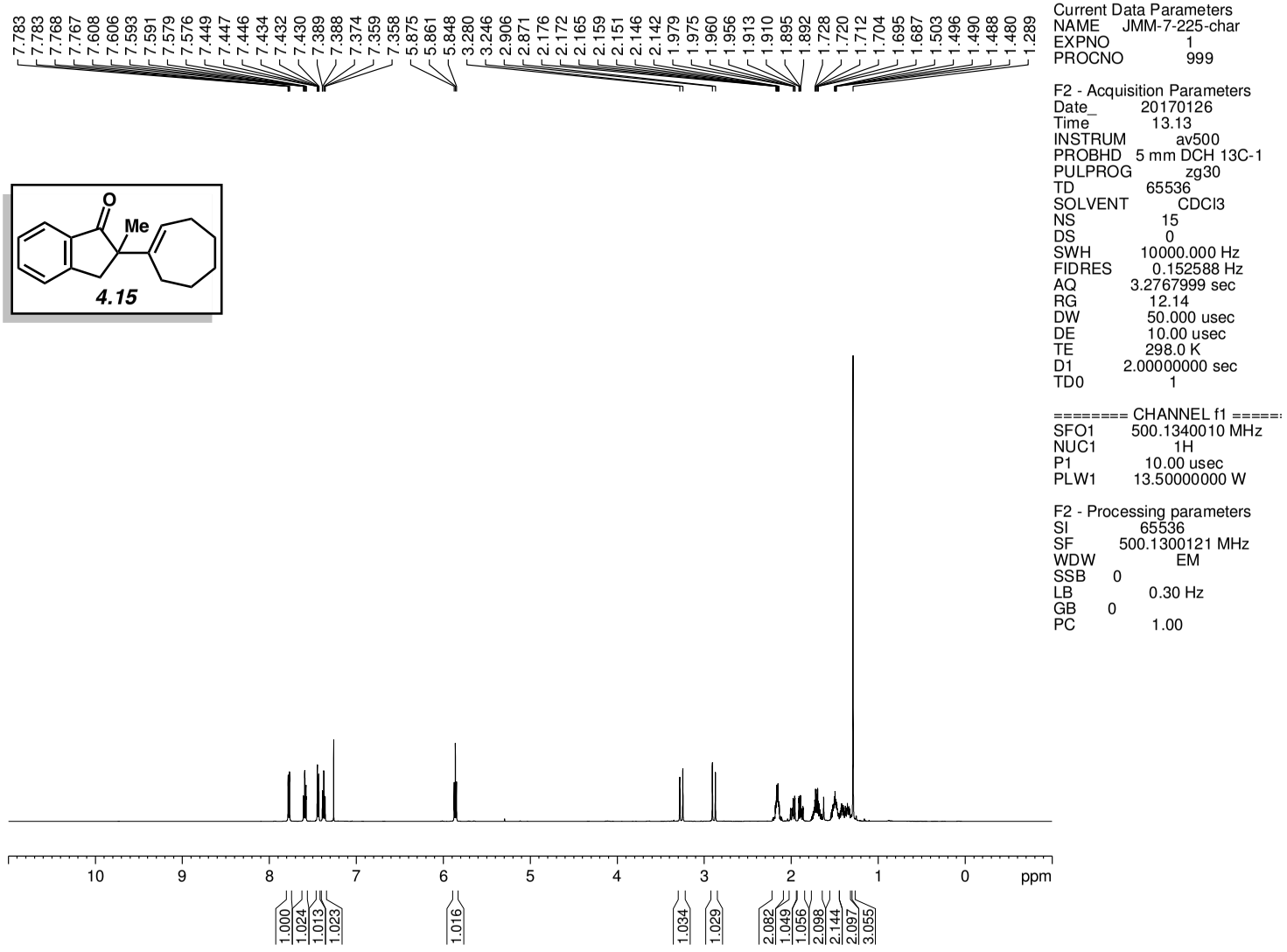

Figure 4.122 ^{1}H NMR (500 MHz, $CDCl_3$) of compound **4.15**.

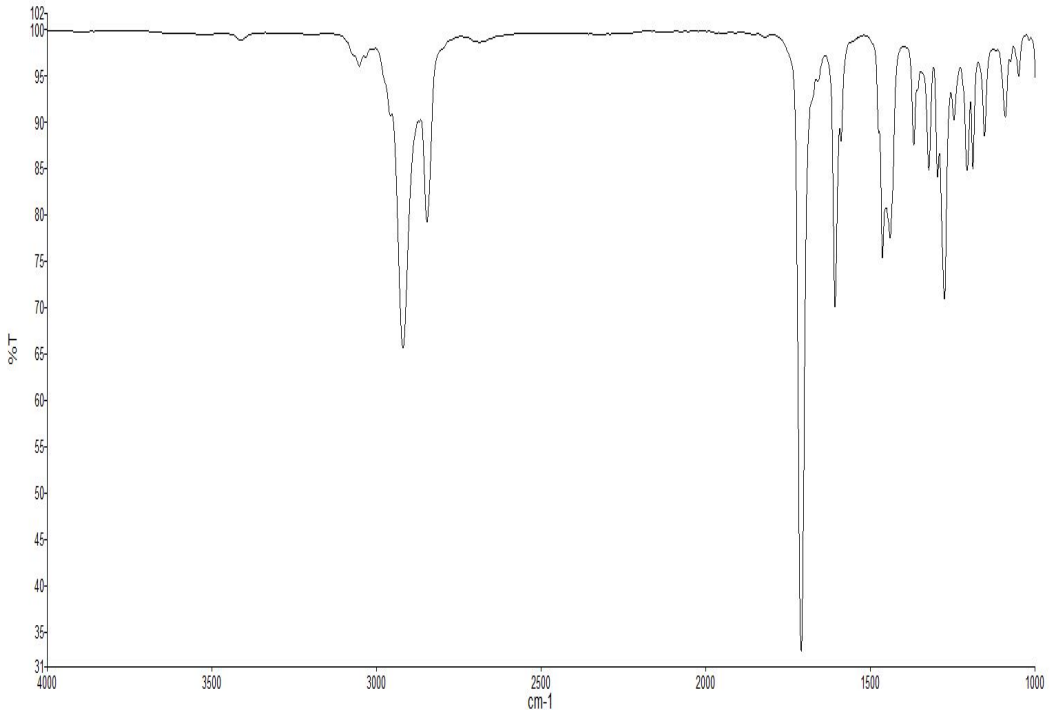

Figure 4.123 Infrared spectrum of compound **4.15**.

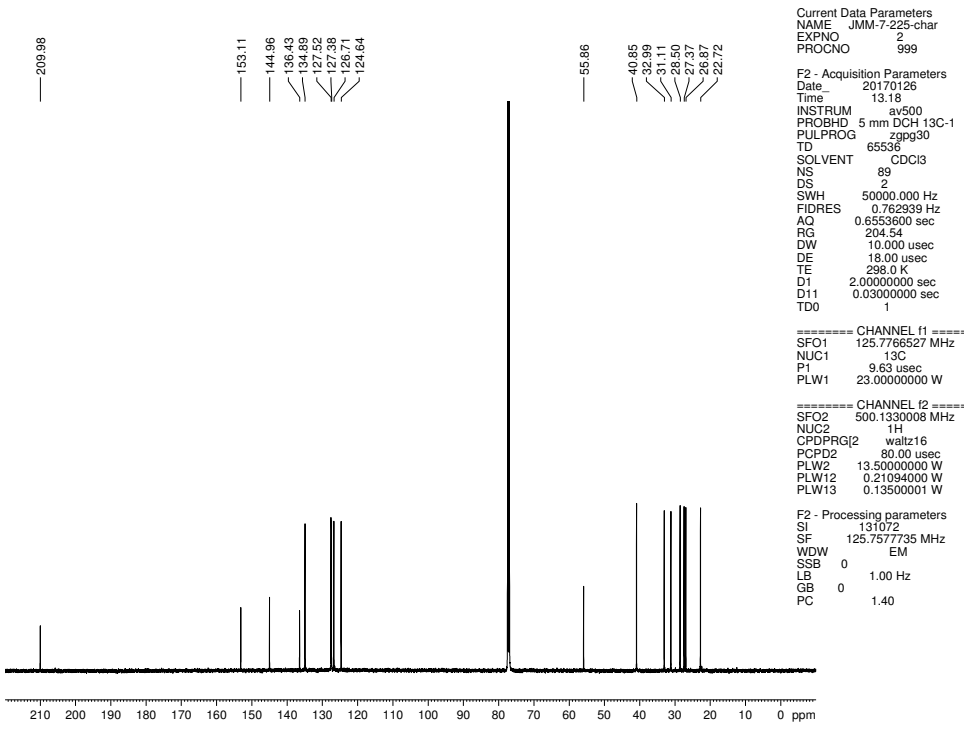

Figure 4.124 ^{13}C NMR (125 MHz, $CDCl_3$) of compound **4.15**.

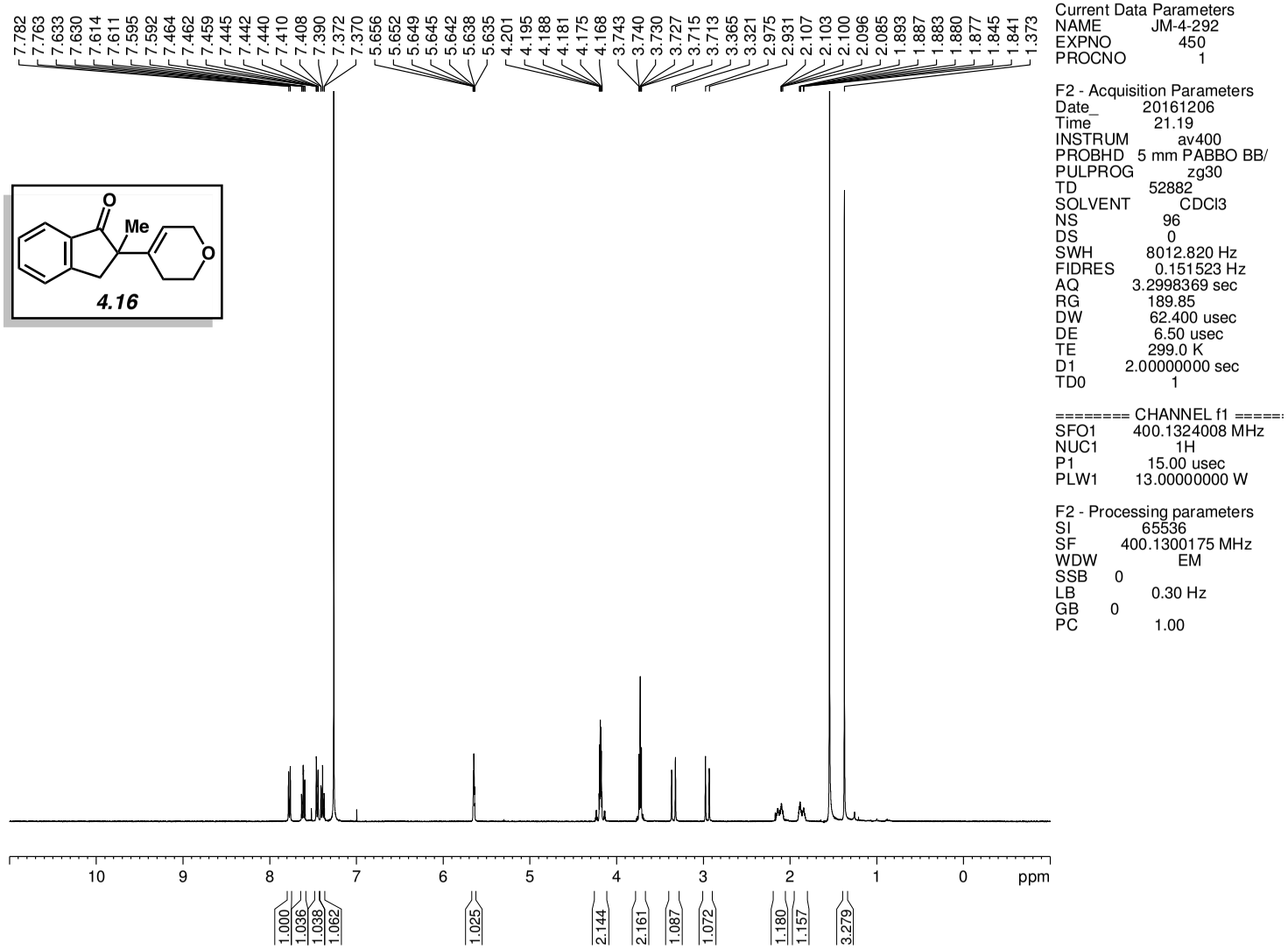

Figure 4.125 ^{1}H NMR (500 MHz, $CDCl_3$) of compound **4.16**.

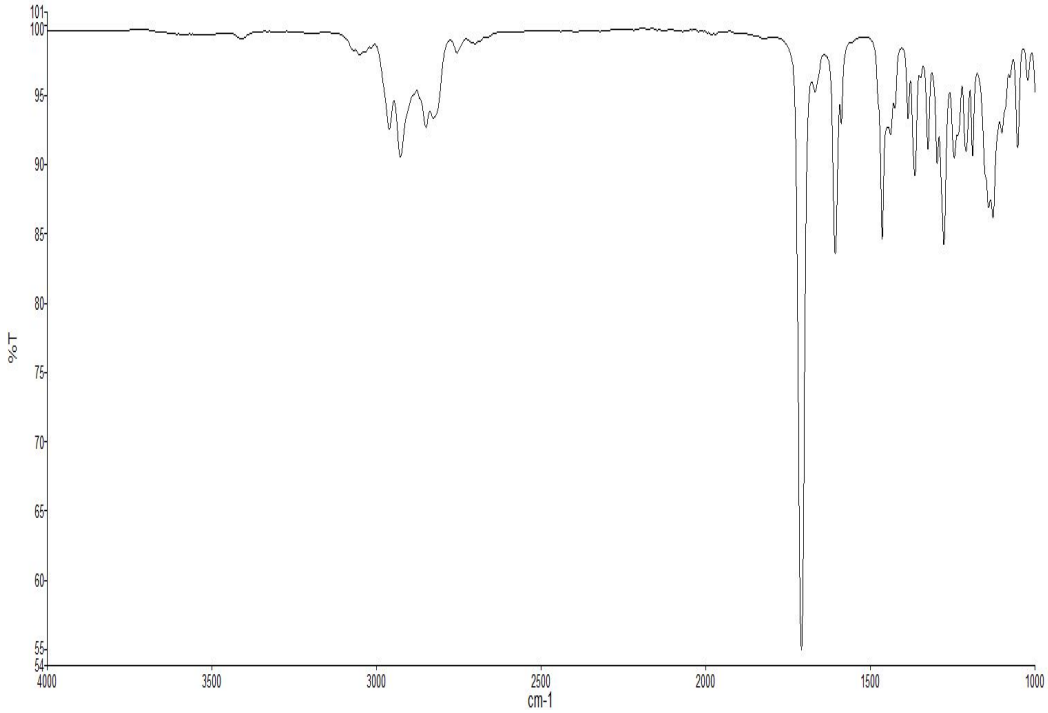

Figure 4.126 Infrared spectrum of compound **4.16**.

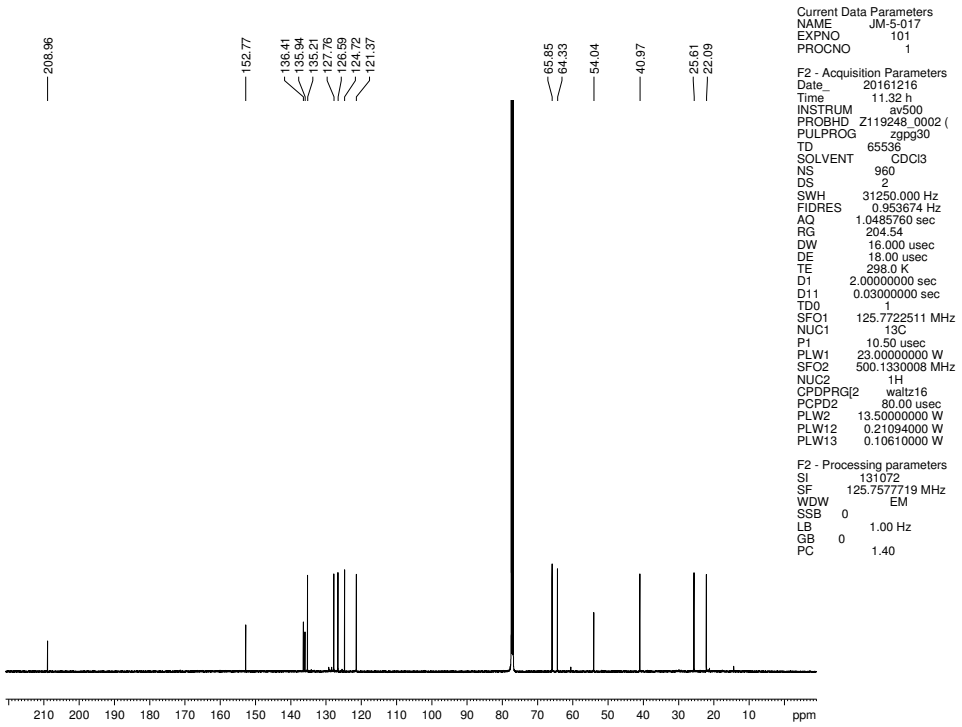

Figure 4.127 ^{13}C NMR (125 MHz, $CDCl_3$) of compound **4.16**.

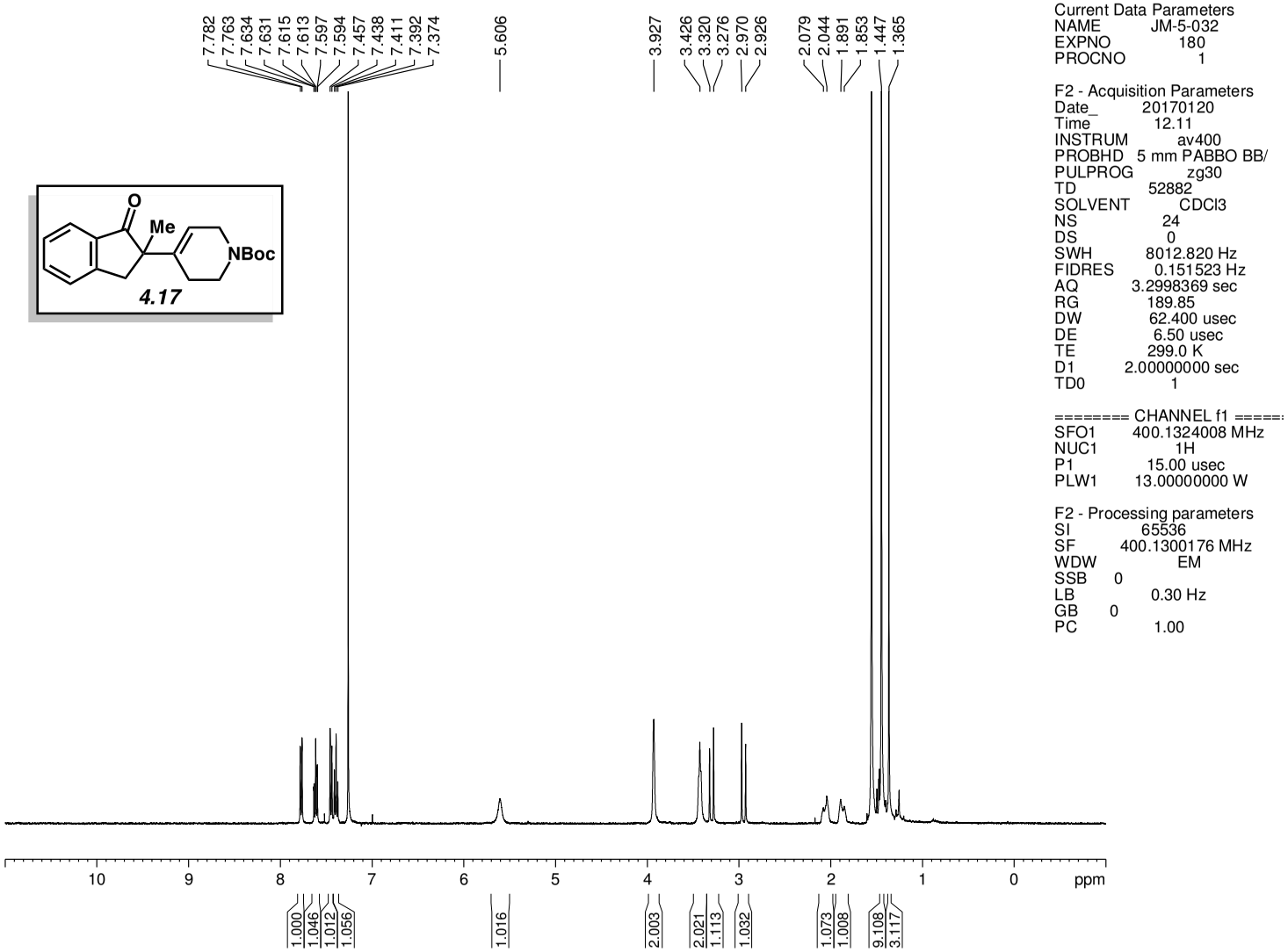

Figure 4.128 ^{1}H NMR (500 MHz, $CDCl_3$) of compound **4.17**.

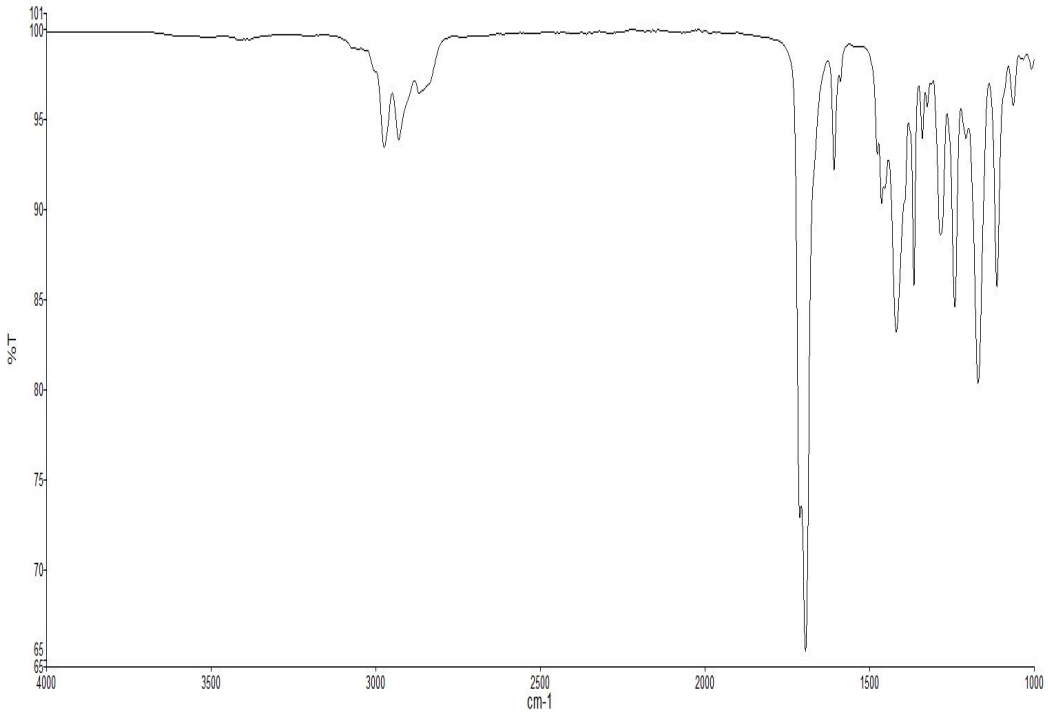

Figure 4.129 Infrared spectrum of compound **4.17**.

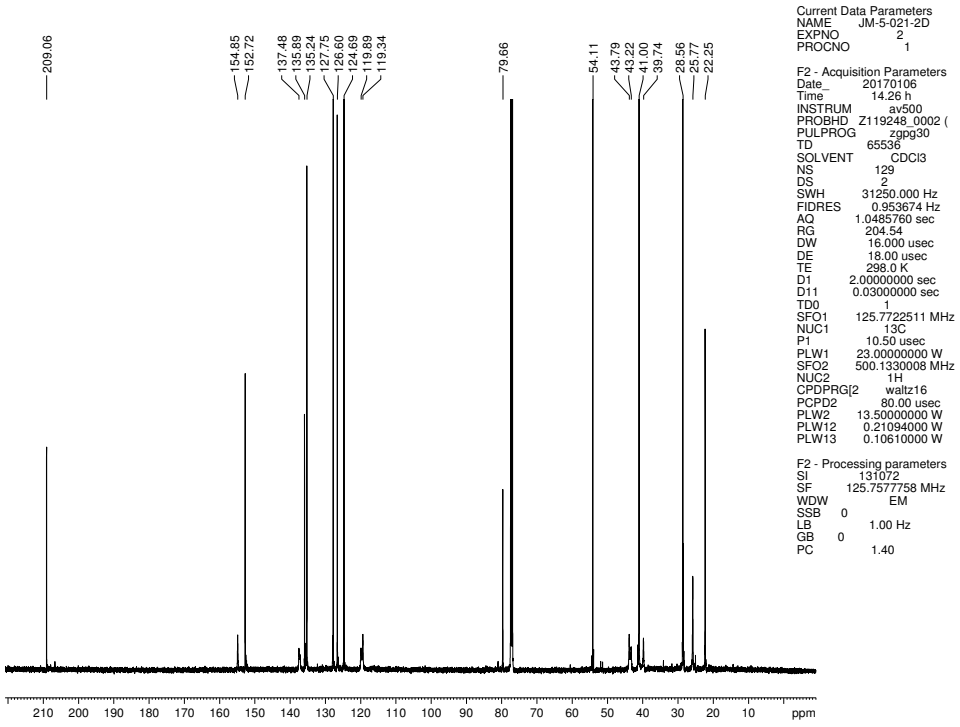

Figure 4.130 ^{13}C NMR (125 MHz, $CDCl_3$) of compound **4.17**.

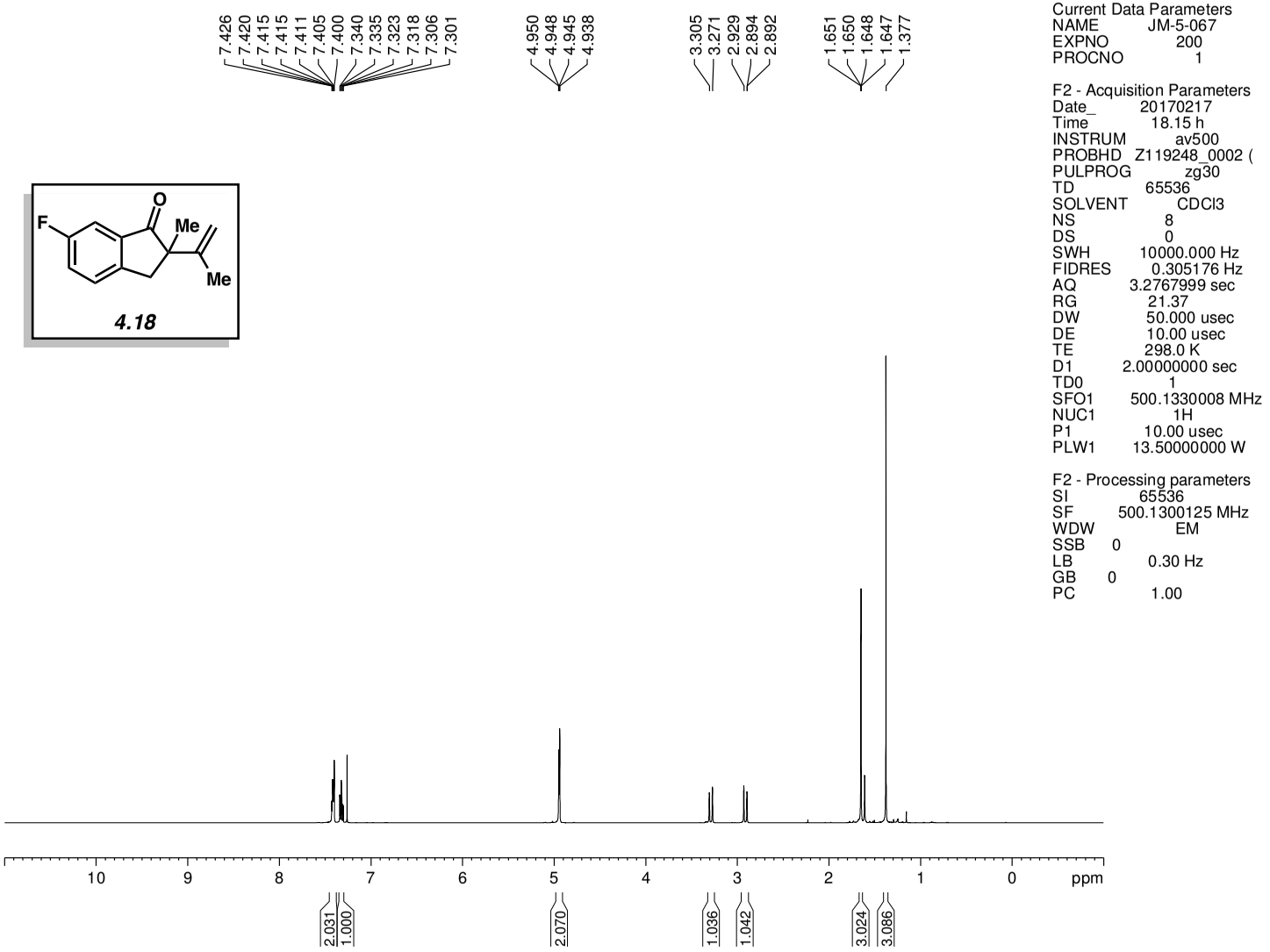

Figure 4.131 ^{1}H NMR (500 MHz, $CDCl_3$) of compound **4.18**.

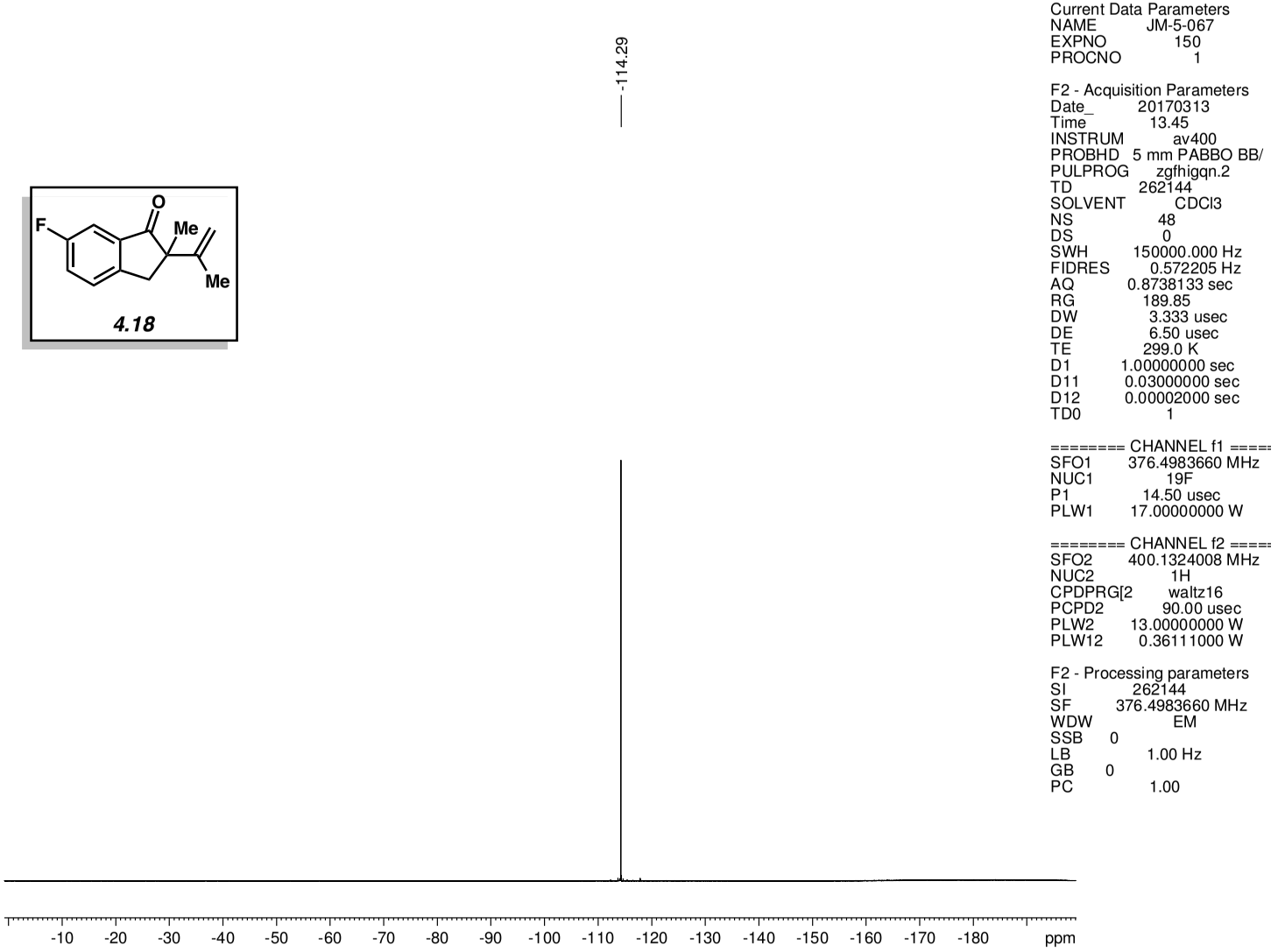

Figure 4.132 ^{19}F NMR (376 MHz, $CDCl_3$) of compound **4.18**.

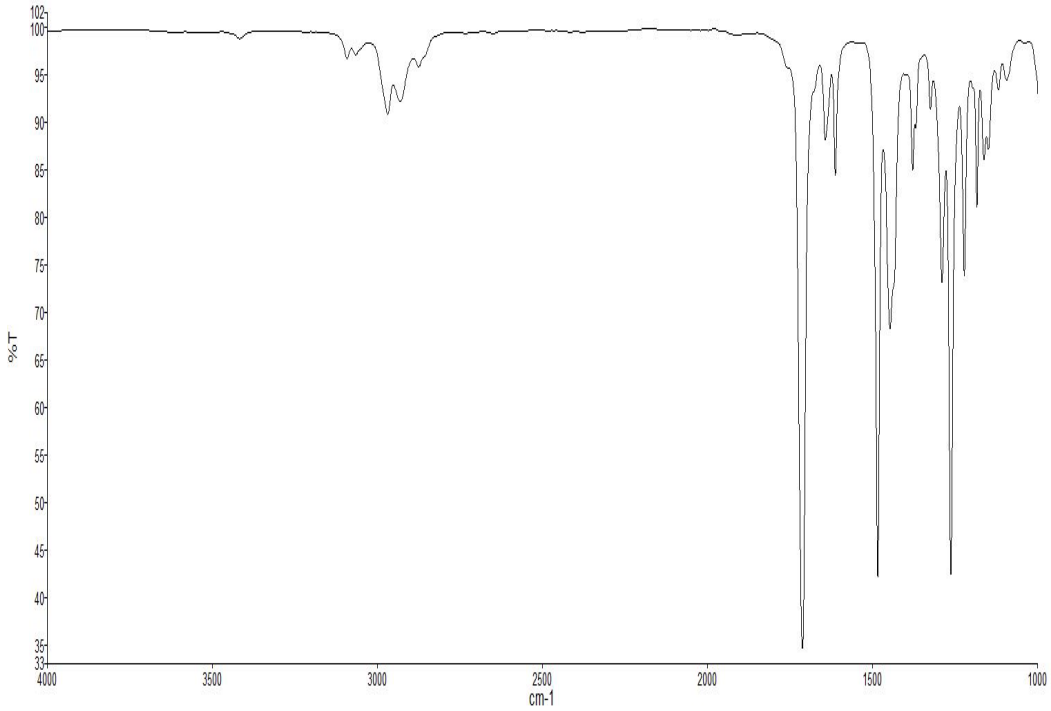

Figure 4.133 Infrared spectrum of compound **4.18**.

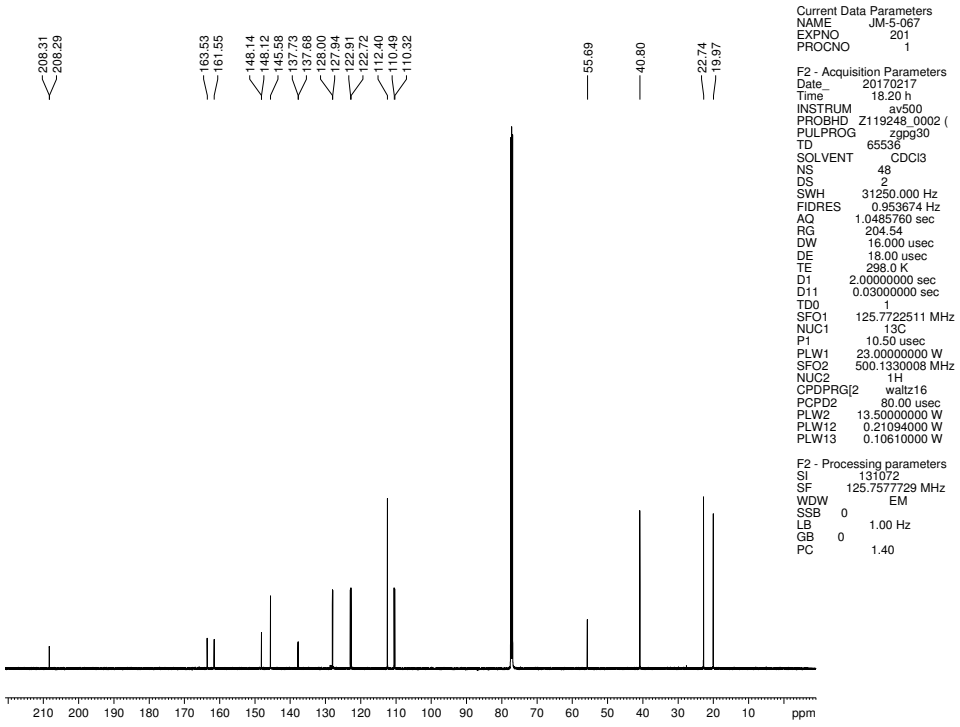

Figure 4.134 ^{13}C NMR (125 MHz, $CDCl_3$) of compound **4.18**.

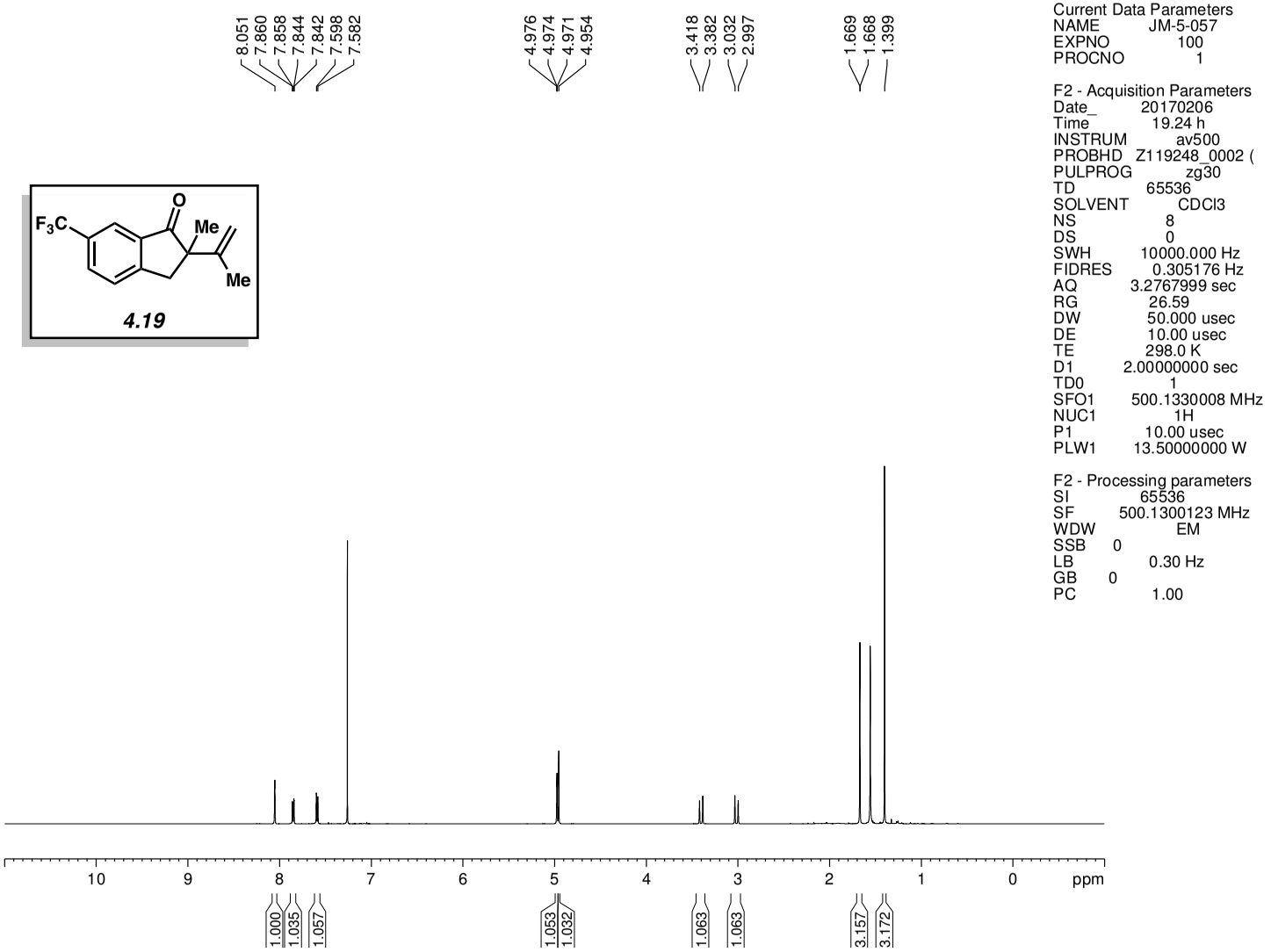

Figure 4.135 ^{1}H NMR (500 MHz, $CDCl_3$) of compound **4.19**.

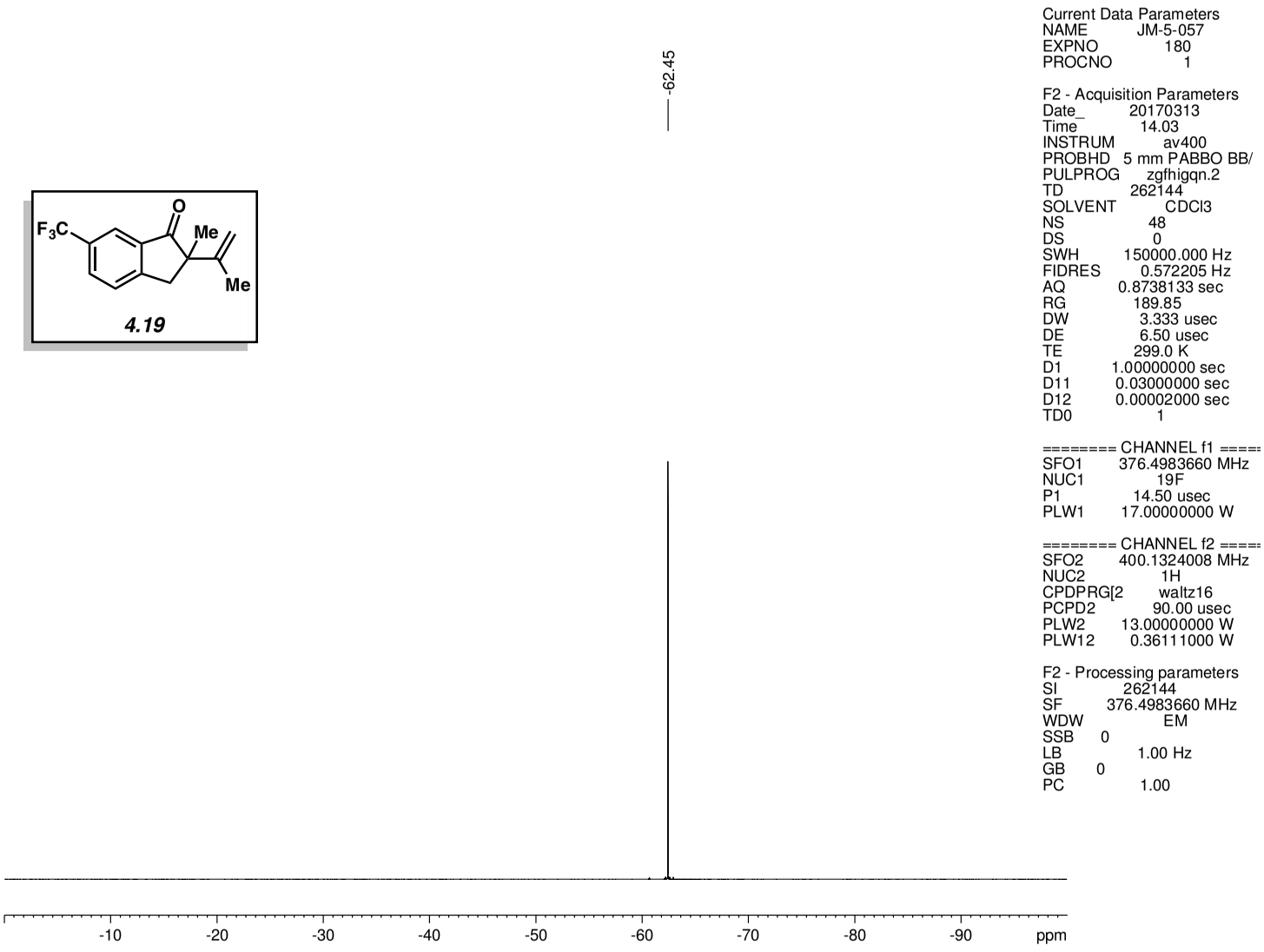

Figure 4.136 ^{19}F NMR (376 MHz, $CDCl_3$) of compound **4.19**.

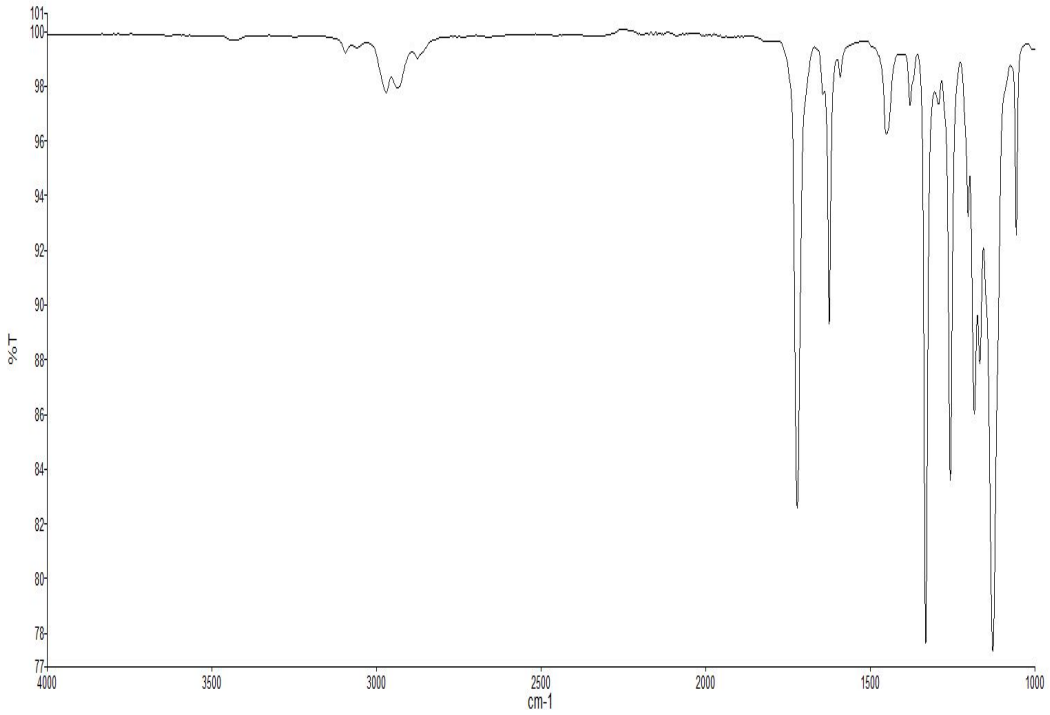

Figure 4.137 Infrared spectrum of compound **4.19**.

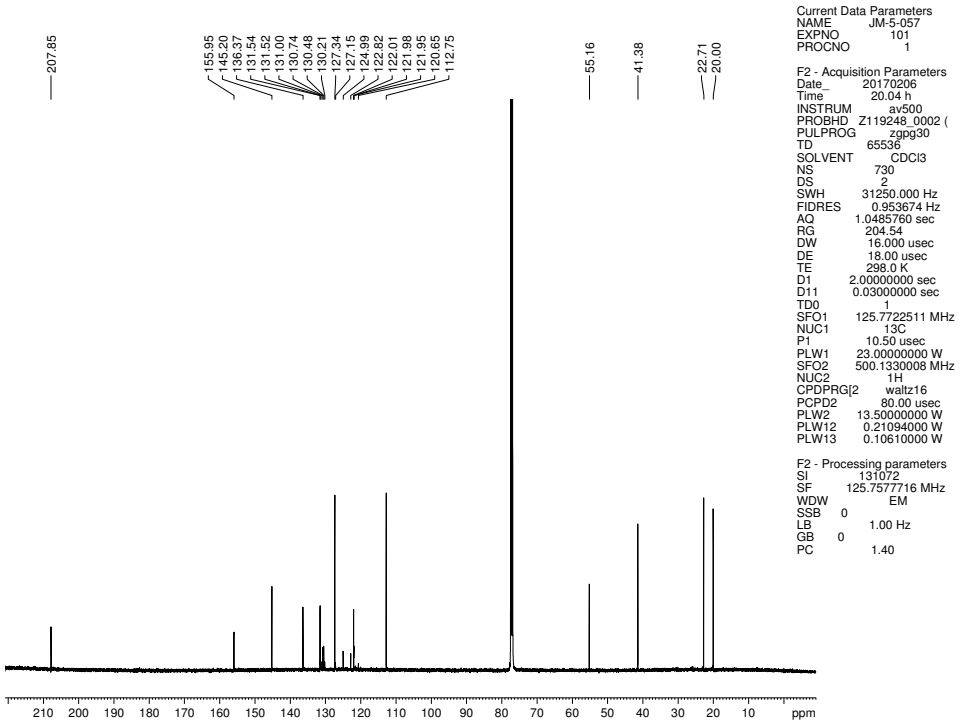

Figure 4.138 ^{13}C NMR (125 MHz, $CDCl_3$) of compound **4.19**.

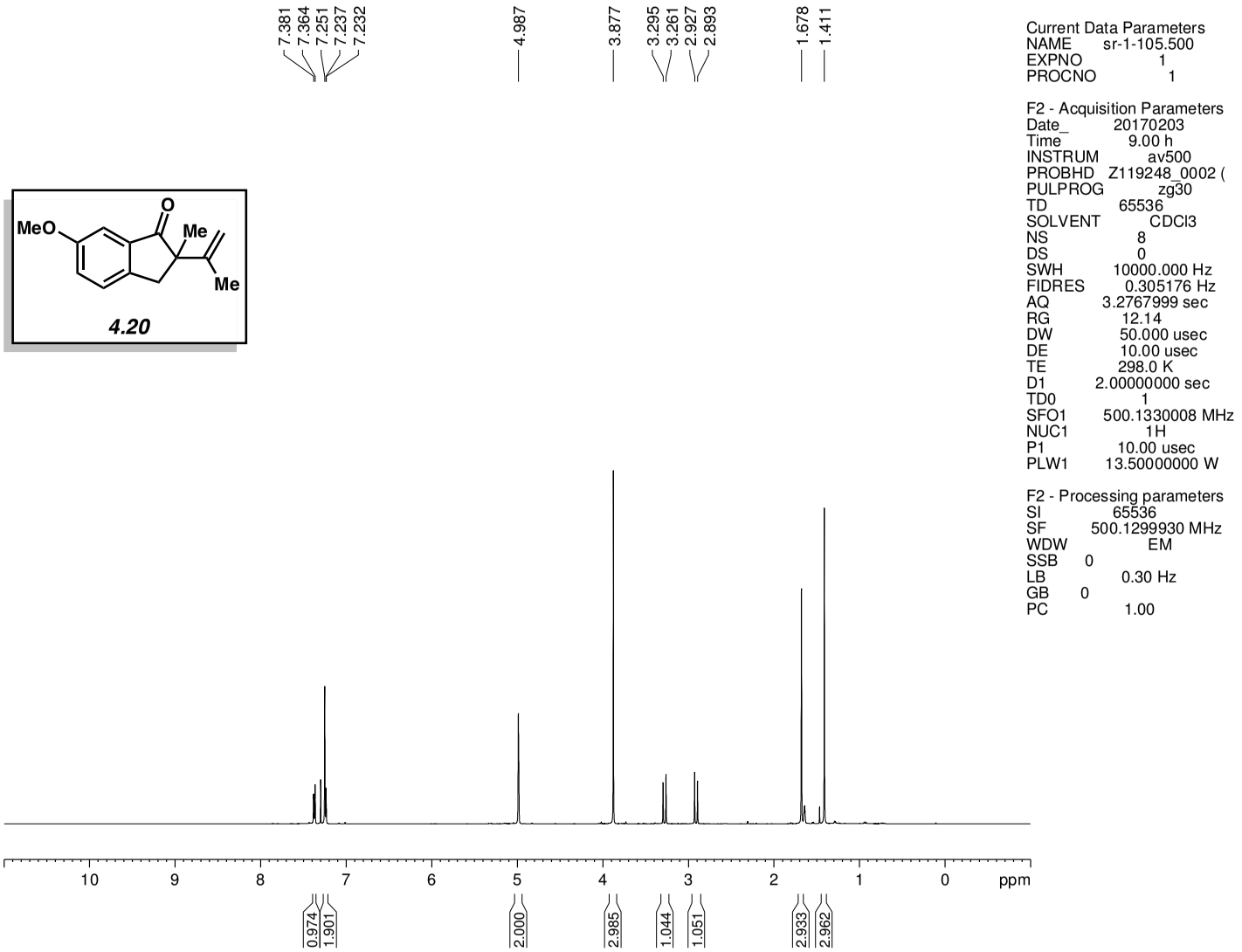

Figure 4.139 ^{1}H NMR (500 MHz, $CDCl_3$) of compound **4.20**.

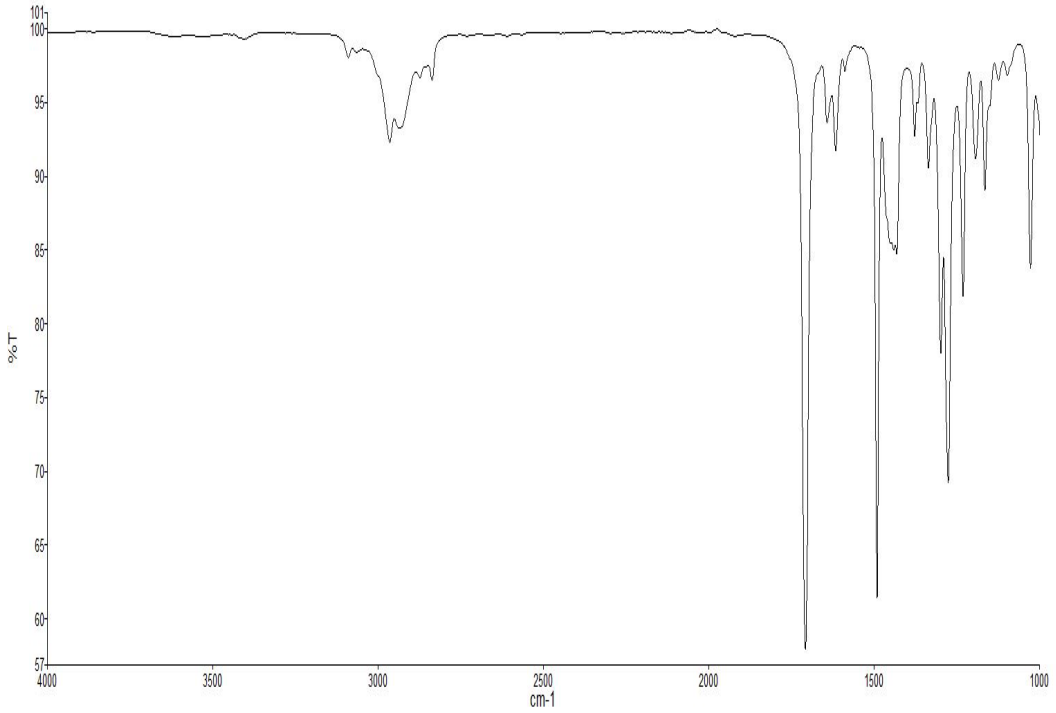

Figure 4.140 Infrared spectrum of compound **4.20**.

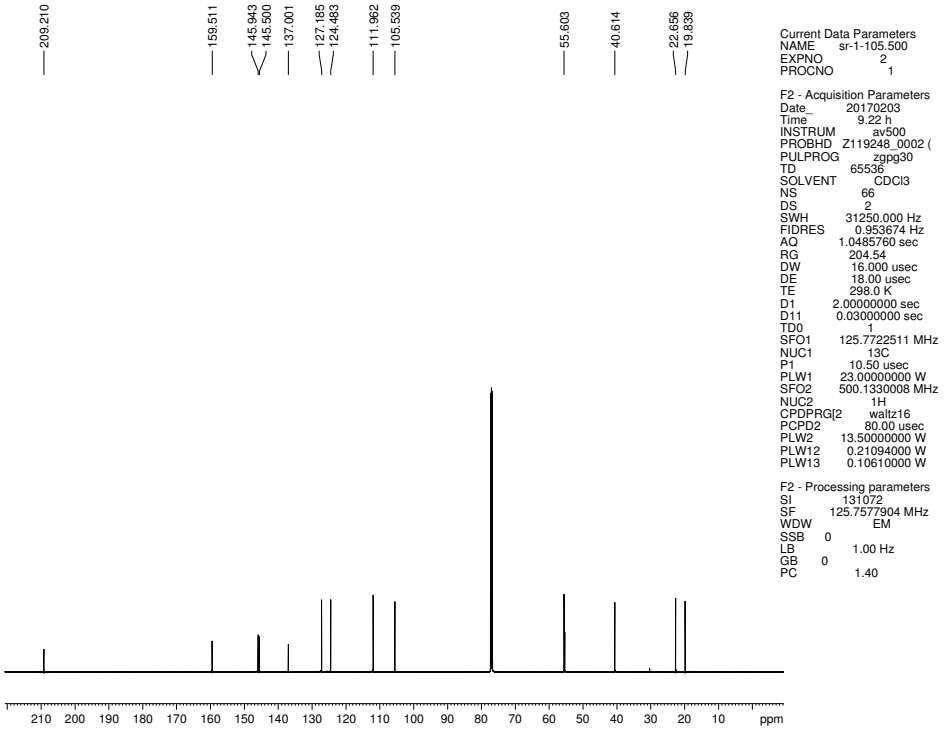

Figure 4.141 ^{13}C NMR (125 MHz, $CDCl_3$) of compound **4.20**.

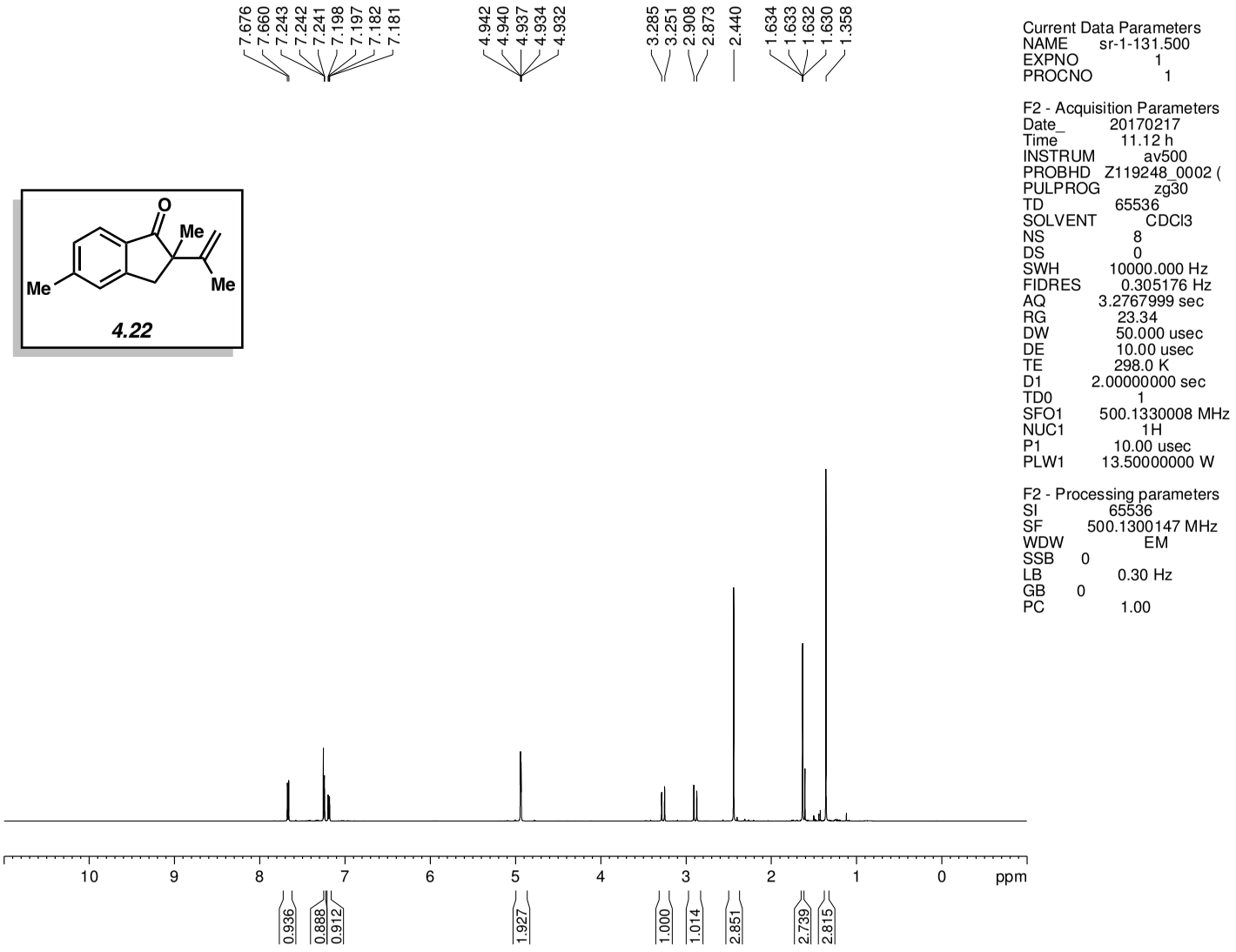

Figure 4.142 ^{1}H NMR (500 MHz, $CDCl_3$) of compound **4.22**.

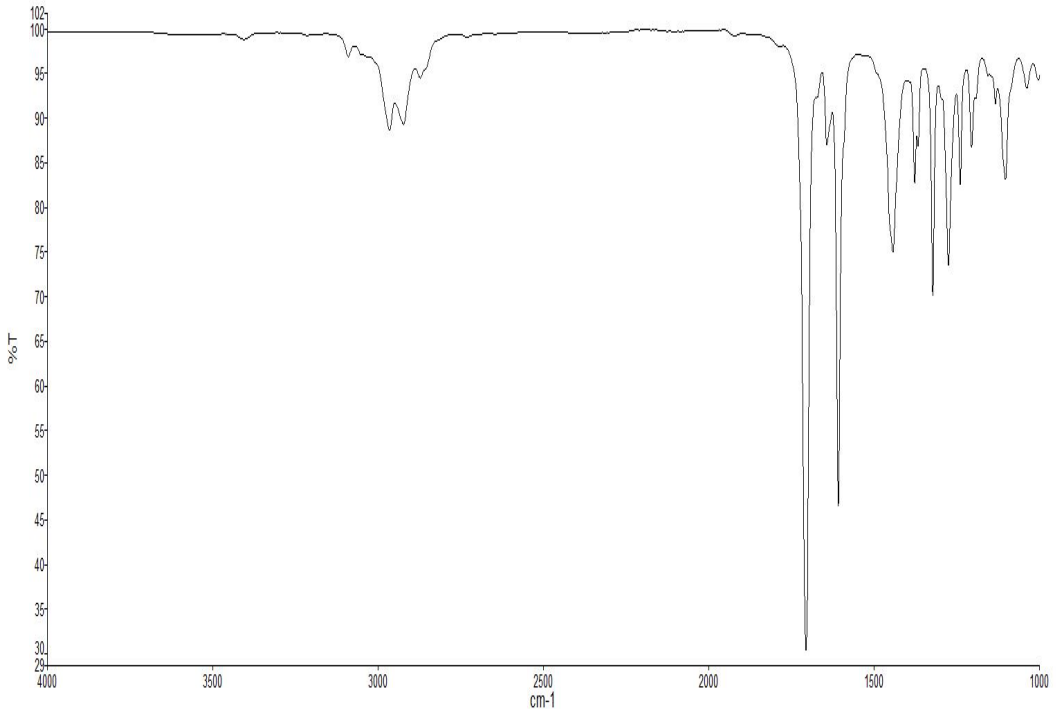

Figure 4.143 Infrared spectrum of compound **4.22**.

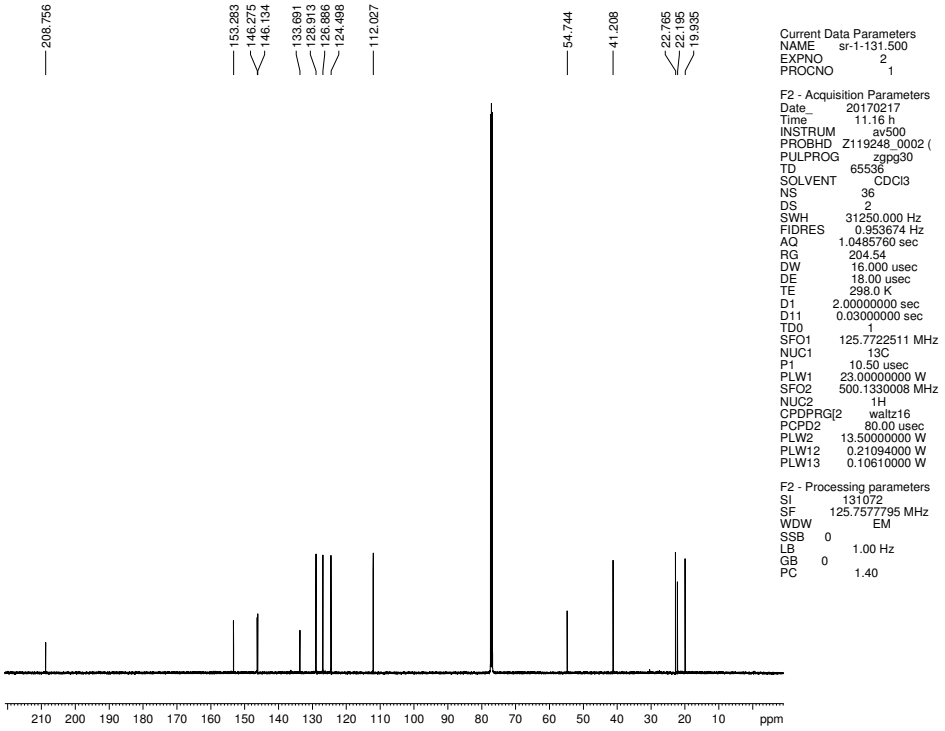

Figure 4.144 ^{13}C NMR (125 MHz, $CDCl_3$) of compound **4.22**.

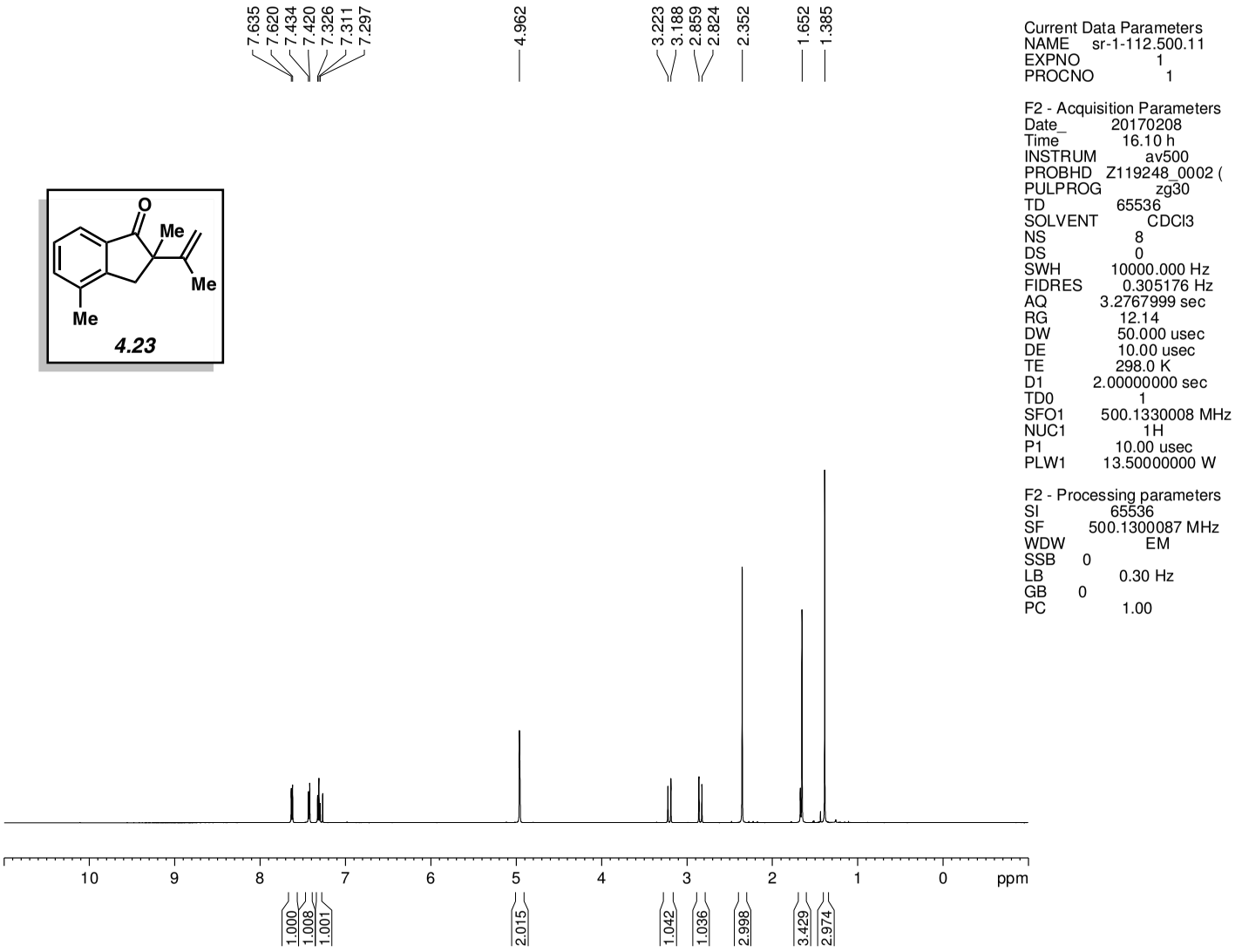

Figure 4.145 ^{1}H NMR (500 MHz, $CDCl_3$) of compound **4.23**.

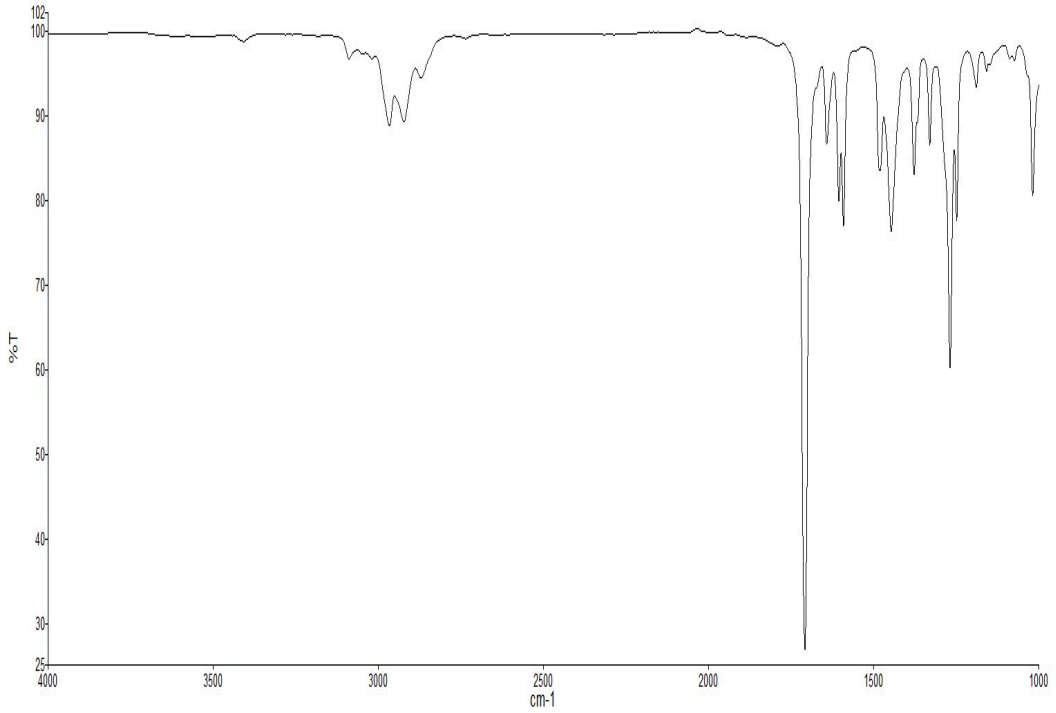

Figure 4.146 Infrared spectrum of compound **4.23**.

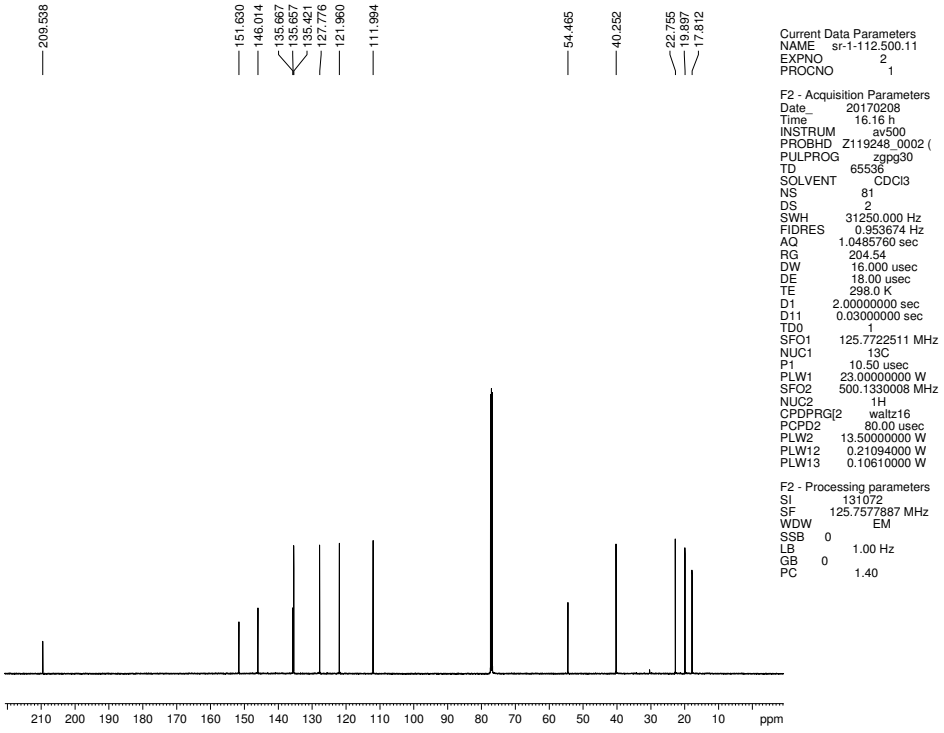

Figure 4.147 ^{13}C NMR (125 MHz, $CDCl_3$) of compound **4.23**.

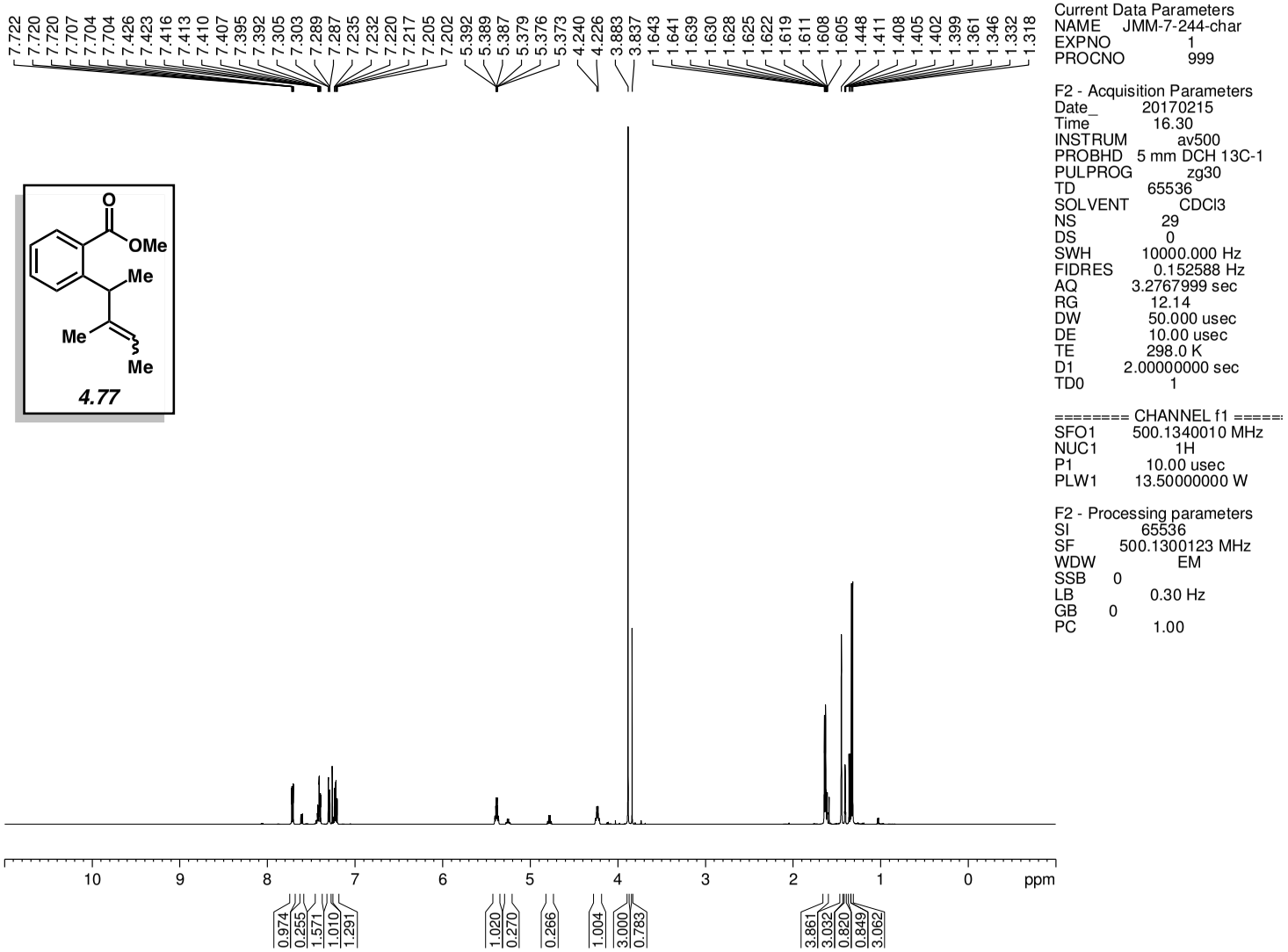

Figure 4.148 ^{1}H NMR (500 MHz, $CDCl_3$) of compound **4.77**.

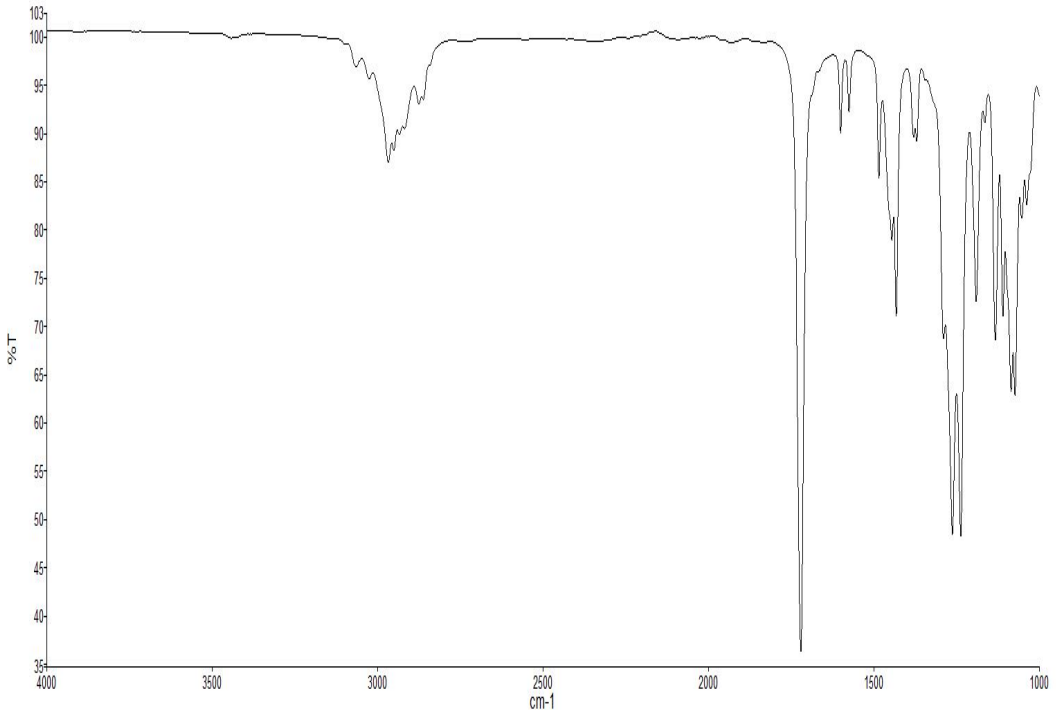

Figure 4.149 Infrared spectrum of compound **4.77**.

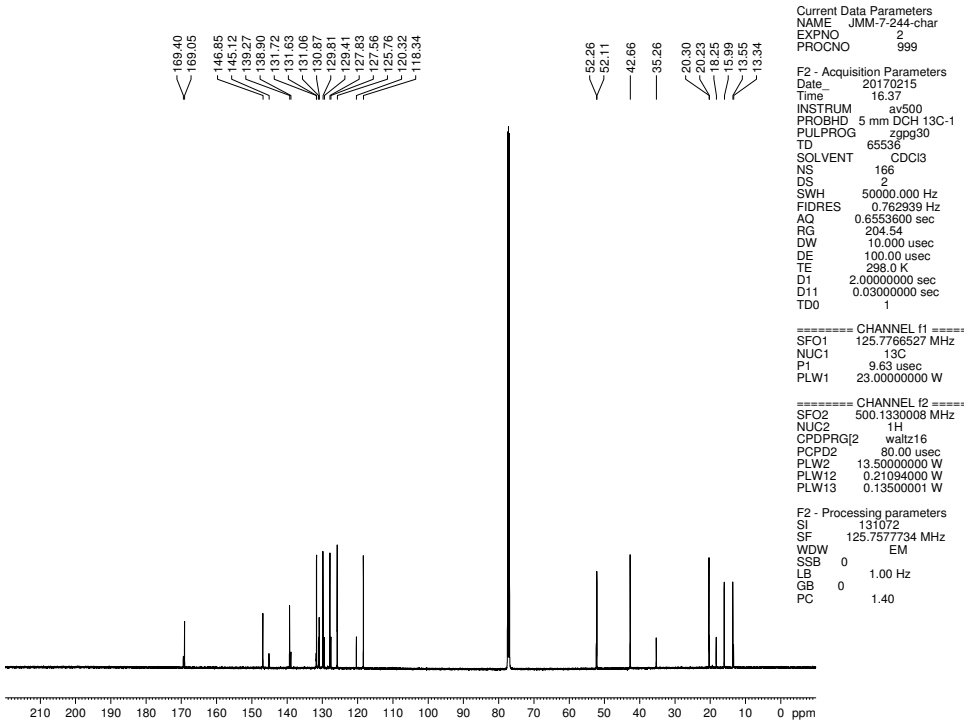

Figure 4.150 ^{13}C NMR (125 MHz, $CDCl_3$) of compound **4.77**.

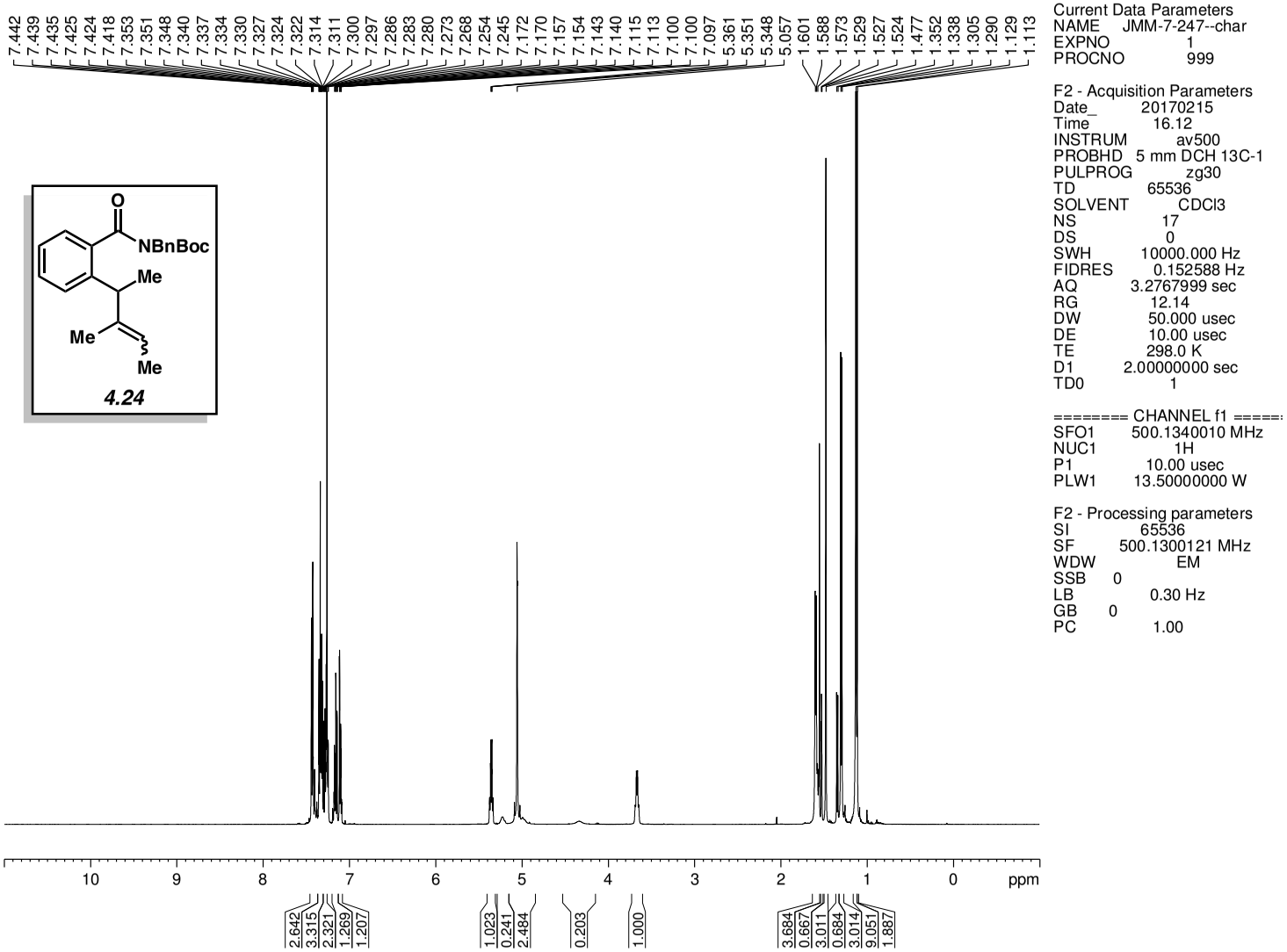

Figure 4.151 ^{1}H NMR (500 MHz, $CDCl_3$) of compound **4.24**.

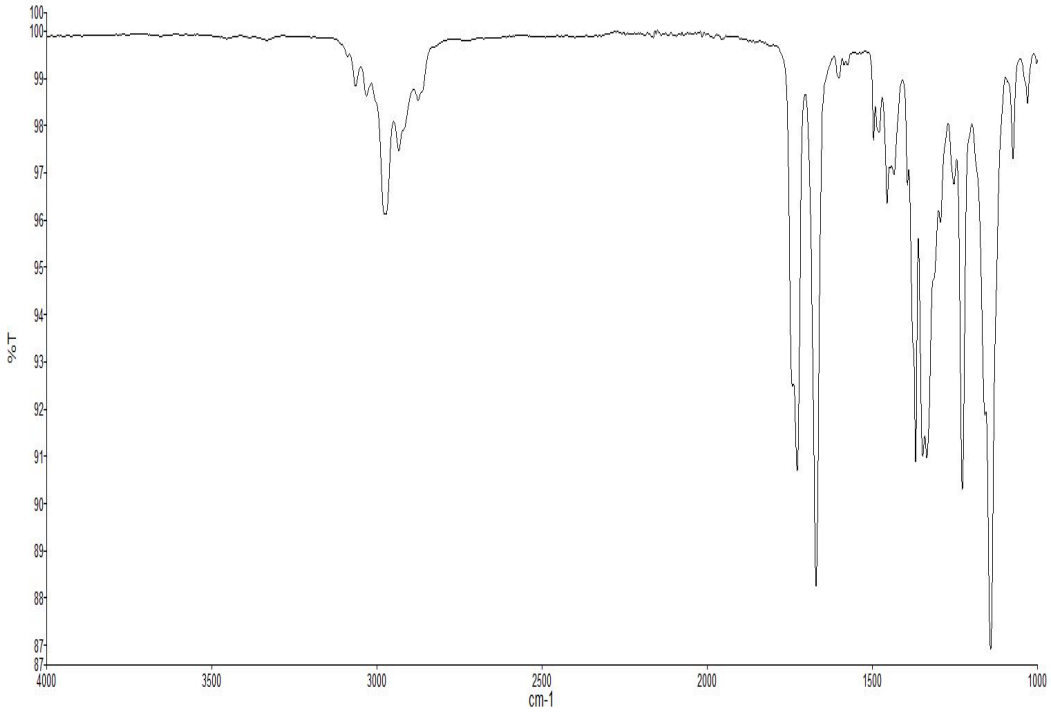

Figure 4.152 Infrared spectrum of compound **4.24**.

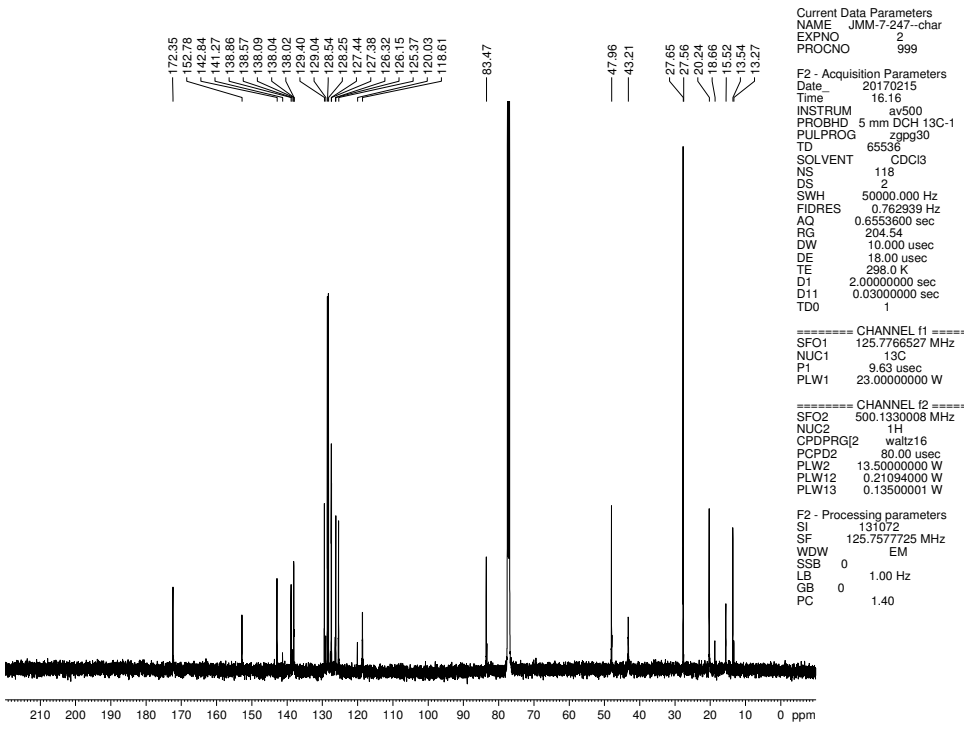

Figure 4.153 ^{13}C NMR (125 MHz, $CDCl_3$) of compound **4.24**.

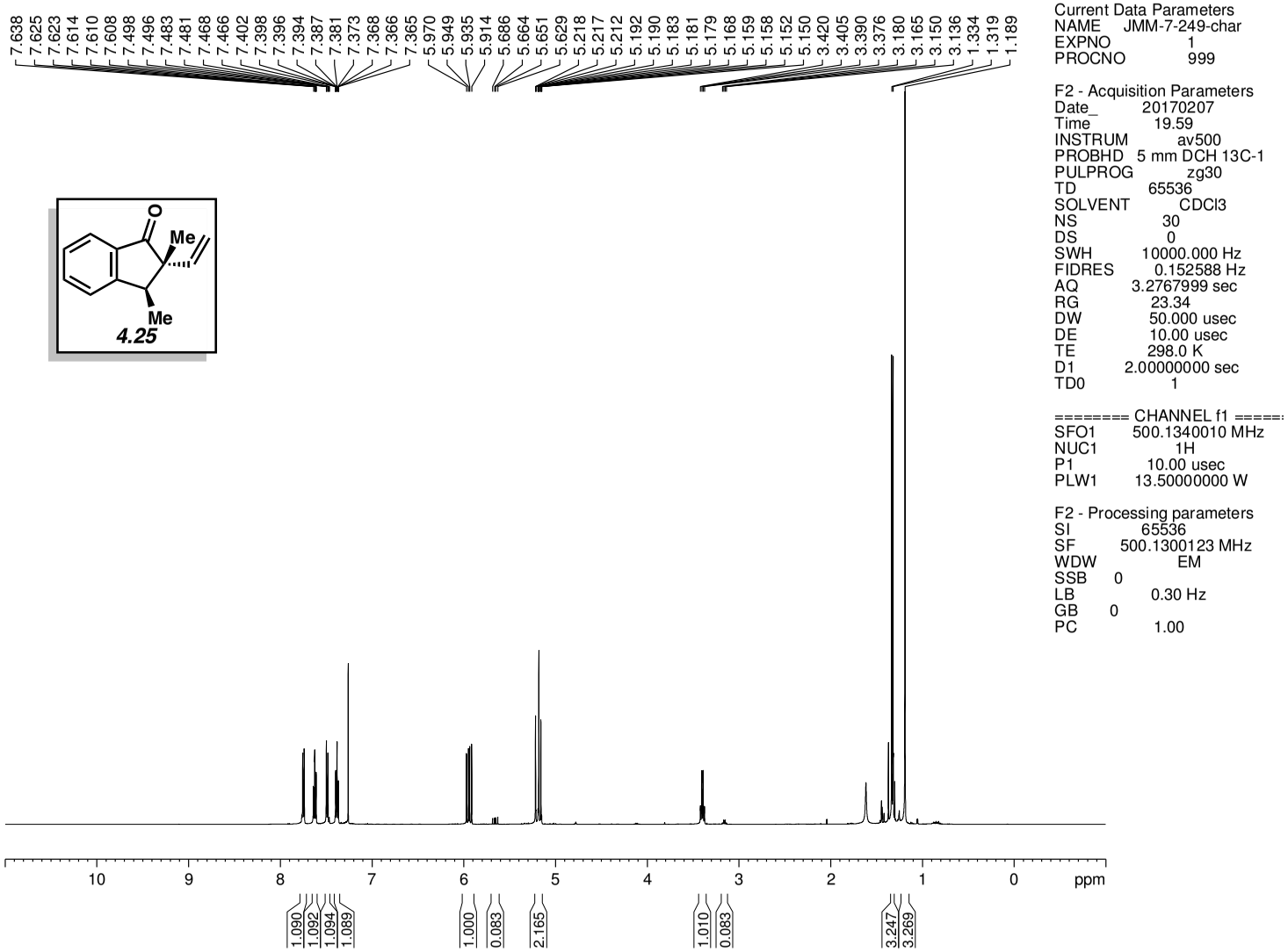

Figure 4.154 ^{1}H NMR (500 MHz, $CDCl_3$) of compound **4.25**.

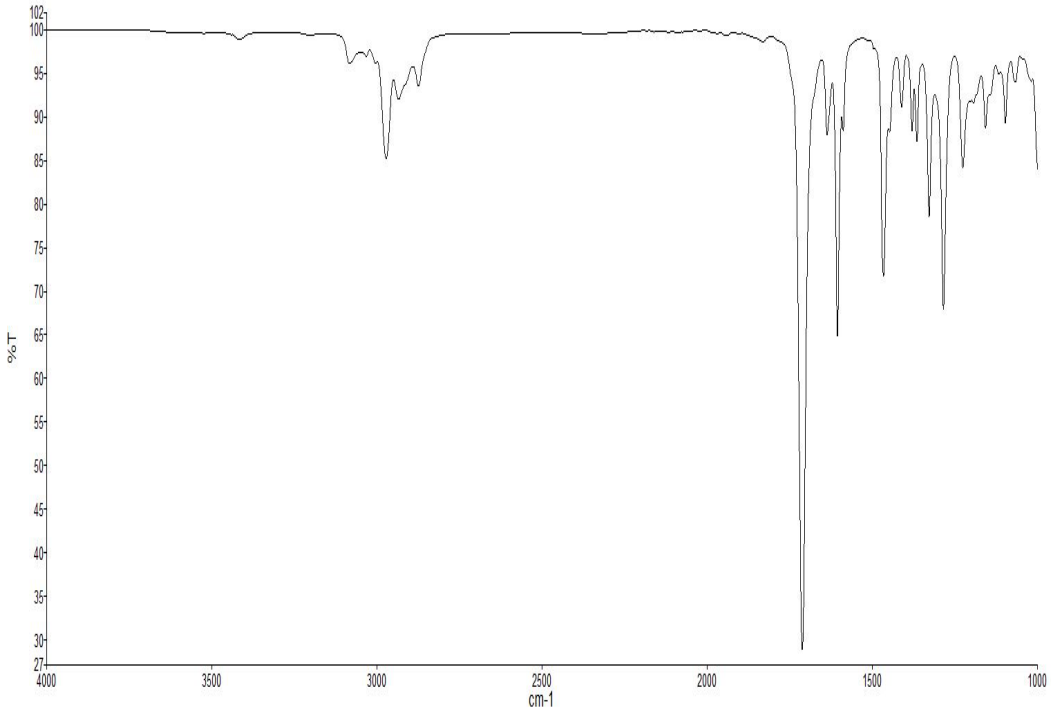

Figure 4.155 Infrared spectrum of compound **4.25**.

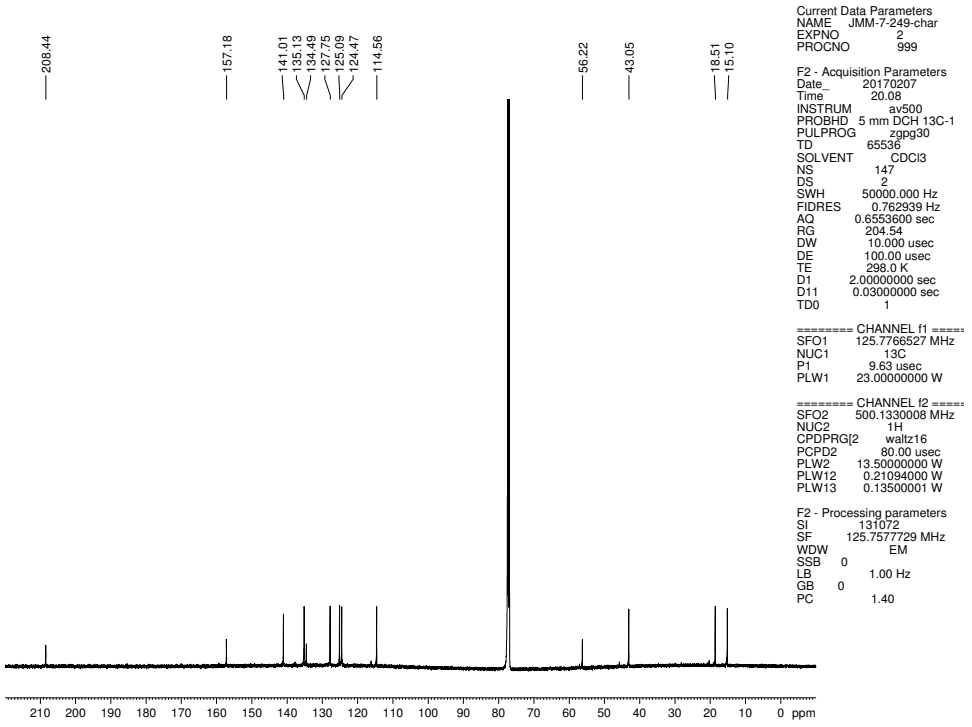

Figure 4.156 ^{13}C NMR (125 MHz, $CDCl_3$) of compound **4.25**.

4.9 Notes and References

(1) For reviews on quaternary stereocenters, see: (a) Christoffers, J.; Baro, A. *Adv. Synth. Catal.* **2005**, *347*, 1473–1482. (b) Trost, B. M.; Jiang, C. *Synthesis* **2006**, *3*, 369–396. (c) Quasdorf, K. W.; Overman, L. E. *Nature* **2014**, *516*, 181–191. (d) Marek, I.; Minko, Y.; Pasco, M.; Mejuch, T.; Gilboa, N.; Chechik, H.; Das, J. P. *J. Am. Chem. Soc.* **2014**, *136*, 2682–2694. (e) Liu, Y.; Han, S.-J.; Liu, W.-B.; Stoltz, B. M. *Acc. Chem. Res.* **2015**, *48*, 740–751. (f) Long, R.; Huang, J.; Gong, J.; Yang, Z. *Nat. Prod. Rep.* **2015**, *32*, 1584–1601. (g) Zeng, X.-P.; Cao, Z.-Y.; Wang, Y.-H.; Zhou, F.; Zhou, J. *Chem. Rev.* **2016**, *116*, 7330–7396. (h) Christoffers, J.; Baro, A. John Wiley & Sons. *Quaternary stereocenters: challenges and solutions for organic synthesis*; Wiley-VCH: Weinheim, **2005**.

(2) (a) Beletskaya, I. P.; Cheprakov, A. V. *Chem. Rev.* **2000**, *100*, 3009–3066. (b) Whitcombe, N. J.; Hii, K. K.; Gibson, S. E. *Tetrahedron* **2001**, *57*, 7449–7476. (c) Dounay, A. B.; Overman, L. E. *Chem. Rev.* **2003**, *103*, 2945–2964. (d) Shibasaki, M.; Vogl, E. M.; Ohshima, T. *Adv. Synth. Catal.* **2004**, *346*, 1533–1552. (e) Oestreich, M. *Top. Organomet. Chem.* **2007**, *24*, 169–192. (f) Shibasaki, M.; Ohshima, T.; Itano, W. *Sci. Synth.* **2011**, *3*, 483–512. (g) Mc Cartney, D.; Guiry, P. J. *Chem. Soc. Rev.* **2011**, *40*, 5122–5150. (h) Le Bras, J.; Muzart, J. *Chem. Rev*. **2011**, *111*, 1170–1214. (i) Jones, A. C.; May, J. A.; Sarpong, R.; Stoltz, B. M. *Angew. Chem., Int. Ed.* **2014**, *53*, 2556–2591.

(3) β-hydride elimination of Ni(II) intermediates is known to be challenging; see: Lin, B.-L.; Liu, L.; Fu, Y.; Luo, S.-W.; Chen, Q.; Guo, Q.-X. *Organometallics* **2004**, *23*, 2114–2123.

(4) For Ni-catalyzed reactions of amide derivatives to build C–O or C–N bonds, see: (a) Hie, L.; Fine Nathel, N. F.; Shah, T.; Baker, E. L.; Hong, X.; Yang, Y.-F.; Liu, P.; Houk, K. N.; Garg, N. K. *Nature* **2015**, *524*, 79–83. (b) Baker, E. L.; Yamano, M. M.; Zhou, Y.; Anthony, S. M.;

Garg, N. K. *Nat. Commun*. **2016**, *7*, 11554. (c) Hie, L.; Baker, E. L.; Anthony, S. M.; Desrosiers, J.-N.; Senanayake, C.; Garg, N. K. *Angew. Chem., Int. Ed.* **2016**, *55*, 15129–15132.

(5) For Ni-catalyzed reactions of amide derivatives to build C–C bonds, see: (a) Weires, N. A.; Baker, E. L.; Garg, N. K. *Nat. Chem*. **2016**, *8*, 75–79. (b) Simmons, B. J.; Weires, N. A.; Dander, J. E.; Garg, N. K. *ACS Catal*. **2016**, *6*, 3176–3179. (c) Dander, J. E.; Weires, N. A.; Garg, N. K. *Org. Lett*. **2016**, *18*, 3934–3936. (d) Shi, S.; Szostak, M. *Chem. Eur. J.* **2016**, *22*, 10420–10424. (e) Liu, L.; Chen, P.; Sun, Y.; Wu, Y.; Chen, S.; Zhu, J.; Zhao, Y. *J. Org. Chem.* **2016**, *81*, 11686–11696.

(6) For Pd-catalyzed reactions of amide derivatives to build C–C bonds, see: (a) Li, X.; Zou, G. *Chem. Commun.* **2015**, *51*, 5089–5092. (b) Li, X.; Zou, G. *J. Organomet. Chem.* **2015**, *794*, 136–145. (c) Yada, A.; Okajima, S.; Murakami, M. *J. Am. Chem. Soc.* **2015**, *137*, 8708–8711. (d) Meng, G.; Szostak, M. *Org. Lett.* **2015**, *17*, 4364–4367. (e) Meng, G.; Szostak, M. *Org. Biomol. Chem.* **2016**, *14*, 5690–5705. (f) Liu, C.; Meng, G.; Liu, Y.; Liu, R.; Lalancette, R.; Szostak, R.; Szostak, M. *Org. Lett.* **2016**, *18*, 4194–4197. (g) Meng, G.; Shi, S.; Szostak, M. *ACS Catal.* **2016**, *6*, 7335–7339. (h) Cui, M.; Wu, H.; Jian, J.; Wang, H.; Liu, C.; Daniel, S.; Zeng, Z. *Chem. Commun.* **2016**, *52*, 12076–12079.

(7) For decarbonylative couplings of amide derivatives, see: (a) Meng, G.; Szostak, M. *Angew. Chem., Int. Ed.* **2015**, *54*, 14518–14522. (b) Hu, J.; Zhao, Y.; Zhang, Y.; Shi, Z. *Angew. Chem., Int. Ed.* **2016**, *55*, 8718–8722. (c) Shi, S.; Meng, G.; Szostak, M. *Angew. Chem., Int. Ed.* **2016**, *55*, 6959–6963. (d) Shi, S.; Szostak, M. *Org. Lett.* **2016**, *18*, 5872–5875. (e) Liu, C.; Meng, G.; Szostak, M. *J. Org. Chem.* **2016**, *81*, 12023–12030. (f) Yue, H.; Guo, L.; Liao, H.-H.; Cai, Y.; Zhu, C.; Rueping, M. *Angew. Chem., Int. Ed.* **2017**, *56*, 4282–4285.

(8) For pertinent reviews, see: (a) Meng, G.; Shi, S.; Szostak, M. *Synlett* **2016**, *27*, 2530–2540. (b) Dander, J. E.; Garg, N. K. *ACS Catal.* **2017**, *7*, 1413–1423. (c) Liu, C.; Szostak, M. *Chem. Eur. J.* [Online early access]. DOI: 10.1002/chem.201605012.

(9) Miles, K. C.; Le, C. C.; Stambuli, J. P. *Chem. Eur. J.* **2014**, *20*, 11336–11339.

(10) For the Pd-catalyzed Mizoroki–Heck cyclization of thioesters to give ortho-quinone methide products, see: Thottumkara, A. P.; Kurokawa, T.; Du Bois, J. *Chem. Sci.* **2013**, *4*, 2686-2689.

(11) (a) Negishi, E.-I.; Copéret, C.; Ma, S.; Mita, T.; Sugihara, T.; Tour, J. M. *J. Am. Chem. Soc.* **1996**, *118*, 5904–5918. (b) Hayashi, T.; Tang, J.; Kato, K. *Org. Lett.* **1999**, *1*, 1487–1489. (c) Wu, X.-F.; Neumann, H.; Spannenberg, A.; Schulz, T.; Jiao, H.; Beller, M. *J. Am. Chem. Soc.* **2010**, *132*, 14596–14602. (d) Goegsig, T. M.; Nielsen, D. U.; Lindhardt, A. T.; Skrydstrup, T. *Org. Lett.* **2012**, *14*, 2536–2539.

(12) Amide derivatives are considered to be ideally suited for use as synthons in chemical synthesis because of their directing group ability and stability to a variety of reaction conditions.

(13) For pertinent reviews concerning nickel catalysis, see: (a) Rosen, B. M.; Quasdorf, K. W.; Wilson, D. A.; Zhang, N.; Resmerita, A.-M.; Garg, N. K.; Percec, V. *Chem. Rev*. **2011**, *111*, 1346−1416. (b) Tasker, S. Z.; Standley, E. A.; Jamison, T. F. *Nature* **2014**, *509*, 299−309. (c) Mesganaw, T.; Garg, N. K. *Org. Process Res. Dev.* **2013**, *17*, 29−39. (d) Ananikov, V. P. *ACS Catal*. **2015**, *5*, 1964−1971.

(14) Substrates described in this manuscript were derived from commercially available 2-halobenzoic acid derivatives and readily available allylic electrophiles, either via lithiation/displacement or reductive coupling methodologies (see the SI). For reductive couplings, see: (a) Weix, D. J.; *Acc. Chem. Res.* **2015**, *48*, 1767–1775. (b) Anka-Lufford, L. L.; Prinsell, M. R.; Weix, D. J. *J. Org. Chem.* **2012**, *77*, 9989–10000. (c) Cui, X.; Wang, S.;

Zhang, Y.; Deng, W.; Qian, Q.; Gong, H. *Org. Biomol. Chem.* **2013**, *11*, 3094–3097. (d) Hansen, E. C.; Pedro, D. J.; Wotal, A. C.; Gower, N. J.; Nelson, J. D.; Caron, S.; Weix, D. J. *Nat. Chem.* **2016**, *8*, 1226–1230.

(15) Other classes of amide derivatives were also evaluated, such as *N*-Me,Ph, *N*-Me,Ts, *N*-Ph,Boc, *N*-Ph,Ts. However, these efforts either led to no product or the Mizoroki–Heck cyclization product in diminished yields. Similarly, efforts to generate 6- or 7-membered ring products were unsuccessful.

(16) Extensive variations in bases (e.g. Cs_2CO_3, K_3PO_4, NaH), ligands (e.g. terpyridine, IMes, Benz-I*t*Bu), solvents (DME, DMA, $PhCF_3$), Ni and ligand loadings, and temperature were explored.

(17) NHC precursors **4.7**–**4.9** are commercially available.

(18) Additives such as morpholine, aniline, Et_2NH, and 1-hexanol were also tested. Of all additives examined, *t*-amyl alcohol proved most successful. For the use of alcohols as additives in Ni-catalyzed cross couplings, see: Harris, M. R.; Hanna, L. E.; Greene, M. A.; Moore, C. E.; Jarvo, E. R. *J. Am. Chem. Soc.* **2013**, *135*, 3303–3306.

(19) (a) Using entry 7 conditions, cyclized product **4.6** was obtained in 74% isolated yield, respectively. Product **4.6** is volatile as described in the SI. (b) Product **4.6** could also be obtained in comparable yield by Mizoroki–Heck cyclization of the *N*-*n*Bu,Boc derivative of **4.5**, thus demonstrating that this methodology is not restricted to *N*-benzyl amide derivatives.

(20) For the Ni-catalyzed Mizoroki–Heck cyclization of *aryl* halides, albeit without tetrasubstituted olefins, see: Desrosiers, J.-N.; Hie, L.; Biswas, S.; Zatalochnaya, O. V.; Rodriguez, S.; Lee, H.; Grinberg, N.; Haddad, N.; Yee, N. K.; Garg, N. K.; Senanayake, C. *Angew. Chem., Int. Ed.* **2016**, *55*, 11921–11924; see also references therein.

(21) For examples of Mizoroki–Heck reactions involving tetrasubstituted olefins, see: (a) Shuler, S. A.; Yin, G.; Krause, S. B.; Vesper, C. M.; Watson, D. A. *J. Am. Chem. Soc*. **2016**, *138*, 13830–13833. (b) Seo, J. H.; Liu, P.; Weinreb, S. M. *J. Org. Chem*. **2010**, *75*, 2667–2680. (c) Liu, P.; Seo, J. H.; Weinreb, S. M. *Angew. Chem., Int. Ed*. **2010**, *49*, 2000–2003. (d) Abelman, M. M.; Oh, T.; Overman, L. E. *J. Org. Chem*. **1987**, *52*, 4130–4133. (e) Madin, A.; O'Donnell, C. J.; Oh, T.; Old, D. W.; Overman, L. E.; Sharp, M. J. *J. Am. Chem. Soc*. **2005**, *127*, 18054–18065.

(22) 2-Vinylindanones bearing quaternary stereocenters can also be synthesized by the Pd- or Ni-catalyzed α-vinylation of lithium enolates; see (a) Huang, J.; Bunel, E.; Faul, M. M. *Org. Lett*. **2007**, *9*, 4343–4346. (b) Grigalunas, M.; Ankner, T.; Norrby, P.-O.; Wiest, O.; Helquist, P. *Org. Lett.* **2014**, *16*, 3970–3973. (c) Grigalunas, M.; Ankner, T.; Norrby, P.-O.; Wiest, P. Helquist, O. *J. Am. Chem. Soc*. **2015**, *137*, 7019–7022. (d) Chieffi, A.; Kamikawa, K.; Ahman, J.; Fox, J. M.; Buchwald, S. L. *Org. Lett*. **2001**, *3*, 1897–1900.

(23) A substrate containing a phenyl (Ph) group at the R' position was also tested, but was deemed unreactive.

(24) This substrate was employed as a 7:1 mixture of *E* to *Z* olefins.

(25) See the Supporting Information for details.

(26) (a) Böhm, H.-J.; Banner, D.; Bendels, S.; Kansy, M.; Kuhn, B.; Müller, K.; Obst-Sander, U.; Stahl, M. *ChemBioChem*, **2004**, *5*, 637–643. (b) Wang, J.; Sánchez-Roselló, M.; Aceña, J. L.; del Pozo, C.; Sorochinsky, A. E.; Fustero, S.; Soloshonok, V. A.; Liu, H. *Chem. Rev.* **2014**, *114*, 2432–2506. (c) Gillis, E. P.; Eastman, K. J.; Hill, M. D.; Donnelly, D. J.; Meanwell, N. A. *J. Med. Chem.* **2015**, *58*, 8315–8359.

(27) This substrate was employed as a 4:1 mixture of *E* to *Z* olefins.

(28) Based on calculated rotational energies for conformers of 3-methyl-1-butene and allylic strain arguments, **TS2** is estimated to be roughly 0.7 kcal/mol higher in energy compared to **TS1**. For a review, see: Hoffmann, R. W. *Chem. Rev.* **1989**, *89*, 1841–1860.

(29) Querolle, O.; Dubois, J.; Thoret, S.; Roussi, F.; Guéritte, F.; Guénard, D. *J. Med. Chem.* **2004**, *47*, 5937–5944.

(30) Clennan, E. L.; Chen, X. *J. Am. Chem. Soc.* **1989**, *111*, 5787–5792.

(31) Tanaka, K.; Uneme, H.; Ono, N.; Kaji, A. *Chem. Lett*. **1979**, *9*, 1039–1040.

(32) Friese, A.; Hell-Momeni, K.; Zundorf, I.; Winckler, T.; Dingermann, T.; Dannhardt, G. *J. Med. Chem*. **2002**, *45*, 1535–1542.

(33) Shimano, M.; Kamei, N.; Tanaka, T.; Harada, T.; Haino, M.; Okuyama, A.; Arakawa, Y. Murakami, Y. Reverse Hydroxamic Acid Derivatives. Eur. Pat. Appl. 1431285. June 23rd, 2004.

(34) Sato, K.; Sugimoto, H.; Rikimaru, K.; Imoto, H.; Kamaura, M.; Negoro, N.; Tsujihata, Y.; Miyashita, H.; Odani, T.; Murata, T. *Bioorg. Med. Chem.* **2014**, *22*, 1649–1666.

(35) (a) Mori, M.; Kaneta, N.; Isono, N.; Shibasaki, M. *J. Organomet. Chem*. **1993**, *455*, 255–260. (b) Kotha, S.; Mandal, K.; Tiwari, A.; Mobin, S. M. *Chem. Eur. J*. **2006**, *12*, 8024–8038.

(36) Van Zyl. C. M.; McKeeby, J. L.; Van Dort, P. C.; Larson, E. J.; Silver, M. E. *Inorg. Chim. Acta*. **1987**, *133*, 289–294.